

# SATURN

MPR-SAT-FE-72-1

JUNE 19, 1972

(NASA-TM-X-69535) SATURN 5 LAUNCH  
VEHICLE FLIGHT EVALUATION REPORT-AS-511  
APOLLO 16 MISSION (NASA) 317 p HC  
\$18.00

N73-33823

CSC 22C

Unclas  
63/30 19846

## SATURN V LAUNCH VEHICLE FLIGHT EVALUATION REPORT-AS-511 APOLLO 16 MISSION

PREPARED BY  
SATURN FLIGHT EVALUATION  
WORKING GROUP



NATIONAL AERONAUTICS AND SPACE ADMINISTRATION

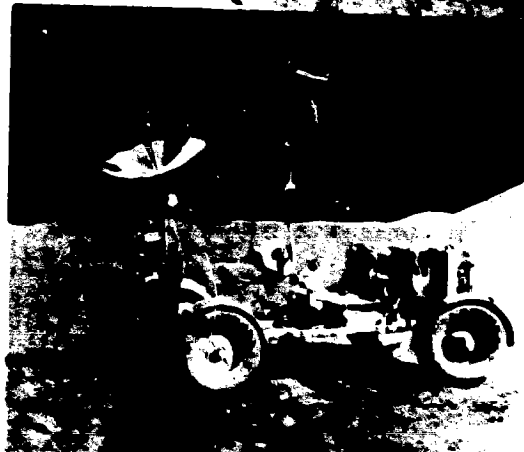
GEORGE C. MARSHALL SPACE FLIGHT CENTER

MPR-SAT-FE-72-1      JUNE 19, 1972

**SATURN V LAUNCH VEHICLE  
FLIGHT EVALUATION  
REPORT-AS-511  
APOLLO 16 MISSION**

**PREPARED BY  
SATURN FLIGHT EVALUATION  
WORKING GROUP**

REPRODUCIBILITY OF THE ORIGINAL PAGE IS POOR.



MPR-SAT-FE-72-1

SATURN V LAUNCH VEHICLE FLIGHT EVALUATION REPORT - AS-511

APOLLO 16 MISSION

BY

Saturn Flight Evaluation Working Group  
George C. Marshall Space Flight Center

ABSTRACT

Saturn V AS-511 (Apollo 16 Mission) was launched at 12:54:00 Eastern Standard Time (EST) on April 16, 1972, from Kennedy Space Center, Complex 39, Pad A. The vehicle lifted off on a launch azimuth of 90 degrees east of north and rolled to a flight azimuth of 72.034 degrees east of north. The launch vehicle successfully placed the manned spacecraft in the planned translunar coast mode. The S-IVB/IU impacted the lunar surface within the planned target area.

This was the second Apollo Mission to employ the Lunar Roving Vehicle (LRV) during Extravehicular Activity (EVA). The performance of the LRV was satisfactory and as on Apollo 15 Mission resulted in a significant increase in lunar exploration capability. The total distance traveled on the lunar surface with the LRV on this Mission was 27 kilometers (17 miles).

All launch vehicle Mandatory and Desirable Objectives were accomplished except the precise determination of the lunar impact point and time. No failures or anomalies occurred that seriously affected the mission.

Any questions or comments pertaining to the information contained in this report are invited and should be directed to:

Director, George C. Marshall Space Flight Center  
Huntsville, Alabama 35812  
Attention: Chairman, Saturn Flight Evaluation Working  
Group, S&E-CSE-LA (Phone 205-453-2462)

# PRECEDING PAGE BLANK NOT FILMED

## TABLE OF CONTENTS

	Page		Page
TABLE OF CONTENTS	iii	4.2.2 Parking Orbit Phase	4-7
LIST OF ILLUSTRATIONS	vii	4.2.3 Injection Phase	4-9
LIST OF TABLES	xi	4.2.4 Early Translunar Orbit Phase	4-10
ACKNOWLEDGEMENT	xiii	<b>SECTION 5 - S-IC PROPULSION</b>	
ABBREVIATIONS	xiv	5.1 Summary	5-1
MISSION PLAN	xviii	5.2 S-IC Ignition Transient Performance	5-1
FLIGHT SUMMARY	xxi	5.3 S-IC Mainstage Performance	5-3
MISSION OBJECTIVES ACCOMPLISHMENT	xxviii	5.4 S-IC Engine Shutdown Transient Performance	5-5
FAILURES AND ANOMALIES	xxvix	5.5 S-IC Stage Propellant Management	5-6
<b>SECTION 1 - INTRODUCTION</b>		5.6 S-IC Pressurization Systems	5-7
1.1 Purpose	1-1	5.6.1 S-IC Fuel Pressurization System	5-7
1.2 Scope	1-1	5.6.2 S-IC LGX Pressurization System	5-9
<b>SECTION 2 - EVENT TIMES</b>		5.7 S-IC Pneumatic Control Pressure System	5-10
2.1 Summary of Events	2-1	5.8 S-IC Purge Systems	5-10
2.2 Variable Time and Commanded Switch Selector Events	2-1	5.9 S-IC POGO Suppression System	5-10
<b>SECTION 3 - LAUNCH OPERATIONS</b>		5.10 S-IC Hydraulic System	5-10
3.1 Summary	3-1	<b>SECTION 6 - S-II PROPULSION</b>	
3.2 Prelaunch Milestones	3-1	6.1 Summary	6-1
3.2.1 S-IC Stage Prelaunch Problems	3-1	6.2 S-II Chilldown and Buildup Transient Performance	6-2
3.2.2 S-II Stage Prelaunch Problems	3-1	6.3 S-II Mainstage Performance	6-7
3.2.3 S-IVB Prelaunch Problems	3-3	6.4 S-II Shutdown Transient Performance	6-9
3.2.4 IU Stage Prelaunch Problems	3-3	6.5 S-II Stage Propellant Management	6-11
3.3 Terminal Countdown	3-4	6.6 S-II Pressurization System	6-13
3.4 Propellant Loading	3-4	6.6.1 S-II Fuel Pressurization System	6-13
3.4.1 RP-1 Loading	3-4	6.6.2 S-II LOX Pressurization System	6-15
3.4.2 LOX Loading	3-4	6.7 S-II Pneumatic Control Pressure System	6-19
3.4.3 LH <sub>2</sub> Loading	3-5		
3.5 Ground Support Equipment	3-6		
3.5.1 Ground/Vehicle Interface	3-6		
3.5.2 MSFC Furnished Ground Support Equipment	3-7		
<b>SECTION 4 - TRAJECTORY</b>			
4.1 Summary	4-1		
4.2 Trajectory Evaluation	4-1		
4.2.1 Ascent Phase	4-1		

## TABLE OF CONTENTS (CONTINUED)

		Page		Page
6.8	S-II Helium Injection System	6-19	8.2.2	Bending Moments 8-3
6.9	POGO Suppression System	6-20	8.2.3	Vehicle Dynamic Characteristics 8-3
6.10	S-II Hydraulic System	6-20	8.2.3.1	Longitudinal Dynamic Characteristics 8-3
<b>SECTION 7 - S-IVB PROPULSION</b>			8.2.4	Vibration 8-5
7.1	Summary	7-1	8.3	S-II POGO Limiting Backup Cutoff System 8-7
7.2	S-IVB Chillydown and Buildup Transient Performance for First Burn	7-2	<b>SECTION 9 - GUIDANCE AND NAVIGATION</b>	
7.3	S-IVB Mainstage Performance for First Burn	7-5	9.1	Summary 9-1
7.4	S-IVB Shutdown Transient Performance for First Burn	7-7	9.2	Guidance Comparisons 9-1
7.5	S-IVB Parking Orbit Coast Phase Conditioning	7-7	9.3	Navigation and Guidance Scheme Evaluation 9-10
7.6	S-IVB Chillydown and Buildup Transient Performance for Second Burn	7-7	9.4	Navigation and Guidance System Components 9-22
7.7	S-IVB Mainstage Performance For Second Burn	7-13	9.4.1	ST-124M Stabilized Platform System 9-24
7.7.1	Mainstage Prediction Technique	7-15	9.4.2	LVDC and LVDA 9-24
7.8	S-IVB Shutdown Transient Performance for Second Burn	7-17	<b>SECTION 10 - CONTROL AND SEPARATION</b>	
7.9	S-IVB Stage Propellant Management	7-17	10.1	Summary 10-1
7.10	S-IVB Pressurization System	7-18	10.2	S-IC Control System Evaluation 10-1
7.10.1	S-IVB Fuel Pressurization System	7-18	10.2.1	Liftoff Clearances 10-1
7.10.2	S-IVB LOX Pressurization System	7-20	10.2.2	Inflight Dynamics 10-1
7.11	S-IVB Pneumatic Control Pressure System	7-24	10.3	S-II Control System Evaluation 10-8
7.12	S-IVB Auxiliary Propulsion System	7-24	10.4	S-IVB Control System Evaluation 10-9
7.12.1	APS Module 1 Performance	7-24	10.4.1	Control System Evaluation During First Burn 10-9
7.12.1.1	Propellant System	7-24	10.4.2	Control System Evaluation During Parking Orbit 10-14
7.12.1.2	Helium Pressurization System	7-29	10.4.3	Control System Evaluation During Second Burn 10-15
7.12.1.3	Results of Failure Investigation	7-31	10.4.4	Control System Evaluation After S-IVB Second Burn 10-18
7.12.1.4	APS External Leakage Corrective Action	7-31	10.5	Instrument Unit Control Components Evaluation 10-24
7.12.1.5	Thrust System	7-31	10.6	Separation 10-24
7.12.2	APS Module 2 Performance	7-31	10.6.1	S-IC/S-II Separation 10-24
7.12.2.1	Propellant System	7-34	10.6.2	S-II Second Plane Separation Evaluation 10-26
7.12.2.2	Helium Pressurization System	7-34	10.6.3	S-II/S-IVB Separation 10-26
7.12.2.3	APS Internal Leakage Corrective Action	7-38	10.6.4	S-IVB/CSM Separation 10-26
7.12.2.4	Thrust System	7-39	<b>SECTION 11- ELECTRICAL NETWORKS AND EMERGENCY DETECTION SYSTEM</b>	
7.13	S-IVB Orbital Safing Operations	7-40	11.1	Summary 11-1
7.13.1	Fuel Tank Safing	7-40	11.2	S-IC Stage Electrical System 11-1
7.13.2	LOX Tank Dumping and Safing	7-41	11.3	S-II Stage Electrical System 11-1
7.13.3	Cold Helium Dump	7-41	11.3.1	S-II Ignition System Electrical Network Anomaly 11-2
7.13.4	Ambient Helium Dump	7-41	11.4	S-IVB Stage Electrical System 11-3
7.13.5	Stage Pneumatic Control Sphere Safing	7-43	11.4.1	Summary 11-3
7.13.6	Engine Start Tank Safing	7-43	11.4.2	S-IVB Forward Battery No. 2 Battery Performance 11-3
7.13.7	Engine Control Sphere Safing	7-44	11.5	Instrument Unit Electrical System 11-9
7.14	Hydraulic System	7-44	11.5.1	Summary 11-9
<b>SECTION 8 - STRUCTURES</b>			11.5.2	Battery Analysis 11-14
8.1	Summary	8-1		
8.2	Total Vehicle Structures Evaluation	8-1		
8.2.1	Longitudinal Loads	8-1		

## TABLE OF CONTENTS (CONTINUED)

		Page			Page
11.6	Saturn V Emergency Detection System (EDS)	11-15	SECTION 18 - SPACECRAFT SUMMARY		18-1
	SECTION 12 - VEHICLE PRESSURE ENVIRONMENT		SECTION 19 - APOLLO 16 INFLIGHT DEMONSTRATION		19-1
12.1	Summary	12-1	SECTION 20 - LUNAR ROVING VEHICLE		
12.2	Base Pressures	12-1	20.1	Summary	20-1
12.2.1	S-IC Base Pressures	12-1	20.2	Deployment	20-3
12.2.2	S-II Base Pressures	12-1	20.3	LRV to Stowed Payload Interface	20-3
	SECTION 13 - VEHICLE THERMAL ENVIRONMENT		20.4	Lunar Trafficability Environment	20-3
13.1	Summary	13-1	20.5	Wheel Soil Interaction	20-6
13.2	S-IC Base Heating	13-1	20.6	Locomotion Performance	20-6
13.3	S-II Base Heating	13-1	20.7	Mechanical Systems	20-6
13.4	Vehicle Aeroheating Thermal Environment	13-6	20.7.1	Harmonic Drive	20-6
13.5	S-IC/S-II Separation Thermal Environment	13-7	20.7.2	Wheels and Suspension	20-6
	SECTION 14 - ENVIRONMENTAL CONTROL SYSTEMS		20.7.3	Brakes	20-8
14.1	Summary	14-1	20.7.4	Stability	20-8
14.2	S-IC Environmental Control	14-1	20.7.5	Hand Controller	20-8
14.3	S-II Environmental Control	14-2	20.7.6	Loads	20-8
14.4	IU Environmental Control	14-2	20.8	Electrical Systems	20-8
14.4.1	Thermal Conditioning System (TCS)	14-2	20.8.1	Batteries	20-8
14.4.2	ST-124M Gas Bearing System (GBS)	14-7	20.8.2	Traction Drive System	20-8
	SECTION 15 - DATA SYSTEMS		20.8.3	Distribution System	20-9
15.1	Summary	15-1	20.8.4	Steering	20-9
15.2	Vehicle Measurement Evaluation	15-1	20.8.5	Amp-Hour Integrator	20-9
15.3	Airborne VHF Telemetry Systems Evaluation	15-1	20.9	Control and Display Console	20-10
15.4	C-Band Radar System Evaluation	15-4	20.10	Navigation System	20-10
15.5	Secure Range Safety Command Systems Evaluation	15-7	20.11	Crew Station	20-15
15.6	Command and Communication System Evaluation	15-7	20.12	Thermal	20-16
15.6.1	Command Communication System Summary	15-7	20.12.1	Summary	20-16
15.6.2	CCS Performance	15-7	20.12.2	Transportation Phase	20-16
15.6.3	CCS Signal Loss	15-10	20.12.3	Extravehicular Activity Periods	20-16
15.7	Ground Engineering Cameras	15-12	20.13	Structural	20-19
	SECTION 16 - MASS CHARACTERISTICS		20.14	Lunar Roving Vehicle Configuration	20-19
16.1	Summary	16-1	APPENDIX A - ATMOSPHERE		
16.2	Mass Evaluation	16-1	A.1	Summary	A-1
	SECTION 17 - LUNAR IMPACT		A.2	General Atmospheric Conditions at Launch Time	A-1
17.1	Summary	17-1	A.3	Surface Observations at Launch Time	A-1
17.2	Translunar Coast Maneuvers	17-1	A.4	Upper Air Measurements	A-1
17.3	Trajectory Evaluation	17-5	A.4.1	Wind Speed	A-1
17.4	Lunar Impact Conditions	17-5	A.4.2	Wind Direction	A-2
17.5	Tracking Data	17-8	A.4.3	Pitch Wind Component	A-2
			A.4.4	Yaw Wind Component	A-2
			A.4.5	Component Wind Shears	A-2
			A.4.6	Extreme Wind Data in the High Dynamic Region	A-2
			A.5	Thermodynamic Data	A-2
			A.5.1	Temperature	A-3
			A.5.2	Atmospheric Density	A-3
			A.5.3	Optical Index of Refraction	A-3

## TABLE OF CONTENTS (CONTINUED)

A.6	Comparison of Selected Atmospheric Data for Saturn V Launches	A-3
APPENDIX B - AS-511 SIGNIFICANT CONFIGURATION CHANGES		
B.1	Introduction	B-1



## LIST OF ILLUSTRATIONS

Figure	Page	Figure	Page
		6-9	S-II Fuel Pump Inlet Conditions 6-16
2-1	Ground Station Time to Vehicle Time Conversion 2-2	6-10	S-II LOX Tank Ullage Pressure 6-17
4-1	Ascent Trajectory Position Comparison 4-2	6-11	S-II LOX Pump Inlet Conditions 6-18
4-2	Ascent Trajectory Space-Fixed Velocity and Flight Path Angle Comparisons 4-2	6-12	S-II Center Engine LOX Feedline Accumulator Bleed System Performance 6-21
4-3	Ascent Trajectory Acceleration Comparison 4-3	6-13	S-II Center Engine LOX Feedline Accumulator Fill Transient 6-21
4-4	Dynamic Pressure and Mach Number Comparison 4-7	6-14	S-II Center Engine LOX Feedline Accumulator Helium Supply System Performance 6-22
4-5	Launch Vehicle Groundtrack 4-8	7-1	S-IVB Start Box and Run Requirements - First Burn 7-3
4-6	Injection Phase Space-Fixed Velocity and Flight Path Angle Comparisons 4-9	7-2	S-IVB Thrust Buildup Transient for First Burn 7-4
4-7	Injection Phase Acceleration Comparison 4-10	7-3	S-IVB Steady State Performance - First Burn 7-6
5-1	S-IC LOX Start Box Requirements 5-2	7-4	S-IVB Thrust Decay 7-8
5-2	S-IC Engines Thrust Buildup 5-3	7-5	S-IVB CVS Performance - Coast Phase 7-9
5-3	S-IC Stage Propulsion Performance 5-4	7-6	S-IVB Ullage Conditions During Repressurization Using O <sub>2</sub> /H <sub>2</sub> Burner 7-10
5-4	F-1 Engine Thrust Decay 5-6	7-7	S-IVB O <sub>2</sub> /H <sub>2</sub> Burner Thrust and Pressurant Flowrate 7-11
5-5	S-IC Thrust Decay 5-7	7-8	S-IVB Start Box and Run Requirements - Second Burn 7-12
5-6	S-IC Fuel Tank Ullage Pressure 5-8	7-9	S-IVB Steady State Performance - Second Burn 7-14
5-7	S-IC LOX Tank Ullage Pressure 5-9	7-10	S-IVB Engine Steady State Performance During Stage Acceptance Test 7-16
6-1	S-II Engine Start Tank Performance 6-3	7-11	S-IVB LH <sub>2</sub> Ullage Pressure - First Burn and Parking Orbit 7-19
6-2	S-II Engine Helium Tank Pressures 6-4	7-12	S-IVB LH <sub>2</sub> Ullage Pressure - Second Burn and Translunar Coast 7-19
6-3	S-II J-2 Engine Schematic 6-5	7-13	S-IVB Fuel Pump Inlet Conditions - First Burn 7-21
6-3a	J-2 Engine Configuration Changes 6-8	7-14	S-IVB Fuel Pump Inlet Conditions - Second Burn 7-22
6-4	S-II Engine Pump Inlet Start Requirements 6-8		
6-5	S-II Single Engine Thrust Buildup Characteristics 6-9		
6-6	S-II Propulsion Performance 6-10		
6-7	S-II J-2 Outboard Engine Thrust Decay 6-12		
6-8	S-II Fuel Tank Ullage Pressure 6-15		

## LIST OF ILLUSTRATIONS (CONTINUED)

Figure	Page	Figure	Page
7-15	S-1VB LOX Tank Ullage Pressure - First Burn and Earth Parking Orbit	7-23	
7-16	S-1VB LOX Pump Inlet Conditions - First Burn	7-25	
7-17	S-1VB LOX Pump Inlet Conditions - Second Burn	7-26	
7-18	S-1VB Cold Helium Supply History	7-27	
7-19	APS Module 1 Helium Supply Pressure	7-28	
7-20	S-1VB APS Accumulated Helium Leakage for Modules 1 and 2	7-30	
7-21	APS Regulator Outlet Pressure	7-32	
7-22	S-1VB Ambient Helium Interconnect Spheres Schematic	7-33	
7-23	APS Module 2 Supply Pressure	7-35	
7-24	APS Helium Bottle/Regulator Discharge Transducer Mounting	7-36	
7-25	APS Helium Pressure Regulator 1B54601	7-36	
7-26	APS Helium Regulator Outlet Pressure During Pressurization	7-37	
7-27	APS Module 2 Regulator Outlet Pressure	7-38	
7-28	APS Helium Bottle/Regulator Discharge Transducer Mounting (Proposed Redesign)	7-39	
7-29	S-1VB LOX Dump and Orbital Safing Sequence	7-40	
7-30	S-1VB LOX Dump Parameter Histories	7-42	
7-31	S-1VB LOX Tank Ullage Pressure - Second Burn and Translunar Coast	7-43	
8-1	Longitudinal Acceleration at IU and CM During Thrust Buildup and Launch	8-2	
8-2	Longitudinal Load at Time of Maximum Bending Moment, CECO and OECCO	8-2	
8-3	Bending Moment and Load Factor Distribution at Time of Maximum Bending Moment	8-3	
8-4	IU Accelerometer Five Hertz Response During S-IC Burn (Longitudinal)	8-4	
8-5	IU and CM Longitudinal Acceleration After S-IC CECO	8-5	
8-6	IU and CM Longitudinal Acceleration After S-IC OECCO	8-6	
8-7	AS-511/AS-510 Acceleration and Pressure Oscillations During S-II Burn (8 to 20 Hz Filter)	8-8	
8-8	AS-511 Pump Inlet Pressure and Thrust Pad Acceleration Oscillations During Accumulator Fill Transient (1 to 110 Hz Filter)	8-8	
8-9	S-1VB Stage vibration envelopes	8-9	
8-10	S-1VB Vibration Spectral Analysis	8-9	
9-1	Trajectory and ST-124M Platform Velocity Comparisons, Boost-to-EPO (Trajectory Minus LVDC)	9-2	
9-2	Trajectory and ST-124M Platform Velocity Comparisons, Boost-to-TLI (Trajectory Minus LVDC)	9-2	
9-3	Comparison of LVDC and Post-flight Trajectory During EPO, X Position and Velocity	9-6	
9-4	Comparison of LVDC and Post-flight Trajectory During EPO, Y Position and Velocity	9-7	
9-5	Comparison of LVDC and Post-flight Trajectory During EPO, Z Position and Velocity	9-8	
9-6	Comparison of LVDC and Post-flight Trajectory During EPO, Radius and Velocity	9-9	
9-7	Comparison of LVDC and Post-flight Trajectory During Boost to TLI, X Position and Velocity	9-11	
9-8	Comparison of LVDC and Post-flight Trajectory During Boost to TLI, Y Position and Velocity	9-12	
9-9	Comparison of LVDC and Post-flight Trajectory During Boost to TLI, Z Position and Velocity	9-13	
9-10	Comparisons of LVDC and Post-flight Trajectory During Boost to TLI, Radius and Velocity	9-14	
9-11	Continuous Vent System (CVS) Thrust and Acceleration During EPO	9-15	
9-12	AS-511 Pitch Attitude Angle, First Burn	9-18	
9-13	AS-511 Yaw Attitude Angle, First Burn	9-19	
9-14	AS-511 Roll Attitude Angle, First Burn	9-20	
9-15	Commanded and Actual Pitch Attitude - Second Burn	9-23	
9-16	Commanded and Actual Yaw Attitude - Second Burn	9-23	
9-17	Amplitude of Cross-Analysis	9-25	
10-1	AS-511 Liftoff Yaw Maneuver	10-2	
10-2	AS-511 Reconstructed Liftoff Trajectory	10-3	
10-3	Pitch Plane Dynamics During S-IC Burn	10-4	
10-4	Yaw Plane Dynamics During S-IC Burn	10-5	
10-5	Pitch and Yaw Plane Free Stream Angle of Attack During S-IC Burn	10-6	

## LIST OF ILLUSTRATIONS (CONTINUED)

Figure	Page	Figure	Page
10-6	Pitch Plane Dynamics During S-II Burn	10-10	
10-7	Yaw Plane Dynamics During S-II Burn	10-11	
10-8	Pitch Plane Dynamics During S-IVB First Burn	10-12	
10-9	Yaw Plane Dynamics During S-IVB First Burn	10-13	
10-10	Pitch Plane Dynamics During Parking Orbit	10-14	
10-11	Pitch Plane Dynamics During S-IVB Second Burn	10-16	
10-12	Yaw Plane Dynamics During S-IVB Second Burn	10-17	
10-13	Pitch Plane Dynamics During Translunar Coast (Sheet 1 of 5)	10-19	
10-14	AS-511 S-IC/S-II Separation Distance	10-25	
11-1	S-IVB Stage Forward No. 1 Battery Voltage and Current	11-4	
11-2	S-IVB Stage Forward No. 2 Battery Voltage and Current	11-5	
11-3	AS-510 S-IVB Stage Forward No. 2 Battery Voltage and Current	11-6	
11-4	S-IVB Stage Aft No. 1 Battery Voltage and Current	11-7	
11-5	S-IVB Stage Aft No. 2 Battery Voltage and Current	11-8	
11-6	6D10 Battery Measurements	11-10	
11-7	6D20 Battery Measurements	11-11	
11-8	6D30 Battery Measurements	11-12	
11-9	6D40 Battery Measurements	11-13	
12-1	S-IC Base Heat Shield Differential Pressure	12-2	
12-2	S-II Heat Shield Forward Face Pressure	12-2	
12-3	S-II Thrust Cone Pressure	12-3	
12-4	S-II Heat Shield Aft Face Pressure	12-3	
13-1	S-IC Base Region Total Heating Rate	13-2	
13-2	S-IC Base Region Gas Temperature	13-2	
13-3	S-IC Ambient Gas Temperature Under Engine Cocoon	13-3	
13-4	S-II Heat Shield Aft Heat Rate	13-4	
13-5	S-II Heat Shield Recovery Temperature	13-4	
13-6	S-II Heat Shield Aft Radiation Heat Rate	13-5	
13-7	Forward Location of Separated Flow on S-IC Stage	13-6	
14-1	IU TCS GN <sub>2</sub> Sphere Pressure	14-3	
14-2	IU Thermal Control System (TCS)	14-4	
14-3	IU TCS Hydraulic Performance	14-5	
14-4	Selected IU Component Temperatures	14-6	
14-5	IU Pressure Regulator Operation	14-8	
14-6	TCS Pressurization Schematic	14-6	
14-7	IU Sublimator Performance During Ascent	14-9	
14-8	IU Inertial Platform GN <sub>2</sub> Pressures	14-10	
14-9	IU GBS GN <sub>2</sub> Sphere Pressure	14-10	
15-1	VHF Telemetry Coverage Summary	15-5	
15-2	C-Band Radar Coverage Summary	15-8	
15-3	CCS Coverage Summary	15-9	
15-4	CCS Down Link Signal Strength Indications	15-12	
17-1	Translunar Coast Maneuvers Overview	17-4	
17-2	Modeled Translunar Coast Maneuvers and Early PTC Residuals	17-4	
17-3	Late Residuals Showing PTC Frequency Decrease	17-6	
17-4	Lunar Landmarks of Scientific Interest	17-7	
17-5	Tracking Data Availability	17-9	
20-1	Apollo 16 LRV-2 Traverses	20-2	
20-2	Lunar Surface Photographs	20-4	
20-3	LRV Power Usage	20-7	
20-4	Navigation Subsystem Block Diagram	20-11	
20-5	LRV Power Schematic (Sheet 1 of 2)	20-12	
20-6	Control and Display Panel Configuration	20-14	
20-7	Battery No. 1 Temperature	20-17	
20-8	Battery No. 2 Temperature	20-18	
A-1	Surface Weather Map Approximately 6 Hours Before Launch of AS-511	A-8	
A-2	500 Millibar Map Approximately 6 Hours Before Launch of AS-511	A-9	
A-3	Scalar Wind Speed at Launch Time of AS-511	A-10	
A-4	Wind Direction at Launch Time of AS-511	A-11	
A-5	Pitch Wind Velocity Component ( $W_x$ ) at Launch Time of AS-511	A-12	

## LIST OF ILLUSTRATIONS (CONTINUED)

Figure		Page
A-6	Yaw Wind Velocity Component ( $W_z$ ) at Launch Time of AS-511	A-13
A-7	Pitch ( $S_x$ ) and Yaw ( $S_z$ ) Component Wind Shears at Launch Time of AS-511	A-14
A-8	Relative Deviation of Temperature and Pressure from the PRA-63 Reference Atmosphere, AS-511	A-15
A-9	Relative Deviation of Density and Absolute Deviation of the Index of Refraction From the PRA-63 Reference Atmosphere, AS-511	A-16

## LIST OF TABLES

Table	Page	Table	Page
1	Mission Objectives Accomplishment	xxvii	
2	Summary of Significant Anomalies	xxvix	
3	Summary of Anomalies	xxx	
2-1	Time Base Summary	2-2	
2-2	Significant Event Times Summary	2-4	
2-3	Variable Time and Command Switch Selector Events	2-10	
3-1	AS-511/Apollo 16 Prelaunch Milestones	3-2	
4-1	Comparison of Significant Trajectory Events	4-4	
4-2	Comparison of Cutoff Events	4-5	
4-3	Comparison of Separation Events	4-6	
4-4	Parking Orbit Insertion Conditions	4-8	
4-5	Translunar Injection Conditions	4-11	
5-1	F-1 Engine Systems Buildup and Start Times	5-2	
5-2	S-1C Individual Standard Sea Level Engine Performance	5-5	
5-3	S-1C Propellant Mass History	5-8	
6-1	S-1I Engine Performance	6-10	
6-2	AS-511 Flight S-1I Propellant Mass History	6-13	
7-1	S-1VB Steady State Performance - First Burn (STDV Open +140-Second Time Slice at Standard Altitude Conditions)	7-5	
7-2	S-1VB Steady State Performance - Second Burn (STDV Open +140-Second Time Slice at Standard Altitude Conditions)	7-13	
7-3	S-1VB Engine Mainstage Performance Averages	7-15	
7-4	S-1VB Stage Propellant Mass History	7-18	
7-5	S-1VB APS Propellant Consumption	7-29	
7-6	APS External Leakage Summary	7-30	
8-1	Post S-1I CECO 11 Hertz Engine No. 1 Gimbal Pad Oscillations	8-7	
9-1	Inertial Platform Velocity Comparisons (PACSS-12 Coordinate System)	9-4	
9-2	Guidance Comparisons (PACSS 13)	9-5	
9-3	State Vector Differences at Translunar Injection	9-16	
9-4	AS-511 Guidance System Accuracy	9-16	
9-5	Coast Phase Guidance Steering Commands at Major Events	9-21	
10-1	AS-511 Misalignment and Liftoff Conditions Summary	10-7	
10-2	Maximum Control Parameters During S-1C Burn	10-7	
10-3	Maximum Control Parameters During S-1I Burn	10-8	
10-4	Maximum Control Parameters During S-1VB First Burn	10-14	
10-5	Maximum Control Parameters During S-1VB Second Burn	10-15	
11-1	S-1C Stage Battery Power Consumption	11-1	
11-2	S-1I Stage Battery Current Consumption	11-2	
11-3	S-1VB Stage Battery Power Consumption	11-9	
11-4	IU Battery Power Consumption	11-14	
15-1	AS-511 Measurement Summary	15-2	
15-2	AS-511 Flight Measurements Waived Prior to Flight	15-2	
15-3	AS-511 Measurement Malfunctions	15-3	
15-4	AS-511 Questionable Flight Measurements	15-4	
15-5	AS-511 Launch Vehicle Telemetry Links	15-6	
15-6	Command and Communication System Command History, AS-511	15-11	

## LIST OF TABLES (CONTINUED)

Table	Page	Table	Page
16-1	Total Vehicle Mass - S-1C Burn Phase - Kilograms	16-3	B-4 IU Significant Configuration Changes
16-2	Total Vehicle Mass - S-1C Burn Phase - Pounds	16-3	B-3
16-3	Total Vehicle Mass - S-1I Burn Phase - Kilograms	16-4	
16-4	Total Vehicle Mass - S-1I Burn Phase - Pounds	16-4	
16-5	Total Vehicle Mass - S-1VB First Burn Phase - Kilograms	16-5	
16-6	Total Vehicle Mass - S-1VB First Burn Phase - Pounds Mass	16-5	
16-7	Total Vehicle Mass - S-1VB Second Burn Phase - Kilograms	16-6	
16-8	Total Vehicle Mass - S-1VB Second Burn Phase - Pounds Mass	16-6	
16-9	Flight Sequence Mass Summary	16-7	
16-10	Mass Characteristics Comparison	16-9	
17-1	Translunar Coast Maneuvers	17-3	
17-2	Geocentric Orbit Parameters Following APS Impact Burn	17-5	
17-3	Lunar Impact Conditions	17-9	
17-4	Lunar Impact Seismic Data	17-9	
17-5	S-1VB/IU Tracking Stations	17-10	
20-1	LRV Performance Summary	20-5	
20-2	LRV Significant Configuration Changes	20-20	
A-1	Surface Observations at AS-511 Launch Time	A-4	
A-2	Systems Used to Measure Upper Air Wind Data for AS-511	A-4	
A-3	Maximum Wind Speed in High Dynamic Pressure Region for Apollo/Saturn 501 through Apollo/Saturn 511 Vehicles	A-5	
A-4	Extreme Wind Shear Values in the High Dynamic Pressure Region for Apollo/Saturn 501 through Apollo/Saturn 511 Vehicles	A-6	
A-5	Selected Atmospheric Observa- tions for Apollo/Saturn 501 through 511 Vehicle Launches at Kennedy Space Center, Florida	A-7	
B-1	S-1C Significant Configuration Changes	B-1	
B-2	S-1I Significant Configuration Changes	B-2	
B-3	S-1VB Significant Configuration Changes	B-2	

## ACKNOWLEDGEMENT

This report is published by the Saturn Flight Evaluation Working Group, composed of representatives of Marshall Space Flight Center, John F. Kennedy Space Center, and MSFC's prime contractors, and in cooperation with the Manned Spacecraft Center. Significant contributions to the evaluation have been made by:

George C. Marshall Space Flight Center

Science and Engineering

Central Systems Engineering  
Aero-Astroynamics Laboratory  
Astrionics Laboratory  
Computation Laboratory  
Astronautics Laboratory  
Space Sciences Laboratory

Program Management

John F. Kennedy Space Center

Manned Spacecraft Center

The Boeing Company

McDonnell Douglas Astronautics Company

International Business Machines Corporation

North American Rockwell/Space Division

North American Rockwell/Rocketdyne Division

## ABBREVIATIONS

ACN	Ascension Island	DAC	Data Acquisition Camera
ACS	Alternating Current Power Supply	DDAS	Digital Data Acquisition System
ALSEP	Apollo Lunar Surface Experiments Package	DEE	Digital Events Evaluator
ANT	Antigua	DGU	Directional Gyro Unit
AOS	Acquisition of Signal	DO	Desirable Objective
APS	Auxiliary Propulsion System	DOM	Data Output Multiplexer
ARIA	Apollo Range Instrument Aircraft	DTS	Data Transmission System
ASC	Accelerometer Signal Conditioner	EBW	Exploding Bridge Wire
ASI	Augmented Spark Igniter	ECO	Engine Cutoff
BDA	Bermuda	ECP	Engineering Change Proposal
BST	Boost	ECS	Environmental Control System
CCS	Command and Communications System	EDS	Emergency Detection System
C&DC	Control and Display Console	EMR	Engine Mixture Ratio
CDDT	Countdown Demonstration Test	EMR	Error Monitor Register
CDR	Commander	EMU	Extra-Vehicular Mobility Unit
CECO	Center Engine Cutoff	EPO	Earth Parking Orbit
CIF	Central Instrumentation Facility	ESC	Engine Start Command
CG	Center of Gravity	EST	Eastern Standard Time
CM	Command Module	ETC	Goddard Experimental Test Center
CNV	Cape Kennedy	ETW	Error Time Word
CRO	Carnarvon	EVA	Extra-Vehicular Activity
CRP	Computer Reset Pulse	FCC	Flight Control Computer
CSM	Command and Service Module	FM/FM	Frequency Modulation/ Frequency Modulation
CT4	Cape Telemetry 4	FMR	Flight Mission Rule
CVS	Continuous Vent System	FRT	Flight Readiness Test
CYI	Grand Canary Island	GBI	Grand Bahama Island
		GBS	Gas Bearing System



ABBREVIATIONS ( CONTINUED)

GDS	Goldstone	LVDC	Launch Vehicle Digital Computer
GDSW	Goldstone Wing	LVGSE	Launch Vehicle Ground Support Equipment
GG	Gas Generator	MAD	Madrid
GOX	Gaseous Oxygen	MADW	Madrid Wing
GRR	Guidance Reference Release	MAP	Message Acceptance Pulse
GSE	Ground Support Equipment	MCC-H	Mission Control Center - Houston
GSFC	Goddard Space Flight Center	MESA	Modularized Equipment Storage Assembly
GTK	Grand Turk Island	MFV	Main Fuel Valve
GWM	Guam	MILA	Merritt Island Launch Area
HAW	Hawaii	ML	Mobile Launcher
HDA	Holddown Arm	MO	Mandatory Objective
HE	Helium	MOV	Main Oxidizer Valve
HFCV	Helium Flow Control Valve	MR	Mixture Ratio
HSK	Honeysuckle Creek	MRCV	Mixture Ratio Control Valve
ICD	Interface Control Document	MSC	Manned Spacecraft Center
IGM	Iterative Guidance Mode	MSFC	Marshall Space Flight Center
IMU	Inertial Measurement Unit	MSFN	Manned Space Flight Network
IU	Instrument Unit	MSS	Mobile Service Structure
KSC	Kennedy Space Center	MTF	Mississippi Test Facility
LCRU	Lunar Communication Relay Unit	M/W	Methanol Water
LET	Launch Escape Tower	NASA	National Aeronautics and Space Administration
LH <sub>2</sub>	Liquid Hydrogen	NPSP	Net Positive Suction Pressure
LIT	Lunar Impact Team	NPV	Nonpropulsive Vent
LM	Lunar Module	OAT	Overall Test
LMP	Lunar Module Pilot	OCP	Orbital Correction Program
LMR	Launch Mission Rule	OECO	Outboard Engine Cutoff
LOI	Lunar Orbit Insertion	OFSO	Overfill Shutoff Sensor
LOS	Loss of Signal	OMPT	Post Flight Trajectory
LOX	Liquid Oxygen	OT	Operational Trajectory
LRV	Lunar Roving Vehicle	OTBV	Oxidizer Turbine Bypass Valve
LSS	Lunar Soil Simulant		
LUT	Launch Umbilical Tower		
LV	Launch Vehicle		
LVDA	Launch Vehicle Data Adapter		

ABBREVIATIONS (CONTINUED)

PACSS	Project Apollo Coordinate System Standards	SSDO	Switch Selector and Discrete Output Register
PAFB	Patrick Air Force Base	STDV	Start Tank Discharge Valve
PCM	Pulse Code Modulation	SV	Space Vehicle
PCM/FM	Pulse Code Modulation/Frequency Modulation	TCS	Thermal Conditioning System
PEA	Platform Electronics Assembly	TD&E	Transportation, Docking and Ejection
PIO	Process Input/Output	TEI	Tranearth Injection
PLSS	Portable Life Support System	TEX	Corpus Christi (Texas)
POI	Parking Orbit Insertion	TLC	Translunar Coast
PMR	Programmed Mixture Ratio	TLI	Translunar Injection
PRA	Patrick Reference Atmosphere	TM	Telemetry
PTCS	Propellant Tanking Computer System	TMR	Triple Module Redundant
PTC	Passive Thermal Control	TSM	Tail Service Mast
PU	Propellant Utilization	TVC	Thrust Vector Control
PWM	Pulse Width Modulator	UCR	Unsatisfactory Condition Report
RF	Radiofrequency	USAE	U. S. Army Engineer
RFI	Radiofrequency Interference	USB	Unified S-Band
RMS	Root Mean Square	UT	Universal Time
PP-1	S-IC Stage Fuel	VA	Volt Amperes
SA	Service Arm	VAN	Vanguard (ship)
SC	spacecraft	VHF	Very High Frequency
SCFM	Standard Cubic Feet per Minute	WES	Waterways Experimental Station
SCIM	Standard Cubic Inch per Minute	Z	Zulu Time (equivalent to UT)
SIM	Scientific Instrument Module		
SLA	Spacecraft/LM Adapter		
SM	Service Module		
SPS	Service Propulsion System		
SPS	Stabilized Platform Subsystem		
SPU	Signal Processing Unit		
SRSCS	Secure Range Safety Command System		

## MISSION PLAN

The AS-511 flight (Apollo 16 mission) is the eleventh flight in the Apollo/Saturn V flight program, the sixth mission planned for lunar landing, and the fourth mission planned for landing in the lunar highlands. The primary mission objectives are: a) perform selenological inspection, survey, and sampling of materials and surface features in a preselected area of the Descartes region; b) deploy and activate the Apollo Lunar Surface Experiments Package (ALSEP); and c) conduct inflight experiments and photographic tests from lunar orbit. The crew consists of J. W. Young (Mission Commander), T. K. Mattingly, II (Command Module Pilot), and C. M. Duke, Jr. (Lunar Module Pilot).

The AS-511 Launch Vehicle (LV) is composed of the S-IC-11, S-II-11, S-IVB-511, and Instrument Unit (IU)-511 stages. The Spacecraft (SC) consists of SC/Lunar Module Adapter (SLA)-20, Command Module (CM)-113, Service Module (SM)-113, and Lunar Module (LM)-11. The LM has been modified for this flight and will include the Lunar Roving Vehicle (LRV)-2.

Vehicle launch from Complex 39A at Kennedy Space Center (KSC) is along a 90 degree azimuth with a roll to a flight azimuth of approximately 72 degrees measured east of true north. Vehicle mass at ignition is 6,538,395 lbm.

The S-IC stage powered flight is approximately 162 seconds; the S-II stage provides powered flight for approximately 395 seconds. The S-IVB stage first burn of approximately 142 seconds inserts the S-IVB/IU/SLA/LM/Command and Service Module (CSM) into a circular 90 n mi. altitude (referenced to the earth equatorial radius) Earth Parking Orbit (EPO). Vehicle mass at orbit insertion is 308,916 lbm.

At approximately 10 seconds after EPO insertion, the vehicle is aligned with the local horizontal. Continuous hydrogen venting is initiated shortly after EPO insertion and the LV and Spacecraft (SC) systems are checked in preparation for the Translunar Injection (TLI) burn. During the second revolution in EPO, the S-IVB stage is restarted and burns for approximately 344 seconds. This burn inserts the S-IVB/IU/SLA-CSM into an earth-return, translunar trajectory.

Within 15 minutes after TLI, the vehicle initiates a maneuver to an inertial attitude hold for CSM separation, docking, and CSM/LM ejection. Following the attitude freeze, the CSM separates from the LV and the

SLA panels are jettisoned. The CSM then transposes and docks to the LM. After docking, the CSM/LM is spring ejected from the S-IVB/IU. Following separation of the combined CSM/LM from the S-IVB/IU, the S-IVB/IU performs a yaw maneuver and then an 80-second burn of the S-IVB Auxiliary Propulsion System (APS) ullage engines as an evasive maneuver to decrease the probability of S-IVB/IU recontact with the spacecraft. Subsequent to the completion of the S-IVB/IU evasive maneuver, the S-IVB/IU is placed on a trajectory such that it will impact the lunar surface in the vicinity of the Apollo 12 landing site. The actual lunar impact target is at 2.3°S latitude and 31.7°W longitude. The impact trajectory is achieved by propulsive venting of hydrogen (H<sub>2</sub>), dumping of residual liquid oxygen (LOX), and by firing the APS ullage engines. The S-IVB/IU impact will be recorded by the seismographs deployed during the Apollo 12, 14, and 15 missions. S-IVB/IU lunar impact is predicted at approximately 74 hours 30 minutes 8 seconds after launch.

Several inflight experiments will be flown on Apollo 16. Several experiments are to be conducted by use of the Scientific Instrument Module (SIM) located in Sector I of the SM. A subsatellite is launched from the SIM into lunar orbit and several experiments are performed by it. The inflight experiments are conducted during earth orbit, translunar coast, lunar orbit, and transearth coast mission phases.

During the 71-hour 50-minute translunar coast, the astronauts will perform star-earth landmark sightings, Inertial Measurement Unit (IMU) alignments, general lunar navigation procedures, and possibly four midcourse corrections. At approximately 74 hours and 28 minutes, a Service Propulsion System (SPS), Lunar Orbit Insertion (LOI) burn of approximately 375 seconds is initiated to insert the CSM/LM into a 58 by 170 n mi. altitude parking orbit. Approximately two revolutions after LOI, a 24.1-second burn will adjust the orbit into an 11 by 59 n mi. altitude. The LM is entered by astronauts Young and Duke, and checkout is accomplished. During the twelfth revolution in orbit, at 96.2 hours, the LM separates from the CSM and prepares for the lunar descent. The CSM is then inserted into an approximately 52 by 68 n mi. altitude orbit using a 5.9-second SPS burn. The LM descent propulsion system is used to brake the LM into the proper landing trajectory and maneuver the LM during descent to the lunar surface.

Following lunar landing, three EVA time periods of 7 hours each are scheduled during which the astronauts will explore the lunar surface in the LRV, examine the LM exterior, photograph the lunar surface, and deploy scientific instruments. Sorties in the LRV will be limited in radius such that the life support system capability will not be exceeded if LRV failure necessitates the astronauts walking back to the LM. Total stay time on the lunar surface is open-ended, with a planned maximum of 73.3 hours depending upon the outcome of current lunar surface operations planning and of real-time operational decisions. After the EVA, the astronauts prepare the LM ascent propulsion system for lunar ascent.

The CSM performs a plane change approximately 20 hours before rendezvous. At approximately 171.9 hours, the ascent stage inserts the LM into a 9 by 45 n mi. altitude lunar orbit. At approximately 173.7 hours the rendezvous and docking with the CSM are accomplished.

Following docking, equipment transfer, and decontamination procedures, the LM ascent stage is jettisoned and targeted to impact the lunar surface at a point near the Apollo 16 landing site, but far enough away so as not to endanger the scientific packages. During the third revolution before transearth injection, the CSM will perform an SPS maneuver to achieve a 55 by 85 n mi. altitude orbit. Shortly thereafter the subsatellite will be launched into the same orbit. Transearth Injection (TEI) is accomplished at the end of revolution 76 at approximately 222 hours and 23 minutes with a 150-second SPS burn.

During the 67-hour 59-minute transearth coast, the astronauts will perform navigation procedures, star-earth-moon sightings, the electrophoretic separation demonstration, and as many as three midcourse corrections. The SM will separate from the CM 15 minutes before re-entry. Splashdown will occur in the Pacific Ocean 290 hours and 36 minutes after liftoff.

After the recovery operations, a biological quarantine is not imposed on the crew and CM. However, biological isolation garments will be available for use in the event of unexplained crew illness.

## FLIGHT SUMMARY

The ninth manned Saturn Apollo space vehicle, AS-511 (Apollo 16 Mission) was launched at 12:54:00 Eastern Standard Time (EST) on April 16, 1972, from Kennedy Space Center, Complex 39, Pad A. The performance of the launch vehicle and Lunar Roving Vehicle was satisfactory and all Mandatory and Desirable Objectives were accomplished except the precise determination of the lunar impact point and time.

The ground systems supporting the AS-511/Apollo 16 countdown and launch performed satisfactorily with no unscheduled holds. Propellant tanking was accomplished satisfactorily. Damage to the pad, Launch Umbilical Tower (LUT) and support equipment was considered minimal.

The vehicle was launched on an azimuth 90 degrees east of north. A roll maneuver was initiated at 12.7 seconds that placed the vehicle on a flight azimuth of 72.034 degrees east of north. The trajectory parameters from launch to Command and Service Module (CSM) separation were close to nominal. Earth parking orbit insertion conditions were achieved 0.72 second later than nominal with altitude nominal and velocity 0.2 meter per second greater than nominal. Translunar Injection (TLI) conditions were achieved 1.78 seconds earlier than nominal with altitude 2.0 kilometers less than nominal and velocity 1.9 meters per second greater than nominal. The trajectory parameters at Command and Service Module (CSM) separation deviated somewhat from nominal since the event occurred 38.6 seconds later than predicted.

All S-IC propulsion systems performed satisfactorily. In all cases, the propulsion performance was very close to the predicted nominal. Overall stage site thrust was 0.05 percent higher than predicted. Total propellant consumption rate was 0.36 percent lower than predicted and the total consumed mixture ratio 0.40 percent higher than predicted. Specific impulse was 0.41 percent higher than predicted. Total propellant consumption from Holddown Arm (HDA) release to Outboard Engines Cutoff (OECO) was low by 0.51 percent. Center Engine Cutoff (CECO) was initiated by the Instrument Unit (IU) at 137.85 seconds range time, 0.11 second earlier than planned. Outboard Engine Cutoff (OECO) was initiated by the LOX low level sensors at 161.78 seconds, 0.31 seconds earlier than predicted. This is well within the +4.60, -3.60 second 3-sigma limits. At OECO, the LOX residual was 34,028 lbm compared to the predicted 36,283 lbm and the fuel residual was 31,601 lbm compared to the predicted 28,248 lbm.

The S-II propulsion system performed satisfactorily throughout the flight. The S-II Engine Start Command (ESC), as sensed at the engines, occurred at 164.20 seconds. Center Engine Cutoff (CECO) was initiated by the Instrument Unit (IU) at 461.77 seconds as planned. Outboard Engine Cutoff (OECO), initiated by LOX depletion ECO sensors, occurred at 559.54 seconds giving an outboard engine operating time of 395.34 seconds or 0.63 seconds longer than predicted. The later than predicted S-II OECO was a result of an earlier than predicted Engine Mixture Ratio (EMR) shift and lower than planned EMR after the step. Engine mainstage performance was satisfactory throughout flight. The total stage thrust at the standard time slice (61 seconds after S-II ESC) was 0.04 percent above predicted. Total propellant flowrate, including pressurization flow, was 0.01 percent below predicted, and the stage specific impulse was 0.07 percent above predicted at the standard time slice. Stage propellant mixture ratio was 0.36 percent below predicted. Engine thrust buildup and cutoff transients were within the predicted envelopes. During the S-II engine start transient, an unusually large amount of helium was expended from the engine 4 helium tank. The most probable cause of the anomaly is slow closing of the engine purge control valve allowing excessive helium to be vented overboard. Tests, analysis, and examination of valves from service are being conducted to determine the cause and solutions for engines on subsequent stages. The center engine LOX feedline accumulator performance was satisfactory. The accumulator bleed and fill subsystems operations were within predictions and the accumulator system was effective in suppressing POGO type oscillations. The propellant management system performance was satisfactory throughout loading and flight, and all parameters were within expected limits. Propellant residuals at OECO were 1405 lbm LOX, 1 lbm more than predicted and 2612 lbm LH<sub>2</sub>, 239 lbm less than predicted. Control of engine mixture ratio was accomplished with the two-position pneumatically operated Mixture Ratio Control Valves (MRCV). The low EMR step occurred 2.0 seconds earlier than predicted. The performance of the LOX and LH<sub>2</sub> tank pressurization systems was satisfactory. This was the second stage to utilize pressurization orifices in place of regulators to control in-flight pressurization of the propellant tanks. Ullage pressure in both tanks was adequate to meet or exceed engine inlet Net Positive Suction Pressure (NPSP) minimum requirements throughout mainstage.

The S-IVB propulsion system performed satisfactorily throughout the operational phase of first burn and had normal start and cutoff transients. S-IVB first burn time was 142.6 seconds, 0.4 second longer than predicted. This difference is composed of 1.0 second due to the combined first and second stage performance and -0.6 second due to the higher S-IVB performance. The engine performance during first burn, as determined from standard altitude reconstruction analysis, deviated from the predicted Start Tank Discharge Valve (STDV) open +140-second time slice by 0.38 percent for thrust and zero percent for specific impulse. The S-IVB stage first burn Engine Cutoff (ECO) was initiated by the Launch Vehicle

Digital Computer (LVDC) at 706.21 seconds. The Continuous Vent System (CVS) adequately regulated LH<sub>2</sub> tank ullage pressure at an average level of 19.4 psia during orbit and the Oxygen/Hydrogen (O<sub>2</sub>/H<sub>2</sub>) burner satisfactorily achieved LH<sub>2</sub> and LOX tank repressurization for restart. Engine restart conditions were within specified limits. The restart at full open Mixture Ratio Control Valve (MRCV) position was successful. S-IVB second burn time was 341.9 seconds, 2.4 seconds less than predicted. This difference is primarily due to the slightly higher S-IVB performance during second burn, as determined from the standard altitude reconstruction analysis, deviated from the STDV open +140-second time slice by 0.57 percent for thrust and zero percent for specific impulse. Second burn ECO was initiated by the LVDC at 9,558.41 seconds (02:39:18.41). The S-IVB high pressure systems were safed following J-2 engine second burn cutoff. The thrust developed during the LOX dump provided a satisfactory contribution to the velocity change for lunar impact. Momentary ullage gas ingestion occurred three times during the LOX dump as a result of LOX sloshing. The greater than nominal slosh activity was attributed to the additional vehicle maneuver to the LOX dump attitude for optimum velocity increment following the programmed LOX dump maneuver. As a result of the ullage ingestion, liquid flow was impeded and dump performance was decreased. Auxiliary Propulsion System (APS) Module 1 experienced an external helium leak which started at approximately 3600 seconds and continued to 22,800 seconds (06:20:00). The maximum leak rate experienced was 585 psi/hour. The other Module 1 systems functioned normally. Module 2 experienced internal leakage from the high pressure system to the low pressure system during the flight. The regulator outlet pressure began to increase above the regulator setting at approximately 970 seconds. The pressure continued to increase to 344 psia, the relief setting of the low pressure module relief valve. The regulator outlet pressure remained between 344 and 203 psia out to loss of data. During periods of high propellant usage the regulator outlet pressure decreased, but not low enough for regulator operation. The prime suspect for this internal helium leakage is leakage through the regulator. Data from preflight pressurization of the APS indicates that the APS probably was on the secondary regulator at liftoff. Another leak path being examined is the common mounting block for the high and low pressure He system pressure transducer.

The structural loads experienced during the S-IC boost phase were well below design values. The maximum bending moment was  $71 \times 10^6$  lbf-in at the S-IC LOX tank (approximately 27 percent of the design value). Thrust cutoff transients experienced by AS-511 were similar to those of previous flights. The maximum longitudinal dynamic responses at the Instrument Unit (IU) were  $\pm 0.25$  g and  $\pm 0.32$  g at S-IC Center Engine Cutoff (CECO) and Outboard Engine Cutoff (OECO), respectively. The magnitudes of the thrust cutoff responses are considered normal. During S-IC stage boost, four to five hertz oscillations were detected beginning at approximately 100 seconds. The maximum amplitude measured at the IU was  $\pm 0.06$  g.



Oscillations in the four to five hertz range have been observed on previous flights and are considered to be normal vehicle response to flight environment. POGO did not occur during S-IC boost. The S-II stage center engine LOX feedline accumulator successfully inhibited the 16 hertz POGO oscillations. A peak response of  $\pm 0.5$  g in the 14 to 20 hertz frequency range was measured on engine No. 5 gimbal pad during steady-state engine operation. As on previous flights, low amplitude 11 hertz oscillations were experienced near the end of S-II burn. Peak engine No. 1 gimbal pad response was  $\pm 0.07$  g. POGO did not occur during S-II boost. The POGO limiting backup cutoff system performed satisfactorily during the prelaunch and flight operations. The system did not produce any discrete outputs and should not have since there was no POGO. The structural loads experienced during the S-IVB stage burns were well below design values. During first burn the S-IVB experienced low amplitude, 16 to 20 hertz oscillations. The amplitudes measured on the gimbal block were comparable to previous flights and within the expected range of values. Similarly, S-IVB second burn produced intermittent low amplitude oscillations in the 11 to 16 hertz frequency range which peaked near second burn cutoff.

The Guidance and Navigation System satisfactory supported accomplishment of the mission objectives. The end condition errors at parking orbit insertion and translunar injection were insignificant. Three anomalies occurred in the Guidance and Navigation System, although their effect on the mission were not significant. The anomalies were: a) An anomalous one meter/second shift in the crossrange integrating accelerometer output just after liftoff, b) A one second delay in ending the tower clearance yaw maneuver, c) Intermittent setting of Error Monitor Register bits 13 and 14.

The control and separation systems functioned correctly throughout the flight of AS-511. Engine gimbal deflections were nominal and APS firings predictable. Bending and slosh dynamics were adequately stabilized. No undue dynamics accompanied any separation.

The AS-511 launch vehicle electrical systems and Emergency Detection System (EDS) performed satisfactorily throughout the required period of flight. There was, however, an anomaly in the S-II ignition bus voltage indications during and after the ignition sequence. The S-IVB forward Battery No. 2 depleted early as on AS-510 and did not deliver its rated capacity. Operation of all other batteries, power supplies, inverters, Exploding Bridge Wire (EBW) firing units and switch selectors was normal.

The S-IC base heat shield was instrumented with two differential pressure measurements. The AS-511 flight data have trends and magnitudes similar to those seen on previous flights. The AS-511 S-II base pressure environments are consistent with the trends and magnitudes seen on previous flights.

The AS-511 S-IC base region thermal environments exhibited trends and magnitudes similar to those seen on previous flights. The base thermal environments of the S-II stage were consistent with the trends and magnitudes seen on previous flights and were well below design limits. Aerodynamic heating environments and S-IVB base thermal environments were not measured on AS-511.

The S-IC stage forward compartment ambient temperatures were maintained above the minimum performance limit during AS-511 countdown. The S-IC stage aft compartment environmental conditioning system performed satisfactorily. The S-II thermal control and compartment conditioning system apparently performed satisfactorily since the ambient temperatures external to the containers were normal, and there were no problems with the equipment in the containers. The Instrument Unit (IU) Environmental Control Systems (ECS) performed satisfactorily up until approximately 18,000 seconds (05:00:00). At this time coolant fluid circulation ceased due to an excessively high GN<sub>2</sub> usage rate which depleted the Thermal Conditioning System (TCS) storage sphere. After cooling ceased, temperatures began to increase but were within acceptable values at the time IU telemetry was terminated.

All data systems performed satisfactorily throughout the flight. Flight measurements from onboard telemetry were 99.9 percent reliable. Telemetry performance was normal except for noted problems. Radio Frequency (RF) propagation was satisfactory, though the usual problems due to flame effects and staging were experienced. Usable VHF data were received until 18,720 seconds (5:12:00). The Secure Range Safety Command Systems (SRSCS) on the S-IC, S-II, and S-IVB stages were ready to perform their functions properly, on command, if flight conditions during launch phase had required destruct. The system properly safed the S-IVB on a command transmitted from Bermuda (BDA) at 716.2 seconds. The performance of the Command and Communications System (CCS) was satisfactory from liftoff through the first part of lunar coast when the CCS downlink signal was lost. Usable CCS telemetry data were received to 27,645 seconds (7:40:43) at which time the telemetry subcarrier was inhibited. Madrid (MAD and MADW), Ascension (ACN), Goldstone (GDS), Bermuda (BDA) and Merritt Island Launch Area (MILA) were receiving CCS signal carrier at the abrupt loss of signal at 97,799 seconds (27:09:59). Good tracking data were received from the C-Band radar, with MILA indicating final Loss of Signal (LOS) at 38,837 seconds (10:47:17). In general ground engineering camera coverage was good.

Total vehicle mass, determined in post-flight analysis, was within 0.36 percent of prediction from ground ignition through S-IVB stage final shutdown. This small variation indicates that hardware weights, propellant loads, and propellant utilization were close to predicted values during flight.

All aspects of the S-IVB/IU Lunar Impact Mission objectives were accomplished successfully except the precise determination of the impact

point and time of impact. Preliminary analysis of available tracking data plus calculations based upon three lunar seismometer recordings of the impact indicate the S-IVB/IU was successfully maneuvered to impact the lunar surface within 350 kilometers (189 n mi) of the target. The loss of tracking data at 97,799 seconds (27:09:59) has precluded determining the impact time and location within the mission objectives of one second and five kilometers (2.7 n mi), but these objectives may be eventually determined by analytical techniques not previously used. Based upon analysis to date the S-IVB/IU impacted the lunar surface at 270,482 seconds (75:08:02) at approximately 2.1 degrees north latitude and 22.1 degrees west longitude with a velocity of 2,655 meters per second (8,711 ft/s). This preliminary impact point is approximately 320 kilometers (173 n mi) from the target of 2.3 degrees south latitude and 31.7 degrees west longitude. Real time targeting activities were changed considerably from preflight planned operations because of the following real time indications:

1. IU GN<sub>2</sub> cooling pressurant leakage
2. Unanticipated IU velocity accumulations during Timebase 7 (later identified as primarily platform biases)
3. Early S-IVB APS Module 1 propellant depletion (later identified as a He leakage problem)
4. Unsymmetrical APS ullage performance

Because of these indications, a more efficient LOX dump attitude was selected to reduce the APS targeting burn requirement. Due to the problems with the vehicle, there would have been no opportunity to perform a second APS burn even if it had been required.

An inflight demonstration was conducted as proposed by the Marshall Space Flight Center to demonstrate Electrophoretic Separation in a zero g environment. The Electrophoretic Separation Demonstration, a chemical separation process based on the motion of particles in a fluid due to the force of an electric field, was conducted to show the advantages of the almost weightless environment. The preliminary assessment of the demonstration indicates that the electrophoresis was more distinct than on earth and fluid convection effects were minimal. The photographs were clear and sharp and the crew commentary thorough.

The Lunar Roving Vehicle (LRV) satisfactorily supported the lunar exploration objectives. The total odometer distance traveled during the three traverses was 26.9 kilometers at an average velocity of 7.30 km/hr. The maximum velocity attained was 17.0 km/hr and the maximum slope negotiated was 20 degrees. The average LRV energy consumption rate was 2.00 amp-hours/km with a total consumed energy of 86.0 amp-hours (including the Lunar Communication Relay Unit [LCRU]) out of an

approximate total available energy of 242 amp-hours. The navigation system gyro drift and closure error at the Lunar Module (LM) were negligible. Controllability was good. There were no problems with steering, braking, or obstacle negotiation, except downslope at speeds above 10 kph, where the vehicle reacted like an "auto driven on ice." Brakes were used at least partially on all downslopes. Driving down sun was difficult because of poor visibility of the "washed out" terrain. All interfaces between crew and LRV and between LRV and stowed payload were satisfactory.

The following anomalies were noted during lunar surface operation:

Anomaly 1. Insufficient Battery Cooledown

The LRV Battery Cooledown between EVA's 1 and 2 and between EVA's 2 and 3 was insufficient causing battery over temperature before the end of the mission.

Anomaly 2. LRV Electrical Reconfiguration

- a. Navigation system distance, range, and bearing computations stopped on EVA 2.
- b. Zero amps on Battery #2 on EVA 2.

Anomaly 3. LRV Instrumentation

- a. Four meters off scale low at post deployment checkout.
- b. No rear steering at post deployment checkout.
- c. Loss of vehicle attitude indicator pitch meter scale.
- d. Battery #1 temperature meter off scale low.
- e. Amp-Hour meter malfunction.

Anomaly 4. LRV Fender Extension Missing

## MISSION OBJECTIVES ACCOMPLISHMENT

Table 1 presents the MSFC Mandatory Objectives and Desirable Objectives as defined in the "Saturn V Apollo 16/AS-511 Mission Implementation Plan," MSFC Document PM-SAT-8010.9 (Rev. A), dated December 20, 1971, and revised on February 24, 1972. An assessment of the degree of accomplishment of each objective is shown. Discussion supporting the assessment can be found in other sections of this report as shown in Table 1.

Table 1. Mission Objectives Accomplishment

NO.	MSFC MANDATORY OBJECTIVES (MO) AND DESIRABLE OBJECTIVES (DO)	DEGREE OF ACCOMPLISHMENT	DISCREPANCIES	SECTION IN WHICH DISCUSSED
1	Launch on a flight azimuth between 72 and 100 degrees and insert the S-IVB/IU/SC into the planned circular earth parking orbit (MO).	Complete	None	4.1
2	Restart the S-IVB during either the second or third revolution and inject the S-IVB/IU/SC onto the planned translunar trajectory (MO).	Complete	None	4.2.3, 7.6
3	Provide the required attitude control for the S-IVB/IU/SC during TD&E (MO).	Complete	None	10.4.4
4	Perform an evasive maneuver after ejection of the CSM/LM from the S-IVB/IU (DO).	Complete	None	10.4.4
5	Target the S-IVB/IU stages for impact on the lunar surface at 2.3 degrees South latitude and 31.7 degrees West longitude (DO).	Complete	None	17.4
6	Determine actual impact point within 5 kilometers and time of impact within one second (DO).	Not Accomplished	Desired accuracy not achieved, but determined still in progress.	17.4
7	After final LV/SC separation, vent, and dump the remaining gases and propellants to save the S-IVB/IU (DO).	Complete	None	7.4

## FAILURES AND ANOMALIES

Evaluation of the Launch Vehicle and Lunar Roving Vehicle data revealed fifteen anomalies, five of which were considered significant. There were no failures. The significant anomalies are summarized in Table 2 and the other anomalies summarized in Table 3.

Previous Saturn Launch Vehicle reports classified problems either as Failures, Anomalies, or Deviations. Effective with this AS-511 Report, problems are now reported as per Apollo Program Directive 19C (APD 19C) Failures, Significant Anomalies, or Anomalies. Significant Anomalies reported herein are comparable to previously reported Anomalies. Anomalies reported herein are comparable to previously reported Deviations.

Problems are defined per APD 19C as:

a. Failure

The inability of a system, subsystem, and/or hardware to perform its required function.

b. Significant Anomaly

Any anomaly which creates or could create a hazardous situation or condition; results or could result in a launch delay or endanger the accomplishment of a primary or secondary mission objective; would indicate a serious design deficiency; or could have serious impact on future missions.

c. Anomaly

Any deviation of system, subsystem, and/or hardware performance beyond previously established limits.

Table 2. Summary of Significant Anomalies

ANOMALY IDENTIFICATION					RECOMMENDED CORRECTIVE ACTION			
ITEM	VEHICLE SYSTEM	DESCRIPTION (CAUSE)	EFFECT ON MISSION	OCCURRENCE RANGE TIME SECS.	DESCRIPTION	ACTION STATUS	VEHICLE EFFECTIVITY	SECTION REFERENCE
1	S-II/Propulsion	J-2 Engine No. 4 helium consumption during engine start operations excessive. Pressure in system dropped 890 psi compared to normal 325 psi. (Failure of engine purge control valve to completely close for approximately 10 secs.)	None, pressure decay lasted 10 secs. If decay had lasted 40 secs, engine cut-off would have resulted and the primary mission not accomplished. (All outboard engines must burn for 184 secs for primary mission.)	164.2	Replace purge control valve assemblies in the S-II and S-IVB stages effective with AS-512 with assemblies that have had: a. The deactivation setting increased. b. An orifice added to the valve vent outlet. c. A redundant check valve added.	ECP in-work	AS-512	6.2
2	S-IVB/Propulsion	Excessive helium leakage in the APS module #1 propellant pressurization system. (Unknown)	Degraded lunar impact targeting accuracy. The leakage rate indicated that there would be insufficient helium supply for the second APS scheduled burn. This anomaly and item 4 anomaly were contributing factors in the decision not to attempt the burn.	From 3600 sec to 22,800 sec.	1. Provide additional He supply by connecting the stage supply to the APS He system. 2. Replace bulkhead fittings with adapter unions. 3. More stringent leak checks and reduce pre-launch allowable leakage. 4. Replace Teflon "O" rings with K-seals and Buna-N "O" rings.	ECP in-work	AS-512	7.12.1
3	S-IVB/Propulsion	APS Module #2 propellant pressurization system experienced an excessive pressure decay in the helium supply bottle and an accompanying pressure build-up downstream of the dual pressure regulators which at times reached the relief valve setting and caused helium overboard. (1. Probably leakage through the helium primary and secondary regulators. 2. Leakage through common transducer mounting block housing the upstream and downstream helium pressure transducers.)	None, however, if anomalies in items 2 and 4 had not existed and a second lunar impact burn attempted, the burn would have required modification due to excessive propellant expulsion pressure and early helium supply depletion.	Throughout flight after 970 sec.	1. Redesign transducer mounting block to increase sealing reliability. 2. Provide additional He supply by connecting the stage supply to the APS He system. 3. More stringent contamination avoidance program. 4. Modify pre-launch procedures and redlines.	ECP's in-work	AS-512	7.12.2
4	IS/Thermal Conditioning System	Excessive gly leakage in the IS coolant pressurization system. Lost coolant flow at 5 hours (Probably 1/2" K-seal leak at plug near #12 inlet to Orville accumulator.)	Possibly degraded lunar impact targeting accuracy.	18,000 (5 hours)	Improved pre-launch leak test requirements and procedures.	In-work	AS-512	14.4
5	IS/Command Communication System (CCS)	Madrid and Goldstone tracking stations reported a loss of signal at 27 hours, 10 minutes and were unable to reacquire. (Failure of CCS transmitter)	Degraded lunar impact determination accuracy. Could not track FN/S-IVB to lunar impact.	97,799 (27 hours, 10 minutes)	Under investigation	--	--	15.6

Table 3. Summary of Anomalies

ITEM	VEHICLE SYSTEM	ANOMALY	PROBABLE CAUSE	SIGNIFICANCE	PARAGRAPH REFERENCE
1	S-II/Electrical	One volt drop in ignition voltage during ignition sequence and drop to zero 1.2 seconds after ignition off.	Measurement or electrical network failure.	None on this mission. If problem was in electrical networks and had occurred earlier, availability of proper ignition voltage would be questionable.	11.3
2	S-IVB/Electrical	Forward battery No. 2 depleted at approximately 6 hours and 27 minutes and did not deliver its rated capacity of 24.6 amp-hrs.	Inflight thermal environment, coupled with excessive negative plate limiting of the battery.	None on this mission. Although the battery fulfilled its mission requirements, it was not known prior to flight that plate limiting coupled with the cooler in-flight environment and battery temperature gradient would cause a reduction in service capacity.	11.4.2
3	IU/LVDA & LVDC	Error Monitor Register bits 13 and 14 set intermittently. Logic signal disagreements occurred at approximately 6 hours, 43 minutes.	Failure of the 44 .sec Delay line.	None, since system is triple redundant.	9.4.2
4	IU/Guidance	The crossrange (Y) accelerometer experienced a 1 meter/sec velocity shift just after liftoff.	Contact of accelerometer float with mechanical stop.	Probably none, although the AS-513 guidance scheme will not use accelerometers for first ten seconds of flight.	9.4
5	IU/Control & EDS	During a prelaunch test, the backup yaw rate gyro channel had an unexplained drop in output from 0.25 deg/sec to 0.15 deg/sec.	Shorted or open transistor (probably 08) on Demodulator Card of Control Signal Processor.	A decrease in flight redundancy if the same failure occurred in flight, although analyses indicate vehicle would still be controllable.	3.2.4
6	IU/Guidance	Tower clearance yaw maneuver was extended approximately one second longer than nominal.	Method of implementing yaw maneuver termination in LVDC software provides approximately 10% probability of this situation occurring. (Yaw maneuver is implemented by priority interrupt and can be erroneously delayed for approximately one second if the attempt to implement occurs between calculating the minor loop yaw command rate stored in temporary location and its subsequent storage in normal location.)	None on this mission. Since a similar delay could occur in performance of tower clearance maneuver initiation with a resulting decrease in clearance distances, the flight program will be reprogrammed to prevent such an occurrence on a future mission.	9.3 10.2.1
7	LRV Batteries	Insufficient battery cool-down.	LRV was parked closer to LH than anticipated and dust on battery mirrors.	Required departure from standard procedure for operating electrical system, causing electrical system anomalies. Battery exceeded temperature specification.	20.12
8	LRV Electrical System	Amp-hour readings divergent (EVA-2).	Unknown.	None.	20.8.5
		Navigation system distance, range, and bearing outputs inert (EVA-2).	No forward drive power.	None, was operational during EVA 1.	20.10
		No rear steering at post deployment checkout.	Unknown.	None. Operated properly during traverses.	20.8.4
		Loss of rear drive power (EVA-2).	PAR select switch inadvertently moved by crewman.	None.	20.8.4
9	LRV Instrumentation	Four of six meters off-scale-low at post deployment checkout.	Unknown.	None. Operated properly during traverses.	20.8.3
		Pitch indicator scale fell off (EVA-2).	Scale debanding.	None.	20.10
		Battery #1 temperature meter off-scale-low (EVA-3).	Meter failure.	None.	20.8.3, 20.8.5
10	LRV Fender Extension	Missing (EVA-2).	Bumped by crewman and dislodged.	Excessive lunar dust on crew and equipment.	20.13



SECTION 1  
INTRODUCTION

1.1 PURPOSE

This report provides the National Aeronautics and Space Administration (NASA) Headquarters, and other interested agencies, with the launch vehicle and Lunar Roving Vehicle (LRV) evaluation results of the AS-511 flight (Apollo 16 Mission). The basic objective of flight evaluation is to acquire, reduce, analyze, evaluate and report on flight data to the extent required to assure future mission success and vehicle reliability. To accomplish this objective, actual flight problems are identified, their causes determined, and recommendations made for appropriate corrective action.

1.2 SCOPE

This report contains the performance evaluation of the major launch vehicle systems and LRV, with special emphasis on problems. Summaries of launch operations and spacecraft performance are included.

The official George C. Marshall Space Flight Center (MSFC) position at this time is represented by this report. It will not be followed by a similar report unless continued analysis or new information should prove the conclusions presented herein to be significantly incorrect.

## SECTION 2

### EVENT TIMES

#### 2.1 SUMMARY OF EVENTS

Range zero time, the basic time reference for this report is 12:54:00 Eastern Standard Time (EST) (17:54:00 Universal Time [UT]) April 16, 1972. Range time is the elapsed time from range zero time and, unless otherwise noted, is the time used throughout this report. Time From Base time is the elapsed time from the start of the indicated time base. Table 2-1 presents the time bases used in the flight sequence program, the vehicle and corresponding range time and the signal for initiating each time base.

The start times of  $T_0$ ,  $T_1$ , and  $T_2$  were nominal.  $T_3$ ,  $T_4$ , and  $T_5$  were initiated approximately 0.3 seconds early, 0.3 seconds late, and 0.7 seconds late, respectively, due to variations in the stage burn times. These variations are discussed in Sections 5, 6 and 7 of this document. Start times of  $T_6$  and  $T_7$  were 0.7 seconds late and 1.8 seconds early, respectively.  $T_8$ , which was initiated by the receipt of a ground command, started 293.1 seconds early.

Figure 2-1 shows the mean difference between ground station time and vehicle time including the adjustments for telemetry transmission time and Launch Vehicle Digital Computer (LVDC) clock errors.

A summary of significant event times for AS-511 is given in Table 2-2. The preflight predicted times were adjusted to include the actual first motion time. The predicted times for establishing actual minus predicted times in Table 2-2 were taken from 40M33627D, "Interface Control Document Definition of Saturn SA-511, 512 and 514 Flight Sequence Program" and from the "Revised AS-511 Launch Vehicle Operational Trajectory for the April 16, 1972, Launch Day."

#### 2.2 VARIABLE TIME AND COMMANDED SWITCH SELECTOR EVENTS

Table 2-3 lists the switch selector events which were issued during the flight, but were not programmed for specific times. The water coolant valve open and close switch selector commands were issued by the LVDC based on the temperatures sensed in the Environmental Control System (ECS).

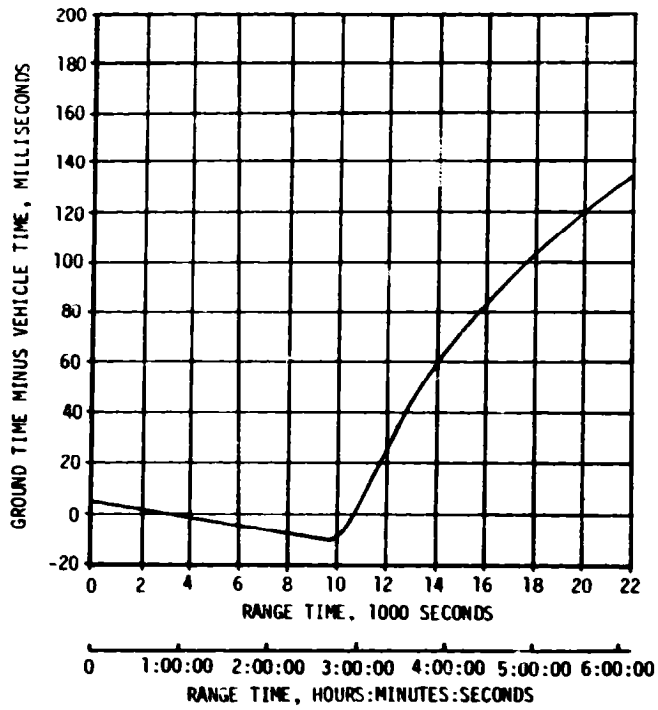


Figure 2-1. Ground Station Time to Vehicle Time Conversion

Table 2-1. Time Base Summary

TIME BASE	VEHICLE TIME SECONDS (HR:MIN:SEC)	GROUND TIME SECONDS (HR:MIN:SEC)	SIGNAL START
T <sub>0</sub>	-16.96	-16.96	Guidance Reference Release
T <sub>1</sub>	0.59	0.59	IU Umbilical Disconnect Sensed by LVDC
T <sub>2</sub>	138.00	138.00	Initiated by LVDC 0.010 Seconds after T <sub>1</sub> +137.4 Seconds
T <sub>3</sub>	161.81	161.81	S-IC OECD Sensed by LVDC
T <sub>4</sub>	559.54	559.54	S-II OECD Sensed by LVDC
T <sub>5</sub>	706.43	706.43	S-IVB ECO (Velocity) Sensed by LVDC
T <sub>6</sub>	8638.58 (02:23:58.58)	8638.57 (02:23:58.57)	Restart Equation Solution
T <sub>7</sub>	9558.65 (02:39:08.65)	9558.64 (02:39:08.64)	S-IVB ECO (Velocity) Sensed by LVDC
T <sub>8</sub>	15,487.09 (04:18:07.09)	15,487.16 (04:18:07.16)	Initiated by Ground Command

Table 2-3 also contains the special sequence of switch selector events which were programmed to be initiated by telemetry station acquisition and included the following calibration sequence:

FUNCTION	STAGE	TIME (SEC)
Telemetry Calibrator Inflight Calibrate, ON	IU	Acquisition + 60.0
TM Calibrate, ON	S-IVB	Acquisition + 60.4
TM Calibrate, OFF	S-IVB	Acquisition + 61.4
Telemetry Calibrator Inflight Calibrate, OFF	IU	Acquisition + 65.0

Table 2-2. Significant Event Times Summary

ITEM	EVENT DESCRIPTION	RANGE TIME		TIME FROM BASE	
		ACTUAL SEC	ACT-PRED SEC	ACTUAL SEC	ACT-PRED SEC
1	GUIDANCE REFERENCE RELEASE (GRR)	-17.0	0.0	-17.6	0.1
2	S-IC ENGINE START SEQUENCE COMMAND (GROUND)	-8.9	-0.1	-9.5	0.0
3	S-IC ENGINE NO.5 START	-6.7	-0.1	-7.3	0.0
4	S-IC ENGINE NO.1 START	-6.4	0.0	-7.3	0.1
5	S-IC ENGINE NO.3 START	-6.4	0.0	-7.0	0.1
6	S-IC ENGINE NO.2 START	-6.1	0.0	-6.7	0.1
7	S-IC ENGINE NO.4 START	-6.4	0.0	-7.0	0.1
8	ALL S-IC ENGINES THRUST OK	-1.9	-0.4	-2.5	-0.3
9	RANGE ZERO	0.0		-0.6	
10	ALL HOLDDOWN AFMS RELEASED (FIRST MOTION)	0.3	0.0	-0.3	0.1
11	TU UMBILICAL DISCONNECT, START OF TIME BASE 1 (T1)	0.6	-0.1	0.0	0.0
12	BEGIN TOWER CLEARANCE YAW MANEUVER	1.7	0.0	1.1	0.1
13	END YAW MANEUVER	10.9	1.2	10.3	1.3
14	BEGIN PITCH AND ROLL MANEUVER	12.7	0.2	12.1	0.3
15	S-IC OUTBOARD ENGINE CANT	20.5	-0.2	20.0	0.0
16	END ROLL MANEUVER	31.8	-0.7	31.2	-0.6
17	MACH 1	67.5	0.4	66.9	0.4
18	MAXIMUM DYNAMIC PRESSURE (MAX Q)	86.0	4.1	85.4	4.2
19	S-IC CENTER ENGINE CUTOFF (CECO)	137.85	-0.11	137.26	-0.04
20	START OF TIME BASE 2 (T2)	138.0	-0.1	0.0	0.0
21	END PITCH MANEUVER (TILT ARREST)	158.9	-0.5	20.9	-0.4
22	S-IC OUTBOARD ENGINE CUTOFF (OECO)	161.78	-0.31	23.78	-0.25
23	START OF TIME BASE 3 (T3)	161.8	-0.3	0.0	0.0

Table 2-2. Significant Event Times Summary (Continued)

ITEM	EVENT DESCRIPTION	RANGE TIME		TIME FROM BASE	
		ACTUAL SEC	ACT-PRED SEC	ACTUAL SEC	ACT-PRED SEC
24	START S-II LM2 TANK HIGH PRESSURE VENT MODE	161.9	-0.3	0.1	0.0
25	S-II LM2 RECIRCULATION PUMPS OFF	162.0	-0.3	0.2	0.0
26	S-IC/S-II SEPARATION COMMAND TO FIRE SEPARATION DEVICES AND RETRO MOTORS	163.5	-0.3	1.7	0.0
27	S-II ENGINE SOLENOID ACTIVATION (AVERAGE OF FIVE)	164.2	-0.3	2.4	0.0
28	S-II ENGINE START SEQUENCE COMMAND (ESCI)	164.2	-0.3	2.4	0.0
29	S-II IGNITION-STOP OPEN	165.2	-0.3	3.4	0.0
30	S-II CHILLDOWN VALVES CLOSE	167.1	-0.3	5.3	0.0
31	S-II MAINSTAGE	167.2	-0.3	5.4	0.0
32	S-II HIGH (5.5) EMP NO. 1 ON	169.7	-0.3	7.9	0.0
33	S-II HIGH (5.5) EMP NO. 2 ON	169.9	-0.3	8.1	0.0
34	S-II SECOND PLANE SEPARATION COMMAND (JETTISON S-II AFT INTERSTAGE)	193.5	-0.3	31.7	0.0
35	LAUNCH ESCAPE TOWER (LET) JETTISON	199.8	0.3	38.0	0.6
36	ITERATIVE GUIDANCE MODE (IGM) PHASE 1 INITIATED	204.5	0.4	42.7	0.7
37	S-II CENTER ENGINE CUTOFF (CECO)	461.77	-0.33	299.96	-0.04
38	START OF ARTIFICIAL TAU MODE	494.3	-0.5	332.5	-0.2
39	S-II LOW ENGINE MIXTURE RATIO (EMR) SHIFT (ACTUAL)	494.5	-2.3	332.7	-2.0
40	END OF ARTIFICIAL TAU MODE	506.7	0.7	344.9	1.0
41	S-II OUTBOARD ENGINE CUTOFF (OECO)	559.54	0.33	397.73	0.62
42	S-II ENGINE CUTOFF INTERRUPT, START OF TIME BASE 4 (T4)	559.5	0.3	397.7	0.0
43	S-IVB ULLAGE MOTOR IGNITION	560.4	0.3	399.9	0.0
44	S-II/S-IVB SEPARATION COMMAND TO FIRE SEPARATION DEVICES AND RETRO MOTORS	560.5	0.3	400.0	0.0

Table 2-2. Significant Event Times Summary (Continued)

ITEM	EVENT DESCRIPTION	RANGE TIME		TIME FROM BASE	
		ACTUAL SEC	ACT-PRED SEC	ACTUAL SEC	ACT-PRED SEC
45	S-IVR ENGINE START COMMAND (FIRST ESC)	560.6	0.3	1.1	0.0
46	FUEL CHILDOOWN PUMP OFF	561.7	0.3	2.2	0.0
47	S-IVB IGNITION (STDV OPEN)	563.6	0.3	4.1	0.0
48	S-IVB MAINSTAGE	566.1	0.3	6.6	0.0
49	START OF ARTIFICIAL TAU MODE	568.1	0.2	8.5	-0.2
50	S-IVB ULLAGE CASE JETTISON	572.3	0.3	12.8	0.0
51	END OF ARTIFICIAL TAU MODE	579.4	2.1	19.8	1.8
52	BEGIN TERMINAL GUIDANCE	673.6	2.6	114.0	2.2
53	END IGM PHASE 3	698.3	-0.5	138.8	-0.7
54	BEGIN CHI FREEZE	698.3	-0.5	138.8	-0.7
55	S-IVB VELOCITY CUTOFF COMMAND NO. 1 (FIRST ECO)	706.21	0.72	-0.22	-0.01
56	S-IVB VELOCITY CUTOFF COMMAND NO. 2	706.35	0.75	-0.09	0.01
57	S-IVB ENGINE CUTOFF INTERRUPT, START OF TIME BASE 5 (T5)	706.4	0.7	0.0	0.0
58	S-IVB APS ULLAGE ENGINE NO. 1 IGNITION COMMAND	706.7	0.7	0.3	0.0
59	S-IVB APS ULLAGE ENGINE NO. 2 IGNITION COMMAND	706.8	0.7	0.4	0.0
60	LOX TANK PRESSURIZATION OFF	707.6	0.7	1.2	0.0
61	PARKING ORBIT INSERTION	716.2	0.7	9.8	0.0
62	BEGIN MANEUVER TO LOCAL HORIZONTAL ATTITUDE	727.8	1.9	21.3	1.1
63	S-IVB CONTINUOUS VENT SYSTEM (CVS) ON	765.4	0.7	59.0	0.0
64	S-IVB APS ULLAGE ENGINE NO. 1 CUTOFF COMMAND	793.4	0.7	87.0	0.0
65	S-IVB APS ULLAGE ENGINE NO. 2 CUTOFF COMMAND	793.5	0.7	87.1	0.0
66	BEGIN ORBITAL NAVIGATION	806.1	0.2	99.7	-0.5
67	BEGIN S-IVB RESTART PREPARA- TIONS, START OF TIME BASE 6 (T6)	8638.6	0.7	0.0	0.0

Table 2-2. Significant Event Times Summary (Continued)

ITEM	EVENT DESCRIPTION	RANGE TIME		TIME FROM PASE	
		ACTUAL SEC	ACT-PRED SEC	ACTUAL SEC	ACT-PRED SEC
68	S-IVR O2/H2 BURNER LH2 ON	8679.8	0.6	41.3	0.0
69	S-IVR O2/H2 BURNER EXCITERS ON	8680.1	0.6	41.6	0.0
70	S-IVR O2/H2 BURNER LOX ON (HELIUM HEATER ON)	8680.5	0.6	42.0	0.0
71	S-IVR CVS OFF	8680.7	0.6	42.2	0.0
72	S-IVB LH2 REPRESSURIZATION CONTROL VALVE ON	8686.6	0.6	48.1	0.0
73	S-IVR LOX REPRESSURIZATION CONTROL VALVE ON	8686.8	0.6	48.3	0.0
74	S-IVB AUX HYDRAULIC PUMP FLIGHT MODE ON	8857.5	0.6	219.0	0.0
75	S-IVR LOX CHILDDOWN PUMP ON	8987.5	0.6	249.0	0.0
76	S-IVR LH2 CHILDDOWN PUMP ON	8992.5	0.6	254.0	0.0
77	S-IVR PNEVALVES CLOSED	8897.5	0.6	259.0	0.0
78	S-IVR MIXTURE RATIO CONTROL VALVE OPEN	9088.6	0.6	450.1	0.0
79	S-IVR APS ULLAGE ENGINE NO. 1 IGNITION COMMAND	9134.8	0.6	496.3	0.0
80	S-IVR APS ULLAGE ENGINE NO. 2 IGNITION COMMAND	9134.9	0.6	496.4	0.0
81	S-IVB O2/H2 BURNER LH2 OFF (HELIUM HEATER OFF)	9135.3	0.6	496.8	0.0
82	S-IVR O2/H2 BURNER LOX OFF	9139.8	0.6	501.3	0.0
83	S-IVR LH2 CHILDDOWN PUMP OFF	9207.9	0.6	569.4	0.0
84	S-IVR LOX CHILDDOWN PUMP OFF	9208.1	0.6	569.6	0.0
85	S-IVR ENGINE RESTART COMMAND (FUEL LEAD INITIATION) (SECOND ESC)	9208.5	0.6	570.0	0.0
86	S-IVR APS ULLAGE ENGINE NO. 1 CUTOFF COMMAND	9211.5	0.6	573.0	0.0
87	S-IVR APS ULLAGE ENGINE NO. 2 CUTOFF COMMAND	9211.6	0.6	573.1	0.0
88	S-IVR SECOND IGNITION (STDV OPEN)	9216.5	0.6	578.0	0.0
89	S-IVR MAINSTAGE	9219.0	0.6	580.5	0.0



Table 2-2. Significant Event Times Summary (Continued)

ITEM	EVENT DESCRIPTION	RANGE TIME		TIME FROM BASE	
		ACTUAL SEC	ACT-PRED SEC	ACTUAL SEC	ACT-PRED SEC
90	ENGINE MIXTURE RATIO (EMR) CONTROL VALVE SHIFT (BEGIN VALVE MOVEMENT)	9264.9	1.0	626.3	0.3
91	S-IVB LH2 STEP PRESSURIZATION (SECOND PURN RELAY OFF)	9488.5	0.0	850.0	0.0
92	BEGIN TERMINAL GUIDANCE	9530.7	-1.2	892.2	-1.8
93	BEGIN CHI FREEZE	9555.8	-2.3	917.2	-3.1
94	S-IVB SECOND GUIDANCE CUTOFF COMMAND NO. 1 (SECOND ECO)	9558.41	-1.79	-0.23	-0.03
95	S-IVB SECOND GUIDANCE CUTOFF COMMAND NO. 2	9558.52	-1.78	-0.12	-0.02
96	S-IVB ENGINE CUTOFF INTERRUPT, START OF TIME BASE 7 (T7)	9558.6	-1.8	0.0	0.0
97	S-IVB CVS ON	9559.1	-1.8	0.5	0.0
98	TRANSLUNAR INJECTION (TLI)	9568.4	-1.8	9.9	0.0
99	S-IVB CVS OFF	9711.3	0.0	152.7	1.8
100	BEGIN ORBITAL NAVIGATION	9710.3	-1.1	151.6	0.6
101	BEGIN MANEUVER TO LOCAL HORIZONTAL ATTITUDE	9710.3	-1.1	151.6	0.6
102	BEGIN MANEUVER TO TRANSPOSITION AND DOCKING ATTITUDE (TDC)	10459.3	-5.1	900.6	-3.4
103	CSM SEPARATION	11099.0	38.6	1540.3	40.3
104	CSM DOCK	12113.4	453.6	2554.7	455.4
105	SC/LV FINAL SEPARATION	14355.1	-4.7	4796.4	-2.9
106	START OF TIME BASE 8 (T8)	15487.2	-293.1	0.0	0.0
107	S-IVB APS ULLAGE ENGINE NO. 1 IGNITION COMMAND	15488.3	-293.2	1.2	0.0
108	S-IVB APS ULLAGE ENGINE NO. 2 IGNITION COMMAND	15488.5	-293.2	1.4	0.0
109	S-IVB APS ULLAGE ENGINE NO. 1 CUTOFF COMMAND	15568.3	-293.2	81.2	0.0
110	S-IVB APS ULLAGE ENGINE NO. 2 CUTOFF COMMAND	15568.5	-293.2	81.4	0.0

Table 2-2. Significant Event Times Summary (Continued)

ITEM	EVENT DESCRIPTION	RANGE TIME		TIME FROM USE	
		ACTUAL SEC	ACT-PRED SEC	ACTUAL SEC	ACT-PRED SEC
111	INITIATE MANEUVER TO LOX DUMP ATTITUDE	16068.4	-292.1	581.2	1.1
112	S-IVR CVS ON	16487.1	-293.3	1000.0	0.0
113	BEGIN LOX DUMP	16767.1	-293.3	1280.0	0.0
114	S-IVR CVS OFF	16787.1	-293.3	1300.0	0.0
115	END LOX DUMP	16815.1	-293.3	1328.0	0.0
116	M2 NONPROPULSIVE VENT (NPV) ON	17064.1	-291.3	1577.0	2.0
117	INITIATE MANEUVER TO ATTITUDE REQUIRED FOR S-IVR APS BURN	19837.2	936.9	4350.0	1230.1
118	S-IVR APS ULLAGE ENGINE NO. 1 IGNITION COMMAND	20407.2	606.9	4920.0	900.1
119	S-IVR APS ULLAGE ENGINE NO. 2 IGNITION COMMAND	20407.4	607.1	4920.2	900.3
120	S-IVR APS ULLAGE ENGINE NO. 1 CUTOFF COMMAND	20461.2	502.9	4974.0	796.1
121	S-IVR APS ULLAGE ENGINE NO. 2 CUTOFF COMMAND	20461.4	503.1	4974.2	796.3
122	INITIATE THREE-AXIS TUMBLE COMMAND	21306.2	14094.1	5819.0	13800.8
123	S-IVR/TU LUNAR IMPACT (HOURS)	270,482	2274		
	(HR:MIN:SEC)	75:08:02	00:37:54		

Table 2-3. Variable Time and Command Switch Selector Events

FUNCTION	STAGE	RANGE TIME (SEC)	TIME FROM BASE (SEC)	REMARKS
Water Coolant Valve CLOSED	IU	780.2	T <sub>5</sub> +73.8	LVDC Function
Telemetry Calibrator Inflight Calibrate ON	IU	1106.7	T <sub>5</sub> +400.3	Acquisition by Canary Rev. 1
TM Calibrate ON	S-IVB	1107.2	T <sub>5</sub> +400.7	Acquisition by Canary Rev. 1
TM Calibrate OFF	S-IVB	1108.2	T <sub>5</sub> +401.7	Acquisition by Canary Rev. 1
Telemetry Calibrator In-Flight Calibrate OFF	IU	1111.7	T <sub>5</sub> +405.3	Acquisition by Canary Rev. 1
Water Coolant Valve CLOSED	IU	3180.2	T <sub>5</sub> +2473.8	LVDC Function
Telemetry Calibrator In-Flight Calibrate ON	IU	3242.7	T <sub>5</sub> +2536.3	Acquisition by Carnarvon Rev 1
TM Calibrate ON	S-IVB	3243.1	T <sub>5</sub> +2536.7	Acquisition by Carnarvon Rev 1
TM Calibrate OFF	S-IVB	3244.1	T <sub>5</sub> +2537.7	Acquisition by Carnarvon Rev 1
Telemetry Calibrator In-Flight Calibrate OFF	IU	3247.7	T <sub>5</sub> +2541.3	Acquisition by Carnarvon Rev 1
Telemetry Calibrator In-Flight Calibrate ON	IU	3674.8	T <sub>5</sub> +2968.3	Acquisition by Honeysuckle Rev 1
TM Calibrate ON	S-IVB	3675.1	T <sub>5</sub> +2968.7	Acquisition by Honeysuckle Rev 1
TM Calibrate OFF	S-IVB	3676.1	T <sub>5</sub> +2969.7	Acquisition by Honeysuckle Rev 1
Telemetry Calibrator In-Flight Calibrate OFF	IU	3679.7	T <sub>5</sub> +2973.3	Acquisition by Honeysuckle Rev 1

Table 2-3. Variable Time and Command Switch Selector Events (Cont'd)

FUNCTION	STAGE	RANGE TIME (SEC)	TIME FROM BASE (SEC)	REMARKS
Telemetry Calibrator In-Flight Calibrate ON	IU	6706.7	T <sub>5</sub> +6000.3	Acquisition by Canary Rev 2
TM Calibrate ON	S-IVB	6707.1	T <sub>5</sub> +6000.7	Acquisition by Canary Rev 2
TM Calibrate OFF	S-IVB	6708.1	T <sub>5</sub> +6001.7	Acquisition by Canary Rev 2
Telemetry Calibrator In-Flight Calibrate	IU	6711.7	T <sub>5</sub> +6005.3	Acquisition by Canary Rev 2
Water Coolant Valve OPEN	IU	13380.2	T <sub>7</sub> +3821.6	LVDC Function
Water Coolant Valve CLOSED	IU	13680.2	T <sub>7</sub> +4121.5	LVDC Function
Start of Time Base 8 (T <sub>8</sub> )	IU	15487.2	T <sub>8</sub> +0.0	CCS Command
Water Coolant Valve OPEN	IU	16380.2	T <sub>8</sub> +893.1	LVDC Function
Water Coolant Valve CLOSED	IU	16680.2	T <sub>8</sub> +1193.1	LVDC Function
Switch CCS to Low Gain Antenna	IU	20249.0	T <sub>8</sub> +4761.9	CCS Command
Switch CCS to Low Gain Antenna	IU	20250.3	T <sub>8</sub> +4763.2	CCS Command
Switch CCS Antenna to OMNI	IU	21476.3	T <sub>8</sub> +5989.2	CCS Command
Water Coolant Valve OPEN	IU	22980.2	T <sub>8</sub> +7493.1	LVDC Function
S-IVB Ullage Engine No. 1 ON	S-IVB	20407.2	T <sub>8</sub> +4920.0	Lunar Impact CCS Command
S-IVB Ullage Engine No. 2 ON	S-IVB	20407.4	T <sub>8</sub> +4920.2	Lunar Impact CCS Command
S-IVB Ullage Engine No. 1 OFF	S-IVB	20461.2	T <sub>8</sub> +4974.0	Lunar Impact CCS Command
S-IVB Ullage Engine No. 2 OFF	S-IVB	20461.4	T <sub>8</sub> +4974.2	Lunar Impact CCS Command
FCC Power OFF "A"	IU	21323.9	T <sub>8</sub> +5836.7	CCS Command
FCC Power OFF "B"	IU	21337.2	T <sub>8</sub> +5850.0	CCS Command

SECTION 3  
LAUNCH OPERATIONS

3.1 SUMMARY

The ground systems supporting the AS-511/Apollo 16 countdown and launch performed satisfactorily with no unscheduled holds. Propellant tanking was accomplished satisfactorily. The space vehicle was launched on schedule at 12:54:00 Eastern Standard Time (EST) on April 16, 1972, from pad 39A of the Kennedy Space Center, Saturn Complex. Damage to the pad, Launch Umbilical Tower (LUT) and support equipment was considered minimal.

3.2 PRELAUNCH MILESTONES

A chronological summary of prelaunch milestones for the AS-511 launch is contained in Table 3-1.

3.2.1 S-IC Stage Prelaunch Problems

One minor S-IC problem occurred during the Countdown Demonstration Test (CDDT). The LOX tank ullage pressure measurement, D94-119, was erratic for a five minute period during the T-9 hour hold. The problem cleared and could not be duplicated; however, the transducer was replaced. Failure analysis could not determine the cause of the problem.

3.2.2 S-II Stage Prelaunch Problems

During an engine helium bottle decay test, engine No. 2 emergency vent was two minutes slow in closing. The pneumatic package was replaced on February 2, and the replaced unit returned to the engine contractor where the problem could not be repeated. The failure was attributed to contamination.

During the Flight Readiness Test (FRT), prior to application of hydraulic pressure, engine No. 4 yaw actuator position showed a step from 0 degrees to approximately 1.5 degrees extended. Review of test data revealed similar steps occurring on other actuators during the Overall Test (OAT-1) and Backup Guidance System (BUGS) test. Engine No. 4 yaw actuator was replaced on March 23, 1972, and returned to the supplier where testing failed to reveal the cause of the problem. Analysis and lab tests revealed that movement of the cylinder bypass valve was the most likely suspect, therefore, mechanical clamps were installed on the valves to prevent valve motion. Launch Mission Rule (LMR), items 2-394 through 2-401, were implemented to assure detection in the event of recurrence during countdown operations.

Table 3-1. AS-511/Apollo 16 Prelaunch Milestones

DATE	ACTIVITY OR EVENT
July 1, 1970	S-IVB-511 Stage Arrival
August 17, 1970	Spacecraft/Lunar Module Adapter (SLA)-20 Arrival
September 30, 1970	S-II-11 Stage Arrival
May 5, 1971	Lunar Module (LM)-11 Descent Stage Arrival
May 14, 1971	Lunar Module (LM)-11 Ascent Stage Arrival
July 29, 1971	Command and Service Module (CSM)-113 Arrival
September 1, 1971	Lunar Roving Vehicle (LRV)-2 Arrival
September 17, 1971	S-IC-11 Stage Arrival
September 21, 1971	S-IC Erection on Mobile Launcher (ML)-3
September 29, 1971	Instrument Unit (IU)-511 Arrival
October 1, 1971	S-II Erection
October 5, 1971	S-IVB Erection
October 6, 1971	IU Erection
October 15, 1971	Launch Vehicle (LV) Electrical Systems Test
November 8, 1971	LV Propellant Dispersion/Malfunction Overall Test (OAT) Complete
November 16, 1971	LRV Installation
November 18, 1971	LV Service Arm OAT Complete
December 8, 1971	Spacecraft (SC) Erection
December 13, 1971	Space Vehicle (SV)/ML Transfer to Pad 39A
January 27, 1972	SV/ML Returned to VAB
February 9, 1972	SV/ML Second Transfer to Pad 39A
February 22, 1972	SV Electrical Mate
February 23, 1972	SV OAT No. 1 (Plugs In) Complete
March 2, 1972	SV FLight Readiness Test (FRT) Completed
March 20, 1972	RP-1 Loading
March 30, 1972	Countdown Demonstration Test (CDDT) Completed (Wet)
March 31, 1972	CDDT Completed (Dry)
April 14, 1972	SV Terminal Countdown Started (T-28 Hours)
April 16, 1972	SV Launch

During the CDDT, the check valve in the LOX recirculation valve actuation system was found to be leaking in the reverse direction. Special post CDDT tests failed to repeat the failure; however, the valve was replaced. Failure analysis found a mark on the valve seat and the failure was attributed to contamination.

During the CDDT engine start tank vent valve settling test, venting from engine No. 2 helium bottle continued after vent valve closing subsequent to the sixth vent cycle. Following extensive special tests at the engine contractor facility and on S-II-11, the problem was attributed to "stiction" in the bleed regulator of the engine helium regulator. The system was determined to be flight worthy.

### 3.2.3 S-IVB Prelaunch Problems

During the CDDT LOX alternate loading tests, the S-IVB LOX fill and drain valve closing response times got progressively longer. During the three loading tests the valve was cycled three times. An investigation revealed that all conditions appeared to be nominal except for the thermal environment. This environment was abnormal since this was the first test in which LOX was repeatedly drained and replenished. During the CDDT terminal count the closing response time recovered to a normal value. A post CDDT ambient leakage test of the pneumatic system showed no abnormal leakage. Since the valve would not be exposed to a similar thermal environment associated with repeated LOX fill and drain during the launch countdown, no problems were anticipated or encountered.

A leak was noted in a facilities line at approximately four hours prior to liftoff, while scanning the area with TV. An investigation revealed the leak was in the 3000 psi cold helium facility line, at the union fitting closest to Model 433A inlet port. At the time the leak was discovered, the cold helium bottles had already been pressurized. The line was isolated until approximately 15 minutes prior to launch. During post launch inspection, the B-nuts on each side of the union were found to be undertorqued. All fittings in the cryogenic lines will be retorqued prior to AS-512 CDDT and the torque rechecked during CDDT post loading checks.

### 3.2.4 IU Stage Prelaunch Problems

On April 14, 1972, a problem occurred during the Control/EDS Rate Gyro Test (CTC4) when the program displayed an Emergency Detection System (EDS) interface error. The error was found to be due to a program problem. This problem was transferred to programming and dispositioned "Use As Is" for AS-511 and will be corrected for AS-512.

On April 16, 1972, during a special running of the CTC5, Auxiliary Propulsion System (APS) automatic gain test, the group 2 (backup) yaw control/EDS rate gyro was torqued at 0.25 degree/second. The flight control computer (FCC) spatial amplifier outputs decreased

below the APS threshold and the same time the Control Signal Processor (CSP) demodulator output voltage decreased approximately 40% to 0.15 degree/second, as monitored on measurement R5-602. The problem occurred just once, for approximately 1.9 seconds, and could not be duplicated. Countdown continued on schedule.

The most probable cause is considered to be an open circuit condition of the Q8 transistor of the CSP.

If this failure had occurred during flight, the result would have been a decrease in rate gyro signals redundancy. This is a backup gyro and is used whenever the primary and reference gyro outputs disagree. If such a disagreement had occurred in flight and the prelaunch failure recurred, analysis indicates the vehicle would still be controllable.

### 3.3 TERMINAL COUNTDOWN

The AS-511/Apollo 16 terminal countdown was picked up at T-28 hours on April 14, 1972, at 22:54:00 EST. Scheduled holds were initiated at T-9 hours for a duration of 9 hours, and at T-3 hours 30 minutes for a duration of one hour. Launch occurred on schedule at 12:54:00 EST on April 16, 1972, from pad 39A of the Kennedy Space Center (KSC), Saturn Launch Complex.

### 3.4 PROPELLANT LOADING

#### 3.4.1 RP-1 Loading

The RP-1 system successfully supported countdown and launch without incident. Tail Service Mast (TSM) 1-2 fill and replenish was accomplished at T-13 hours and S-IC level adjust and fill line inert at T-60 minutes as planned. Launch countdown support consumed 213,814 gallons of RP-1.

The S-IC/RP-1 continuous level probe values did not correlate with the Propellant Tanking Computer System (PTCS) readout. This measurement provides data for the RP-1 loading/level adjust secondary backup mode in the event that both segments of the PTCS should fail. An investigation of this problem is underway.

#### 3.4.2 LOX Loading

The LOX system supported countdown and launch satisfactorily. The fill sequence began with S-IVB fill command at 3:40 EST on April 16, 1972, and was completed 2 hours and 33 minutes later with all stage replenish normal at 6:13 EST. Replenish was as planned until about T-1 hour and 23 minutes when the S-IC replenish valve stuck closed. At this time the PTCS was placed in the manual replenish mode and full open to full



closed commands applied. On the third cycle the valve responded. Manual control for S-IC replenish was then continued through Thermal Conditioning System (TCS) start at T-187 seconds. Post launch inspection of the valve indicates the probability of a packing leak. A leak check is planned with corrective maintenance to follow.

LOX consumption during launch countdown was 588,000 gallons.

Launch damage to the LOX loading system was limited to several broken cabinet latches; scorched cable identification tags at the 30 foot level; a damaged gauge and two warped enclosure doors. No internal damage was noted as a result of the latter.

During S-IC fast fill operations at about T-6 hours on April 16, 1972, filter A224 began leaking. No corrective action was required or taken at that time. A post launch leak check and component disassembly and inspection are planned. Corrective action will depend on the results.

At about T-1 hour, the position indication from the replenish pump bypass valve surged to full scale where it remained. Normal valve operation was verified by flowrate, line pressure and pump speed. Consequently, no corrective action was taken. During post launch inspection it was found that the welds holding the valve position potentiometer had failed allowing it to become dislocated. The unit will be replaced. An evaluation to determine if additional bracing is required to prevent problem recurrence is also planned.

### 3.4.3 LH<sub>2</sub> Loading

The LH<sub>2</sub> system successfully supported countdown and launch. The fill sequence began with start of S-II loading at 6:29 EST on April 16, 1972, and was completed 80 minutes later when all stage replenish was established at 7:49 EST. S-II replenish was automatic until terminated with TCS start at T-187 seconds. S-IVB automatic replenish was established but switched to manual a short time later due to loading systems probe excursions. Manual replenish was continued until TCS start.

The S-IVB heat exchanger supply valve failed to open during plus time drain operations. This problem was first encountered after AS-509 launch and repeated after AS-510. All subsequent change requests submitted on this problem have been disapproved. No further action is recommended for the Apollo Program. The problem has received design corrective action for Skylab (SL)-2.

Near the end of S-IVB loading on April 16, 1972, liquid air was observed falling onto the S-IVB LH<sub>2</sub> valve skid. The source of the liquid air could not be definitely identified visually, however, temperature data indicates that it may have originated around the S-IVB heat exchanger vent check valve or vent pipe. In addition, liquid air was visually noted to be falling from the S-II heat exchanger vent flex hose.

Liquid air impingement could weaken or cause the failure of system components or structural members not designed to withstand low temperatures. Design action may be required to protect sensitive equipment or insulate the appropriate heat exchanger elements to prevent problem recurrence.

At about T-15 hours the S-IVB debris valve failed to respond following a system revert command. Relay K335-1 in ML patch distributor 6600 was replaced and system operation returned to normal.

Launch countdown support consumed about 460,000 gallons of LH<sub>2</sub>.

Launch damage to the LH<sub>2</sub> launch system was not excessive or serious. Scorched handles were noted on two regulators; the back was blown out of gauge A5292; paint was scorched and blistered on the vent line purge panel; cabling on the disconnect mechanism limit switch was scorched; three leak detection sensors were dislocated; disconnect mechanism jack covers were damaged; vacuum line 4D2 was scorched; an expansion joint was scorched; and an electrical terminal strip on the 200 foot level purge console was broken.

### 3.5 GROUND SUPPORT EQUIPMENT

#### 3.5.1 Ground/Vehicle Interface

In general, performance of the ground service systems supporting all stages of the launch vehicle was satisfactory. Overall damage to the pad, LUT, and support equipment from blast and flame impingement was considered minimal. Detailed discussion of the Ground Support Equipment (GSE) is contained in KSC Apollo/Saturn V (AS-511) "Ground Support Evaluation Report."

The PTCS satisfactorily supported countdown and launch operations.

The ECS performed satisfactorily throughout countdown and launch. Change-over from air to GN<sub>2</sub> purge occurred 23 minutes before resuming the count at T-9 hours. The changeover pressure/flow spike was significantly reduced from CDDT results due to procedural changes that reduced flowrates. The air to GN<sub>2</sub> changeover sequence will be evaluated further to determine if a modification is warranted. The S-II Aft-Engine interstage temperature did not reach the 200 +15°F requirement during thrust chamber chilldown until T-1 minute 40 seconds (specified at T-3 minutes). The temperature ramp-up was commenced 10 minutes before the nominal schedule, however, the starting temperature was very low (136°F). This item has been experienced during previous thrust chamber chilldowns and had no significant effect on system support.

The Holddown Arms and Service Arm Control Switches (SACS) satisfactorily supported countdown and launch. All Holddown Arms released pneumatically within a 12 millisecond period. The retraction and explosive release lanyard pull was accomplished in advance of ordnance actuation with a

41 millisecond margin. Pneumatic release valves 1 and 2 opened simultaneously 24 milliseconds after SACS armed signal. The SACS primary switches closed within 6 milliseconds of each other at 423 and 417 milliseconds after commit. SACS secondary switches closed simultaneously 1.112 seconds after commit. Fixed hood attach bolts on Holddown Arm 4 sheared on one side of the arm resulting in severe warping of both fixed and movable hoods.

Overall performance of the Tail Service Masts was satisfactory. Mast retraction times were nominal; 2.649 seconds for TSM 1-2, 2.292 seconds for TSM 3-2 and 2.505 seconds for TSM 3-4, measured from umbilical plate separation to mast retracted.

The Preflight and Inflight Service Arms (S/A's 1 through 8) supported countdown in a satisfactory manner. Performance was nominal during terminal count and liftoff. On S/A 1, there is an indication that the carrier connected switches are affected by cryogenic conditions. During S/A 1 disconnect the elapsed time from the Carrier Retract Command to loss of Carrier Connected indication was 35.9 seconds. The elapsed time during the Launch Control Room Integration Test was .240 second and during S/A OAT was .276 second, both of which were under non-cryogenic conditions. The slow switch actuation did not impair system operation.

### 3.5.2 MSFC Furnished Ground Support Equipment

The S-IC Mechanical GSE performance for countdown and launch was satisfactory. There was no visible damage to the system and only one minor problem was noted. On April 4, 1972, while setting up the S-IC pneumatic console He bottle fill module an indication of internal leakage was noted. Subsequent trouble-shooting failed to duplicate the problem or isolate a faulty component. As a precautionary measure, the regulator was replaced and performed satisfactorily throughout countdown and launch.

The S-IC ESE satisfactorily supported countdown and launch. No anomalies were noted in any of the ese systems and launch damage was minor.

All Ground Power and Battery equipment operated satisfactorily from the start of precount through launch. Two problems occurred, however, no down-time during countdown was attributed to the Ground Power or Battery equipment. At T-40 hours the Flight Battery Checkout Console (FBC) power supply tripped off. The FBC power supply was being used as the power source for S-II flight battery tests at the time it tripped. On all previous vehicles external power supply had been used for the heater tests. Investigation revealed that an incompatibility existed in using the FBC power supply as the power source for S-II flight battery heater tests. The flight battery activation procedures are being revised to use an external power supply for heater tests.

At about T-2 seconds the 400 cycle generator dropped off line. Switchover

to the 23T200 unit prevented the loss of 400 cycle power. Preliminary post launch checks revealed no abnormal behavior. Further testing will be accomplished when the Mobile Launcher is returned to the VAB. Recommended design action, if any, is pending results of this testing.

The Hazardous Gas Detection System successfully supported AS-511 count-down; support started at 2:24 EST (T-9 hours 30 minutes), and concluded at 12:54 EST. System operation was normal throughout the support period and no detections were reported.

## SECTION 4

### TRAJECTORY

#### 4.1 SUMMARY

The vehicle was launched on an azimuth 90 degrees east of north. A roll maneuver was initiated at 12.7 seconds that placed the vehicle on a flight azimuth of 72.034 degrees east of north. The reconstructed trajectory was generated by merging the following four trajectory segments: the ascent phase, the parking orbit phase, the injection phase, and the early translunar orbit phase. The analysis for each phase was conducted separately with appropriate end point constraints to provide trajectory continuity. Available C-Band radar and Unified S-Band (USB) tracking data plus telemetered guidance velocity data were used in the trajectory reconstruction.

The trajectory parameters from launch to Command and Service Module (CSM) separation were close to nominal. Earth parking orbit insertion conditions were achieved 0.72 second later than nominal with altitude nominal and velocity 0.2 meter per second greater than nominal. Translunar Injection (TLI) conditions were achieved 1.78 seconds earlier than nominal with altitude 2.0 kilometers less than nominal and velocity 1.9 meters per second greater than nominal. The trajectory parameters at Command and Service Module (CSM) separation deviated somewhat from nominal since the event occurred 38.6 seconds later than predicted.

#### 4.2 TRAJECTORY EVALUATION

##### 4.2.1 Ascent Phase

The ascent phase spans the interval from guidance reference release through parking orbit insertion. The ascent trajectory was established by using guidance velocity data as generating parameters to fit tracking data from five C-Band stations (Merritt Island, Patrick Air Force Base, Grand Turk, Bermuda FPQ-6, and Bermuda FPS-16M) and two S-Band stations (Merritt Island and Bermuda). Approximately 25 percent of the C-Band tracking data and 40 percent of the S-Band tracking were eliminated due to inconsistencies. The launch phase portion of the ascent phase (liftoff to approximately 20 seconds) was established by constraining guidance velocity data to the best estimate trajectory.

Actual and nominal altitude, surface range, and crossrange for the ascent phase are presented in Figure 4-1. Actual and nominal space-fixed velocity and flight path angle during ascent are shown in Figure 4-2.

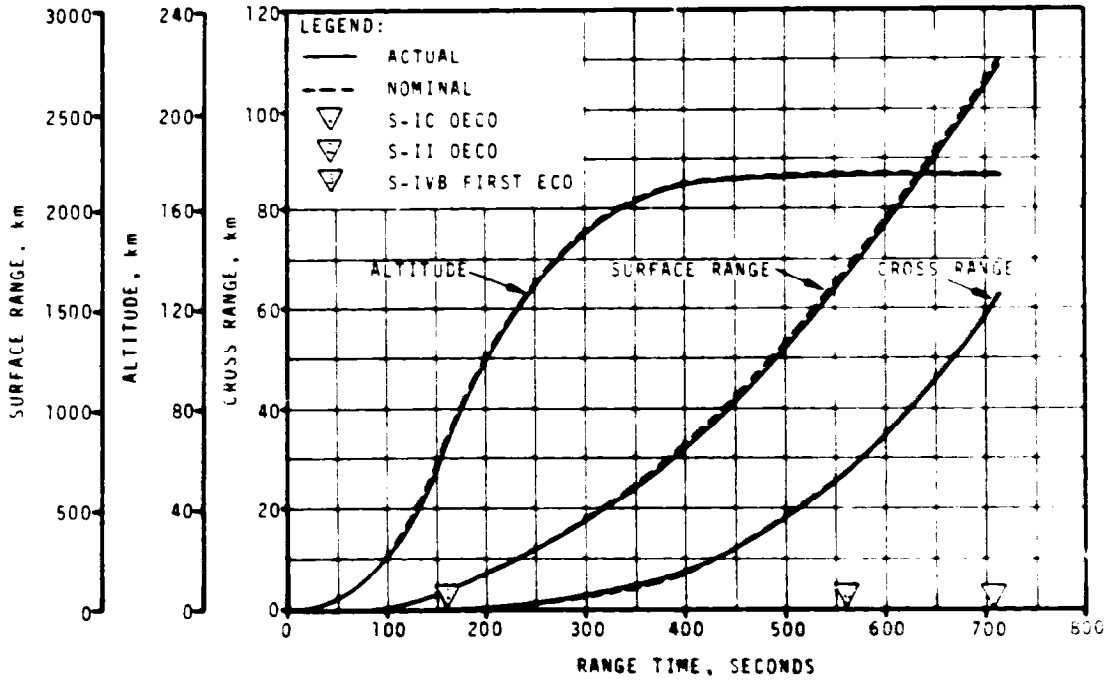


Figure 4-1. Ascent Trajectory Position Comparison

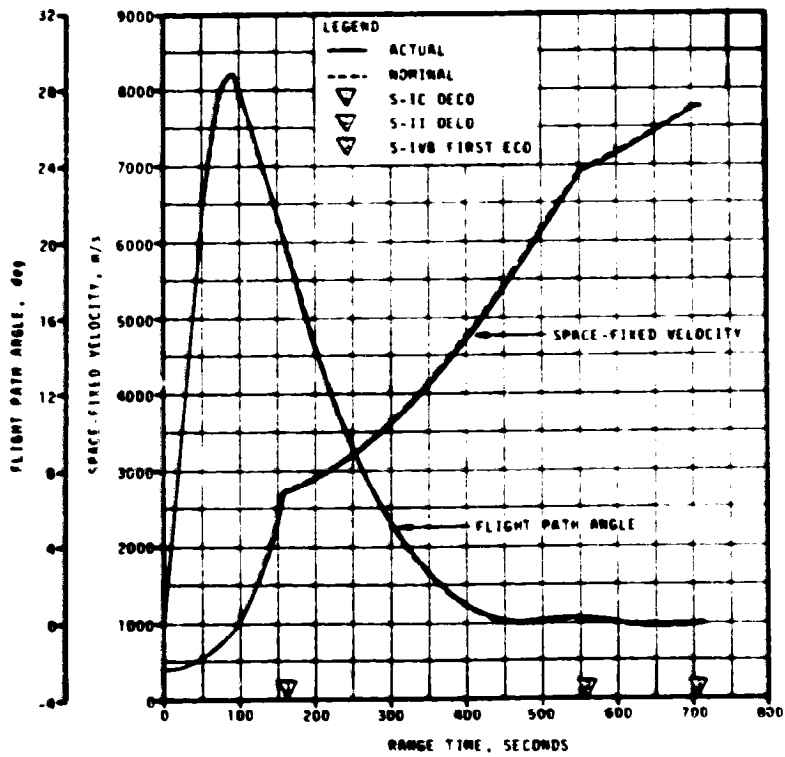


Figure 4-2. Ascent Trajectory Space-Fixed Velocity and Flight Path Angle Comparisons

Actual and nominal comparisons of ascent accelerations are shown in Figure 4-3. The maximum acceleration during S-IC burn was 3.85 g.

Mach number and dynamic pressure are shown in Figure 4-4. Differences from the nominal values are consistent with previous flight experience. These parameters were calculated using meteorological data measured to an altitude of 61.0 kilometers (32.9 n mi). Above this altitude, the measured data were merged into the U. S. Standard Reference Atmosphere.

Actual and nominal values of parameters at significant trajectory event times, cutoff events, and separation events are shown in Tables 4-1, 4-2, and 4-3, respectively.

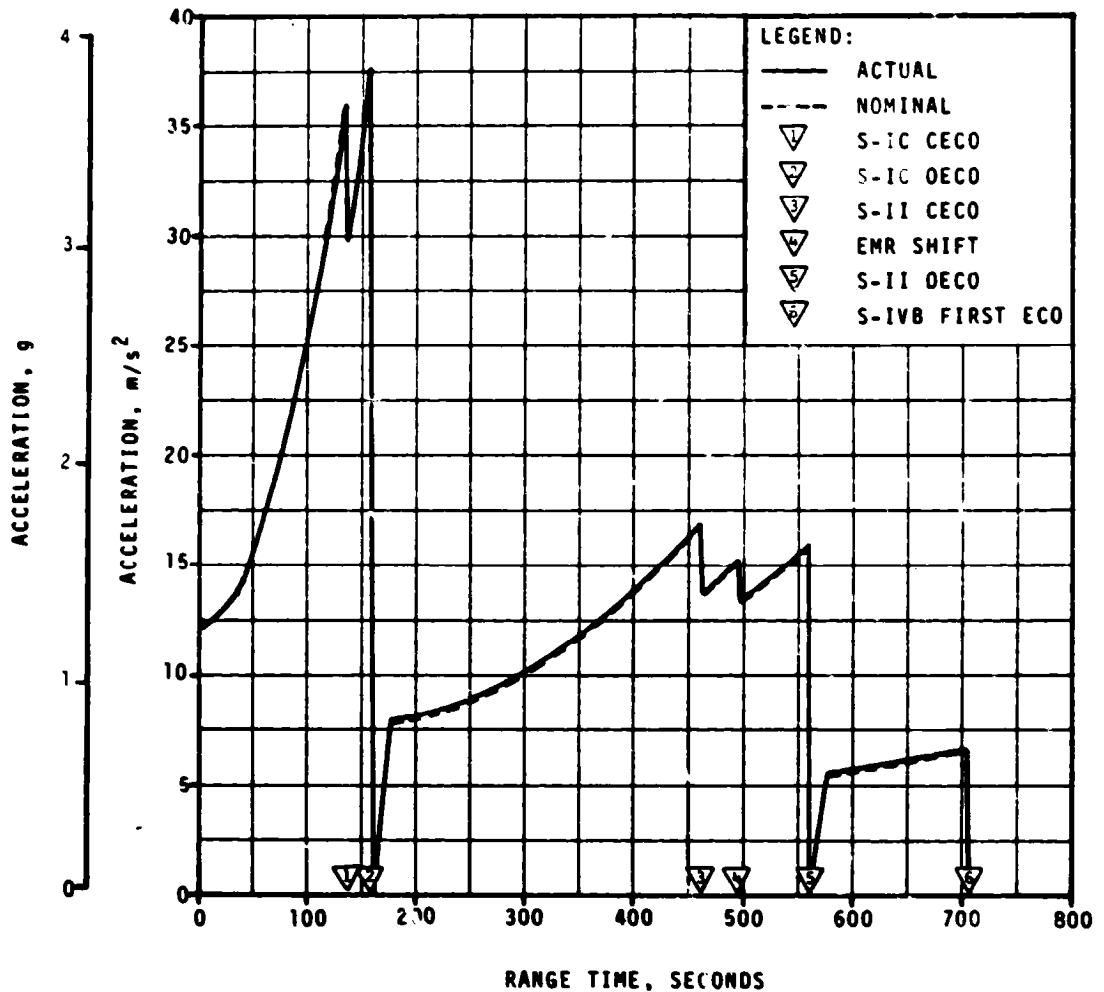


Figure 4-3. Ascent Trajectory Acceleration Comparison

Table 4-1. Comparison of Significant Trajectory Events

EVENT	PARAMETER	ACTUAL	NOMINAL	ACT-NOM
First Motion	Range Time, sec	0.3	0.3	0.0
	Non-gravitational Acceleration, $m/s^2$ ( $ft/s^2$ ) (g)	10.58 (34.71) (1.08)	10.53 (34.55) (1.07)	0.05 (0.16) (0.01)
Mach 1	Range Time, sec	67.5	67.1	0.4
	Altitude, km (n mi)	7.9 (4.3)	7.8 (4.2)	0.1 (0.1)
Maximum Dynamic Pressure	Range Time, sec	86.0	81.9	4.1
	Dynamic Pressure, $N/cm^2$ ( $lb/ft^2$ )	3.48 (726.81)	3.10 (689.22)	0.18 (37.59)
	Altitude, km (n mi)	14.3 (7.7)	12.7 (6.9)	1.6 (0.8)
Non-gravitational Acceleration, S-1C	Range Time, sec	161.78	161.26	0.52
	Acceleration, $m/s^2$ ( $ft/s^2$ ) (g)	37.70 (123.69) (3.85)	37.34 (122.51) (3.81)	0.36 (1.18) (0.04)
S-11	Range Time, sec	461.77	462.10	-0.33
	Acceleration, $m/s^2$ ( $ft/s^2$ ) (g)	17.08 (56.04) (1.74)	17.04 (55.91) (1.74)	0.04 (0.13) (0.00)
S-1VB First Burn	Range Time, sec	706.21	705.49	0.72
	Acceleration, $m/s^2$ ( $ft/s^2$ ) (g)	6.58 (21.59) (0.67)	6.56 (21.52) (0.67)	0.02 (0.07) (0.00)
S-1VB Second Burn	Range Time, sec	9,558.42	9,560.20	1.78
	Acceleration, $m/s^2$ ( $ft/s^2$ ) (g)	13.97 (45.83) (1.42)	13.92 (45.67) (1.42)	0.05 (0.16) (0.00)
Maximum Earth-Fixed Velocity: S-1C	Range Time, sec	162.5	163.3	-0.8
	Velocity, m/s (ft/s)	2,371.6 (7,780.8)	2,321.9 (7,614.6)	-10.3 (-33.8)
S-11	Range Time, sec	560.0	560.3	-0.3
	Velocity, m/s (ft/s)	6,568.2 (21,549.2)	6,572.5 (21,563.3)	-4.3 (-14.1)
S-1VB First Burn	Range Time, sec	707.0	706.3	0.7
	Velocity, m/s (ft/s)	7,402.1 (24,285.1)	7,401.7 (24,283.8)	0.4 (1.3)
S-1VB Second Burn	Range Time, sec	9,559.0	9,560.4	-1.4
	Velocity, m/s (ft/s)	10,446.1 (34,272.0)	10,443.9 (34,264.8)	2.2 (7.2)

NOTE: Times used are vehicle times.  
All maximums are at the nearest time point available.



Table 4-2. Comparison of Cutoff Events

PARAMETER	ACTUAL	NOMINAL	ACT-NOM	ACTUAL	NOMINAL	ACT-NOM
S-1C OECO (ENGINE SOLENOID)			S-1C OECO (ENGINE SOLENOID)			
Range Time, sec	137.84	137.86	-0.02	161.78	162.09	-0.31
Altitude, km (n mi)	45.4 (24.5)	45.8 (24.7)	-0.4 (-0.2)	66.1 (35.7)	66.9 (36.7)	-0.8 (-0.4)
Space-Fixed Velocity, m/s (ft/s)	2,028.4 (6,654.9)	2,033.6 (6,671.9)	-5.2 (-17.0)	2,731.7 (8,961.6)	2,742.0 (8,986.1)	-10.3 (-34.5)
Flight Path Angle, deg	23.110	23.337	-0.227	19.900	20.137	-0.237
Heading Angle, deg	76.125	76.118	0.007	75.324	75.312	0.012
Surface Range, km (n mi)	49.7 (26.8)	49.7 (26.8)	0.0 (0.0)	92.5 (49.9)	93.0 (50.2)	-0.5 (-0.2)
Cross Range, km (n mi)	0.0 (0.0)	0.1 (0.1)	-0.1 (-0.1)	0.1 (0.1)	0.2 (0.1)	-0.1 (0.0)
Cross Range Velocity, m/s (ft/s)	2.5 (8.2)	2.4 (7.9)	0.1 (0.3)	6.4 (21.0)	6.1 (20.0)	0.3 (1.0)
S-1I OECO (ENGINE SOLENOID)			S-1I OECO (ENGINE SOLENOID)			
Range Time, sec	461.77	462.10	-0.33	559.54	559.27	0.27
Altitude, km (n mi)	171.1 (92.8)	177.4 (93.1)	-6.3 (-0.7)	173.0 (93.4)	173.3 (93.6)	-0.3 (-0.2)
Space-Fixed Velocity, m/s (ft/s)	5,596.5 (18,361.2)	5,605.1 (18,389.4)	-8.6 (-28.2)	6,966.0 (22,857.0)	6,972.0 (22,874.0)	-6.0 (-19.0)
Flight Path Angle, deg	0.119	-0.001	0.120	0.369	0.287	0.082
Heading Angle, deg	79.538	79.563	-0.025	82.595	82.585	0.010
Surface Range, km (n mi)	1,097.5 (592.7)	1,100.3 (594.1)	-2.8 (-1.4)	1,655.0 (894.1)	1,655.5 (893.9)	-0.5 (0.2)
Cross Range, km (n mi)	13.2 (7.1)	13.3 (7.2)	-0.1 (-0.1)	27.0 (14.6)	27.0 (14.6)	0.0 (0.0)
Cross Range Velocity, m/s (ft/s)	107.6 (353.0)	108.9 (357.3)	-1.3 (-4.3)	179.0 (587.3)	178.3 (585.0)	0.7 (2.3)
S-1VB 1ST GUIDANCE CUTOFF SIGNAL			S-1VB 2ND GUIDANCE CUTOFF SIGNAL			
Range Time, sec	706.21	705.49	0.72	9,558.42	9,560.20	-1.78
Altitude, km (n mi)	172.9 (93.4)	172.9 (93.4)	0.0 (0.0)	303.4 (163.8)	305.2 (164.8)	-1.8 (-1.0)
Space-Fixed Velocity, m/s (ft/s)	7,802.7 (25,599.4)	7,802.5 (25,598.8)	0.2 (0.6)	10,847.8 (35,589.8)	10,846.3 (35,585.8)	1.5 (4.9)
Flight Path Angle, deg	0.903	-0.001	0.904	7.012	7.162	-0.150
Heading Angle, deg	88.504	88.471	0.033	59.695	59.620	0.075
Surface Range, km (n mi)	2,648.6 (1,430.1)	2,646.0 (1,428.7)	2.6 (1.4)			
Cross Range, km (n mi)	60.2 (32.5)	59.9 (32.3)	0.3 (0.2)			
Cross Range Velocity, m/s (ft/s)	278.5 (913.7)	276.8 (905.5)	1.7 (5.2)			
Inclination, deg				32.512	32.519	-0.007
Descending Node, deg				122.465	122.457	0.008
Eccentricity				0.9726	0.9726	0.0000
$C_3$ (ft <sup>2</sup> /s <sup>2</sup> )				-1,457,301 (-17,039,039)	-1,658,570 (-17,052,705)	1,277 (13,746)

NOTE: Times used are vehicle times.  
 $C_3$  is twice the specific energy of orbit  
 $C_3 = V^2 - \frac{2\mu}{R}$   
 where V = Inertial Velocity  
 $\mu$  = Gravitational Constant  
 R = Radius vector from center of earth

Table 4-3. Comparison of Separation Events

Parameter	A 7-A	NOMINAL	A 7-400
S-11/11 SEPARATION			
Range Time, sec	163.5	163.8	0.3
Altitude, km (n mi)	87.7 (54.6)	84.5 (52.6)	3.2 (2.0)
Space-fixed velocity, m/s (ft/s)	2,727.1 (8,981.0)	2,748.4 (9,018.7)	-21.3 (-69.7)
Flight Path Angle, deg	19.642	19.869	-0.227
Heading Angle, deg	75.335	75.421	-0.086
Surface Range, km (n mi)	96.2 (59.8)	91.7 (57.2)	4.5 (2.8)
Cross Range, km (n mi)	0.1 (0.1)	0.2 (0.1)	-0.1 (0.0)
Cross Range Velocity, m/s (ft/s)	0.6 (21.2)	0.3 (10.7)	0.3 (1.0)
Geodetic Latitude, deg N	28.872	28.871	-0.001
Longitude, deg E	-79.667	-79.661	-0.006
S-11/S-11B SEPARATION			
Range Time, sec	560.5	560.2	0.3
Altitude, km (n mi)	173.0 (107.4)	173.3 (107.6)	-0.3 (-0.2)
Space-fixed Velocity, m/s (ft/s)	6,970.3 (22,868.8)	6,974.6 (22,882.5)	-4.3 (-14.1)
Flight Path Angle, deg	0.360	0.277	0.083
Heading Angle, deg	82.630	82.625	0.005
Surface Range, km (n mi)	1,661.9 (1032.4)	1,661.9 (1032.4)	0.0 (0.0)
Cross Range, km (n mi)	27.1 (16.8)	27.2 (16.9)	-0.1 (-0.1)
Cross Range Velocity, m/s (ft/s)	179.8 (588.6)	178.8 (586.6)	0.6 (2.0)
Geodetic Latitude, deg N	31.949	31.948	0.001
Longitude, deg E	-63.746	-63.745	-0.001
S-11B/CSM SEPARATION			
Range Time, sec	11,099.0	11,060.4	38.6
Altitude, km (n mi)	7,168.0 (4454.4)	6,967.3 (4328.0)	200.7 (125.7)
Space-fixed Velocity, m/s (ft/s)	7,566.5 (24,824.5)	7,624.5 (25,014.8)	-58.0 (-180.3)
Flight Path Angle, deg	45.397	44.995	0.402
Heading Angle, deg	69.807	69.452	0.355
Geodetic Latitude, deg N	26.180	25.840	0.260
Longitude, deg E	-134.563	-135.211	0.648

NOTE: Times used are vehicle times.

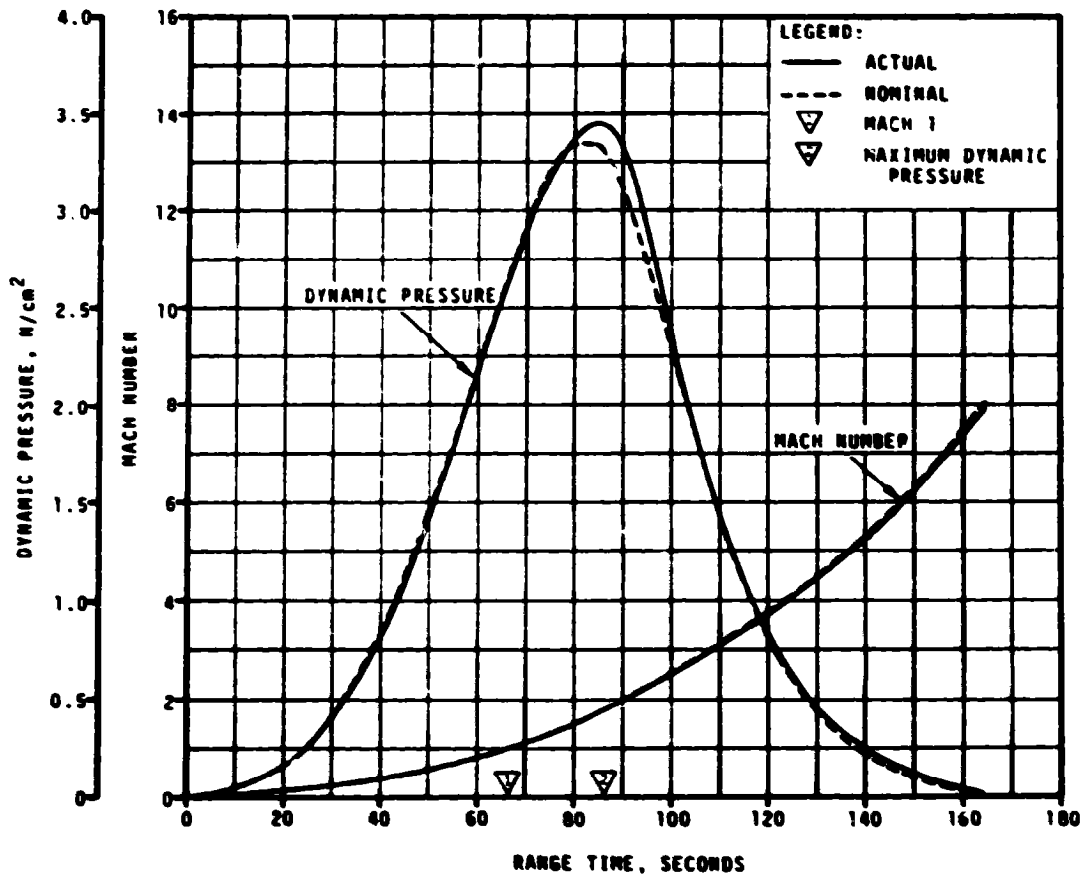


Figure 4-4. Dynamic Pressure and Mach Number Comparison

#### 4.2.2 Parking Orbit Phase

Orbital tracking was conducted by the NASA Manned Space Flight Network. Four C-Band stations (Merritt Island, two Bermuda radars and Carnarvon) provided seven data passes. Four S-Band stations (Honeysuckle, Bermuda, Texas, and Merritt Island) furnished four additional tracking passes.

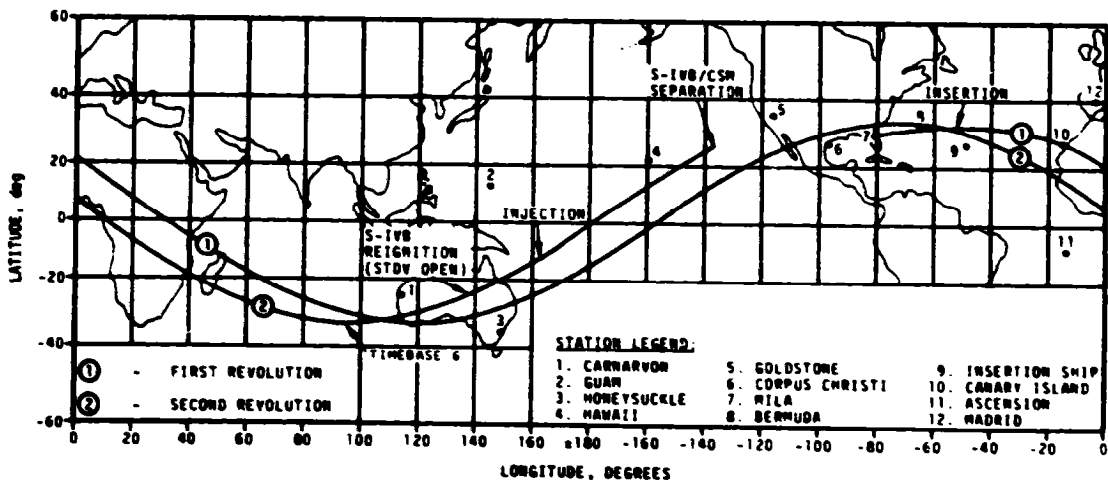
The parking orbit trajectory was obtained by integrating a comprehensive orbit model with corrected insertion conditions forward to the initiation of S-IVB restart preparation ( $T_6$ ) at 8,638.6 seconds (2:23:58.6). The final insertion conditions were obtained through a differential correction procedure in the Orbital Correction Program (OCP) which adjusted the preliminary estimate of insertion conditions to final values in accordance with relative weights assigned to the tracking data. The orbital venting acceleration model was derived from telemetered guidance velocity data generated by the ST-124M guidance platform.

A comparison of actual and nominal parking orbit insertion parameters is presented in Table 4-4. The groundtrack from insertion to S-IVB/CSM separation is given in Figure 4-5.

Table 4-4. Parking Orbit Insertion Conditions

PARAMETER	ACTUAL	NOMINAL	ACT- NOM
Range Time, sec	716.21	715.49	0.72
Altitude, km (n mi)	172.9 (93.4)	172.9 (93.4)	0.0 (0.0)
Space-Fixed Velocity, m/s (ft/s)	7,804.4 (25,605.0)	7,804.2 (25,604.3)	0.2 (0.7)
Flight Path Angle, deg	0.003	0.000	0.003
Heading Angle, deg	88.940	88.907	0.033
Inclination, deg	32.540	32.542	-0.002
Descending Node, deg	123.107	123.138	-0.031
Eccentricity	0.0001	0.0000	0.0001
Apogee*, km (n mi)	168.0 (90.7)	167.1 (90.2)	0.9 (0.5)
Perigee*, km (n mi)	166.6 (90.0)	166.7 (90.0)	-0.1 (0.0)
Period, min	87.84	87.83	0.01
Geodetic Latitude, deg N	32.695	32.696	-0.001
Longitude, deg E	-52.530	-52.558	0.028

NOTE: Times used are vehicle times.  
\*Based on a spherical earth of radius 6,378.165 km (3,443.934 n mi).



### 4.2.3 Injection Phase

The injection phase spans the interval from  $T_6$  to TLI and was established in two parts (the initiation of S-IVB restart preparation  $T_6$  to 9,150 seconds and 9,150 seconds to TLI). The first part was obtained by fitting Carnarvon C-Band tracking data available prior to S-IVB restart. The second part was obtained by integrating a state vector taken from the first part at 9,150 seconds (2:32:30) through second burn and constraining the integration to a final TLI state vector taken from the early translunar orbit trajectory. Telemetered guidance velocity data were used as generating parameters for both parts.

Comparisons between the actual and nominal space-fixed velocity and flight path angle are shown in Figure 4-6. The actual and nominal injection phase acceleration comparisons are presented in Figure 4-7. The actual and nominal targeting parameters at S-IVB second guidance cutoff are presented in Table 4-2.

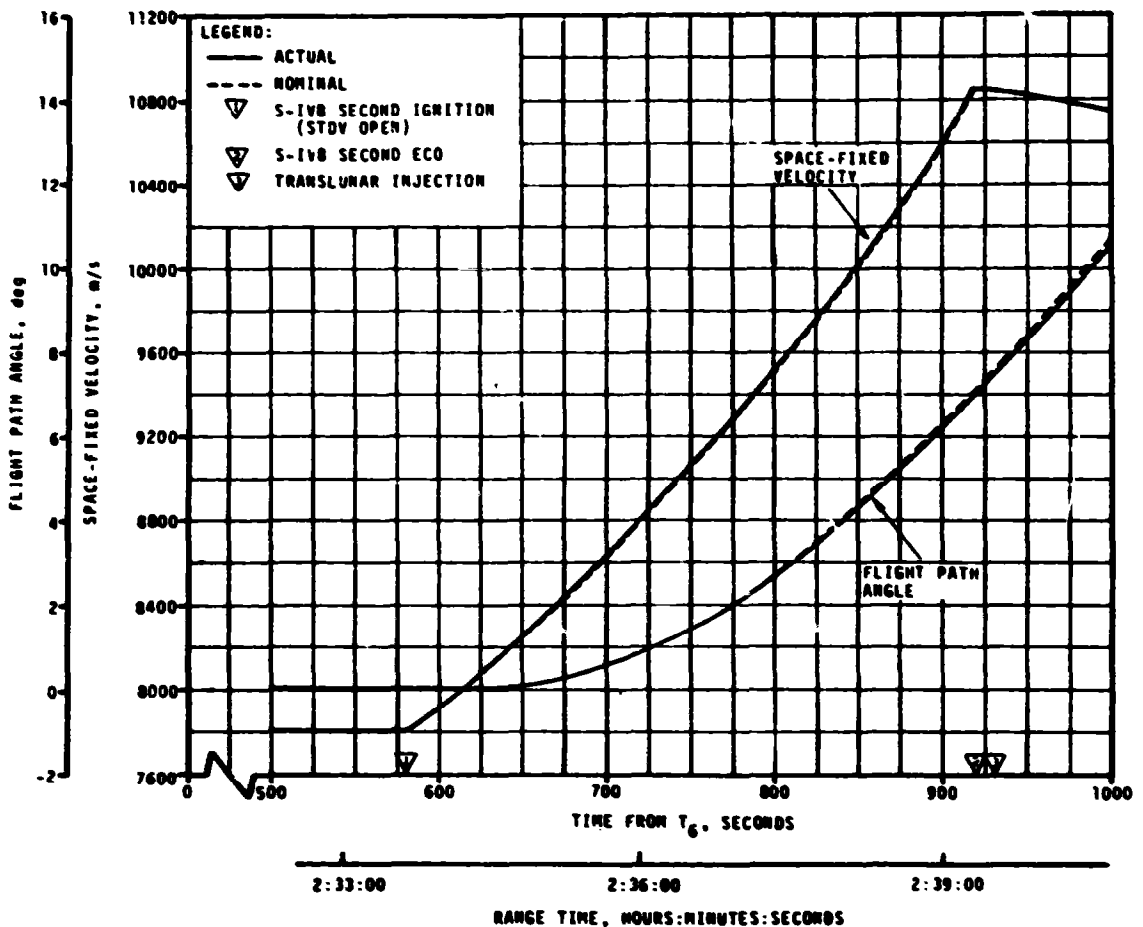


Figure 4-6. Injection Phase Space-Fixed Velocity and Flight Path Angle Comparisons

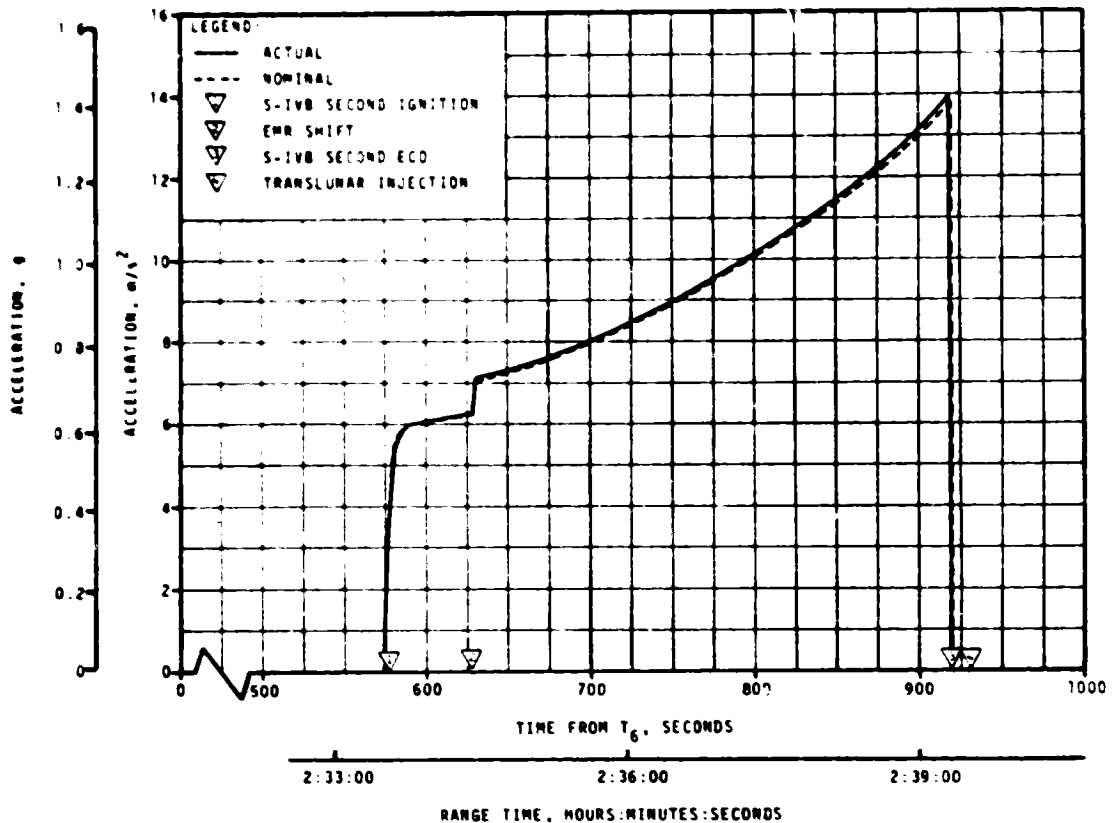


Figure 4-7. Injection Phase Acceleration Comparison

#### 4.2.4 Early Translunar Orbit Phase

The early translunar orbit trajectory spans the interval from translunar injection to S-IVB/CSM separation. Tracking data from one C-Band station (Merritt Island) and two S-Band stations (Hawaii and Goldstone Wing) were utilized in the reconstruction of this trajectory segment. Telemetered guidance velocity data were used to derive non-gravitational accelerations during this phase. The early translunar orbit trajectory was reconstructed by the method as outlined in paragraph 4.2.2. The actual and nominal translunar injection conditions are compared in Table 4-5. The S-IVB/CSM separation conditions are presented in Table 4-3.

Table 4-5. Translunar Injection Conditions

PARAMETER	ACTUAL	NOMINAL	ACT-NOM
Range Time, sec	9,568.42	9,570.20	-1.78
Altitude, km (n mi)	317.0 (171.2)	319.0 (172.2)	-2.0 (-1.0)
Space-Fixed Velocity, m/s (ft/s)	10,840.4 (35,565.6)	10,838.5 (35,559.4)	1.9 (6.2)
Flight Path Angle, deg	7.466	7.615	-0.149
Heading Angle, deg	59.524	59.451	0.073
Inclination, deg	32.512	32.519	-0.007
Descending Node, deg	122.465	122.456	0.009
Eccentricity	0.9740	0.9740	0.0000
$C_3$ , $m^2/s^2$ ( $ft^2/s^2$ )	-1,574,297 (-16,945,592)	-1,578,558 (-16,991,457)	4,261 (45,865)

NOTE: Times used are vehicle times.

## SECTION 5

### S-IC PROPULSION

#### 5.1 SUMMARY

All S-IC propulsion systems performed satisfactorily. In all cases, the propulsion performance was very close to the predicted nominal. Overall stage site thrust was 0.05 percent higher than predicted. Total propellant consumption rate was 0.36 percent lower than predicted and the total consumed mixture ratio was 0.40 percent higher than predicted. Specific impulse was 0.41 percent higher than predicted. Total propellant consumption from Holddown Arm (HDA) release to Outboard Engines Cutoff (OECO) was low by 0.51 percent.

Center Engine Cutoff (CECO) was initiated by the Instrument Unit (IU) at 137.85 seconds range time, 0.11 second earlier than planned. Outboard Engine Cutoff (OECO) was initiated by the LOX low level sensors at 161.78 seconds, 0.31 seconds earlier than predicted. This is well within the +4.60, -3.60 second 3-sigma limits. At OECO, the LOX residual was 34,028 lbm compared to the predicted 36,283 lbm and the fuel residual was 31,601 lbm compared to the predicted 28,248 lbm.

The S-IC hydraulic system performed satisfactorily.

#### 5.2 S-IC IGNITION TRANSIENT PERFORMANCE

The fuel pump inlet preignition pressure of 45.9 psia was within the F-1 engine acceptable starting region of 43.3 to 110 psia.

The LOX pump inlet preignition pressure and temperature were 80.9 psia and -285.8°F and were within F-1 engine acceptable starting region, as shown by Figure 5-1.

The planned 1-2-2 start was attained. Engine position starting order was 5, 3-1, and 4-2. By definition, two engines are considered to start together if their thrust chamber pressures reach 100 psig in a 100-millisecond time period. The time difference to reach 100 psig thrust chamber pressure was approximately 18 milliseconds for engines 3 and 1, and 57 milliseconds for engines 4 and 2, both well within the 100 millisecond planned sequence.

Although within specifications, the start times as measured from engine control valve open signal to 100-psig chamber pressure, was faster than predicted for all engines. Table 5-1 shows actual and predicted times to 100 psig chamber pressure corrected to nominal prestart conditions. The programmed time for engine control valve open signal is calculated for each F-1 engine to minimize start sequence dispersions and is historically



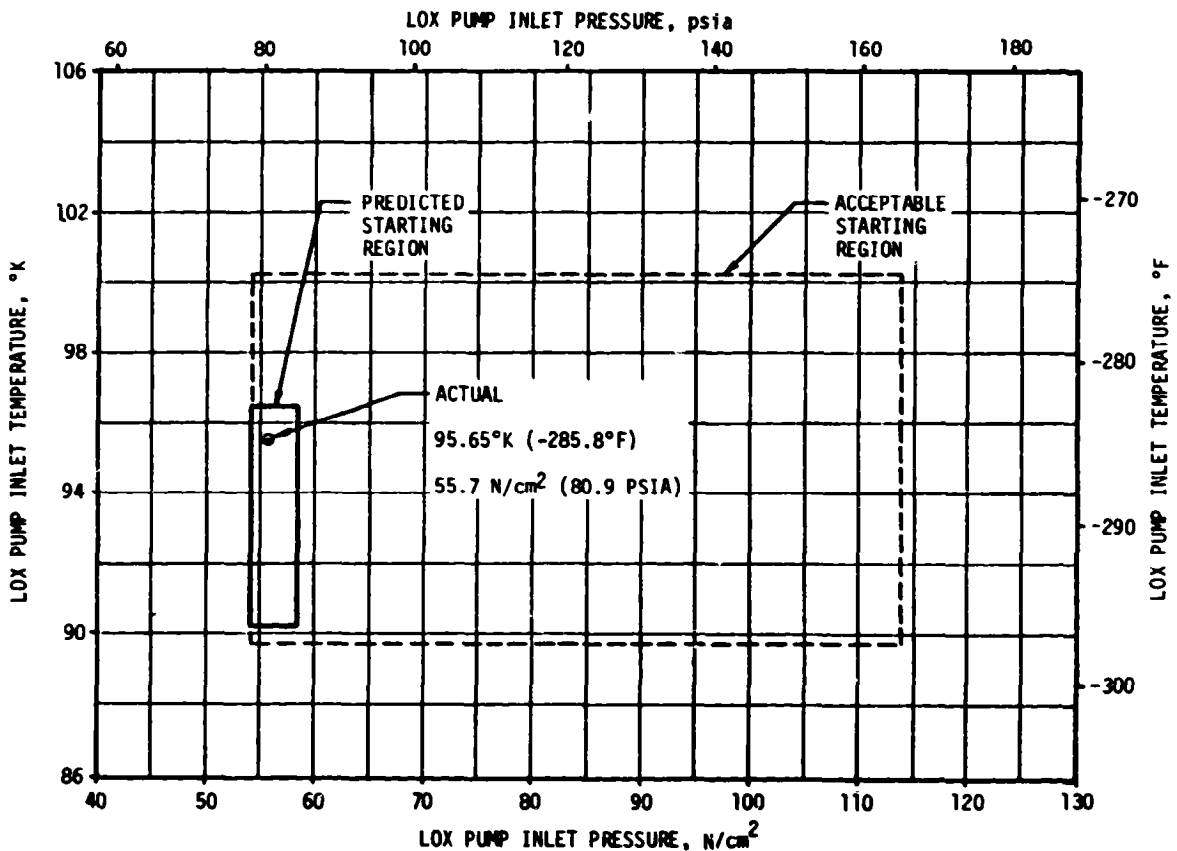


Figure 5-1. S-IC LOX Start Box Requirements

based on static test hardware data since this has been the most consistent base for making the calculations. As experienced on static tests of previous stages, there was a difference between the hardware data and telemetry data taken during the static test. The actual engine start times, for this flight, agree more closely with the static test telemetry data than the hardware data. Thus, it appears that the hardware data and the resulting control valve open signal programmed times were biased and resulted in faster starts. Although the AS-511 difference was greater than seen on previous flights, no concern is apparent since the desired staggered start sequence was attained and the vehicle dynamics at lift-off were well within previous flight bands.

Table 5-1. F-1 Engine Systems Buildup and Start Times

BUILDUP TIME, SECONDS					
	ENGINE 1	ENGINE 2	ENGINE 3	ENGINE 4	ENGINE 5
Predicted*	3.785	3.799	3.761	4.112	3.739
Actual*	3.546	3.434	3.514	3.678	3.532
Difference	0.239	0.365	0.247	0.434	0.207
Direction	FAST	FAST	FAST	FAST	FAST

\*Time from 4-way control valve open signal to 100 psig thrust chamber pressure  
All times corrected to nominal prestart conditions

Thrust buildup rates were as expected, as shown in Figure 5-2. The shift in thrust buildup near the 1100 Klbf level on the outboard engines is attributed to ingestion of helium from the LOX prevalves during startup and is a normal occurrence. The thrust shift is absent on the inboard engine (engine 5) because the POGO suppression helium injection system is not used on this engine.

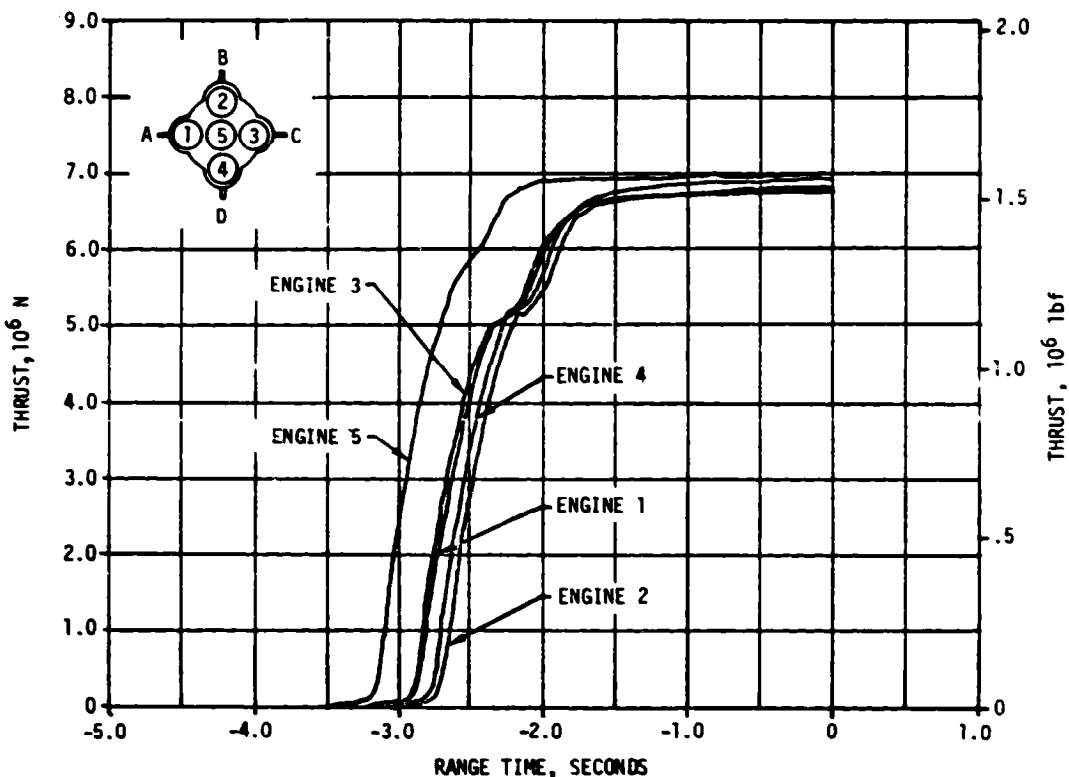


Figure 5-2. S-IC Engines Thrust Buildup

The engine ignition transient Main Oxidizer Valve (MOV), Main Fuel Valve (MFV), and Gas Generator (GG) ball valve opening times were nominal.

The reconstructed propellant consumption during holddown (from ignition command to holddown arm release) was 82,229 lbm LOX (66,900 lbm predicted) and 25,431 lbm fuel (18,888 lbm predicted). This is greater than experienced on previous flights and was due to the faster engine start and longer burn before holddown release. The reconstructed propellant load at holddown arm release was 3,228,997 lbm LOX (3,243,506 predicted) and 1,414,463 lbm fuel (1,422,121 lbm predicted).

### 5.3 S-IC MAINSTAGE PERFORMANCE

S-IC stage propulsion performance was satisfactory. Stage thrust, specific impulse, mixture ratio, and propellant flowrate were near nominal predictions as shown in Figure 5-3. The stage site thrust (averaged from time zero to OECO) was 0.05 percent higher than predicted. Total propellant consumption rate was 0.36 percent lower than predicted and the

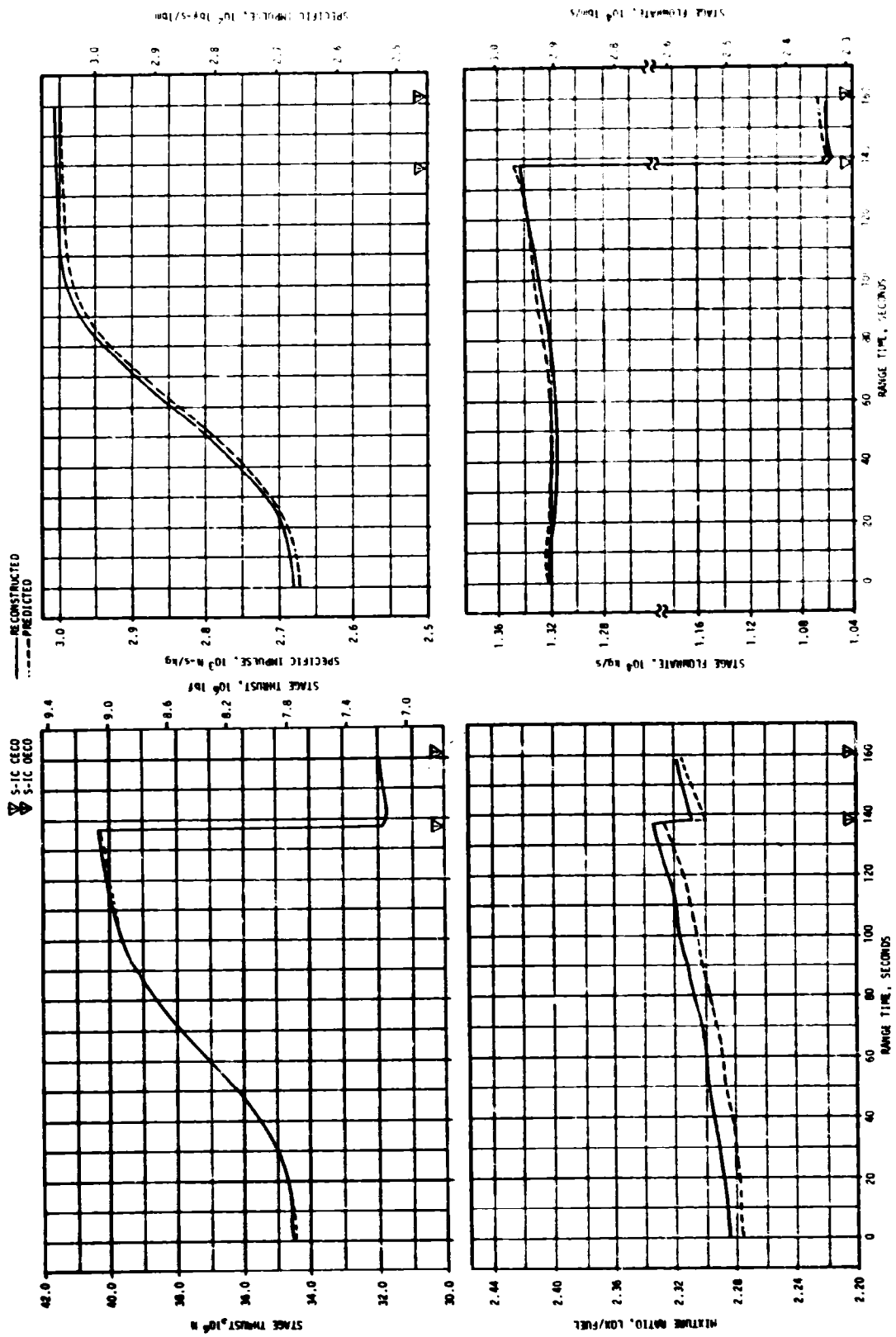


Figure 5-3. S-IC Stage Propulsion Performance

total consumed mixture ratio was 0.40 percent higher than predicted. The specific impulse was 0.41 percent higher than predicted. Total propellant consumption from HDA release to OECO was low by 0.51 percent.

For comparison of F-1 engine flight performance with predicted performance, the flight performance has been analytically reduced to standard conditions and compared to the predicted performance which is based on ground firings and also reduced to standard conditions. These comparisons are shown in Table 5-2 for the 35 to 38-second time slice. The largest thrust deviation from the predicted value was 10 Klbf for engine 1. Engines 3, 4 and 5 had lower thrusts than predicted by 5, 1, and 8 Klbf, respectively. Engine 2 thrust was higher than predicted by 3 Klbf. Total stage thrust was 1 Klbf lower than predicted for an average of -0.2 Klbf/engine. These performance values are derived from a reconstruction math model that uses a chamber pressure and pump speed match.

Table 5-2. S-IC Individual Standard Sea Level Engine Performance

PARAMETER	ENGINE	PREDICTED	RECONSTRUCTION ANALYSIS	DEVIATION PERCENT	STAGE DEVIATION PERCENT
Thrust 10 <sup>3</sup> lbf	1	1515	1525	0.660	-0.013
	2	1523	1526	0.197	
	3	1527	1522	-0.327	
	4	1534	1533	-0.065	
	5	1522	1514	-0.526	
Specific Impulse, lbf-s/lbm	1	266.0	266.2	0.075	-0.008
	2	265.3	265.4	0.038	
	3	265.2	265.1	-0.038	
	4	266.1	266.0	-0.038	
	5	264.9	264.7	-0.075	
Total Flowrate lbm/s	1	5698	5729	0.545	-0.012
	2	5739	5749	0.178	
	3	5758	5743	-0.273	
	4	5764	5760	-0.071	
	5	5745	5720	-0.435	
Mixture Ratio LOX/Fuel	1	2.259	2.256	-0.133	-0.176
	2	2.272	2.268	-0.176	
	3	2.277	2.273	-0.176	
	4	2.248	2.245	-0.133	
	5	2.262	2.256	-0.265	
NOTE: Performance levels were reduced to standard sea level and pump inlet conditions. Data were taken from the 35 to 38-second time slice.					

#### 5.4 S-IC ENGINE SHUTDOWN TRANSIENT PERFORMANCE

The F-1 engine thrust decay transient was normal. Thrust decay of the F-1 engines is shown in Figure 5-4. The cutoff impulse, measured from cutoff signal to zero thrust, was 775,690 lbf-s for the center engine (10.9 percent greater than predicted) and 2,700,932 lbf-s for all outboard engines (2.6 percent less than predicted). The total stage cutoff impulse

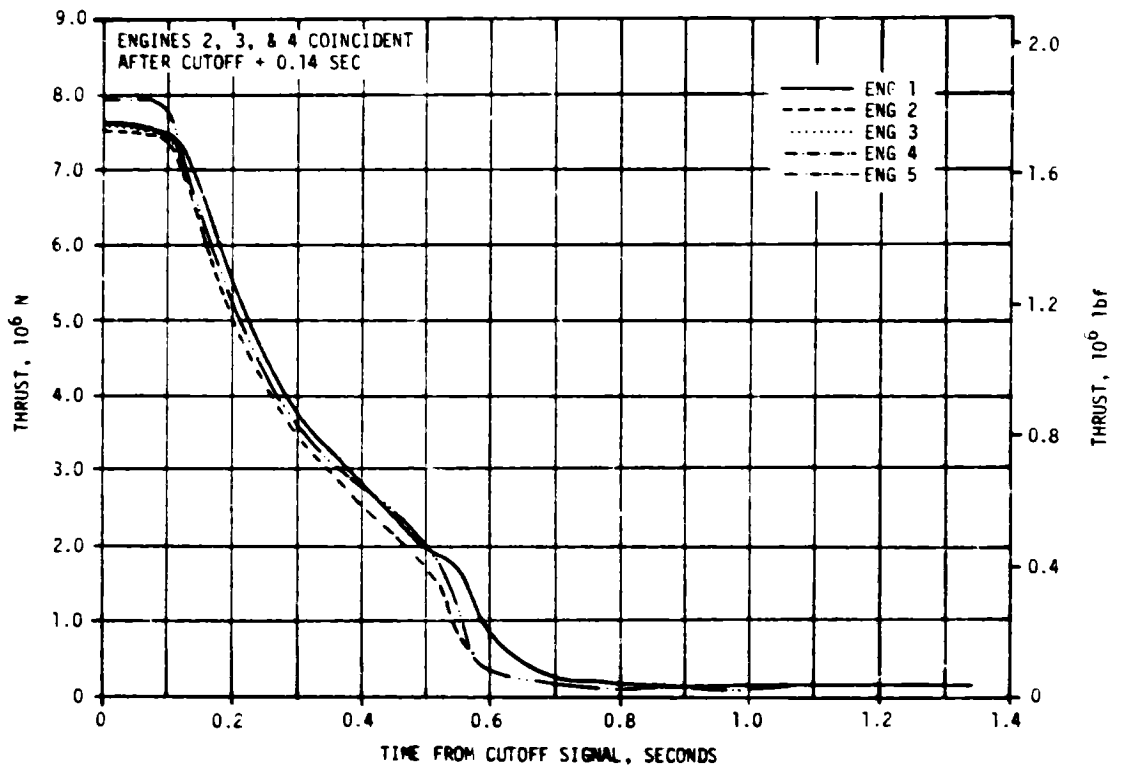


Figure 5-4. F-1 Engine Thrust Decay

of 3,476,622 lbf-s was 0.16 percent greater than predicted.

Center engine cutoff, initiated by a signal from the IU at 137.85 seconds, was 0.11 second earlier than planned. Outboard engine cutoff, initiated by a signal from the LOX low level sensors at 161.78 seconds, was 0.31 second earlier than the nominal predicted time. Most of the OECO deviation, which was small when compared to the 3-sigma limits of +4.60, -3.60 seconds, can be attributed to higher than predicted bulk fuel temperature.

Stage tailoff thrust from 162.5 seconds until zero thrust is compared to the predicted +3-sigma maximum tailoff thrust in Figure 5-5. Data were averaged over 110 millisecond time slices and the curve was fitted through these points. The curve was interpolated through noise caused by retromotor burn, and extrapolated to zero thrust from approximately 167 seconds.

## 5.5 S-IC STAGE PROPELLANT MANAGEMENT

The S-IC stage does not have an active propellant utilization system. Minimum residuals are obtained by attempting to load the mixture ratio expected to be consumed by the engines plus the predicted unusable residuals. An analysis of the usable residuals experienced during a flight is a good measure of the performance of the passive propellant utilization system.

The residual LOX at OECO was 34,028 lbm compared to the predicted value

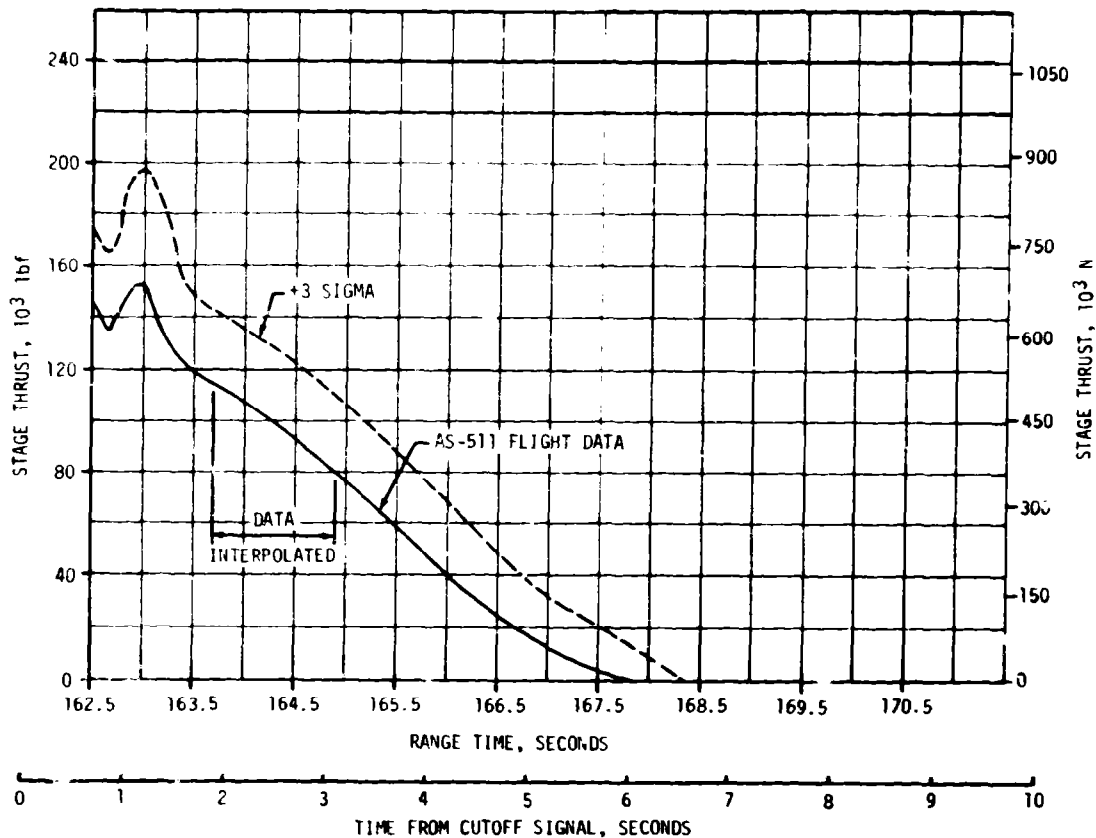


Figure 5-5. S-IC Thrust Decay

of 36,283 lbm. The fuel residual at OECO was 31,601 lbm compared to the predicted value of 28,248 lbm. A summary of the propellants remaining at major event times is presented in Table 5-3.

## 5.6 S-IC PRESSURIZATION SYSTEMS

### 5.6.1 S-IC Fuel Pressurization System

The fuel tank pressurization system performed satisfactorily, keeping ullage pressure within acceptable limits during flight. Helium Flow Control Valves (HFCV) No. 1 through 4 opened as planned and HFCV No. 5 was not required.

The low flow prepressurization system was commanded on at -97.0 seconds. The low flow system was cycled on a second time at -3.0 seconds. High flow pressurization, accomplished by the onboard pressurization system, performed as expected. HFCV 1 was commanded on at -2.7 seconds and was supplemented by the ground high flow prepressurization system until umbilical disconnect.

Fuel tank ullage pressure was within the predicted limits throughout flight as shown by Figure 5-6. HFCV's 2, 3 and 4 were commanded open

Table 5-3. S-IC Propellant Mass History

EVENT	PREDICTED, LBM		LEVEL SENSOR DATA, LBM		RECONSTRUCTED, LBM	
	LOX	FUEL	LOX	FUEL	LOX	FUEL
Ignition Command	3,310,406	1,441,009	-----	1,440,846	3,311,226	1,439,894
Holddown Arm Release	3,243,506	1,422,121	3,231,626	1,415,311	3,228,997	1,414,463
CECC	433,385	199,914	423,295	200,066	425,225	200,329
OECC	36,283	28,248	-----	31,676	34,028	31,601
Separation	30,826	25,271	-----	-----	29,107	28,906
Zero Thrust	30,704	25,184	-----	-----	28,991	28,324

Note: Predicted and reconstructed values do not include pressurization gas so they will compare with level sensor data.

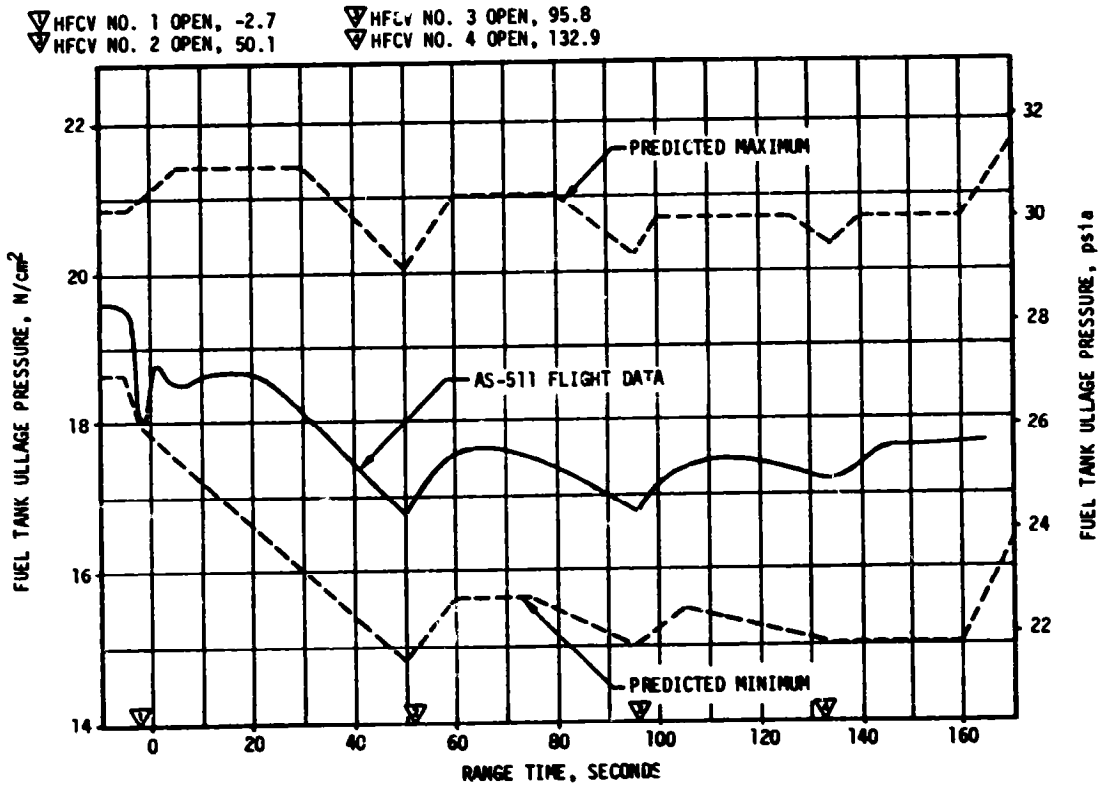


Figure 5-6. S-IC Fuel Tank Ullage Pressure

during flight by the switch selector within acceptable limits. Helium bottle pressure was 2907 psia at -2.8 seconds and decayed to 425 psia at OECO. Total helium flowrate was as expected.

Fuel pump inlet pressure was maintained above the required minimum Net Positive Suction Pressure (NPSP) during flight.

### 5.6.2 S-IC LOX Pressurization System

The LOX pressurization system performed satisfactorily and all performance requirements were met. The ground prepressurization system maintained ullage pressure within acceptable limits until launch commit. The onboard pressurization system performed satisfactorily during flight.

The prepressurization system was initiated at -72.0 seconds. Ullage pressure increased to the prepressurization switch band and flow was terminated at -56.8 seconds. The low flow system was cycled on three additional times at -42.0, -21.0, and -5.3 seconds. At -4.7 seconds, the high flow system was commanded on and maintained ullage pressure within acceptable limits until launch commit.

Ullage pressure was within the predicted limits throughout flight as shown in Figure 5-7. GOX flowrate to the tank was as expected. The maximum GOX flowrate after the initial transient was 46.4 lbm/s at CECO.

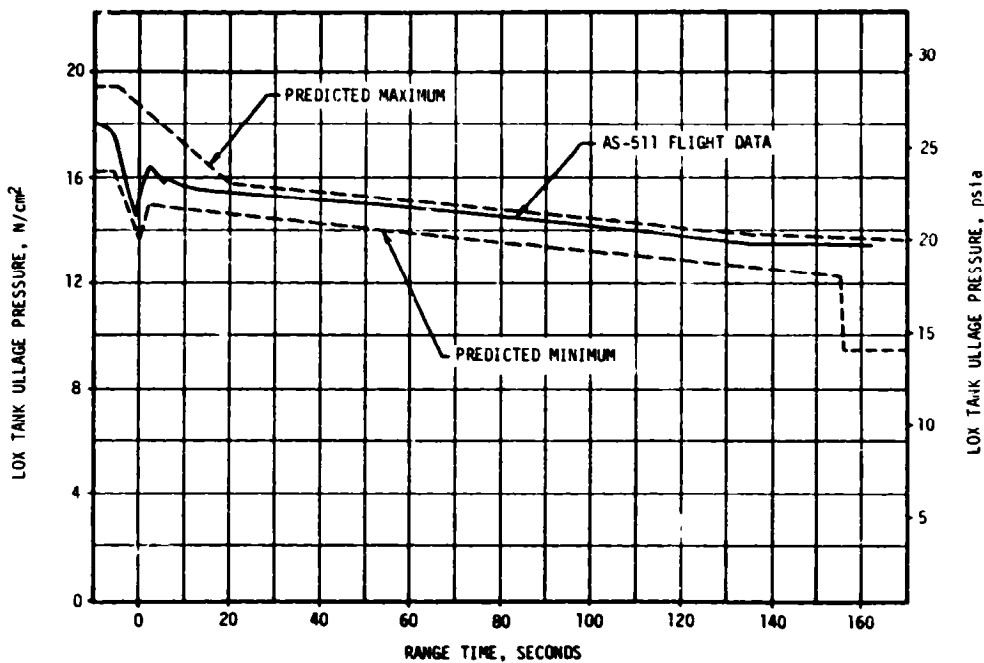


Figure 5-7. S-IC LOX Tank Ullage Pressure



The LOX pump inlet pressure met the minimum NPSP requirement throughout flight.

#### 5.7 S-IC PNEUMATIC CONTROL PRESSURE SYSTEM

The control pressure system functioned satisfactorily throughout the S-IC flight.

Sphere pressure was 2946 psia at liftoff and remained steady until CECO when it decreased to 2840 psia. The decrease was due to center engine pre-valve actuation. There was a further decrease to 2472 psia after OECO. Pressure regulator performance was within limits.

The engine pre valves were closed after CECO and OECO as required.

#### 5.8 S-IC PURGE SYSTEMS

Performance of the purge systems was satisfactory during flight.

The turbopump LOX seal storage sphere pressure of 2940 psia at liftoff was within the preignition limits of 2700 to 3300 psia. Pressure was within the predicted envelope throughout flight and was 2640 psia at OECO.

The pressure regulator performance throughout the flight was within the 85  $\pm$ 10 psig limits.

#### 5.9 S-IC POGO SUPPRESSION SYSTEM

The POGO suppression system performed satisfactorily during S-IC flight.

Outboard LOX pre valve temperature measurements indicated that the pre valve cavities were filled with gas prior to liftoff as planned. The four resistance thermometers behaved during the AS-511 flight similarly to the flights of AS-510 and AS-509. The temperature measurements in the outboard LOX pre valve cavities remained warm (off scale high) throughout flight, indicating helium remained in the pre valves as planned. The two thermometers in the center engine pre valve were cold, indicating LOX in this valve as planned. The pressure and flowrate in the system were nominal.

#### 5.10 S-IC HYDRAULIC SYSTEM

The performance of the S-IC hydraulic system was satisfactory. All servo-actuator supply pressures were within required limits.

Engine control system return pressures were within predicted limits and the engine hydraulic control system valves operated as planned.

## SECTION 6

### S-II PROPULSION

#### 6.1 SUMMARY

The S-II Propulsion systems performed satisfactorily throughout the flight. The S-II Engine Start Command (ESC), as sensed at the engines, occurred at 164.2 seconds. Center Engine Cutoff (CECO) was initiated by the Instrument Unit (IU) at 461.77 seconds as planned. Outboard Engine Cutoff (OECO), initiated by LOX depletion ECO sensors, occurred at 559.54 seconds giving an outboard engine operating time of 395.34 seconds or 0.63 seconds longer than predicted. The later than predicted S-II OECO was a result of an earlier than predicted Engine Mixture Ratio (EMR) shift and lower than planned EMR after the step.

Engine mainstage performance was satisfactory throughout flight. The total stage thrust at the standard time slice (61 seconds after S-II ESC) was 0.04 percent above predicted. Total propellant flowrate, including pressurization flow, was 0.01 percent below predicted, and the stage specific impulse was 0.07 percent above predicted at the standard time slice. Stage propellant mixture ratio was 0.36 percent below predicted. Engine thrust buildup and cutoff transients were within the predicted envelopes.

During the S-II engine start transient, an unusually large amount of helium was expended from the engine 4 helium tank. The most probable cause of the anomaly is slow closing of the engine purge control valve allowing excessive helium to be vented overboard. Tests, analysis, and examination of valves from service are being conducted to determine the cause and solutions for engines on subsequent stages.

Performance of the center engine LOX feedline accumulator system for POGO suppression was satisfactory. The accumulator bleed and fill subsystems operations were within predictions.

The propellant management system performance was satisfactory throughout loading and flight, and all parameters were within expected limits. Propellant residuals at OECO were 4105 lbm LOX, 1 lbm more than predicted and 2612 lbm LH<sub>2</sub>, 239 lbm less than predicted. Control of engine mixture ratio was accomplished with the two-position pneumatically operated Mixture Ratio Control Valves (MRCV). The low EMR step occurred 2.0 seconds earlier, relative to ESC, than predicted.

The performance of the LOX and LH<sub>2</sub> tank pressurization systems was

satisfactory. This was the second stage to utilize pressurization orifices in place of regulators to control inflight pressurization of the propellant tanks. Ullage pressure in both tanks was adequate to meet or exceed engine inlet Net Positive Suction Pressure (NPSP) minimum requirements throughout mainstage.

The engine servicing, recirculation, helium injection, and valve actuation systems performed satisfactorily.

S-II hydraulic system performance was normal throughout the flight.

## 6.2 S-II CHILLDOWN AND BUILDUP TRANSIENT PERFORMANCE

The engine servicing operations required to condition the engines prior to S-II engine start were satisfactorily accomplished. Thrust chamber jacket temperatures were within predicted limits at both prelaunch and S-II ESC. Thrust chamber chilldown requirements are  $-200^{\circ}\text{F}$  maximum at prelaunch commit and  $-150^{\circ}\text{F}$  maximum at engine start. Thrust chamber temperatures ranged between  $-281$  and  $-258^{\circ}\text{F}$  at prelaunch commit and between  $-231$  and  $-198^{\circ}\text{F}$  at ESC. Thrust chamber temperature warmup rates during S-IC boost agreed closely with those experienced on previous flights.

Start tank system performance was satisfactory. Both temperature and pressure conditions of the engine start tanks were within the required prelaunch and engine start boxes as shown in Figure 6-1. Start tank temperature and pressure heat-up rates were normal and no indication of start tank relief valve operation was noted during prelaunch and S-IC boost.

During launch operations, all engine helium tank pressures were within the prelaunch and engine start limits of 2800 to 3450 psia. Engine helium tank pressures ranged between 3050 and 3200 psia at prelaunch commit and between 3190 and 3340 psia at S-II ESC.

Engine number 4 helium consumption during engine start operations was larger than expected. Nominal helium pressure drop during start is approximately 400 psi. Engine number 4 experienced an 890 psi pressure drop lasting over a period of approximately 10 seconds, as shown in Figure 6-2; eight seconds longer duration and 490 psi greater pressure drop than expected.

Prior to Mainstage Command, the helium tank pressure decay rates of all engines were essentially as expected. After Mainstage Command, the pressure decay rate of engine 4 did not decrease to the normal rate during start sequence (approximately two psi/sec) but decreased to 73 psi/sec for 7.8 seconds before changing abruptly to the mainstage rate. At this time, the helium tank pressure of 2406 psia was still adequate for engine propellant valve sequencing and engine thrust during buildup, mainstage and cutoff was nominal. If the decay rate had continued at 73 psi/sec, the helium pressure would have dropped below that required to hold the engine propellant valves open and

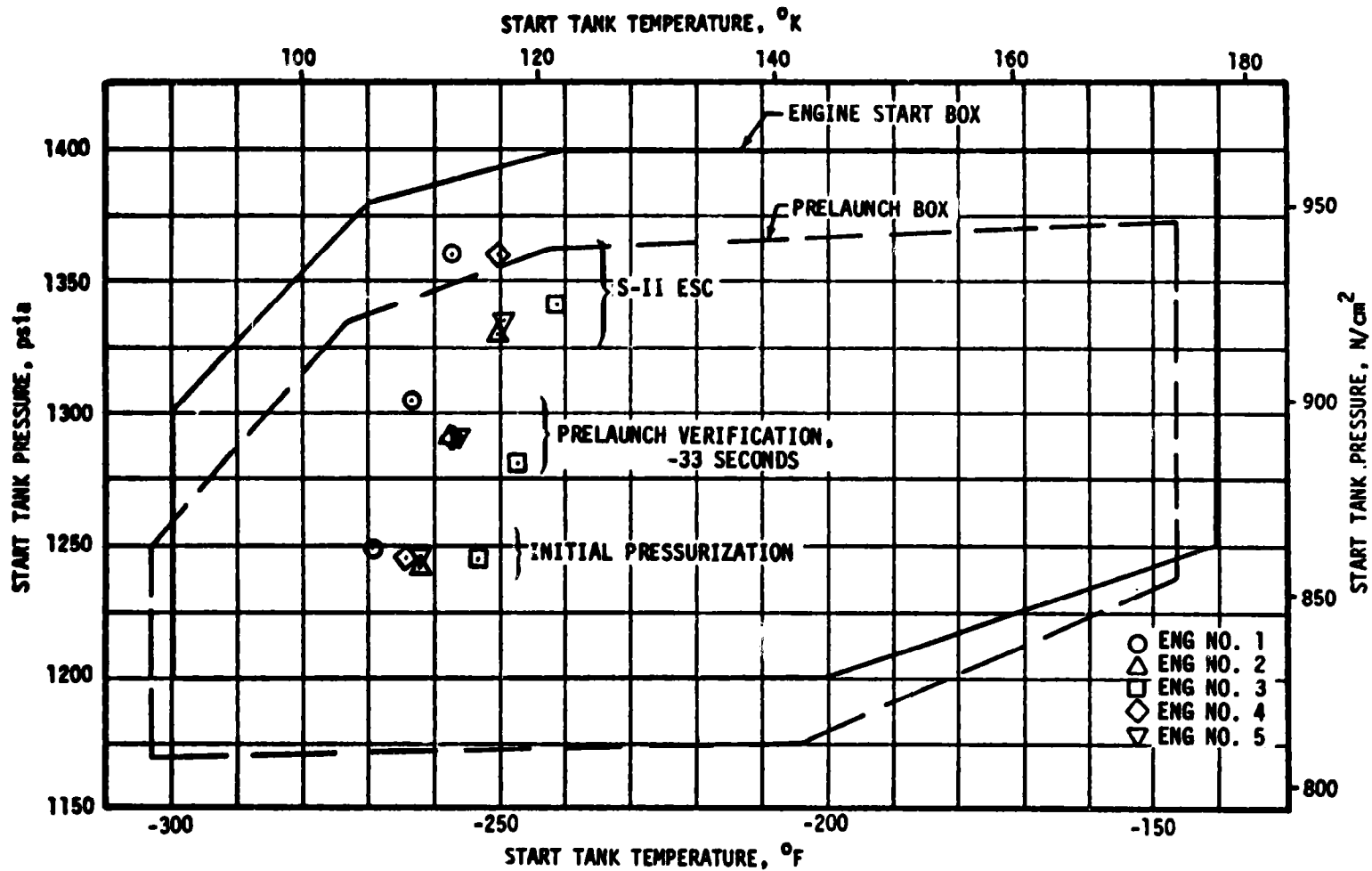


Figure 6-1. S-II Engine Start Tank Performance

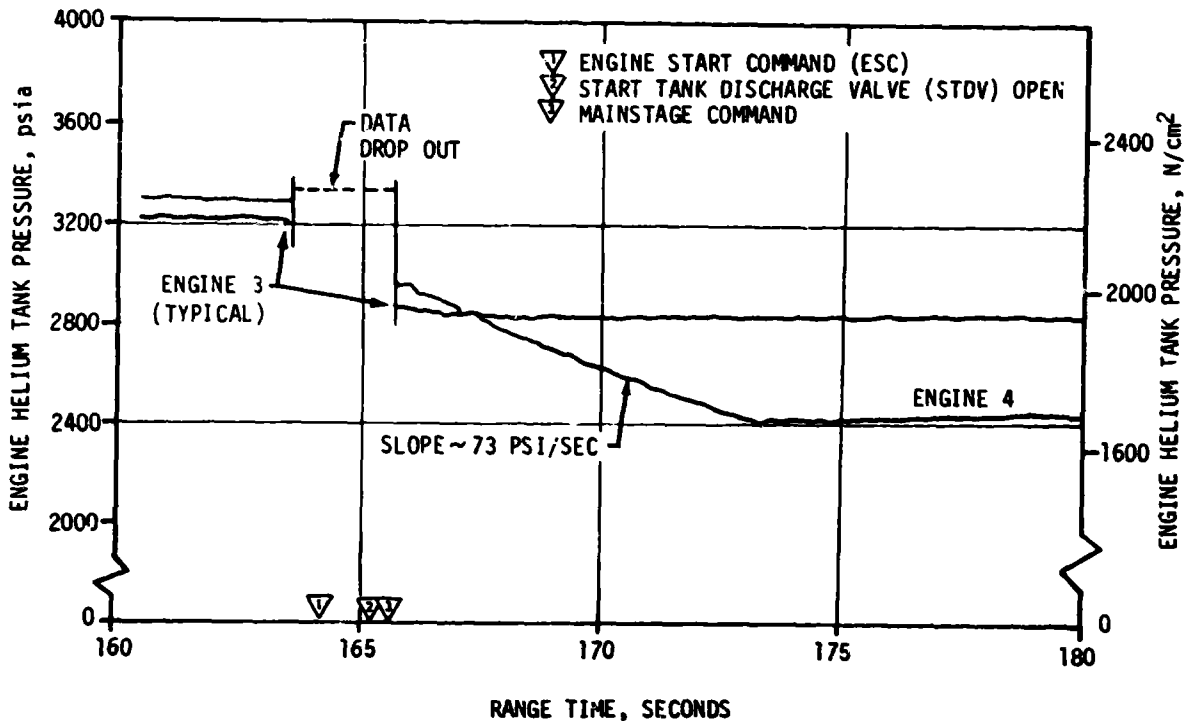


Figure 6-2. S-II Engine Helium Tank Pressures

engine shutdown would have occurred at approximately 40 seconds after ESC. Such a premature engine shutdown would have resulted in primary mission loss, since all outboard engines are required for 184 seconds.

The most probable cause of the excessive helium venting is slow closing of the engine 4 purge control valve (Figure 6-3). The engine purge control valve provides helium from the engine helium tank to purge the oxidizer dome and the gas generator oxidizer injector. The purge valve normally closes at Mainstage Command to terminate the purge. Slow closing of the valve allows excessive helium to be vented overboard while the valve is in the mid-position, thus causing a larger than normal pressure decay following Mainstage Command as shown in Figure 6-2. This large pressure decay following mainstage command in conjunction with the normal sequencing of the propellant valves and the inability of a number of the pneumatic system components to flow the quantity of helium involved isolates the cause of the high usage to the engine purge control valve.

A similar occurrence on flight AS-501 was attributed to slow closing of the engine purge control valve due to contamination, and a filter was added in the J-2 system at the purge control valve inlet prior to the AS-502 flight. The high helium consumption rates on AS-501 and AS-511 flights are the only two observed in the J-2 program; none have been observed in acceptance or R&D testing (approximately 4500 ground tests).

——— PURGE SUPPLY LINE  
 - - - - PURGE FLOW LINE  
 - · - · CONTROL PRESSURE LINE

PURGE  
 CONTROL  
 VALVE

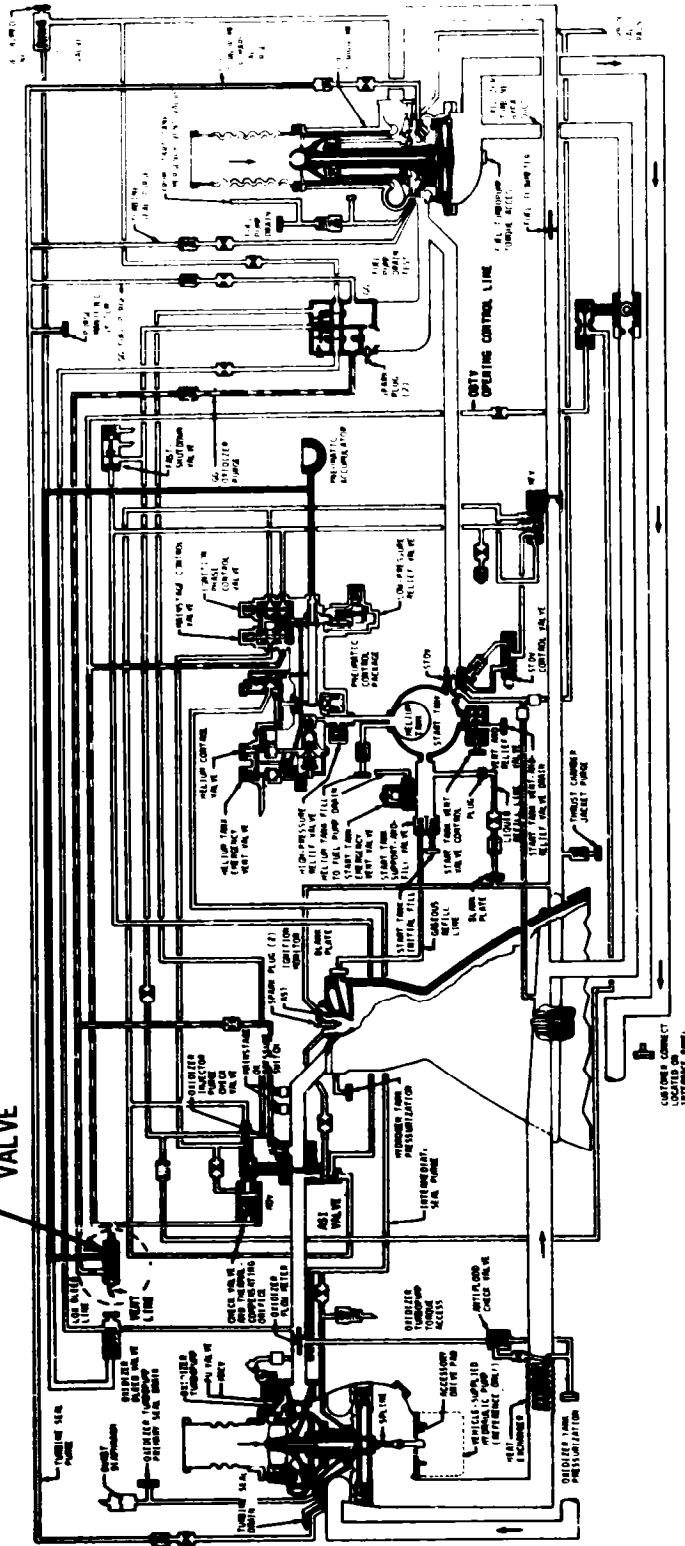


Figure 6-3. S-II J-2 Engine Schematic

During the AS-511 prelaunch operations at KSC, two failed components in the S-II helium system were replaced and subsequent failure analysis assigned the most probable cause to be contamination. The replaced components were: (1) Engine No. 2 Helium Regulator Assembly and (2) LOX Recirculation Check Valve (helium actuated).

This history of satisfactory operation of the purge control valve in ground test and flight combined with the evidence of other failures in the helium system because of contamination leads to the hypothesis that the most probable cause of the AS-511 engine purge valve anomaly was contamination, perhaps in conjunction with thermal and/or vibration environments. In that two failures of this type have occurred in 66 flight cases and no failures have occurred in the approximately 4500 ground tests, the evidence suggests that the flight failure rate is peculiar to the Launch Complex 39 and/or the stacked configuration.

Corrective actions are in process effective with AS-512, for S-II and S-IVB stage J-2 engines, to reduce the probability of leakage and to limit the impact of a leak if it should occur. Existing purge control valve assemblies will be replaced with assemblies that are modified as follows:

- a. Increase the deactivation setting to reduce the effect of blockage of the control pressure line, combined with vibration,
- b. Restrict the Purge Control Valve vent area by adding an orifice at valve outlet to limit the leakage to an acceptable level in the event it should recur.
- c. Add a check valve for additional protection against oxidizer back-flow into the helium system in order to retain the degree of redundancy lost in this mode by orificing of the Purge Control Valve Vent. These configuration changes are shown schematically in Figure 6-3a.

The LOX and LH<sub>2</sub> recirculation systems used to chill the feed ducts, turbopumps, and other engine components performed satisfactorily during prelaunch and S-IC boost. Engine pump inlet temperatures and pressures at S-II ESC were well within the requirements as shown in Figure 6-4. The LOX pump discharge temperatures at S-II ESC were approximately 14.0°F subcooled, well below the 3°F subcooling requirement.

Again as on AS-510, the deletion of the S-II ullage motors did not adversely affect the recirculation system. The characteristic rise of the LOX pump discharge temperature between S-IC OECO and S-II ESC was approximately 1.5°F, similar to that experienced on stages with ullage motors installed.

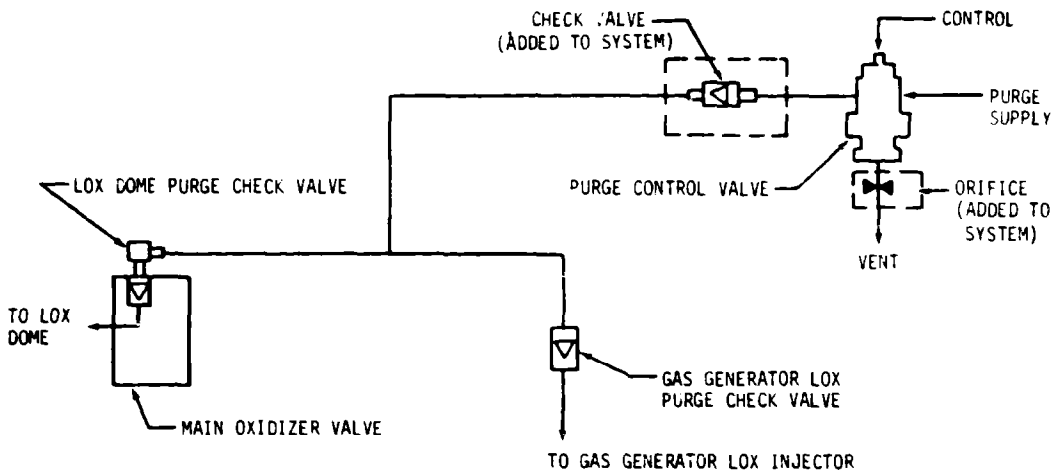


Figure 6-3a. J-2 Engine Configuration Changes

Prepressurization of the propellant tanks was accomplished satisfactorily. Tank ullage pressures at S-II ESC were 41.0 psia for LOX and 29.0 psia for LH<sub>2</sub>, well above the minimum requirement of 33.0 and 27.0 psia, respectively.

S-II ESC was received at 164.20 seconds and the Start Tank Discharge Valve (STDV) solenoid activation signal occurred 1.0 second later. The engine thrust buildup was satisfactory and well within the predicted thrust buildup envelope as shown in Figure 6-5. All engines reached 90 percent thrust within 3.24 seconds after S-II ESC.

### 6.3 S-II MAINSTAGE PERFORMANCE

The propulsion reconstruction analysis showed that stage site performance during mainstage operation was satisfactory. A comparison of predicted and reconstructed performance of thrust, specific impulse, total flow-rate, and mixture ratio versus time is shown in Figure 6-6. Stage performance during the high EMR portion of flight (prior to CECO) was very close to predicted. At the time of ESC +61 seconds, total stage thrust was 1,163,547 lbf which was 473 lbf (0.04 percent) above the preflight prediction. Total propellant flowrate including pressurization flow, was 2755.5 lbm/s, 0.01 percent below predicted. Stage specific impulse, including the effect of pressurization gas flowrate, was 422.3 lbf-s/lbm, 0.07 percent above predicted. The stage propellant mixture ratio was 0.36 percent below predicted.

Center Engine Cutoff was initiated at ESC +297.57 seconds as planned. This action reduced total stage thrust by 236,071 lbf to a level of



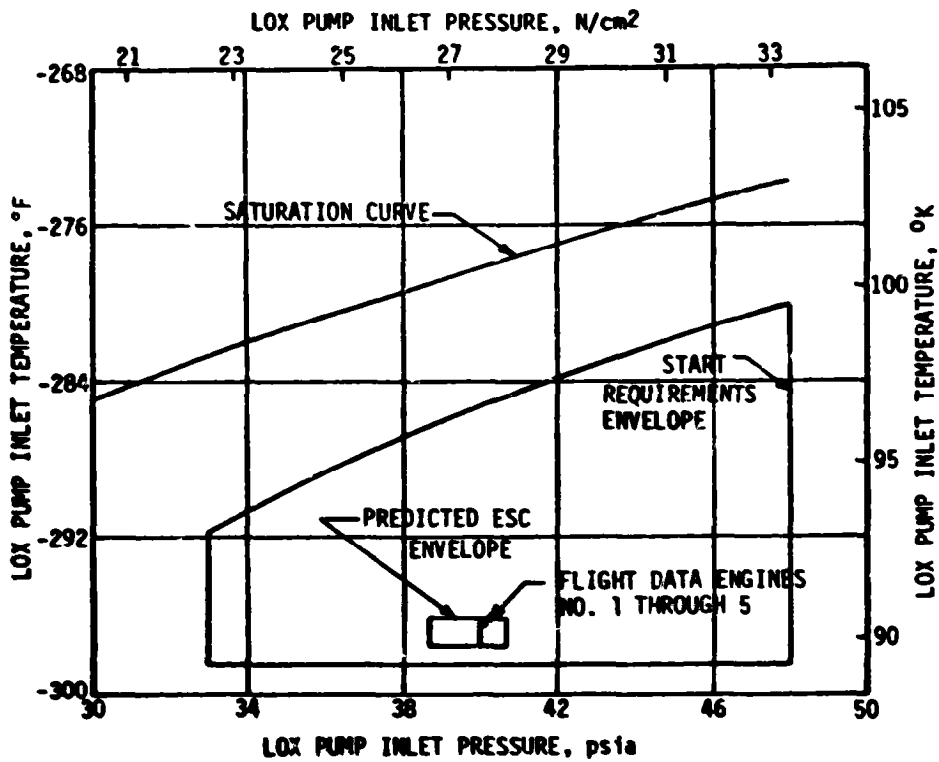
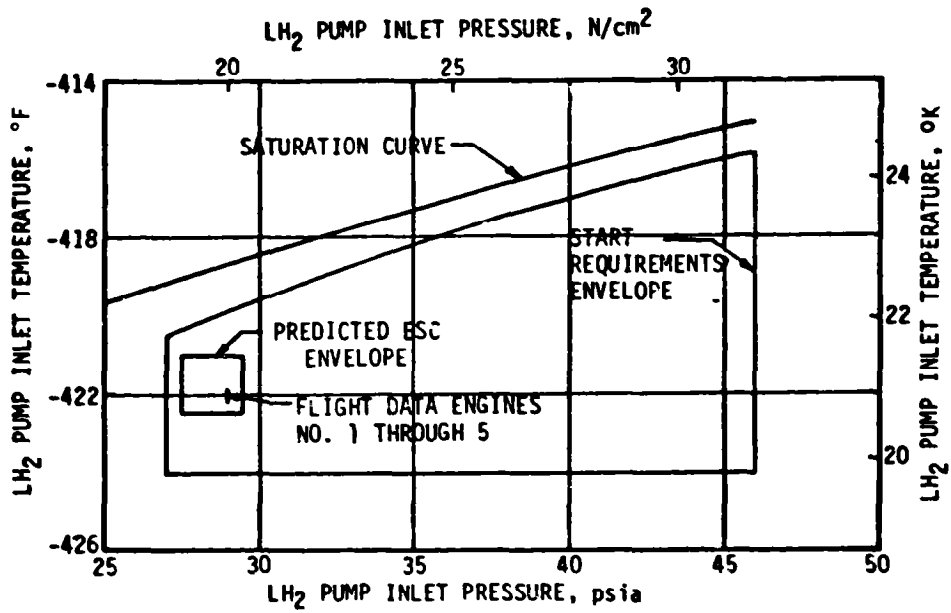


Figure 6-4. S-II Engine Pump Inlet Start Requirements

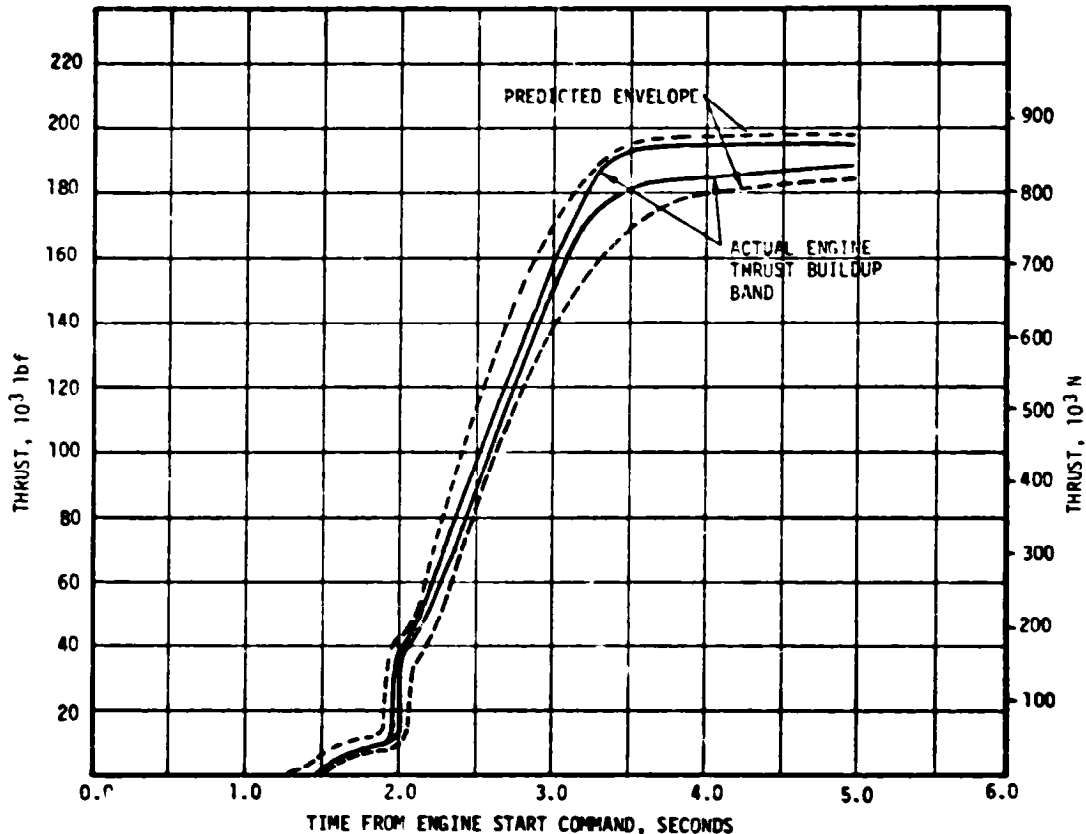


Figure 6-5. S-II Single Engine Thrust Buildup Characteristics

923,267 lbf. The EMR shift from high to low occurred 330.3 seconds after ESC and the reduction in stage thrust occurred as expected. At ESC +357 seconds, the total stage thrust was 787,380 lbf; thus, a decrease in thrust of 135,266 lbf was indicated between high and low EMR operation. S-II burn duration was 395.34 seconds, which was 0.63 seconds longer than predicted.

Individual J-2 engine data are presented in Table 6-1 for the ESC +61 second time slice. Good correlation exists between predicted and reconstructed flight performance. The performance levels shown in Table 6-1 have not been adjusted to standard J-2 altitude conditions and do not include the effects of pressurization flow.

#### 6.4 S-II SHUTDOWN TRANSIENT PERFORMANCE

S-II OEEO was initiated by the stage LOX depletion cutoff system as planned. The LOX depletion cutoff system again included a 1.5 second delay timer. As in previous flights (AS-504 and subsequent), this resulted in engine thrust decay (observed as a drop in thrust chamber pressure) prior to receipt of the cutoff signal. The pre-cutoff decay was less than that observed on AS-510 due to lower engine thrust and EMR levels at OEEO.

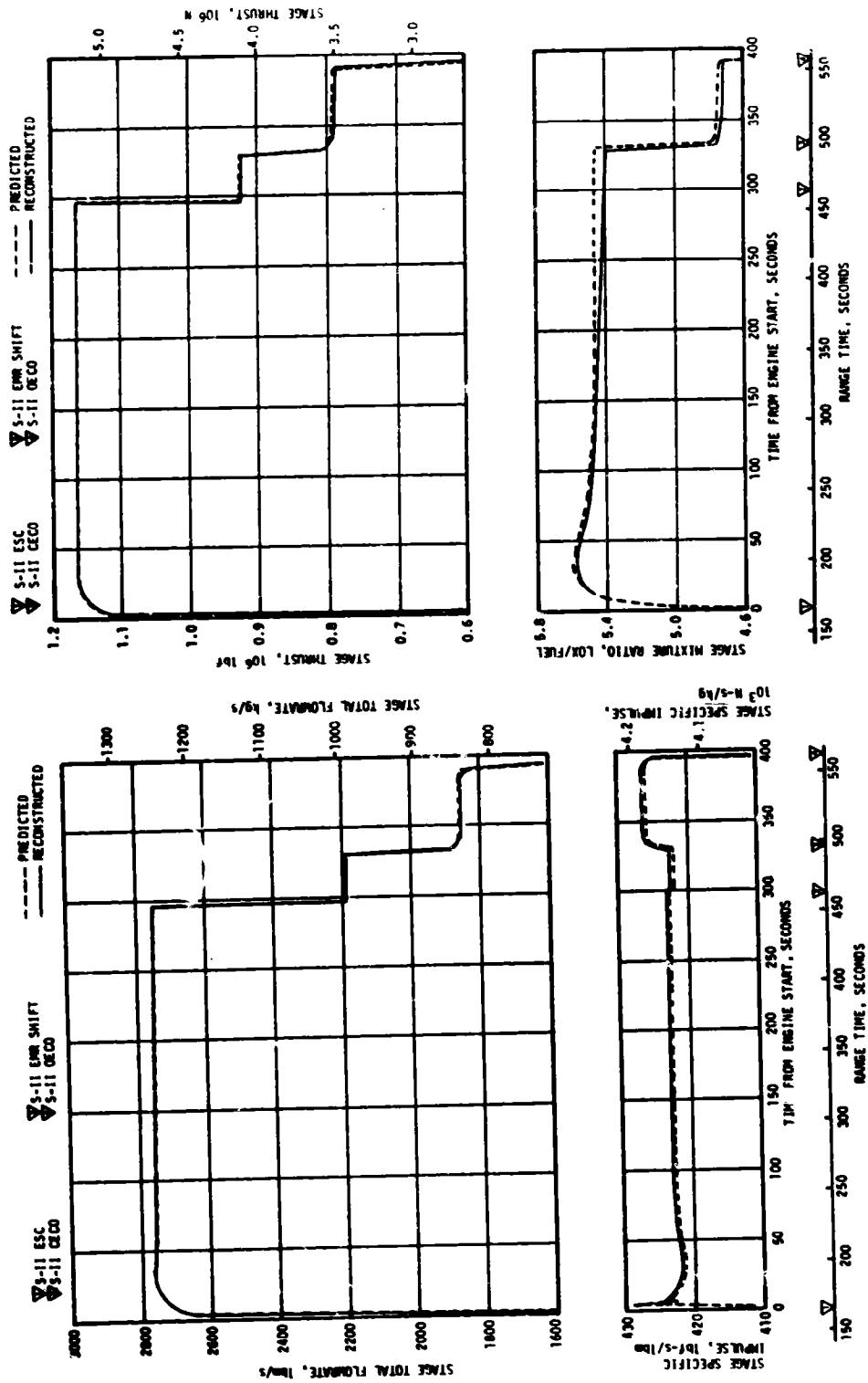


Figure 6-6. S-II Propulsion Performance

Table 6-1. S-II Engine Performance

PARAMETER	ENGINE	PREDICTED	RECONSTRUCTION ANALYSIS	PERCENT INDIVIDUAL DEVIATION	PERCENT STAGE DEVIATION
THRUST, lbf	1	232,485	232,451	-0.01	0.04
	2	231,778	231,549	-0.10	
	3	232,427	232,580	0.06	
	4	232,195	231,445	-0.32	
	5	234,190	235,509	0.56	
SPECIFIC IMPULSE, lbf-s/lbm	1	424.9	425.2	0.07	0.03
	2	423.1	423.1	0	
	3	424.2	424.5	0.07	
	4	424.4	424.7	0.07	
	5	424.5	424.2	-0.07	
ENGINE FLOWRATE, lbm/s	1	547.15	546.71	-0.08	0.01
	2	547.81	547.26	-0.10	
	3	547.92	547.92	0	
	4	547.97	544.97	-0.38	
	5	551.66	555.16	0.63	
ENGINE MIXTURE RATIO, LOX/LH <sub>2</sub>	1	5.608	5.567	-0.73	-0.34
	2	5.595	5.589	-0.11	
	3	5.582	5.537	-0.81	
	4	5.576	5.540	-0.64	
	5	5.551	5.584	0.59	

Note: Performance values at ESC + 61 seconds. Values are site conditions and do not include effect of pressurization flow.

The outboard engine thrust decay performance was within the predicted band as shown in Figure 6-7. First indications of thrust decay were noted 0.60 seconds prior to cutoff signal on engine 2. On previous vehicles, engine 1 has led the performance degradation. In order of engine position, thrust decay began at 0.59, 0.60, 0.45, and 0.40 seconds prior to cutoff signal and corresponding chamber pressure decays were 140, 160, 130 and 120 psi.

At S-II OECO total thrust was down to 637,450 lbf. Stage thrust dropped to five percent of this level within 0.4 second. The stage cutoff impulse through the five percent thrust level is estimated to be 143,360 lbf-s.

#### 6.5 S-II STAGE PROPELLANT MANAGEMENT

Flight and ground loading performance of the propellant management system was nominal and all parameters were within expected limits.

The Propellant Tanking Computer System (PTCS) and the stage propellant management system properly controlled S-II loading and replenishment. The newly added loading and overflow point sensors (LOX and LH<sub>2</sub>) on the S-II stage and the point sensor percent wet indication system on the PTCS consoles all functioned properly. The over-fill point sensor percent wet indications were all within the redlines at the -187 second commit point.

The LOX depletion ECO sensor No. 4 indicated open for two minutes 20

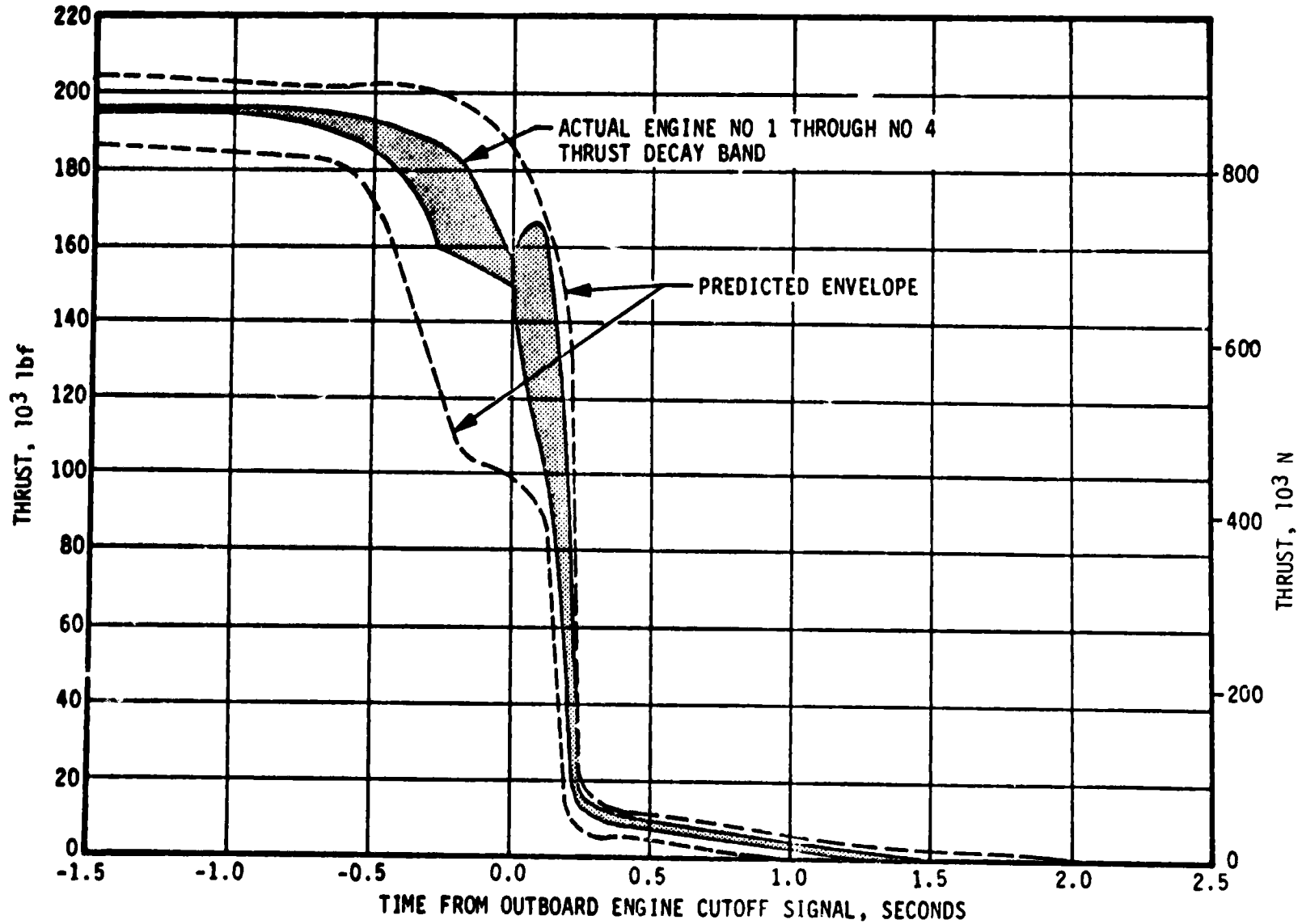


Figure 6-7. S-II J-2 Outboard Engine Thrust Decay

seconds during the early phases of LOX loading which is similar to past occurrences on S-II-11 and other stages. This phenomenon is attributed to a thermal problem in the LOX tank feed-through electrical connectors. The occurrence is not considered a problem since three or more sensors have to be open before mission rules are violated.

Open-loop control of EMR during flight was successfully accomplished through use of the engine two-position pneumatically operated Mixture Ratio Control Valves (MRCV). At ESC, helium pressure drove the valves to the engine start position corresponding to the 4.8 EMR. The high EMR (5.5) command was received at ESC +5.5 seconds as expected, providing a nominal high EMR of 5.5 for the first phase of the Programmed Mixture Ratio (PMR)

The low EMR step occurred at ESC +330.3 seconds, which is 2.0 seconds earlier than predicted. This time difference is most likely caused by engine performance deviations, IU computational cycle and slight under-loading of propellants on the S-II and S-IVB stages. The average EMR at the low step was 4.75 as compared to a predicted 4.78. This lower than planned EMR is well within the two sigma  $\pm 0.06$  mixture ratio tolerance.

Outboard Engine Cutoff (OECO) was initiated by the LOX depletion ECO sensors at ESC +395.34 seconds compared to the planned ESC +394.71 seconds. Based on point sensor and flowmeter data, propellant residuals (mass in tanks) at OECO were 1405 lbm LOX and 2612 lbm LH<sub>2</sub> versus 1404 lbm LOX and 2851 lbm LH<sub>2</sub> predicted. The late OECO and low LH<sub>2</sub> residuals were primarily due to the early low EMR step and lower than planned EMR after the step. The open-loop PU error at OECO was -239 lbm LH<sub>2</sub> which is well within the estimated three sigma dispersion of  $\pm 2500$  lbm LH<sub>2</sub>.

Table 6-2 presents a comparison of propellant masses as measured by the PU probes and engine flowmeters. The best estimate propellant mass is based on integration of flowmeter data utilizing the propellant residuals determined from point sensor data. The full load mass values were 0.13 percent less than predicted for LOX and 0.06 percent greater than predicted for LH<sub>2</sub>.

## 6.6 S-II PRESSURIZATION SYSTEM

### 6.6.1 S-II Fuel Pressurization System

LH<sub>2</sub> tank ullage pressure, actual and predicted, is presented in Figure 6-8 for autosequence, S-1C boost, and S-II boost. The LH<sub>2</sub> vent valves were closed at -93.4 seconds and the ullage volume pressurized to 35.8 psia in 17.6 seconds. One make-up cycle was required at approximately -41.0 seconds and the ullage pressure was increased from 34.7 psia to 35.6 psia. Ullage pressure decayed to 35.0 psia at S-1C ESC at which time the pressure decay rate increased for about 20 seconds. The

Table 6-2. AS-511 Flight S-II Propellant Mass History

EVENT	PREDICTED, LBM		PU SYSTEM ANALYSIS, LBM*		ENGINE FLOWMETER INTEGRATION (BEST ESTIMATE), LBM	
	LOX	LH <sub>2</sub>	LOX	LH <sub>2</sub>	LOX	LH <sub>2</sub>
LIFTOFF	845,613	160,216	845,506	160,251	844,532	160,320
S-II ESC	845,613	160,202	841,918	159,519	844,532	160,306
S-II PU VALVE STEP COMMAND	94,670	22,516	99,986	23,497	100,376	23,639
2 PERCENT POINT SENSOR	16,489	4,338	17,899	4,199	17,803	4,336
S-II OECO	1,404	2,851	DATA NOT USABLE	2,425	1,405	2,612
S-II RESIDUAL AFTER THRUST DECAY	1,193	2,730	DATA NOT USABLE	DATA NOT USABLE	1,196	2,524

NOTE: Table is based on mass in tanks and sump only. Propellant trapped external to tanks and LOX sump is not included. PU data are not corrected for tank/probe mismatch.

\*Liftoff data based on pressurized ground data system. All other PU system propellant quantities based on flight data system.

increased decay rate was attributed to an increase in LH<sub>2</sub> surface agitation caused by S-IC engine firing. This decay is normal and has occurred on previous launches.

The LH<sub>2</sub> vent valves opened during S-IC boost, limiting tank pressure; however, no main poppet operation was indicated. During valve action, differential pressure across the vent valve was maintained by the primary pilot valve within the allowable low-mode band of 27.5 to 29.5 psi. Ullage pressure at engine start was 29.0 psia exceeding the minimum engine start requirement of 27 psia. The LH<sub>2</sub> vent valves were switched to the high vent mode prior to S-II engine start.

The LH<sub>2</sub> ullage pressure during S-II boost was controlled by an orifice in the LH<sub>2</sub> tank pressurization line, with maximum tank pressure controlled by the LH<sub>2</sub> vent valves. Except for the normal low pressure spike during start transient, the ullage pressure throughout the S-II boost period was controlled by the LH<sub>2</sub> vent valves within the 30.5 to 33 psia allowable band. LH<sub>2</sub> tank vent valve 1 opened at 177.0 seconds and remained open until 200.9 seconds. LH<sub>2</sub> tank vent valve 2 opened at 171.8 seconds and remained open until 560.7 seconds. The LH<sub>2</sub> ullage pressure was approximately one psi higher than the predicted pressure because the vent valves controlled the pressure in mid-cracking pressure range rather than the minimum crack level. This

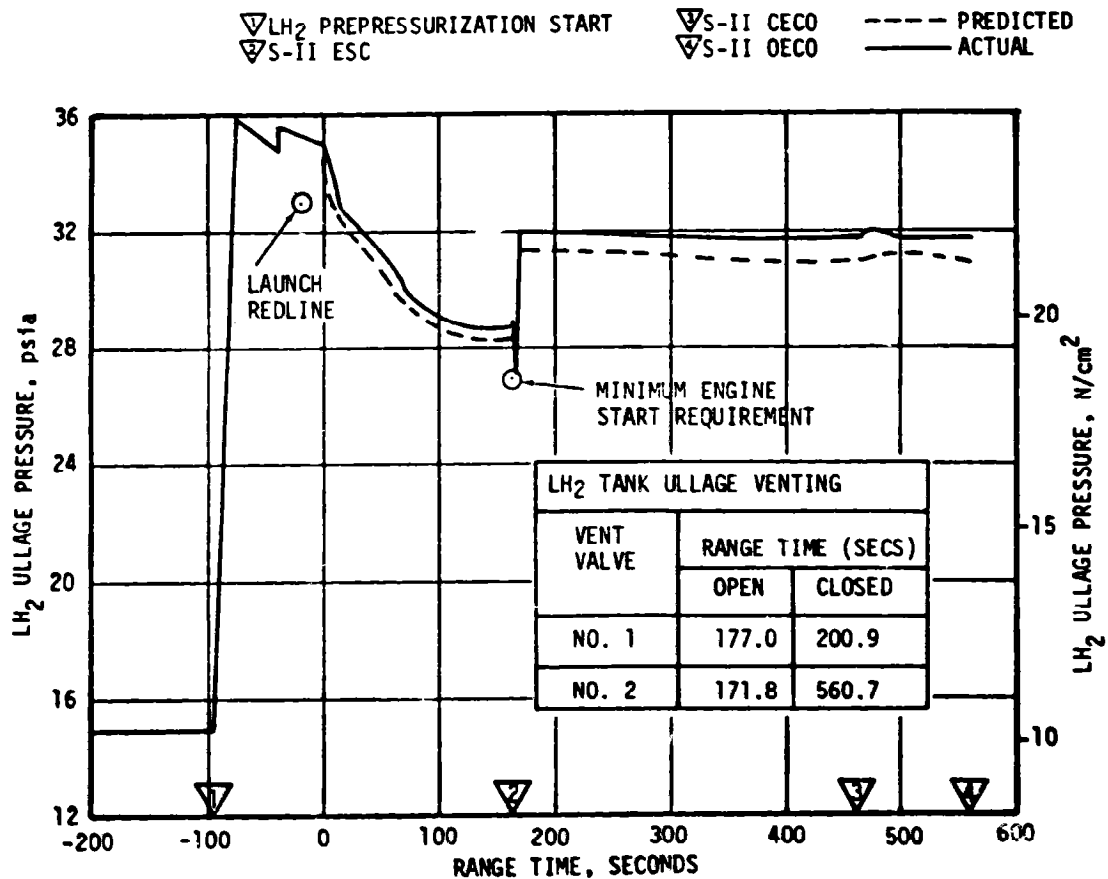


Figure 6-8. S-II Fuel Tank Ullage Pressure is an acceptable condition and no corrective action is necessary.

Figure 6-9 shows LH<sub>2</sub> pump total inlet pressure, temperature and Net Positive Suction Pressure (NPSP) for the J-2 engines. The parameters were in close agreement with the predicted values throughout the S-II flight period. NPSP remained above the minimum requirement throughout the S-II burn phase.

### 6.6.2 S-II LOX Pressurization System

LOX tank ullage pressure, actual and predicted, is presented in Figure 6-10 for autosequence, S-IC boost, and S-II burn. After a 107 second cold helium chilldown flow through the LOX tank, the chilldown flow was terminated at -200 seconds. The vent valves were closed at -184 seconds and the LOX tank was pressurized to the pressure switch No. 2 setting of 38.6 psia in 30.9 seconds. No pressure make-up cycles were required. The LOX tank ullage pressure increased to 40.5 psia because of common bulkhead flexure due to LH<sub>2</sub> tank prepressurization. The LOX vent valves performed satisfactorily during all prelaunch operations. The extended LOX vent valve closing time experienced on AS-510 was not repeated.



- ▽ S-II ESC
- ▽ S-II CECO
- ▽ S-II EMR SHIFT
- ▽ S-II OECS

- PREDICTED
- ACTUAL, OE
- MINIMUM NPSP REQUIREMENT
- ACTUAL, CE

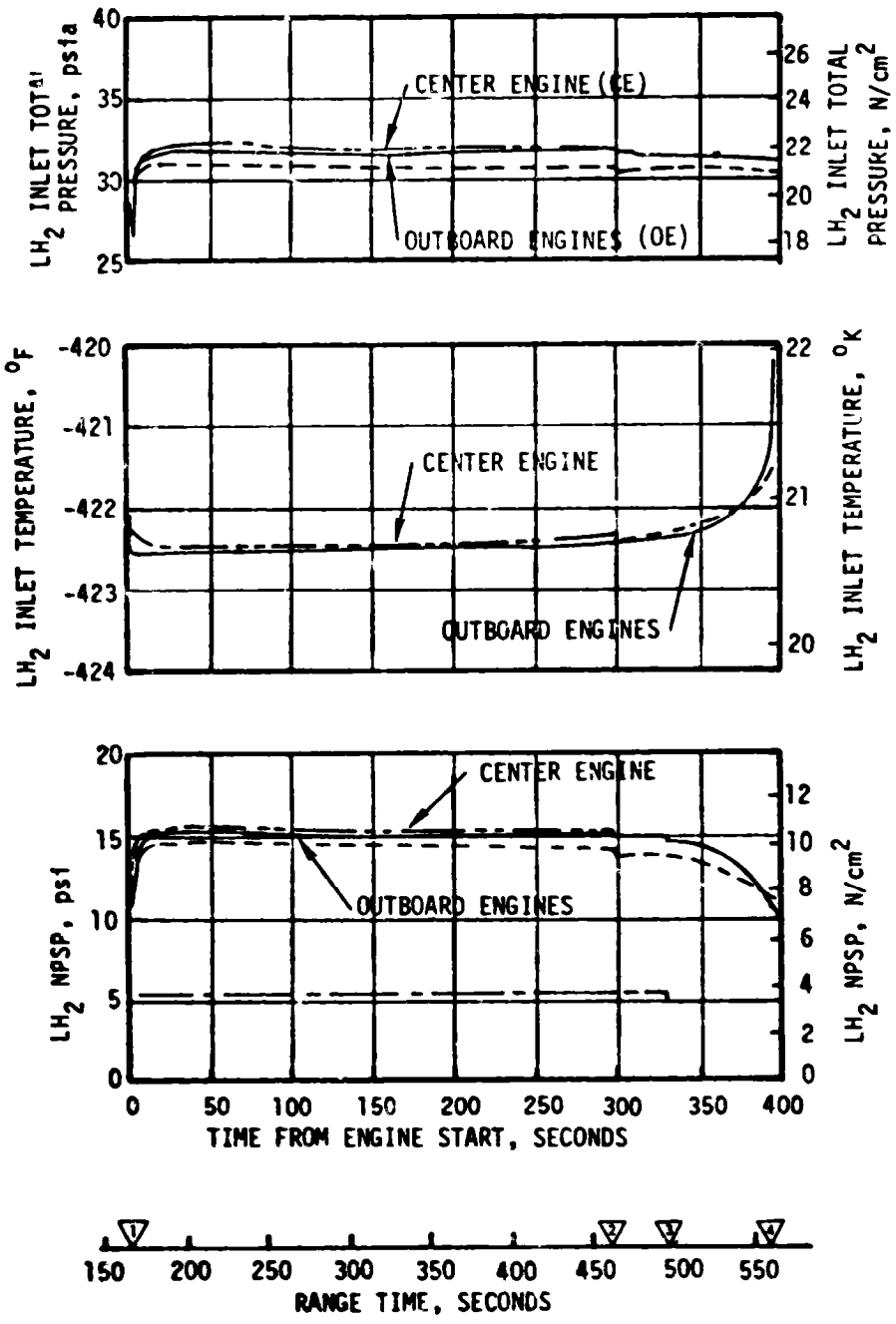


Figure 6-9. S-II Fuel Pump Inlet Conditions

The LOX vent valves remained closed during the S-IC boost and the LOX tank ullage pressure prior to S-II ESC was 41.0 psia. During the S-II boost, the LOX tank pressure varied from a maximum of 41.8 psia at 192 seconds to a minimum of 38.3 psia at S-II OECO. The LOX tank pressurization was controlled in-flight by an orifice, with the LOX tank vent valves controlling excessive pressure buildup within a pressure range setting of 39.0 to 42.0 psia. The LOX tank vent valve 1 opened at 193.5 seconds and remained open until 193.6 seconds. LOX tank vent valve 2 opened and closed four times between 165.6 seconds and 237.9 seconds. The LOX tank vent valve 2 open durations ranged from 0.3 second to 12.2 seconds.

The LOX tank ullage pressure was controlled within one psi of the pressure predicted for S-II boost, as shown in Figure 6-10. Comparisons of the LOX pump total inlet pressure, temperature, and NPSP are presented in Figure 6-11. Throughout S-II boost, the LOX pump NPSP was well above the minimum requirement.

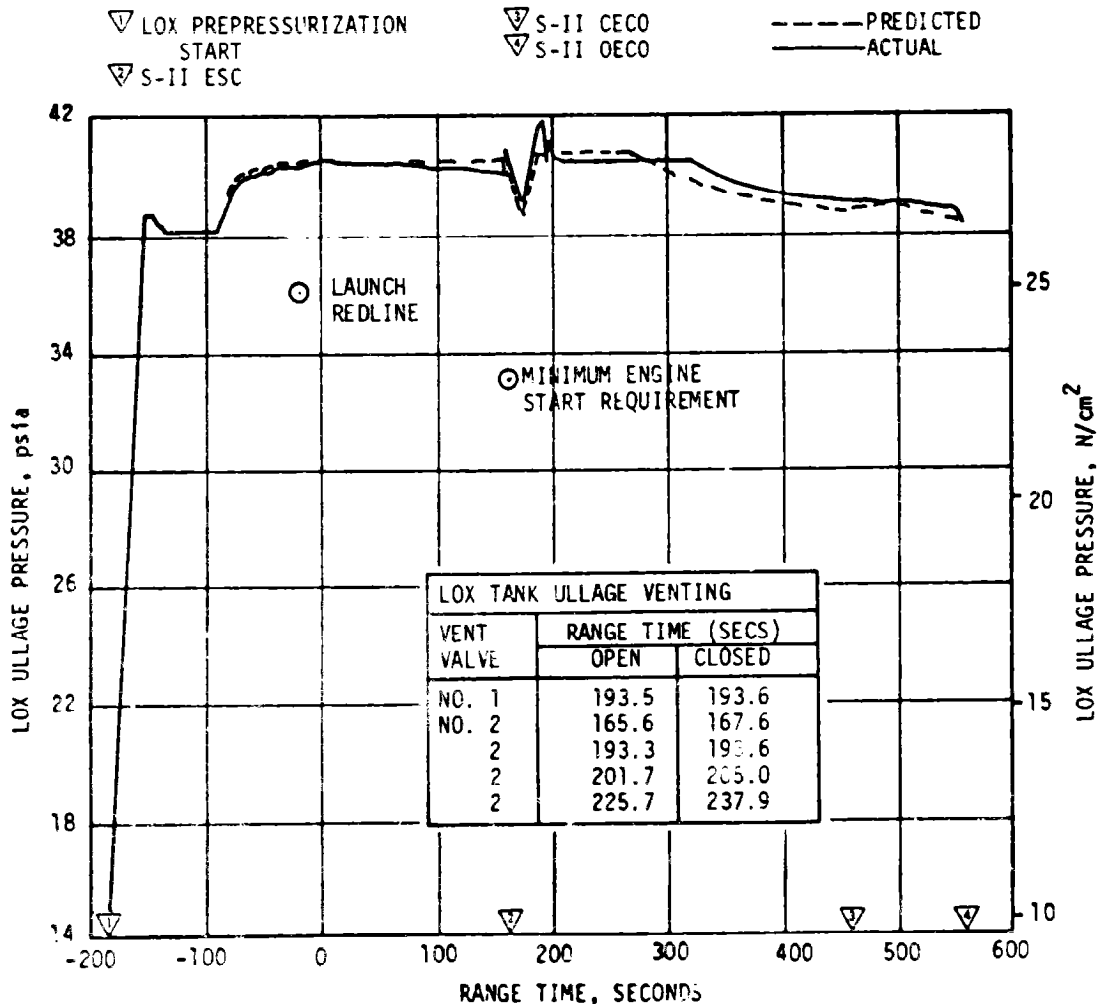


Figure 6-10. S-II LOX Tank Ullage Pressure

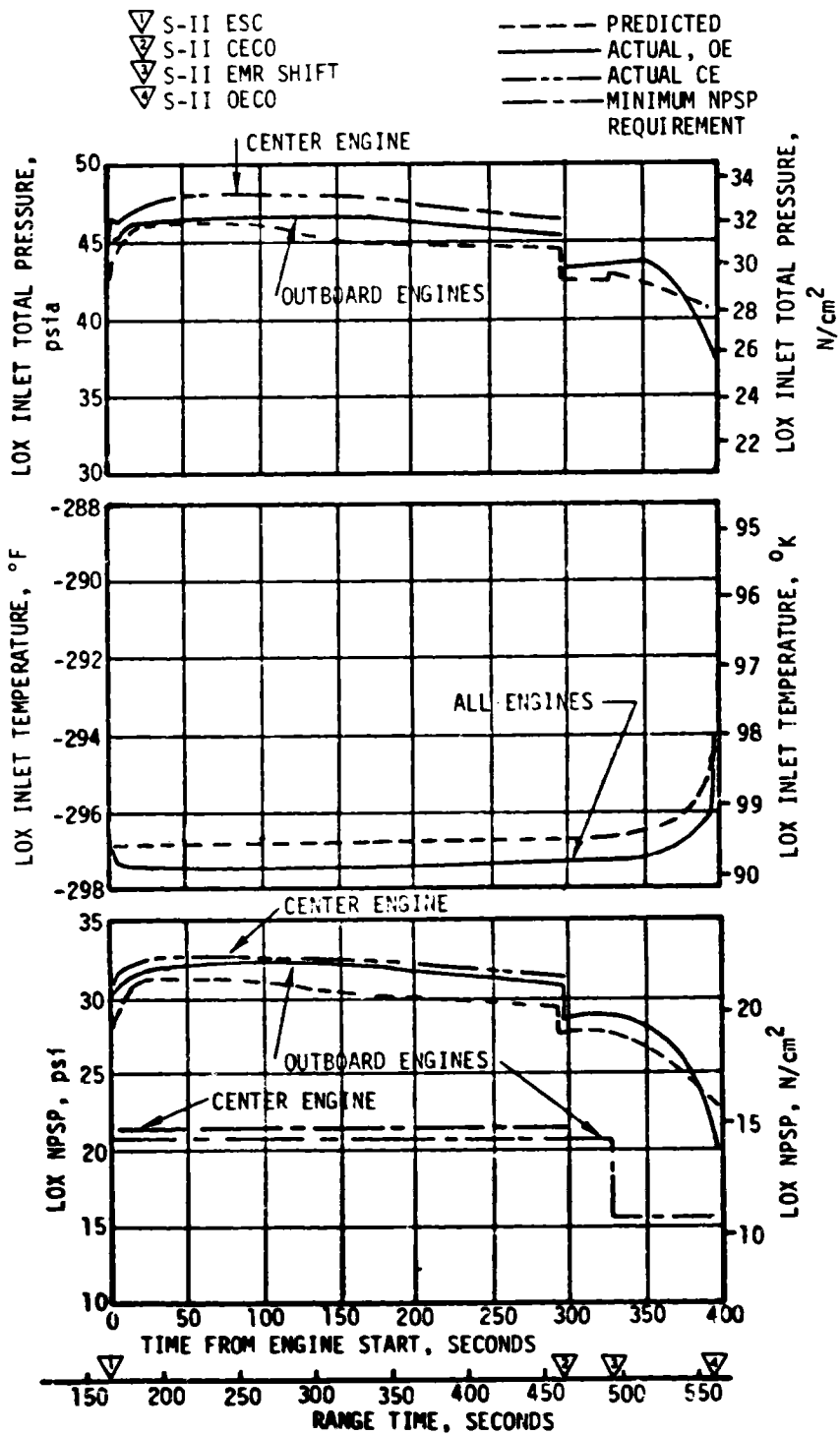


Figure 6-11. S-II LOX Pump Inlet Conditions

One configuration change was made to the LOX pressurization system for this flight. A LOX tank pressure switch purge was installed, effective AS-511 and subsequent vehicles. The purge system was incorporated to preclude a potential LOX/GOX incompatibility situation within the LOX pressure switch assembly. The purge is connected to the helium injection and accumulator fill helium supply system. No instrumentation is available to evaluate the purge system. However, since the helium injection and accumulator fill supply pressure was within predicted (Figure 6-14), it is concluded that the purge system also functioned properly.

#### 6.7 S-II PNEUMATIC CONTROL PRESSURE SYSTEM

The pneumatic control system functioned satisfactorily throughout S-IC and S-II boost periods. Bottle pressure was 2960 psia at -19 seconds. The bottle pressure decay to approximately 2930 psia just prior to S-II ESC is attributed to a decreasing temperature in the thrust cone area and system leakage due to the vibrations caused by going through Mach 1 and maximum dynamic pressure. The pressure decayed from 2930 psia prior to S-II engine start to 2560 psia after S-II OECO because of normal valve activities during S-II burn.

The regulator outlet pressure at -187 seconds was 700 psia which was within the revised regulation-relief band of 670 to 815 psia. The minimum redline limit was revised from 690 to 670 psia for this and subsequent flights. The regulator pressure decreased from 700 psia to approximately 695 psia at the S-II engine start for the same reasons the supply bottle pressure decreased during the same time period. After S-II engine start, the regulator pressure decreased to approximately 690 psia and remained relatively constant at that pressure level for the remainder of S-II boost except for allowable pressure drops during recirculation or pre valve actuations at S-II engine start, at CECO, and at OECO.

The LH<sub>2</sub> recirculation pump valve No. 1 (open and closed) indications, and the LH<sub>2</sub> recirculation pump valve No. 5 open indication were not functioning properly at liftoff and S-II engine start. However, proper valve positions were verified by monitoring other system parameters.

The pre valves functioned as required at S-II engine start and at CECO and OECO.

#### 6.8 S-II HELIUM INJECTION SYSTEM

The performance of the helium injection system was satisfactory. The supply bottle was pressurized to 2940 psia prior to liftoff and by S-II ESC the pressure was 1700 psia. Helium injection average total flowrate during supply bottle blowdown (-30 to 163 seconds) was 70 SCFM.

## 6.9 POGO SUPPRESSION SYSTEM

A center engine LOX feedline accumulator is installed on the S-II stage as a POGO suppression device. This was the third flight stage to incorporate an accumulator system to suppress S-II POGO and the analysis indicates that there was no POGO.

The accumulator bleed subsystem performance was satisfactory. Figure 6-12 shows the required accumulator temperature at engine start, the predicted temperatures during prelaunch and S-IC boost, and the actual temperatures experienced during AS-511 flight. As can be seen, the maximum allowable temperature of  $-281.5^{\circ}\text{F}$  at engine start was adequately met ( $-294.5^{\circ}\text{F}$  actual).

Accumulator fill was initiated 4.1 seconds after engine start. Figure 6-13 shows the accumulator LOX level versus time during accumulator fill. The fill time was 6.8 seconds, within the required five to seven second requirement. The helium fill flow rate, during the fill transient, was 0.0052 lbm/s and the accumulator pressure was 43.7 psia.

After the accumulator was filled with helium, it remained in that state until S-II CECO when the helium flow was terminated by closing the two fill solenoid valves. There was no sloshing or abnormal liquid level behavior in the accumulator during center engine operation. Figure 6-14 shows the helium injection and accumulator fill supply pressure during accumulator fill operation. The supply bottle pressure was within the predicted band, indicating that the helium usage rates were as predicted.

## 6.10 S-II HYDRAULIC SYSTEM

S-II hydraulic system performance was normal throughout the flight. System supply and return pressures, reservoir volumes, and system fluid temperatures were within predicted ranges. Reservoir fluid temperatures increased at close to predicted rate. All servoactuators responded to commands with good precision. The maximum engine deflection was approximately 1.1 degrees in pitch on engine 1 at initiation of Iterative Guidance Mode (IGM). Actuator loads were well within design limits. The maximum actuator load was approximately 7,800 lbf on the pitch actuator of engine 2 at IGM.

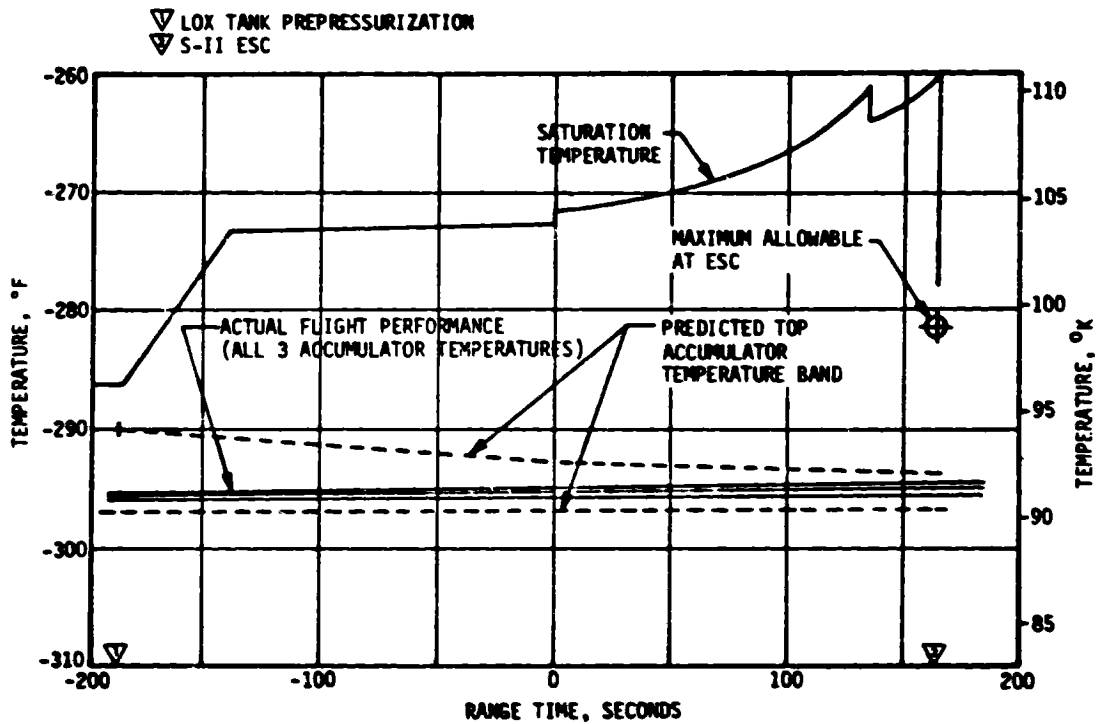


Figure 6-12. S-II Center Engine LOX Feedline Accumulator Bleed System Performance

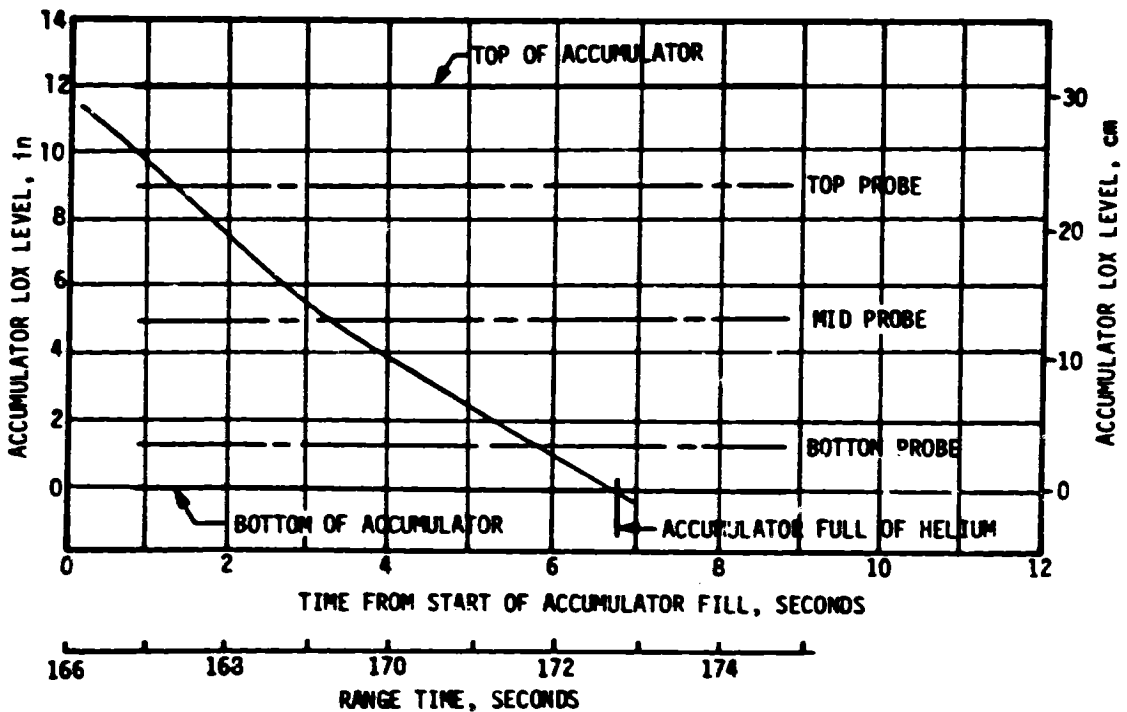


Figure 6-13. S-II Center Engine LOX Feedline Accumulator Fill Transient

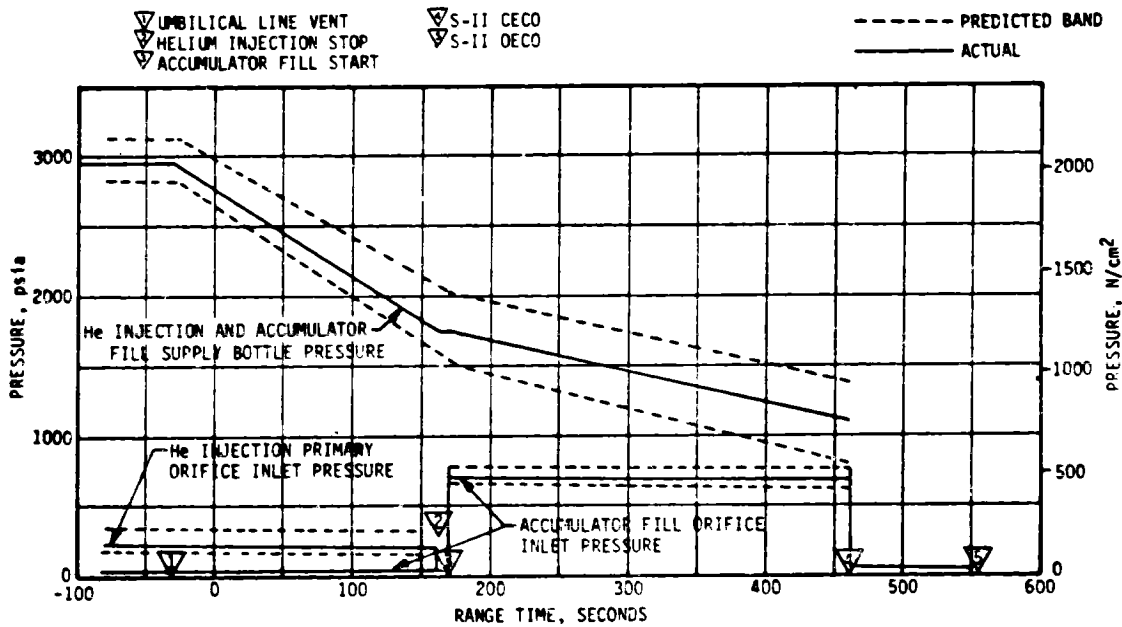


Figure 6-14. S-II Center Engine 'OX Feedline Accumulator Helium Supply System Performance

## SECTION 7

### S-IVB PROPULSION

#### 7.1 SUMMARY

The S-IVB propulsion system performed satisfactorily throughout the operational phase of first burn and had normal start and cutoff transients. S-IVB first burn time was 142.6 seconds, 0.4 seconds longer than predicted. This difference is composed of 1.0 second due to the combined first and second stage performance and -0.6 second due to higher S-IVB performance. The engine performance during first burn, as determined from standard altitude reconstruction analysis, deviated from the predicted Start Tank Discharge Valve (STDV) open +140-second time slice by 0.38 percent for thrust and zero percent for specific impulse. The S-IVB stage first burn Engine Cutoff (ECO) was initiated by the Launch Vehicle Digital Computer (LVDC) at 706.21 seconds.

The Continuous Vent System (CVS) adequately regulated LH<sub>2</sub> tank ullage pressure at an average level of 19.4 psia during orbit and the Oxygen/Hydrogen (O<sub>2</sub>/H<sub>2</sub>) burner satisfactorily achieved LH<sub>2</sub> and LOX tank repressurization for restart. Engine restart conditions were within specified limits. The restart at full open Mixture Ratio Control Valve (MRCV) position was successful.

S-IVB second burn time was 341.9 seconds, 2.4 seconds less than predicted. This difference is primarily due to the slightly higher S-IVB performance and lighter vehicle mass during second burn. The engine performance during second burn, as determined from the standard altitude reconstruction analysis, deviated from the STDV open +140-second time slice by 0.57 percent for thrust and zero percent for specific impulse. Second burn ECO was initiated by the LVDC at 9,558.41 seconds (02:39:18.41).

The S-IVB high pressure systems were safed following J-2 engine second burn cutoff. The thrust developed during the LOX dump provided a satisfactory contribution to the velocity change for lunar impact. Momentary ullage gas ingestion occurred three times during the LOX dump as a result of LOX sloshing. The greater than nominal slosh activity was attributed to the additional vehicle maneuver to the LOX dump attitude for optimum velocity increment following the programmed LOX dump maneuver. As a result of the ullage ingestion, liquid flow was impeded and dump performance was decreased.

Auxiliary Propulsion System (APS) Module 1 experienced an external helium leak which started at approximately 3600 seconds and continued to 22,800



seconds (06:20:00). The maximum leak rate experienced was 585 psi/hr. The other Module 1 systems functioned normally.

Module 2 experienced internal leakage from the high pressure system to the low pressure system during the flight. The regulator outlet pressure began to increase above the regulator setting at approximately 970 seconds. The pressure continued to increase to 344 psia, the relief setting of the low pressure module relief valve. The regulator outlet pressure remained between 344 and 203 psia out to loss of data. During periods of high propellant usage the regulator outlet pressure decreased, but not low enough for regulator operation. The prime suspect for this internal helium leakage is leakage through the regulator. Data from preflight pressurization of the APS indicates that the APS probably was on the secondary regulator at liftoff. Another leak path being examined is the common mounting block for the high and low pressure helium system pressure transducer.

## 7.2 S-IVB CHILLDOWN AND BUILDUP TRANSIENT PERFORMANCE FOR FIRST BURN

The thrust chamber temperature at launch was below the maximum allowable redline limit of  $-130^{\circ}\text{F}$ . At S-IVB first burn Engine Start Command (ESC), the temperature was  $-138^{\circ}\text{F}$ , which was within the requirements of  $-189.6 \pm 110^{\circ}\text{F}$ .

The chilldown and loading of the engine  $\text{GH}_2$  start tank and pneumatic control bottle prior to liftoff was satisfactory.

The engine control sphere pressure and temperature at liftoff were 3025 psia and  $-158^{\circ}\text{F}$ . At first burn ESC the start tank conditions were 1308 psia and  $-163.4^{\circ}\text{F}$ , within the required region of  $1325 \pm 75$  psia and  $-170 \pm 30^{\circ}\text{F}$  for start. The discharge was completed and the refill initiated at first burn ESC +3.8 seconds. The refill was satisfactory with 1163 psia and  $-233^{\circ}\text{F}$  at cutoff.

The propellant recirculation systems operation, which was continuous from before liftoff until just prior to first ESC, was satisfactory. Start and run box requirements for both fuel and LOX were met, as shown in Figure 7-1. At first ESC the LOX pump inlet temperature was  $-295^{\circ}\text{F}$  and the  $\text{LH}_2$  pump inlet temperature was  $-420.8^{\circ}\text{F}$ . The oxidizer recirculation chilldown system flowmeter failed to indicate recirculation flow when chilldown was initiated. However, other chilldown measurements indicated that recirculation flow was normal. During boost the measurement failed sporadically (Section 15, Table 15-3).

First burn fuel lead followed the expected pattern and resulted in satisfactory conditions as indicated by the fuel injector temperature.

The first burn start transient was satisfactory, and the thrust buildup was within the limits set by the engine manufacturer. Thrust data during the start transient is presented in Figure 7-2. This buildup was similar

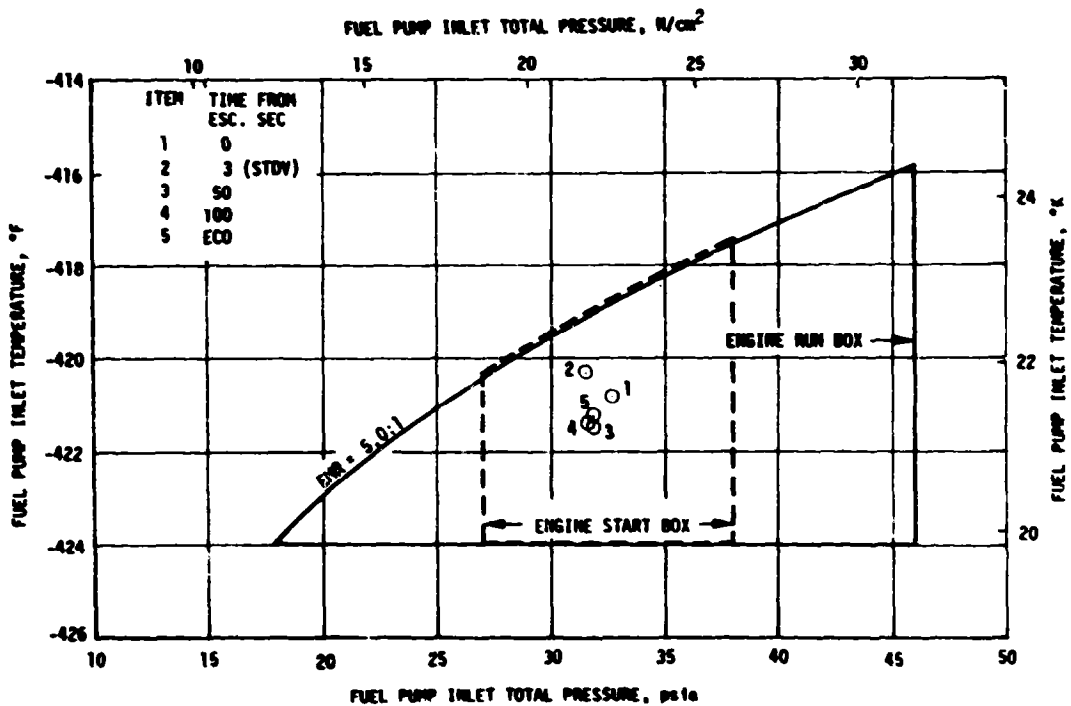
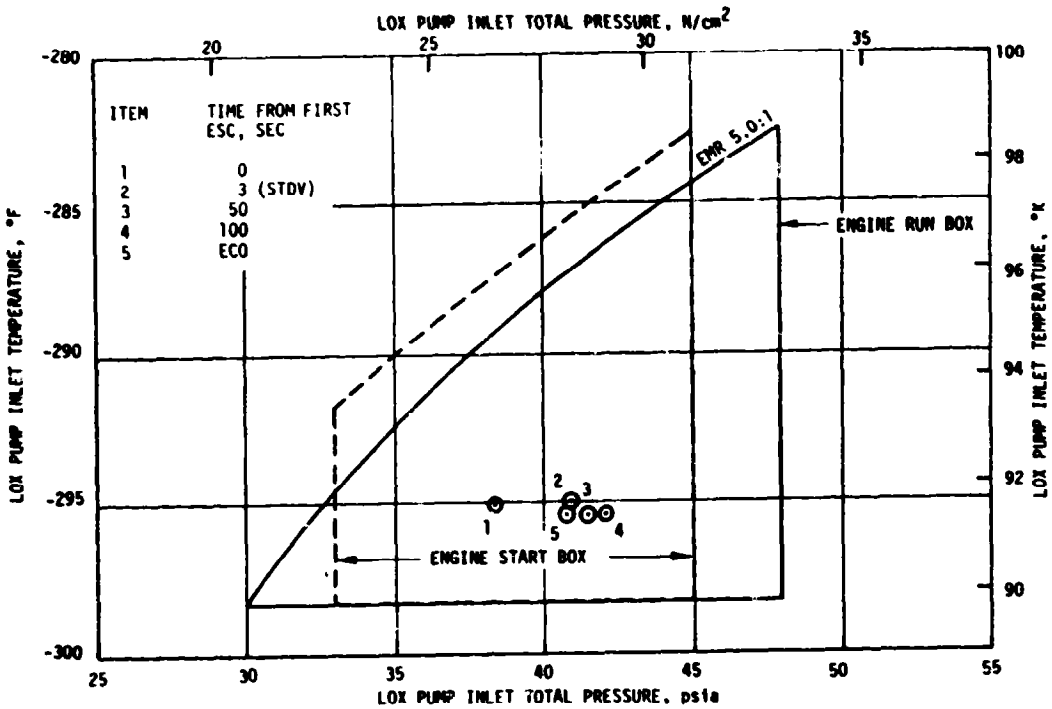


Figure 7-1. S-IVB Start Box and Run Requirements - First Burn

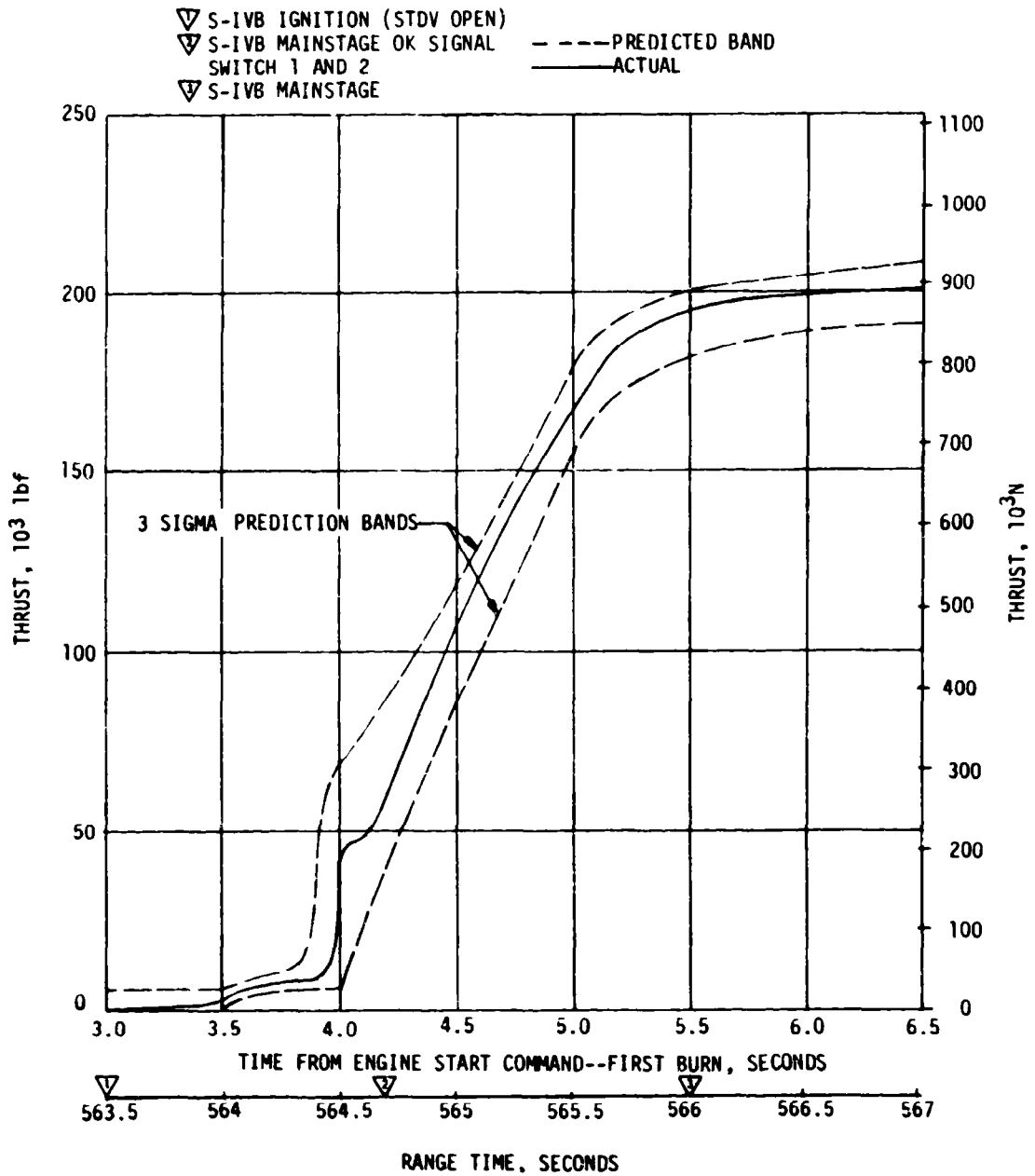


Figure 7-2. S-IVB Thrust Buildup Transient for First Burn

to the thrust buildups observed on AS-506 through AS-510. The MRCV was in the closed position (5.0 EMR) prior to first start, and performance indicates it remained closed during first burn. The total impulse from STDV to STDV open +2.5 seconds was 198,939 lbf-s.

### 7.3 S-IVB MAINSTAGE PERFORMANCE FOR FIRST BURN

The propulsion reconstruction analysis showed that the stage performance during mainstage operation was satisfactory. A comparison of predicted and actual performance of thrust, specific impulse, total flowrate, and Engine Mixture Ratio (EMR) versus time is shown in Figure 7-3. Table 7-1 shows the thrust, specific impulse, flowrates, and ERM deviations from the predicted at the STDV open +140-second time slice at standard altitude conditions.

Table 7-1. S-IVB Steady State Performance - First Burn  
(STDV Open +140-Second Time Slice at Standard Altitude Conditions)

PARAMETER	PREDICTED	RECONSTRUCTION	FLIGHT DEVIATION	PERCENT DEVIATION FROM PREDICTED
Thrust, lbf	205,637	206,439	802	0.38
Specific Impulse, lbf-s/lbm	429.5	429.5	0	0
LOX Flowrate, lbm/s	397.55	399.29	1.74	0.44
Fuel Flowrate, lbm/s	81.22	81.33	0.11	0.13
Engine Mixture Ratio, LOX/Fuel	4.895	4.909	0.014	0.29

Thrust, specific impulse, and EMR were well within the predicted bands. The thrust and propellant flowrates were slightly higher than nominal. The higher thrust and flowrates for flight can be attributed to a higher than nominal MRCV setting of approximately 30.8 degrees as compared to the predicted nominal setting of 30.4 degrees. The MRCV setting was within the requirement of  $30.0 \pm 1$  degrees. It should be noted that the estimated higher MRCV setting is based on engine performance reconstruction. The MRCV position indicator can only be used as a gross measurement.

The first burn time was 142.6 seconds which was 0.4 seconds longer than predicted. This difference is composed of 1.0 second longer due to the combined first and second stage performance and 0.6 second shorter due to higher S-IVB performance. Total impulse from STDV open +2.5 seconds to ECO was  $29.06 \times 10^6$  lbf-s which was 160,000 lbf-s more than predicted.

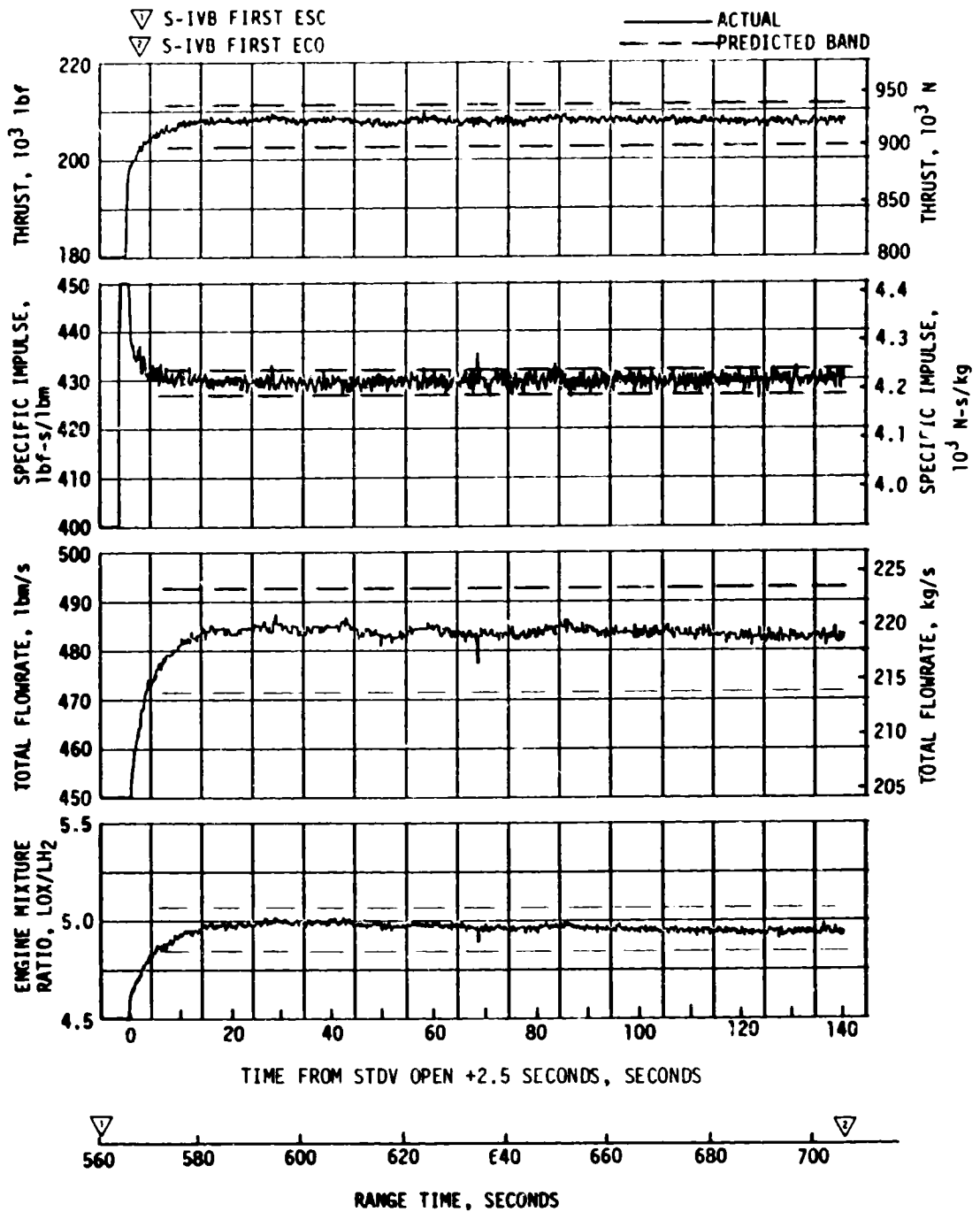


Figure 7-3. S-IVB Steady State Performance - First Burn

The engine helium control system performed satisfactorily during mainstage operation. The engine control bottle was connected to the stage ambient repressurization bottles, which resulted in a small pressure decay. An estimated 0.30 lbm of helium was consumed during first burn.

#### 7.4 S-IVB SHUTDOWN TRANSIENT PERFORMANCE FOR FIRST BURN

S-IVB first ECO was initiated at 706.2 seconds by a guidance velocity cutoff command. The ECO transient was satisfactory. The total cutoff impulse to zero thrust was 46,073 lbf-s which was 1781 lbf-s lower than the nominal predicted value of 47,854 lbf-s and within the  $\pm 4,100$  lbf-s predicted band. Cutoff occurred with the MRCV in the 5.0 EMR position. Thrust data during the cutoff transient is presented in Figure 7-4.

#### 7.5 S-IVB PARKING ORBIT COAST PHASE CONDITIONING

The LH<sub>2</sub> CVS performed satisfactorily, maintaining the fuel tank ullage pressure at an average level of 19.4 psia. This was well within the 18 to 21 psia band of the inflight specification.

The continuous vent regulator was activated at 765.4 seconds and was terminated at 8680.7 seconds (02:24:40.7). The CVS performance is shown in Figure 7-5.

Calculations based on estimated temperatures indicate that the mass vented from the fuel tank during parking orbit was 1803 lbm and that the boiloff mass was 2183 lbm, compared to predicted values of 1987 lbm and 2090 lbm, respectively.

LOX boiloff during the parking orbit coast phase was approximately 20 lbm.

#### 7.6 S-IVB CHILLDOWN AND BUILDUP TRANSIENT PERFORMANCE FOR SECOND BURN

Repressurization of the LOX and LH<sub>2</sub> tanks was satisfactorily accomplished by the O<sub>2</sub>/H<sub>2</sub> burner. Burner "ON" command was initiated at 8680.5 seconds (02:24:40.5). The LH<sub>2</sub> repressurization control valves were opened at burner "ON" +6.1 seconds, and the fuel tank was repressurized from 19.6 to 30.6 psia in 185 seconds. There were 25.6 lbm of cold helium used to repressurize the LH<sub>2</sub> tank. The LOX repressurization control valves were opened at burner "ON" +6.3 seconds, and the LOX tank was repressurized from 36.9 to 40.0 psia in 107 seconds. There were 2.9 lbm of cold helium used to repressurize the LOX tank. LH<sub>2</sub> and LOX ullage pressures are shown in Figure 7-6. The burner continued to operate for a total of 455 seconds providing nominal propellant settling forces. The performance of the AS-511 O<sub>2</sub>/H<sub>2</sub> burner was satisfactory as shown in Figure 7-7.

The S-IVB LOX recirculation system satisfactorily provided conditioned oxidizer to the J-2 engine for restart. Fuel recirculation system

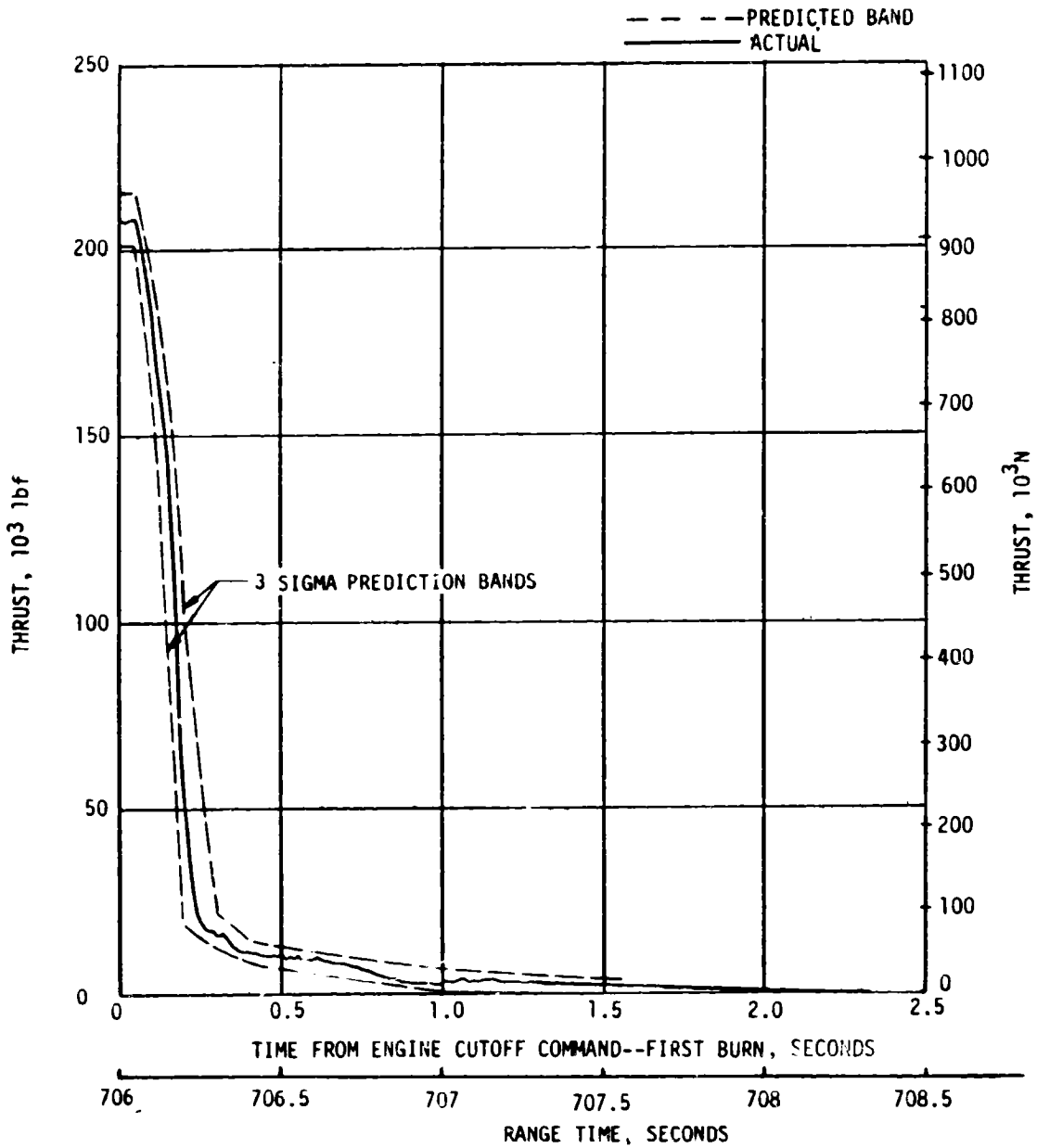


Figure 7-4. S-IVB Thrust Decay

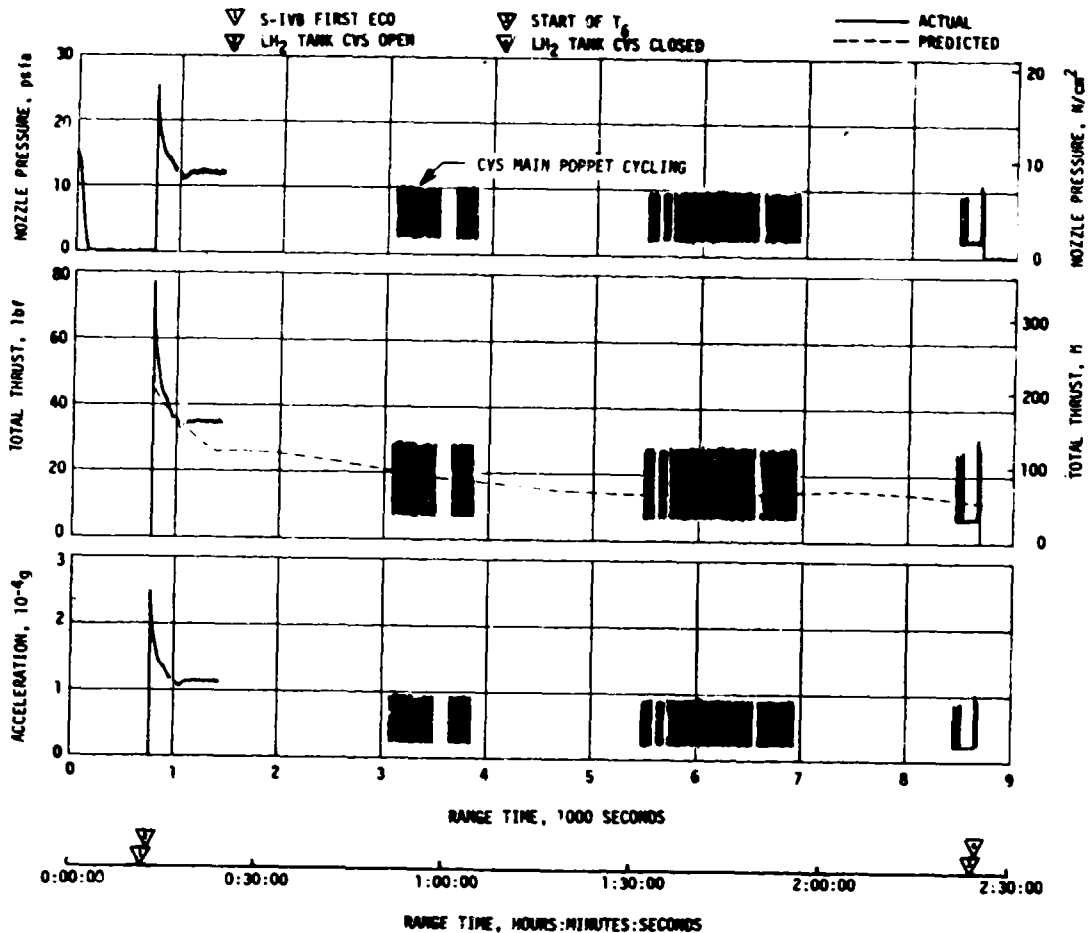


Figure 7-5. S-IVB CVS Performance - Coast Phase

performance was adequate and conditions at the pump inlet were satisfactory at second STDV open. The LOX and fuel pump inlet conditions are plotted in the start and run boxes in Figure 7-8. At second ESC, the LOX and fuel pump inlet temperatures were  $-294.3$  and  $-419.1^{\circ}\text{F}$ , respectively.

The oxidizer recirculation chilldown system flowmeter operated normally during the first 200 seconds of chilldown and then failed completely (Table 15-3). Second burn fuel lead generally followed the predicted pattern and resulted in satisfactory conditions, as indicated by the fuel injector temperature. Since J-2 start system performance was nominal during coast and restart, no helium recharge was required from the LOX ambient repressurization system (bottle No. 2). The start tank performed satisfactorily during second burn blowdown and recharge sequence. The engine start tank was recharged properly and it maintained sufficient



- ▽ O<sub>2</sub>/H<sub>2</sub> BURNER ON
- ▽ LH<sub>2</sub> AND LOX CRYOGENIC REPRESSURIZATION VALVES OPEN
- ▽ TERMINATION OF LOX TANK REPRESSURIZATION
- ▽ TERMINATION OF LH<sub>2</sub> TANK REPRESSURIZATION
- ▽ O<sub>2</sub>/H<sub>2</sub> BURNER OFF

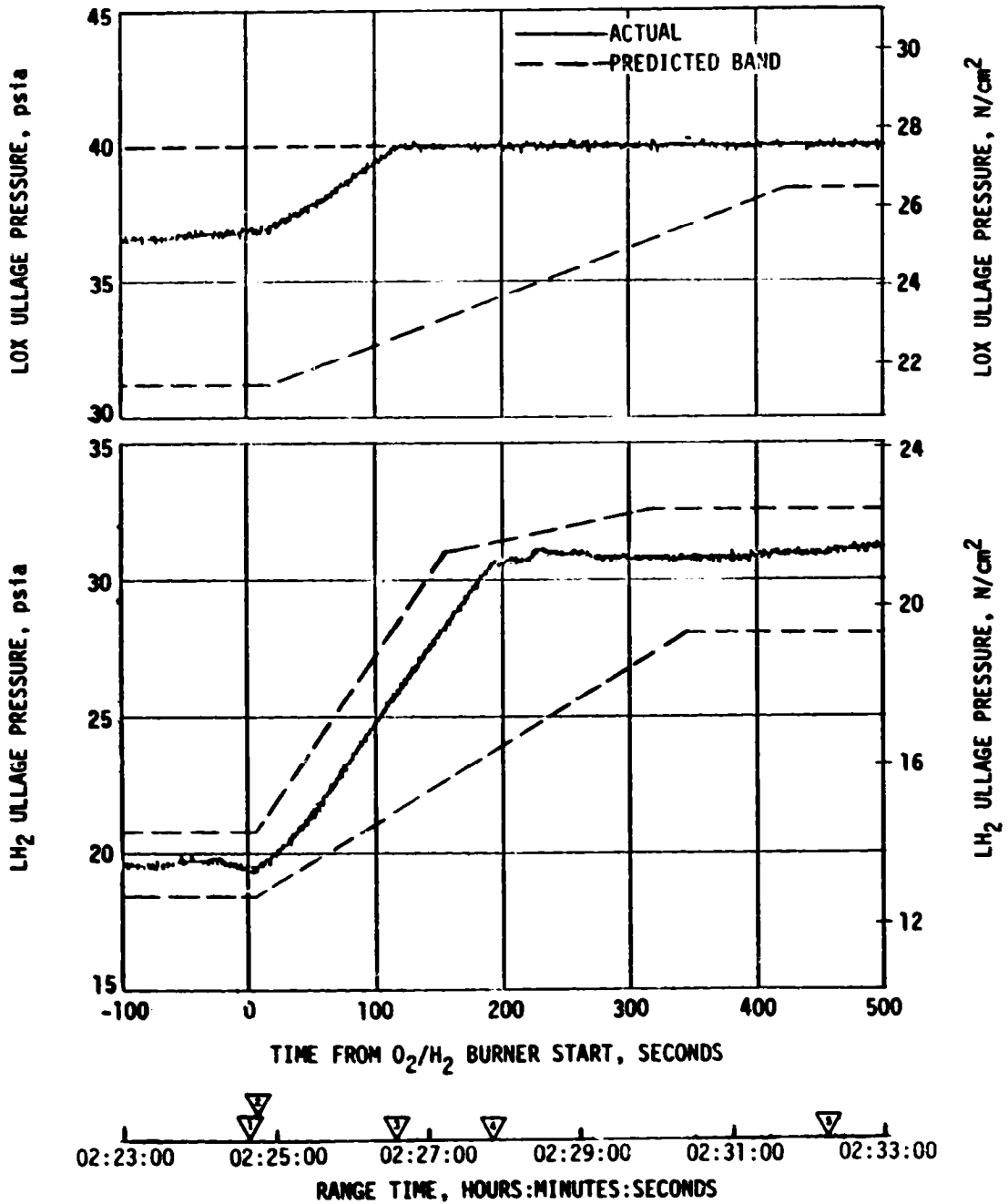


Figure 7-6. S-IVB Ullage Conditions During Repressurization Using O<sub>2</sub>/H<sub>2</sub> Burner

- ▽ BURNER START COMMAND
- ▽ LH<sub>2</sub> AND LOX TANK REPRESSURIZATION VALVES OPEN
- ▽ TERMINATION OF LOX TANK REPRESSURIZATION
- ▽ TERMINATION OF LH<sub>2</sub> TANK REPRESSURIZATION
- ▽ BURNER CUTOFF

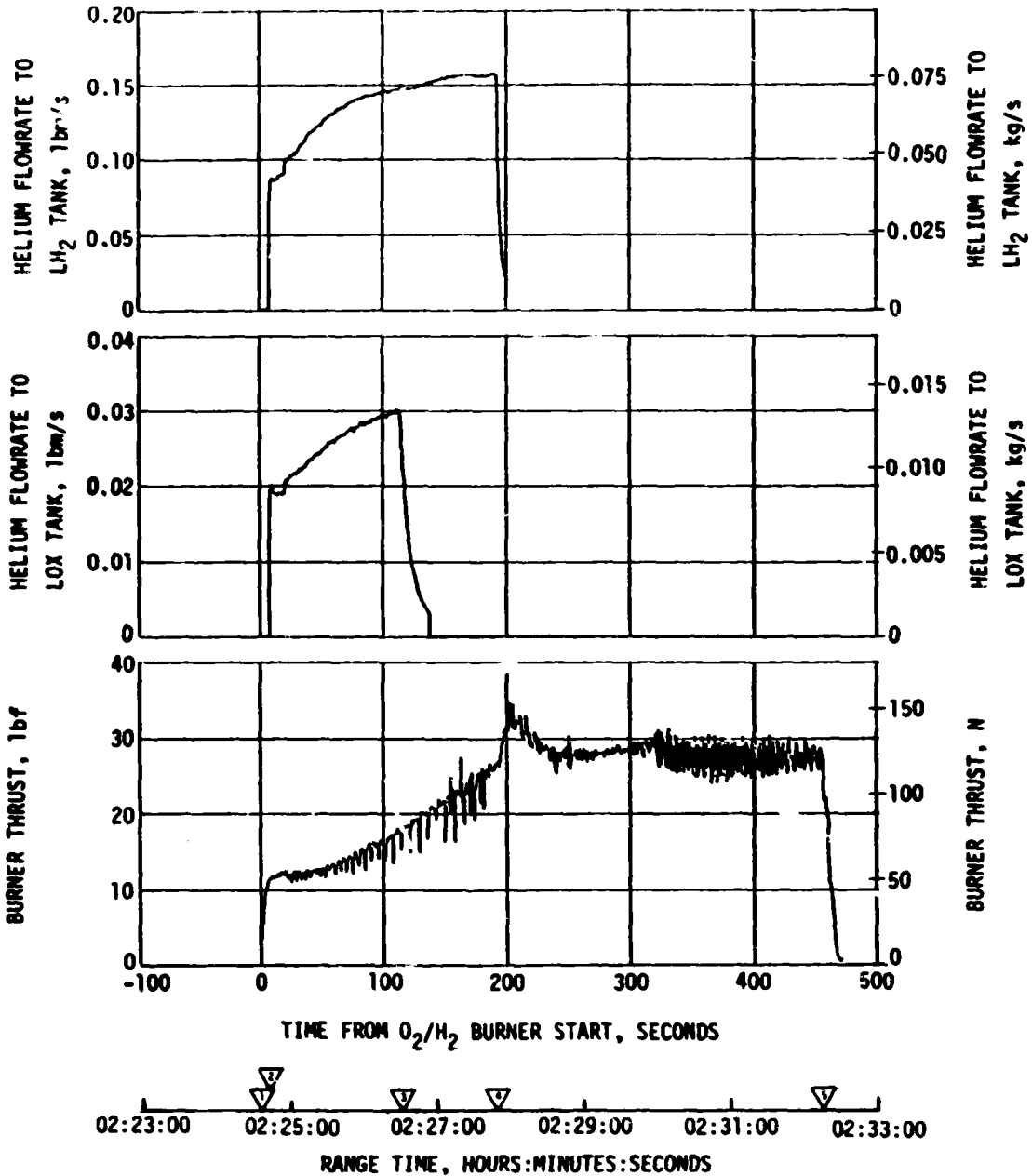


Figure 7-7. S-IVB O<sub>2</sub>/H<sub>2</sub> Burner Thrust and Pressurant Flowrate

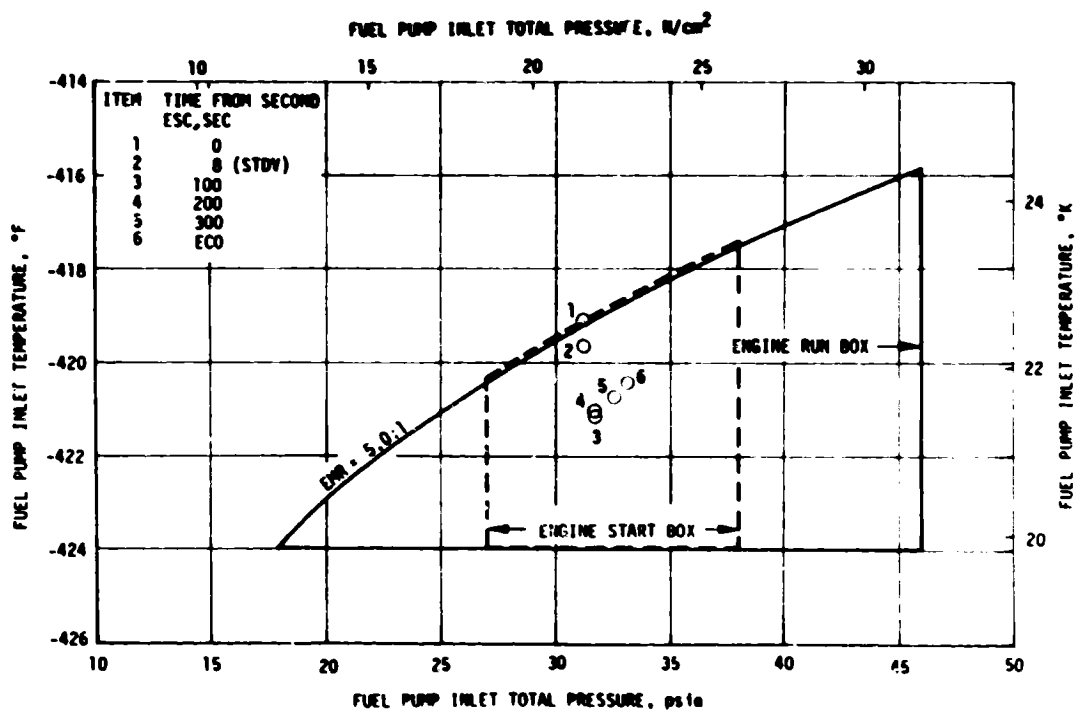
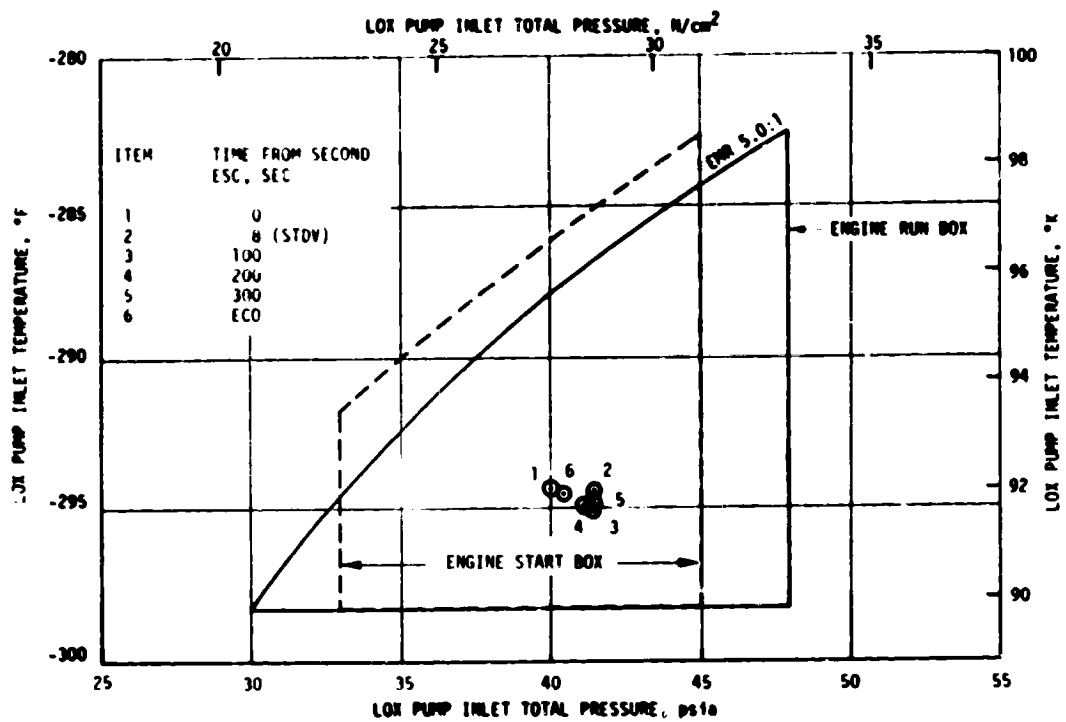


Figure 7-8. S-IVB Start Box and Run Requirements - Second Burn

pressure during coast. The engine control sphere first burn gas usage was as predicted; the ambient helium spheres recharged the control sphere to a nominal level for restart.

The second burn start transient was satisfactory. The thrust buildup was within the limits set by the engine manufacturer and was similar to the thrust buildup on AS-506 through AS-510. The MRCV was in the proper full open (4.5 EMR) position prior to the second start. The total impulse from STDV open to STDV open +2.5 seconds was 196,139 lbf-s.

### 7.7 S-IVB MAINSTAGE PERFORMANCE FOR SECOND BURN

The propulsion reconstruction analysis showed that the stage performance during mainstage operation was satisfactory. A comparison of predicted and actual performance of thrust, specific impulse, total flowrate, and MR versus time is shown in Figure 7-9. Table 7-2 shows the thrust, specific impulse, flowrates, and EMR deviations from the predicted at the STDV open +140-second time slice at standard altitude conditions.

Table 7-2. S-IVB Steady State Performance - Second Burn  
(STDV Open +140-Second Time Slice at Standard Altitude Conditions)

PARAMETER	PREDICTED	RECONSTRUCTION	FLIGHT DEVIATION	PERCENT DEVIATION FROM PREDICTED
Thrust, lbf	205,637	206,807	1,170	0.57
Specific Impulse, lbf-s/lbm	429.5	429.5	0	0
LOX Flowrate, lbm/s	397.55	399.98	2.43	0.61
Fuel Flowrate, lbm/s	81.22	81.49	0.22	0.33
Engine Mixture Ratio, LOX/Fuel	4.895	4.909	0.014	0.28

Thrust, specific impulse, and EMR were well within the predicted bands. The thrust and propellant flowrates were slightly higher than nominal. The higher thrust and flowrates during second burn are attributed to the same reason as for first burn.

The second burn time was 341.9 seconds which was 2.4 seconds less than predicted. This difference is primarily due to the slightly higher S-IVB

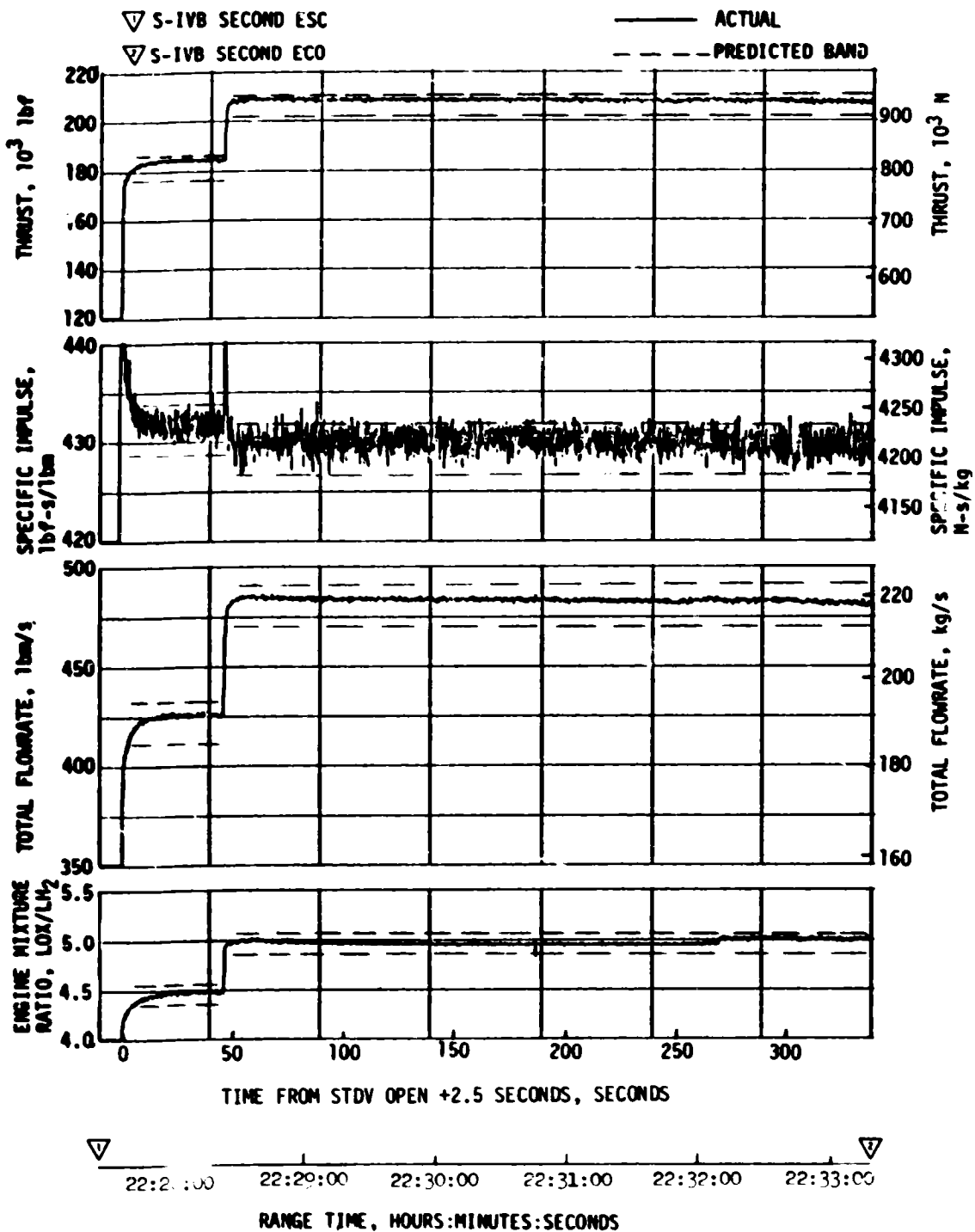


Figure 7-9. S-IVB Steady State Performance - Second Burn

performance and lighter second burn vehicle mass. The total impulse from STDV open +2.5 seconds to ECO was  $69.33 \times 10^6$  lbf-s which was 40,000 lbf-s less than predicted.

The engine helium control system performed satisfactorily during mainstage operation. The engine control bottle was connected to the stage ambient repressurization bottles, which resulted in only a small pressure decay. An estimated 1.1 lbm of helium was consumed during second burn.

### 7.7.1 Mainstage Prediction Technique

The AS-511 flight prediction was revised prior to flight to incorporate the results of the AS-510 flight evaluation. The "old" and "new" mainstage average performance levels are compared to AS-511 reconstructed performance levels in Table 7-3. The changes to the prediction were caused primarily by the following:

Table 7-3. S-IVB Engine Mainstage Performance Averages\*

PARAMETER	5.0 EMR - 1st BURN			RECONSTRUCTED MINUS PREDICTED		4.5 EMR - 2nd BURN			RECONSTRUCTED MINUS PREDICTED	
	PREDICTED		RECONSTRUCTION	OLD	NEW	PREDICTED		RECONSTRUCTION	OLD	NEW
	OLD	NEW				OLD	NEW			
Thrust, lbf	205,065	206,937	207,463	2,398	526	181,947	181,758	182,921	974	1,163
Specific Impulse, lbf-s/lbm	427.8	429.3	429.8	2.0	0.5	429.9	431.3	432.4	2.5	1.1
LOX Flowrate, lbm/s	398.98	401.03	401.61	2.63	0.58	345.27	344.07	345.21	-0.06	1.14
Fuel Flowrate, lbm/s	80.33	81.05	81.13	0.80	0.08	76.94	77.39	77.81	0.87	0.42
Engine Mixture Ratio, LOX/Fuel	4.97	4.95	4.95	0.22	0	4.50	4.45	4.44	-0.06	-0.01

\*Averages calculated from STDV Open +2.5 seconds.

- The prediction was changed to reflect the specific impulse/mixture ratio correlation from the engine contractor logbook. Recent studies indicated that the specific impulse correlation as quoted in the logbook, has been in good agreement with the observed flight data.
- The assembly methods and tolerances associated with the MRCV position were reviewed. The results indicated that the true nominal at the high stop position (5.0 EMR) is 30.4 degrees rather than 30.0 degrees; the true nominal for the low stop position (4.5 EMR) is 11.5 degrees rather than 12.5 degrees. The AS-511 prediction incorporated these new nominal values.
- The AS-511 stage acceptance test data (Figure 7-10) after ESC + 420 seconds was used for the "old" 5.0 EMR flight prediction. However, further analysis indicated that a performance shift occurred at this time and that the performance level prior to the 4.5 EMR operation was more typical. Also, past flight data more nearly corresponds to the acceptance test 5.0 EMR level prior to operation at the 4.5 EMR level, therefore the earlier in-run data was used for the "new" 5.0 EMR flight prediction for AS-511.

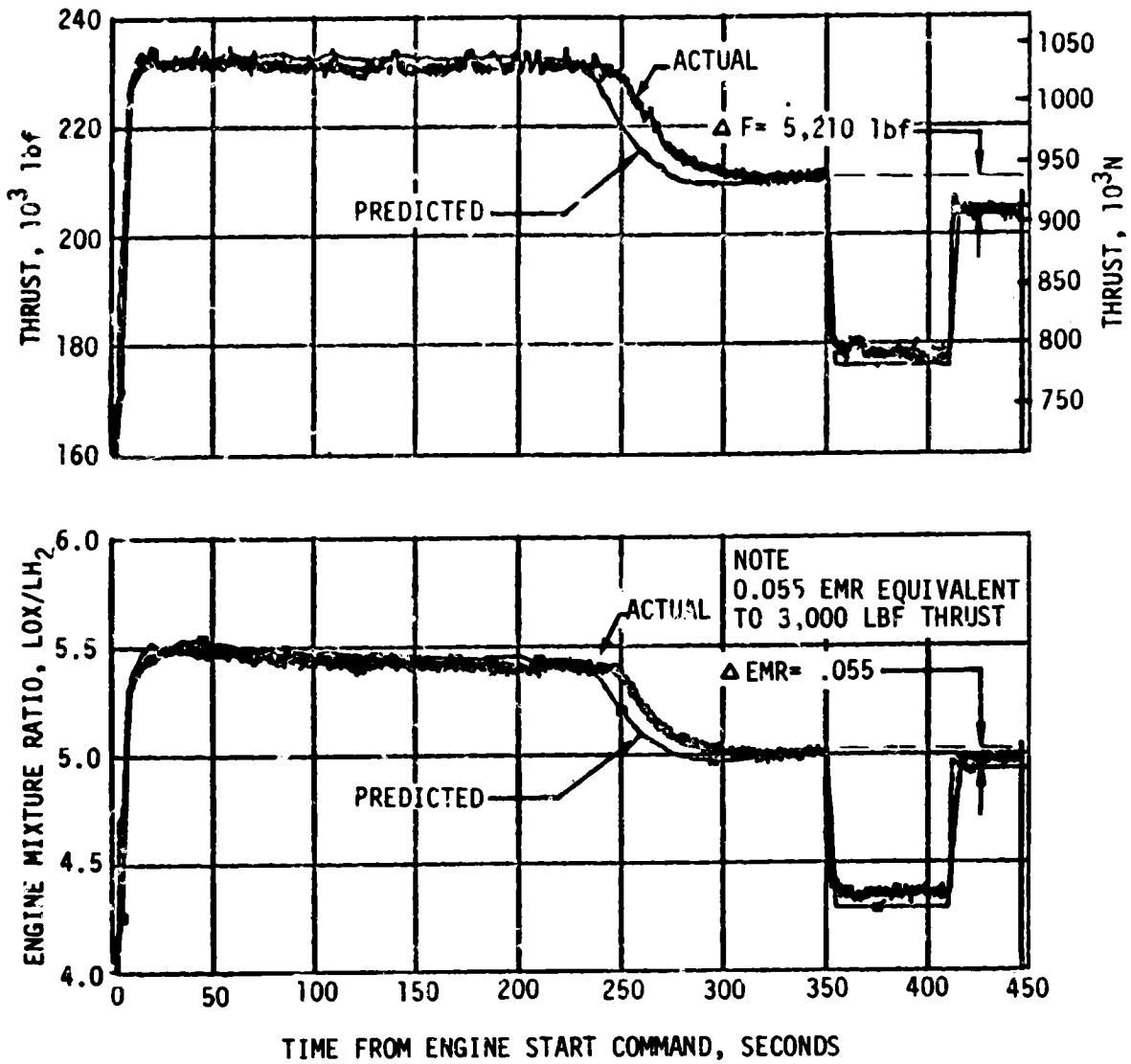


Figure 7-10. S-IVB Engine Steady State Performance During Stage Acceptance Test

- d. The engine in-run trends were changed to reflect previous flight data at 5.0 EMR. Previous predictions used the in-run trends as observed during the stage acceptance firing at 5.5 EMR.

The AS-511 flight 5.0 EMR prediction was, therefore, generated based on the established stage acceptance test power level at ESC + 328 seconds and engine contractor acceptance test data. The 4.5 EMR power level was based on the acceptance test data at ESC + 380 seconds and engine contractor acceptance test data. It should be noted that the engine contractor acceptance tests did not include the rotated PU valve baffle. Modification of the PU valve occurred between the engine contractor test series and the stage acceptance test. Consequently, the stage acceptance test provided a better EMR reference value for the prediction.

A comparison between the "old" and "new" reconstructed minus predicted values from Table 7-3 show that in general the "new" method of prediction provides much better agreement with reconstructed.

#### 7.8 S-IVB SHUTDOWN TRANSIENT PERFORMANCE FOR SECOND BURN

S-IVB second ECO was initiated at 9558.41 seconds (02:39:18.41) by a guidance velocity cutoff command. The ECO transient was satisfactory. The total cutoff impulse to zero thrust was 46,667 lbf-s which was 1674 lbf-s lower than the nominal predicted value of 48,341 lbf-s and within the  $\pm 4,100$  lbf-s predicted band. Cutoff occurred with the MRCV in the 5.0 EMR position.

#### 7.9 S-IVB STAGE PROPELLANT MANAGEMENT

A comparison of propellant masses at critical flight events, as determined by various analyses, is presented in Table 7-4. The best estimate full load propellant masses were 0.12 percent greater for LOX and 0.07 percent less for LH<sub>2</sub> than predicted. This deviation was well within the required loading accuracy.

Extrapolation of best estimate residuals data to depletion, using the propellant flowrates, indicated that a LOX depletion would have occurred approximately 8.24 seconds after second burn velocity cutoff.

During first burn, the pneumatically controlled two position Mixture Ratio Control Valve (MRCV) was positioned at the closed position for start and remained there, as programmed, for the duration of the burn.

The MRCV was commanded to the 4.5 EMR position 119.9 seconds prior to second ESC. The MRCV moved to the 4.5 EMR position when it received engine pneumatic power at ESC +0.6 second. The MRCV took less than 250 milliseconds to reach the open (4.5 EMR) position.



Table 7-4. S-IVB Stage Propellant Mass History

EVENT	UNITS	PREDICTED		PU INDICATED (CORRECTED)		PU VOLUMETRIC		FLOW INTEGRAL		BEST ESTIMATE	
		LOX	LH <sub>2</sub>	LOX	LH <sub>2</sub>	LOX	LH <sub>2</sub>	LOX	LH <sub>2</sub>	LOX	LH <sub>2</sub>
S-IC Liftoff	LBM	195,000	43,720	195,009	43,598	195,474	43,858	194,770	43,677	195,266	43,683
First S-IVB ESC	LBM	194,997	43,719	195,009	43,598	195,474	43,858	194,770	43,677	195,266	43,682
First S-IVB Cutoff	LBM	138,573	32,184	138,480	32,006	138,940	32,108	138,094	32,095	138,609	32,092
Second S-IVB ESC	LBM	138,421	29,964	138,405	29,908	138,771	30,006	138,019	29,997	138,487	29,971
Second S-IVB Cutoff	LBM	4,038	2,081	3,795	2,300	3,815	2,300	3,839	2,203	3,839	2,203

THE MASSES SHOWN DO NOT INCLUDE MASS BELOW THE MAIN ENGINE VALVES, AS PRESENTED IN SECTION 16.

At second ESC + 56 seconds, the valve was commanded to the closed position (approximately 5.0 EMR) and remained there throughout the remainder of the flight.

## 7.10 S-IVB PRESSURIZATION SYSTEM

### 7.10.1 S-IVB Fuel Pressurization System

The LH<sub>2</sub> pressurization system met all of its operational requirements. The LH<sub>2</sub> pressurization system indicated acceptable performance during prepressurization, boost, first burn, coast phase, and second burn.

The LH<sub>2</sub> tank prepressurization command was received at -96.4 seconds and the tank pressurized signal was received 12.0 seconds later. Following the termination of prepressurization, the ullage pressure reached relief conditions (approximately 31.7 psia) and remained at that level until liftoff, as shown in Figure 7-11. A small ullage collapse occurred during the first 15 seconds of boost. The ullage pressure returned to the relief level by 90 seconds due to self pressurization. A similar ullage collapse occurred at S-IC/S-II separation. The ullage pressure returned to the relief level 30 seconds later. Ullage collapse during boost has been experienced on previous flights and is considered normal.

During first burn, the average pressurization flowrate was approximately 0.69 lbm/s, providing a total flow of 97.6 lbm. Throughout the burn, the ullage pressure was at the relief level, as predicted.

The LH<sub>2</sub> tank was satisfactorily repressurized for restart by the O<sub>2</sub>/H<sub>2</sub> burner. The LH<sub>2</sub> ullage pressure was 31.2 psia at second burn ESC, as shown in Figure 7-12. The average second burn pressurization flowrate was 0.70 lbm/s until step pressurization, when it increased to 1.39 lbm/s.

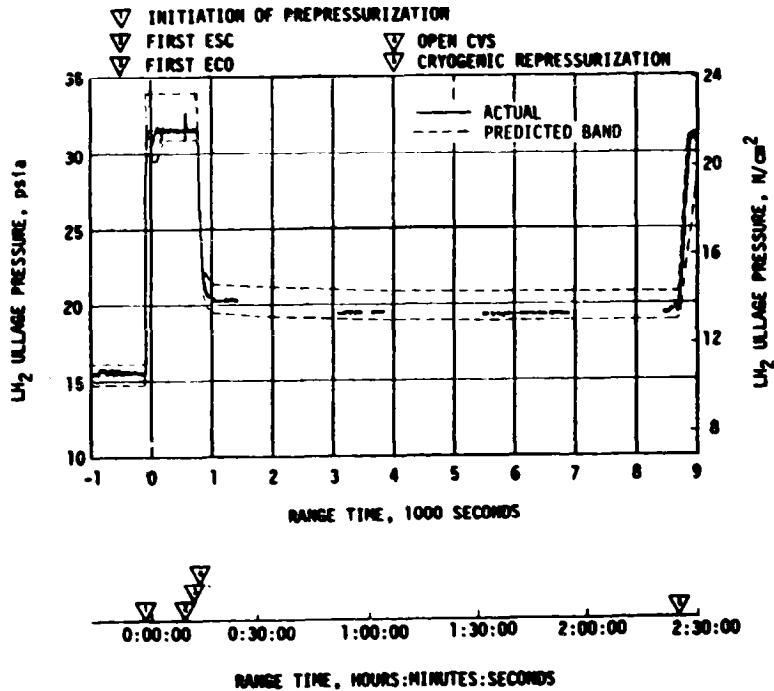


Figure 7-11. S-IVB LH<sub>2</sub> Ullage Pressure - First Burn and Parking Orbit

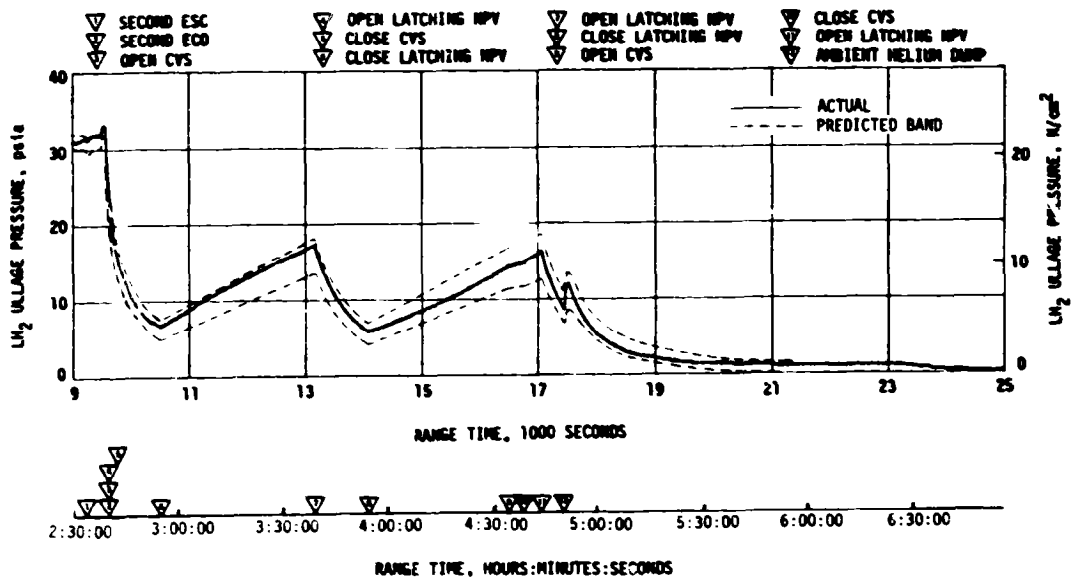


Figure 7-12. S-IVB LH<sub>2</sub> Ullage Pressure - Second Burn and Translunar Coast

This provided a total flow of 287.4 lbm during second burn. The increase in pressurization flowrate resulting from the EMR change increased the ullage pressure to relief pressure (31.7 psia) at second ESC + 106 seconds. The initiation of step pressurization at second ESC + 280 seconds increased the relief level to 32.9 psia.

The LH<sub>2</sub> pump inlet Net Positive Suction Pressure (NPSP) was calculated from the pump interface temperature and total pressure. These values indicated that the NPSP at first burn ESC was 14.1 psi. At the minimum point, the NPSP was 5.0 psi above the minimum required value. Throughout the burn, the NPSP had satisfactory agreement with the predicted values.

The NPSP at second burn STDV open was 5.7 psi, which was 1.2 psi above the minimum required value but lower than that experienced on previous flights. The fuel pump inlet temperature response included upward shifts that are attributed to changes in flow conditions around the temperature probe. Similar temperature responses have been seen on previous flights. When the temperature shifts are accounted for, the NPSP at second burn STDV open is about 7.3 psi and is comparable to the 7.5 psi average value for previous flights. The indicated temperature returned to a nominal level during burn. Figures 7-13 and 7-14 summarize the fuel pump inlet conditions for first and second burns.

#### 7.10.2 S-IVB LOX Pressurization System

LOX tank prepressurization was initiated at -167 seconds and increased the LOX tank ullage pressure from ambient to 40 psia in 14.3 seconds, as shown in Figure 7-15. Three makeup cycles were required to maintain the LOX tank ullage pressure before the ullage temperature stabilized. At -96 seconds the LOX tank ullage pressure increased from 40.0 to 41.5 psia due to fuel tank prepressurization. The pressure then decreased to 40.9 psia at liftoff.

During boost there was a nominal rate of ullage pressure decay caused by an acceleration effect and ullage collapse. No makeup cycles can occur because of an inhibit until after Timebase 4 (T4). LOX tank ullage pressure was 36.5 psia just prior to ESC and was increasing at ESC due to a makeup cycle.

During first burn, five over-control cycles were initiated, including the programmed over-control cycle initiated prior to ESC. The LOX tank pressurization flowrate variation was 0.24 to 0.31 lbm/s during under-control system operation. This variation is normal and is caused by temperature effects. Heat exchanger performance during first burn was satisfactory.

The LOX NPSP calculated at the interface was 21.7 psi at the first burn ESC. This was 8.9 psi above the NPSP minimum requirement for start. The

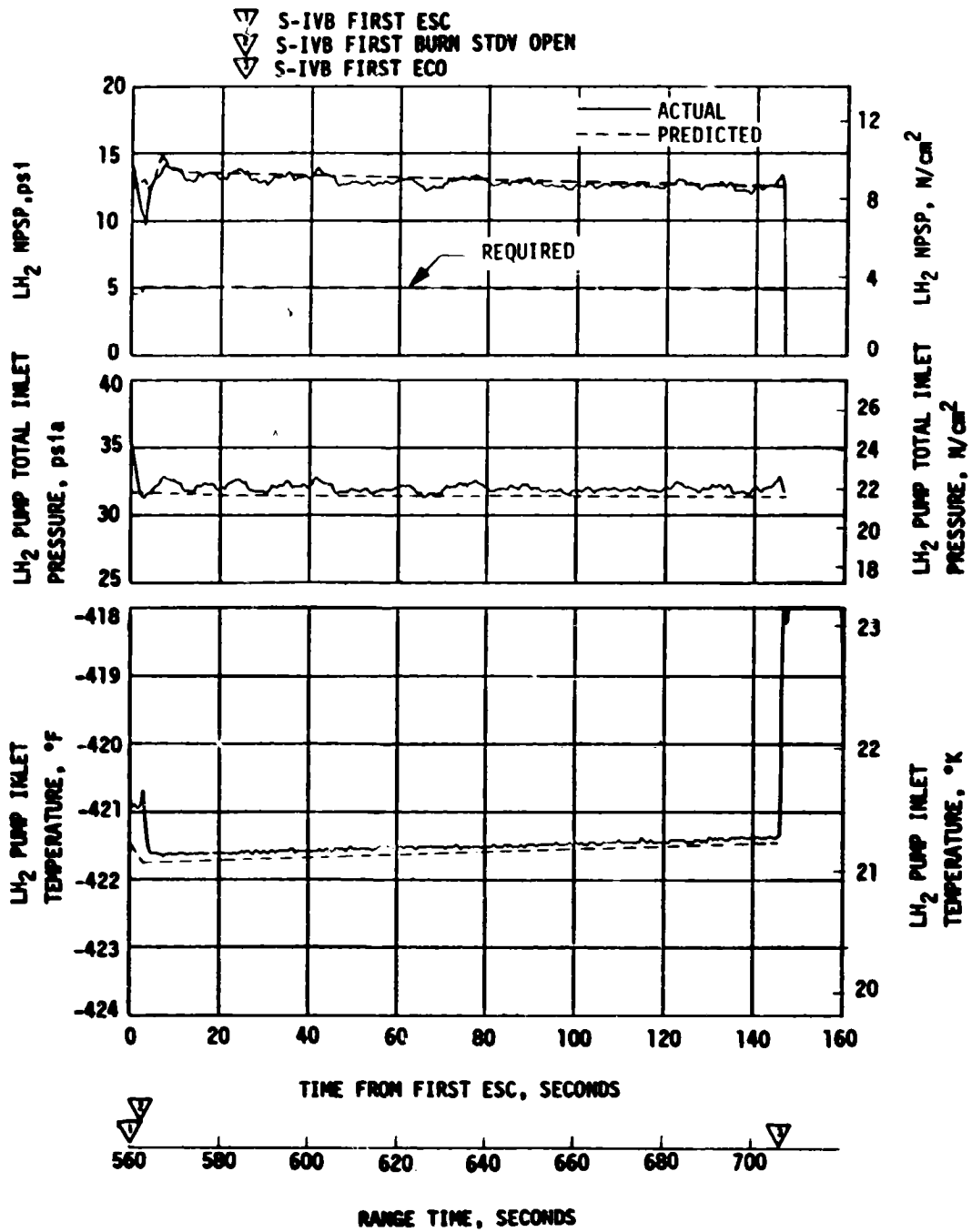


Figure 7-13. S-IVB Fuel Pump Inlet Conditions - First Burn

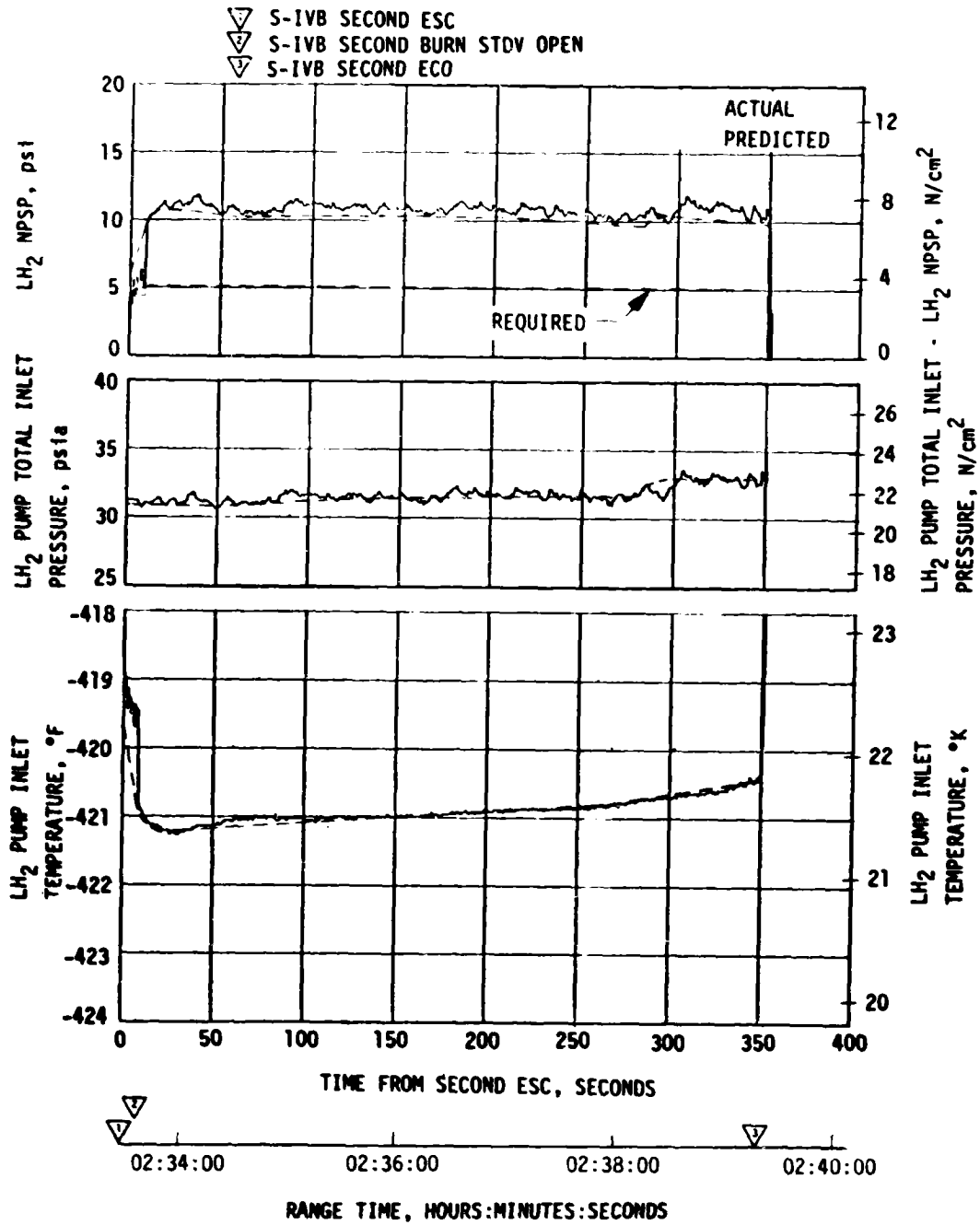


Figure 7-14. S-IVB Fuel Pump Inlet Conditions - Second Burn

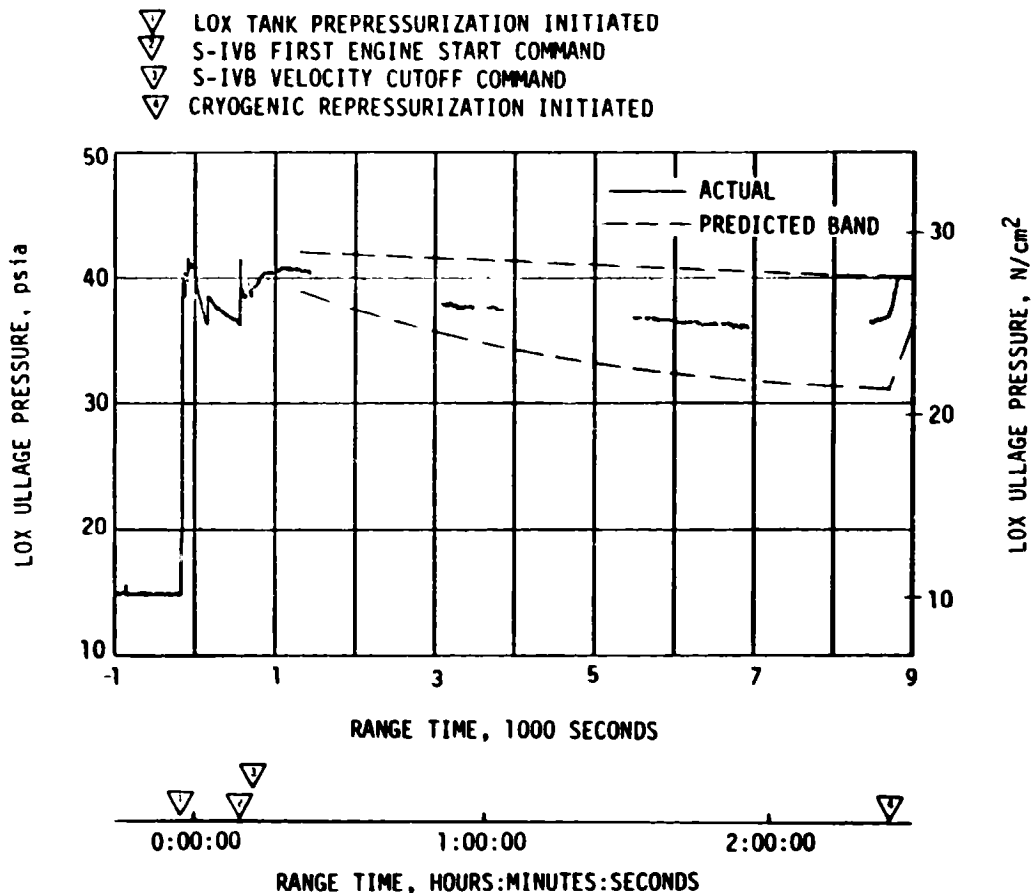


Figure 7-15. S-IVB LOX Tank Ullage Pressure - First Burn and Earth Parking Orbit

LOX pump static interface pressure during first burn follows the cyclic trends of the LOX tank ullage pressure.

During orbital coast, the LOX tank ullage pressure experienced a decay similar to that experienced on the AS-510 flight. This decay was within the predicted band, and was not a problem.

On AS-511 the vehicle pitch rate at insertion was reduced from the AS-510 value in order to minimize sloshing that resulted in LOX venting. No liquid was vented. Mass addition to the ullage from LOX evaporation was minimal and the ullage pressure stayed below the relief range. For additional information, see Section 10.4.2.

Repressurization of the LOX tank prior to second burn was required and was satisfactorily accomplished by the O<sub>2</sub>/H<sub>2</sub> burner. The tank ullage pressure was 40.0 psia at second ESC and satisfied the engine start requirements.

Pressurization system performance during second burn was satisfactory. There was one over-control cycle, which was nominal. Helium flowrate varied between 0.32 and 0.39 lbm/s. Heat exchanger performance was satisfactory.

The LOX NPSP calculated at the engine interface was 22.5 psi at second burn ESC. This was 10.7 psi above the minimum required NPSP for second engine start. At all times during second burn, NPSP was above the required level. Figures 7-16 and 7-17 summarize the LOX pump conditions for first burn and second burn, respectively. The LOX pump run requirements for first and second burns were satisfactorily met.

The cold helium supply was adequate to meet all flight requirements. At first burn ESC, the cold helium spheres contained 375 lbm of helium. At the end of second burn, the helium mass had decreased to 152 lbm. Figure 7-18 shows helium supply pressure history.

#### 7.11 S-IVB PNEUMATIC CONTROL PRESSURE SYSTEM

The stage pneumatic system performed satisfactorily during all phases of the mission. The pneumatic sphere pressure was 2450 psia at initiation of safing.

#### 7.12 S-IVB AUXILIARY PROPULSION SYSTEM

The S-IVB Auxiliary Propulsion System (APS) provided attitude control throughout the mission. The Flight Control Computer (FCC) was shut off at approximately 21,338 seconds (05:55:38). The APS ullage engines provided thrust for propellant settling following first J-2 engine cutoff and prior to second J-2 engine start, and for S-IVB/CSM evasive burn and first lunar impact velocity change requirements. Both Module 1 and 2 experienced helium leaks during the mission. Module 1 experienced excessive external helium leakage from the propellant pressurization system and Module 2 experienced internal leakage from the high pressure side to the low pressure side of the propellant pressurization system.

##### 7.12.1 APS Module 1 Performance

The helium pressurant system, the propellant systems, and thrust system all performed nominally during flight, with the exception of the external helium leak. Figure 7-19 presents the Module 1 helium bottle pressure corrected to 80°F and compares it with the predicted values.

##### 7.12.1.1 Propellant System

The oxidizer and fuel propellant systems performed as expected during the flight. The propellant temperatures ranged from 81°F to 91°F.

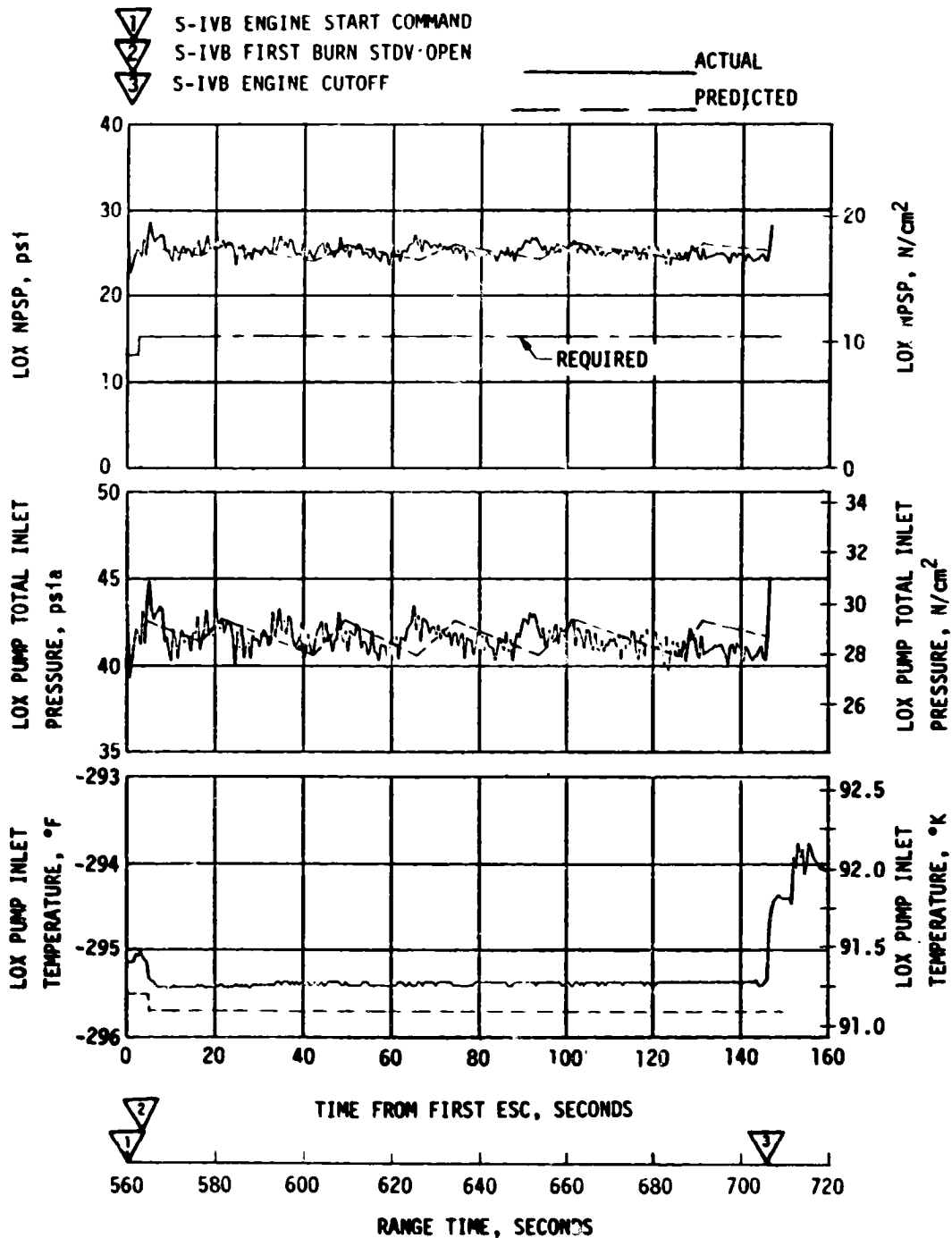


Figure 7-16. S-IVB LOX Pump Inlet Conditions - First Burn



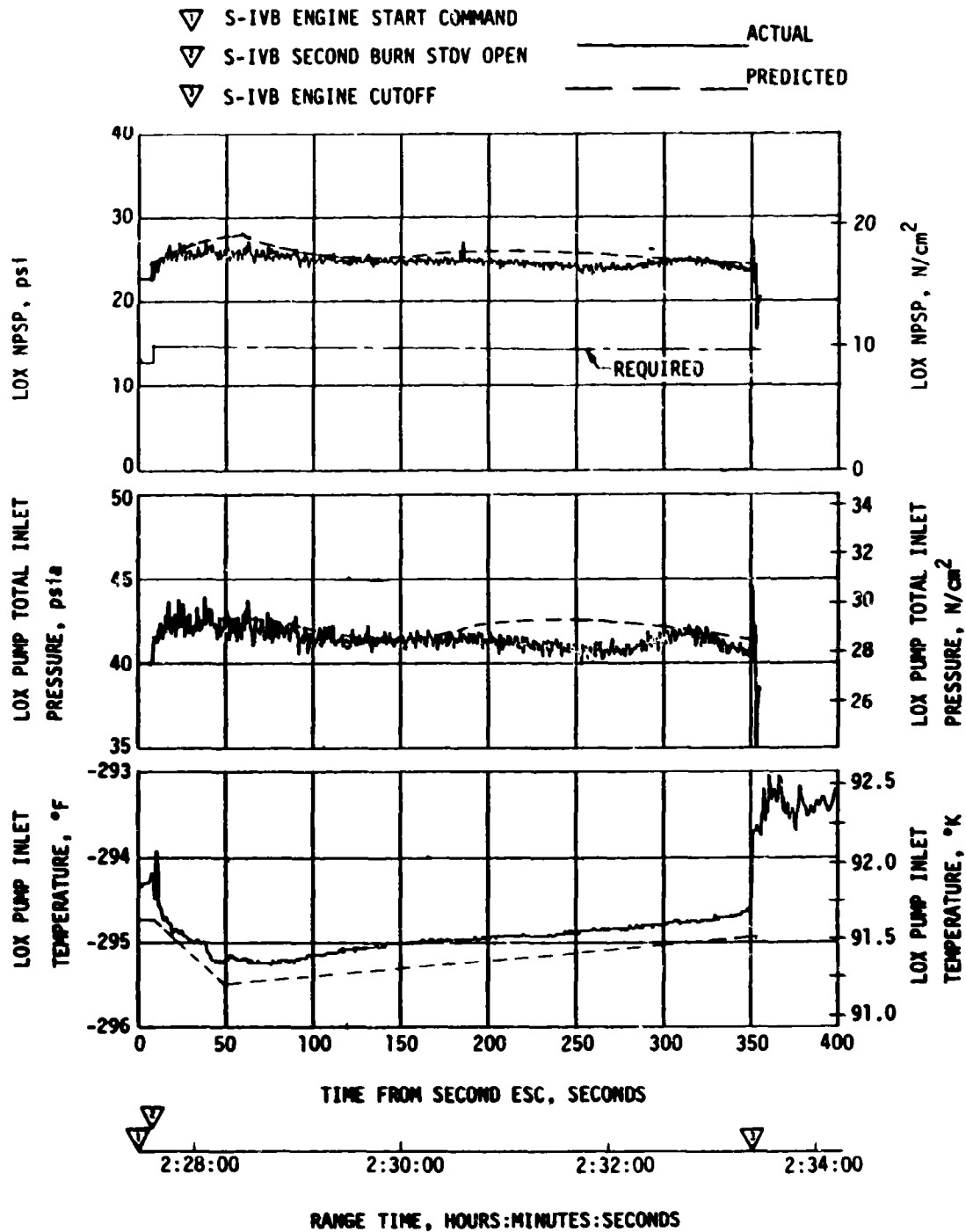


Figure 7-17. S-IVB LOX Pump Inlet Conditions - Second Burn

- ▽ S-IVB FIRST ESC
- ▽ S-IVB FIRST ECO
- ▽ START CRYOGENIC REPRESSURIZATION
- ▽ S-IVB SECOND ESC
- ▽ S-IVB SECOND ECO
- ▽ START COLD HELIUM DUMP
- ▽ END COLD HELIUM DUMP
- ▽ START COLD HELIUM DUMP
- ▽ END COLD HELIUM DUMP
- ▽ START COLD HELIUM DUMP
- ▽ END COLD HELIUM DUMP

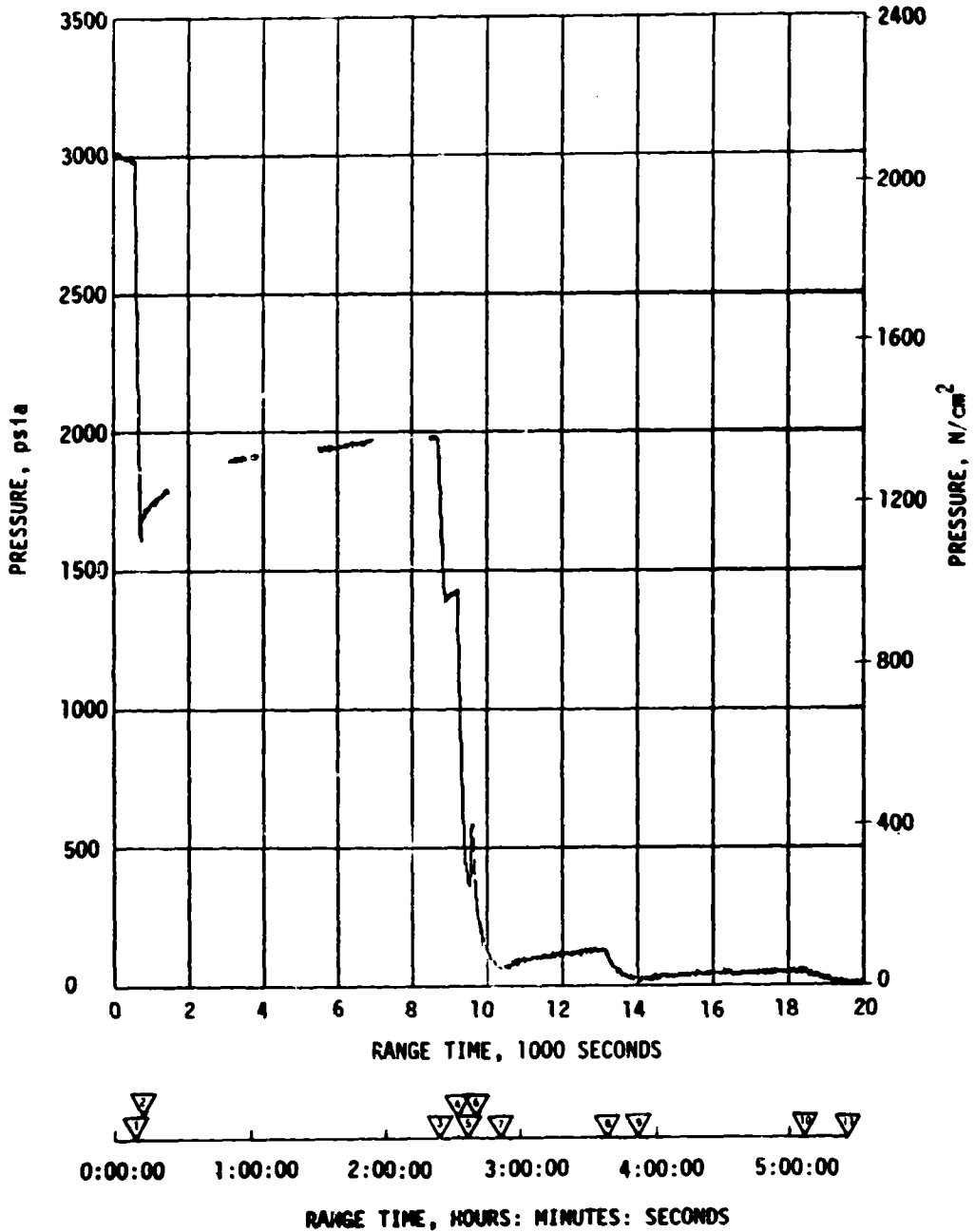


Figure 7-18. S-IVB Cold Helium Supply History

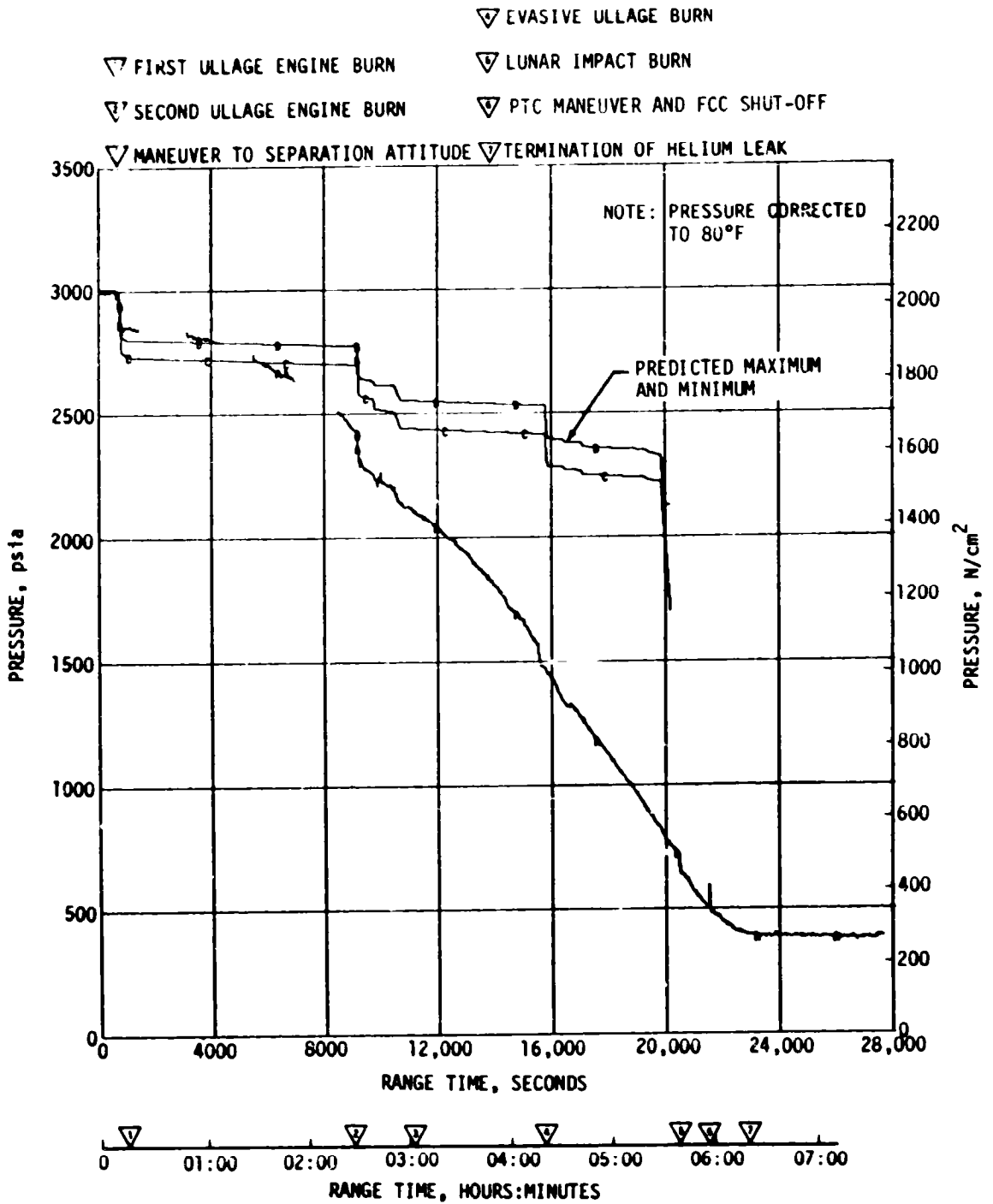


Figure 7-19. APS Module 1 Helium Supply Pressure

The APS Module 1 propellant usage was less than the predicted nominal usage. Table 7-5 presents the APS propellant usage during specific portions of the mission.

Table 7-5. S-IVB APS Propellant Consumption

TIME PERIOD	MODULE NO. 1				MODULE NO. 2			
	OXIDIZER		FUEL		OXIDIZER		FUEL	
	LBM	PERCENT	LBM	PERCENT	LBM	PERCENT	LBM	PERCENT
Initial Load	204.1	100	126.0	100	204.3	100	126.1	100
First Burn (Roll Control)	0.7	0.3	0.4	0.3	0.7	0.3	0.4	0.3
ECO to End of First APS Ullaging (86.7 sec time period)	16.5	7.8	12.1	9.6	13.3	6.5	10.4	8.2
End of First Ullage Burn to Start of Second Ullage Burn	4.6	2.3	2.8	2.2	5.2	2.5	3.2	2.5
Second Ullage Burn (76.7 sec duration)	11.3	5.5	9.0	7.1	15.1	7.4	11.7	9.3
Second Burn (Roll Control)	0.3	0.1	0.2	0.2	0.3	0.1	0.2	0.2
ECO to Start of Evasive Burn at 15,488 sec	11.0	5.4	7.4	5.9	12.7	6.2	7.9	6.3
Evasive Ullage Burn (80 sec duration)	11.6	5.7	8.5	6.7	19.9	9.7	14.9	11.8
From End of Evasive Burn to Start of Lunar Impact Burn at 20,407 sec	6.1	3.0	3.7	2.9	9.5	4.6	5.9	4.7
From Start of Lunar Impact Burn to FCC Cutoff (approximately 21,324 sec)	9.2	4.5	7.1	5.6	13.0	6.4	9.7	7.7
Total Propellant Usage	70.8	34.7	51.2	40.6	89.7	43.9	64.4	51.0

NOTE: The APS propellant consumption presented in this table calculated from APS engine total impulse calculations.

### 7.12.1.2 Helium Pressurization System

An external leak developed at approximately one hour into the mission as shown in Figure 7-19. On previous flights external leakage has been experienced, but never as early in the mission or at so large a rate. Table 7-6 presents a comparison of previous missions in which external helium leakage was experienced. It should also be noted that Module 1 experienced a 38 psi/hour leakage prior to liftoff, which is within the allowable limit of 60 psi/hour. Previous pre-liftoff decay checks have been less than 10 psi/hour. The adequacy of the present prelaunch acceptable leakage rate to allow for the colder inflight environment is being investigated and a proposal to reduce this limit to a value between 0 and 10 psi/hr is in progress.

Figure 7-20 presents the total helium mass leakage during the flight. It should be noted from Figure 7-20 that the leakage appears to terminate at approximately 22,800 seconds (06:20:00) following the Passive Thermal Control (PTC) maneuver.

Table 7-6. APS External Leakage Summary

STAGE NO.	APS MODULE NO.	START TIME (GET)	MAX. LEAKAGE PSI/HR	DURATION
AS-504	2	4 HR 25 MIN	375	*2 HR 35 MIN.
AS-505	1	6 HR 15 MIN	180	**>4 HR 39 MIN.
AS-509	1	5 HR	50	*2 HR 30 MIN.
AS-511	1	1 HR	585	*≈5:20 MIN.

\*LEAKRATE WENT TO APPROXIMATELY ZERO  
 \*\*LEAKRATE CONTINUED TO LOSS OF SIGNAL

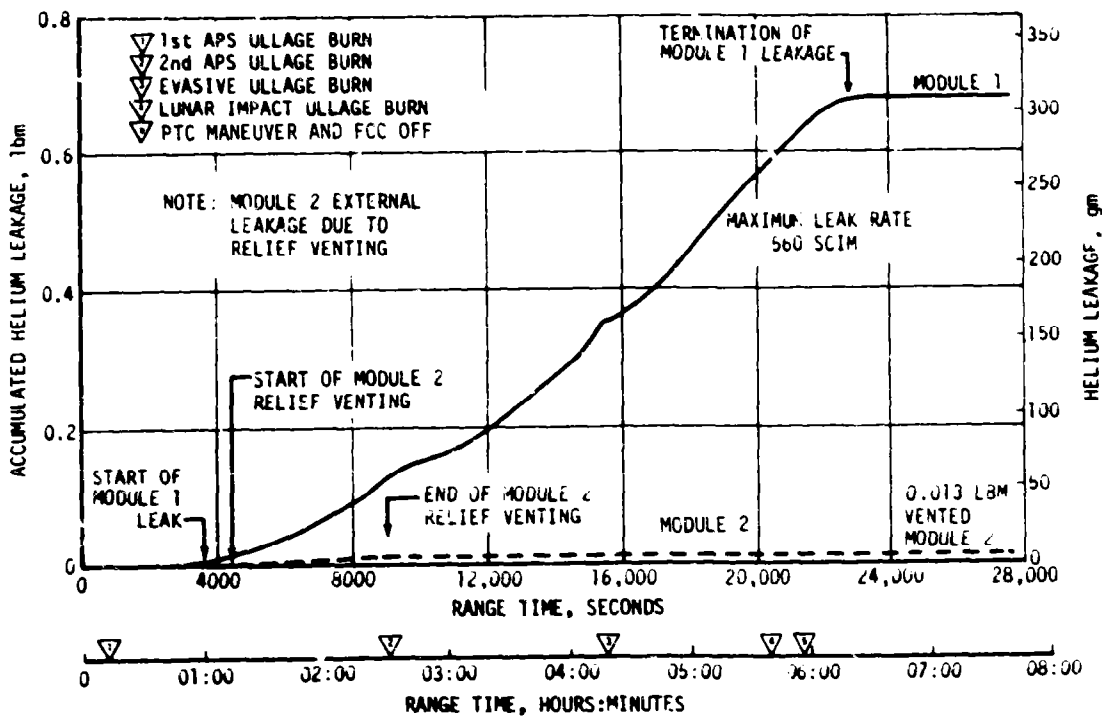


Figure 7-20. S-IVB APS Accumulated Helium Leakage for Modules 1 and 2

#### 7.12.1.3 Results of Failure Investigation

Laboratory tests showed that joints located at bulkhead fittings were temperature sensitive in that at selected torque values the leakage rate increased as the temperature decreased. Similar tests performed on adapter fittings indicated insensitivity to temperature extremes. It was also noted that the bulkhead fitting leaks ceased when the temperatures were increased.

#### 7.12.1.4 APS External Leakage Corrective Action

Corrective action in process includes hardware modifications and procedural changes as follows:

- a. Replace all APS bulkhead fittings with adapter unions.
- b. Replace Teflon "O" rings with K-seals where exposed to propellants.
- c. Replace Teflon "O" rings with Buna-N "O" rings where compatibility is acceptable.
- d. Connect APS helium system to stage helium supply to provide backup capability (Figure 7-22).
- e. Perform 3000 psi pressure leak checks of pressurization system in KSC laboratory and on the pad prior to propellant tank connection.
- f. Reduce allowable pressure decay rate after propellant loading.

#### 7.12.1.5 Thrust System

The performance of the attitude control thrusters and ullage thruster was satisfactory throughout the mission. The thrust chamber pressures ranged from 95 to 102 psia. The ullage thruster successfully completed three sequenced burns of 86.7, 76.7 and 80 seconds duration; and one ground commanded lunar impact burn of 54 seconds duration at 20,407.2 seconds (05:40:07.2). The PTC maneuver was successfully initiated prior to Flight Control Computer (FCC) shutoff.

#### 7.12.2 APS Module 2 Performance

The internal Helium leakage from the high pressure side of the low pressure side of the APS Module 2 propellant pressurization system resulted in

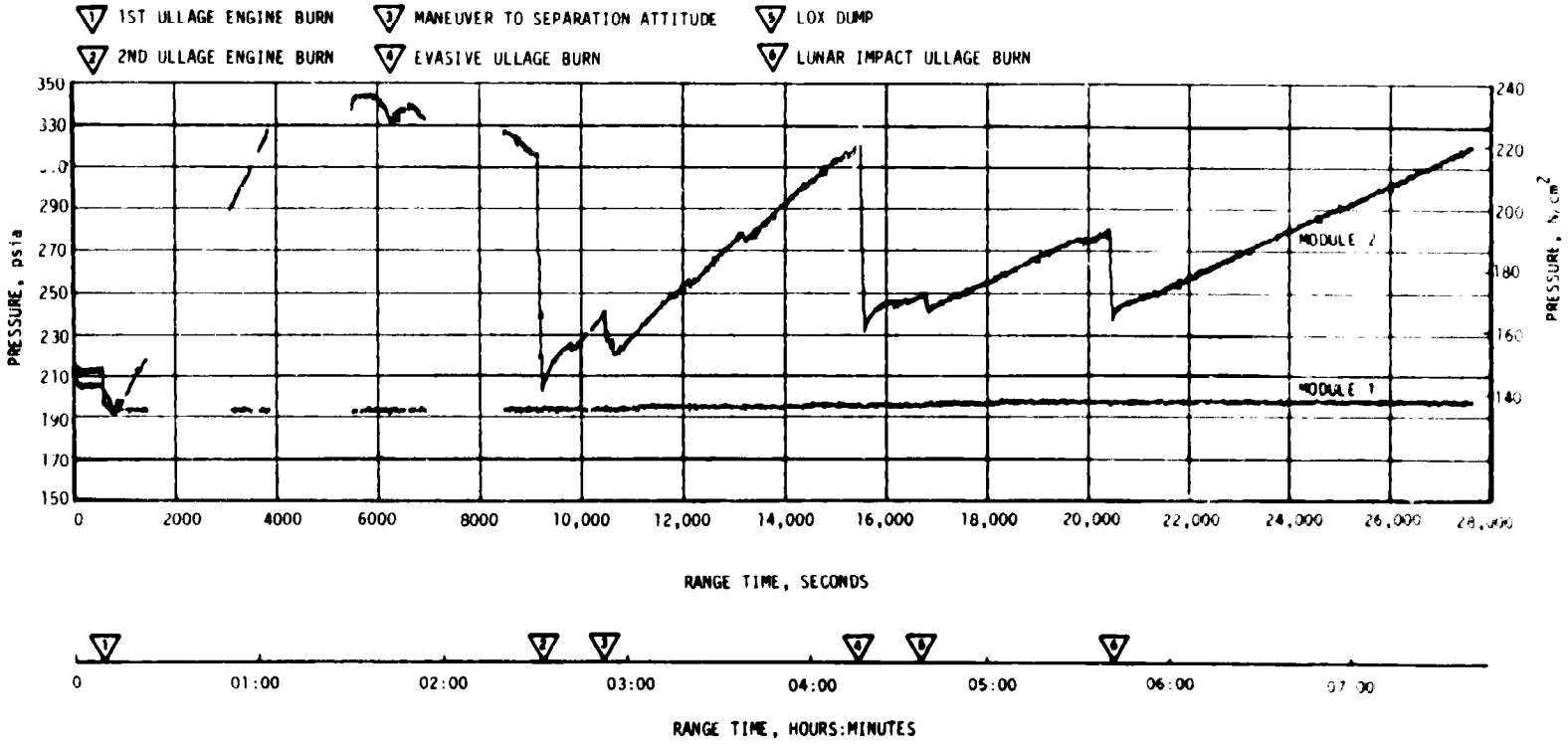


Figure 7-21. APS Regulator Outlet Pressure

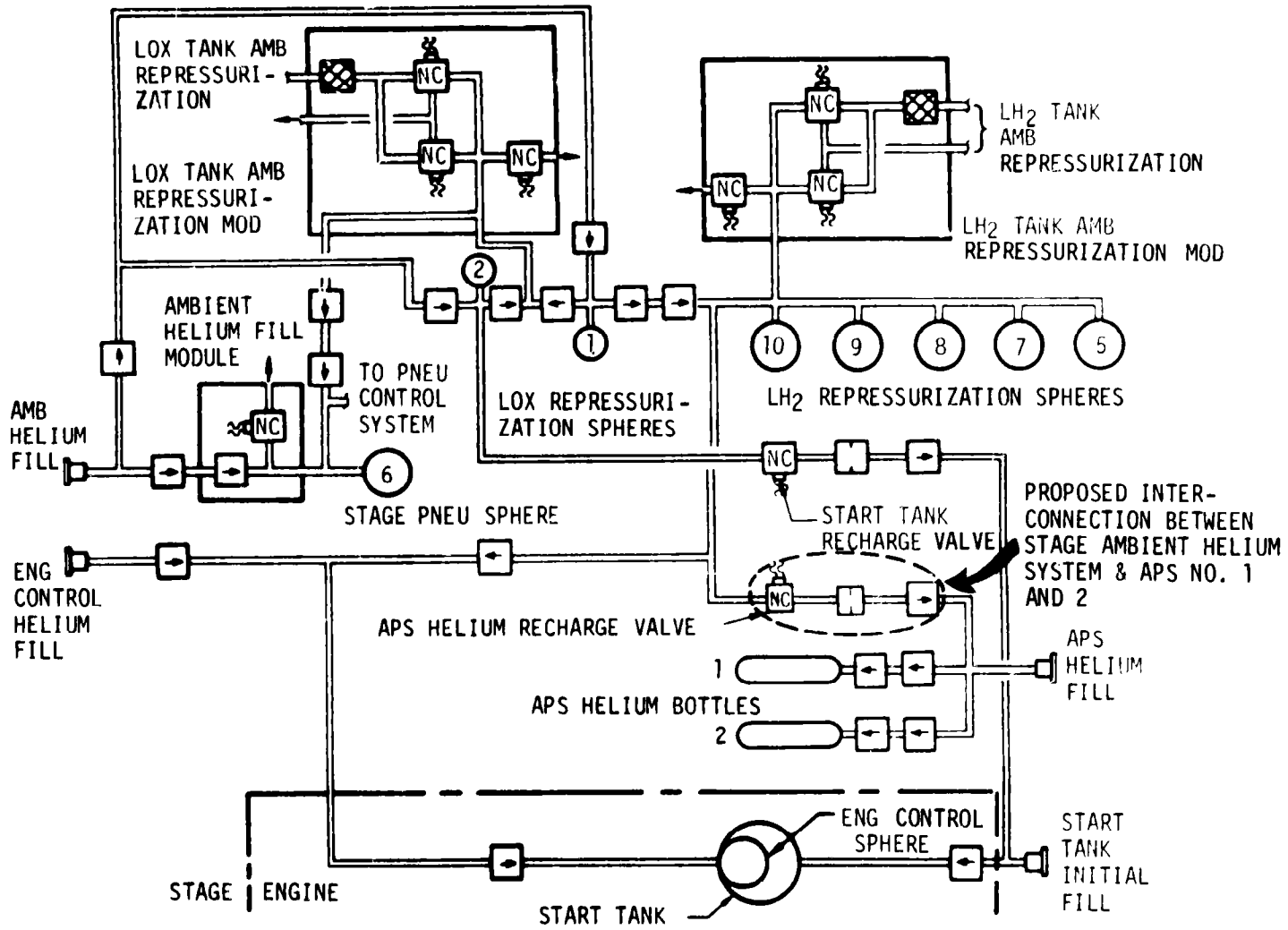


Figure 7-22. S-IVB Ambient Helium Spheres Interconnect Schematic



higher than normal propellant supply pressures and thruster chamber pressures. The greater than nominal thrust from the Module 2 ullage engine created a vehicle pitching moment that required compensating Module 2 pitch engine thrusting. The performance appeared to be consistent with the higher propellant supply pressure.

#### 7.12.2.1 Propellant System

The oxidizer and fuel propellant systems performed as expected during flight. The propellant temperatures ranged from 84 to 110°F. The APS Module 2 propellant usage was slightly above the upper three sigma predicted limit. Module 2 had higher than predicted propellant usage because of higher than nominal ullage engine propellant flow rate resulting from the increased propellant supply pressure and the increased pitch engine thrusting activity. Table 7-5 presents a summary of APS propellant usage.

#### 7.12.2.2 Helium Pressurization System

The internal leakage experienced on Module 2 started at approximately 970 seconds. The internal leakage resulted in a continually decreasing helium bottle pressure (Figure 7-23). The leakage rate corresponded to an equivalent constant orifice diameter of 0.0013 inches with a variation of 10 percent to -27 percent. The regulator discharge pressure increased from the nominal 197 psia at 970 seconds and reached 344 psia, the low pressure module relief valve setting, at approximately 4100 seconds (01:08:20) as shown in Figure 7-21. Figure 7-20 presents a plot of Module 2 external helium loss as a function of time. Venting apparently occurred between the time the ullage pressure reached the relief setting at approximately 4100 seconds (01:08:20) until the start of the second ullage burn at 9135 seconds (02:32:15).

The regulator discharge pressure remained close to relief until the ullage engine burn prior to restart, at which time it dropped to 203 psia. It should be noted that this level is not low enough to result in regulator operation. Following this event, the regulator outlet pressure varied between 220 and 320 psia in response to APS usage until loss of data at 27,640 seconds (07:04:40).

Two possible paths of internal leakage are through the two conoseals in the common mounting block for the helium bottle pressure transducer and the regulator outlet pressure transducer as shown in Figure 7-24, or through the dual regulators as shown in Figure 7-25.

During the launch countdown while pressurizing the APS Module 2 helium sphere at approximately T-8.5 hours the pressure stabilized at 208 psia for approximately six seconds and gradually increased to 212 psia (Figure 7-26). During the same period the Module 1 pressure stabilized

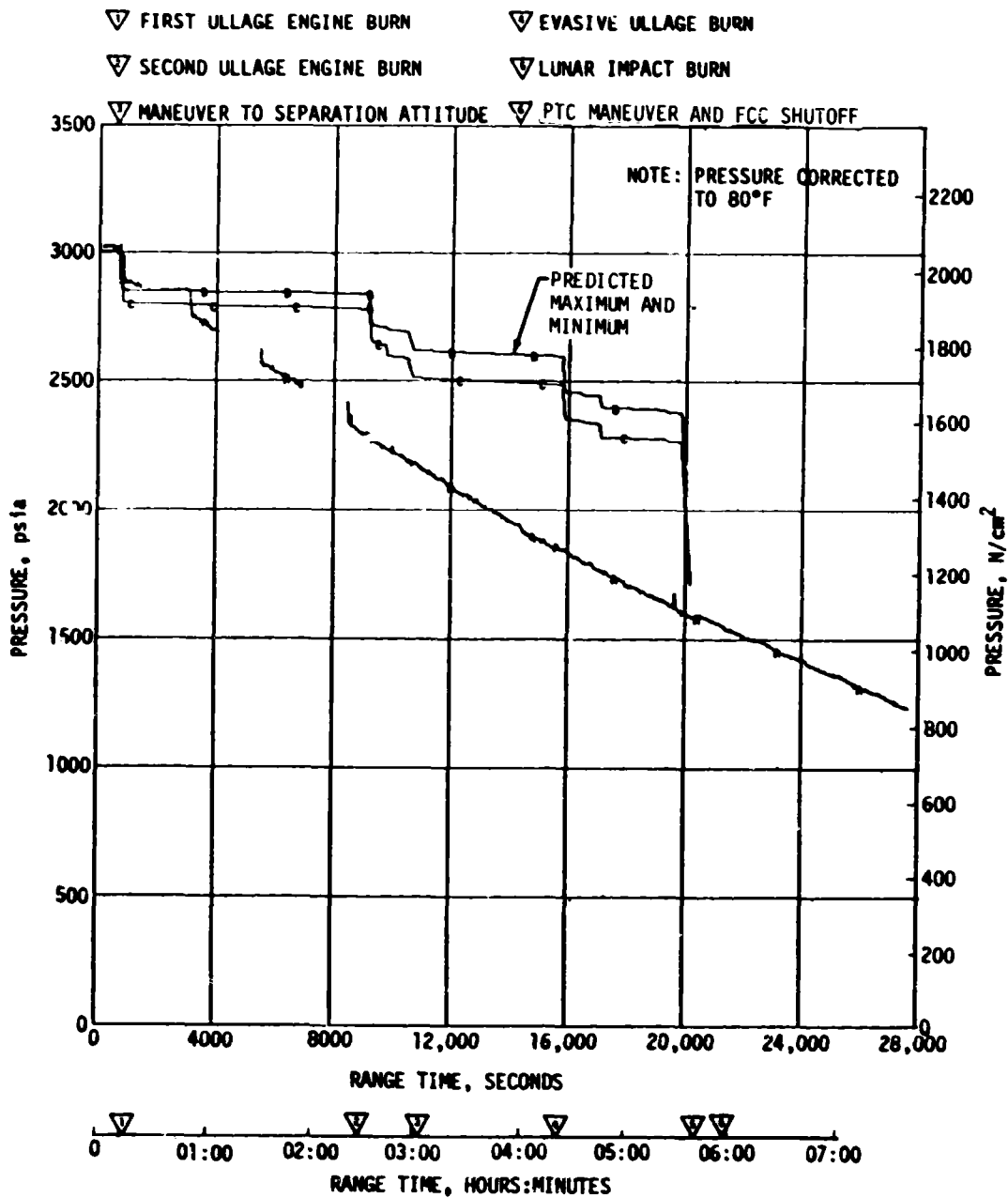


Figure 7-23. APS Module 2 Supply Pressure

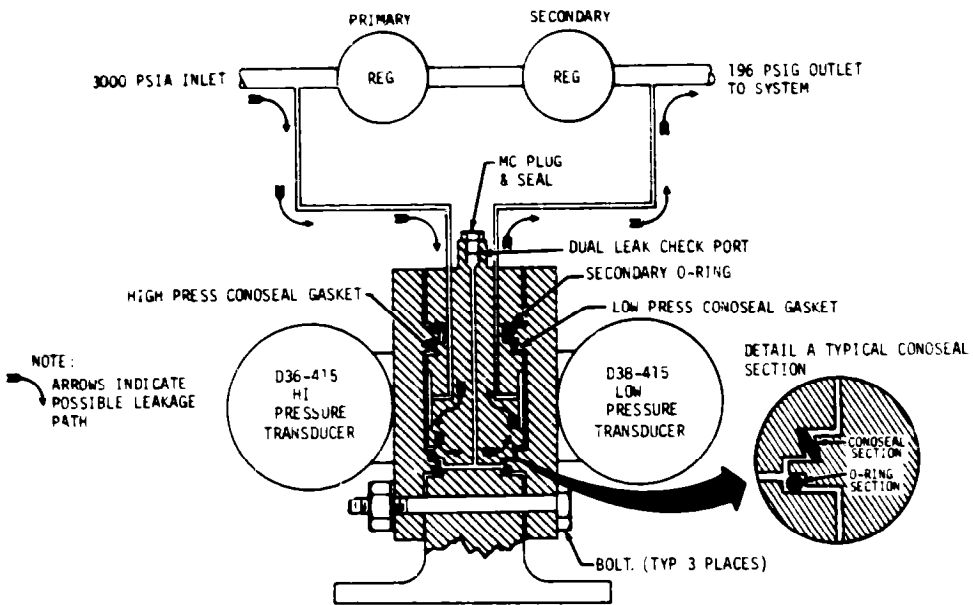


Figure 7-24. APS Helium Bottle/Regulator Discharge Transducer Mounting

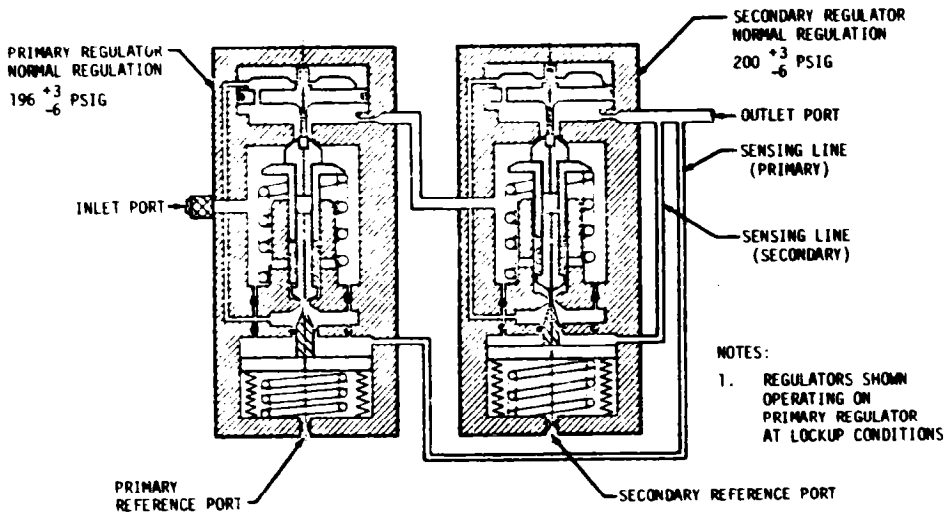


Figure 7-25. APS Helium Pressure Regulator 1B54601

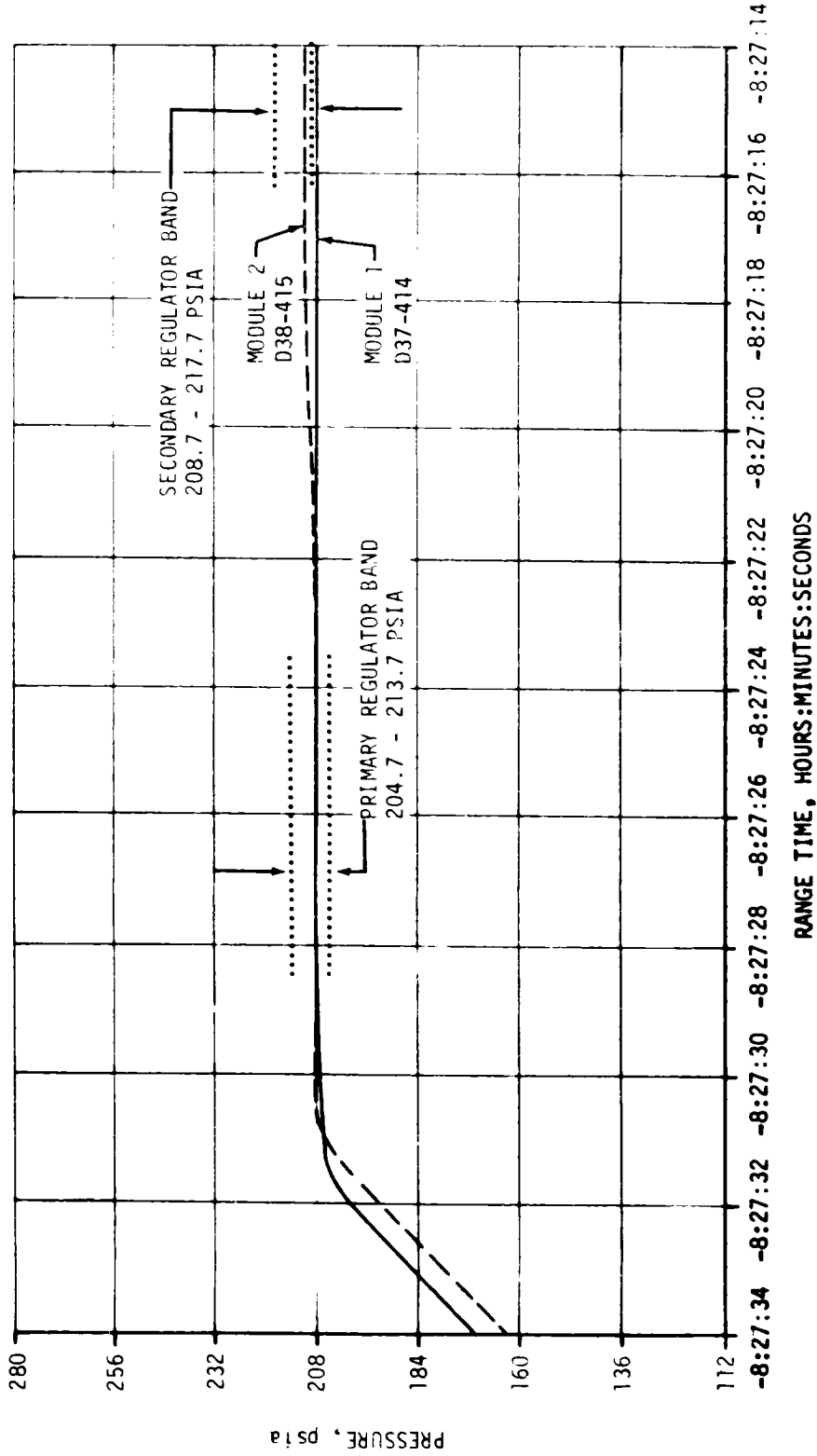


Figure 7-26. APS Helium Regulator Outlet Pressure During Pressurization

and held at 208 psia. Based on postflight data, it has been concluded that the Module 2 regulator first began to regulate on the primary at 208 psia and then shifted to the secondary at 212 psia where it remained throughout the count. AS-506 through AS-510 preflight pressurization data has been examined without revealing similar behavior. The possible cause of the shift from primary to secondary is leakage through the regulator main poppet seat, pilot poppet seat, or body "O" ring seal. The Module 2 pressure remained near the secondary regulator setting as discussed above, except for a slight decrease due to altitude effects (Figure 7-21), during the boost phase of flight until the first ullage engine burn when the regulator outlet pressure decreased to 192 psia and held throughout the burn (Figure 7-27). This occurrence supports the conclusion that the primary regulator was functioning normally, except for leakage, because the primary regulator range is 190 to 199 psia and the secondary regulator range is 194 to 203 psia. Following ullage engine burn the pressure slowly increased to 197 psia where it stabilized for approximately 150 seconds. This increase in regulator pressure can be interpreted as leakage past the primary regulator that results in secondary regulator operation. Subsequent leakage past the secondary regulator then allowed a slow increase in regulator outlet pressure to the relief setting as previously discussed.

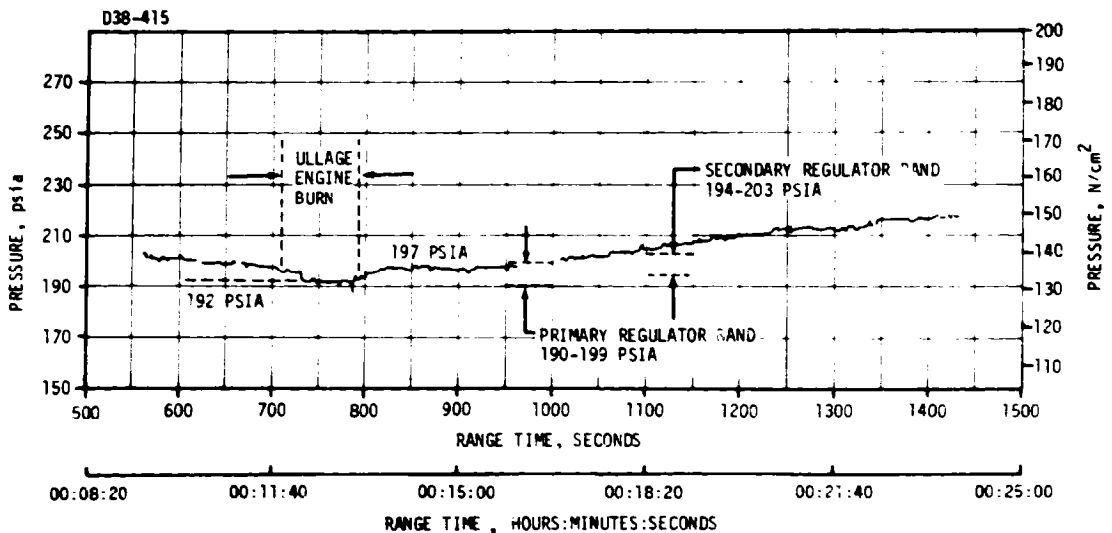


Figure 7-27. APS Module 2 Regulator Outlet Pressure

### 7.12.2.3 APS Internal Leakage Corrective Action

Corrective action in process includes hardware and procedural changes as follows:

- a. Connect APS helium system to stage helium supply to provide backup capability (Figure 7-22). (Same change for external leakage.)

- b. Redesign transducer mounting block. Figure 7-28 shows the new design which replaces the old through bolts with bolts in tapped holes and the leak detection parts redesigned to provide separate leak test ports.
- c. Perform regulator checkout after propellant loading.
- d. Devote closer attention to protect against moisture and particulate contamination of system.
- e. Devote closer attention to regulator outlet pressure during pressurization on launch pad for early detection of primary regulator failure.
- f. Establish regulator outlet pressure as a primary redline measurement.

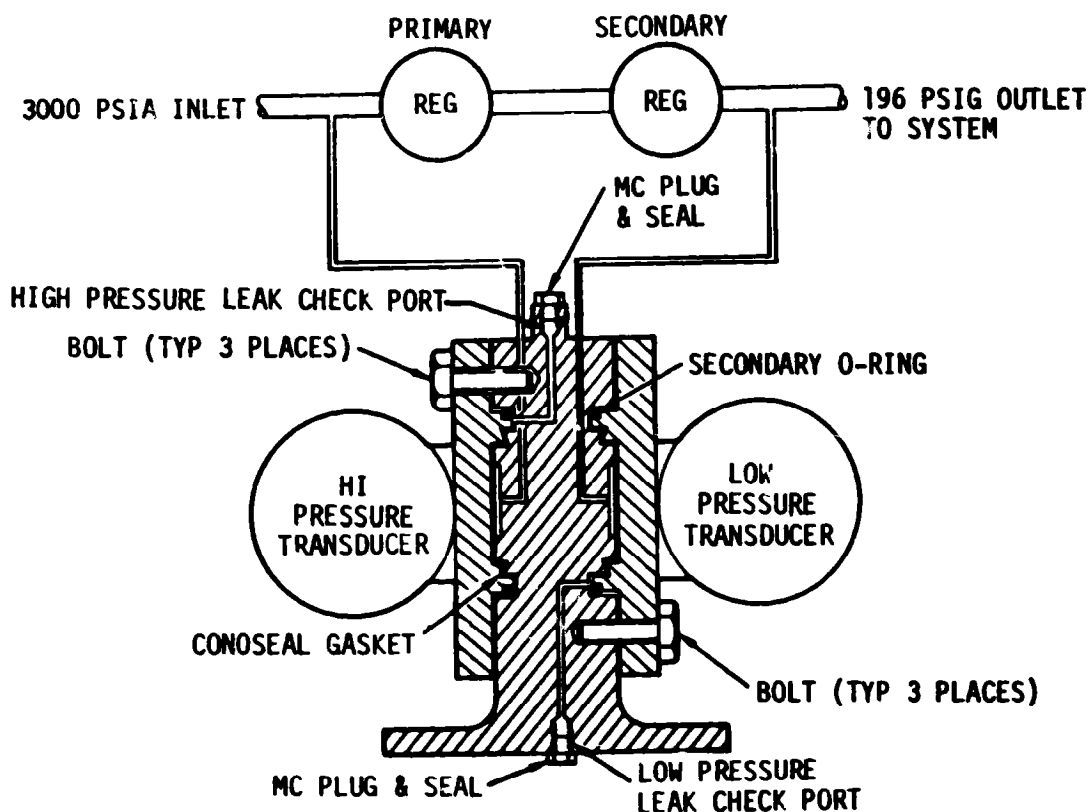


Figure 7-28. APS Helium Bottle/Regulator Discharge Transducer Mounting (Proposed Redesign)

#### 7.12.2.4 Thrust System

The thrusters on Module 2 experienced chamber pressures up to 50 percent above the 100 psia nominal as a result of the high supply pressure. The higher thrusts experienced by the thrusters had no detrimental effect on the performance of the attitude control system. However, the attitude control engines have been qualified over a propellant supply pressure

range of 175 to 275 psia, therefore this mode of operation results in operating the attitude thrusters above the qualification test limits.

The thrust levels of the ullage engine varied with the burn as the supply pressure decreased. The ullage engines have been test fired by Rocketdyne over a propellant supply pressure range of 175 to 375 psia.

### 7.13 S-IVB ORBITAL SAFING OPERATIONS

The S-IVB high pressure systems were safed following J-2 engine cutoff. The thrust developed during the LOX dump was utilized to provide a velocity change for S-IVB lunar impact. The manner and sequence in which the safing was performed is presented in Figure 7-29.

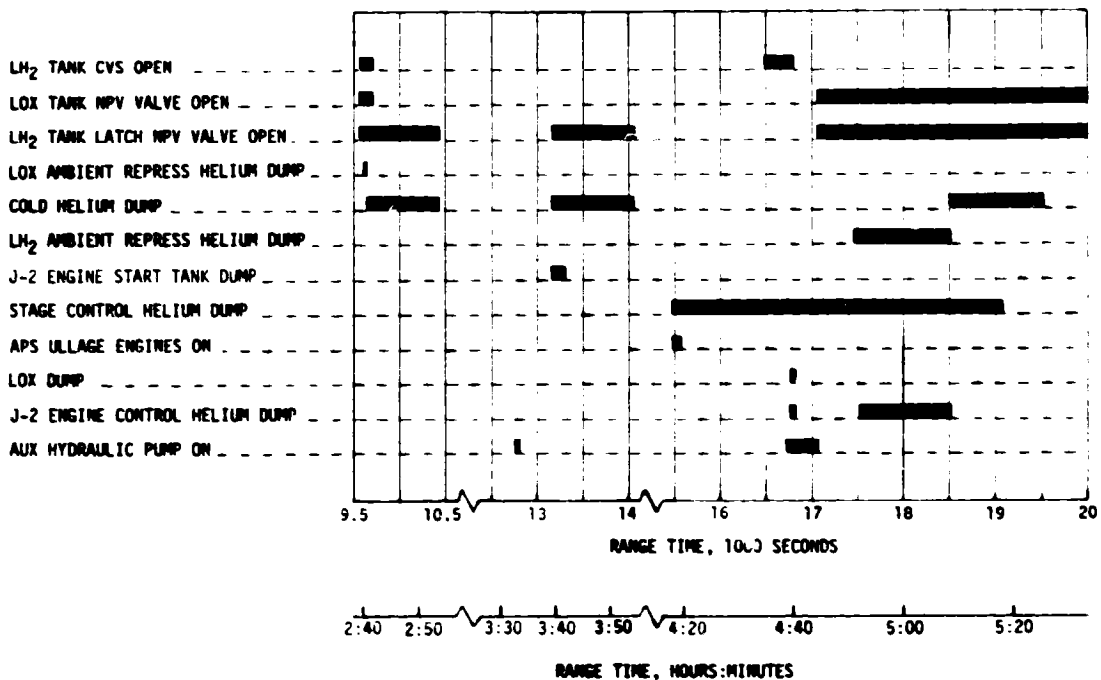


Figure 7-29. S-IVB LOX Dump and Orbital Safing Sequence

#### 7.13.1 Fuel Tank Safing

The LH<sub>2</sub> tank was satisfactorily safed by utilizing both the Nonpropulsive Vent (NPV) and the CVS, as indicated in Figure 7-29. The LH<sub>2</sub> tank ullage pressure during safing is shown in Figure 7-12. At second ECO, the LH<sub>2</sub> tank ullage pressure was 32.9 psia; after three vent cycles, this decayed to zero at approximately 25,000 seconds (06:56:40). The mass of vented GH<sub>2</sub> agrees with the 2203 lbm of residual liquid and approximately 615 lbm of GH<sub>2</sub> in the tank at the end of powered flight.

### 7.13.2 LOX Tank Dumping and Safing

LOX dump performance in thrust, LOX flowrate, oxidizer mass, and LOX ullage pressure is shown in Figure 7-30.

Immediately following second burn cutoff, a programmed 150-second vent reduced the LOX tank ullage pressure from 39.4 to 17.8 psia, as shown in Figure 7-31. Approximately 90 lbm of ullage helium and 65 lbm of GOX were vented overboard. The ullage pressure then rose gradually, due to self-pressurization, to 21.9 psia by the time of initiation of the Transposition, Docking, and Ejection (TD&E) maneuver.

The LOX dump was initiated at 16,767.1 seconds (04:39:27.1) and was satisfactorily accomplished. A steady state liquid flow of 358 gpm was reached in 14 seconds. The LOX residual at the start of dump was 3560 lbm. Calculations indicate that 2288 lbm was dumped. During dump, the ullage pressure decreased from 23.1 to 22.7 psia. A steady state LOX dump thrust of 684 lbf was attained. LOX dump ended at 16,815.1 seconds (04:40:15.1) as scheduled, by closing the Main Oxidizer Valve (MOV). The total impulse before MOV closure was 29,614 lbf-s, resulting in a calculated velocity change of 26.5 ft/sec.

Ullage gas ingestion occurred three times during the LOX dump as a result of LOX sloshing at 16,775 seconds (04:39:36), 16,799 seconds (04:39:59), and 16,813 seconds (04:40:13). The greater than nominal slosh activity was attributed to the additional vehicle maneuver to the optimum LOX dump attitude following the programmed LOX dump maneuver. As a result of the ullage ingestion, liquid flow was impeded and dump performance was decreased. Figure 7-30 shows the effects of ullage gas ingestion on LOX dump thrust, flowrate, and oxidizer mass. Without ullage ingestion 189 lbm additional LOX would have been dumped, resulting in 2294 lbf-s greater impulse and 2.07 ft/sec greater velocity change. Additional information on LOX sloshing is presented in Section 10.4.

At LOX dump termination +242 seconds, the LOX NPV valve was opened and latched. The LOX tank ullage pressure decayed from 23.0 psia at 17,057 seconds (04:44:17) to near zero pressure at approximately 22,000 seconds (06:06:40). Sufficient impulse was derived from the LOX dump, LH2 CVS operation, and APS ullage burn to achieve lunar impact. For further discussion of the lunar impact, refer to Section 17.

### 7.13.3 Cold Helium Dump

A total of approximately 144 lbm of helium was dumped during the three programmed dumps which occurred as shown in Figure 7-29.

### 7.13.4 Ambient Helium Dump

The two LOX ambient repressurization spheres were dumped through the LOX ambient repressurization control module into the LOX tank NPV system for 40 seconds beginning at 9590 seconds (02:39:50). During this dump, the pressure decayed from 2900 psia to approximately 1300 psia.



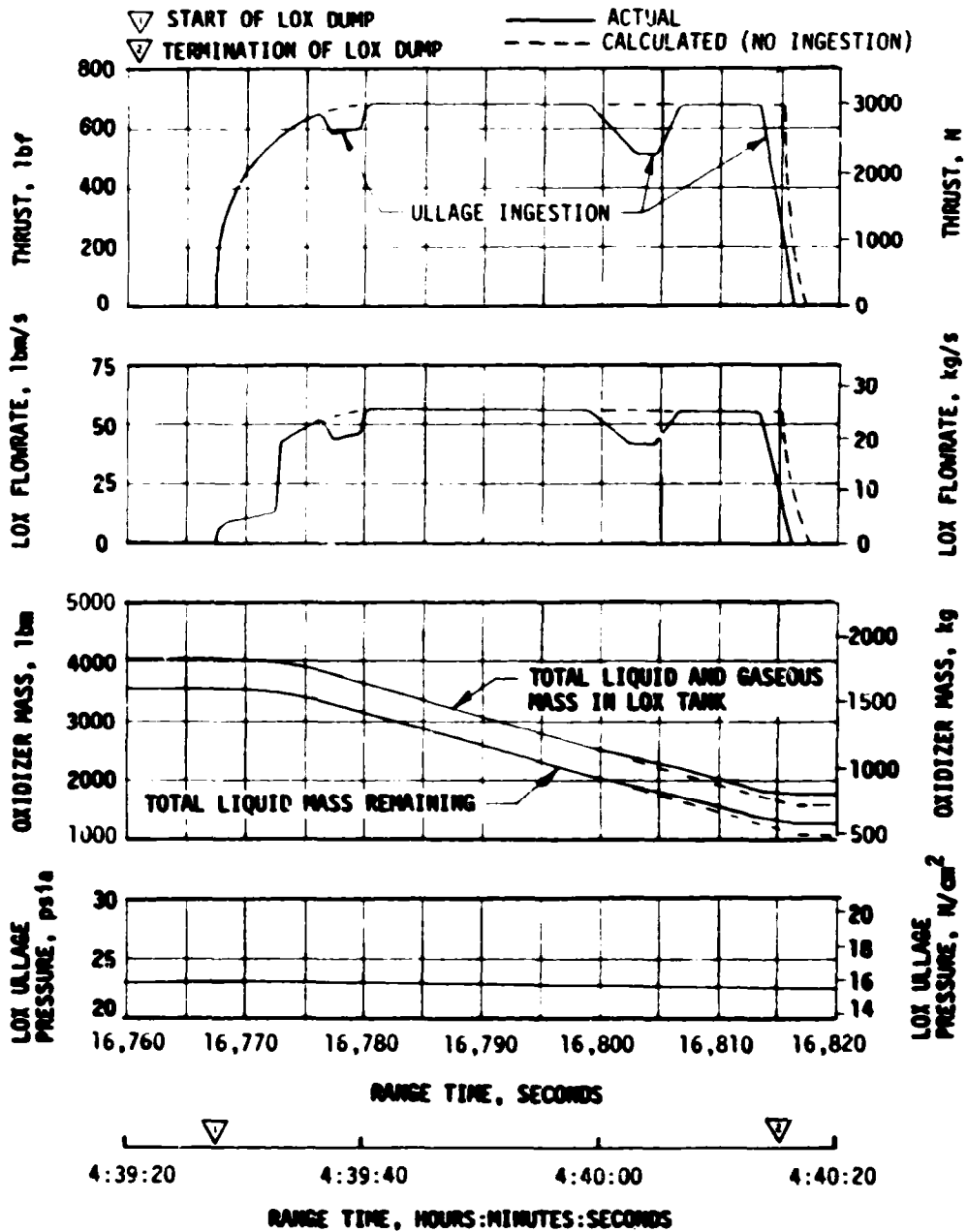


Figure 7-30. S-IVB LOX Dump Parameter Histories

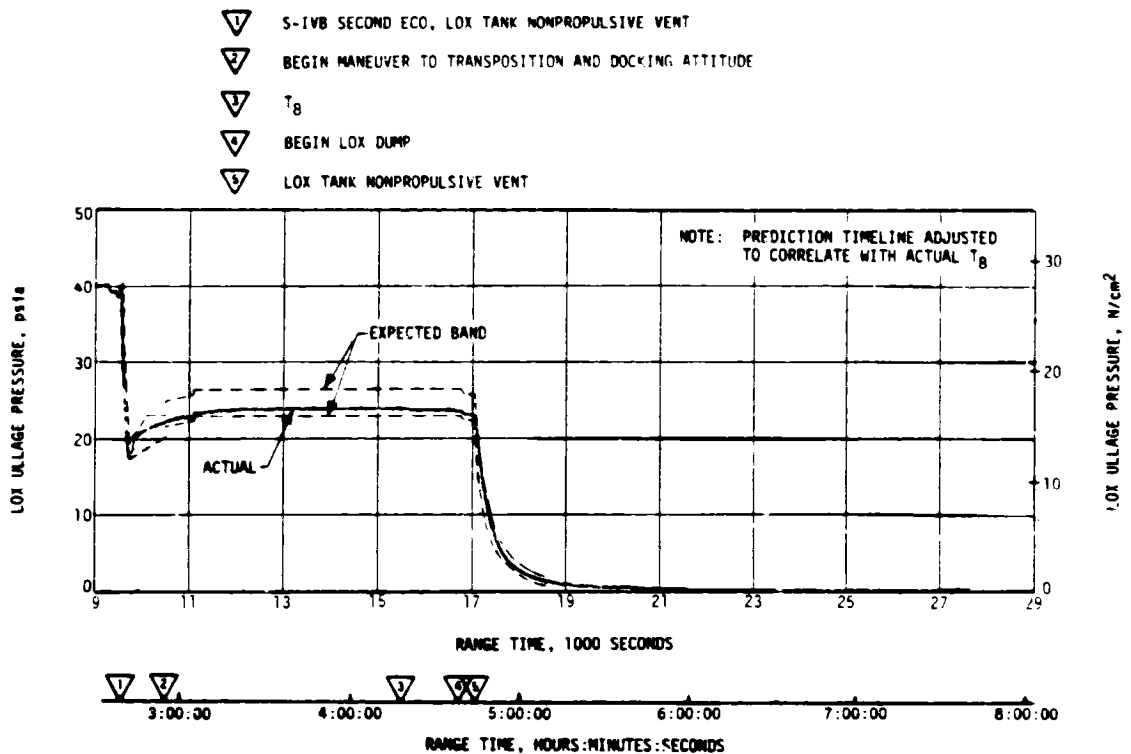


Figure 7-31. S-IVB LOX Tank Ullage Pressure - Second Burn and Translunar Coast

Approximately 49.5 lbm of ambient helium in the LH<sub>2</sub> ambient repressurization spheres and the No. 1 LOX ambient repressurization sphere were dumped via the fuel tank. The 1070-second dump began at 17,448 seconds (04:50:48). The LH<sub>2</sub> repressurization sphere pressure decayed from 2950 psia to 0 psia.

#### 7.13.5 Stage Pneumatic Control Sphere Safing

The stage pneumatic control sphere and LOX repressurization sphere No. 2 were safed by initiating the J-2 engine pump purge for a one hour period. This activity began at 15,487 seconds (04:18:07) and satisfactorily reduced the pressure in the spheres from 2500 to 1310 psia.

#### 7.13.6 Engine start Tank Safing

The engine start tank was safed during a period of approximately 150 seconds beginning at 15,160 seconds (03:39:20). Safing was accomplished by opening the sphere vent valve. Pressure was decreased from 1325 to 30 psia with 2.78 lbm of hydrogen being vented.

#### 7.13.7 Engine Control Sphere Safing

The safing of the engine control sphere began at 17,518.1 seconds (04:51:58.1). The helium control solenoid was energized to vent helium through the engine purge system. The initial pressure in the sphere was approximately 2950 psia. Helium from the control sphere continued to vent until 18,518.1 seconds (05:08:38.1). The sphere pressure had decreased to zero prior to vent termination.

The AS-511 flight sequence was changed to delay the initiation of the engine control helium dump until 70 seconds after initiation of the LH<sub>2</sub> repressurization helium dump. This sequence change prevented any significant helium mass transfer from the LH<sub>2</sub> repressurization spheres to the engine control sphere. The LH<sub>2</sub> repressurization helium was dumped into the LH<sub>2</sub> tank and vented through the NPV. The engine control helium was dumped through the engine thrust chamber.

#### 7.14 HYDRAULIC SYSTEM

The S-IVB Hydraulic System performance was satisfactory during the entire mission (S-IC/S-II boost, first and second burns of S-IVB, and orbital and translunar coast).

The S-IVB hydraulic system was modified by changing the accumulator-reservoir assembly charging valve. The original valve was removed and replaced with a similar Schrader valve, the type presently used on the S-II stage. This change will eliminate a single failure point leak path to improve the reliability of the system.

The performance of the accumulator-reservoir assembly through the first and second burns and LOX dump was nominal. There was no evidence of accumulator GN<sub>2</sub> precharge leakage during the flight.

## SECTION 8 STRUCTURES

### 8.1 SUMMARY

The structural loads experienced during the S-IC boost phase were well below design values. The maximum bending moment was  $71 \times 10^6$  lbf-in at the S-IC LOX tank (approximately 27 percent of the design value). Thrust cutoff transients experienced by AS-511 were similar to those of previous flights. The maximum longitudinal dynamic responses at the Instrument Unit (IU) were  $\pm 0.25$  g and  $\pm 0.32$  g at S-IC Center Engine Cutoff (CECO) and Outboard Engine Cutoff (OECO), respectively. The magnitudes of the thrust cutoff responses are considered normal.

During S-IC stage boost, four to five hertz oscillations were detected beginning at approximately 100 seconds. The maximum amplitude measured at the IU was  $\pm 0.06$  g. Oscillations in the four to five hertz range have been observed on previous flights and are considered to be normal vehicle response to flight environment. POGO did not occur during S-IC boost.

The S-II stage center engine LOX feedline accumulator successfully inhibited the 16 hertz POGO oscillations. A peak response of  $\pm 0.5$  g in the 14 to 20 hertz frequency range was measured on engine No. 5 gimbal pad during steady-state engine operation. As on previous flights, low amplitude 11 hertz oscillations were experienced near the end of S-II burn. Peak engine No. 1 gimbal pad response was  $\pm 0.07$  g. POGO did not occur during S-II boost. The POGO limiting backup cutoff system performed satisfactorily during the prelaunch and flight operations. The system did not produce any discrete outputs and should not have since there was no POGO.

The structural loads experienced during the S-IVB stage burns were well below design values. During first burn the S-IVB experienced low amplitude, 16 to 20 hertz oscillations. The amplitudes measured on the gimbal block were comparable to previous flights and within the expected range of values. Similarly, S-IVB second burn produced intermittent low amplitude oscillations in the 11 to 16 hertz frequency range which peaked near second burn cutoff.

### 8.2 TOTAL VEHICLE STRUCTURES EVALUATION

#### 8.2.i Longitudinal Loads

The structural loads experienced during boost were well below design values. The AS-511 vehicle liftoff occurred at a steady-state acceleration of 1.20 g. Maximum longitudinal dynamic response measured during thrust buildup and release was  $\pm 0.20$  g in the IU and  $\pm 0.50$  g at the Command Module (CM), Figure 8-1. Comparable values have been seen on previous flights.

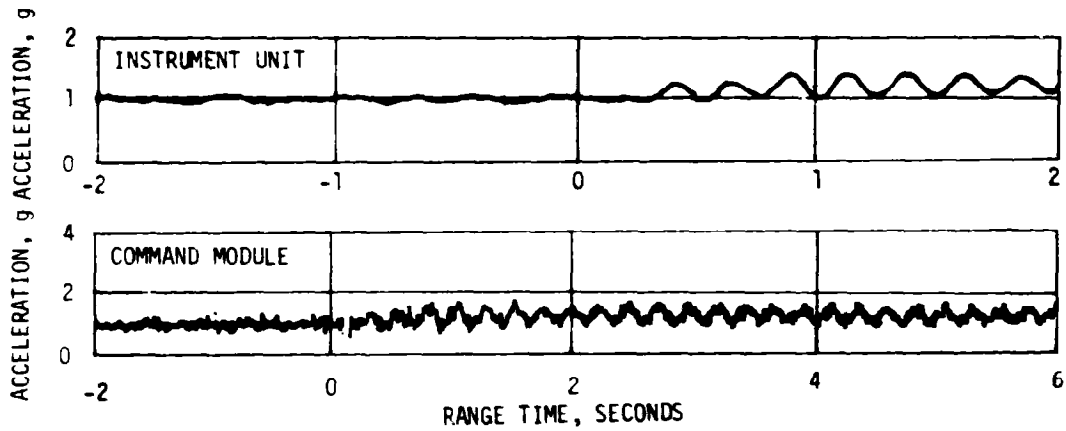


Figure 8-1. Longitudinal Acceleration at IU and CM During Thrust Buildup and Launch

The longitudinal loads experienced at the time of maximum bending moment (86.5 seconds) were as expected and are shown in Figure 8-2. The steady-state longitudinal acceleration was 2.16 g as compared to 2.06 g on AS-510 and 1.9 g on AS-509.

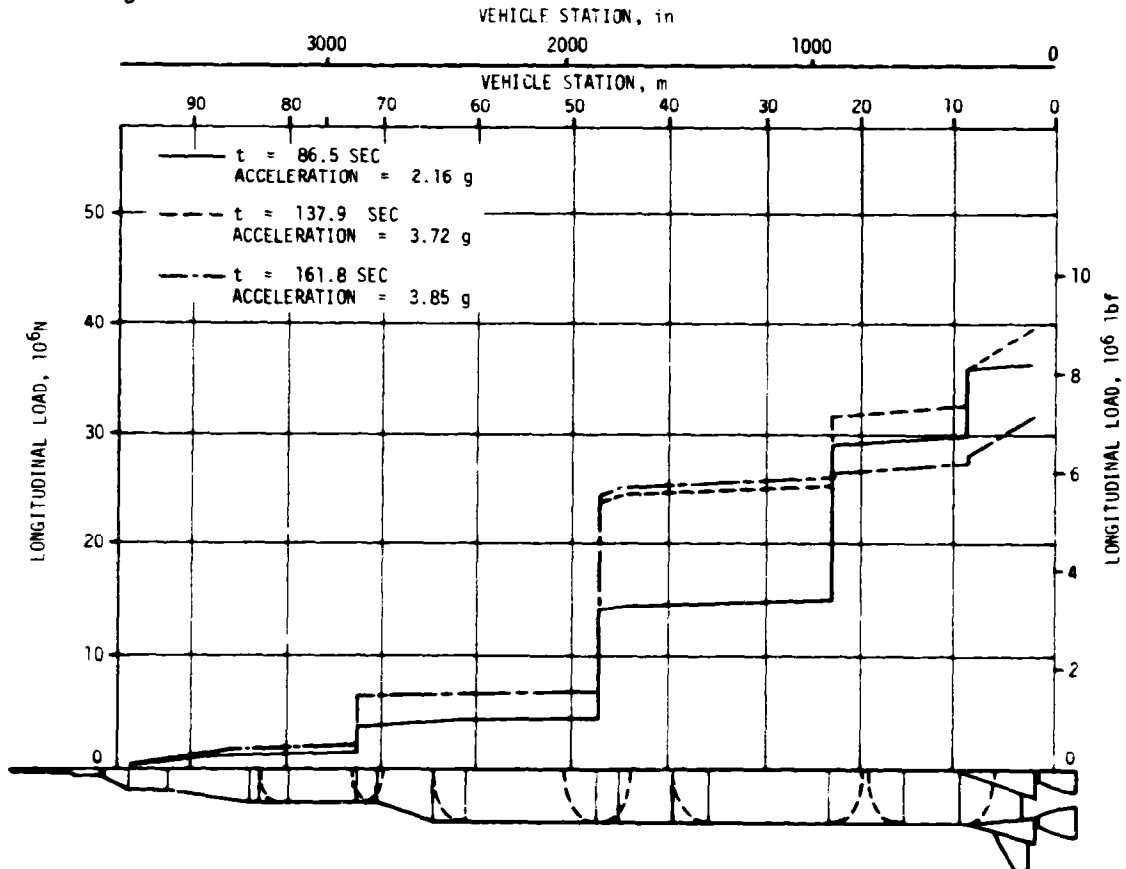


Figure 8-2. Longitudinal Load at Time of Maximum Bending Moment, CECO and OECC

Figure 8-2 also shows that the maximum longitudinal loads imposed on the S-IC stage thrust structure, fuel tank, and intertank area occurred at S-IC CECCO (137.9 seconds) at a longitudinal acceleration of 3.72 g. The maximum longitudinal loads imposed on all vehicle structure above the S-IC intertank area occurred at S-IC OECCO (161.8 seconds) at an acceleration of 3.85 g.

## 8.2.2 Bending Moments

The peak vehicle bending moment occurred during the maximum dynamic pressure phase of boost at 86.5 seconds, Figure 8-3. The maximum bending moment of  $71 \times 10^6$  lbf-in at vehicle station 1156 was approximately 27 percent of design value.

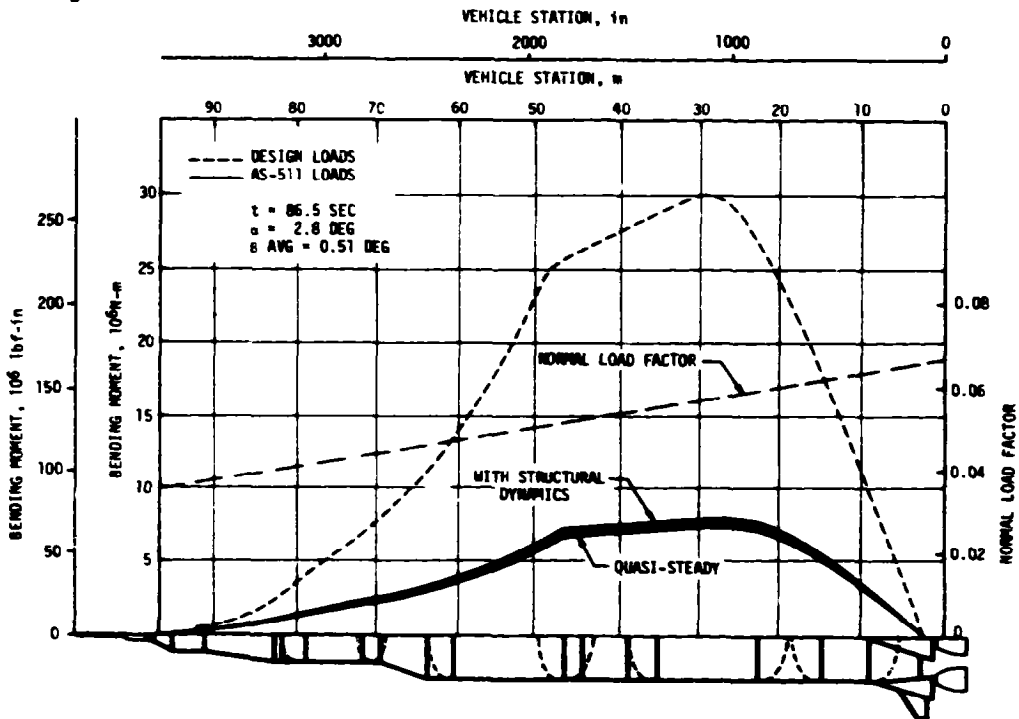


Figure 8-3. Bending Moment and Load Factor Distribution at Time of Maximum Bending Moment

## 8.2.3 Vehicle Dynamic Characteristics

### 8.2.3.1 Longitudinal Dynamic Characteristics

During S-IC stage boost, the significant vehicle response was the expected four to five hertz first longitudinal mode response. The low amplitude oscillations began at approximately 100 seconds and continued until S-IC CECCO. The peak amplitude measured in the IU was +0.06 g, the same as seen on AS-510 and AS-509, but occurred later in flight than previously seen. The AS-511 IU response during the oscillatory period is compared with previous flight data in Figure 8-4. Spectral analysis of engine chamber pressure measurements shows no detectable buildup of structural/propulsion coupled oscillations. POGO did not occur during S-IC boost.

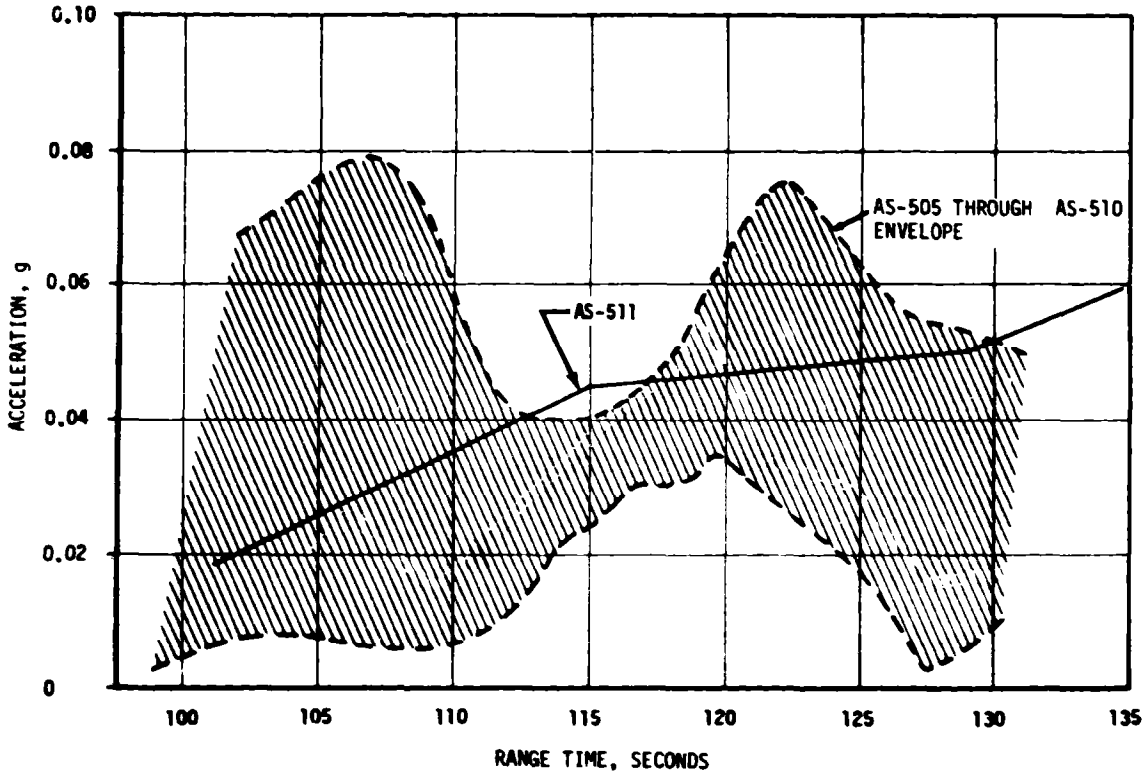


Figure 8-4. IU Accelerometer Five Hertz Response During S-IC Burn (Longitudinal)

The AS-511 S-IC CECO and OECO transient responses were similar to those of previous flights. The maximum longitudinal dynamics resulting from CECO were  $\pm 0.25$  g at the IU and  $\pm 0.50$  g at the CM, Figure 8-5. For OECO the maximum dynamics at the IU were  $\pm 0.32$  g and  $\pm 1.10$  g at the CM, Figure 8-6. The minimum CM acceleration level of  $-0.90$  g occurred at approximately the same time and is of the same magnitude as on previous flights.

The S-II stage center engine accumulator effectively suppressed the 16 hertz POGO phenomenon. The flight data show that the 16 hertz oscillations were inhibited with amplitudes comparable to those seen on AS-510, Figure 8-7. The peak 14 to 20 hertz center engine gimbal response was approximately  $\pm 0.5$  g, as compared to  $\pm 0.6$  g on AS-510. POGO did not occur.

A transient response was experienced shortly after accumulator fill was initiated. The peak response of the LOX pump inlet pressure was approximately 13 psi peak-to-peak with a frequency of 80 hertz, Figure 8-8. The LOX pump inlet pressure on AS-511 had a higher frequency content and a longer duration, but lower amplitude than that experienced on AS-510 (45 psi peak-to-peak at 68 hertz). Such variations are not unique and the causes are attributed to the individual pump characteristics. The response of the center engine gimbal pad at the corresponding time was less than  $\pm 0.5$  g.

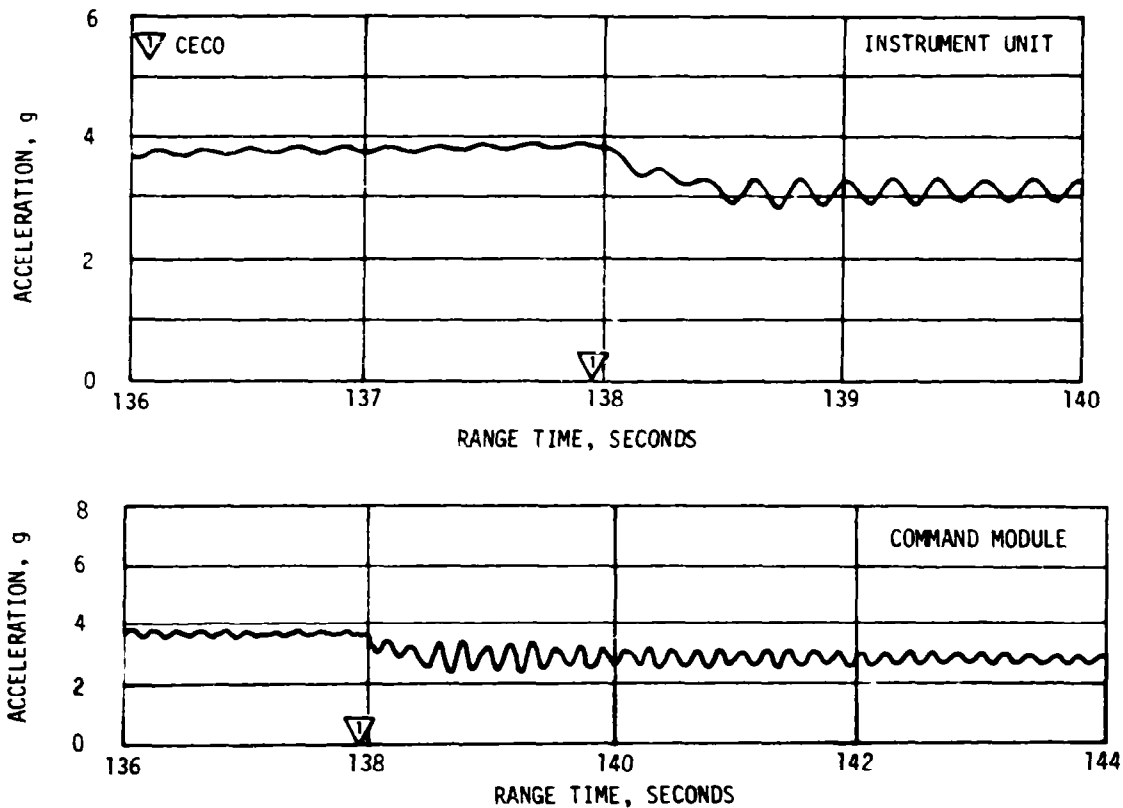


Figure 8-5. IU and CM Longitudinal Acceleration After S-IC CECO

As on prior flights, 11 hertz oscillations were noted near the end of S-II burn. The AS-511 peak engine No. 1 gimbal pad response was  $\pm 0.07$  g as compared to  $\pm 0.06$  g on AS-510. Table 8-1 presents a summary of peak engine No. 1 gimbal pad responses for all flights.

During AS-511 S-IVB first burn, low frequency (16 to 20 hertz) longitudinal oscillations similar to those observed on previous flights were evident. The AS-511 amplitudes ( $\pm 0.16$  g at gimbal block) were well below the maximum measured on AS-505 ( $\pm 0.30$  g) and within the expected range of values.

AS-511 S-IVB second burn produced intermittent 11 to 16 hertz oscillations similar to those experienced on previous flights. The oscillations began approximately 118 seconds prior to cutoff and had a maximum value of  $\pm 0.08$  g measured on the gimbal block. This compared to  $\pm 0.05$  g on AS-510.

#### 8.2.4 Vibration

There were no significant vibration environments identified on AS-511. A comparison of AS-511 data with data from previous flights show similar trends and magnitudes.



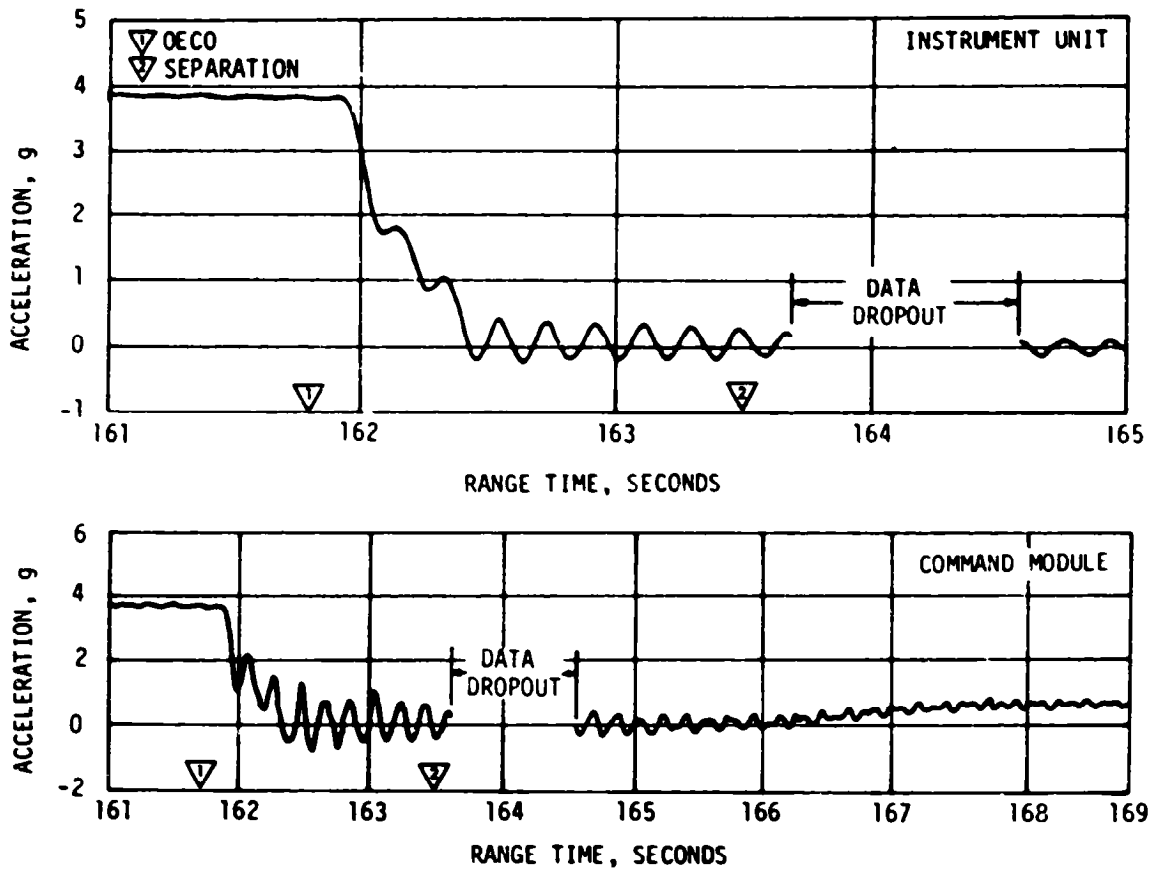
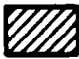


Figure 8-6. IU and CM Longitudinal Acceleration After S-IC OECS

The data from AS-510 and AS-511 were limited in frequency range as compared to previous data. This was caused by the change in the data acquisition system from single-sideband/FM to FM/FM. Direct comparison of similar data can not be made due to frequency roll-off characteristics. However, correlation is obtained when frequency ranges are compatible. Figure 8-9 shows a comparison of AS-511 data with previous flight data for compatible frequency ranges.

In a post-mission debriefing the Apollo 16 crew reported that the vehicle had experienced some low amplitude vibration or "buzz" during portions of the S-II stage burn, and throughout the S-IVB first and second burns. The crew also noted that the vibrations did not appear to be oriented in any particular axis. Analysis of flight data indicates the presence of low amplitude, approximately 65 hertz, vibration during the S-II stage burn and both S-IVB stage burns. The data show lateral amplitudes of  $\pm 0.10$  g at the IU during S-IVB first burn and  $\pm 0.20$  g during second burn. The vibrations can also be seen on selected propulsion pressure measurements (Figure 8-10). A review of AS-510 data shows similar vibration at approximately 72 hertz.

Table 8-1. Post S-II CECO 11 Hertz Engine No. 1 Gimbal Pad Oscillations

FLIGHT	RANGE TIME AT PEAK AMPLITUDE (SECONDS)	ACCELERATION		LOX LEVEL AT PEAK AMPLITUDE (INCHES OF LOX)	LOX LEVELS AT 1/3 AMPLITUDE (INCHES OF LOX)	
		PEAK * AMPLITUDE (G)	FREQUENCY (HZ)		START	STOP
501	NO MEASUREMENT OF ACCELERATION					
502	547	0.07	10.4	30	32	28
503	512	0.22	10.9	23	36	15
504	535	0.14	11.6	8	14	6
505	545	0.11	11.0	16	23	14
506	NO LOW FREQUENCY OSCILLATION INSTRUMENTATION					
507	545	0.10	11.4	15	27	12
508	582	0.19	11.1	19	27	9
509	542	0.16	11.0	26	32	18
510	540	0.06	11.0	18	30	14
511	541	0.07	10.3	24	29	20
 DATA QUESTIONABLE AS-502 - 2 ENGINES OUT AS-502 & AS-503 - LARGE ATTENUATION AT 11 HZ ON E <sub>1</sub> ACCELERATION						
*RESULTS OF LATEST ANALYSIS (502 THROUGH 511)						

Because of the data characteristics, the vibration is suspected to be related to normal stage propulsion system operation and probably characteristic of the J-2 turbomachinery. These vibrations pose no POGO or any other structural concerns, and are of such low amplitude as to be virtually obscured in the measurement background noise.

### 8.3 S-II POGO LIMITING BACKUP CUTOFF SYSTEM

The backup cutoff system provides for automatic S-II CECO if vibration response levels exceed predetermined levels within the preselected frequency band. The system consists of three sensors, a two-out-of-three voting logic, an engine cutoff arming function, and an automatic disable function which is effective until the arming operation has occurred.

The system did not produce discrete outputs at any time. The accelerometer analog outputs were well below the levels which would produce a discrete output even during the engine start period when the system was not armed. After arming, the analog output did not exceed one g.

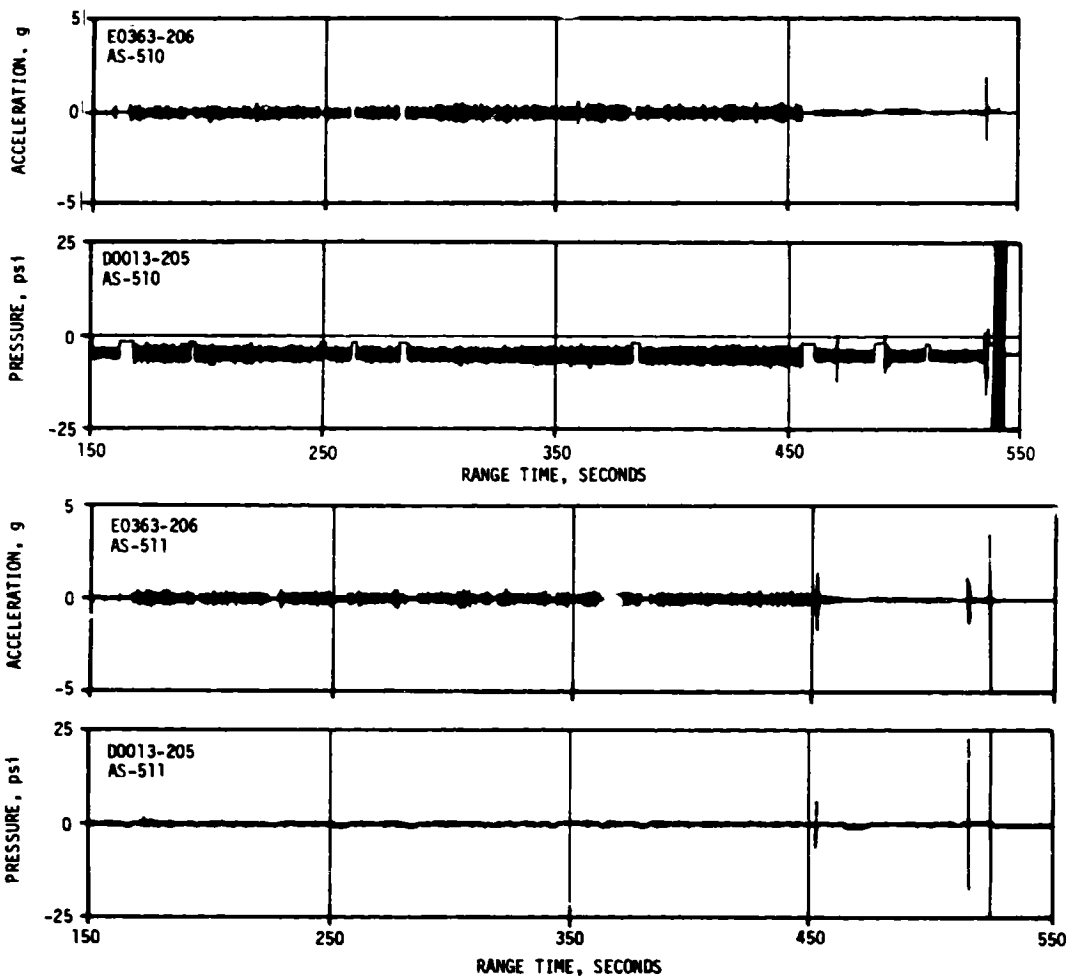


Figure 8-7. AS-511/AS-510 Acceleration and Pressure Oscillations During S-II Burn (8 to 20 Hz Filter)

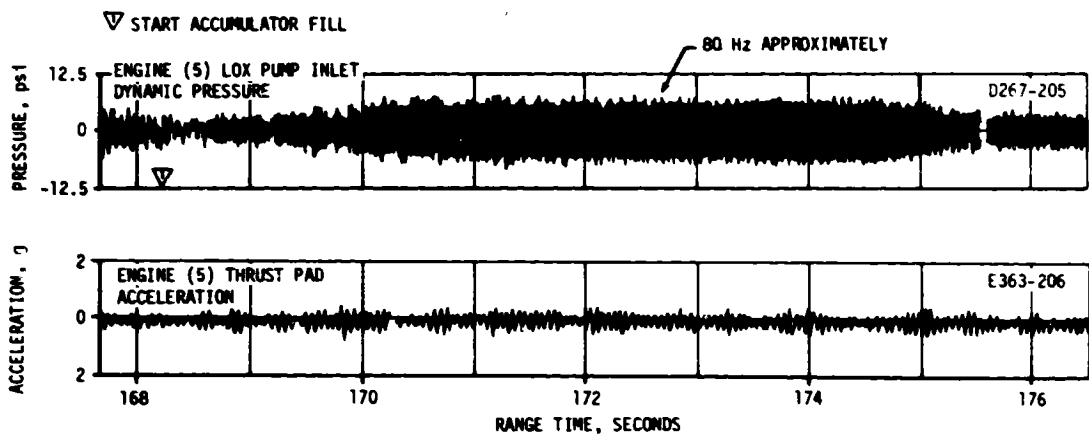


Figure 8-8. AS-511 Pump Inlet Pressure and Thrust Pad Acceleration Oscillations During Accumulator Fill Transient (1 to 110 Hz Filter)

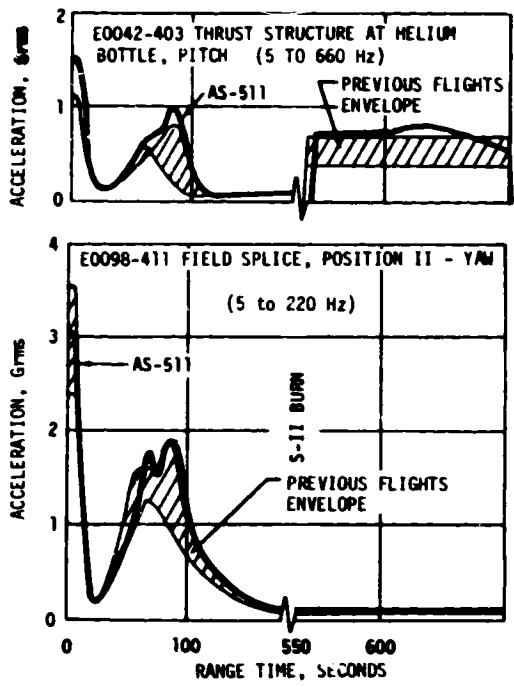


Figure 8-9. S-IVB Stage Vibration Envelopes

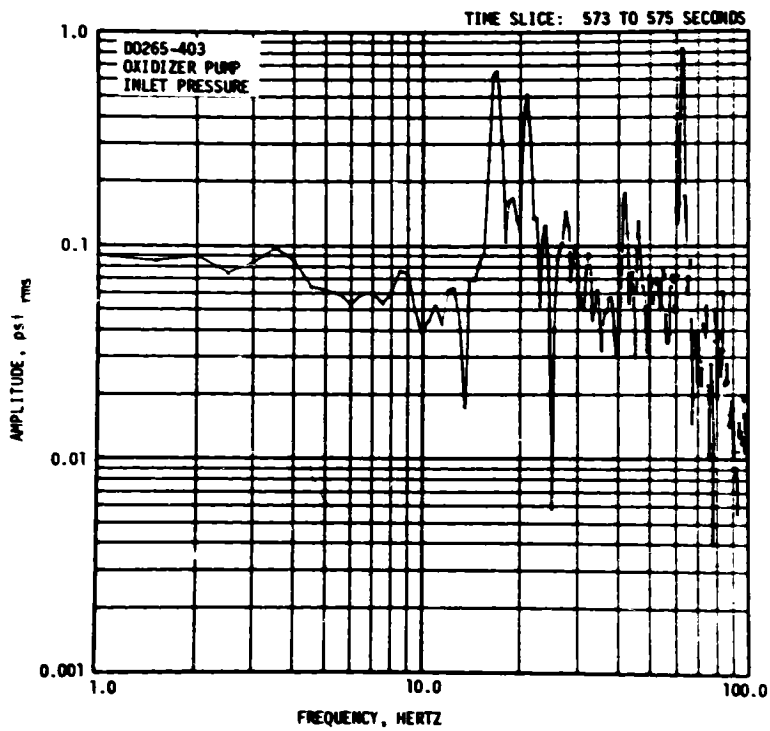


Figure 8-10. S-IVB Vibration Spectral Analysis

## SECTION 9

### GUIDANCE AND NAVIGATION

#### 9.1 SUMMARY

The Guidance and Navigation System satisfactorily supported accomplishment of the mission objectives. The end condition errors at parking orbit insertion and translunar injection were insignificant.

Three anomalies occurred in the Guidance and Navigation System, although their effect on the mission were not significant. The anomalies were:

- a. An anomalous one meter/second shift in the crossrange integrating accelerometer output just after liftoff (Section 9.4.1).
- b. A one second delay in ending the tower clearance yaw maneuver (Section 9.3).
- c. Intermittent setting of Error Monitor Register bits 13 and 14 (Section 9.4.2).

#### 9.2 GUIDANCE COMPARISONS

The post-flight guidance error analysis was based on comparisons of telemetered positions and velocities with corresponding data from the postflight trajectory (21 day Observed Mass Point Trajectory) established from external tracking (see paragraph 4.2). Velocity differences from launch to earth parking orbit (EPO) are shown in Figure 9-1 in a non-rotating vehicle reference coordinate system (PACSS 12). At EPO insertion these differences were 0.18 m/s (0.59 ft/s), 2.18 m/s (7.15 ft/s), and 0.38 m/s (1.25 ft/s) for vertical, crossrange, and down range velocities, respectively. These differences are relatively small and well within the accuracy of the measuring system and/or the tracking. The crossrange accelerometer head apparently hit its mechanical stop at about 0.16 seconds causing a velocity bias of approximately 1.0 m/s (3.28 ft/s). This velocity shift tended to minimize rather than increase the out-of-plane position and velocity deviations at EPO.

Platform velocity differences for the out-of-orbit burn mode are shown in Figure 9-2. At (T6-7.7 seconds), the platform velocity measurements were set to zero in the LVDC. The corresponding trajectory data were adjusted by the values at T6 for comparison with the LVDC outputs. The differences reflect a combination of hardware errors necessary to compute a trajectory initialized to a parking orbit state vector solution that would pass through a post Translunar Injection (TLI) state

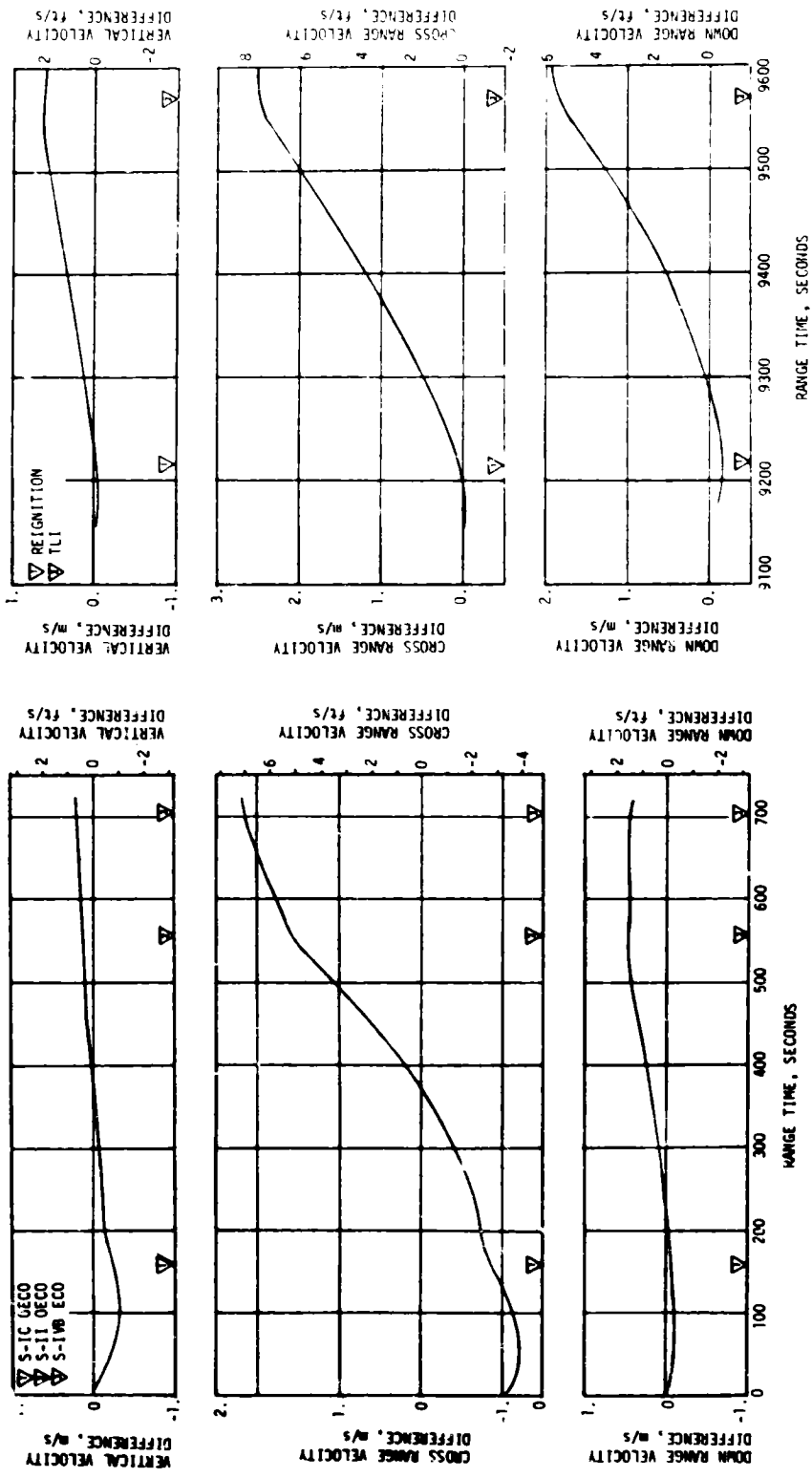


Figure 9-1. Trajectory and ST-124M Platform Velocity Comparisons, Boost-to-EPO (Trajectory Minus LVDC)

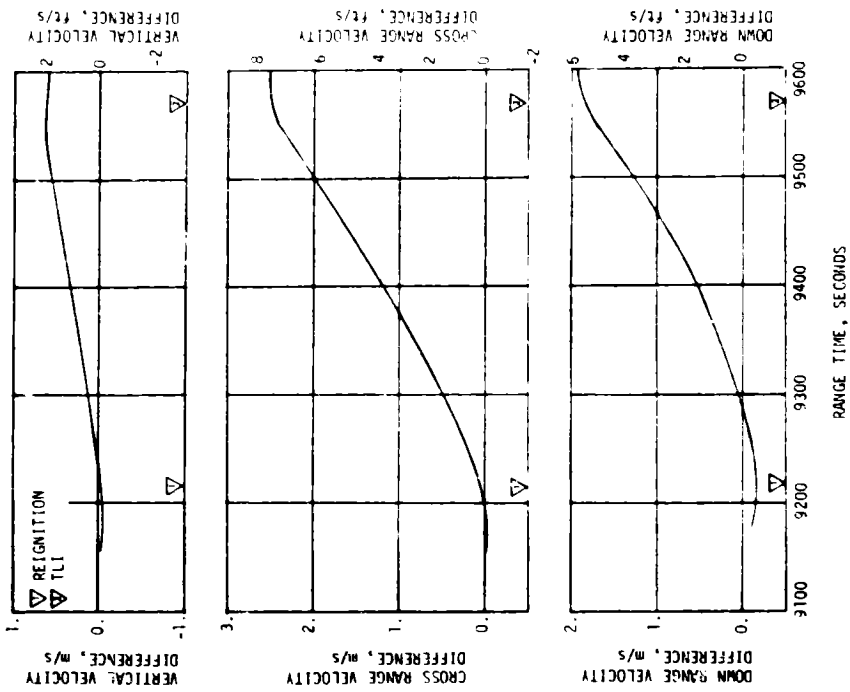


Figure 9-2. Trajectory and ST-124M Platform Velocity Comparisons, Boost-to-TLI (Trajectory Minus LVDC)

vector. There was no tracking coverage during the second burn mode. The trajectory was established by adjusting the telemetered velocity measurements and integrating between the points established from orbital and translunar tracking. The computed velocity differences are small relative to 3 sigma platform dispersions.

Platform system velocity measurements at significant event times are shown in Table 9-1 along with corresponding data from both the postflight and Operational Trajectories (OT). The differences between the telemetered and post-flight trajectory data reflect some combination of small guidance hardware errors and tracking errors along with the crossrange velocity bias of 1.0 m/s (3.28 ft/s) during the boost-to-EPO burn. The differences between the telemetered and OT values reflect differences in actual and nominal performance and environmental conditions. The values shown for the second burn mode represent component velocity change from T<sub>6</sub>. The characteristic velocity determined from the telemetered velocities during second burn to Engine Cutoff (ECO) was 0.38 m/s (1.25 ft/s) less than the OT which indicates slightly less performance was required to meet the targeted end conditions. The telemetered data indicated 0.21 m/s (0.69 ft/s) less than the post-flight trajectory. The total velocity measured by the platform system is considered highly accurate even though the components may be in error due to platform misalignments acquired by gyro drift from launch to re-ignition. The difference in indicated performance between the telemetered and post-flight trajectory data reflects small errors in the state vectors to which the guidance velocities were constrained to generate the out-of-orbit trajectory. The velocity increase due to thrust decay from first S-IVB ECO was 0.01 m/s (0.033 ft/s) less than the OT and 0.13 m/s (0.43 ft/s) greater after second ECO. In constructing the OT, the simulated time delay between guidance cutoff signal and engine solenoid activation was changed from 0.005 second to 0.050 second to account for significantly larger deviations noted on past flights.

Comparisons of navigation (PACSS-13) positions, velocities, and flight path angle at significant event times are shown in Table 9-2. Differences in components of position and velocity between the LVDC and OT values reflect off-nominal flight environment and vehicle performance. Total velocity at first S-IVB ECO was as predicted with a radius vector of 23.4 meters (76.8 feet) less than the OT. Second S-IVB ECO was given with 1338 m<sup>2</sup>/s<sup>2</sup> (OT minus LVDC) orbital energy (C<sub>3</sub>) deviation from the OT value of -1,658,524 m<sup>2</sup>/s<sup>2</sup>. The LVDC and post-flight trajectory were in good agreement during boost to EPO. The shift in the measured cross-range velocity tended to minimize the out-of-plane component errors at EPO. In parking orbit, the position and velocity state vector errors built up as divergent oscillations and added to those amounts simply attributable to the programmed vent thrust. Although the component differences in position and velocity are rather large at TLI, the total velocity and radius vector are in very good agreement. The difference in C<sub>3</sub> at TLI was 2383 m<sup>2</sup>/s<sup>2</sup> (trajectory minus LVDC). Figures 9-3 through 9-6 show the state vector differences between the post-flight trajectory and LVDC during parking orbit. The LVDC data between receiver

Table 9-1. Inertial Platform Velocity Comparisons (PACSS-12 Coordinate System)

EVENT	DATA SOURCE	VELOCITY-M/S (FT/S)		
		VERTICAL (X)	CROSS RANGE (Y)	DOWN RANGE (Z)
S-IC OECO	Guidance (LVDC)	2611.66 (8568.45)	-2.31 (-7.58)	2212.72 (7259.59)
	Postflight Trajectory	2610.99 (8566.24)	-3.14 (-10.30)	2212.56 (7259.06)
	Operational Trajectory	2627.95 (8621.87)	-3.45 (-11.32)	2219.11 (7280.54)
S-II OECO	Guidance (LVDC)	3450.18 (11319.49)	-3.55 (-11.65)	6810.12 (22342.93)
	Postflight Trajectory	3450.45 (11320.37)	-1.84 (-6.04)	6810.18 (22343.11)
	Operational Trajectory	3435.41 (11271.03)	-2.66 (-8.72)	6812.07 (22349.30)
S-IVB FIRST ECO	Guidance (LVDC)	3238.87 (10626.21)	2.15 (7.05)	7624.04 (25013.25)
	Postflight Trajectory	3239.15 (10627.13)	4.24 (13.91)	7624.47 (25014.67)
	Operational Trajectory	3234.13 (10610.66)	1.95 (6.40)	7623.34 (25010.96)
Parking Orbit Insertion	Guidance (LVDC)	3238.35 (10624.51)	2.15 (7.05)	7625.65 (25018.54)
	Postflight Trajectory	3238.53 (10625.10)	4.33 (14.21)	7626.03 (25019.78)
	Operational Trajectory	3233.57 (10608.82)	1.96 (6.43)	7624.98 (25016.34)
S-IVB Second ECO*	Guidance (LVDC)	3103.96 (10183.60)	17.25 (56.59)	-540.24 (-1772.44)
	Postflight Trajectory	3104.48 (10180.30)	19.80 (64.96)	-538.37 (-1766.31)
	Operational Trajectory	3104.03 (10183.84)	17.83 (58.51)	-542.01 (-1778.24)
Translunar Injection*	Guidance (LVDC)	3107.75 (10196.03)	17.25 (56.59)	-540.30 (-1772.64)
	Postflight Trajectory	3108.30 (10197.83)	19.81 (64.99)	-538.50 (-1766.73)
	Operational Trajectory	3107.71 (10195.99)	17.81 (58.44)	-542.07 (-1778.44)

\*Values represent velocity change from Time Base 6 initiation.



Table 9-2. Guidance Comparisons (PACSS 13)

EVENT	DATA SOURCE	POSITIONS (FT)				VELOCITIES (FT/S)				FLIGHT PATH ANGLE (DEG)
		Xs	Ys	Zs	R	Xs	Ys	Zs	R	
S-1C	Guidance (LVD)	6,437,286.2	6,437,229.7	39,161.1	6,439,348.6	118.25	2,588.24	2,737.90	866.20	19.30
		Operational	6,437,998.6	6,437,929.7	39,122,042.7	6,439,289.3	117.12	2,594.44	2,737.90	865.70
S-1C	Trajectory	(21,119,705.5)	(21,119,520.0)	(128,481.3)	(21,126,471.7)	(2,840.93)	(8,491.62)	(8,362.92)	(2,840.52)	19.30
		(129,078.0)	(128,795.6)	(128,795.6)	(128,858.9)	(2,885.77)	(8,426.26)	(8,362.92)	(2,885.77)	19.30
S-11	Guidance (LVD)	6,263,478.7	6,263,431.4	79,746.1	6,263,478.7	87.38	6,679.33	6,966.79	-1,978.64	19.30
		Operational	6,263,794.2	6,263,746.1	79,801.1	6,263,794.2	88.36	6,681.86	6,966.79	-1,988.97
S-11	Trajectory	(20,519,470.7)	(20,549,315.6)	(261,977.5)	(21,473,813.9)	(286.78)	(21,513.81)	(22,856.97)	(-6,490.85)	19.30
		(20,550,505.9)	(20,549,315.6)	(261,814.6)	(21,474,714.9)	(289.91)	(21,922.10)	(22,874.54)	(-6,525.50)	19.30
S-1B	Guidance (LVD)	5,866,687.3	5,866,651.1	91,854.2	5,866,687.3	-3,458.35	6,993.76	7,802.47	-3,458.07	19.30
		Operational	5,867,916.8	5,866,651.1	91,831.6	5,866,687.3	-3,458.35	6,993.76	7,802.47	-3,458.07
S-1B	Trajectory	(19,247,661.7)	(19,247,543.0)	(301,358.9)	(21,472,545.3)	(252.43)	(22,945.41)	(25,598.65)	(-11,345.37)	19.30
		(19,251,695.5)	(19,247,543.0)	(301,997.4)	(21,472,700.1)	(259.74)	(22,946.65)	(25,599.51)	(-11,345.37)	19.30
S-1B	Operational	5,831,672.1	5,831,648.5	92,855.3	5,831,672.1	-3,541.87	6,953.95	7,804.18	-3,541.87	19.30
		Trajectory	5,832,941.9	5,831,648.5	92,596.7	5,831,672.1	-3,541.87	6,953.95	7,804.18	-3,541.87
S-1B	Trajectory	(19,132,782.5)	(19,132,705.1)	(304,577.8)	(21,472,717.8)	(-11,620.31)	(22,814.80)	(25,604.92)	(-11,620.31)	19.30
		(19,136,948.5)	(19,132,705.1)	(303,791.7)	(21,472,623.9)	(-11,611.10)	(22,818.84)	(25,604.92)	(-11,611.10)	19.30
Parking Orbit	Guidance (LVD)	5,831,672.1	5,831,648.5	92,855.3	5,831,672.1	-3,541.87	6,953.95	7,804.18	-3,541.87	19.30
		Operational	5,832,941.9	5,831,648.5	92,596.7	5,831,672.1	-3,541.87	6,953.95	7,804.18	-3,541.87
Parking Orbit	Trajectory	(19,132,782.5)	(19,132,705.1)	(304,577.8)	(21,472,717.8)	(-11,620.31)	(22,814.80)	(25,604.92)	(-11,620.31)	19.30
		(19,136,948.5)	(19,132,705.1)	(303,791.7)	(21,472,623.9)	(-11,611.10)	(22,818.84)	(25,604.92)	(-11,611.10)	19.30
Time Base 6	Guidance (LVD)	-5,770,144.8	-5,781,637.3	-3,078,872.7	-5,770,144.8	-125.18	-6,878.56	7,805.53	-125.18	19.30
		Operational	-5,773,101.6	-5,781,637.3	-3,078,872.7	-5,773,101.6	-125.24	-6,881.35	7,805.53	-125.24
Time Base 6	Trajectory	(-18,940,622.0)	(-18,968,626.3)	(-307,266.4)	(-18,940,622.0)	(-413.32)	(22,596.64)	(25,599.64)	(-413.32)	19.30
		(-18,940,622.0)	(-18,968,626.3)	(-307,266.4)	(-18,940,622.0)	(-410.91)	(22,576.60)	(25,607.66)	(-410.91)	19.30
S-2nd ECO	Guidance (LVD)	567,723.6	578,579.4	-135,838.1	567,723.6	50.27	-430.30	10,848.08	50.27	7.0910
		Operational	578,579.4	578,579.4	-135,933.2	578,579.4	51.20	-416.51	10,846.27	51.20
S-2nd ECO	Trajectory	(1,842,925.2)	(1,761,695.2)	(-446,282.2)	(1,842,925.2)	(-1,411.75)	(-1,411.75)	(35,590.81)	(-1,411.75)	7.0910
		(1,890,226.4)	(1,761,695.2)	(-445,975.1)	(1,890,226.4)	(-1,366.50)	(-1,366.50)	(35,584.87)	(-1,366.50)	7.0910
Translunar Injection	Guidance (LVD)	670,134.7	645,343.2	-135,326.9	670,134.7	52.02	-341.42	10,840.55	52.02	7.5443
		Operational	686,955.8	645,343.2	-135,412.6	686,955.8	52.94	-327.79	10,838.50	52.94
Translunar Injection	Trajectory	(2,190,604.7)	(2,117,267.7)	(-443,985.9)	(2,190,604.7)	(170.67)	(-1,120.14)	(35,566.11)	(170.67)	7.5443
		(2,253,792.0)	(2,117,267.7)	(-444,267.1)	(2,253,792.0)	(-1,075.43)	(-1,203.97)	(35,555.49)	(-1,075.43)	7.5443

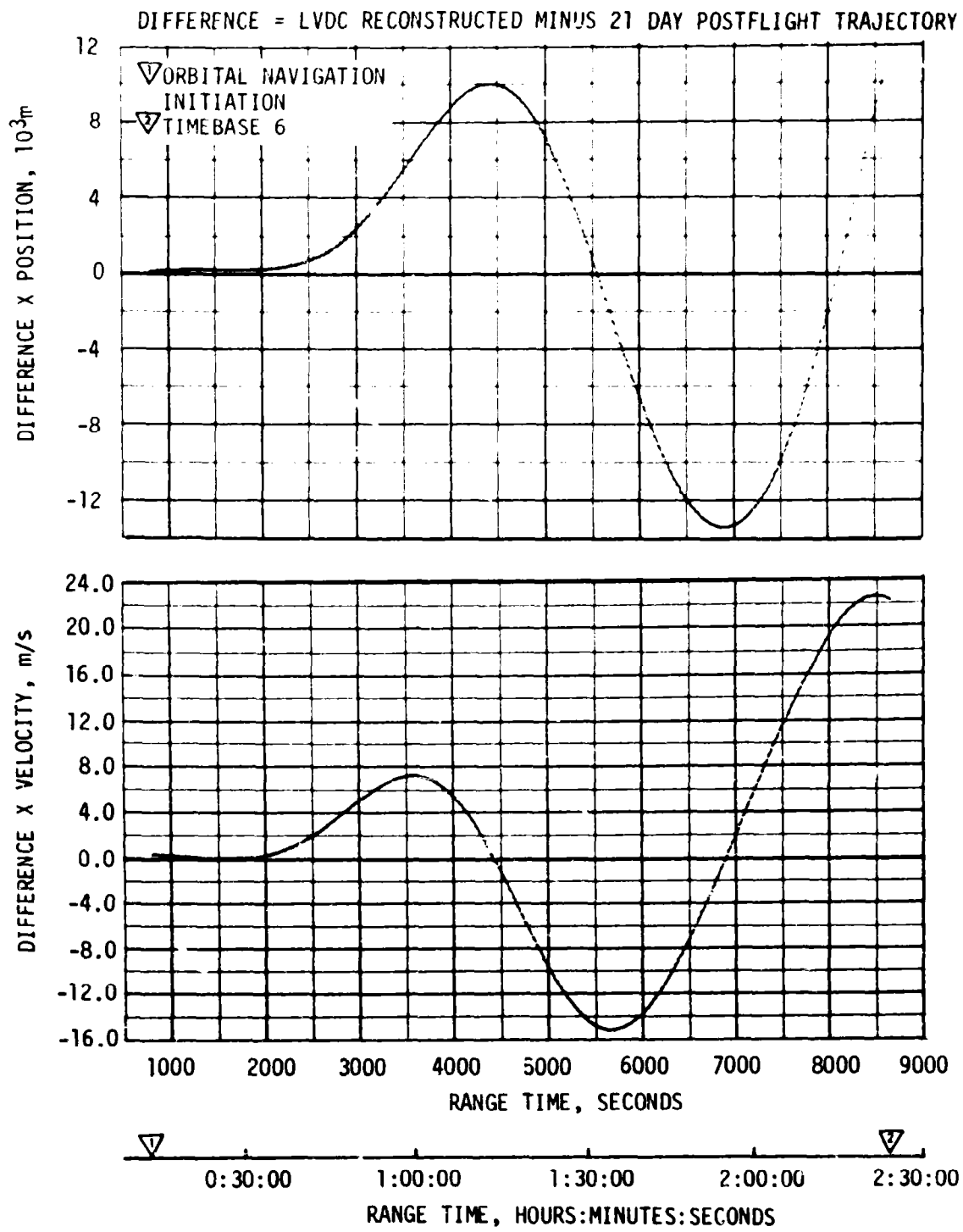


Figure 9-3. Comparison of LVDC and Postflight Trajectory During EPO, X Position and Velocity

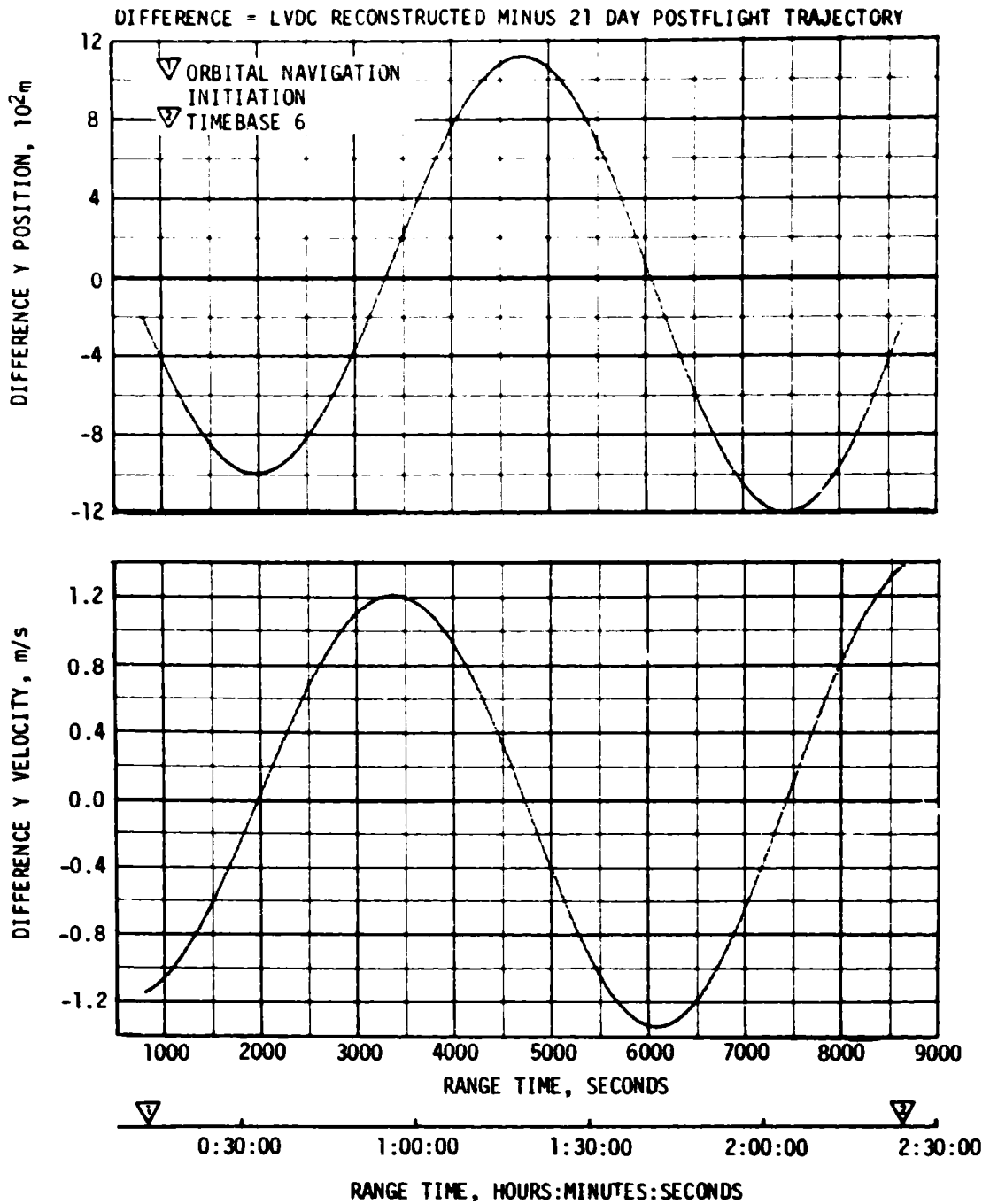


Figure 9-4. Comparison of LVDC and Postflight Trajectory During EPO, Y Position and Velocity

DIFFERENCE = LVDC RECONSTRUCTED MINUS 21 DAY POST FLIGHT TRAJECTORY

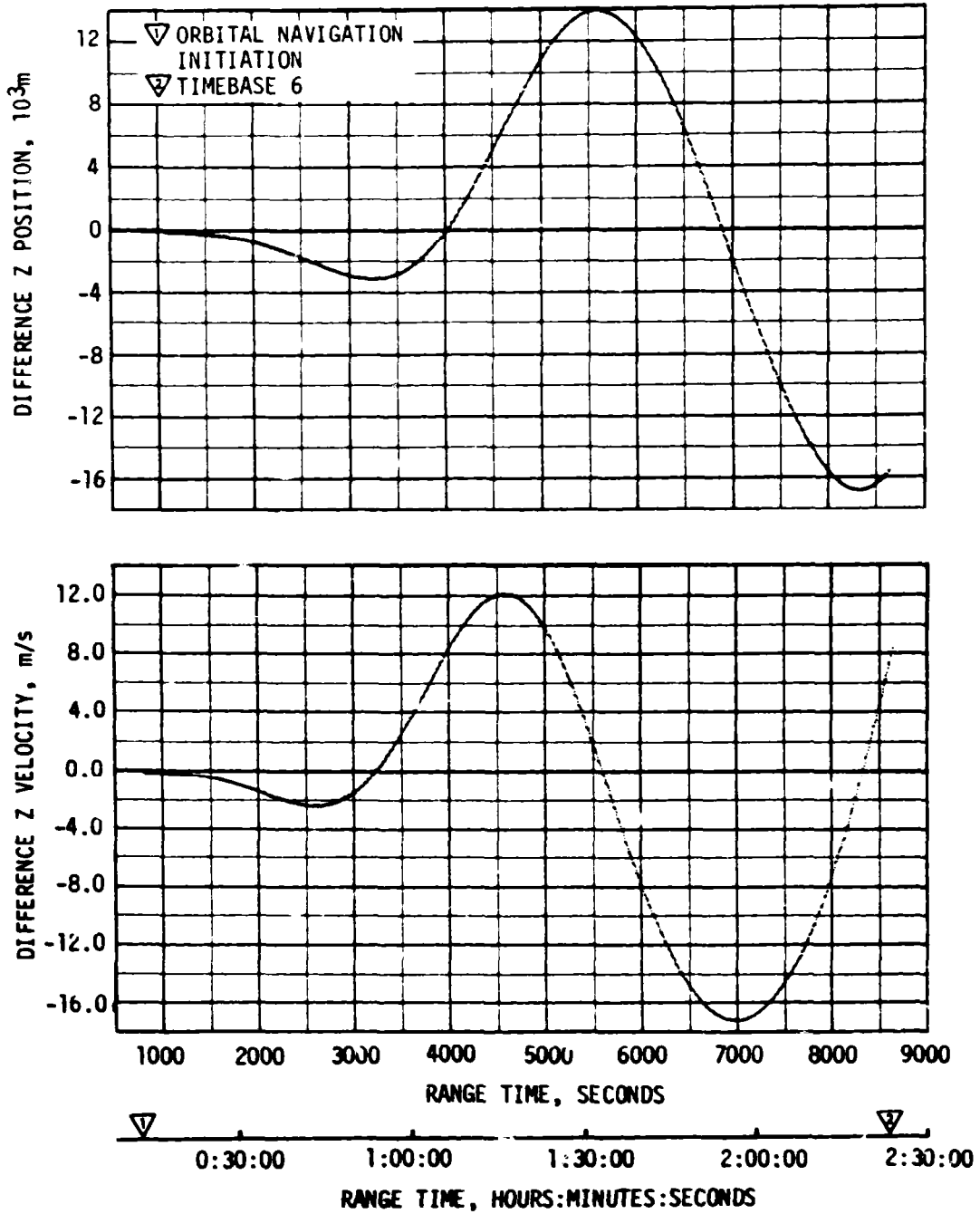


Figure 9-5. Comparison of LVDC and Postflight Trajectory During EPO, Z Position and Velocity

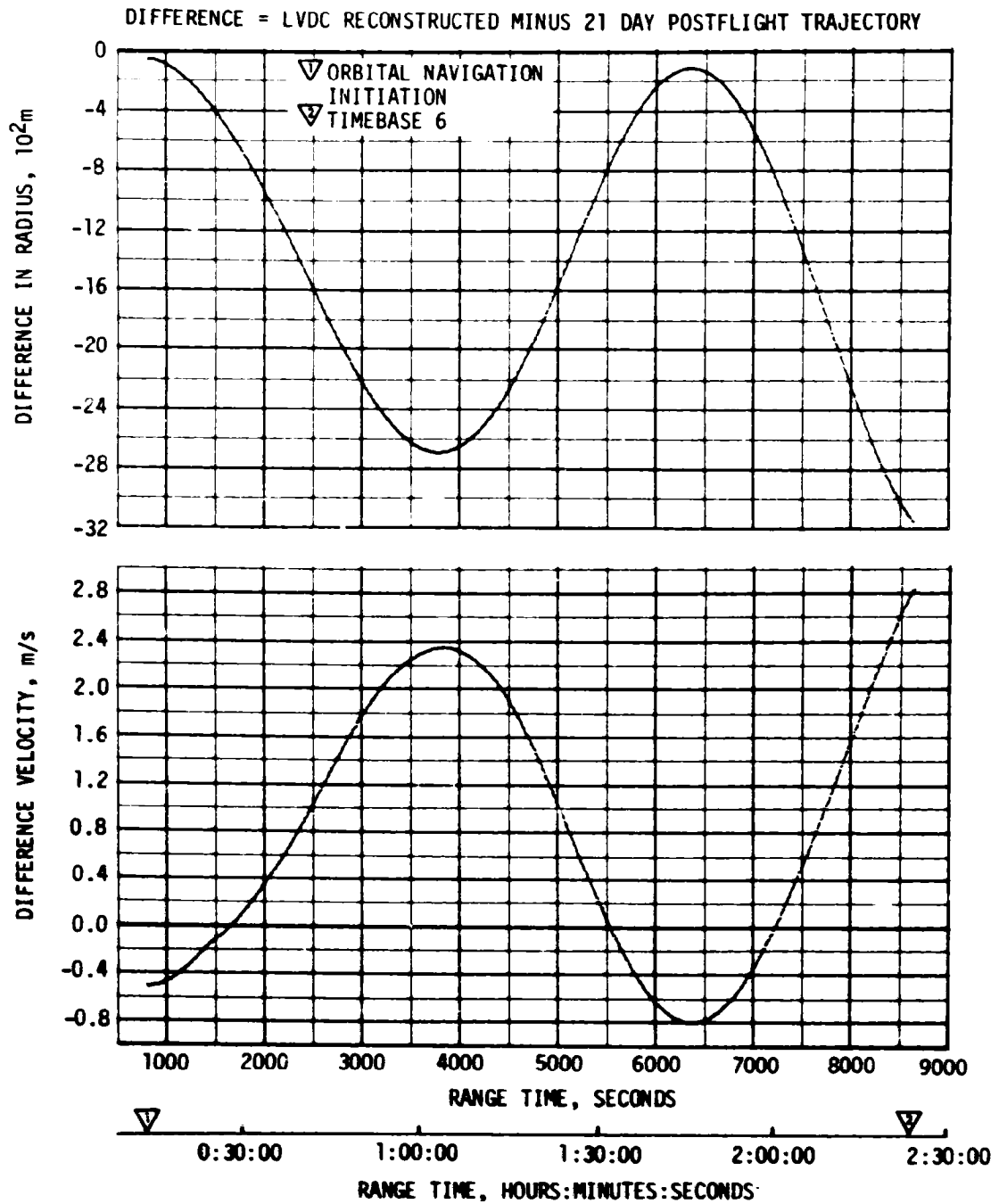


Figure 9-6. Comparison of LVDC and Postflight Trajectory During EPO, Radius and Velocity

stations were simulated using the flight program equations and programmed vent thrust. At T<sub>6</sub>, the state vector deviations were at or approaching a peak or minimum oscillation.

The state vector differences during second burn are shown in Figures 9-7 through 9-10. Although the platform velocity measurements during second burn mode were relatively accurate, the LVDC gravity calculations based on significantly different position components were in error. The velocity differences shown in Figures 9-7 through 9-10 reflect the measurement errors (Figure 9-2) and errors in gravity components in addition to the initial velocity differences at T<sub>6</sub>. The state vector deviations include inaccuracies in the trajectory data. The vehicle was guided to the targeted end conditions with a high degree of accuracy. Vent thrust was higher than the programmed values for about 2000 seconds after orbital navigation initiation (806.1 seconds). Figure 9-11 presents the continuous vent thrust profiles both predicted and reconstructed along with the three-sigma envelope. The upper portion of Figure 9-11 shows the orbital accelerations derived from the platform measurements adjusted for accelerometer bias. Also shown are the programmed and predicted acceleration profiles. The vent thrust was higher than predicted for the early portion of orbital flight, it was well within the three-sigma envelope and essentially nominal after about 2000 seconds into orbit.

LVDC state vector at TLI was compared with the OT and post-flight trajectories and the differences are presented in Table 9-3. The LVDC radius vector was 2392.7 meters (7850.1 feet) lower than the OT and 365.5 meters (1199.1 feet) lower than the post-flight trajectory value. Tele-metered total velocity was 2.05 m/s (6.73 ft/s) and 0.19 m/s (0.62 ft/s) higher than the OT and post-flight trajectory values, respectively. The guidance system was highly successful in measuring the vehicle performance and generating commands to guide to proper terminal conditions as shown in Table 9-4.

### 9.3 NAVIGATION AND GUIDANCE SCHEME EVALUATION

Based upon available data, the flight program performed all functions properly. However, there was an apparent timing flaw at the end of the tower avoidance yaw maneuver.

All events scheduled at preset times occurred within acceptable tolerances with the exception of the termination of the tower avoidance yaw maneuver. All flight program routines, including variable launch azimuth, time tilt, iterative guidance, and minor loop functions, were accomplished properly. The timing problem in yaw maneuver termination has been traced to the Minor Loop Support module. All major navigation and guidance events were implemented within a one computation cycle tolerance following scheduled start and stop times.

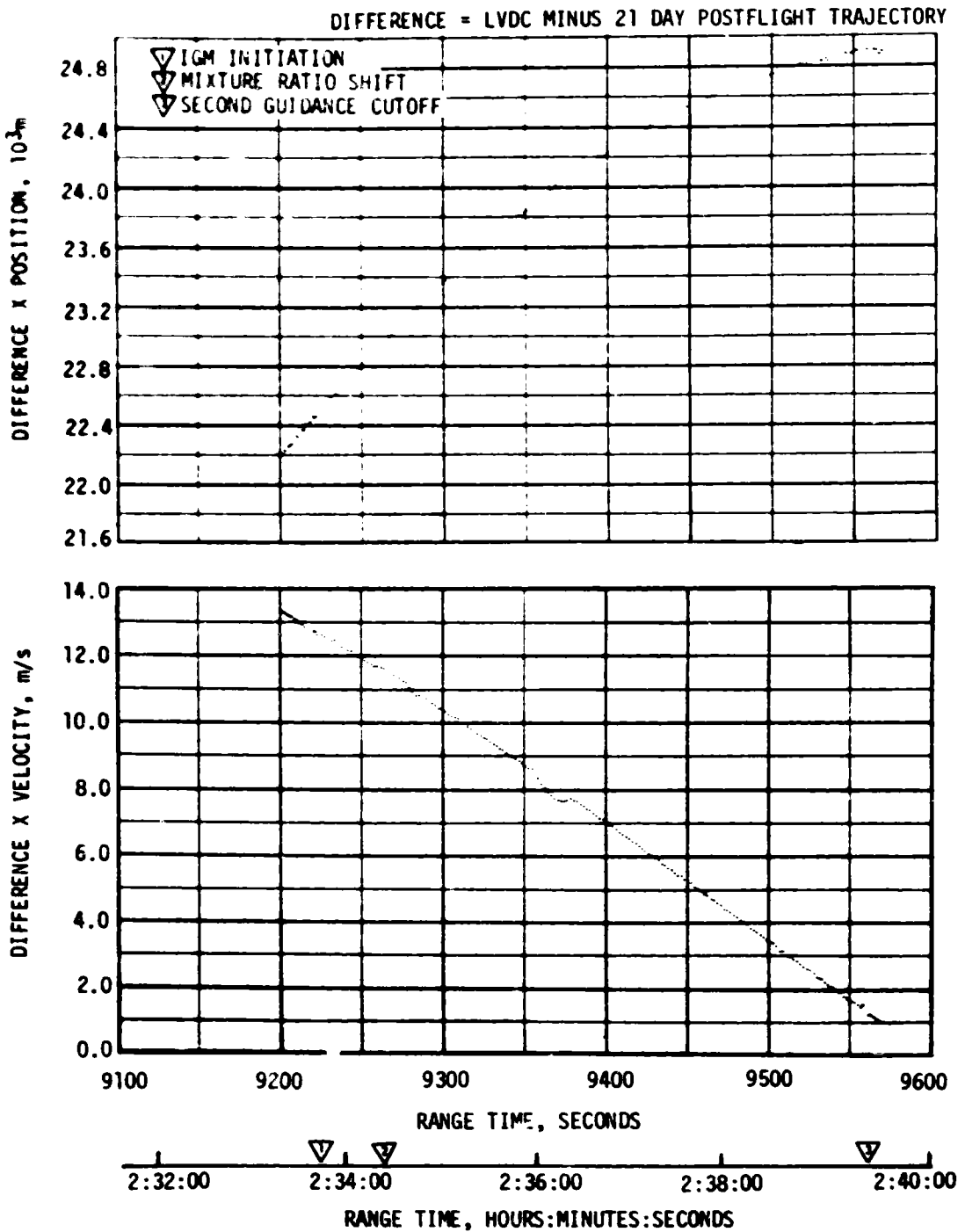


Figure 9-7. Comparison of LVDC and Postflight Trajectory During Boost to TLI, X Position and Velocity

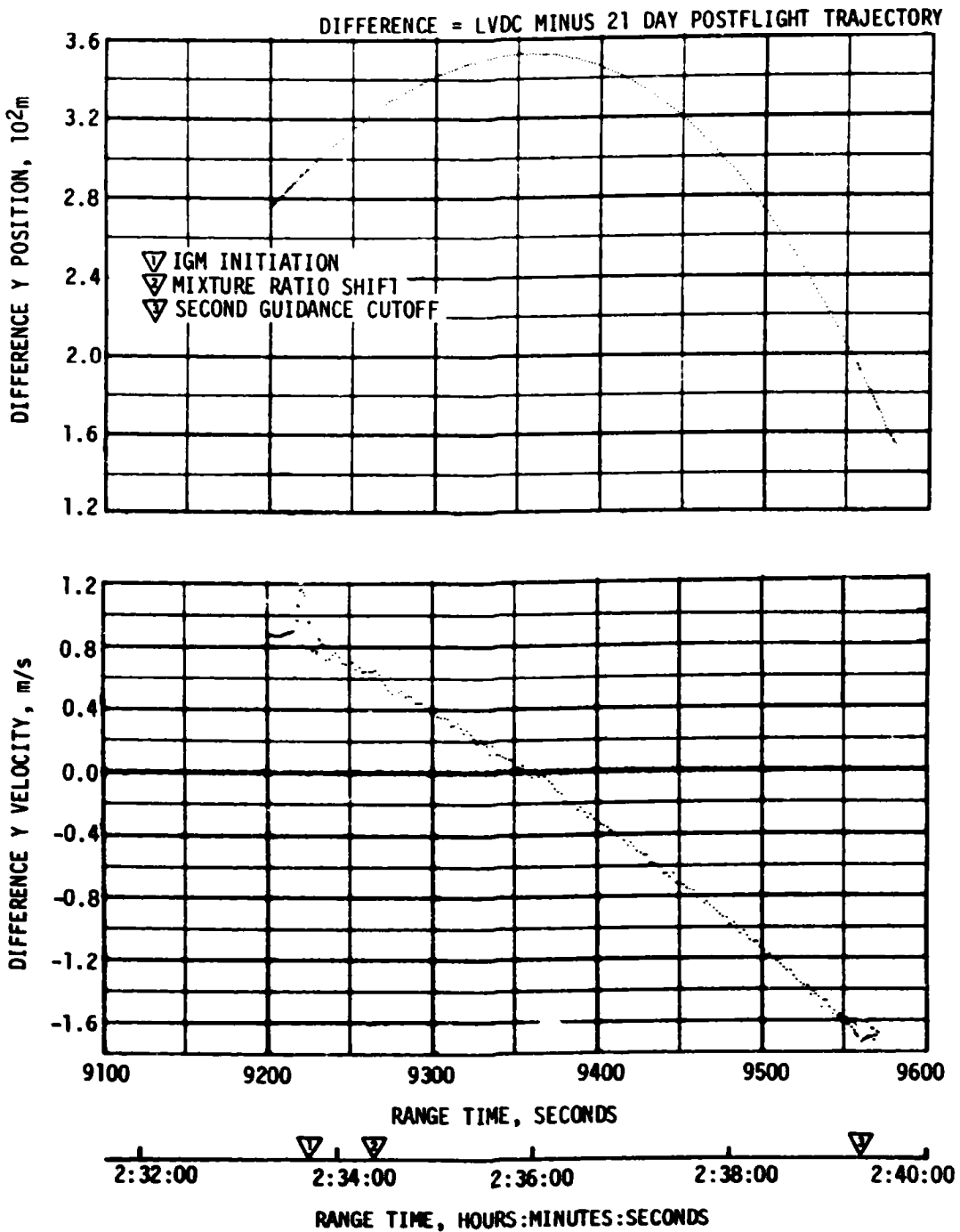


Figure 9-8. Comparison of LVDC and Postflight Trajectory During Boost to TLI, Y Position and Velocity



DIFFERENCE = LVDC MINUS 21 DAY POSTFLIGHT TRAJECTORY

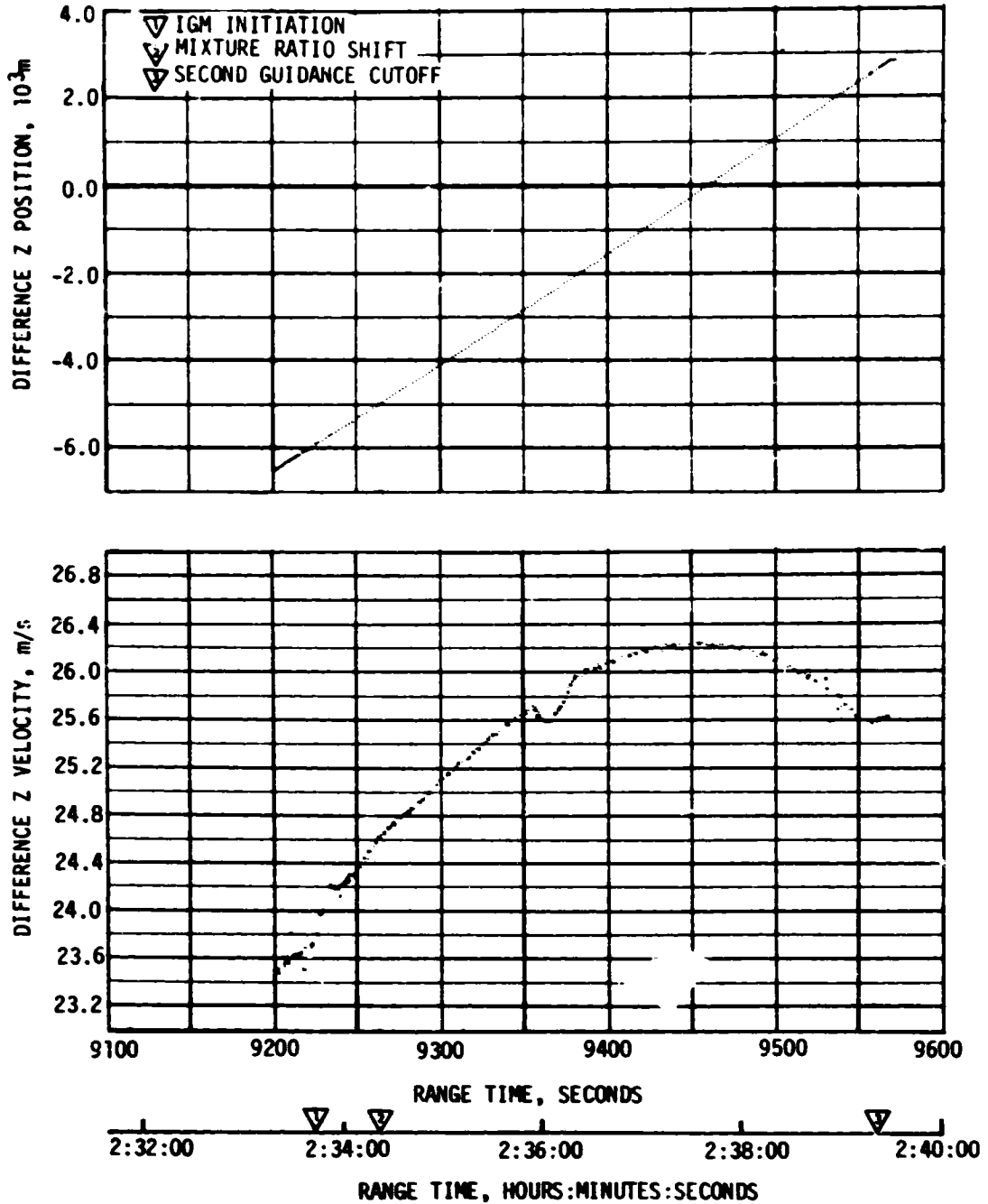


Figure 9-9. Comparison of LVDC and Postflight Trajectory During Boost to TLI, Z Position and Velocity

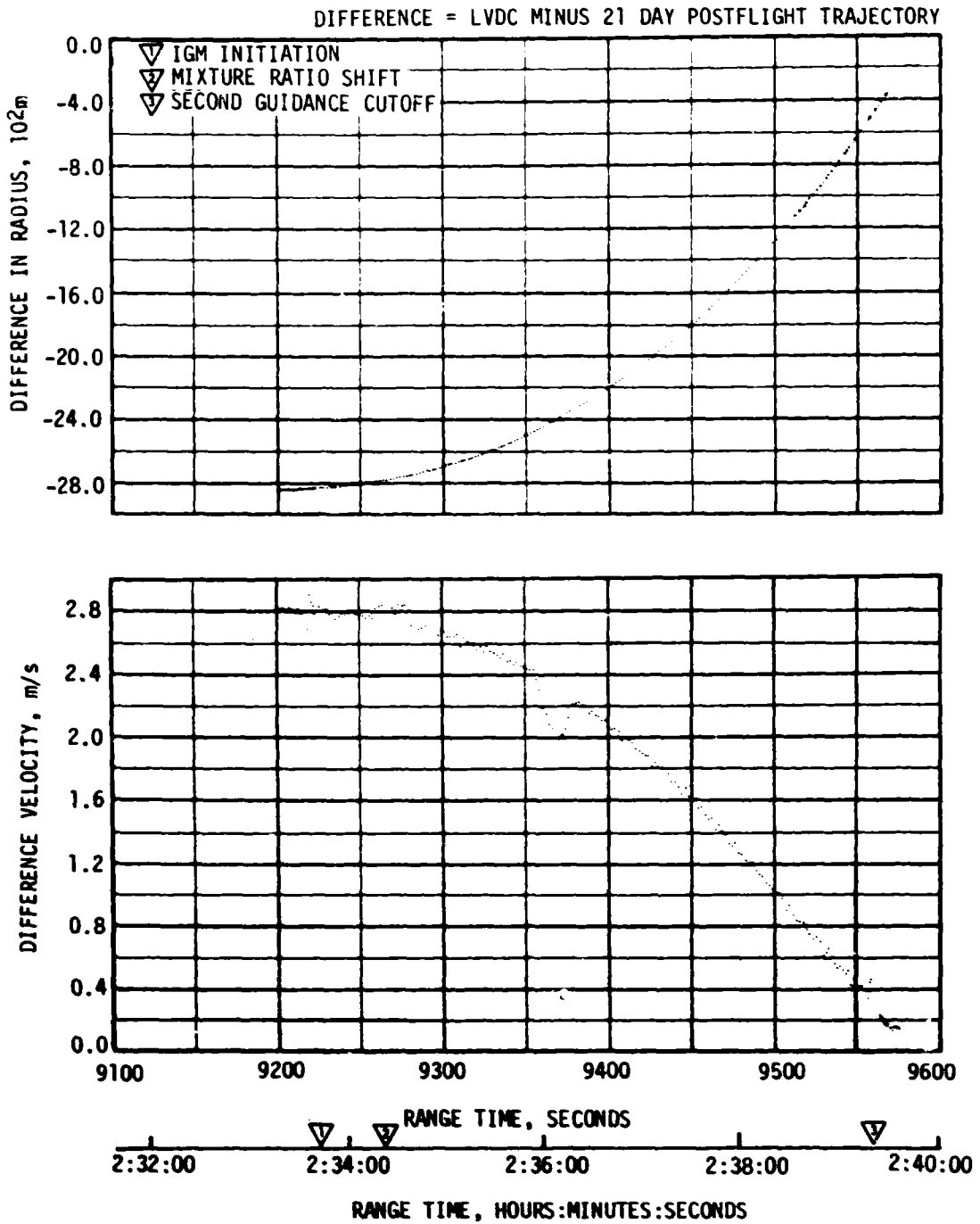


Figure 9-10. Comparisons of LVDC and Postflight Trajectory During Boost to TLI, Radius and Velocity

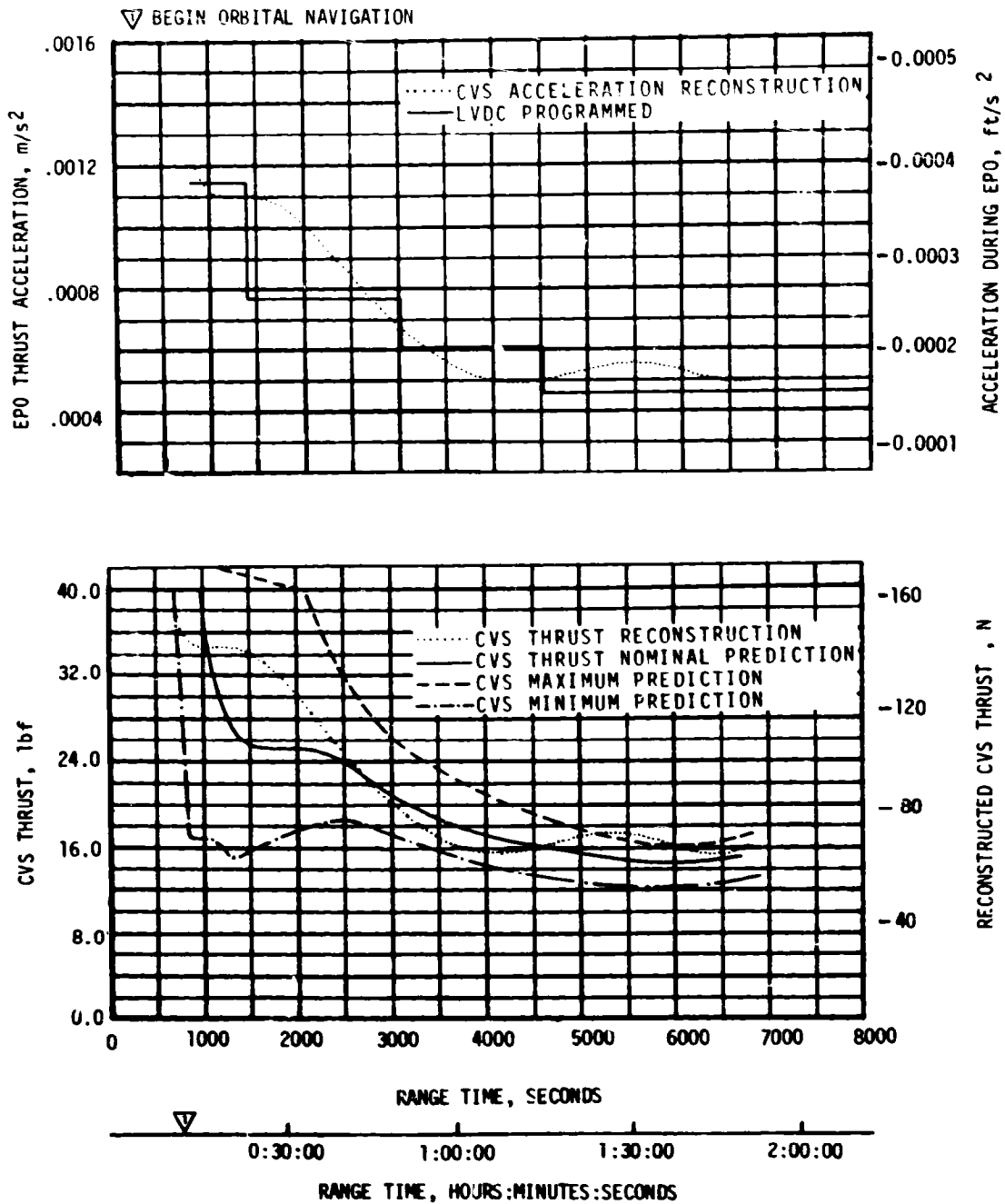


Figure 9-11. Continuous Vent System (CVS) Thrust and Acceleration During EPO

Table 9-3. State Vector Differences at Translunar Injection

PARAMETER	OPERATIONAL TRAJECTORY MINUS LVDC	POSTFLIGHT TRAJECTORY MINUS LVDC
$\Delta X_S$ , meters (feet)	16,821.1 (55,187.3)	-24,791.5 (-81,336.9)
$\Delta Y_S$ , meters (feet)	-85.7 (-281.2)	-172.3 (-565.3)
$\Delta Z_S$ , meters (feet)	-689.9 (-2263.5)	-2812.1 (-9226.0)
$\Delta R$ , meters (feet)	2392.7 (7850.1)	365.5 (1199.1)
$\Delta \dot{X}_S$ , m/s (ft/s)	-1.64 (-5.38)	-1.03 (-3.38)
$\Delta \dot{Y}_S$ , m/s (ft/s)	0.92 (3.02)	1.73 (5.68)
$\Delta \dot{Z}_S$ , m/s (ft/s)	13.63 (44.72)	-25.55 (-83.83)
$\Delta V_S$ , m/s (ft/s)	-2.05 (-6.73)	-0.19 (-0.62)

Table 9-4. AS-511 Guidance System Accuracy

FIRST BURN			
PARAMETER	DESIRED	ACHIEVED	ERROR (ACHIEVED-DESIRED)
Terminal Velocity, $V_T$ (M/Sec)	7804.0613	7804.0759	0.0146
Radius, $R_T$ (Meters)	6,544,846.0	6,544,842.93	-3.07
Path Angle, $\theta_T$ (Degrees)	0.0	-0.000588	-0.000588
Inclination, $I$ (Degrees)	32.542164	32.542099	-0.000065
Descending Node, $\lambda$ (Degrees)	123.140012	123.139111	-0.000901
SECOND BURN			
PARAMETER	DESIRED	ACHIEVED	ERROR (ACHIEVED-DESIRED)
Eccentricity, $E$	0.97402212	0.97403180	0.00000968
Inclination, $I$ (Degrees)	32.522707	32.522531	-0.000176
Descending Node, $\lambda$ (Degrees)	122.455324	122.455304	-0.000020
Argument of Perigee, $\omega$ (Degrees)	-142.339189	-142.345366	-0.006177
Energy, $C_3$ (M <sup>2</sup> /Sec <sup>2</sup> )	-1,574,430.0	-1,573,826.62	603.38

Termination of the tower avoidance yaw maneuver was initiated on time at T1 +9.0 seconds. Termination is accomplished incrementally by reducing the yaw attitude at a rate of -0.4 degrees per minor loop computation cycle. This process was interfered with by a low priority function; namely, the computations required to support the minor loop module. The effect of this interference was to halt the removal of the total yaw attitude error.

Subsequent execution of the Minor Loop Support module re-established the minor loop inertial yaw attitude angular rate and the maneuver was terminated, late, but properly. The effects of the yaw tower avoidance maneuver problem are presented in Section 10.

The flight program will be reprogrammed to save the necessary data required to fulfill the vehicle commanded dynamics.

The acceleration provided by the S-IC was less than that predicted in the Operational Trajectory. This caused negative errors in radius and velocity magnitudes at S-IC OECO and, subsequently, at Iterative Guidance Mode (IGM) initiation. The measured total velocity was approximately 14 meters/second low at IGM initiation and the radius (or altitude) was approximately 1940 meters low. The IGM routines reacted properly and produced a somewhat flatter trajectory profile than that predicted in the Operational Trajectory (OT). The pitch attitude angle during first burn is shown in Figure 9-12.

The crossrange velocity was perturbed by winds during S-IC burn so that the velocity at IGM initiation was different from that shown in the OT. The Flight Program reacted properly and provided satisfactory yaw steering (Figure 9-13). Because the center of gravity does not lay along the longitudinal axis of the vehicle, pitch and yaw motions provide a coupled roll response. The roll attitude is shown in Figure 9-14, and is considered to be within acceptable limits.

Table 9-4 shows the terminal conditions for first burn. Terminal conditions were obtained by linear forward extrapolation.

The coast phase maneuvers were accomplished satisfactorily and at predicted times. Table 9-5 shows the maneuver times and the commanded steering angles.

The initiation of orbital navigation occurred at T5 +100.78 seconds, within the one computation cycle tolerance of the scheduled time, T5 + 100 seconds. Orbital navigation was within the required tolerance for parking orbit. Termination of orbital navigation occurred at T5 +7924.488 seconds (T6 -7.665 seconds).

IGM for the S-IVB stage second burn was implemented satisfactorily producing the terminal conditions shown in Table 9-4. The desired values were based upon telemetered target values and actual terminal values were obtained by linear forward extrapolation. The attitude angles

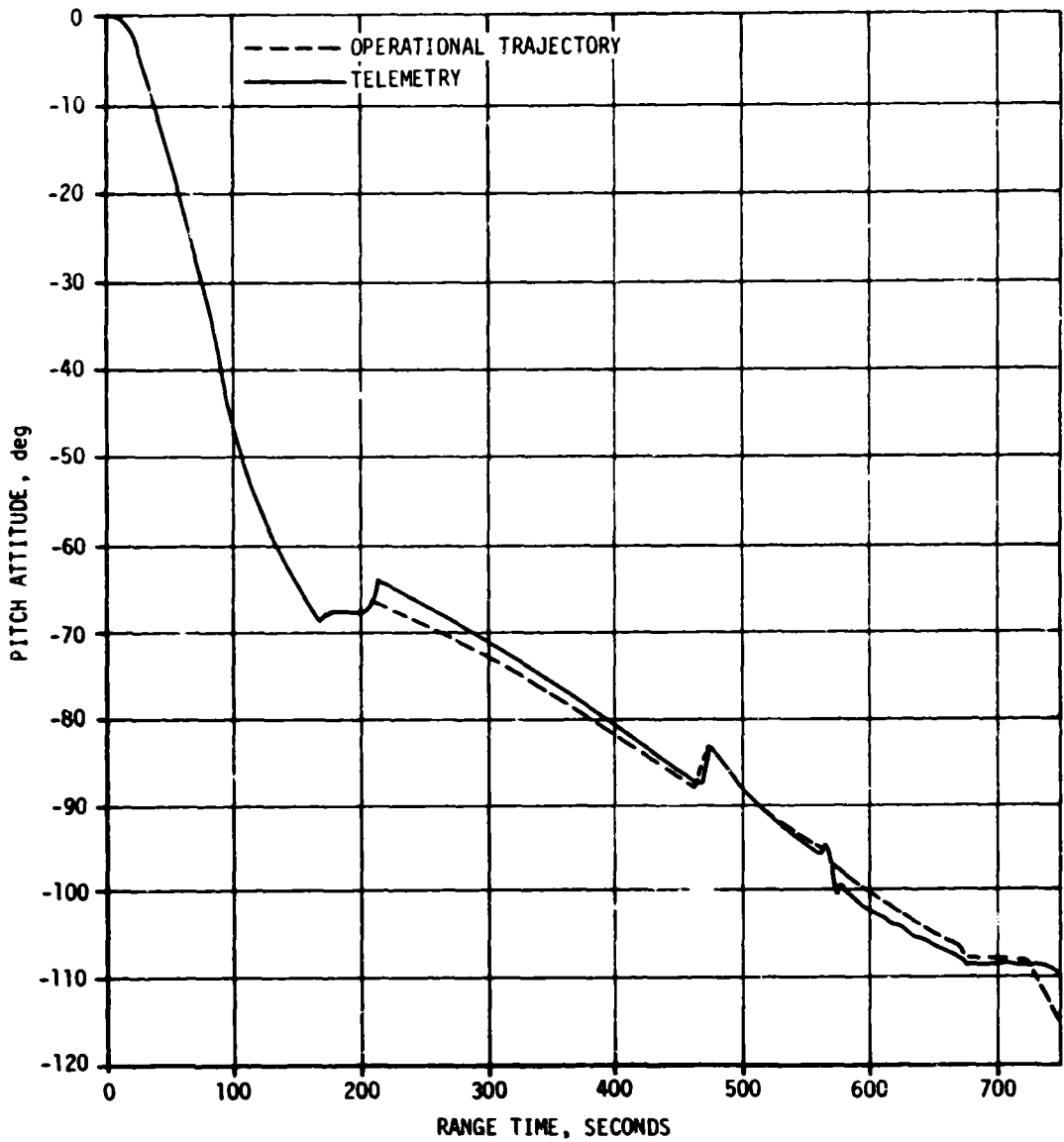


Figure 9-12. AS-511 Pitch Attitude Angle, First Burn

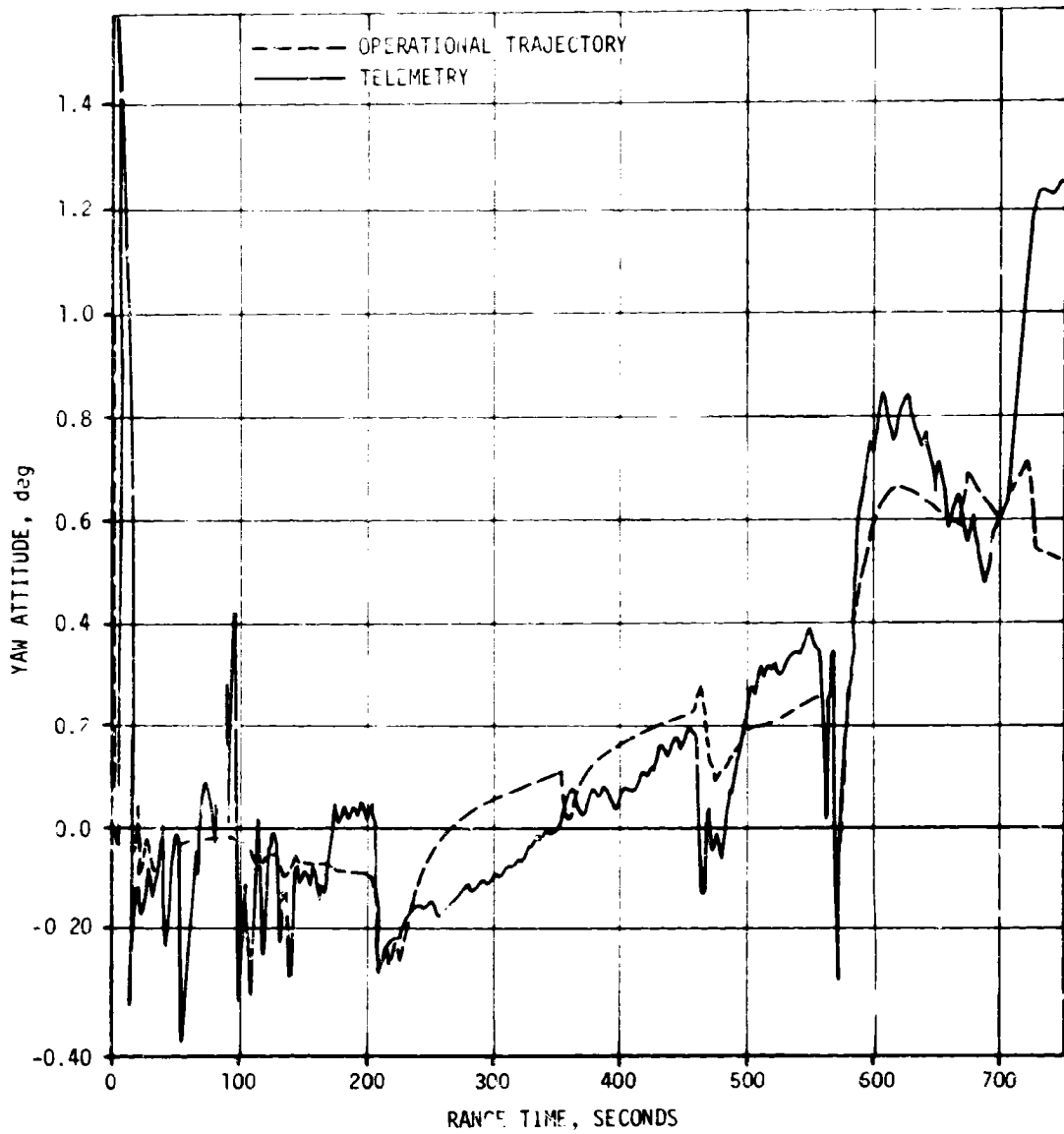


Figure 9-13. AS-511 Yaw Attitude Angle, First Burn

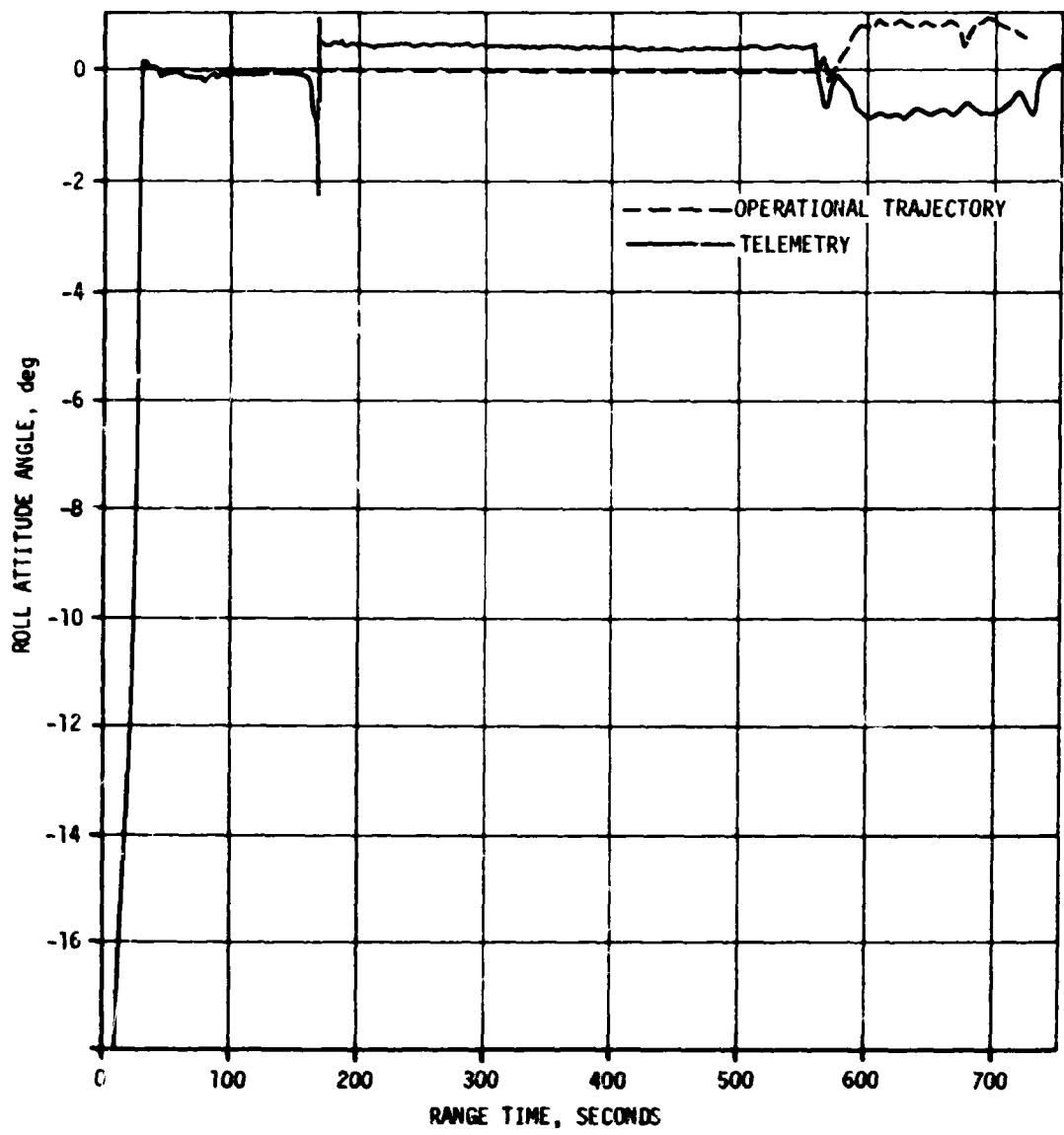


Figure 9-14. AS-511 Roll Attitude Angle, First Burn



Table 9-5. Coast Phase Guidance Steering Commands at Major Events

FLIGHT PERIOD	EVENT	TIME, SECONDS	COMMANDED STEERING ANGLES, DEGREES		
			ROLL (X)	PITCH (Y)	YAW (Z)
Earth Parking Orbit	Initiate Orbital Guidance Chi-Freeze	T <sub>5</sub> + 0.0	-0.7645	-108.3064	0.5971
	Initiate Maneuver to Local Horizontal	T <sub>5</sub> + 21.333	0.0000	-117.7312	0.5444
	Initiate Orbital Navigation	T <sub>5</sub> + 100.788	-	-	-
Post TLI	Initiate Orbital Guidance Chi-Freeze	T <sub>7</sub> + 0.0	-0.9905	1.1886	-0.2149
	Initiate Orbital Navigation	T <sub>7</sub> + 151.395	-	-	-
	Initiate Maneuver to Local Horizontal	T <sub>7</sub> + 151.619	0.0000	-18.2860	0.6721
	Initiate TD&E Maneuver	T <sub>7</sub> + 900.620	180.0000	55.4896	-40.8146
	TD&E Maneuver Complete	T <sub>7</sub> + 11634.0	-	-	-
	Initiate Lunar Impact Local Reference Maneuver	T <sub>8</sub> + 581.195	180.0000	67.0601	13.0220

are shown in Figures 9-15 and 9-16 for pitch and yaw, respectively. The roll attitude angles were nearly nominal, being perturbed only by the roll torque associated with the main engine burn.

The commanded maneuvers occurred predictably at times and with the angles shown in Table 9-5. Some concern caused by the setting of the error monitor bits in the LVDC caused the termination of telemetry from the IU to be initiated earlier than planned, following the initiation of the three-axis tumble at T8 +5819 seconds. This ended the guidance and navigation function for the mission.

All control and error analysis functions in the Minor Loop were accomplished satisfactorily.

The pitch gimbal angle reading failed the Reasonableness Test three consecutive times in the computer cycle beginning at 21,541.07 seconds. The change per minor loop in the output of the pitch gimbal was 0.2148, 0.2427, and 0.4883 degrees for the first, second, and third consecutive readings that exceeded the Reasonableness Test Constant of 0.2 degree per minor loop. The flight program then properly selected the pitch back-up gimbal resolver for all subsequent Minor Loop calculations, and increased the Reasonableness Test Constant from 0.2 to 1.1 degrees per minor loop.

The unreasonable pitch gimbal angle readings were due to contact of the platform yaw gimbal with the mechanical stop. This resulted in translating yaw torque into the pitch axis causing the pitch gimbal torquer to drive unusually fast.

Because Flight Control Computer (FCC) deactivation occurred 204 seconds prior to the first Reasonableness Test failure, this problem is relevant only for the evaluation of flight program error handling. This handling proved to be proper and predictable. No corrective action is needed.

#### 9.4 NAVIGATION AND GUIDANCE SYSTEM COMPONENTS

The navigation and guidance hardware satisfactorily supported the accomplishment of mission objectives. Only two anomalous incidents were observed in flight: the ST-124M Stabilized Platform System (SPS) crossrange accelerometer contacted a mechanical stop during liftoff vibration and the LVDC issued several Error Monitor Register (EMR) indications during the terminal portion of the IU mission.

The Stabilized Platform Subsystem (SPS) showed no evidence of hardware damage and the velocity shift caused by accelerometer contact with a mechanical stop did not impact the mission. The Error Monitor Register indications in the LVDC were caused probably by an intermittent redundant delay line. This intermittent loss of redundancy did not affect any data flow in the LVDC and, therefore, did not impact mission success.

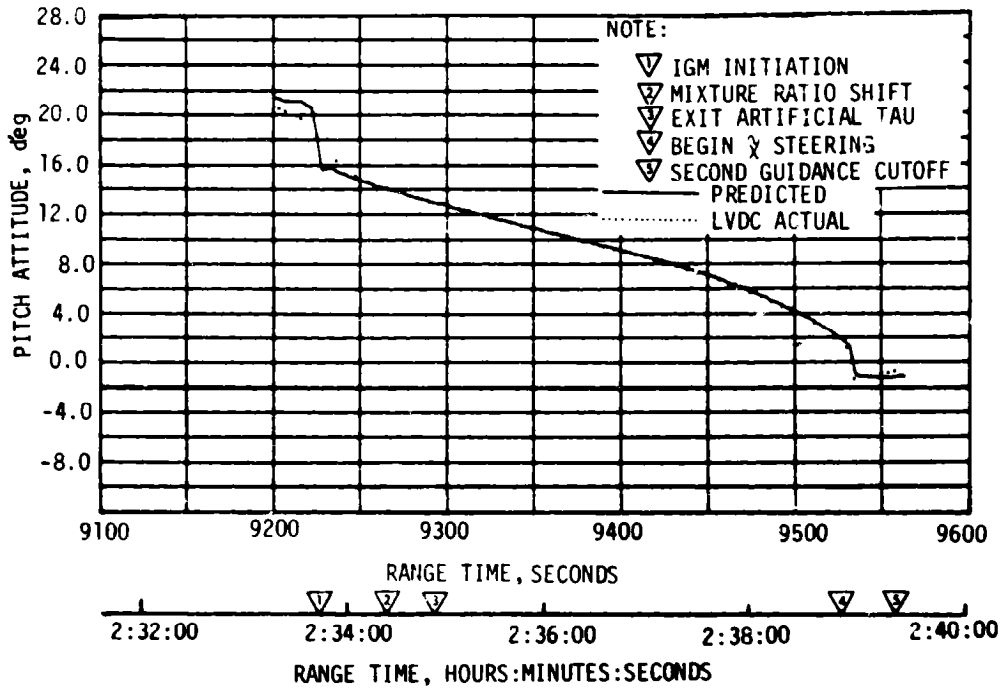


Figure 9-15. Commanded and Actual Pitch Attitude - Second Burn

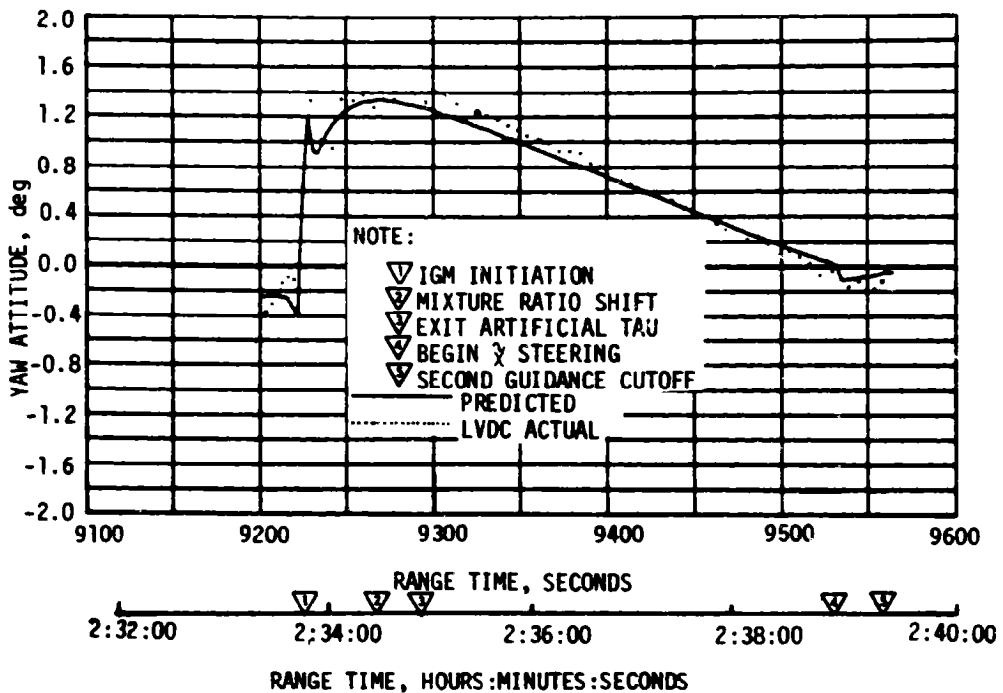


Figure 9-16. Commanded and Actual Yaw Attitude - Second Burn

Starting at 21541.07 seconds, following the establishing of the three-axis tumble, the SPS Z gimbal contacted one of the mechanical stops for three different periods. As described in Section 9.3, this resulted in the three Reasonableness Test failures and a transfer to a backup gimbal resolver.

#### 9.4.1 ST-124M Stabilized Platform System

The three gyro loops were relatively quiet during liftoff. The accelerometer servo loops operated within previously experienced limits.

At 0.16 second, the Y accelerometer pickoff apparently contacted one of the mechanical stops set at  $5.75 \pm 0.25$  degrees either side of null, resulting in an approximate 1 meter/second Y velocity shift. The shift was detected by the LVDA between 0.064 and 0.306 second. A more precise determination of the time of the shift was not possible because continuous telemetry of the velocity output pulses was not provided for this mission. The velocity shift was similar to shifts observed during the liftoff vibration on AS-506 and AS-508.

A cross-analysis was performed on the Power Spectral Densities (PSD) of the pickoff deflection measurement (H12-603) and a vibration measurement (E40-603) located on the upper IU ring at Position IV. Figure 9-17 is the amplitude correlation of these two measurements. It can be seen that significant energy at 33 Hz was present to excite the accelerometer servo loop at its resonant frequency.

A change has been initiated for AS-513 (Skylab 1) to preclude vibration induced shifts during the launch period by taking the ST-124M accelerometer (Y and Z) readings out of the navigation loop from GRR to (T1 +10 seconds). The navigation scheme will employ preflight predictions during this interval of time.

#### 9.4.2 LVDC and LVDA

The LVDA and LVDC performed satisfactorily for the AS-511 mission with the exception of a series of Error Monitor Register (EMR) bits 13 and 14 indications of Triple Modular Redundant (TMR) logic signal disagreements which occurred for approximately 376 seconds beginning at 24,210 seconds. No indication of component malfunction was observed prior to the indications of EMR bits 13 and 14 commencing at 24,210 seconds.

In general, the LVDA Error Monitor Register (EMR) bits are set by disagreement detectors which monitor selected LVDC and LVDA logic signals. Each disagreement detector is gated by one of four clock pulses which comprise the basic computer timing. When an EMR bit is set as a result of a detected signal disagreement, the LVDA automatically generates an Error Time Word (ETW) which can be decoded to give the contents of the LVDC instruction counter, the phase, bit gate, and clock time at the time of failure.

TEST	AS-511	FILTER B.W.	0.999 Hz
LINK/CHAN	DFL-13	SAMPLE RATE	400.000/SEC
SLICE TIME	-0.500 TO 1.500	R-COMP-RRV	453-3323
MEAS. NO.	H12-603	COMP. RMS	0.964
MEAS. NO.	E40-603	COMP. RMS	1.613

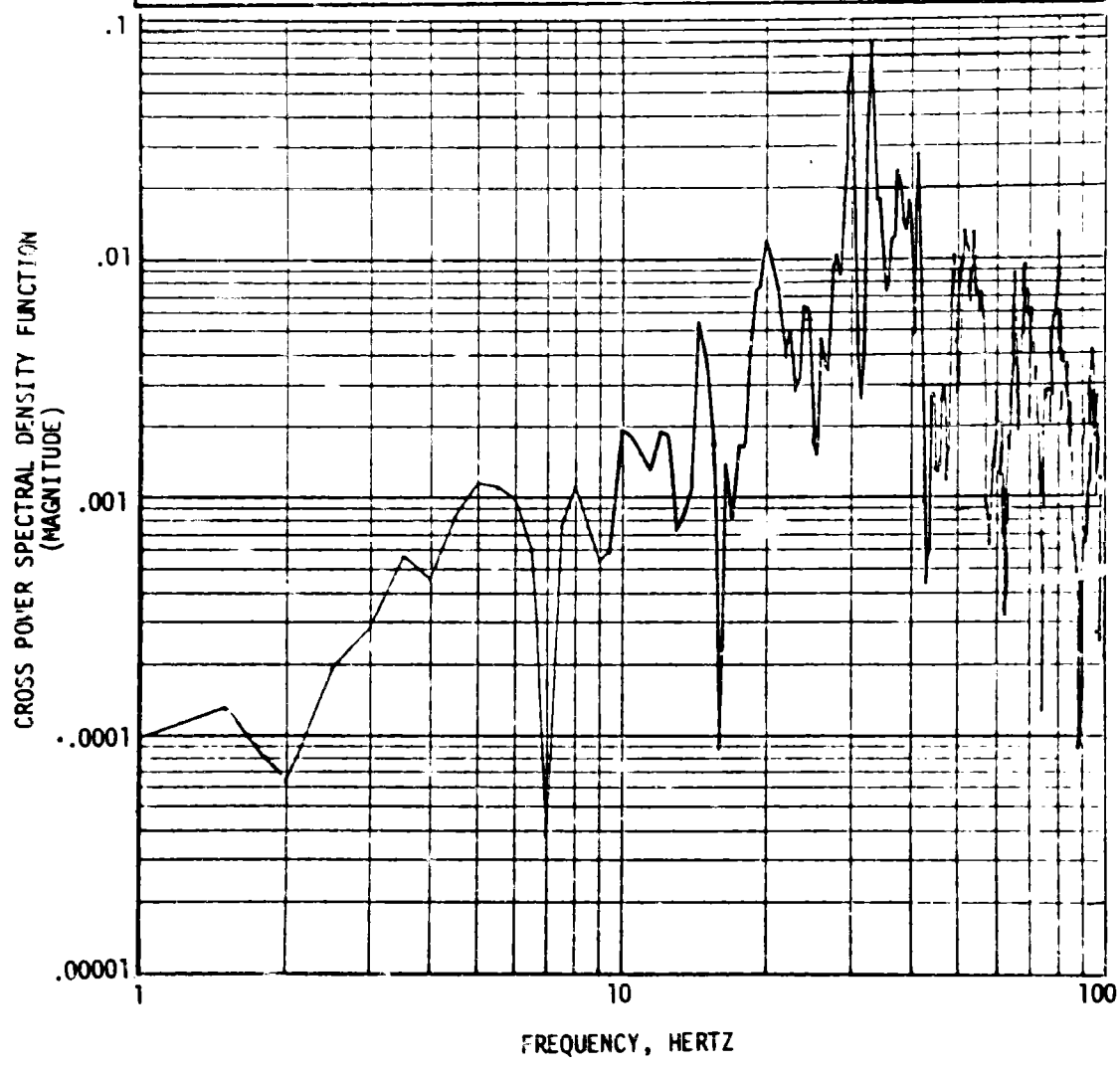


Figure 9-17. Amplitude of Cross-Analysis

The Error Time Word data indicates multiple failure or a single failure common to all channels of DL44 and DL44SA signal flow. The most probable condition was identified as a single failure. Since the delay line element presents a greater contribution to the LVDC failure rate than the other failure candidates, it is concluded that the 44-microsecond delay line failure is the most probable cause of the EMR bits 13 and 14. The safety feature inherent to the triple redundant design prevented the system from deviating from its nominal performance. No corrective action is required.

The LVDA performed satisfactorily. However, three EMR bit 3 indications were observed indicating an interrupt latch signal disagreement as a result of the inherent differences between the rise time responses of the Triple Modular Redundant (TMR) Digital Command System interrupt input circuits. As previously, these disagreements did not impact mission success and are not considered as malfunctions.

## SECTION 10

### CONTROL AND SEPARATION

#### 10.1 SUMMARY

The control and separation systems functioned correctly throughout the flight of AS-511. Engine gimbal deflections were nominal and Auxiliary Propulsion Systems (APS) firings predictable. Bending and slosh dynamics were adequately stabilized. No undue dynamics accompanied any separation. Some problems did appear within the control system and these are discussed below in conjunction with system performance.

#### 10.2 S-IC CONTROL SYSTEM EVALUATION

##### 10.2.1 Liftoff Clearances

The AS-511 postflight data revealed an anomaly in the liftoff yaw maneuver. Figure 10-1 shows that the actual yaw maneuver ended more than one second later than predicted. The control system responded correctly to the yaw guidance commands and the anomaly had little effect on tower clearance for this flight. However, if the same delay would have occurred at the beginning of the yaw maneuver, it may have reduced the clearance significantly, see Section 9.3. Figure 10-2 shows that a liftoff simulation with flight data used less than 10 percent of the available clearance. Even though the yaw maneuver ended more than one second late, the reconstructed yaw attitude and the plume angle were within predicted envelopes (Figure 10-2). The ground wind was from the west (256 degree azimuth) with a magnitude of 5.14 meters/second at the 161.5 meter (530 foot) level. Table 10-1 summarizes liftoff conditions and misalignments.

##### 10.2.2 Inflight Dynamics

The AS-511 control system performed satisfactorily during S-IC boost. The peak measured wind speed was 26.1 meters/second at 11.85 kilometers with an azimuth of 257 degrees. However, the q-ball data indicates that the actual peak wind speed encountered by the vehicle was 21.2 meters/second at the same altitude and azimuth. Both wind speeds are smaller than the 50 percentile April wind. Approximately 10 percent of the available pitch plane engine deflection was used (based on the average pitch engine gimbal angle). Time histories of pitch and yaw control parameters are shown in Figures 10-3 through 10-5, with peaks summarized in Table 10-2.

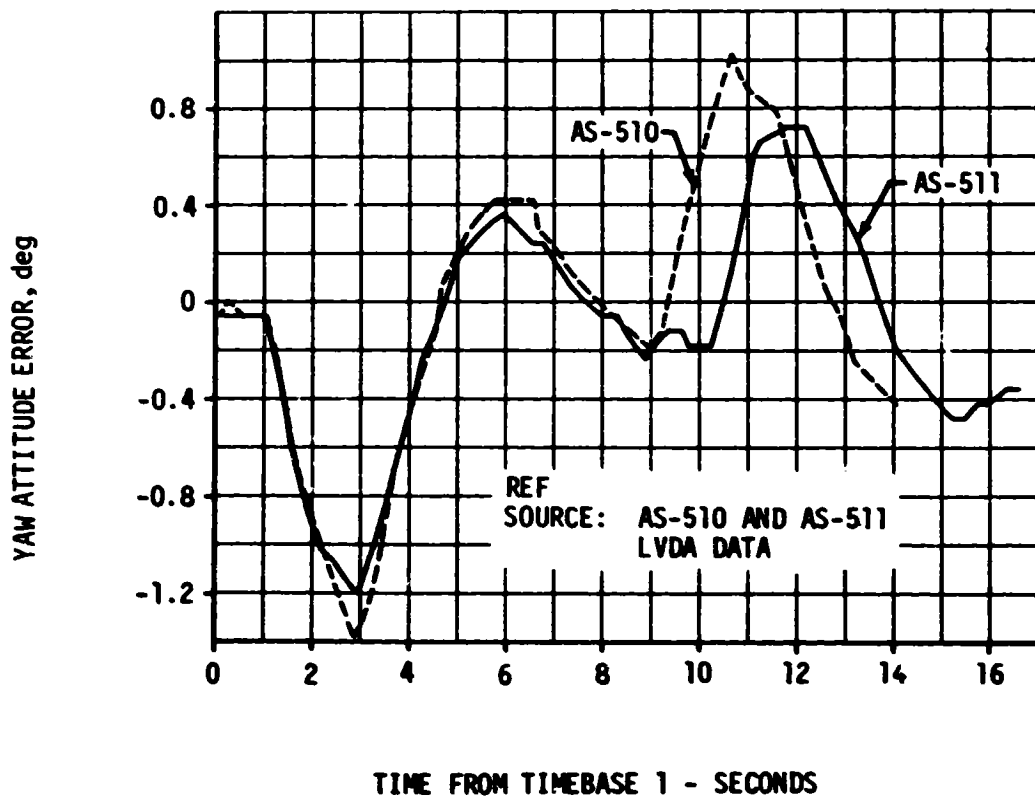
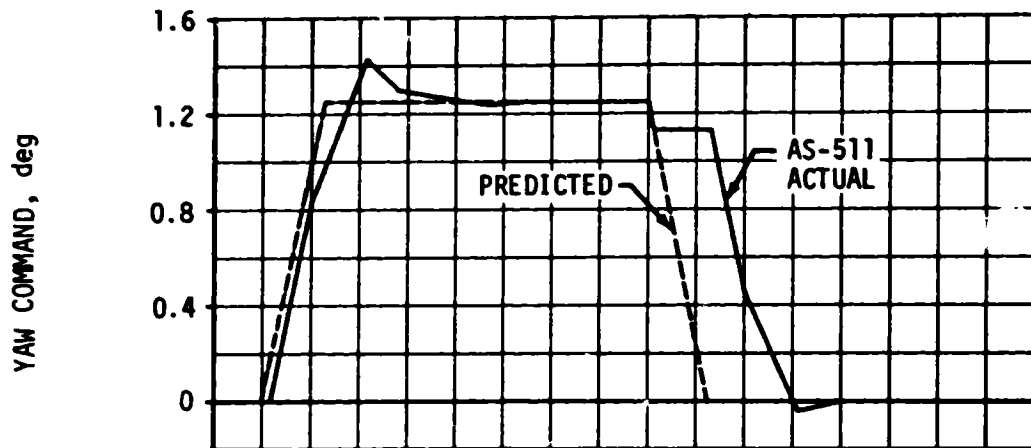


Figure 10-1. AS-511 Liftoff Yaw Maneuver



ε-01

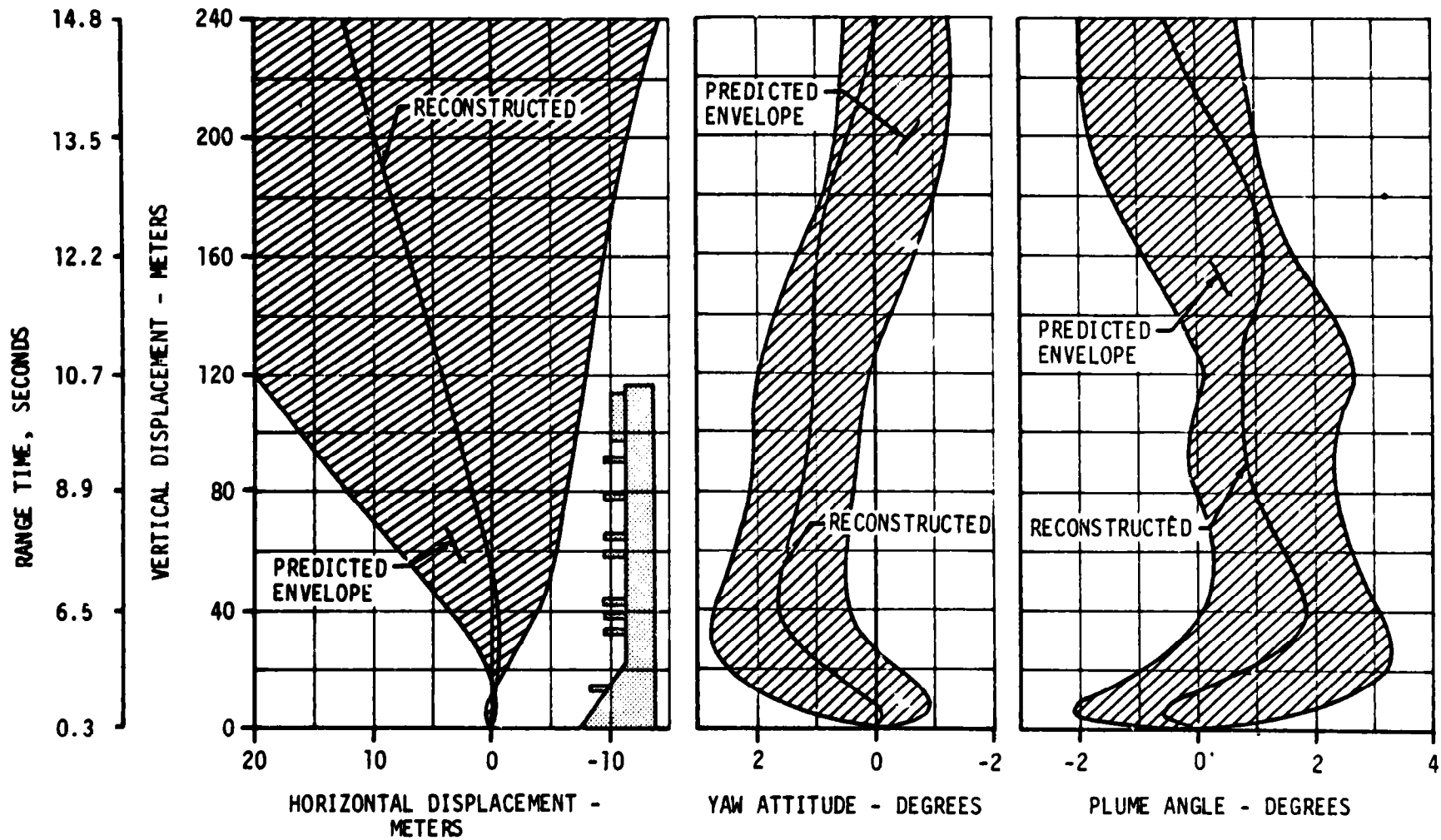


Figure 10-2. AS-511 Reconstructed Liftoff Trajectory

- ▽ BEGIN YAW MANEUVER
- ▽ END YAW MANEUVER, 10.9 SEC
- ▽ BEGIN PITCH/ROLL MANEUVER, 12.7 SEC
- ▽ OUTBOARD ENGINE CANT
- ▽ END ROLL MANEUVER
- ▽ MACH 1
- ▽ MAX q
- ▽ 1st GAIN SWITCH
- ▽ 2nd GAIN SWITCH
- ▽ CENTER ENGINE CUTOFF
- ▽ TILT ARREST
- ▽ OUTBOARD ENGINE CUTOFF
- ▽ STAGING

— MEASURED  
 - - - SIMULATED

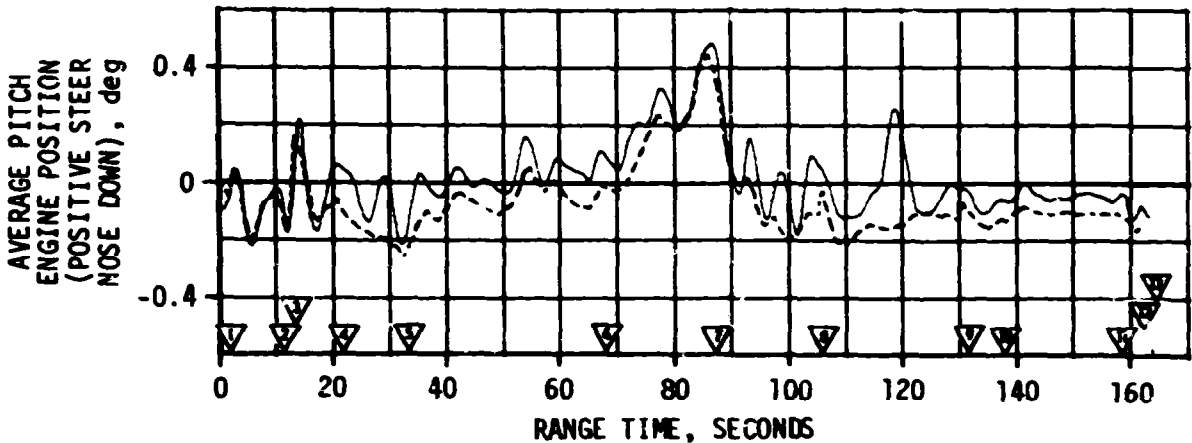
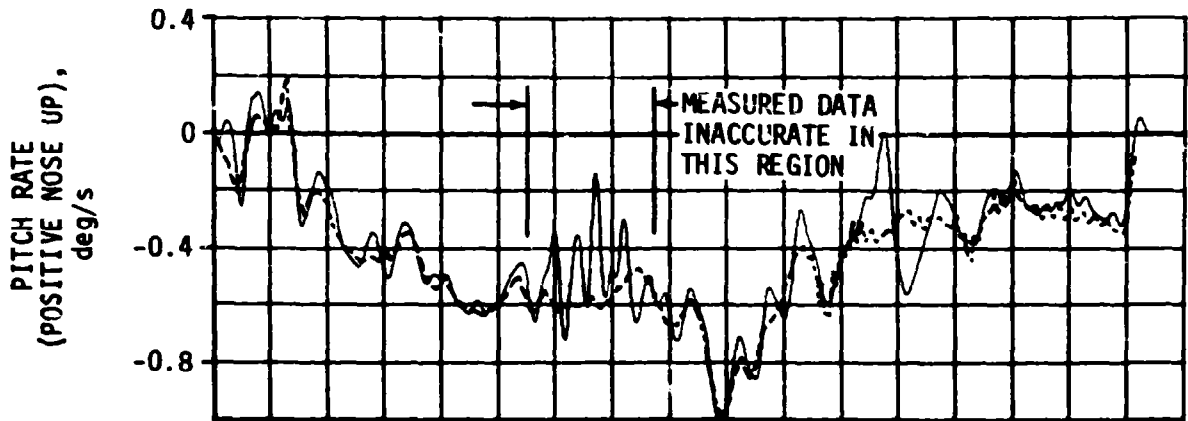
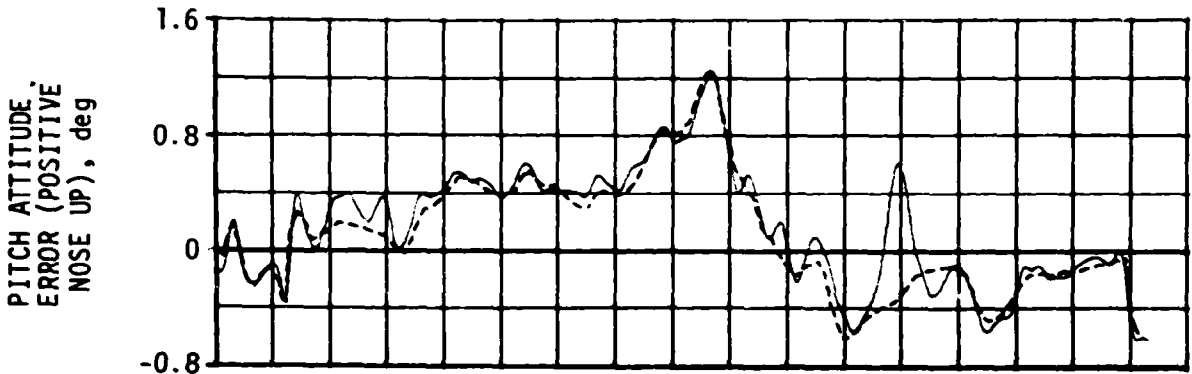


Figure 10-3. Pitch Plane Dynamics During S-IC Burn

- ▽ BEGIN YAW MANEUVER
- ▽ END YAW MANEUVER , 10.9 SEC
- ▽ BEGIN PITCH/ROLL MANEUVER , 12.7 SEC
- ▽ OUTBOARD ENGINE CANT
- ▽ END ROLL MANEUVER
- ▽ MACH 1
- ▽ MAX q
- ▽ 1st GAIN SWITCH
- ▽ 2nd GAIN SWITCH
- ▽ CENTER ENGINE CUTOFF
- ▽ TILT ARREST
- ▽ OUTBOARD ENGINE CUTOFF
- ▽ STAGING

—— MEASURED  
 - - - - SIMULATED

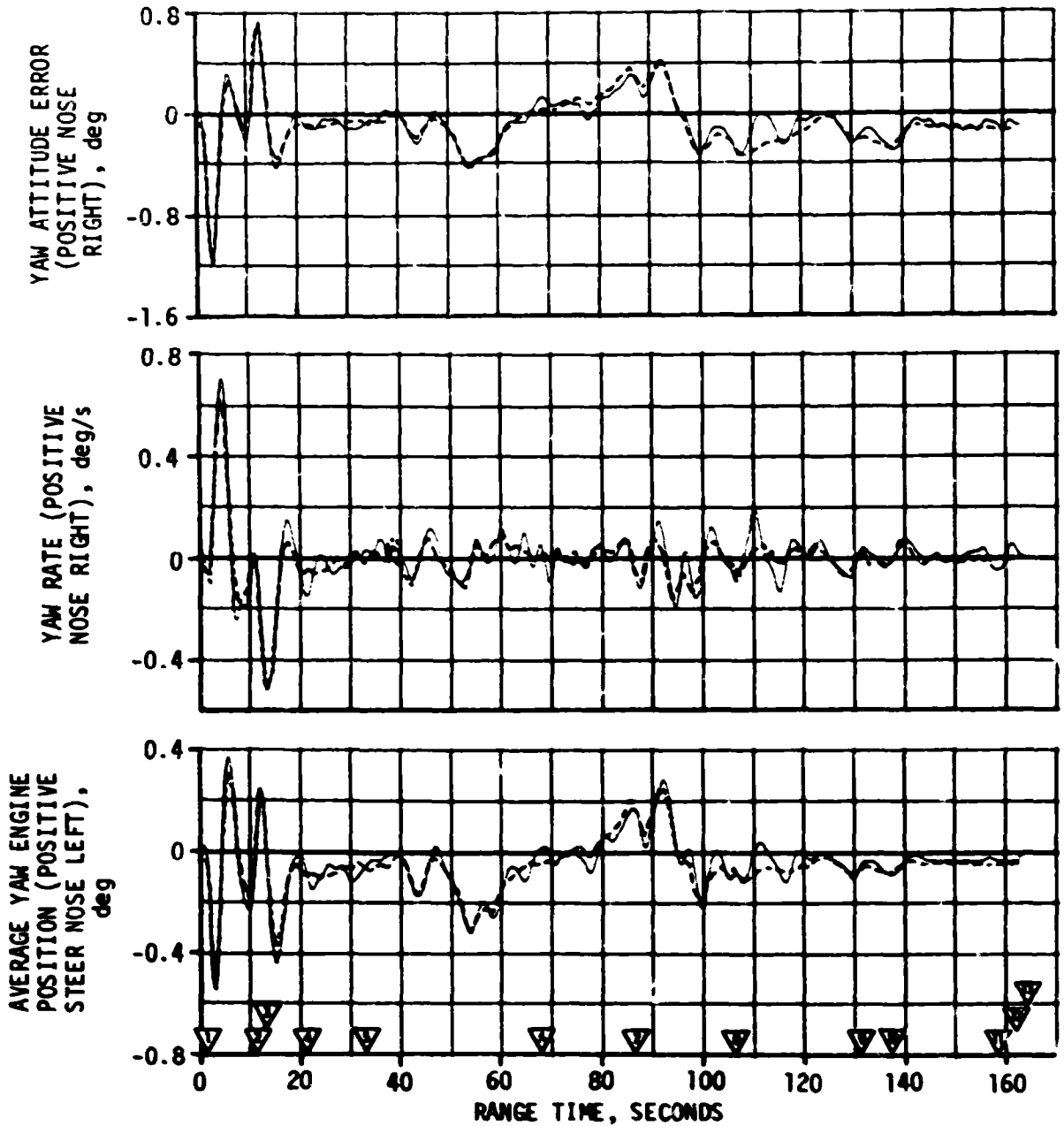


Figure 10-4. Yaw Plane Dynamics During S-IC Burn

- ▽ BEGIN YAW MANEUVER
  - ▽ END YAW MANEUVER, 10.9 SEC
  - ▽ BEGIN PITCH/ROLL MANEUVER, 12.7 SEC
  - ▽ OUTBOARD ENGINE CANT
  - ▽ END ROLL MANEUVER
  - ▽ MACH 1
  - ▽ MAX q
  - ▽ 1st GAIN SWITCH
  - ▽ 2nd GAIN SWITCH
  - ▽ CENTER ENGINE CUTOFF
  - ▽ TILT ARREST
  - ▽ OUTBOARD ENGINE CUTOFF
  - ▽ STAGING
- CALCULATED FROM Q-BALL  
 - - - SIMULATED

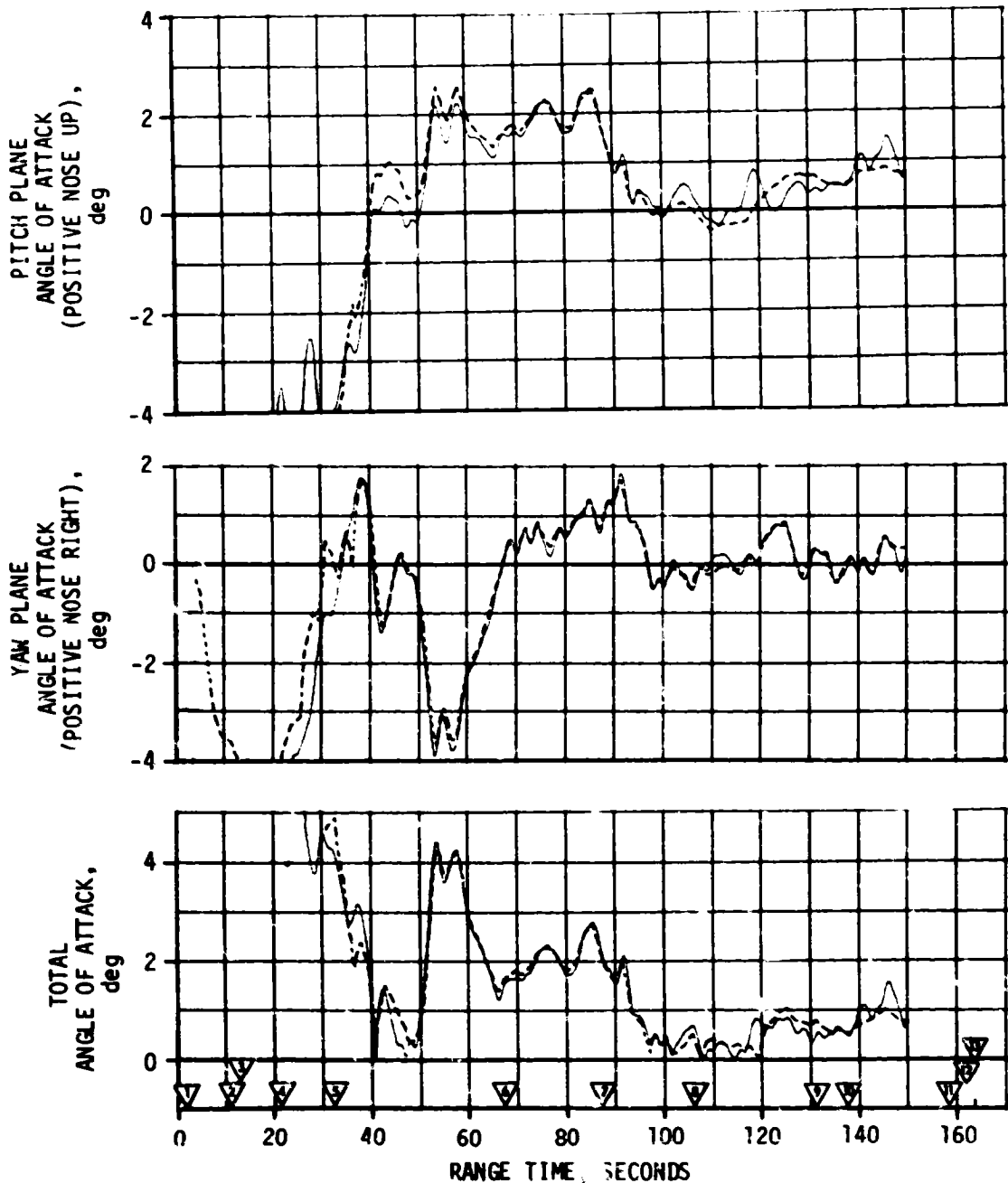


Figure 10-5. Pitch and Yaw Plane Free Stream Angle of Attack During S-1C Burn

Table 10-1. AS-511 Misalignment and Liftoff Conditions Summary

PARAMETER	PREDICTED 3 $\sigma$ RANGE			LAUNCH		
	PITCH	YAW	ROLL	PITCH	YAW	ROLL
Thrust Misalignment, deg	+0.34	+0.34	+0.34	0.01	0.06	0.0
Center Engine Cant, deg	+0.34	+0.34	-	0.11	0.07	-
Vehicle Stacking and Pad Misalignment, deg	+0.29	+0.29	0.0	-0.10	-0.01	0.0
Attitude Error at Holddown Arm Release, deg	-	-	-	-0.16	-0.01	0.03
Peak Soft Release Force Per Rod, N(lbf)	415,900 (93,500)			*		
Wind	19.55 M/S (38 Knots) at 161.5 Meters (530 Feet)			5.14 M/S (10.0 Knots) at 161.5 Meters (530 Feet)		
Thrust to Weight	1.190			1.204**		
*Data not available.						
**Determined by simulating vehicle rise history recorded by camera during liftoff.						

Table 10-2. Maximum Control Parameters During S-IC Burn

PARAMETERS	PITCH PLANE		YAW PLANE		ROLL PLANE	
	AMPLITUDE	RANGE TIME (SEC)	AMPLITUDE	RANGE TIME (SEC)	AMPLITUDE	RANGE TIME (SEC)
Attitude Error, deg	1.24	86.9	-1.18	3.3	-0.88	14.1
Angular Rzte, deg/s	-1.01	88.7	0.70	4.6	1.27	14.8
Average Gimbal Angle, deg	0.48	86.6	-0.55	3.2		
Angle of Attack, deg	2.49	85.9	-3.93	53.3		
Angle of Attack Dynamic Pressure Product, deg-N/CM <sup>2</sup> (deg-lbf/ft <sup>2</sup> )	8.67 (1810)	85.9	5.90 (1250)	91.6		
Normal Acceleration, m/s <sup>2</sup> (ft/s <sup>2</sup> )	-0.56 (-1.84)	86.7	-0.34 (-1.12)	57.5		

Dynamics in the region between 0 and 40 seconds resulted primarily from guidance commands. Between 40 and 110 seconds vehicle dynamics were caused by the pitch guidance program and wind magnitude and shears. Dynamics from 110 seconds to S-IC outboard engine shutdown were caused by separated airflow aerodynamics, inboard engine shutdown, tilt arrest, and high altitude winds.

The attitude errors between liftoff and 20 seconds indicated that the equivalent thrust vector misalignments before the start of outboard engine cant were 0.01, 0.06, and 0.00 degrees in pitch, yaw, and roll, respectively. After a nominal outboard engine cant was introduced these misalignments became 0.1, 0.02, and 0.01 degrees. The transient in the attitude errors at center engine cutoff indicates that the center engine cant was 0.11 degree in pitch and 0.07 degree in yaw.

All dynamics were within vehicle capability. Vehicle attitude errors required to trim out the effects of thrust unbalance, offset center of gravity, thrust vector misalignment, and control system misalignments were within predicted envelopes. The peak angles of attack in the maximum dynamic pressure region were 2.49 degrees in pitch and 1.84 degrees in yaw. In this region wind shears caused maximum average pitch and yaw engine deflections of 0.48 and 0.29 degrees, respectively. No divergent bending or slosh dynamics were observed, indicating that these modes were adequately stabilized. Vehicle dynamics prior to S-IC/S-II first plane separation were within staging requirements.

### 10.3 S-II CONTROL SYSTEM EVALUATION

The S-II stage attitude control system performance was satisfactory. The vehicle dynamics were within expectations at all times. The maximum values of pitch and yaw parameters occurred in response to Iterative Guidance Mode (IGM) Phase I initiation. The maximum values of roll control parameters occurred in response to S-IC/S-II separation conditions. The maximum control parameter values for the period of S-II burn are shown in Table 10-3. The maximum average gimbal angle deflection occurring during S-II flight is shown to be less than the amount developed by the problem which appeared in the Flight Readiness Test (see Section 3.2.2).

Table 10.3 Maximum Control Parameters During S-II Burn

PARAMETER	PITCH PLANE		YAW PLANE		ROLL PLANE	
	AMPLITUDE	RANGE TIME (SEC)	AMPLITUDE	RANGE TIME (SEC)	AMPLITUDE	RANGE TIME (SEC)
Attitude Error, deg	-2.2	207.7	0.3	206.4	-2.3	166.4
Angular Rate, deg/s	1.1	208.4	-0.1	208.0	2.3	167.7
Maximum Gimbal Angle, deg	-0.5	206.7	-0.1	166.8	-	-

Between S-IC OECO and initiation of IGM Phase I, commands were held constant. Significant events occurring during this interval were S-IC/S-II separation, S-II stage J-2 engine start, second plane separation, and Launch Escape Tower (LET) jettison. Pitch and yaw dynamics during this interval indicated adequate control stability as shown in Figures 10-6 and 10-7, respectively. Steady state attitudes were achieved within 10 seconds from S-IC/S-II separation.

At IGM initiation, guidance commands caused the vehicle to pitch up. During IGM, the vehicle pitched down at a constant commanded rate of approximately  $-0.1$  deg/sec. The transient magnitudes experienced were similar to previous flights. At S-II CECO, the guidance routines reacted properly to the decrease in total thrust.

Flight and simulated data comparison, Figures 10-6 and 10-7, show agreement at those events of greatest control system activity. Differences between the two can be accounted for largely by engine location misalignments, thrust vector misalignments, and uncertainties in engine thrust buildup characteristics. The inflight thrust misalignments (with effects of center of gravity offset included) were found to be 0.1 degree about each axis.

#### 10.4 S-IVB CONTROL SYSTEM EVALUATION

The S-IVB Thrust Vector Control (TVC) system provided satisfactory pitch and yaw control during powered flight. The APS provided satisfactory roll control during first and second burns.

During S-IVB first and second burns, control system transients were experienced at S-II/S-IVB separation, guidance initiation, Mixture Ratio (MR) shift, terminal guidance mode, and S-IVB Engine Cutoff (ECO). These transients were expected and were well within the capabilities of the control system.

##### 10.4.1 Control System Evaluation During First Burn

S-IVB first burn pitch attitude error, angular rate, and actuator position are presented in Figure 10-8. First burn yaw plane dynamics are presented in Figure 10-9. The maximum attitude errors and rates occurred at IGM initiation. A summary of the first burn maximum values of critical flight control parameters is presented in Table 10-4.

The pitch and yaw effective thrust vector misalignments during first burn were 0.25 and  $-0.28$  degree, respectively. A steady state roll torque of 15.0 N-m (11.1 lbf-ft) counterclockwise looking forward required roll APS firings during first burn. The steady state roll torque experienced on previous flights has ranged between 61.4 N-m (45.3 lbf-ft) counterclockwise and 54.2 N-m (40.0 lbf-ft) clockwise.

- ▽ S-IC/S-II SEPARATION COMMAND
- ▽ IGM PHASE 1 INITIATED
- ▽ S-II CECCO
- ▽ END OF ARTIFICIAL TAU MODE
- ▽ S-I OECCO

— MEASURED  
 - - - SIMULATED

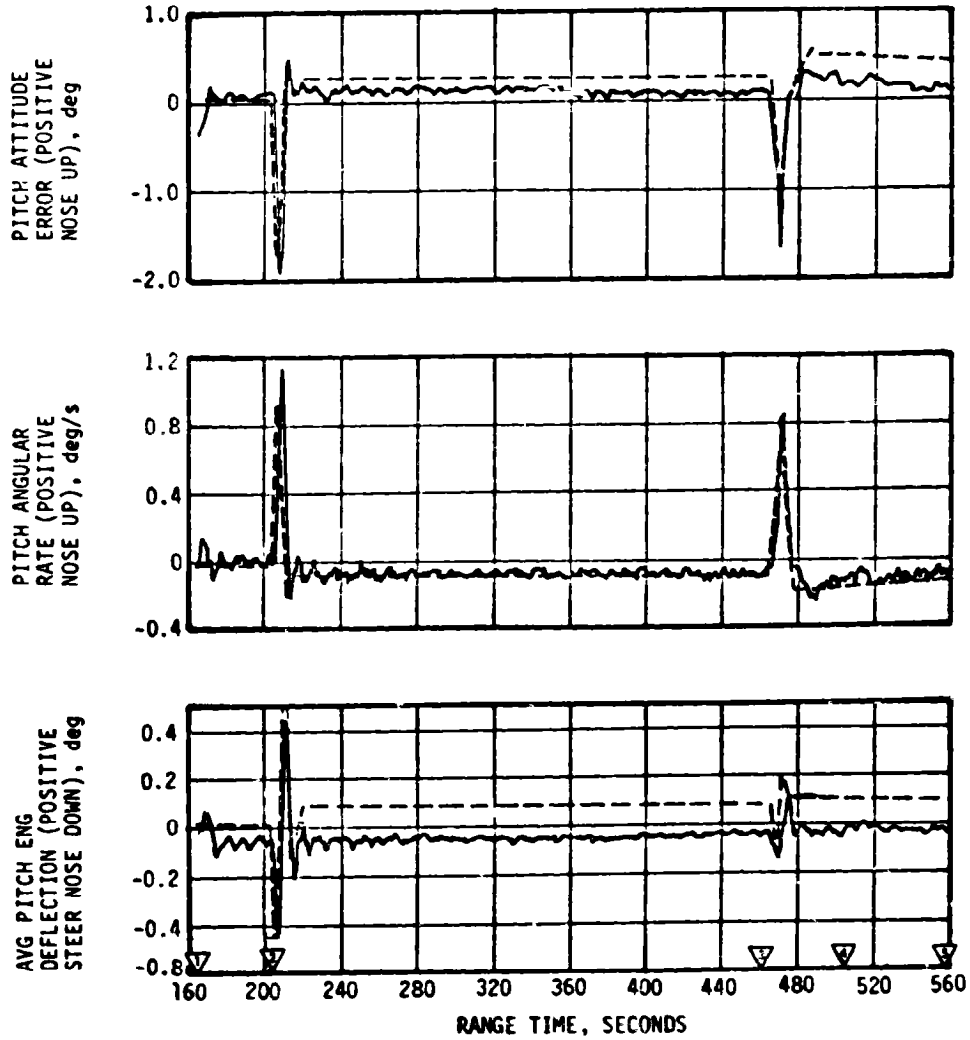


Figure 10-6. Pitch Plane Dynamics During S-II Burn



- ▽ S-IC/S-II SEPARATION COMMAND
- ▽ IGM PHASE 1 INITIATED
- ▽ S-II CECO
- ▽ END OF ARTIFICIAL TAU MODE
- ▽ S-II OECS

—— MEASURED  
 - - - - SIMULATED

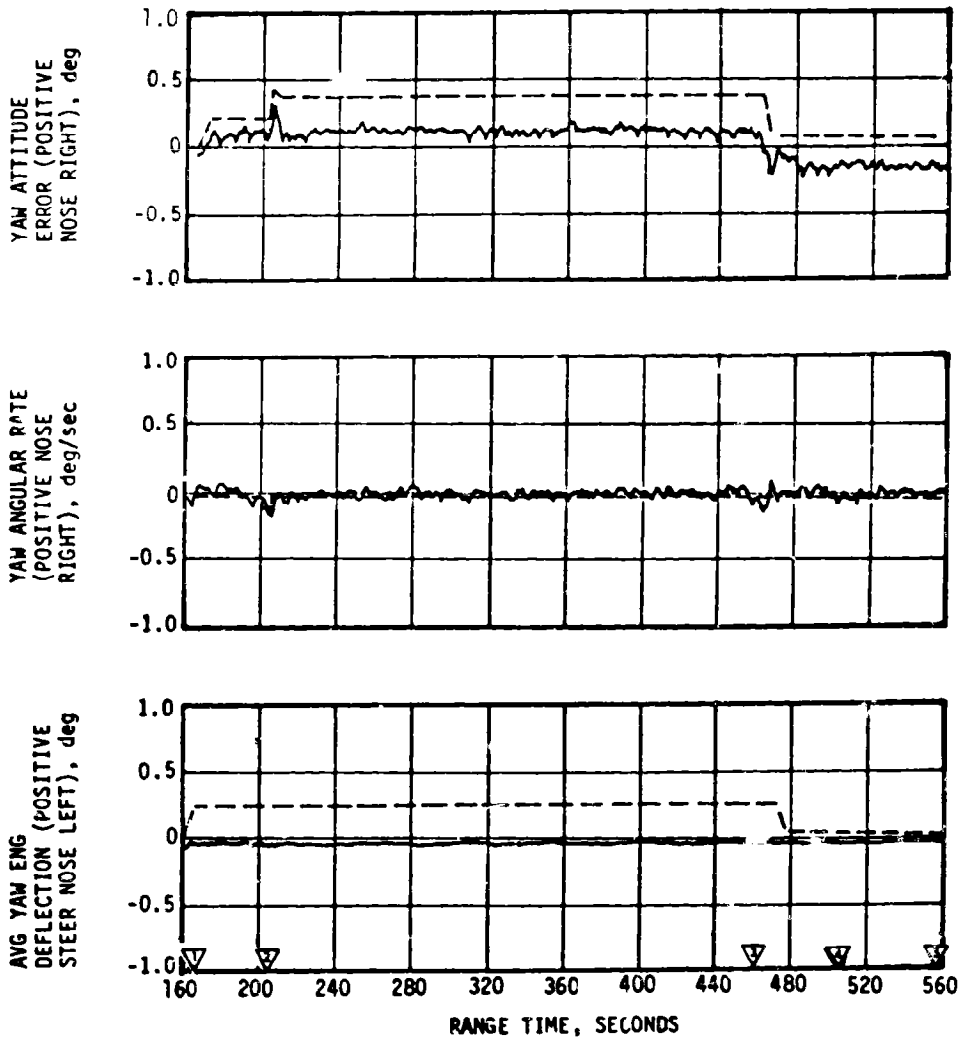


Figure 10-7. Yaw Plane Dynamics During S-II Burn

- ▽ S-IVB BURN MODE ON "B", 560.9 SEC
- ▽ GUIDANCE INITIATION, 568.1 SEC
- ▽ BEGIN TERMINAL GUIDANCE
- ▽ BEGIN CHI FREEZE
- ▽ S-IVB FIRST ECO

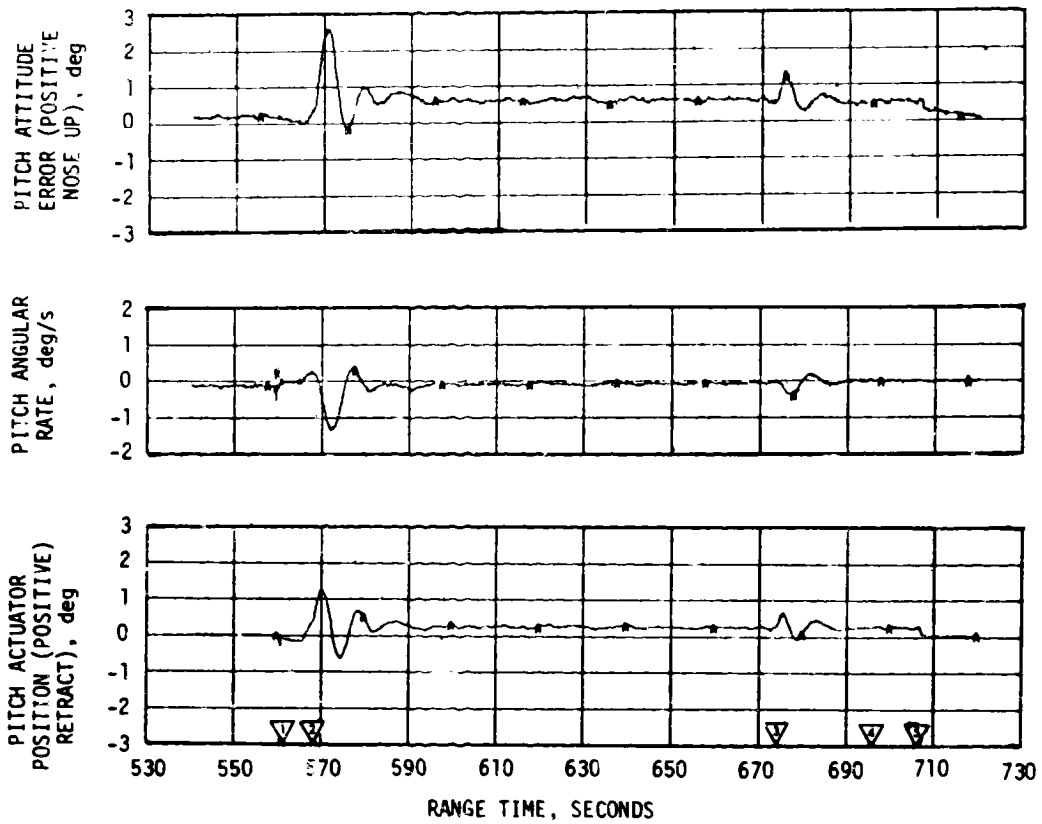


Figure 10-8. Pitch Plane Dynamics During S-IVB First Burn

- ▽ S-IVB BURN MODE ON "B", 560.9 SEC
- ▽ GUIDANCE INITIATION, 568.1 SEC
- ▽ BEGIN TERMINAL GUIDANCE
- ▽ BEGIN CHI FREEZE
- ▽ S-IVB FIRST ECO

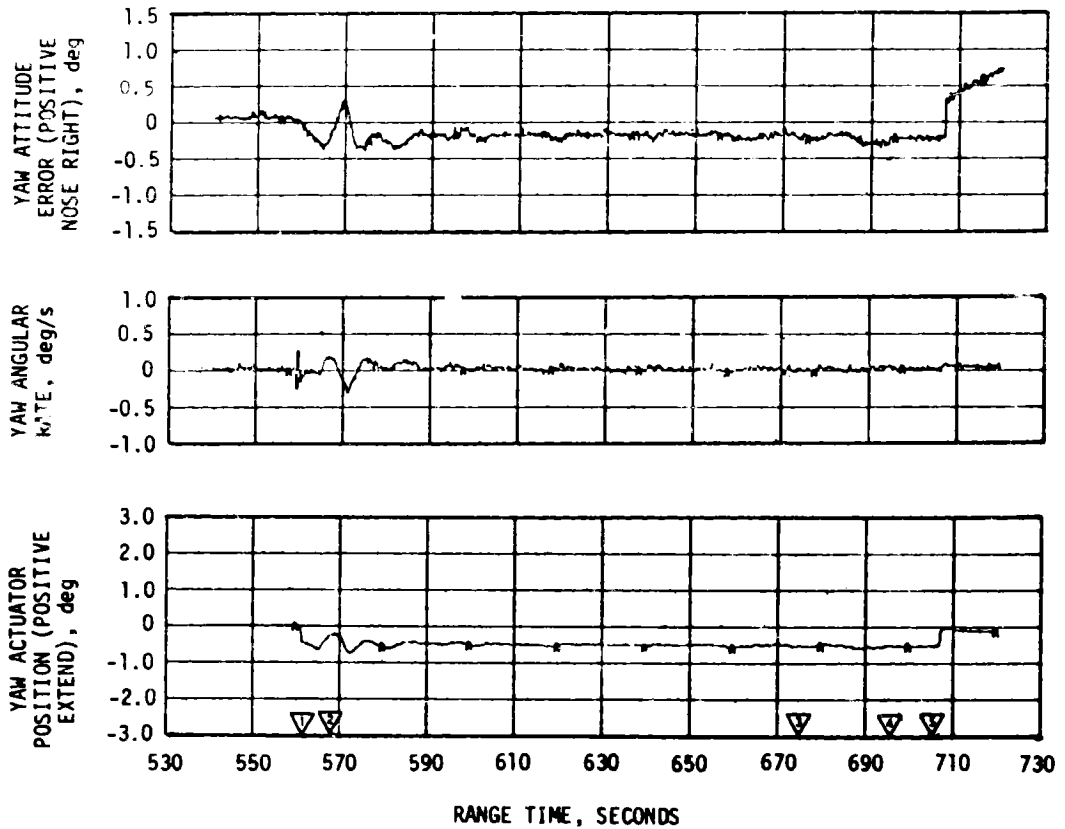


Figure 10-9. Yaw Plane Dynamics During S-IVB First Burn

Table 10-4. Maximum Control Parameters During S-IVB First Burn

PARAMETER	PITCH PLANE		YAW PLANE		ROLL PLANE	
	AMPLITUDE	RANGE TIME (SEC)	AMPLITUDE	RANGE TIME (SEC)	AMPLITUDE	RANGE TIME (SEC)
Attitude Error, deg *	2.3	571	-0.7	572.3	-0.7	630
Angular Rate, deg/s	-1.2	572	-0.25	571.2	-0.25	571.5
Maximum Gimbal Angle, deg	1.2	570	-0.72	572	-	-

\*Biases have been removed from attitude error values.

Propellant sloshing during first burn was observed on data obtained from the Propellant Utilization (PU) mass sensors. The propellant slosh did not have any noticeable effect on the operation of the attitude control system.

#### 10.4.2 Control System Evaluation During Parking Orbit

The APS provided satisfactory orientation and stabilization during parking orbit. Following S-IVB first ECO, the vehicle was maneuvered to the in-plane local horizontal, and the orbital pitch rate was established. The pitch attitude error and pitch angular rate for this maneuver are shown in Figure 10-10.

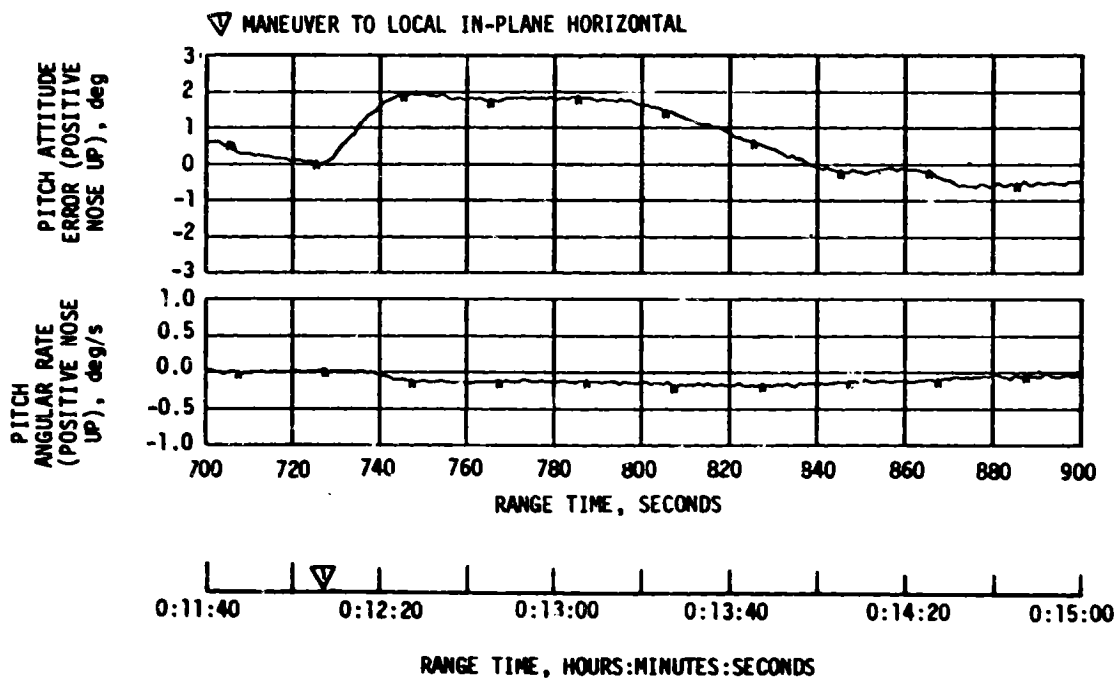


Figure 10-10. Pitch Plane Dynamics During Parking Orbit

The maneuver to the local horizontal on AS-511 incorporated the lower rate of change of minor loop guidance commands (0.14 deg/sec) for TB5 in order to minimize sloshing disturbances which caused venting of LOX on AS-510. Available data indicate that sloshing was significantly reduced on AS-511. The LOX ullage pressure remained below the relief setting throughout parking orbit and did not exhibit as severe a pressure rise during the maneuver to the local horizontal as was observed on AS-510.

At approximately 970 seconds (00:16:10) an APS internal leak of high pressure helium into the propellant tank ullage caused high propellant tank pressure in APS Module 2 (see Section 7.12.2 for complete discussion). This high ullage pressure resulted in relief venting and high thrust for Module 2 attitude control engines and ullage engine for the duration of the mission. The high thrust caused no attitude control problems, but more velocity change than expected was obtained from the remaining ullage burns.

At approximately 3600 seconds (01:00:00) an APS external leak of high pressure helium occurred in Module 1. Because of this leak the lunar impact exercise was modified (see paragraph 10.4.4 and Section 7.12.2).

#### 10.4.3 Control System Evaluation During Second Burn

S-IVB second burn pitch attitude error, angular rate, and actuator position are presented in Figure 10-11. Second burn yaw plane dynamics are presented in Figure 10-12. The maximum attitude errors and rates occurred at guidance initiation. Transients were also observed as a result of the pitch and yaw attitude commands at the termination of the artificial Tau guidance mode (27 seconds before ECO).

A summary of the second burn maximum flight control parameter values is presented in Table 10-5.

Table 10-5. Maximum Control Parameters During S-IVB Second Burn

PARAMETER	AMPLITUDE	RANGE TIME (SEC)	AMPLITUDE	RANGE TIME (SEC)	AMPLITUDE	RANGE TIME (SEC)
Attitude Error, deg*	2.0	9228.5	-1.2	9227.5	-1.3	9255
Angular Rate, deg/s	-1.2	9230.5	0.5	9228.5	0.15	9222
Maximum Gimbal Angle, deg	1.15	9220.3	-0.75	9227.5	-	-
*Biases have been removed from attitude error values.						

- ▽ S-IVB BURN MODE ON "B", 9216.4 SEC
- ▽ GUIDANCE INITIATION, 9222.6 SEC
- ▽ BEGIN TERMINAL GUIDANCE
- ▽ BEGIN CHI FREEZE
- ▽ S-IVB SECOND ECO

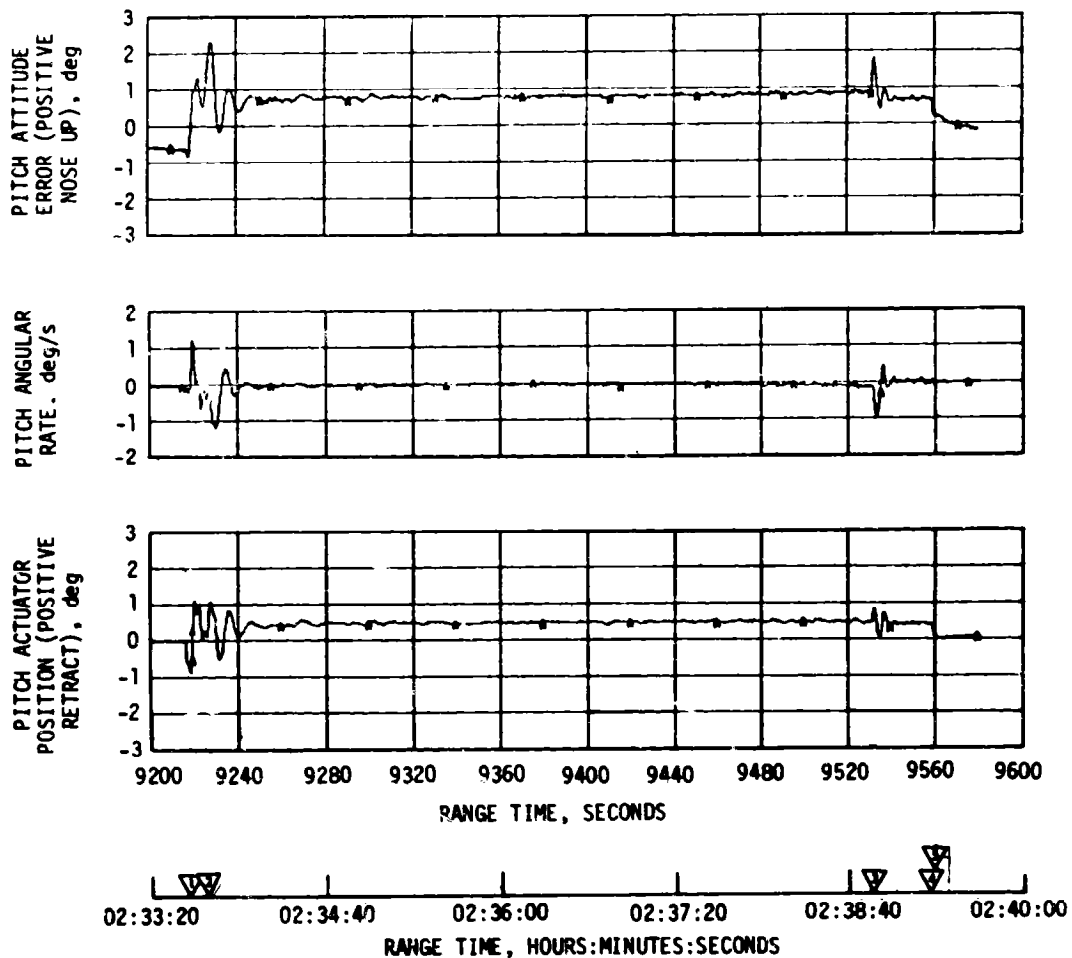


Figure 10-11. Pitch Plane Dynamics During S-IVB Second Burn

- ▽ S-IVB BURN MODE ON "B", 9216.4 SEC
- ▽ GUIDANCE INITIATION, 9222.6 SEC
- ▽ BEGIN TERMINAL GUIDANCE
- ▽ BEGIN CHI FREEZE
- ▽ S-IVB SECOND ECO

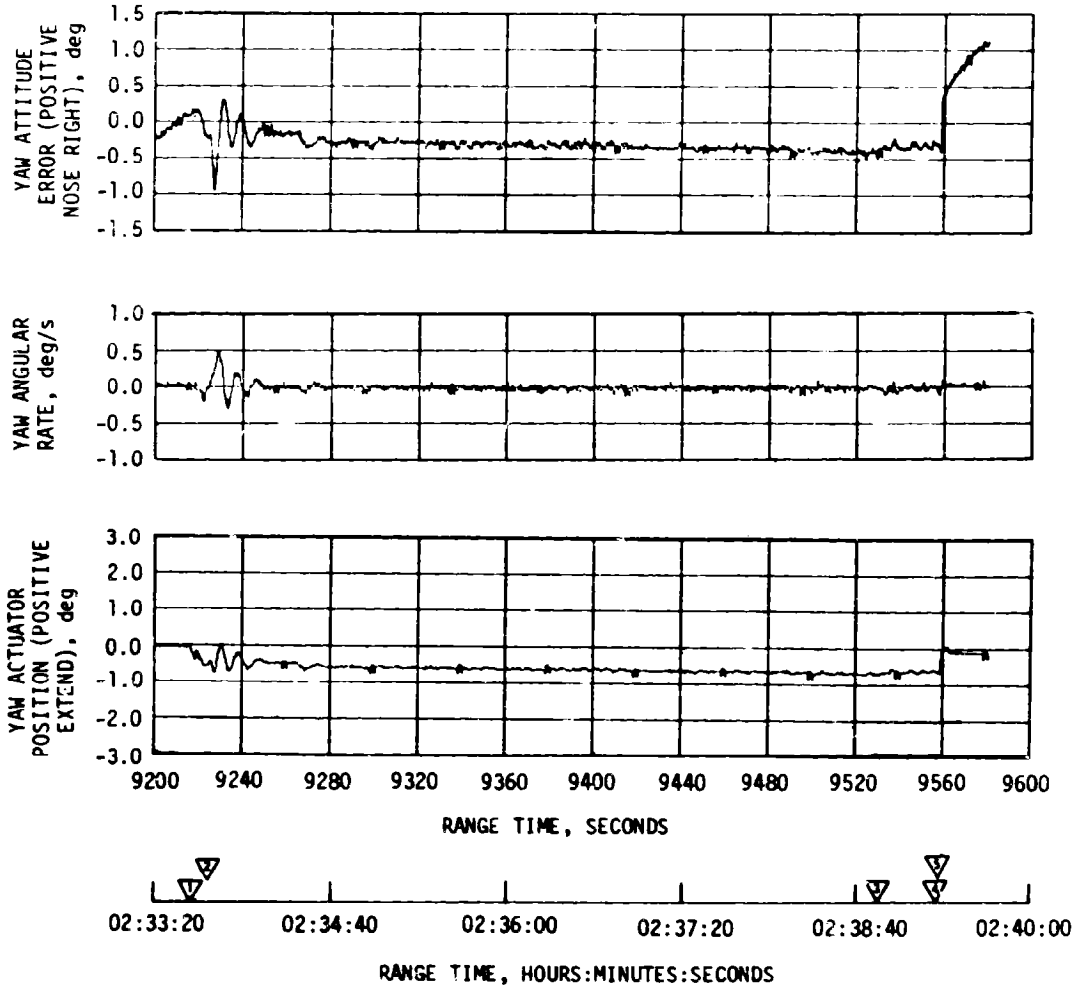


Figure 10-12. Yaw Plane Dynamics During S-IVB Second Burn

The pitch and yaw effective thrust vector misalignments during second burn were approximately 0.43 and -0.44 degree, respectively. The steady state roll torque during second burn ranged from 5.6 N-m (4.2 lbf-ft), counterclockwise looking forward, at the low MR to 19.7 N-m (14.6 lbf-ft) at the 5.0 MR.

Propellant sloshing during second burn was observed on data obtained from the PU mass sensors. The propellant slosh did not have any noticeable effect on the operation of the attitude control system.

#### 10.4.4 Control System Evaluation After S-IVB Second Burn

The APS provided satisfactory orientation and stabilization from translunar injection (TLI) through the S-IVB/iU passive thermal control maneuver (Three-Axis Tumble Maneuver). Each of the planned maneuvers were performed satisfactorily.

Significant periods of interest related to translunar coast attitude control were the maneuver to the in-plane local horizontal following second burn cutoff, the maneuver to the TD&E attitude, spacecraft separation, spacecraft docking, lunar module extraction, the maneuver to the evasive ullage burn attitude, the maneuver to the nominal LOX dump attitude, the maneuver to the optimum LOX dump attitude, the maneuver to the lunar impact ullage burn attitude, and the "Three-Axis Tumble Maneuver."

The pitch attitude error and angular rate for events during which telemetry data were available are shown in Figure 10-13.

Following S-IVB second cutoff, the vehicle was maneuvered to the in-plane local horizontal at 9710 seconds (02:41:50) (through approximately -25 degrees in pitch and -1.0 degree in yaw), and an orbital pitch rate was established. Then the vehicle was commanded to maneuver to the separation TD&E attitude at 10,459 seconds (02:54:19) (through approximately 120, -40, and -180 degrees in pitch, yaw, and roll, respectively).

Spacecraft separation, which occurred at 11,099 seconds (03:04:59), appeared normal, as indicated by the relatively small disturbances induced on the S-IVB.

Disturbances during spacecraft docking, which occurred at 12,113 seconds (03:21:53), were less than on previous flights. Docking disturbances required 1,540 N-sec (346 lbf-sec) of impulse from Module 1 and 1,152 N-sec (259 lbf-sec) of impulse from Module 2. The largest docking disturbances on previous flights occurred on AS-510 and required 3,480 N-sec (783 lbf-sec) of impulse from Module 1 and 3,040 N-sec (683 lbf-sec) of impulse from Module 2. Lunar module extraction occurred at 14,355 seconds (03:59:15) with normal disturbances.



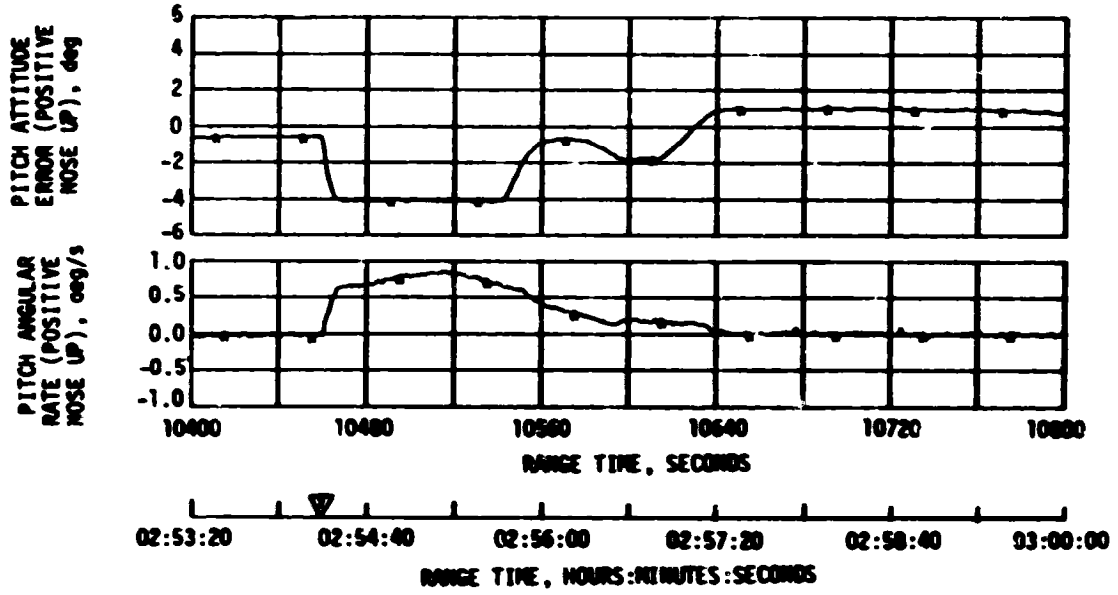
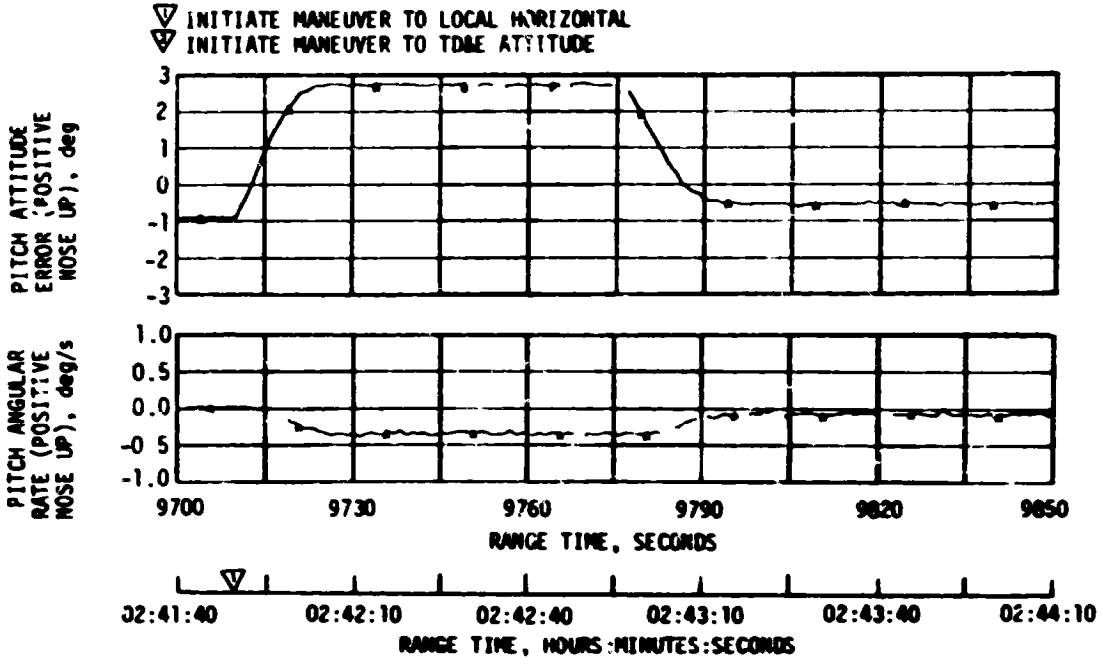


Figure 10-13. Pitch Plane Dynamics During Translunar Coast (Sheet 1 of 5)

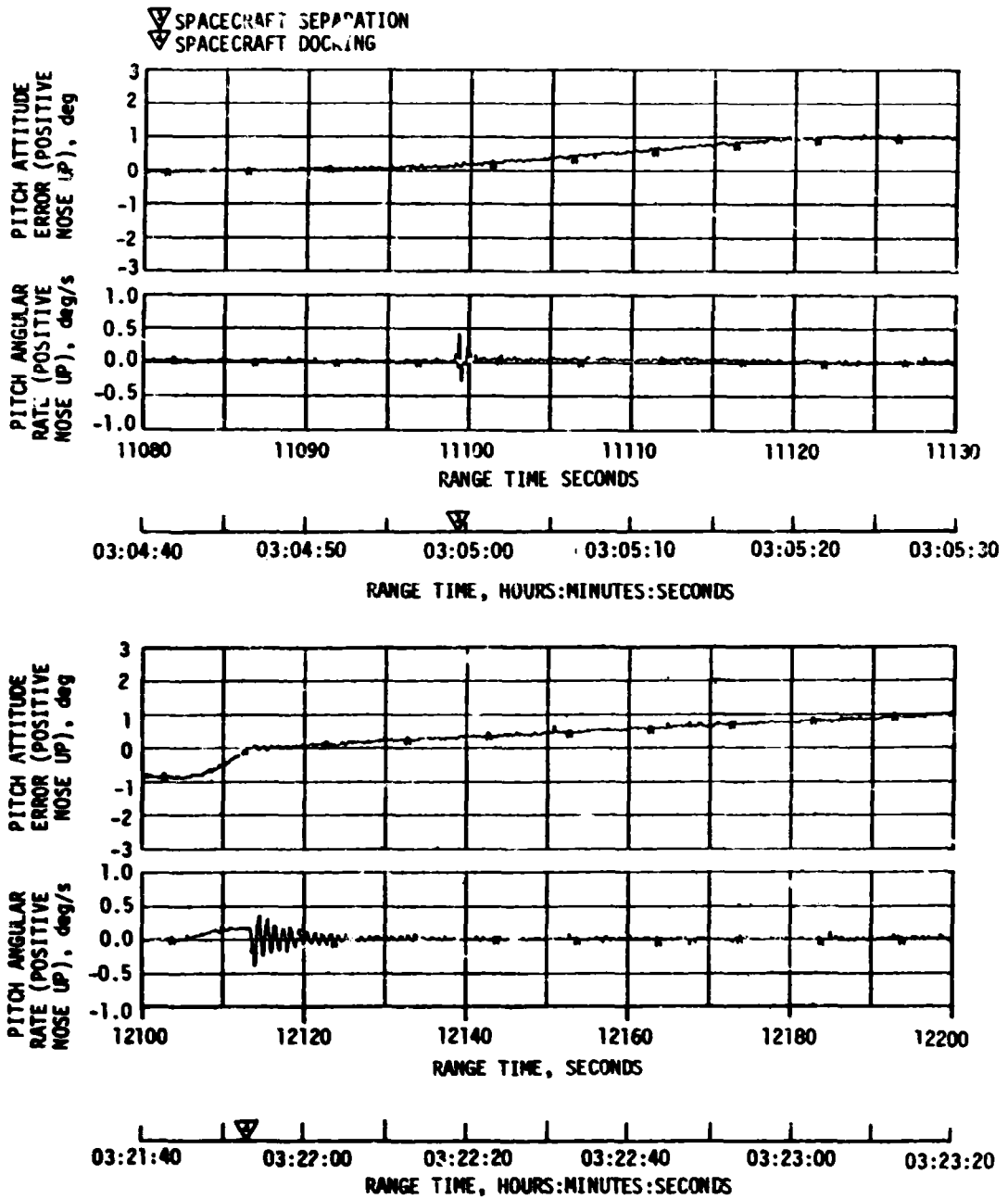


Figure 10-13. Pitch Plane Dynamics During Translunar Coast (Sheet 2 of 5)

▼ LUNAR MODULE EXTRACTION  
 ▼ INITIATE EVASIVE MANEUVER  
 ▼ APS ULLAGE ENGINES ON  
 ▼ APS ULLAGE ENGINES OFF

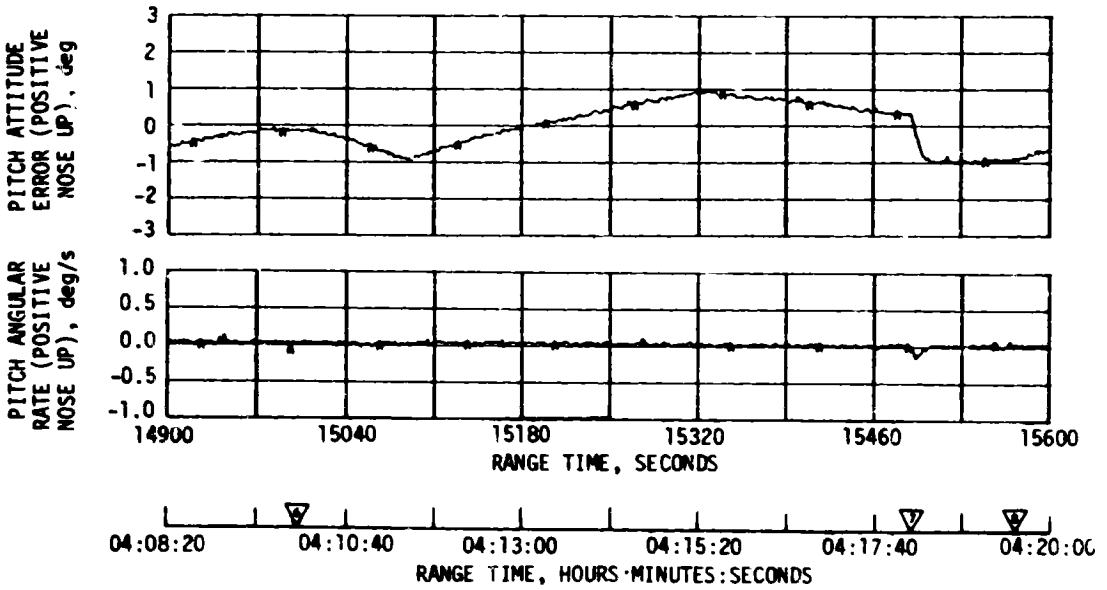
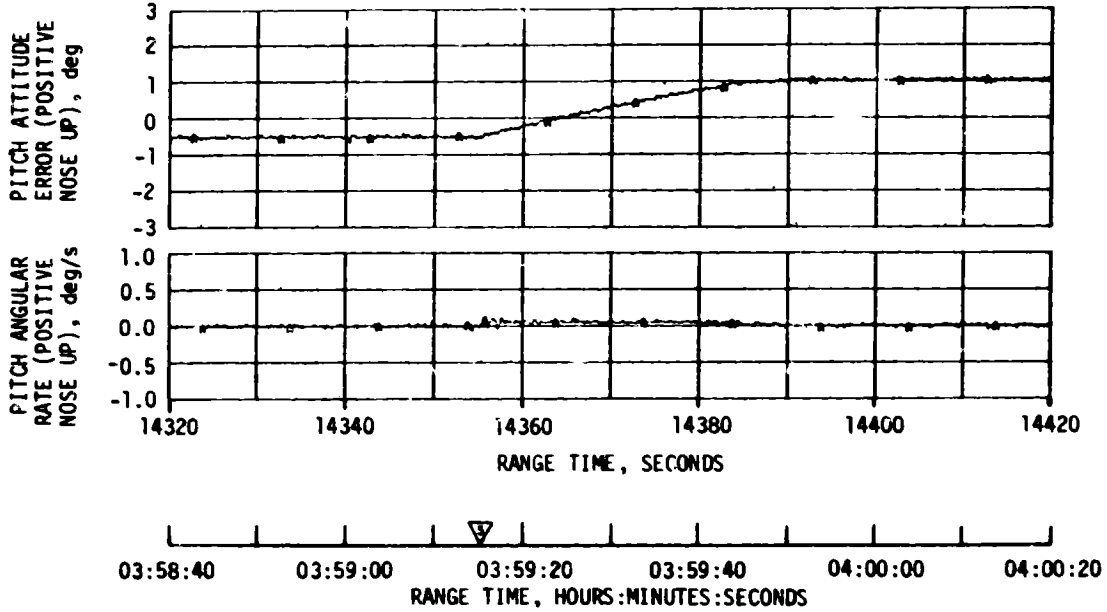


Figure 10-13. Pitch Plane Dynamics During Translunar Coast (Sheet 3 of 5)

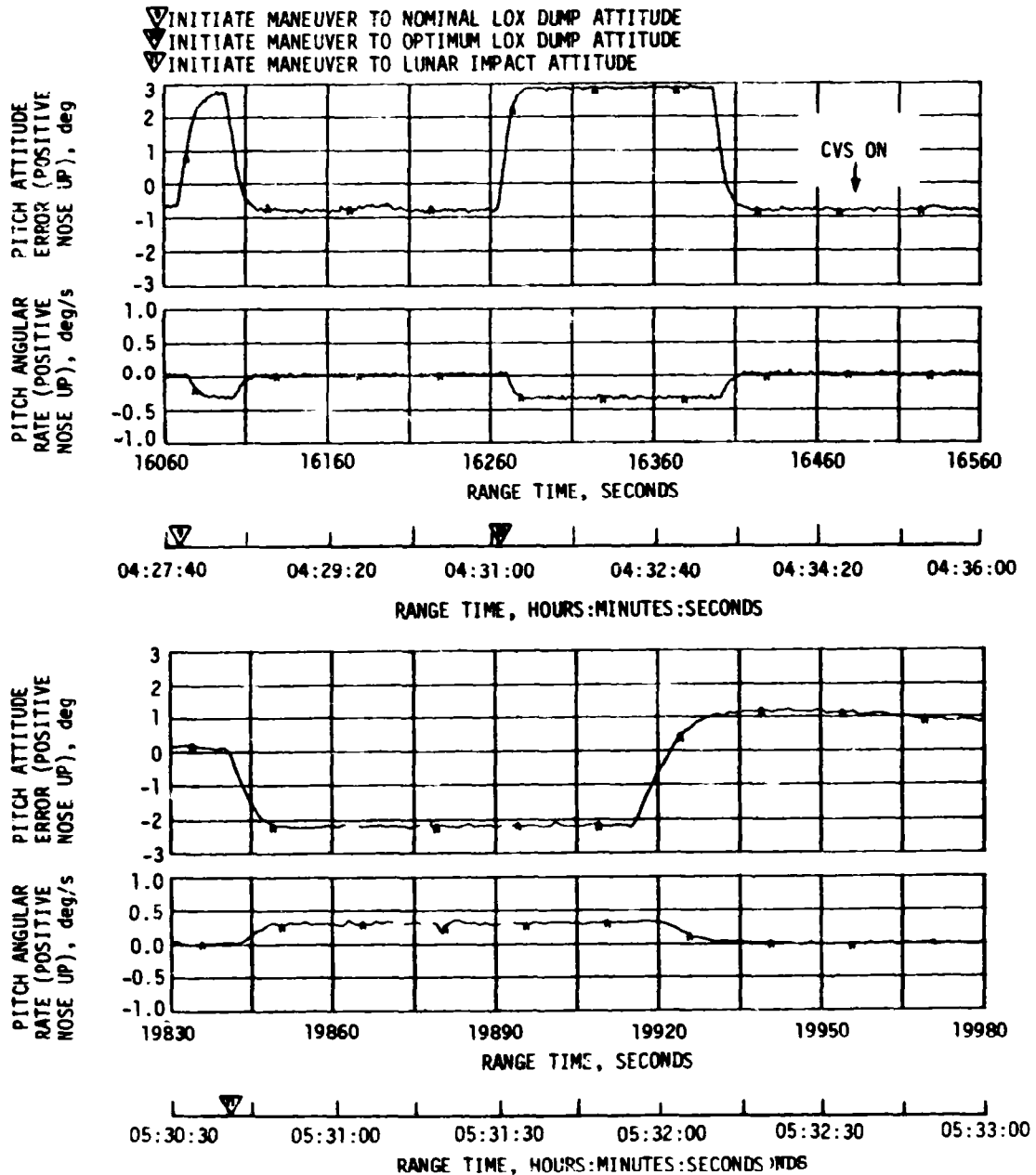


Figure 10-13. Pitch Plane Dynamics During Translunar Coast (Sheet 4 of 5)

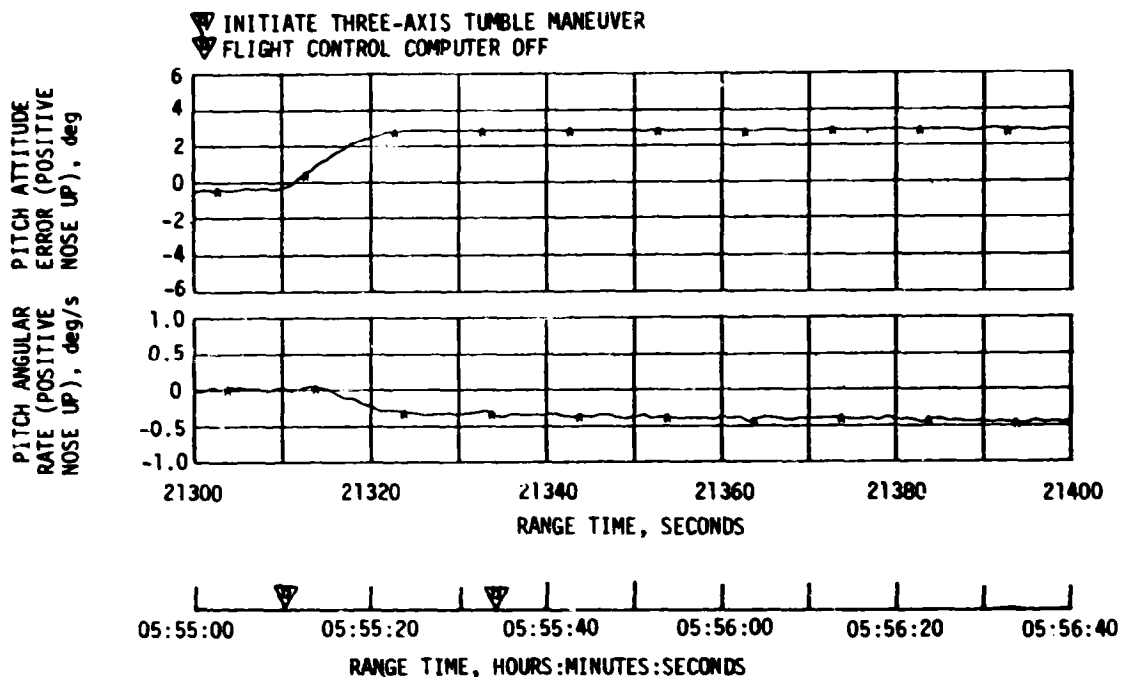


Figure 10-13. Pitch Plane Dynamics During Translunar Coast (Sheet 5 of 5)

At approximately 15,001 seconds (04:10:01) a yaw maneuver from  $-40.8$  degrees (TD&E attitude) to  $40.0$  degrees was initiated to attain the desired attitude for the evasive ullage burn. At 15,488 seconds (04:18:08) the APS ullage engines were commanded on for 80 seconds to increase the separation distance between the S-IVB and spacecraft.

Because of a projected early loss of attitude control, due to the APS leak problem, the LOX dump was performed at an optimum attitude for performance rather than at the preprogrammed attitude. Initial attempts to uplink the desired attitude were unsuccessful and the vehicle maneuvered to the preprogrammed LOX dump attitude 16,068 seconds (04:27:48). This was a two-axis maneuver with pitch commanded from  $176.0$  to  $189.0$  degrees and yaw from  $40.0$  to  $14.0$  degrees referenced to the in-plane local horizontal. Subsequent to the completion of this maneuver the alternate LOX dump attitude command was successfully uplinked and the resulting maneuver was performed at 16,269 seconds (04:31:09). This was also a two-axis maneuver with pitch commanded from  $189.0$  to  $237.0$  degrees and yaw from  $14.0$  to  $6.0$  degrees referenced to the in-plane local horizontal. LOX dump occurred at 16,767 seconds (04:39:27) and lasted for 48 seconds.

Post flight analyses of onboard accelerometer and LOX flowmeter data indicated three periods of momentary ullage gas ingestion during the LOX dump. (See Section 7.13.2 for details on the ullage gas ingestion effect

on LOX dump performance). The gas ingestion is attributed to LOX slosh as the time intervals between the gas ingestion occurrences correspond favorably with calculated LOX slosh frequency. The LOX sloshing was apparently caused by a combination of the large amplitude optimum LOX dump maneuver in the pitch plane and the proximity of the maneuver to LOX dump. On AS-511 there was approximately 300 seconds less time between the termination of LOX dump maneuver activity and the initiation of LOX dump than on previous missions.

At 19,837 seconds (05:30:37) a ground command was sent to perform a maneuver to the desired attitude for the APS ullage burn for lunar target impact. This was also a two-axis maneuver and resulted in a pitch maneuver change from 237.0 to 213.0 degrees and a yaw attitude maneuver change from 6.0 to -33.0 degrees referenced to the in-plane local horizontal. At 20,407 seconds (04:40:07) the APS ullage engines were commanded on for 54 seconds to provide velocity change for lunar target impact.

The command to initiate the "Three-Axis Tumble Maneuver" was received at 21,306 seconds (05:55:06). This maneuver consisted of commanding the vehicle 31 degrees in both pitch and yaw and -31 degrees in roll. After vehicle angular rates of approximately -0.3 degree/second in pitch, -0.3 degree/second in yaw, and 0.4 degree/second in roll were established, a ground command was received (Flight Control Computer Power Off B) at 21,337 seconds (05:55:37) to inhibit the IU Flight Control Computer leaving the vehicle in a three-axis tumble mode.

APS propellant consumption for attitude control and propellant settling prior to the APS burn for lunar target impact was lower than the mean predicted requirement for Module 1 and slightly higher than the plus three sigma requirement for Module 2. The higher propellant usage from Module 2 is attributed to the higher propellant supply pressure. The greater part of this usage occurred during the ullage engine burns prior to restart and for the evasive maneuver. Due to this increased pressure, the propellant flow rate was higher for both the ullage and attitude control engines in Module 2. The unbalanced ullage thrust between Module 1 and 2 also increased pitch attitude control engine propellant usage in Module 2.

## 10.5 INSTRUMENT UNIT CONTROL COMPONENTS EVALUATION

All control functions performed in the Flight Program Minor Loop and in the Flight Control Subsystems were accomplished satisfactorily. One anomaly did occur during the launch countdown in the backup yaw rate gyro channel of the Flight Control System and is discussed in Section 3.3.

## 10.6 SEPARATION

### 10.6.1 S-IC/S-II Separation

S-IC/S-II separation and associated sequencing was accomplished as planned. Subsequent S-IC and S-II stage dynamics provided adequate clearance when S-II fuel lead was initiated, (Figure 10-14).

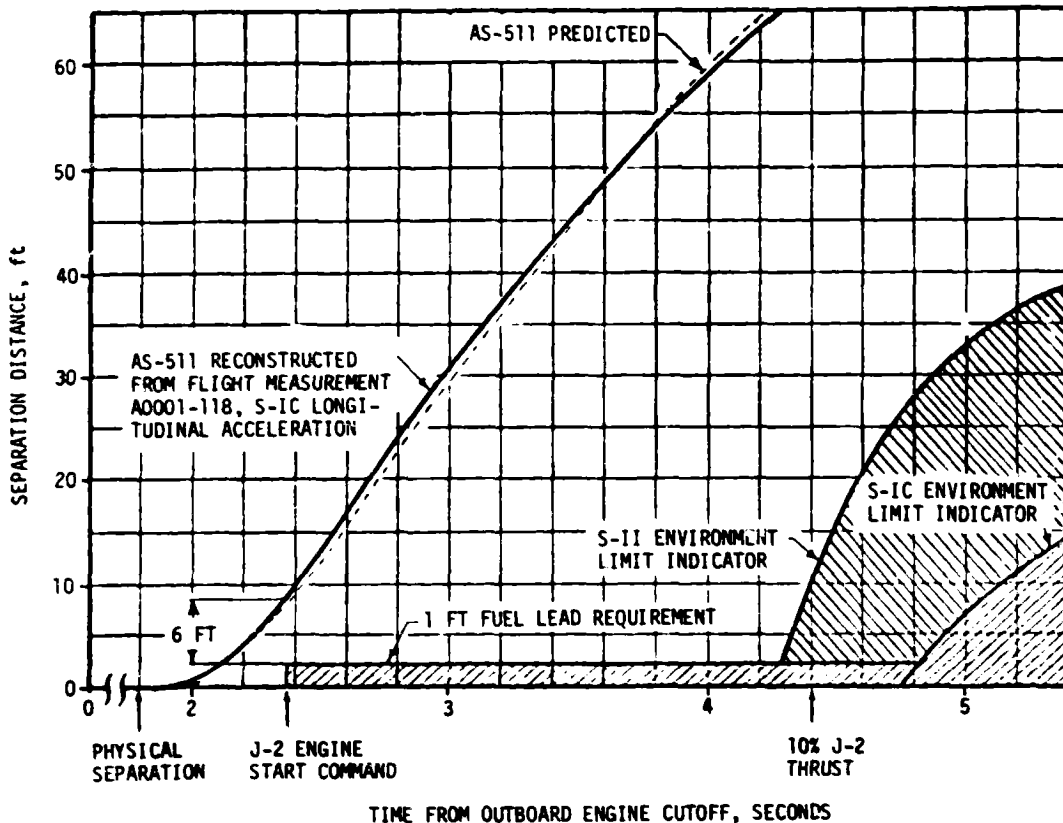


Figure 10-14. AS-511 S-IC/S-II Separation Distance

S-IC-11 was the first stage to use eight retrorockets for separation combined with a 1.7 second delay between OECO and retrorocket ignition signal. By comparison, S-IC-10 used four retrorockets with a 1.7 second delay, and S-IC-1 through S-IC-9 used eight retrorockets with a 0.7 second delay.

Average retrorocket thrust appeared nominal based on partial data obtained from three accelerometer measurements. However, the data were insufficient to determine the burn time or total available impulse of the retrorockets.

Pitch and yaw attitude errors and rates during staging were insignificant. The maximum roll attitude error and angular rate were approximately -2 degrees and 2 degrees per second, respectively, which is within the range experienced in previous flights. Minimum lateral clearance between the J-2 engines and the S-IC stage was approximately 1.3 meters (51 inches). Figure 10-14 shows that clearance distances remained well above the S-IC and S-II stage environment limits.

### 10.6.2 S-II Second Plane Separation Evaluation

The AS-511 flight was not instrumented for monitoring second plane separation. To give an indication of the dynamics of second plane separation, based on available flight data, the dynamics of both the second stage and the separating interstage were calculated. These calculations utilized appropriate initial trajectory conditions, post-flight mass characteristics, engine gimbal angles, J-2 engine thrusts, and predicted J-2 engine plume characteristics.

The calculated dynamics of separation show no significant differences from previous flights. The separation was complete when the interstage passed the bottom of the J-2 engines and occurred at approximately 194.6 seconds.

Attitude errors and rates remained near zero during second plane separation. The lateral clearance between the interstage and the engines was computed to give a minimum clearance of 1.1 meters (41 inches) between engine 4 and the interstage ring at vehicle station 39.7 meters (1564 inches). The separation plane is located at vehicle station 44.7 meters (1760 inches).

### 10.6.3 S-II/S-IVB Separation

S-II/S-IVB Separation Command was verified as sent from the IU, and the S-II retromotor Exploding Bridge Wire (EBW) was fired. The S-IVB ullage motors were fired, and normal acceleration was observed on the S-IVB during ullage motor firing. Vehicle dynamics were normal, and well within staging limits.

### 10.6.4 S-IVB/CSM Separation

At 10,459 seconds (02:54:19) a maneuver to the TD&E attitude was initiated to assure proper lighting and communication conditions for spacecraft separation, docking, and lunar module extraction. The vehicle was commanded to pitch 120 degrees, yaw -40 degrees, and roll -180 degrees. This attitude was held inertially until the beginning of the evasive maneuver. The vehicle motion during the maneuver was close to predicted with maximum vehicle rates of 0.85 deg/sec, 0.66 deg/sec, and -1.00 deg/sec in the pitch, yaw, and roll axes, respectively.

Transients due to spacecraft separation (approximately 11,099 seconds [03:04:59]) appeared normal. Yaw/roll APS firings were observed in response to vibrations experienced at separation. A slight pitch rate (approximately 0.05 deg/sec) was caused by separation and was nulled by three Module 1 pitch firings approximately 20 seconds after separation.

All attitude errors remained within the 1 degree deadband during the separation process.



## SECTION 11

### ELECTRICAL NETWORKS AND EMERGENCY DETECTION SYSTEM

#### 11.1 SUMMARY

The AS-511 launch vehicle electrical systems and Emergency Detection System (EDS) performed satisfactorily throughout the required period of flight. There was, however, an anomaly in the S-II ignition bus voltage indications during and after the ignition sequence. The S-IVB forward Battery No. 2 depleted early as on AS-510 and did not deliver its rated capacity. Operation of all other batteries, power supplies, inverters, Exploding Bridge Wire (EBW) firing units and switch selectors was normal.

#### 11.2 S-IC STAGE ELECTRICAL SYSTEM

The S-IC stage electrical system performance was satisfactory. Battery voltages were within performance limits of 26.5 to 32.0 vdc during powered flight. The battery currents were near predicted and below the maximum limits of 50 amperes for each battery. Battery power consumption was within the rated capacity of each battery, as shown in Table 11-1.

Table 11-1. S-IC Stage Battery Power Consumption

BATTERY	BUS DESIGNATION	RATED CAPACITY (AMP-MIN)	POWER CONSUMPTION*	
			AMP-MIN	PERCENT OF CAPACITY
Operational	1D10	500	27.7	5.5
Instrumentation	1D20	500	81.6	16.3

\*Battery power consumptions were calculated from power transfer (T-50 seconds) until S-IC/S-II separation.

#### 11.3 S-II STAGE ELECTRICAL SYSTEM

The S-II stage electrical system performed satisfactorily. With the exception of the ignition bus, all battery voltages remained within specified limits through the prelaunch and flight periods. Bus currents also remained within required and predicted limits. Main bus current averaged 30 amperes during S-IC boost and varied from 45 to 51 amperes during S-II boost. Instrumentation bus current averaged 21 amperes during S-IC and S-II boost.

Recirculation bus current averaged 88 amperes during S-IC boost. Ignition bus current averaged 30 amperes during the S-II ignition sequence. Battery power consumption was within the rated capacity of each battery, as shown in Table 11-2.

Table 11-2. S-II Stage Battery Current Consumption

BATTERY	BUS DESIGNATION	RATED CAPACITY (AMP-HR)	POWER CONSUMPTION*		TEMPERATURE (°F)	
			AMP-HR	PERCENT OF CAPACITY	MAX	MIN
Main	2D11	35	13.54	38.7	98.0	90.0
Instrumentation	2D21	35	10.21	29.2	92.0	89.0
Recirculation No. 1	2D51	30	11.60	38.7	84.0	80.0
Recirculation No. 2	2D51 and 2D61	30	11.64	38.8	86.0	82.0

\*Battery current consumptions were calculated from activation until S-II/S-IVB separation and include 6.5 to 6.9 Amp-Hr consumed during the battery activation procedure.

### 11.3.1 S-II Ignition System Electrical Network Anomaly

The S-II ignition bus voltage, measurement M0125-207, indicated an anomalous drop of approximately one volt during the ignition sequence and then dropped to zero 1.2 seconds after the ignition sequence was over.

Approximately 4 seconds prior to the drop of the ignition bus voltage, the ignition battery temperature measurement failed. However, it is highly unlikely that the temperature measurement failure is related to the indicated voltage drop. The temperature data has the distinct characteristics of a measurement failure, because the indicated temperature change is too sudden to represent a real thermal environment change.

There was no failure of the ignition system battery since measurement M111-207, which measures the series combination of both the ignition and recirculation batteries, remained close to 60 volts during this period. If either battery had failed, the voltage reading would have been considerably less than 60 volts.

The failure denoted by the ignition voltage measurement (M0125-207) may be a measurement failure but suggests a possible failure in the electrical networks. It is not possible to assign a positive cause for this anomaly with the limited data available. An inspection of the electrical network is planned for S-II-12 to assure that a network problem does not occur.

## 11.4 S-IVB STAGE ELECTRICAL SYSTEM

### 11.4.1 Summary

The S-IVB stage electrical system performance was satisfactory. The battery voltages, currents, and temperatures remained within the normal range beyond the required battery lifetime, except Forward No. 2 Battery which depleted at 23,220 seconds (06:27:00) after supplying only 83.0 percent of the rated capacity. Battery voltage and currents are shown in Figures 11-1 through 11-5. Battery power consumption and capacity for each battery are shown in Table 11-3.

The three 5-vdc and seven 20-vdc excitation modules all performed within acceptable limits. The LOX and LH<sub>2</sub> chilldown inverters performed satisfactorily.

All switch selector channels functioned as commanded by the IU and were within required time limits.

Performance of the EBW circuitry for the separation system was satisfactory. Firing units charge and discharge responses were within predicted time and voltage limits. The range safety command system EBW firing units were in the required state-of-readiness for vehicle destruct, had it been necessary.

### 11.4.2 S-IVB Forward Battery No. 2 Battery Performance

The S-IVB Forward No. 2 Battery completed its mission requirement of 12.7 amp-hours at the time of the evasive maneuver at 15,568 seconds. However, this battery depleted early and did not deliver its rated capacity of 24.6 amp-hours. Forward No. 2 Battery voltage dropped below 26V (depletion by definition) at 23,220 seconds (6 hours 27 minutes). Calculated capacity actually delivered was approximately 20.4-amp-hours.

On AS-510 the S-IVB Forward Battery No. 2 depleted at approximately 26,620 seconds (7 hours 7 minutes) after supplying only 89.7 percent of its rated capacity. Vendor failure analysis on AS-510 backup batteries revealed three problem areas: (1) insufficient silver on positive plate, (2) excessive negative plate limiting\*, and (3) informal (i.e., no formal acceptance or rejection criterion) cell block testing. The AS-510 backup batteries delivered 27 amp-hours capacity under ground test conditions.

\*Negative Plate Limiting is the reduction of chemical action between the cell electrolyte and the negative plate caused by the plate material having a high density.

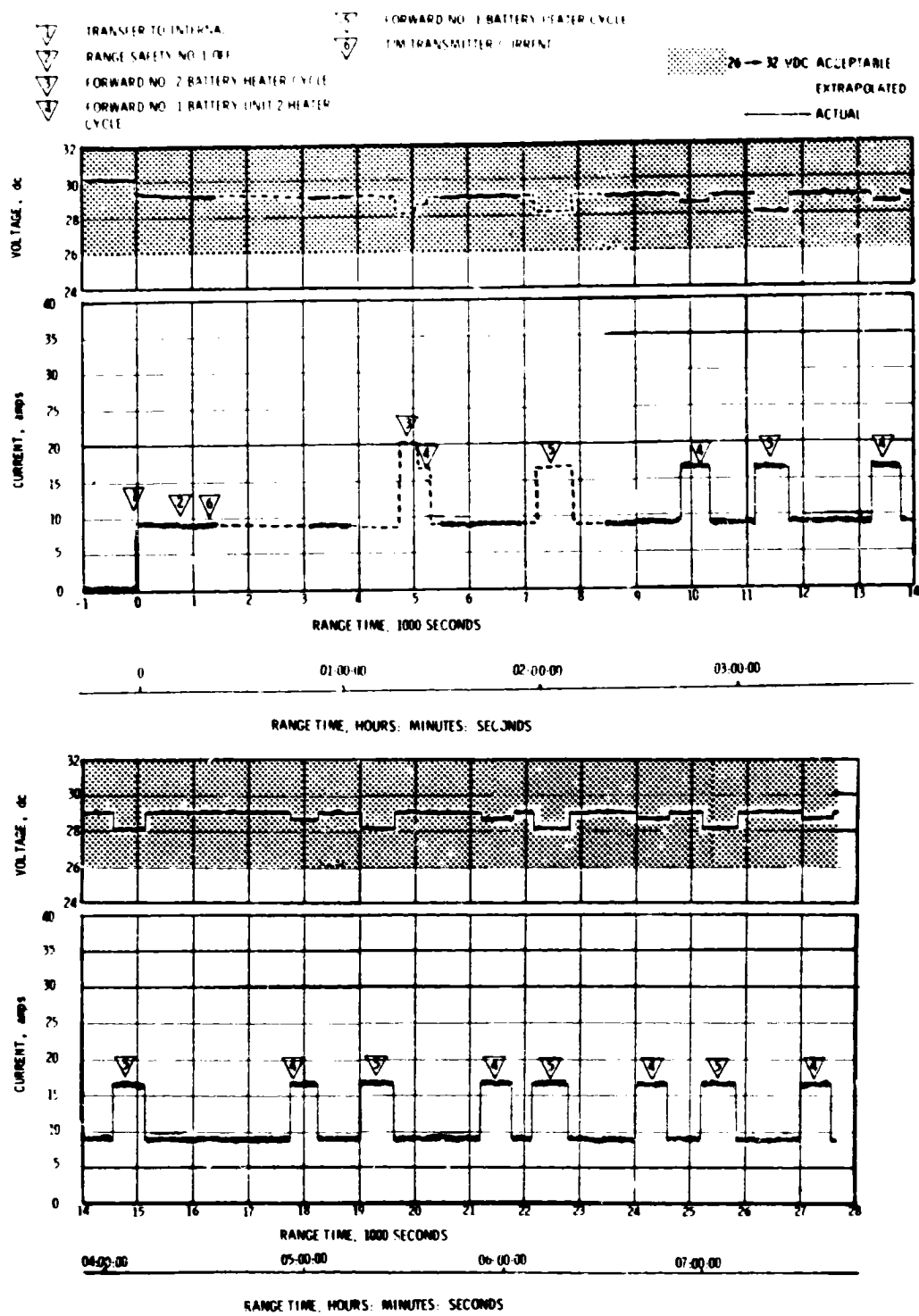


Figure 11-1. S-IVB Stage Forward No. 1 Battery Voltage and Current

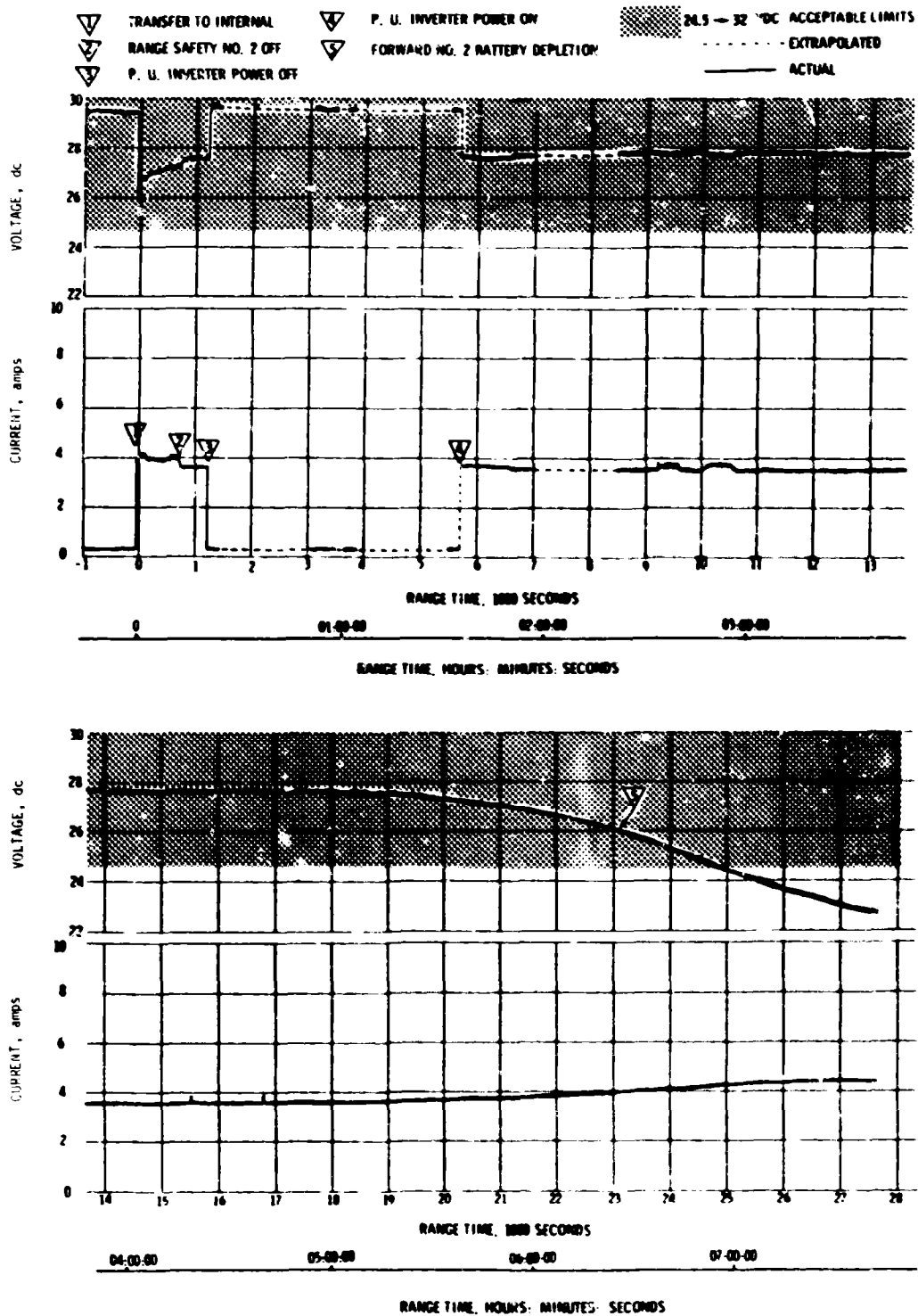


Figure 11-2. S-IVB Stage Forward No. 2 Battery Voltage and Current

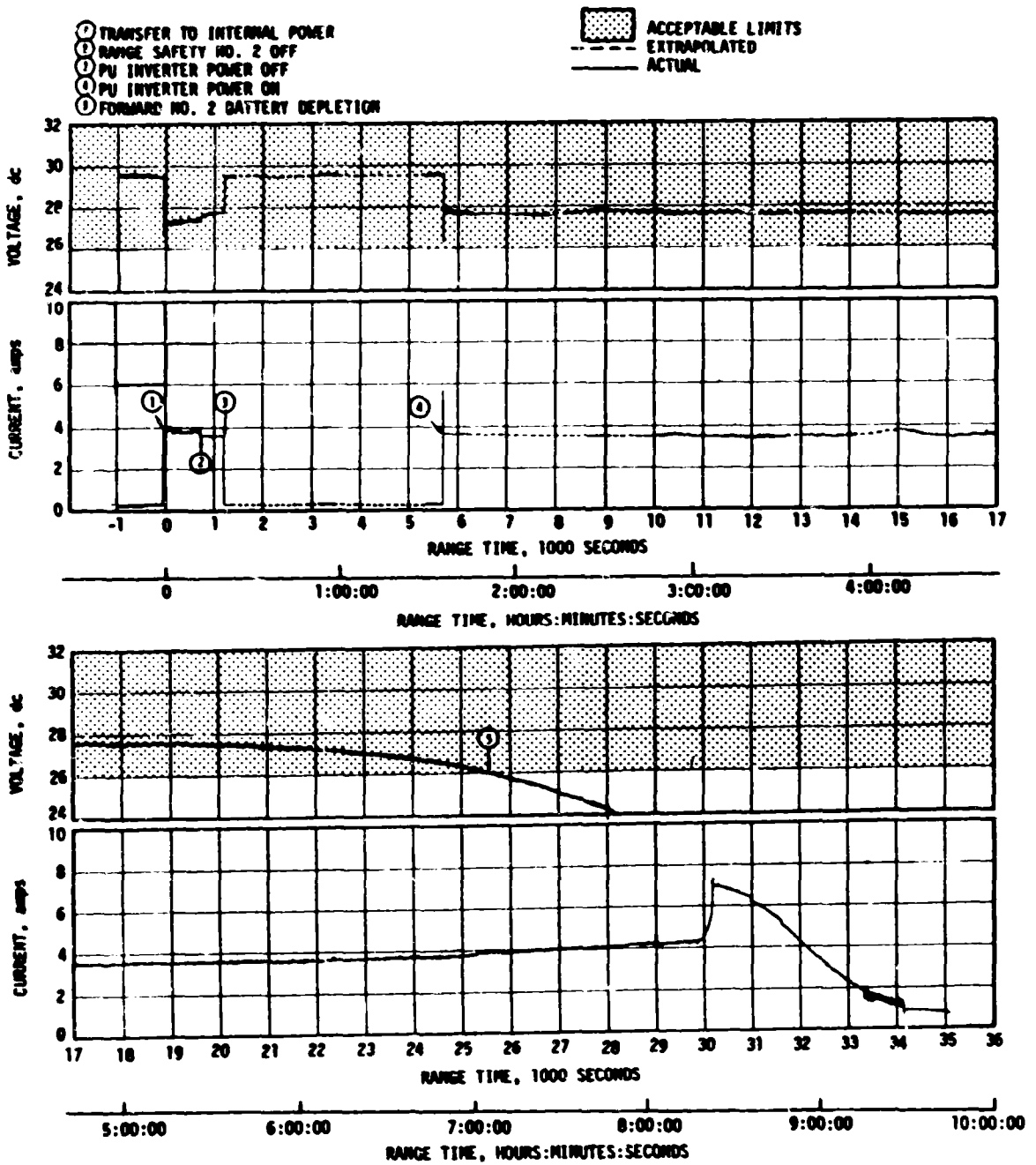


Figure 11-3. AS-510 S-IVB Stage Forward No. 2 Battery Voltage and Current

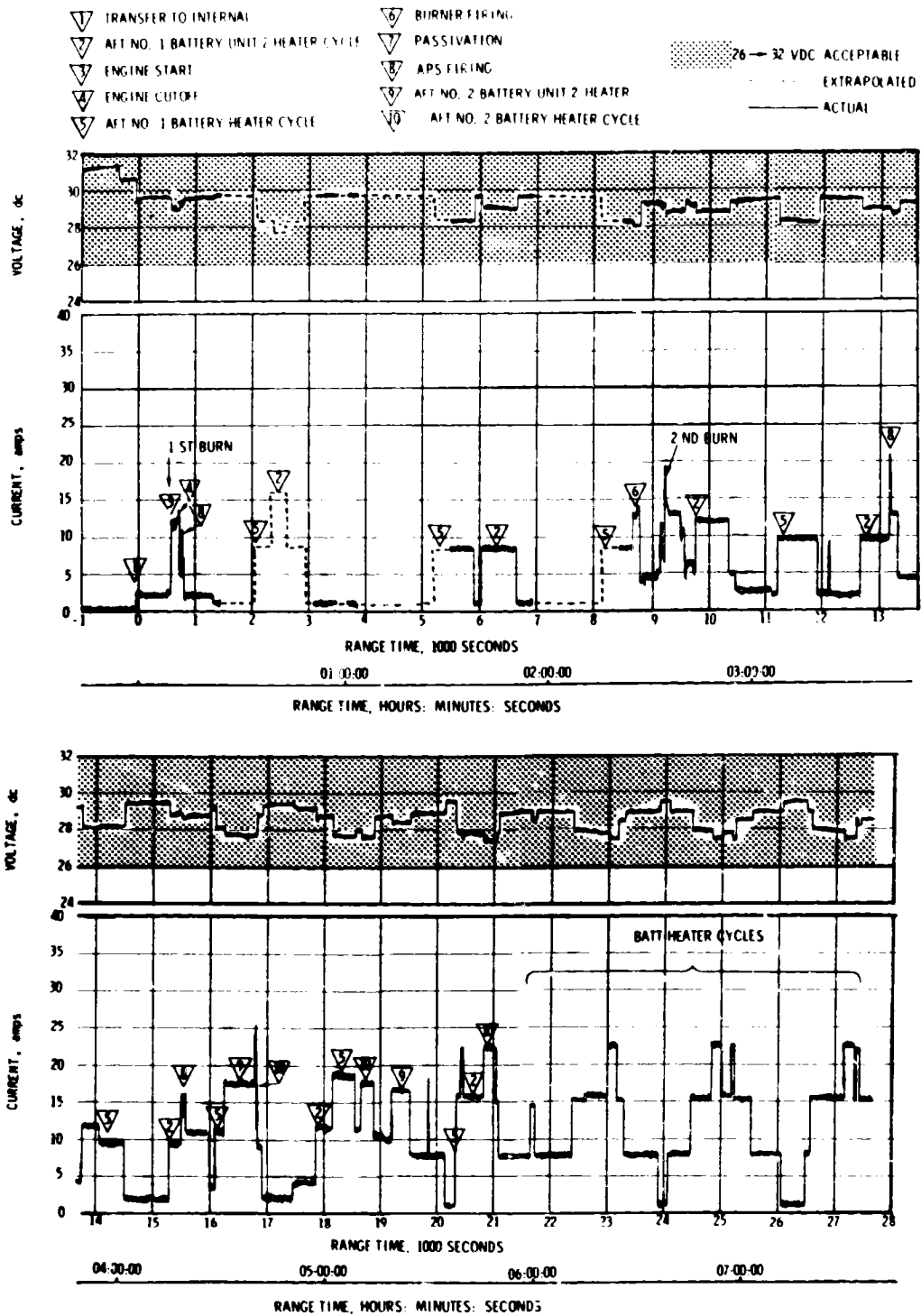


Figure 11-4. S-IVB Stage Aft No. 1 Battery Voltage and Current

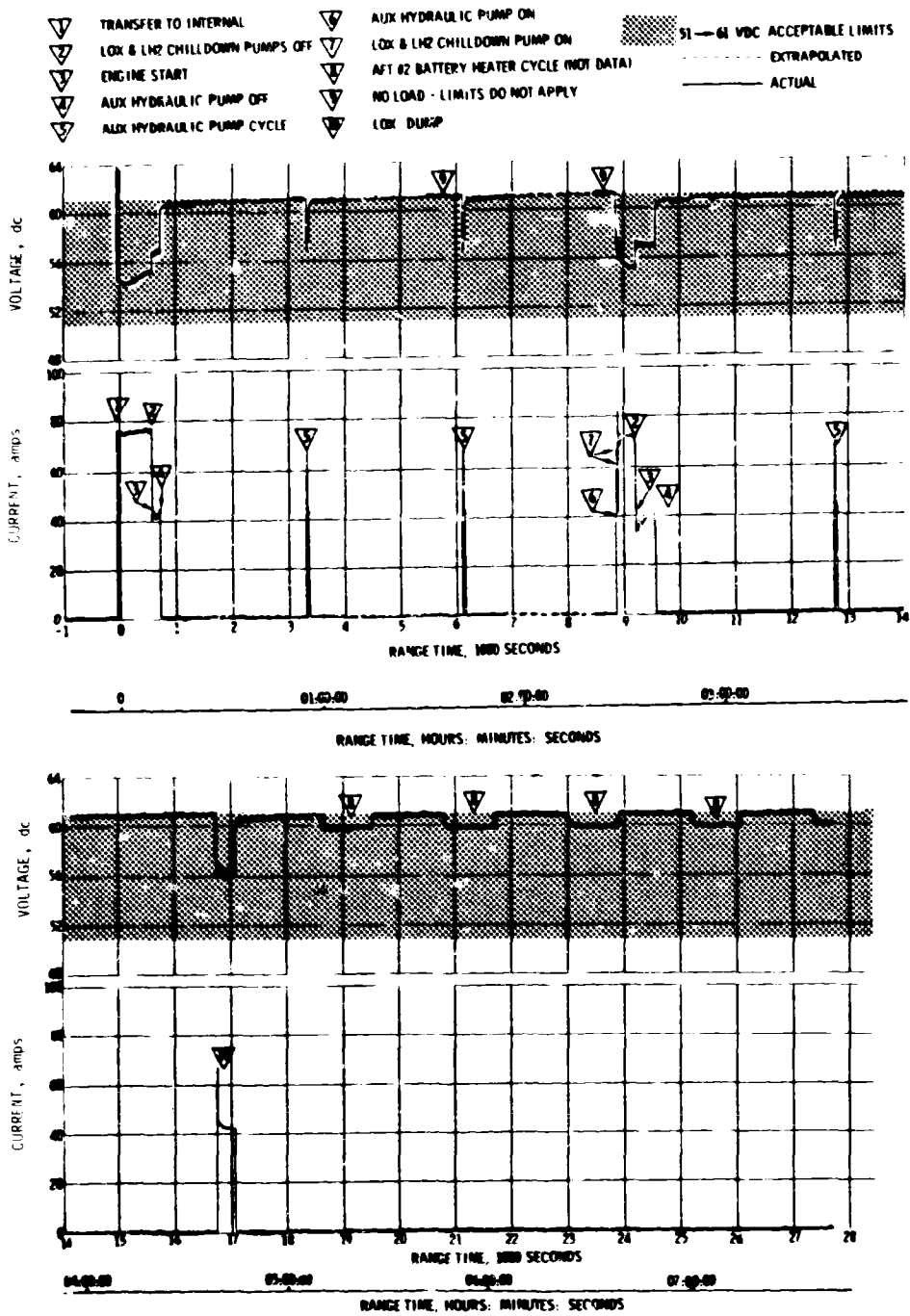


Figure 11-5. S-IVB Stage Aft No. 2 Battery Voltage and Current



Table 11-3. S-IVB Stage Battery Power Consumption

BATTERY	RATED CAPACITY (AMP-HRS)	POWER CONSUMPTION AMP-HRS	PERCENT OF RATED CAPACITY
Forward No. 1	227.5	107.0*	47.0
Forward No. 2	24.6	20.4**	83.0
Aft No. 1	227.5	81.5*	36.0
Aft No. 2	66.5	40.0*	60.0

\* From Battery Activation until Passive Thermal Control (at 21,337 seconds)

\*\* From Battery Activation until battery depleted (dropped below 26.0 volts) at 23,220 seconds.

The roll-off characteristics of the S-IVB #2 batteries during AS-510 and AS-511 flights (Figures 11-2 and 11-3) demonstrated characteristics identified with excessive negative plate limiting as did the four batteries which failed formal cell block testing.

The batch test performed on the AS-511 cells showed that 17% of the cells exhibited excessive negative plate limiting. Excessive negative plate limiting of new cells is difficult to discover except by testing a cell to energy depletion. The most prominent effect of negative limiting identified prior to flight was reduced shelf life. Since the batteries were new, this condition was acceptable. However, the inflight battery temperature gradient characteristics apparently provided a colder active cell temperature than telemetered temperature data indicated. It was not known that plate limiting coupled with the cooler in-flight thermal environment would cause an additional reduction in service capacity. Corrective action for AS-512 includes improved testing and quality control.

## 11.5 INSTRUMENT UNIT ELECTRICAL SYSTEM

### 11.5.1 Summary

The IU power distribution network for AS-511 like AS-510 was configured to provide redundant power to the ST-124 platform and its associated components by diode "OR'ing" the 6D10 and 6D30 batteries. This configuration performed satisfactorily throughout the flight (see paragraph 11.5.2). All battery voltages, currents, and temperatures remained in the normal range during launch and coast periods of flight. Battery voltages, currents, and temperatures are shown in Figures 11-6 through 11-9. Battery power consumption and capacity for each battery are shown in Table 11-4.

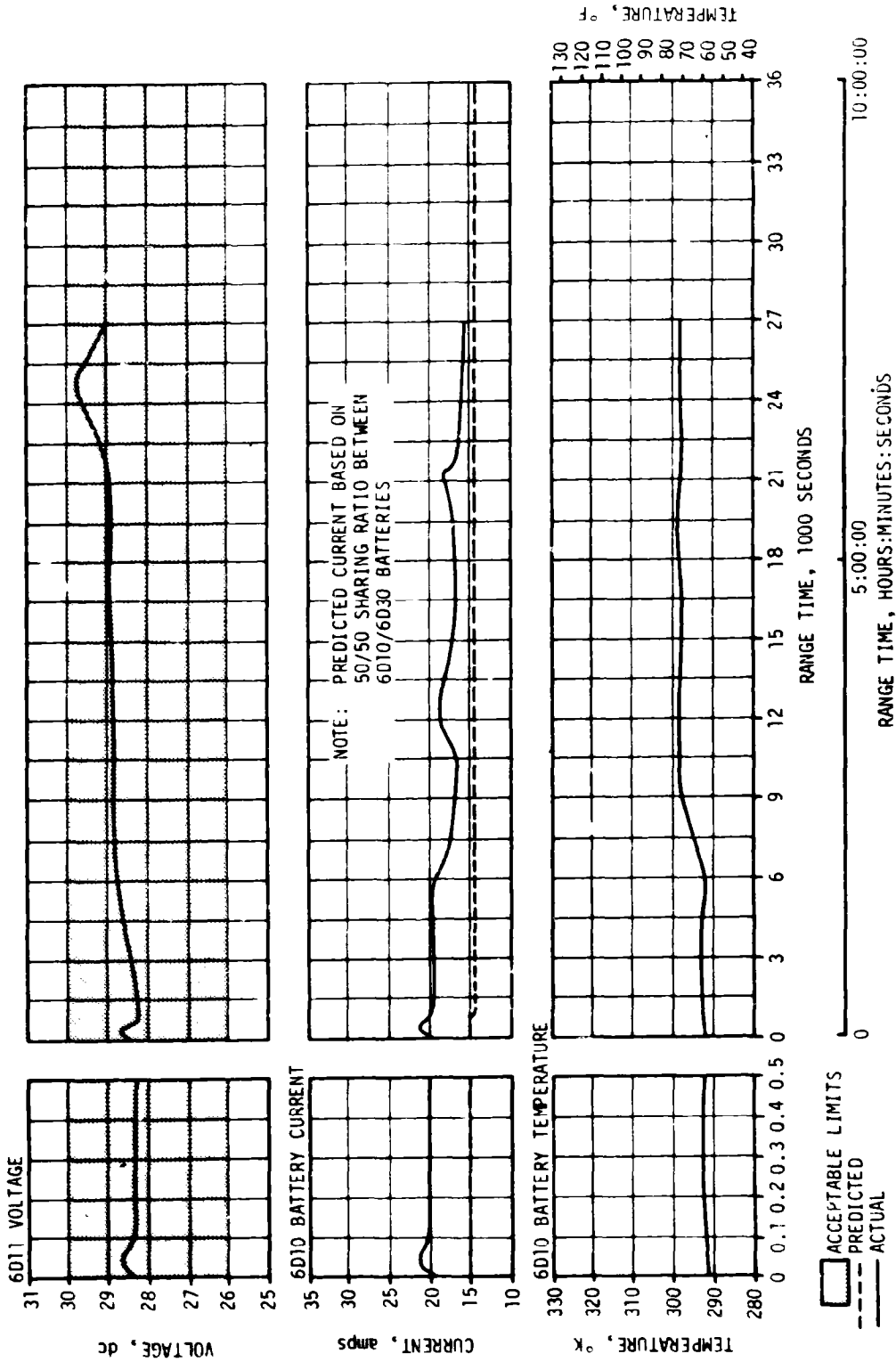


Figure 11-6. 6D10 Battery Measurements

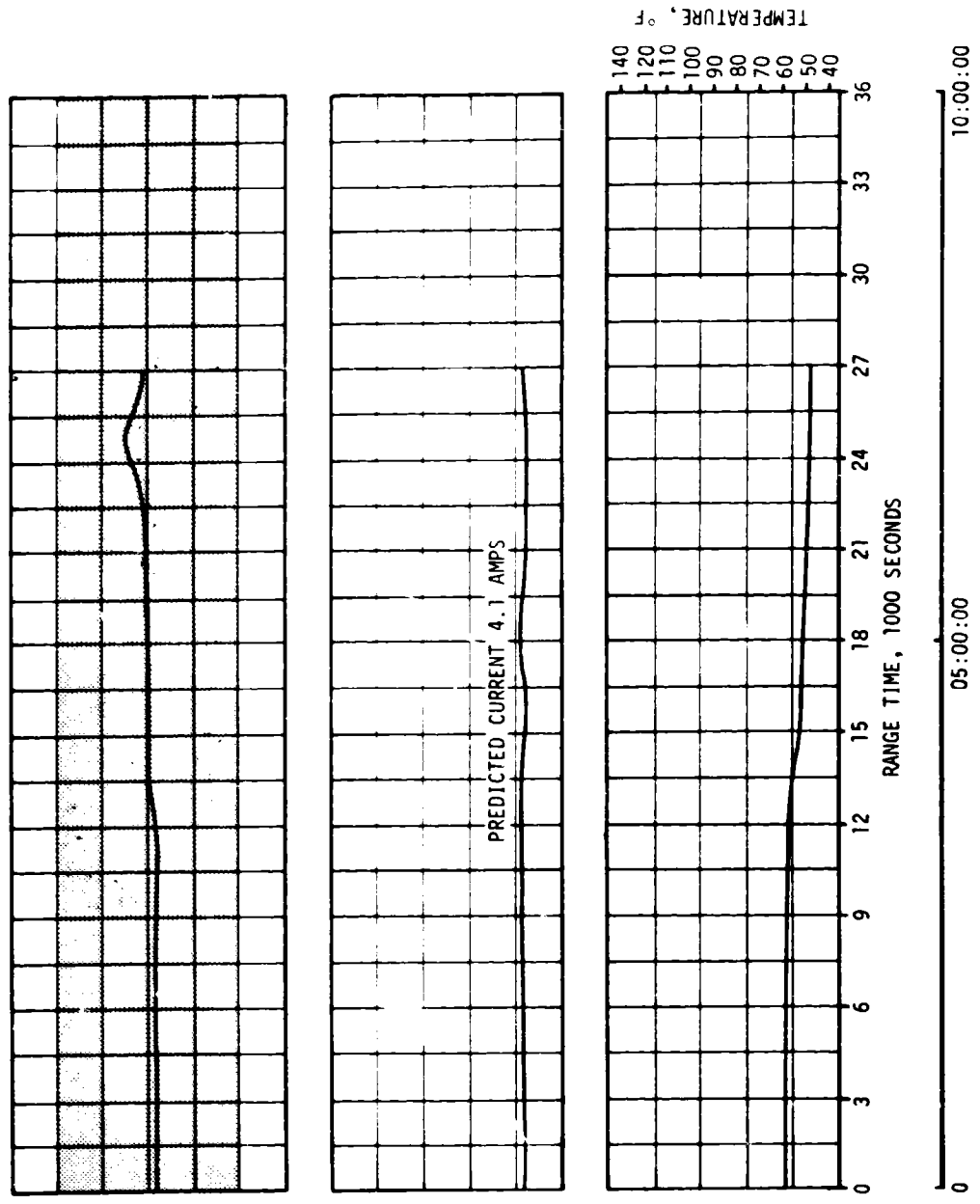
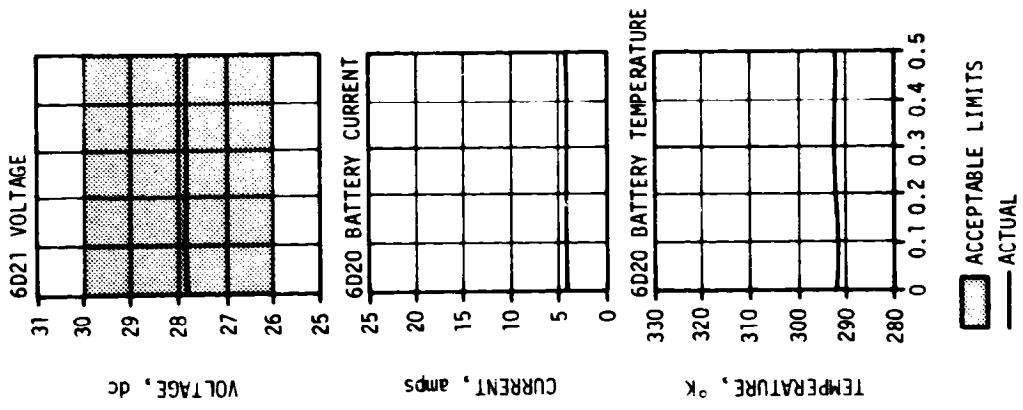


Figure 11-7. 6D20 Battery Measurements

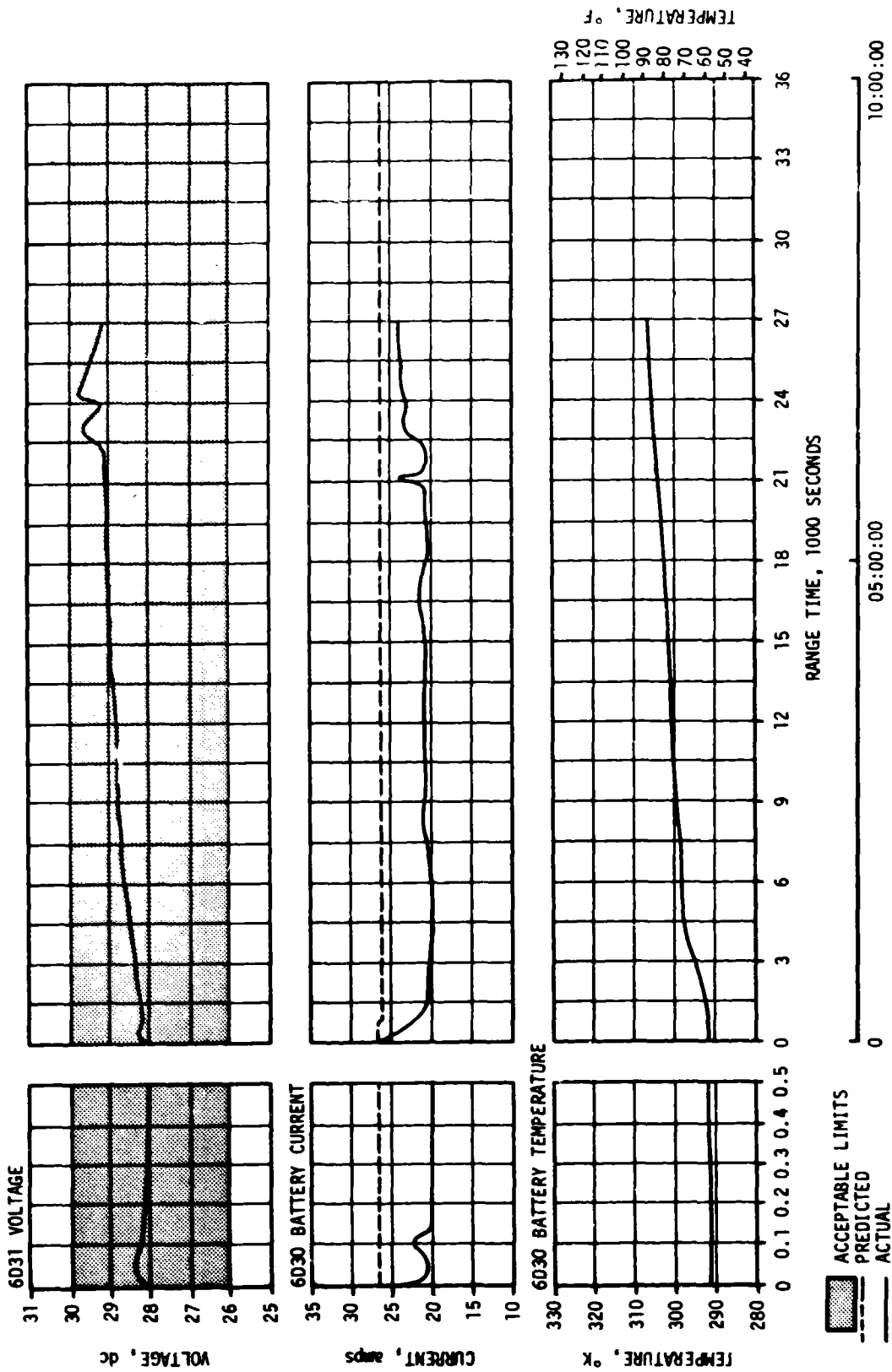


Figure 11-8. 6030 Battery Measurements

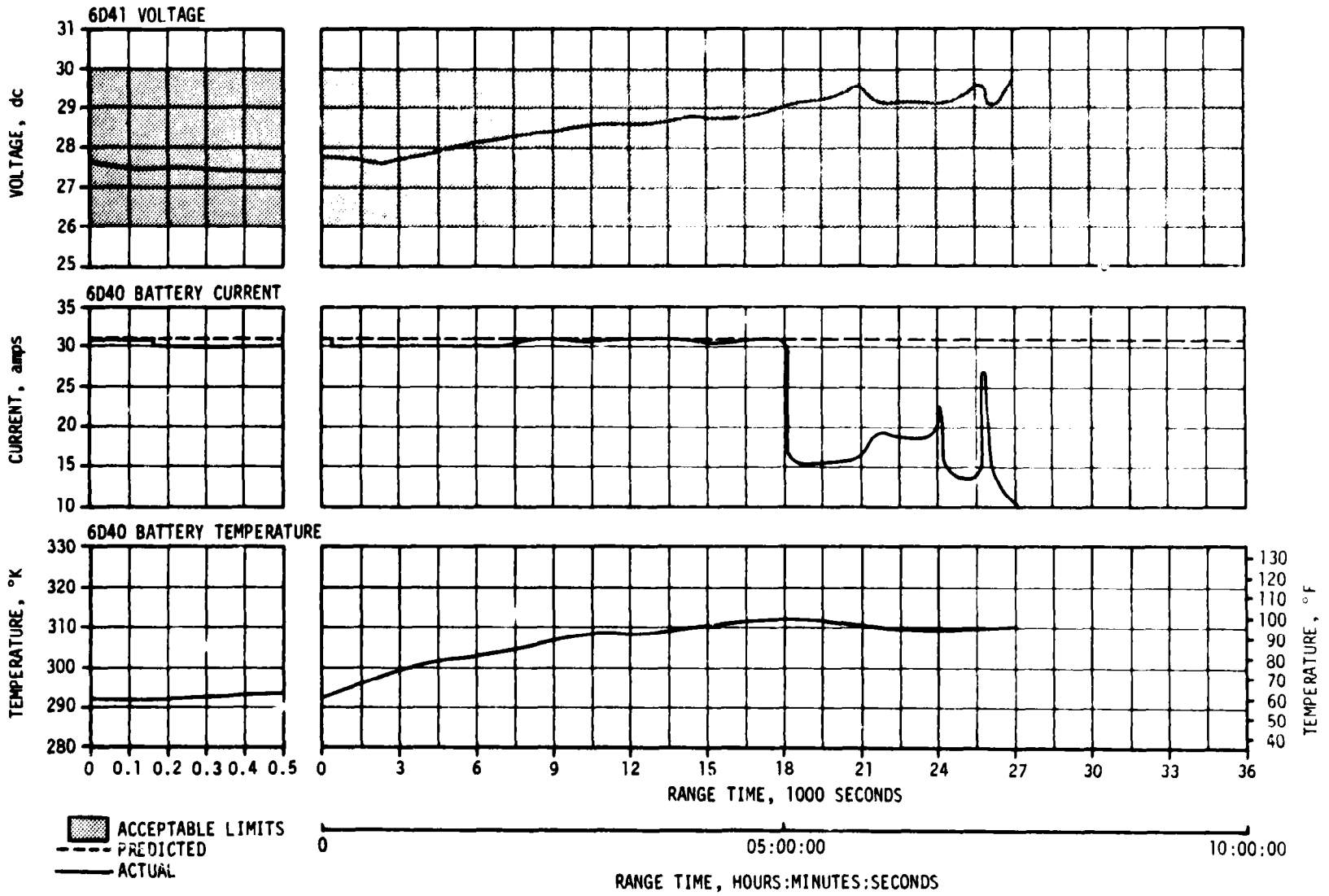


Figure 11-9. 6D40 Battery Measurements

Table 11-4. IU Battery Power Consumption

BATTERY	RATED CAPACITY (AMP-HR)	POWER CONSUMPTION	
		AMP-HR	PERCENT OF CAPACITY
6D10	350	134.0*	38.4
6D20	350	108.6**	31.0
6D30	350	176.2	50.3
6D40	350	204.2	58.3

\* Actual usage was computed from battery activation to 27,643 seconds (7:40:43) when CCS telemetry was inhibited.

\*\* The CCS which was powered by the 6D20 battery failed at 97,799 seconds (27:09:59). Power consumption until CCS failure was calculated based on nominal operation.

The 56-vdc power supply maintained an output voltage of 56.2 to 56.6 vdc, well within the required tolerance of 56 +2.5 vdc.

The 5-vdc measuring power supply performed nominally, maintaining a constant voltage within specified tolerances.

The switch selector, electrical distributors, and network cabling performed nominally.

#### 11.5.2 Battery Analysis

The expected shifts in the 6D10 and 6D30 currents, (during S-IC burn) due to the ST-124 platform requirements and the diode "OR'ed" configuration of the 6D10 and 6D30 batteries, reached a maximum of 24 amperes for 6D10 and 26 amperes for 6D30 and an average of 20 amperes for 6D10 and 22 amperes for 6D30. (See Figure 11-6 and Figure 11-8)

The 6D20 battery temperature varied between 13°C and 19°C indicating a stable condition for the 4.0 amp load. (See Figure 11-7)

Battery 6D40 voltage and current were in the predicted range until approximately 18,000 seconds, when the Environmental Control System (ECS) coolant pump(s) cavitated (see Section 14.4). This condition resulted

in reduced current requirements (32 amps to 18 amps) during the period of pump cavitation (18,000 to 24,900 seconds). At approximately 24,950 through 26,100 seconds high current spikes (with corresponding voltage dips) were recorded, indicating pump failure, and from 26,100 seconds to the end of recorded data, 6D40 current remained at 11 amps which indicates that the coolant pump was no longer drawing current from the battery. (See Figure 11-9)

#### 11.6 SATURN V EMERGENCY DETECTION SYSTEM (EDS)

The performance of the AS-511 EDS was normal and no abort limits were exceeded. All switch selector events associated with EDS for which data are available were issued at the nominal times. The discrete indications for EDS events also functioned normally. The performance of all thrust OK pressure switches and associated voting logic, which monitors engine status, was nominal insofar as EDS operation was concerned. S-II and S-IVB tank ullage pressures remained below the abort limits, and EDS displays to the crew were normal.

The maximum dynamic pressure difference sensed by the Q-ball was 1.1 psid at 57.8 seconds. This pressure was only 34 percent of the EDS abort limit of 3.2 psid.

As noted in Section 10, none of the rate gyros gave any indication of angular overrate in the pitch, yaw, or roll axis. The maximum angular rates were well below the abort limits.

## SECTION 12

### VEHICLE PRESSURE ENVIRONMENT

#### 12.1 SUMMARY

The S-IC base heat shield was instrumented with two differential pressure measurements. The AS-511 flight data have trends and magnitudes similar to those seen on previous flights.

The AS-511 S-II base pressure environments are consistent with the trends and magnitudes seen on previous flights.

#### 12.2 BASE PRESSURES

##### 12.2.1 S-IC Base Pressures

The S-IC base heat shield was instrumented with two differential (internal minus external) pressure measurements. The AS-511 flight data, Figure 12-1, show good agreement with previous flight data with similar trends and magnitudes. The maximum differential pressure of approximately 0.15 psi occurred at an altitude of approximately 4.7 n mi.

##### 12.2.2 S-II Base Pressures

The S-II stage base heat shield forward face pressures are presented in Figure 12-2 together with the postflight analytical values and the data band from previous flights. The AS-511 data was slightly higher than previous flight data prior to interstage separation. A pressure spike occurred during the J-2 engine start transient, however, similar indications do not appear on the thrust cone or heat shield aft face pressure transducers. Consequently, the validity of this pressure spike is questionable.

Figure 12-3 presents the S-II thrust cone pressure history. The flight data fall within the data band of the previous flights prior to interstage separation but fall below zero shortly after. This indicates that the measurement may have a slight bias. However, even considering a negative bias, the data would be comparable to previous flight data.

The heat shield aft face pressures, Figure 12-4, were generally on the high side of the previous flight data band. This could be expected since the J-2 engine precant angle was reduced from 1.3 to 0.6 degree beginning with AS-510.



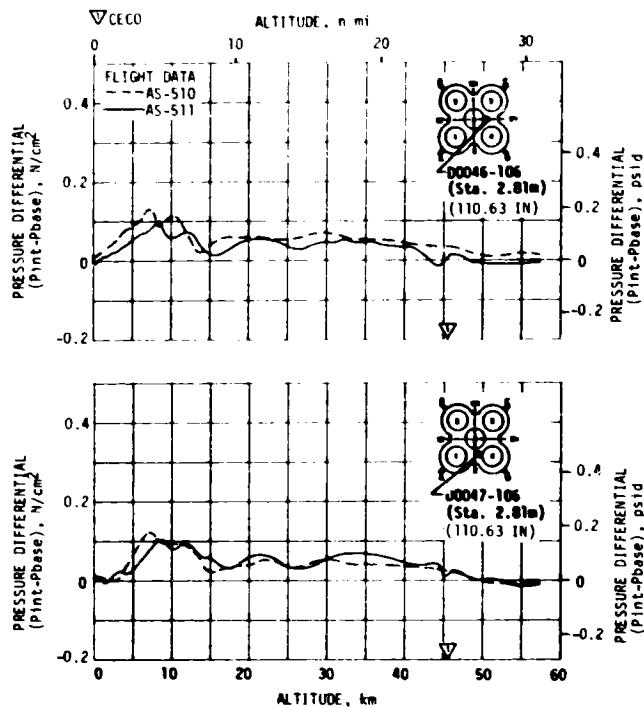


Figure 12-1. S-IC Base Heat Shield Differential Pressure

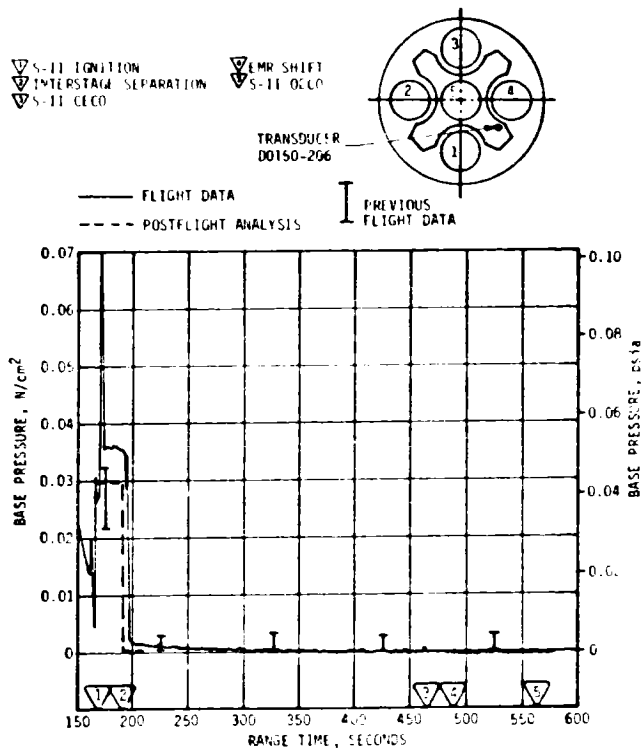


Figure 12-2. S-II Heat Shield Forward Face Pressure

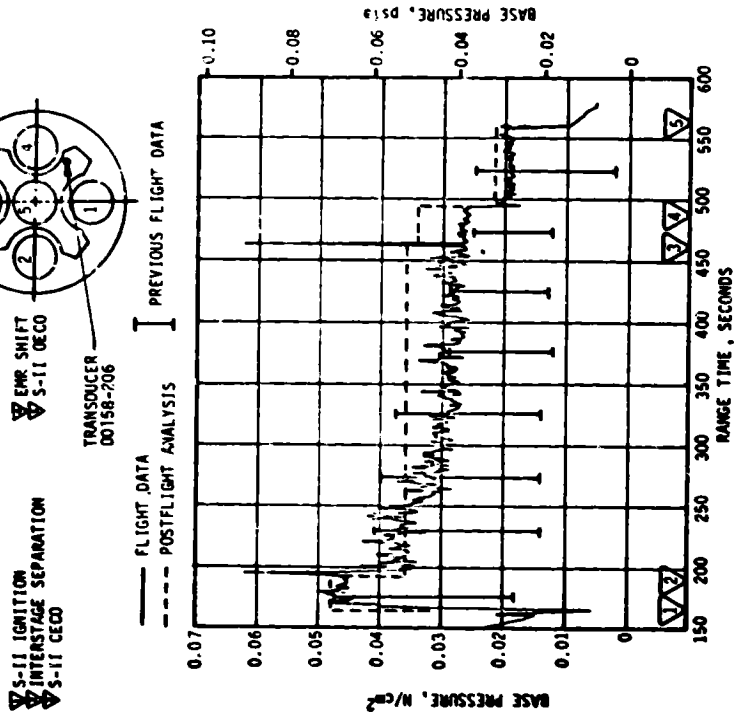


Figure 12-3. S-II Thrust Cone Pressure

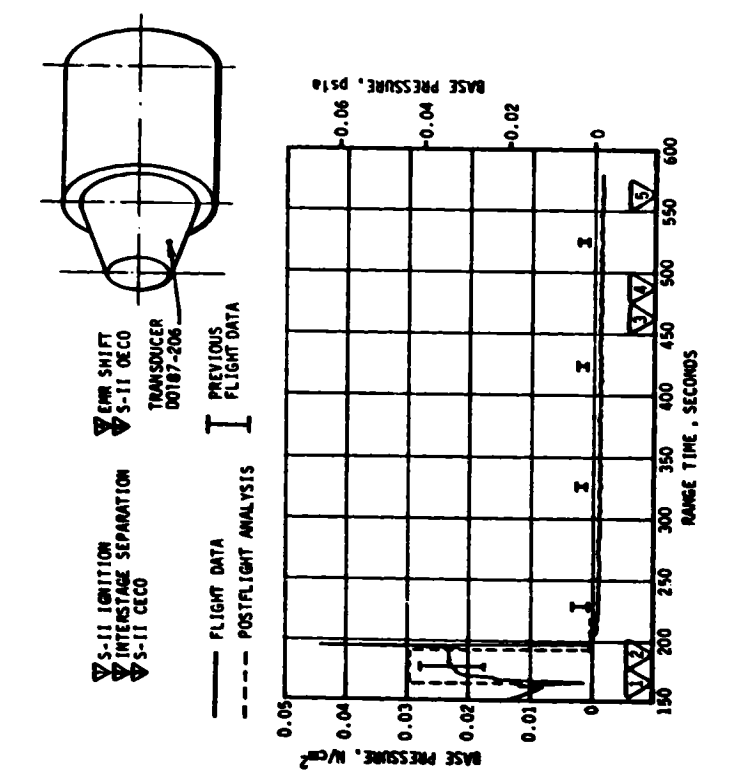


Figure 12-4. S-II Heat Shield Aft Face Pressure

## SECTION 13

### VEHICLE THERMAL ENVIRONMENT

#### 13.1 SUMMARY

The AS-511 S-IC base region thermal environments exhibited trends and magnitudes similar to those seen on previous flights.

The base thermal environments on the S-II stage were consistent with the trends and magnitudes seen on previous flights and were well below design limits.

Aerodynamic heating environments and S-IVB base thermal environments were not measured on AS-511.

#### 13.2 S-IC BASE HEATING

Thermal environments in the base region of the AS-511 S-IC stage were recorded by two total calorimeters and two gas temperature probes which were located on the base heat shield. The sensing surfaces of the total calorimeters were mounted flush with the heat shield surface. The base gas temperature sensing surfaces were mounted at distances aft of the heat shield surface of 0.25 inch (C0050-106) and 2.50 inches (C0052-106). Data from these instruments are compared with AS-510 flight data and are presented in Figures 13-1 and 13-2. The AS-511 data exhibit similar trends and magnitudes as previous flights. The maximum recorded total heating rate was approximately 25 Btu/ft<sup>2</sup>-s and occurred at an altitude of 11.3 n mi.

The maximum gas temperature was approximately 1736°F recorded 2.5 inches aft of the heat shield at an altitude of 11.3 n mi. In general, CECO on AS-511 produced a spike in the thermal environment data with a magnitude and duration similar to previous flight data.

Ambient gas temperatures under the engine cocoons (measurements C0242-101 through C0242-105) were within the band of previous flight data and within predicted values. These temperatures are shown in Figure 13-3.

#### 13.3 S-II BASE HEATING

Figure 13-4 presents the AS-511 total heating rate throughout S-II burn, as recorded by transducer C0722-206 on the aft face of the base heat shield. The postflight analytical curve for this transducer and the previous flight data band are also shown for comparison. The analytical heat rate represents the theoretical response of the transducer to the total thermal environment reflected by thermal math models. Key flight

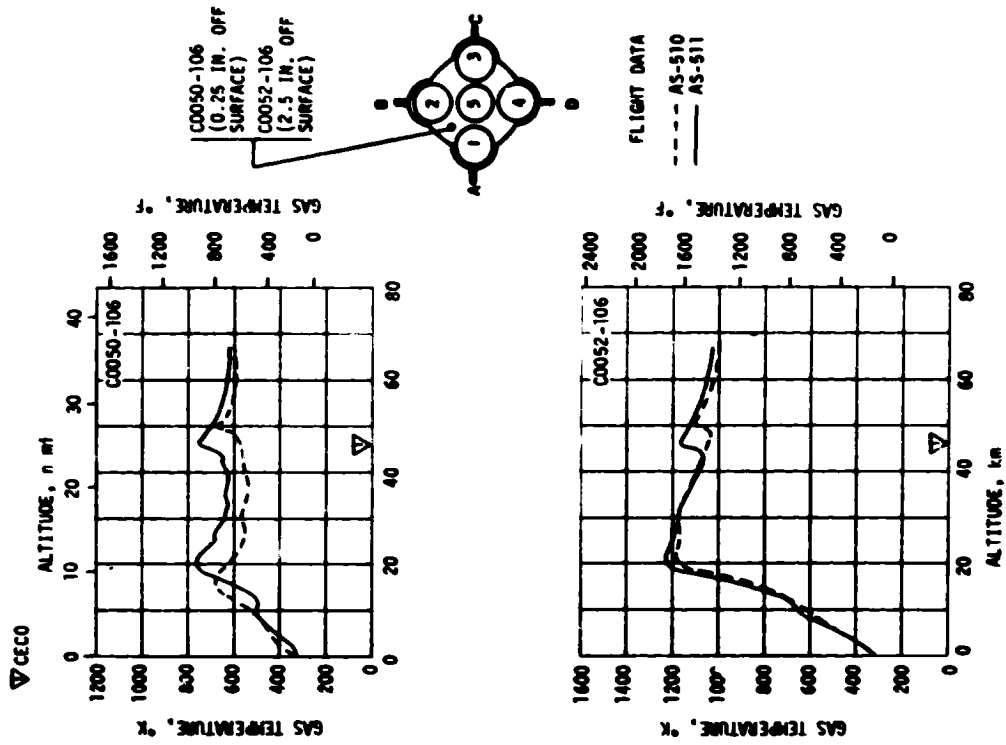


Figure 13-1. S-IC Base Region Total Heating Rate

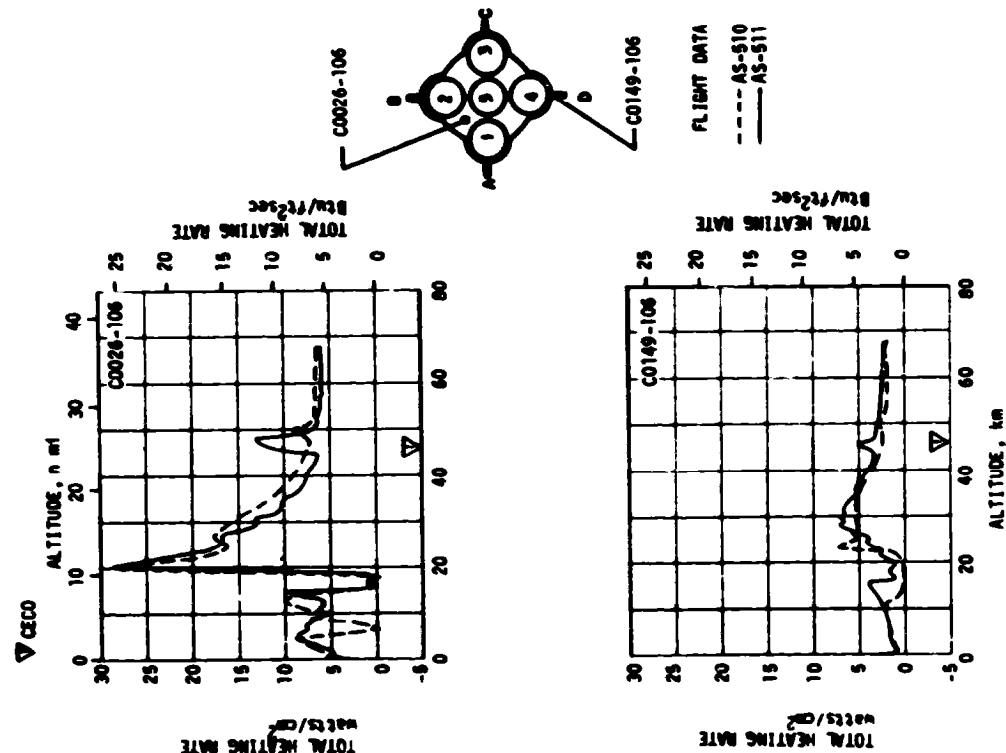


Figure 13-2. S-IC Base Region Gas Temperature

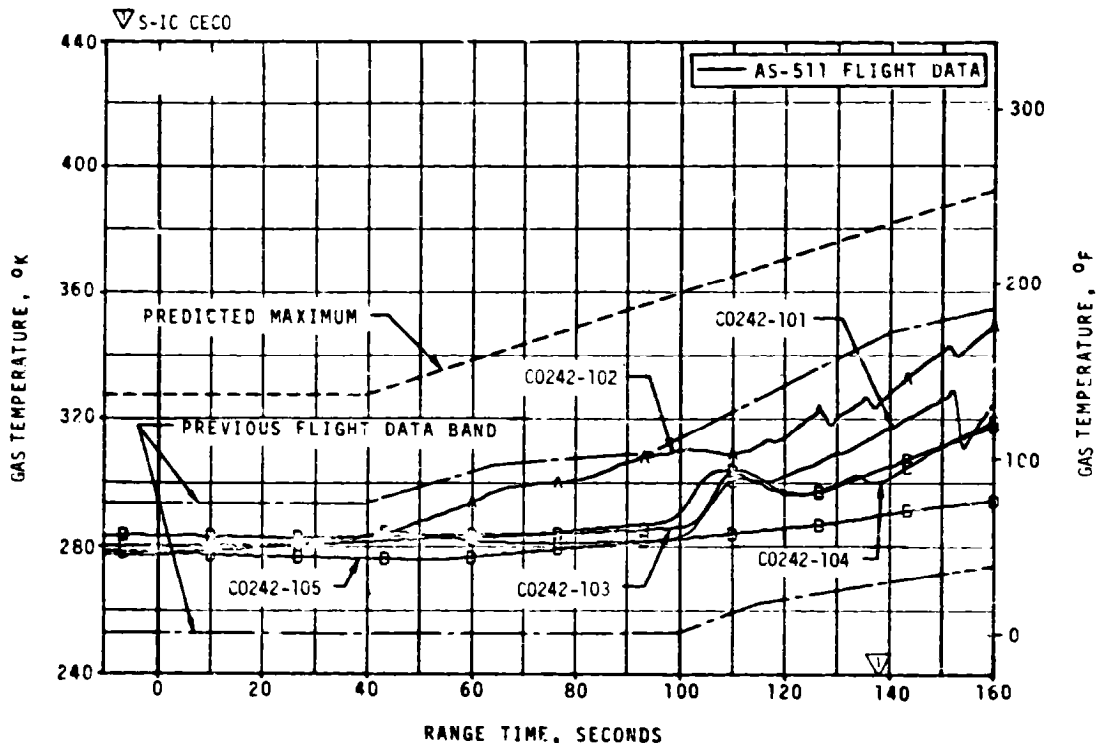


Figure 13-3. S-IC Ambient Gas Temperature Under Engine Cocoon

parameters relating to engine performance, engine position, and reference temperatures are used in the postflight analysis. The math models are based on both theoretical and empirical postulates. The flight data for AS-511 are at the upper end of that recorded during previous flights. This was expected since the J-2 engine precant had been reduced from 1.3 degrees to 0.6 degree since AS-510. The flight measured heating rates are well below the maximum design allowable values.

Figure 13-5 shows the AS-511 flight data and postflight analysis of the heat shield recovery temperature transducer, C0731-206. The analytical temperature curve represents a calculated transducer reading based on math models using key flight parameters. The gas recovery temperature is an analytically derived value computed from the flight measurement data. Note that the flight values are the probe temperatures and not the gas recovery temperatures. The AS-511 flight gas recovery temperature values were expected to be on the high side of the data band from previous flights due to the reduction of the J-2 engine precant angle. It is seen in Figure 13-5 that this is not substantiated by the flight data. However, as indicated by the data envelope from previous flights, a considerable probe temperature variation of the parameters considered in the analysis alone. Also, since the initial temperature is below the probe range, it is not possible to determine if the probe temperature is biased.

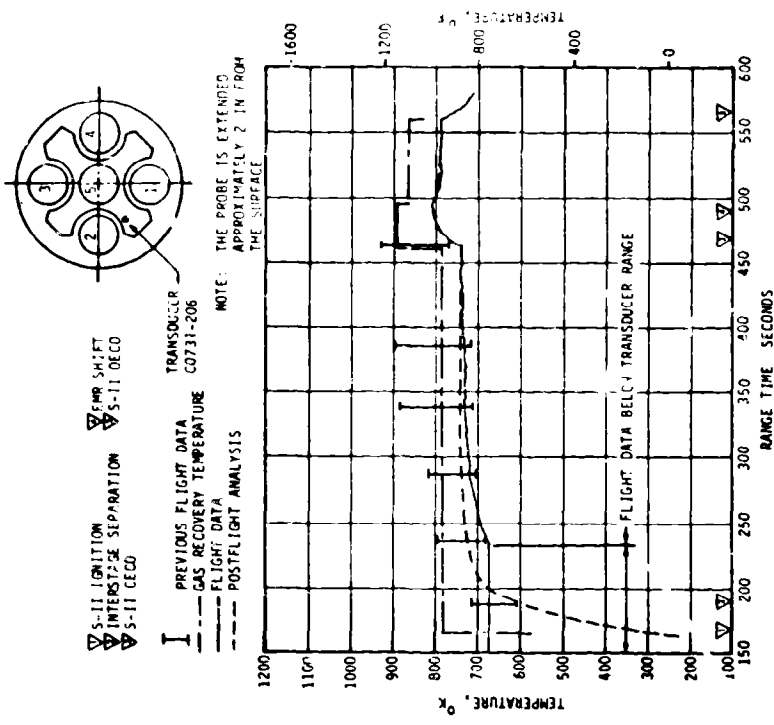


Figure 13-5. S-II Heat Shield Recovery Temperature

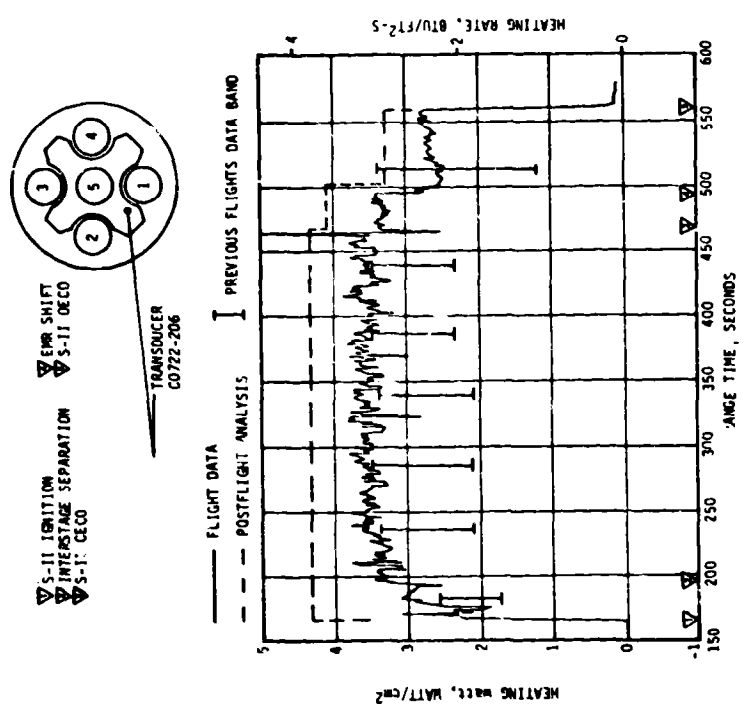


Figure 13-4. S-II Heat Shield Aft Heat Rate

Figure 13-6 shows the AS-511 flight and postflight analytical values of the radiometer measured radiative heat flux to the heat shield aft surface. Also shown is the calculated value of the actual incident radiative heat flux at the same location. The discrepancy between the radiometer indicated value and the incident heat flux is due to the heating of the radiometer quartz window by convection and long-wave plume radiation. Consequently, the radiometer sensor receives additional heat from the quartz window by radiation and convection across the air gap between the window and the sensor. This explains the apparently slow radiometer response at engine start, CECO, Engine Mixture Ratio (EMR) shift and at outboard engine cutoff.

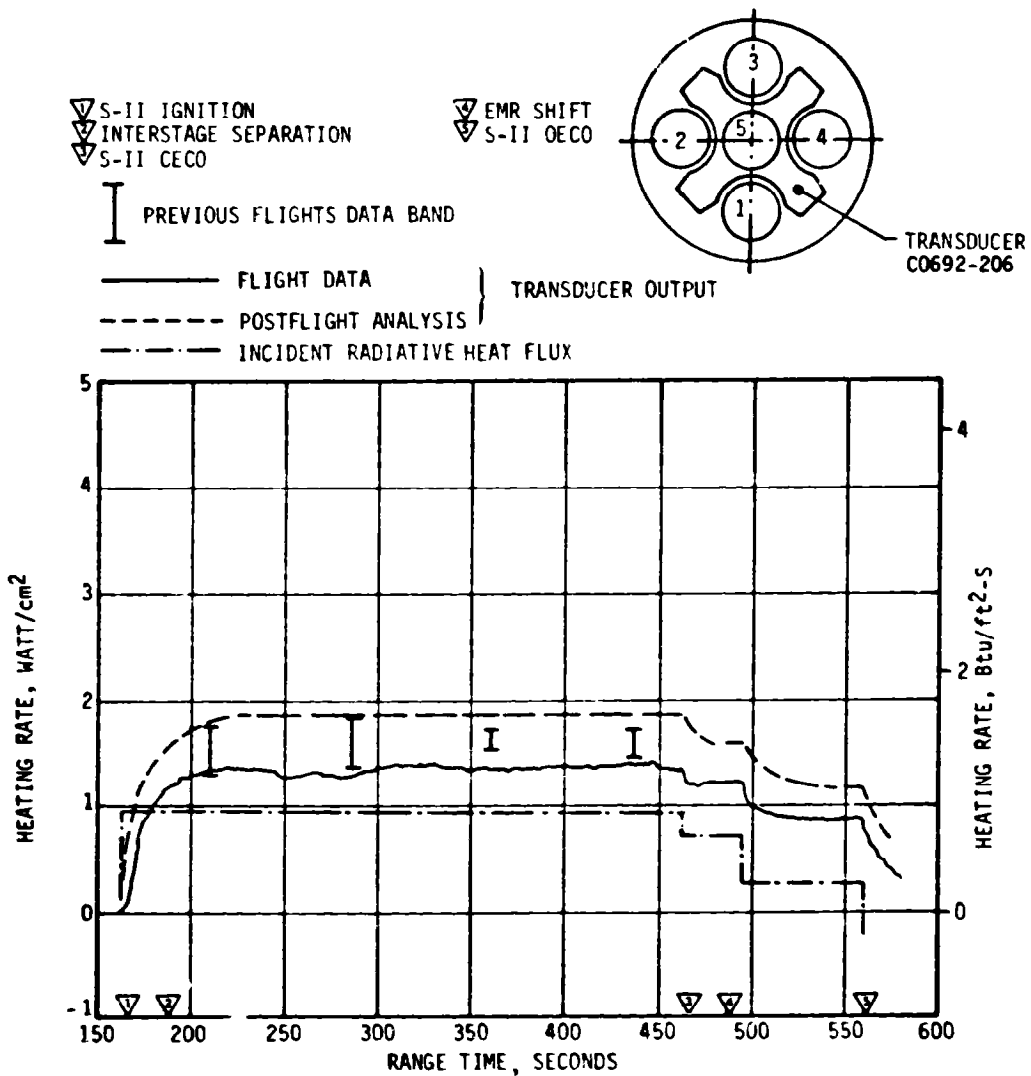


Figure 13-6. S-II Heat Shield Aft Radiation Heat Rate

There were no structural temperature measurements on the base heat shield and only three thrust cone forward surface temperature measurements in the base region. To evaluate the structural temperatures on the aft surface of the heat shield, a postflight analysis was performed using maximum AS-511 postflight analysis base heating rates. The maximum postflight analysis temperature was 885°F which compares favorably with previous flights, and was well below the maximum design temperatures of 1460°F (no engine out) and 1550°F (one control engine out). The effectiveness of the heat shield and flexible curtains was evidenced by the relatively low temperatures recorded on the thrust cone forward surface. The maximum measured temperature on the thrust cone forward surface was 22°F. The measured temperatures were well below design values.

#### 13.4 VEHICLE AEROHEATING THERMAL ENVIRONMENT

Aerodynamic heating environments were not measured on the AS-511 S-IC stage. Due to the similarity in the trajectory, the aerodynamic heating environments are believed to be approximately the same as previous flight environments. Ground optical data were not available to measure flow separation because of cloud interference with the Melbourne Beach camera during the critical period and a loss of timing line on the film from the Ponce de Leon camera. The early flight optical data from Melbourne Beach are shown with AS-509 and AS-510 flight data in Figure 13-7 and indicate that the AS-511 data were probably similar to those flights.

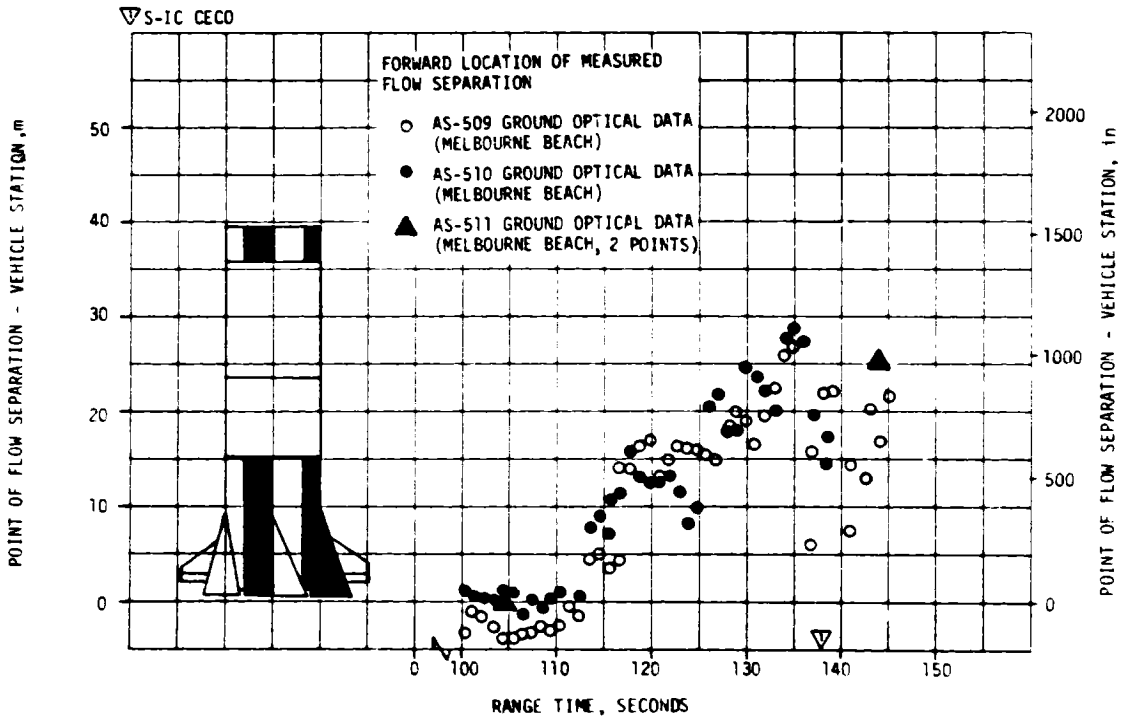


Figure 13-7. Forward Location of Separated Flow on S-IC Stage



### 13.5 S-IC/S-II SEPARATION THERMAL ENVIRONMENT

Since the AS-511 S-IC/S-II separation was nominal, the heating environment to the S-IC LOX tank dome is assumed to be near nominal.

There were no environmental measurements in this area on the flight vehicle and nothing has been observed in other flight data to indicate a more than nominal environment. A detailed discussion of the S-IC/S-II staging is found in Section 10.6.

## SECTION 14

### ENVIRONMENTAL CONTROL SYSTEMS

#### 14.1 SUMMARY

The S-IC stage forward compartment ambient temperatures were maintained above the minimum performance limit during AS-511 countdown. The S-IC stage aft compartment environmental conditioning system performed satisfactorily.

The S-II thermal control and compartment conditioning system apparently performed satisfactorily since the ambient temperatures external to the containers were normal, and there were no problems with the equipment in the containers.

The Instrument Unit (IU) Environmental Control Systems (ECS) performed satisfactorily up until approximately 18,000 seconds (05:00:00). At this time coolant fluid circulation ceased due to an excessively high GN<sub>2</sub> usage rate which depleted the Thermal Conditioning System (TCS) storage sphere. After cooling ceased, temperatures began to increase but were within acceptable values at the time IU telemetry was terminated.

#### 14.2 S-IC ENVIRONMENTAL CONTROL

The S-IC stage forward skirt ECS has three phases of operation during prelaunch operations: (1) when onboard electrical systems are energized, but prior to cryogenic loading, conditioned air is used to maintain the desired environment; (2) when cryogenic loading begins, warmed GN<sub>2</sub> is substituted for the conditioned air; (3) the third phase uses a warmer GN<sub>2</sub> flow to offset the cooling effects caused by S-II stage J-2 engine thrust chamber chilldown. All three phases functioned satisfactorily as evidenced by ambient temperature readings.

The most severe prelaunch forward compartment thermal environment (-74.6°F at C0206-120) occurred during J-2 engine chilldown but was above the minimum performance limit of -90°F. During flight the lowest forward compartment temperature measured was -126.9°F at instrument location C0206-120.

After the initiation of LOX loading, the temperature in the vicinity of the battery (12K10) decreased to 68°F which is within the battery qualification limits of 35 to 95°F. The temperature increased to 78°F at liftoff. Just prior to liftoff, the other ambient temperatures ranged from 75.7°F at instrument location C0203-115 to 88.3°F at instrument

location C0205-115. During flight the lowest aft compartment temperature recorded was 57.2°F at instrument location C0203-115.

#### 14.3 S-II ENVIRONMENTAL CONTROL

The engine compartment conditioning system maintained the ambient temperature and thrust cone surface temperatures within design ranges throughout the launch countdown. The system also maintained an inert atmosphere within the compartment as evidenced by the absence of H<sub>2</sub> or O<sub>2</sub> indications on the hazardous gas monitor.

No equipment container temperature measurements were taken. However, since the ambient measurements external to the containers were satisfactory and there were no problems with the equipment in the containers, it is assumed that the thermal control system performed adequately.

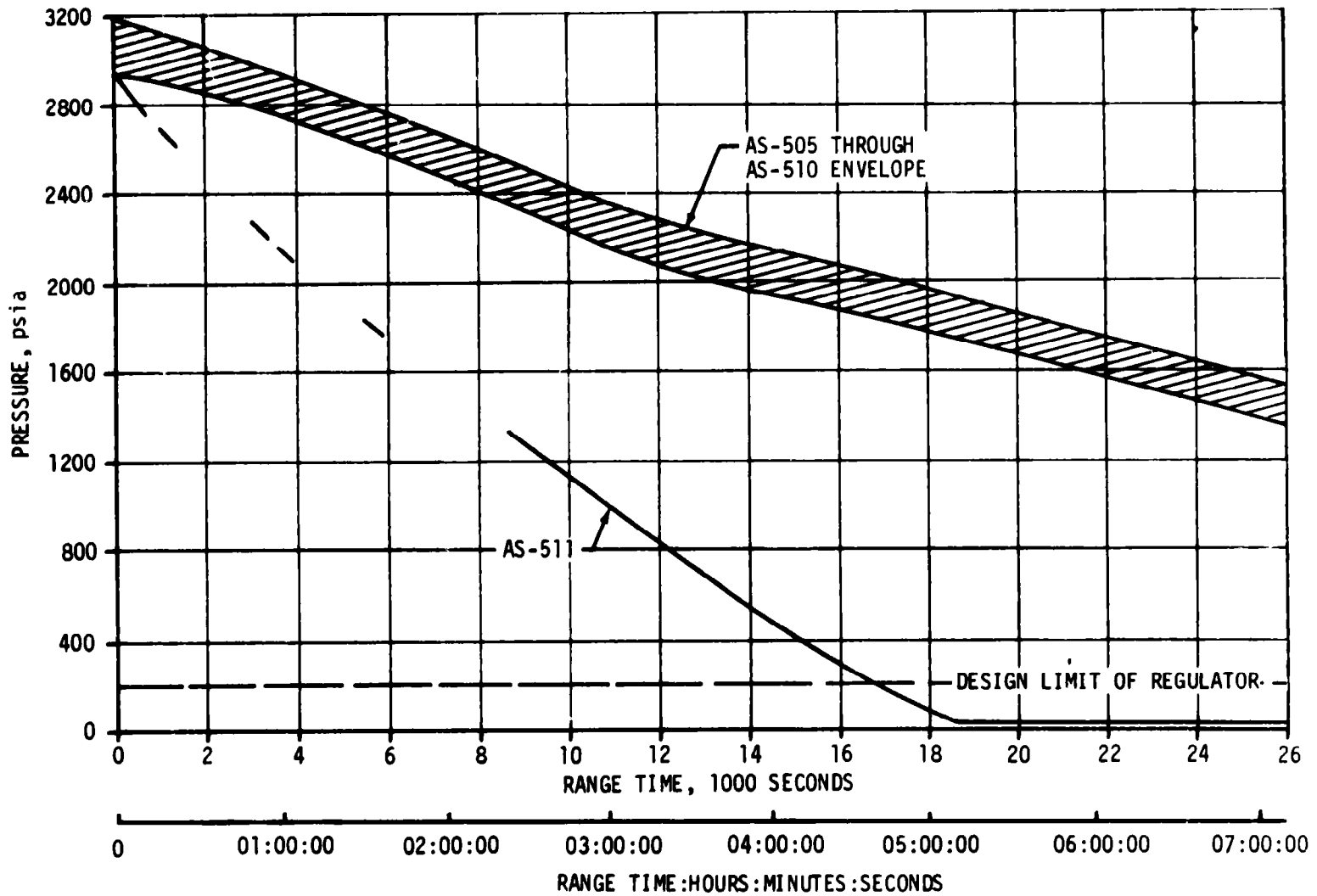
#### 14.4 IU ENVIRONMENTAL CONTROL

##### 14.4.1 Thermal Conditioning System (TCS)

The IU TCS performed satisfactorily for approximately 18,000 seconds (05:00:00). However, an abnormally high GN<sub>2</sub> usage rate (Figure 14-1) attributed to leakage in the system depleted the 165 cubic inch storage sphere at approximately 18,000 seconds (5:00:00). The TCS GN<sub>2</sub> provides pressurization to both the Oronite coolant system and the sublimator water system (Figure 14-2). The loss of GN<sub>2</sub> pressure to the coolant accumulator, and thus to the inlet of the primary coolant pump, caused the pump outlet pressure to decay until the pressure switch activated the redundant pump. The inlet pressure to the redundant pump was such that it could not attain full performance. Cavitation of the redundant pump began at approximately 18,120 seconds (05:02:00) ending coolant circulation (Figure 14-3). The loss of GN<sub>2</sub> in the storage sphere also prevented pressurization of the water accumulator, which provides water to the sublimator. This loss of water to the sublimator is inconsequential as the coolant circulation had ceased.

At the time coolant circulation ceased, most component temperatures began to increase. It would have been possible to subcool the components prior to GN<sub>2</sub> depletion, thereby extending the life of the system. However, the decision was made in realtime not to perform the subcooling due to the S-IVB APS problem and lunar targeting problems. Consequently, the Passive Thermal Control Maneuver was initiated at 21,306 seconds (05:55:06), and the flight control computer was powered down. All component temperatures were below upper limit values at the time telemetry was terminated at 27,643 seconds (7:40:43) (Figure 14-4).

A review and analysis of the available data taken during prelaunch tests and checkout show that an increase in the total TCS GN<sub>2</sub> usage rate occurred between the Service Arm Over-All Test (performed prior to

Figure 14-1. IU TCS GN<sub>2</sub> Sphere Pressure

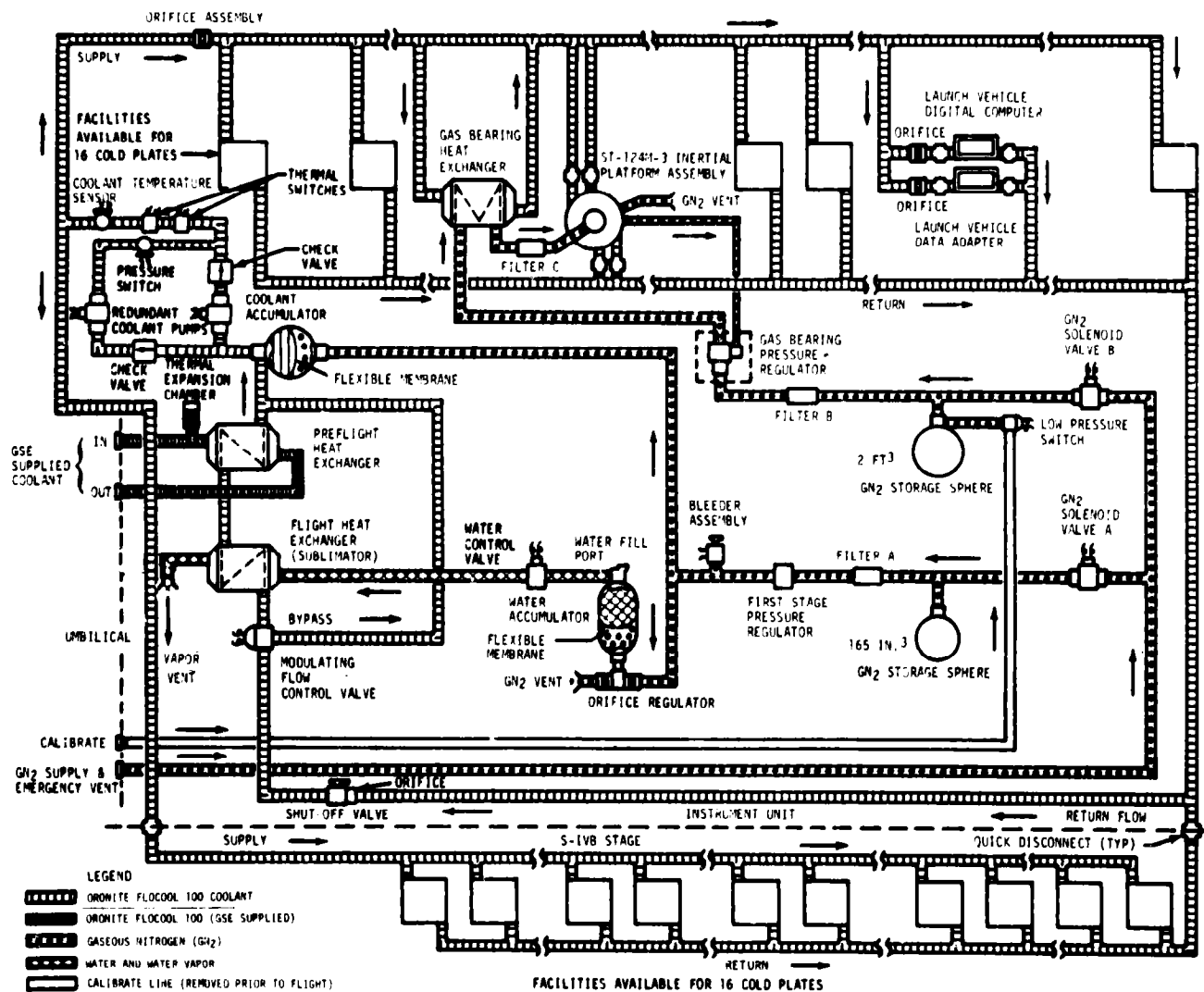


Figure 14-2. IU Thermal Control System (TCS)

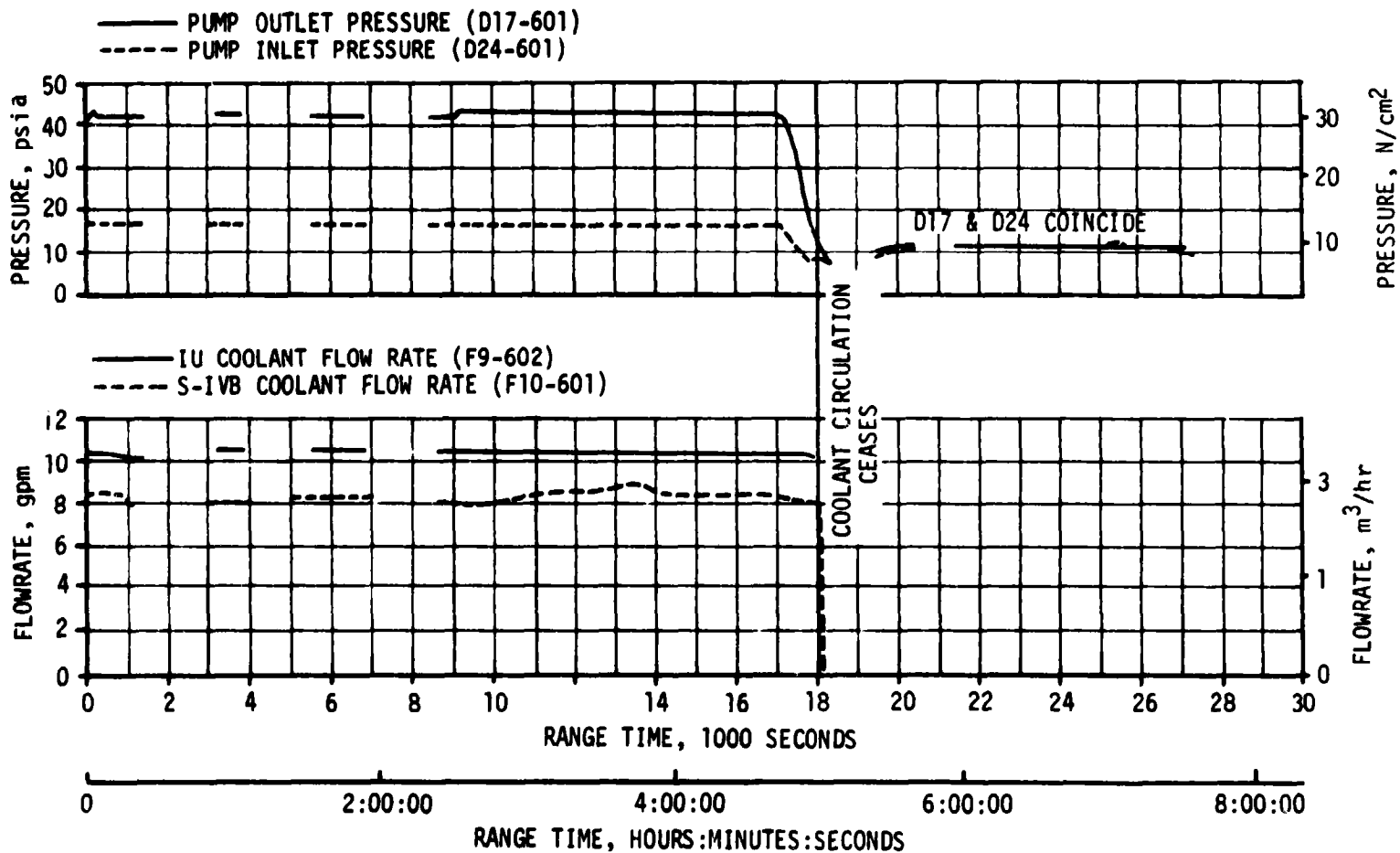


Figure 14-3. IU TCS Hydraulic Performance

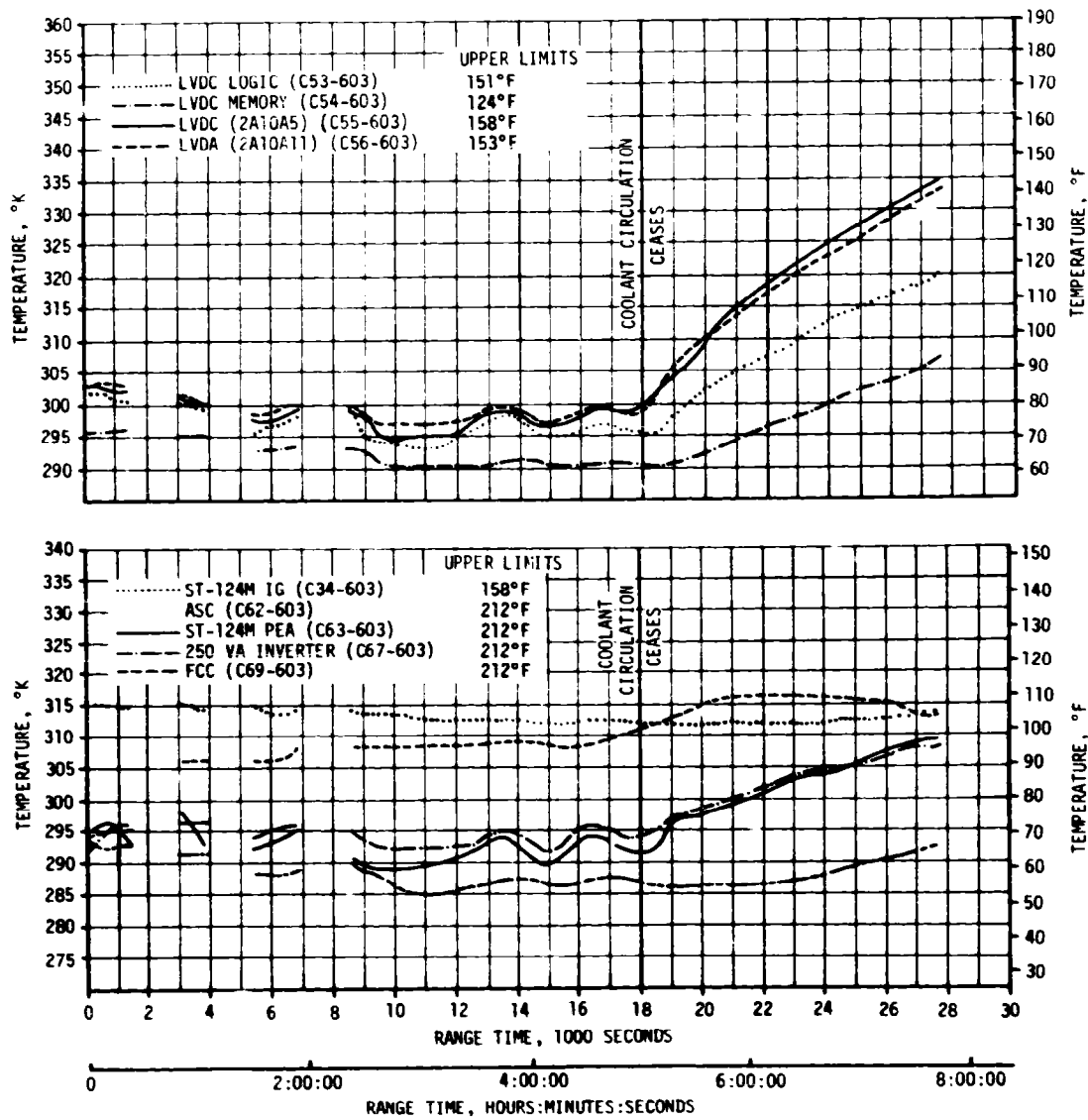


Figure 14-4. Selected IU Component Temperatures

initial roll-out) and preparations for the wet CDDT (performed following second roll-out). Due to problems associated with the GSE dome regulator and the fact that the recorded data was not associated with a scheduled test, the significance of the prelaunch data was obscured. The excessive usage rate during flight was somewhat greater than that recorded pre-launch, but was not inconsistent with the normal increase in flow rate resulting from reducing the ambient pressure to zero (assuming low pressure leak).

As noted in Figure 14-2 the TCS GN<sub>2</sub> flows through the first stage regulator which reduces the supply pressure to 16.5 ±0.5 psia. Analysis of the flight data shows that the regulator ceased to regulate when the inlet pressure fell to approximately 125 psia. Figure 14-5 gives the relationship between the regulator flow rates and minimum inlet pressures. On AS-508 the system was allowed to deplete at the normal usage rate. The regulator ceased to operate at an inlet pressure of approximately 40 psia which is considered to be characteristic of a normally operating system. Assuming the same usage rate for AS-511, a leak on the high pressure side of the regulator would show a loss of pressure regulation considerably above the regulator characteristic curve.

Assuming a leak on the low pressure side, the AS-511 flight data are found to correlate closely with the characteristic curve for full leakage and bleed flow through the regulator. This indicates the leak is most probably on the low pressure side of the regulator.

A review of in-process seal failures on the low pressure side of the regulator is summarized in Figure 14-6. Based on this failure history, the most probable failure point was suggested to be the 1/2 inch K-seal located at a plug near the line connection to the Oronite accumulator. However, this data is not necessarily applicable to KSC operations. While a significant problem was noted with surface finish of or-hand K-seals, this factor was deemed less significant than the greater characteristic tendency of K-seals when once sealed to remain sealed. There are also 3 O-rings in the system which by no means have been exonerated. Therefore, a contemplated change to an all O-ring system was determined to be unwarranted. Improved prelaunch leak test procedures will be incorporated.

Sublimator performance during ascent is presented in Figure 14-7.

The thermal shrouds were effective in shielding the IU components from solar heating as evidenced by the low-normal component temperatures through 18,000 seconds. This is especially significant since all active component cooling ceased at approximately 18,000 seconds.

#### 14.4.2 ST-124M Gas Bearing System (GBS)

The gas bearing subsystem performance was nominal throughout the IU mission. Figure 14-8 depicts ST-124M platform pressure differential (D0011-603) and platform internal ambient pressure (D0012-603).

The GBS GN<sub>2</sub> supply sphere pressure decay was nominal, as shown in Figure 14-9.



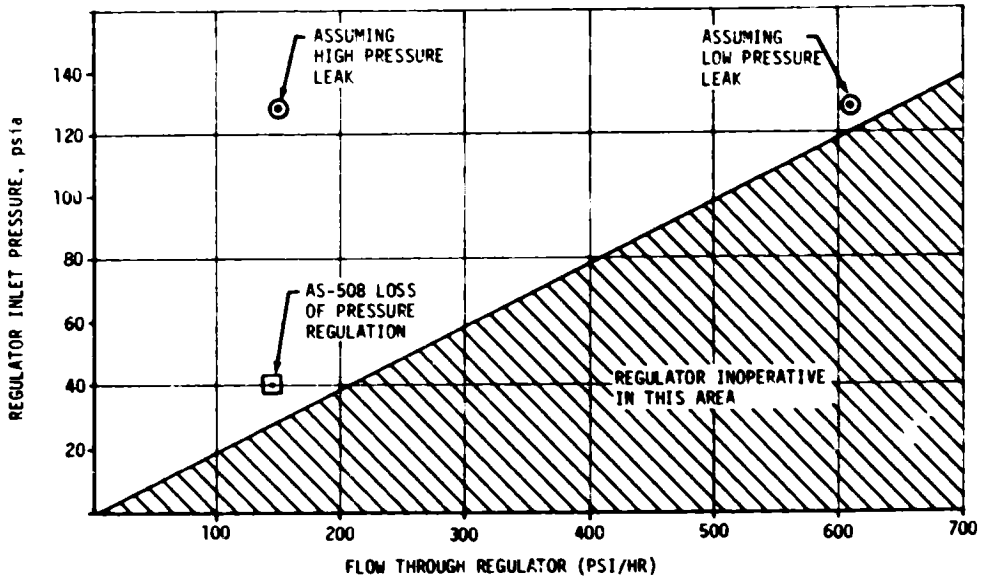


Figure 14-5. IU Pressure Regulator Operation

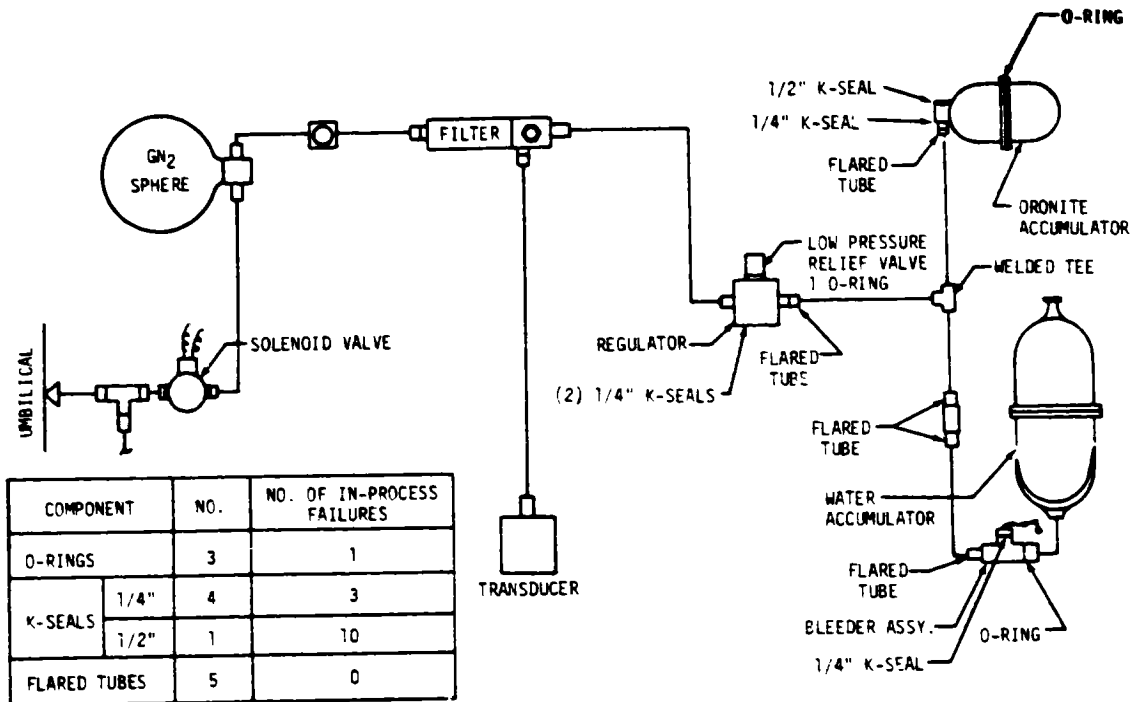


Figure 14-6. TCS Pressurization Schematic

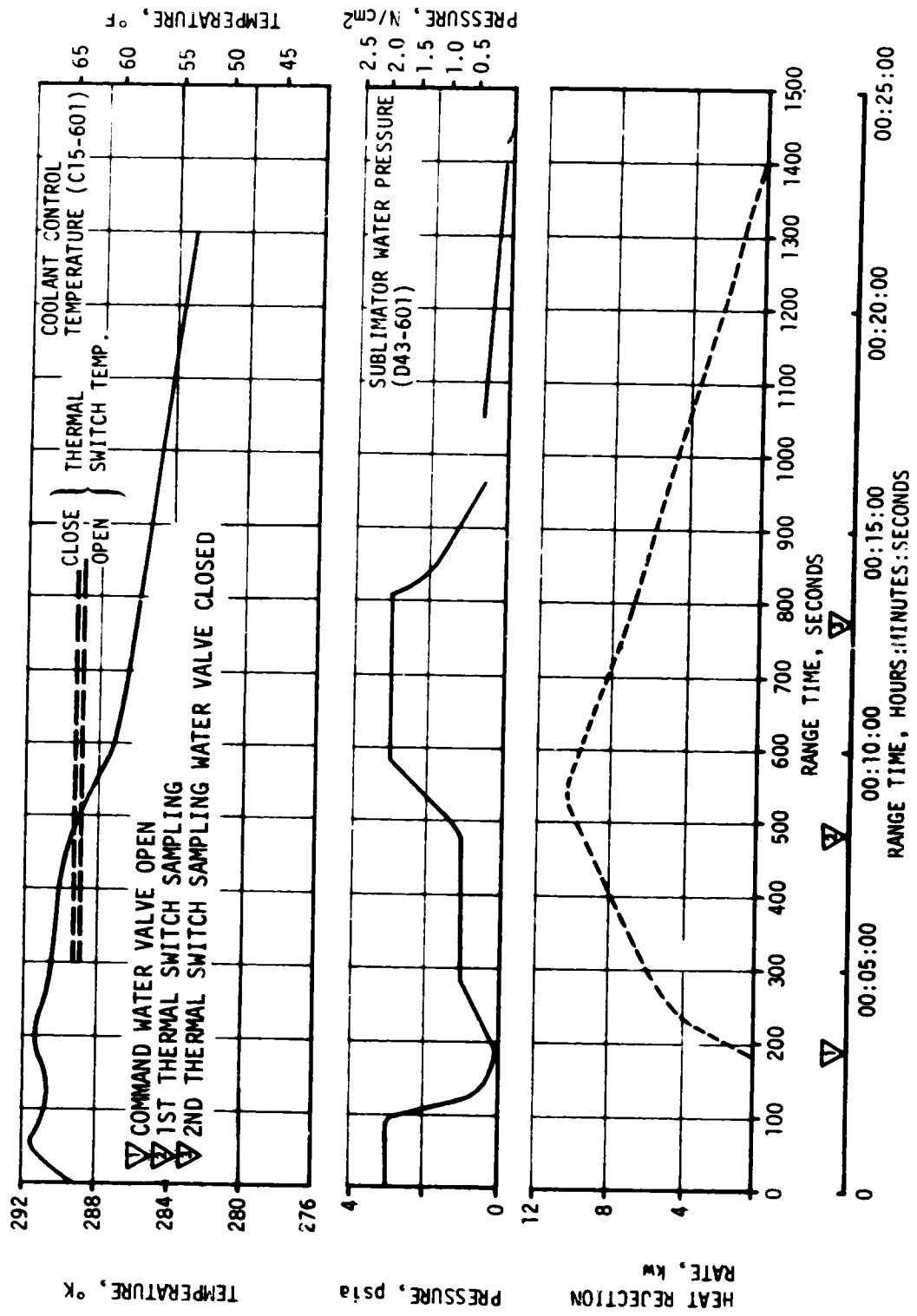


Figure 14-7. IU Sublimator Performance During Ascent

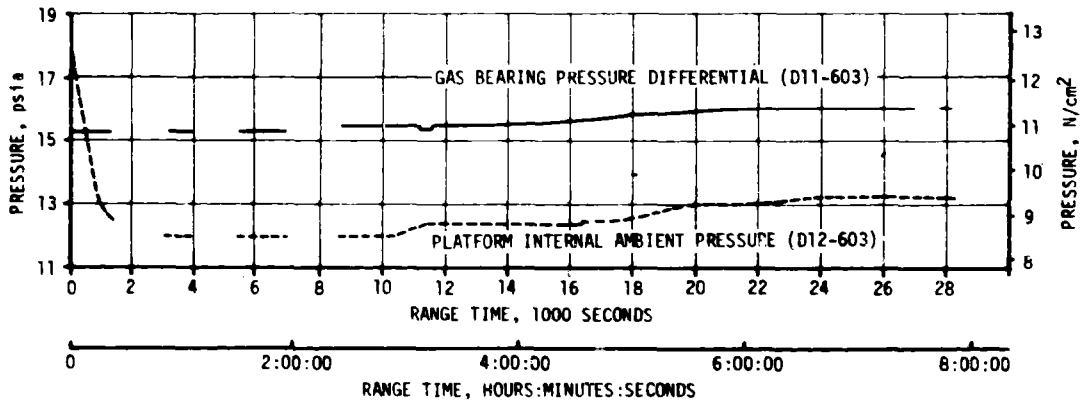


Figure 14-8. IU Inertial Platform GN<sub>2</sub> Pressures

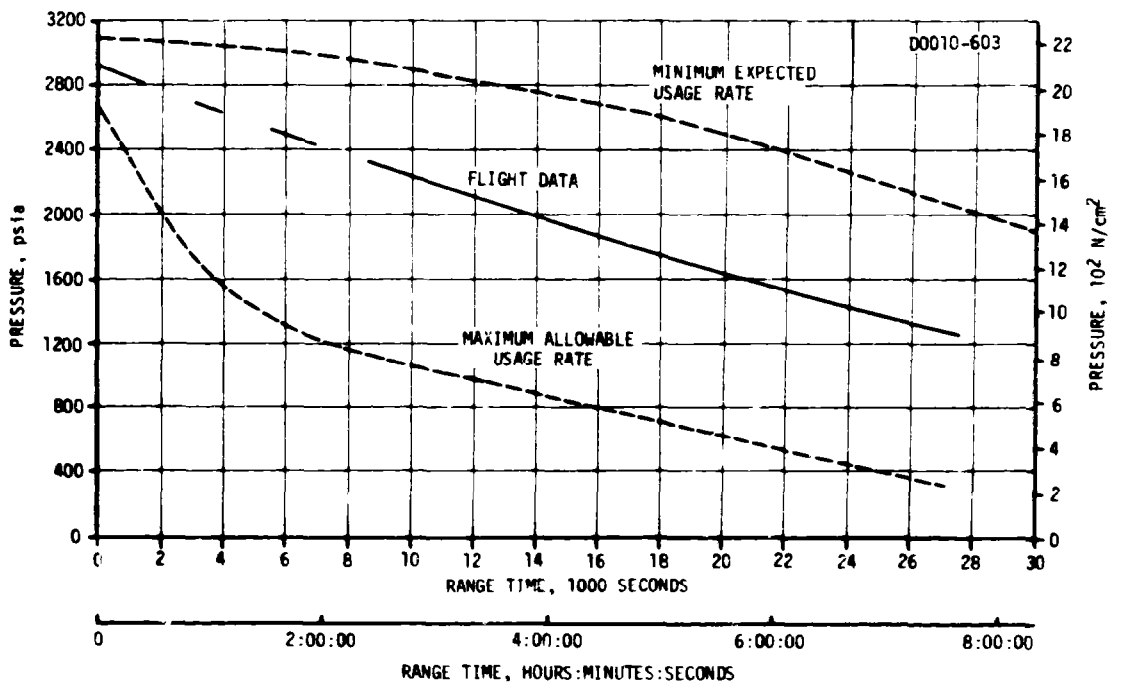


Figure 14-9. IU GBS GN<sub>2</sub> Sphere Pressure

## SECTION 15

### DATA SYSTEMS

#### 15.1 SUMMARY

All data systems performed satisfactorily throughout the flight. Flight measurements from onboard telemetry were 99.9 percent reliable.

Telemetry performance was normal except for noted problems. Radio Frequency (RF) propagation was satisfactory, though the usual problems due to flame effects and staging were experienced. Usable VHF data were received until 18,720 seconds (5:12:00). The Secure Range Safety Command Systems (SRSCS) on the S-IC, S-II, and S-IVB stages were ready to perform their functions properly, on command, if flight conditions during launch phase had required destruct. The system properly safed the S-IVB on a command transmitted from Bermuda (BDA) at 716.2 seconds. The performance of the Command and Communications System (CCS) was satisfactory from liftoff through the first part of lunar coast when the CCS downlink signal was lost. Usable CCS telemetry data were received to 27,643 seconds (7:40:43) at which time the telemetry subcarrier was inhibited. Madrid (MAD and MADW), Ascension (ACN), Goldstone (GDS), Bermuda (BDA) and Merritt Island Launch Area (MILA) were receiving CCS signal carrier at the abrupt loss of signal at 97,799 seconds (27:09:59). Good tracking data were received from the C-Band radar, with MILA indicating final Loss of Signal (LOS) at 38,837 seconds (10:47:17).

In general ground engineering camera coverage was good.

#### 15.2 VEHICLE MEASUREMENT EVALUATION

The AS-511 launch vehicle had 1347 measurements scheduled for flight; three measurements were waived prior to start of the automatic countdown sequence leaving 1344 measurements active for flight. Two measurements failed during flight resulting in an overall measurement system reliability of 99.9 percent.

A summary of measurement reliability is presented in Table 15-1 for the total vehicle and for each stage. The waived measurements, failed measurements, partially failed measurements, and questionable measurements are listed by stage in Tables 15-2, 15-3, and 15-4. None of these listed failures had any significant impact on postflight evaluation.

#### 15.3 AIRBORNE VHF TELEMETRY SYSTEMS EVALUATION

Performance of the eight VHF telemetry links provided good data from liftoff until the vehicle exceeded each subsystem's range limitations, however, data dropouts occurred as indicated in Table 15-5.

Table 15-1. AS-511 Measurement Summary

MEASUREMENT CATEGORY	S-IC STAGE	S-II STAGE	S-IVB STAGE	INSTRUMENT UNIT	TOTAL VEHICLE
Scheduled	293	552	275	227	1347
Waived	2	1	0	0	3
Failures	0	1	1	0	2
Partial Failures	3	4	5	0	12
Questionable	1	0	0	0	1
Reliability, Percent	100.0	99.8	99.6	100.0	99.9

Table 15-2. AS-511 Flight Measurements Waived Prior to Flight

MEASUREMENT NUMBER	MEASUREMENT TITLE	NATURE OF FAILURE	REMARKS
S-IC STAGE			
D119-101	Pressure, Differential, Engine Gimbal System Filter Manifold	Transducer output noisy and shifted in the negative direction.	Waiver I-8-511-215
D119-104	Pressure, Differential, Engine Gimbal System Filter Manifold	Transducer output shifted in the negative direction.	Waiver I-8-511-1
S-II STAGE			
D016-205	Pressure, E5 Start Tank	Low RACS failed to calibrate.	Waiver NR11-3

Table 15-3. AS-511 Measurement Malfunctions

MEASUREMENT NUMBER	MEASUREMENT TITLE	NATURE OF FAILURE	TIME OF FAILURE (RANGE TIME)	DURATION SATISFACTORY OPERATION	REMARKS
MEASUREMENT FAILURES, S-II STAGE					
E362-206	Longitudinal Vibration, LOX Sump/Prevalve	No response	Prior to Liftoff	0 seconds	Suspect coaxial cable open at charge amplifier input
MEASUREMENT FAILURES, S-IVB STAGE					
C0199-401	Temperature, Thrust Chamber Jacket	Improper response to temperature changes	560 seconds	Prior to 560 seconds	Suspect inadequate sensor-to-thrust chamber jacket thermal contact in flight environment
PARTIAL MEASUREMENT FAILURES, S-IC STAGE					
C003-101	Temperature, Turbine Manifold	Failed off scale high	-4.9 to -2.6 seconds -1.3 to -0.6 seconds 42.6 to 154 seconds	69.6 seconds	Probable cable connector problem
C003-104	Temperature, Turbine Manifold	Failed off scale high	30.2 seconds	50.2 seconds	Probable transducer failure
C003-105	Temperature, Turbine Manifold	Failed off scale high	106.7 to 141.6 seconds	149.1 seconds	Probable cable connector problem
PARTIAL MEASUREMENT FAILURES, S-II STAGE					
C003-203	Temperature, E3 Fuel Turbine Inlet	Failed off scale high	202 seconds	0 to 202 seconds	Suspect open in transducer circuit
C443-217	Temperature, LOX Tank Ullage	Improper response to temperature changes	208 seconds	Prior to 208 seconds	Failure mode unknown
C541-200	Temperature, Recirculation Battery 2	Failed off scale high	166 seconds	Prior to 166 seconds	Suspect open in signal return wire at sensor
M125-207	Voltage, Ignition DC Bus Voltage	Failed off scale low	170 seconds	Prior to 170 seconds	Cause unknown. See Section 11.3.1
PARTIAL MEASUREMENT FAILURES, S-IVB STAGE					
D0030-415	Pressure, Attitude Control, Chamber 2-1	Positive data drift	400 seconds	Prior to 400 seconds	Probable amplifier zero drift
D0073-415	Pressure, Oxidizer Supply Manifold, Module 2 (APS)	Exhibited a no-data period	4300 seconds to 9235 seconds	Prior to 4300 sec. after 9235 sec.	Probable transducer wiper open circuit
D0218-403	Pressure Differential, LH <sub>2</sub> Chilldown Pump	Negative data drift	850 seconds	Prior to 850 seconds	Probable amplifier zero drift
F0004-424	Flow Rate, LOX Circulation Pump	Intermittent response	Prior to 0 seconds	9090 to 9220 seconds	Intermittent operation of the frequency to DC converter
H0043-411	Frequency, 5V Excitation Module, Forward 1	Invalid frequency indication	9220 seconds	Prior to 9220 seconds	Probable failure of the frequency converter temperature compensation circuitry

Table 15-4. AS-511 Questionable Flight Measurements

MEASUREMENT NUMBER	MEASUREMENT TITLE	REASON QUESTIONED	REMARKS
QUESTIONABLE MEASUREMENTS, S-IC STAGE			
B003-118	Acoustic/Skin	Measurement lost high frequency content gradually and slowly recovered. Duration 40 to 100 seconds.	Cause unknown.

All inflight calibrations occurred as programmed and were within specifications.

Data degradation and dropouts were experienced at various times during launch and earth orbit as on previous flights, due to the attenuation of RF signals. Signal attenuation was caused by S-IC stage flame and retro-rockets, S-II stage ignition, interstage jettison, vehicle antenna nulls and multipath. As on previous flights data dropouts occurred during retro-rocket effects at S-IC/S-II separation lasting from 163.4 to 164.9 seconds. The S-II stage ignition effects at 166.8 to 172 seconds and the RF interference resulting when the S-IC/S-II interstage passed through the S-II stage flame at 195.0 seconds caused some signal degradation as on previous missions. Loss of this data, however, posed no problem since losses were of such short duration as to have little or no impact on flight analysis. RF signals were received from the S-IC stage until 415.3 seconds and from the S-II stage until 770 seconds.

The performance of S-IVB and IU VHF telemetry systems was normal during earth orbit, S-IVB second burn and final coast. Usable VHF telemetry data were received to 18,720 seconds (5:12:00). A summary of available VHF telemetry coverage showing Acquisition of Signal (AOS) and LOS for each station is shown in Figure 15-1.

#### 15.4 C-BAND RADAR SYSTEM EVALUATION

The C-Band radar performed satisfactorily during flight, although several of the ground stations experienced problems with their equipment which caused some loss of signal. No phase front disturbances were reported as occurred on previous missions.

The VAN FPS/16 radar and both BDA radars experienced signal fade and dropout near PCA (point of closest approach). These dropouts occurred because of the high azimuth rates required when the vehicle was overhead during first and second pass. When these stations attempted to reacquire the signal, they repeatedly acquired on side lobes and had to make several attempts before successfully acquiring the main lobe. MILA was the last station to maintain track and indicated final LOS at 38,837 seconds (10:47:17).

A summary of available C-Band radar coverage showing AOS and LOS for each

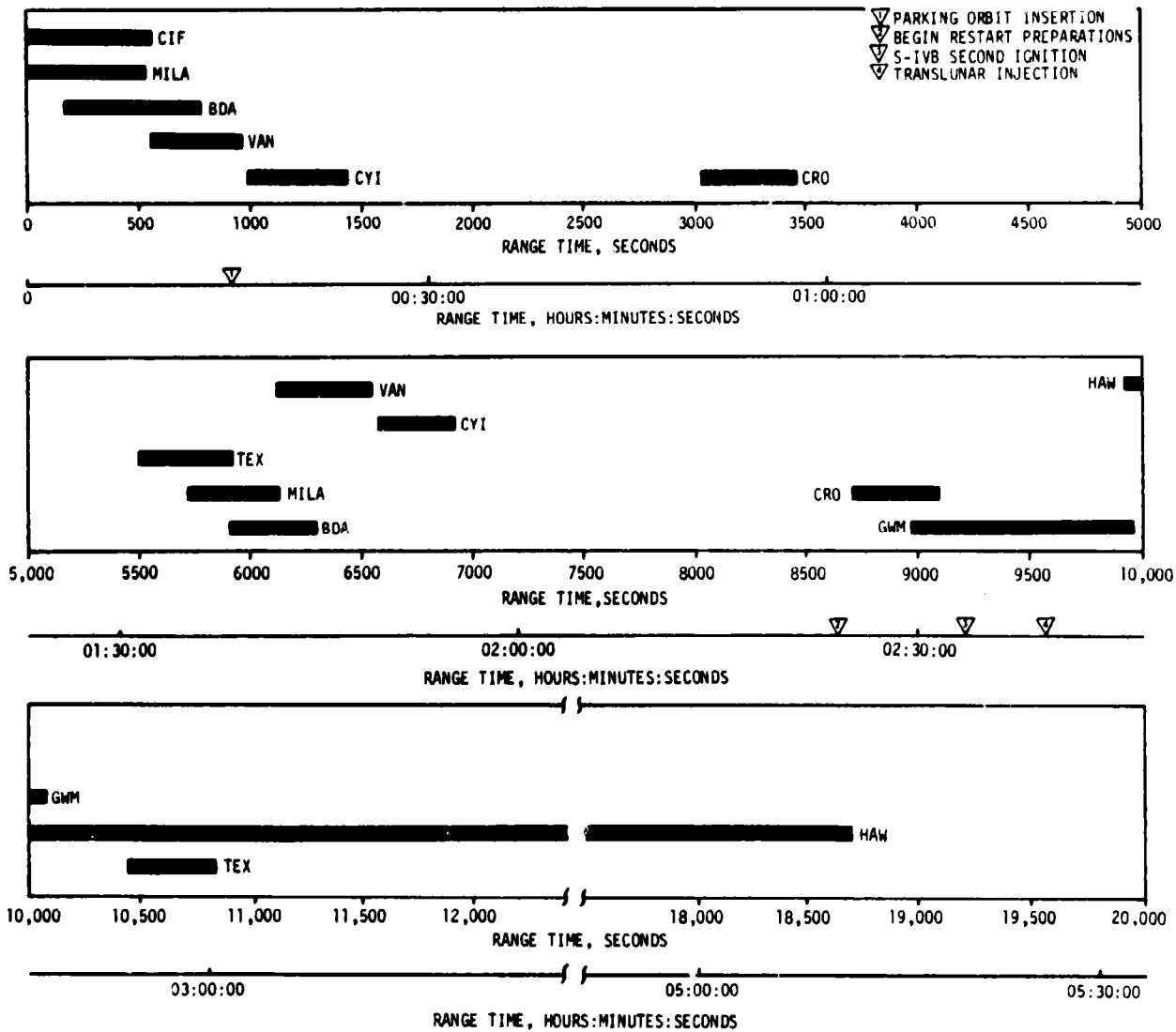


Figure 15-1. VHF Telemetry Coverage Summary



Table 15-5. AS-511 Launch Vehicle Telemetry Links

LINK	FREQUENCY (MHZ)	MODULATION	STAGE	FLIGHT PERIOD (RANGE TIME, SEC)	PERFORMANCE SUMMARY
AF-1	256.2	FM/FM	S-IC	0 to 415.3	Satisfactory
AP-1	244.3	PCM/FM	S-IC	0 to 415.3	Data Dropouts Range Time (sec) Duration (sec) 163.6 1.2
BF-1	241.5	FM/FM	S-II	0 to 770	Satisfactory
BF-2	234.0	FM/FM	S-II	0 to 770	Data Dropouts
BP-1	248.6	PCM/FM	S-II	0 to 770	Range Time (sec) Duration (sec) 163.7 1.2 195.7 1.2
CP-1	258.5	PCM/FM	S-IVB	0 to 16,345	Satisfactory Data Dropouts Range Time (sec) Duration (sec) 163.6 1.1 Intermittent Data 195.0 1.0
DF-1	250.7	FM/FM	IU	0 to 18,720	Satisfactory
DP-1	245.3	PCM/FM	IU	0 to 18,720	Data Dropouts
DP-1B (CCS)	2282.5	PCM/FM	IU	0 to 27,643	Range Time (sec) Duration (sec) 163.4 (DP-1) 0.9 195.0 (DP-1B) 1.0

station is shown in Figure 15-2.

## 15.5 SECURE RANGE SAFETY COMMAND SYSTEMS EVALUATION

Telemetered data indicated that the command antennas, receivers/decoders, Exploding Bridge Wire (EBW) networks, and destruct controllers on each powered stage functioned properly during flight. They were in the required state-of-readiness if flight conditions during the launch had required vehicle destruct. Since no arm/cutoff or destruct commands were required, all data except receiver signal strength remained unchanged during the flight. Power to the S-IVB stage range safety command systems was cut off at 716.2 seconds by ground command, thereby deactivating (safing) the systems.

## 15.6 COMMAND AND COMMUNICATION SYSTEM EVALUATION

### 15.6.1 Command Communication System Summary

Performance of the CCS was satisfactory from liftoff through the first part of Translunar Coast (TLC). At 27,643 seconds (7:40:43) the IU telemetry subcarrier oscillator was commanded off. The CCS signal carrier only was left on for positive tracking to lunar impact.

The Madrid and Goldstone 85-foot tracking antennas were able to track until approximately 27 hours 10 minutes when they suddenly lost track and were unable to reacquire lock-on. Several network stations including a 210-foot antenna at Parkes Observatory attempted the re-acquisition.

A summary of CCS coverage giving AOS and LOS for each station is shown in Figure 15-3.

### 15.6.2 CCS Performance

The CCS should operate through lunar impact. Loss of the CCS downlink signal occurred during TLC at 97,799 seconds (27:09:59). The reason for this loss of signal is unknown at this time and is still under investigation.

Unlike previous Saturn V missions, the CCS did not lose lock during S-IC/S-II separation. However, the dropout occurring on missions previous to AS-510, when the S-IC/S-II interstage passed through the S-II stage flame, did occur on this flight at 195 seconds.

During the earth orbital phase of the mission, three ground tracking stations experienced problems. Canary Island (CYI) had problems tracking because of failure of the antenna to move in the X-axis from 1101 to 1290 seconds. Honeysuckle (HSK) experienced a problem due to keyhole tracking starting at 3856 seconds. Goldstone (GDS) was able to track for only a short period of time at 5430 to 5464 seconds due to poor pointing data and terrain masking.

- ▽ PARKING ORBIT INSERTION
- ▽ BEGIN S-1VB RESTART PREPARATIONS
- ▽ S-1VB SECOND IGNITION
- ▽ TRANSLUNAR INSERTION

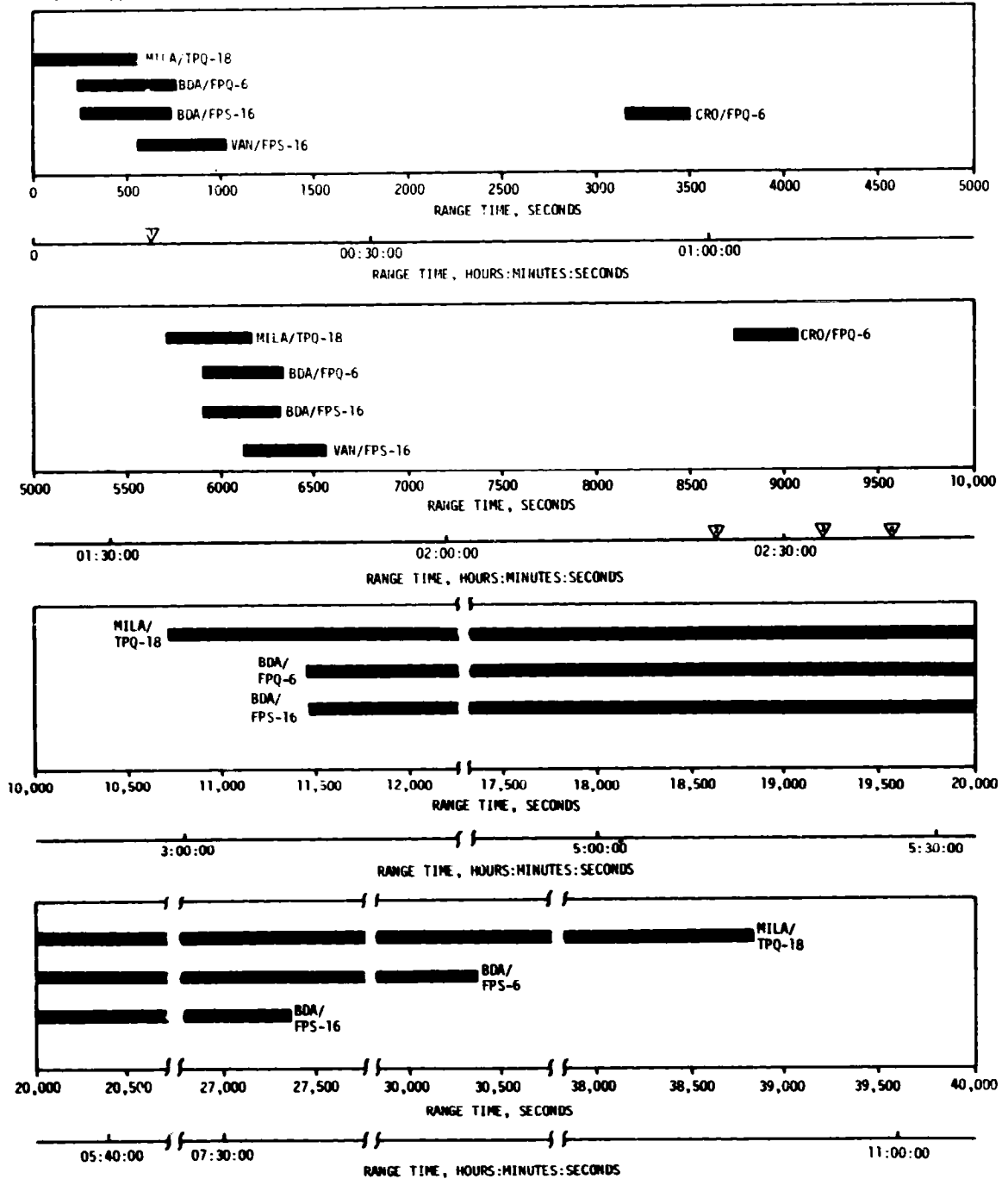


Figure 15-2. C-Band Radar Coverage Summary

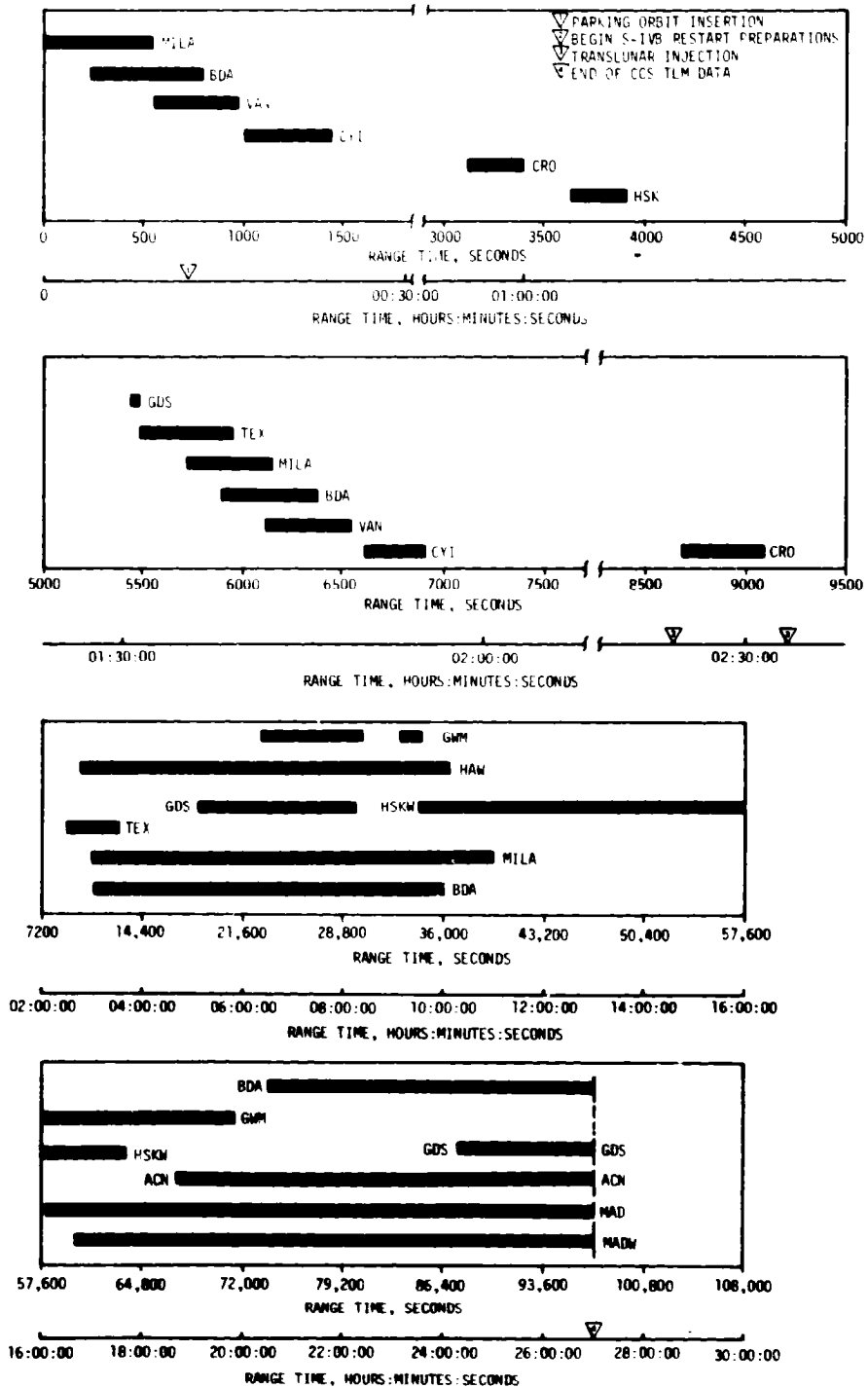


Figure 15-3. CCS Coverage Summary

During the Translunar Coast phase of the mission, numerous dropouts occurred at the 30-foot antenna USB sites starting at 16,380 seconds (4:33:00) and continuing until 20,249.5 seconds (5:37:29.5). At this time the CCS was commanded from OMNI to low gain directional antenna.

The performance of the command section of the CCS was satisfactory. All commands received by the onboard equipment were accepted. A list of commands initiated at MCC Houston and the number of words transmitted in each command is shown in Table 15-6.

At 5:27:03, the mode word of the "lunar impact" command (APS-1) was transmitted from MILA and was accepted by the onboard equipment. However, because of noisy telemetry, the verification pulses were not recognized by MILA.

A terminate command was sent three times at 5:27:48 to reset the computer and each time the subcarrier was out-of-lock. The terminate command was transmitted again at 5:30:16 in the Message Acceptance Pulse (MAP) override mode and was accepted and executed by the onboard equipment.

The MAP override mode was used for transmitting all commands from 5:30:16 through 5:32:08 because of noisy telemetry during that time period.

The command to switch the CCS antenna to low gain at 5:37:28 was sent in the MAP mode, accepted by the vehicle and executed. However, the transmitting ground station did not receive the verification pulses and the command was retransmitted. The command was verified on this transmission.

### 15.6.3 CCS Signal Loss

The only flight hardware related problem encountered during this flight was the premature loss of CCS downlink signal. Investigation of this problem is in process.

Figure 15-4 shows the CCS downlink signal strength spikes as seen at the Madrid Wing and Goldstone stations. The figure also includes a plot of the last CCS signal received at 97,799 seconds (27:09:59).

Repeated efforts by at least four ground stations to acquire the CCS signal were unsuccessful. Therefore, it is assumed the CCS downlink flight hardware was not operational.

There was no telemetry data available for 19 hours 29 minutes 16 seconds prior to the downlink signal dropout. However, all available telemetry data for the measurements associated with the CCS were reviewed for the period prior to disabling the TM subcarrier and no abnormal readings were found.

The most probable cause of the CCS signal loss was failure of the CCS transponder.

Table 15-6. Command and Communication System Command History, AS-511

RANGE TIME		TRANS- MITTING STA.	COMMAND	NO. OF WORDS TRANS- MITTED	REMARKS
SECONDS	HRS:MIN:SECS				
15001	4:10:01	GDS	Evasive Yaw Maneuver	1	
15487	4:18:07	GDS	TB8 Initiate	1	Accepted
16260	4:31:00	MILA	LOX Dump Attitude #1	8	Accepted
16268	4:31:08	MILA	LOX Dump Attitude #2	8	Accepted
19623	5:27:03	MILA	Lunar Impact APS 1	1	*Accepted
19668	5:27:48	MILA	Terminate	4	Not Received
19816	5:30:16	MILA	Terminate (MAP Override)	1	Accepted
19837	5:30:37	MILA	Lunar Impact #1 (MAP Override)	8	Accepted
19850	5:30:50	MILA	Lunar Impact #2 (MAP Override)	8	Accepted
19928	5:32:08	MILA	Single Word Dump Group (MAP Override)	28	Accepted
20248	5:37:28	MILA	Switch Antennas to Low Gain	2	Accepted
21305	5:55:05	MILA	3-Axis Tumble	8	Accepted
21322	5:55:22	MILA	FCC Power Off A	3	Accepted
21335	5:56:35	MILA	FCC Power Off B	3	Accepted
21474	5:57:54	MILA	Switch Antennas to Omni	2	Accepted
27643	7:40:43	GDS	TM Subcarrier Off	3	Accepted

\* Command retransmitted three additional times because signal verification pulse not received by ground station.

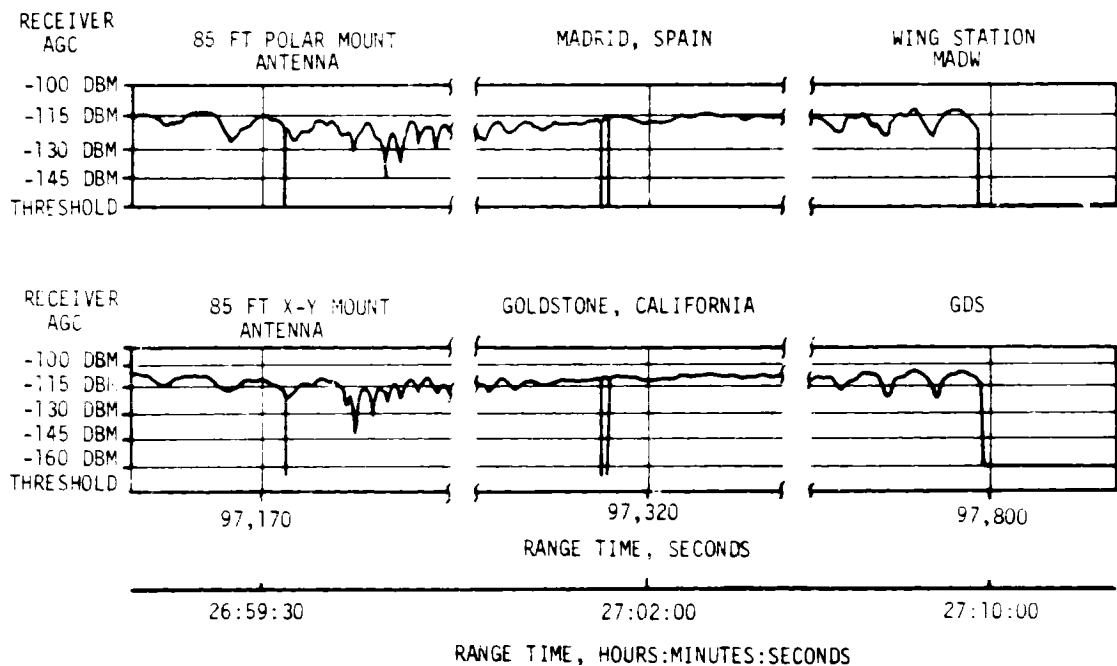


Figure 15-4. CCS Down Link Signal Strength Indications

## 15.7 GROUND ENGINEERING CAMERAS

In general, ground camera coverage was good. Forty-two items were received from KSC and evaluated. Three items did not run, seven items had unusable timing, and two items stopped at ignition. As a result of these 12 failures, system efficiency was 71 percent. Tracking coverage was good with all cameras acquiring data. However, complete engineering analysis from the film could not be accomplished due to cloud cover at Melbourne Beach and due to timing loss at New Smyrna Beach.

## SECTION 16

### MASS CHARACTERISTICS

#### 16.1 SUMMARY

Total vehicle mass, determined from post-flight analysis, was within 0.36 percent of prediction from ground ignition through S-IVB stage final shutdown. This small variation indicates that hardware weights, propellant loads, and propellant utilization were close to predicted values during flight.

#### 16.2 MASS EVALUATION

Post-flight mass characteristics are compared with final predicted mass characteristics (MSFC Memorandum S&E-ASTN-SAE-72-11) and the operational trajectory (MSFC Memorandum S&E-AERO-MFT-72-72).

The post-flight mass characteristics were determined from an analysis of all available actual and reconstructed data from S-IC ignition through S-IVB second burn cutoff. Dry weights of the launch vehicle are based on actual stage weighings and evaluation of the weight and balance log books (MSFC Form 998). Propellant loading and utilization was evaluated from propulsion system performance reconstructions. Spacecraft data were obtained from the Manned Spacecraft Center (MSC).

Differences in dry weights of the inert stages and the loaded spacecraft were all within 0.54 percent of predicted, which was well within acceptable limits.

During S-IC burn phase, the total vehicle mass was less than predicted by 525 kilograms (1157 lbm) (0.02 percent) at ignition, and greater than predicted by 462 kilograms (1018 lbm) (0.06 percent) at S-IC/S-II separation. These differences are respectively attributed to: less than predicted S-IC dry weight and propellant loading at ignition and less than predicted upper stage mass; shorter than predicted S-IC burn resulting in higher residuals. S-IC burn phase total vehicle mass is shown in Tables 16-1 and 16-2.

During S-II burn phase, the total vehicle mass was less than predicted by 318 kilograms (702 lbm) (0.04 percent) at ignition, and greater than predicted by 6 kilograms (15 lbm) (0.003 percent) at S-II/S-IVB separation. These differences are due primarily to a less than predicted LOX loading and a greater than predicted total S-IVB stage mass.

Total vehicle mass for the S-II burn phase is shown in Tables 16-3 and 16-4.



Total vehicle mass during both S-IVB burn phases, as shown in Tables 16-5 through 16-8, was within 0.07 percent of the predicted values. A difference of 119 kilograms (268 lbm) (0.07 percent) greater than predicted at first burn ignition was due largely to a greater than predicted propellant loading. The difference at completion of second burn was 55 kilograms (120 lbm) (0.08 percent) less than predicted resulting from a less than predicted spacecraft weight.

A summary of mass utilization and loss, both actual and predicted, from S-IC stage ignition through spacecraft separation is presented in Table 16-9. A comparison of actual and predicted mass, center of gravity, and moment of inertia is shown in Table 16-10.

Table 16-1. Total Vehicle Mass - S-IC Burn Phase - Kilograms

EVENTS	GROUND IGNITION		HOLDDOWN ARM RELEASE		CENTER ENGINE CUTOFF		OUTBOARD ENGINE CUTOFF		S-IC/S-II SEPARATION	
	PRED	ACT	PRED	ACT	PRED	ACT	PRED	ACT	PRED	ACT
RANGE TIME--SEC	-6.40	-6.40	0.30	0.30	137.96	137.85	162.09	161.76	163.60	163.50
DRY STAGE	130641.	130568.	130641.	130568.	130641.	130568.	130641.	130568.	130641.	130568.
LOX IN TANK	148059.	1480826.	1449354.	1442768.	174720.	171013.	1134.	909.	788.	692.
LOX BELOW TANK	21115.	21120.	21875.	21980.	21859.	21864.	13324.	14524.	13194.	12510.
LOX ULLAGE GAS	190.	190.	239.	224.	2963.	2962.	3435.	3421.	3442.	3427.
FUEL IN TANK	649317.	648798.	639067.	635580.	84683.	84658.	6859.	6362.	5504.	7140.
FUEL BELOW TANK	4313.	4326.	5996.	6009.	5996.	6009.	5958.	5971.	5958.	5971.
FUEL ULLAGE GAS	31.	31.	31.	35.	211.	210.	238.	238.	239.	239.
H2 PURGE GAS	36.	36.	36.	36.	19.	19.	19.	19.	19.	19.
HELIUM IN BOTTLE	288.	288.	288.	284.	109.	109.	82.	81.	80.	80.
FROST	639.	639.	639.	635.	340.	340.	340.	340.	340.	340.
RETROCKET PROP	1026.	1026.	1026.	1026.	1026.	1026.	1026.	1026.	1026.	1026.
OTHER	239.	239.	239.	239.	239.	239.	239.	239.	239.	239.
TOTAL STAGE	2288295.	2288089.	2249428.	2239291.	422811.	419224.	165295.	165705.	161476.	162256.
TOTAL S-IC/S-II IS	4579.	4577.	4579.	4577.	4579.	4577.	4579.	4577.	4579.	4577.
TOTAL S-II STAGE	493986.	493536.	493986.	493536.	493765.	493315.	493765.	493315.	493765.	493315.
TOT S-II/S-IVB IS	3656.	3653.	3656.	3653.	3656.	3653.	3656.	3653.	3656.	3653.
TOTAL S-IVB STAGE	120395.	120393.	120395.	120393.	120304.	120492.	120304.	120492.	120304.	120492.
TOTAL INSTRU UNIT	2053.	2042.	2053.	2042.	2053.	2042.	2053.	2042.	2053.	2042.
TOTAL SPACECRAFT	52798.	52759.	52798.	52759.	52798.	52759.	52798.	52759.	52798.	52759.
TOTAL UPPERSTAGE	677470.	677152.	677470.	677152.	677158.	676840.	677158.	676840.	677158.	676840.
TOTAL VEHICLE	2965766.	2965241.	2926899.	2916643.	1099970.	1098064.	842454.	842549.	838635.	839097.

Table 16-2. Total Vehicle Mass - S-IC Burn Phase - Pounds

EVENTS	GROUND IGNITION		HOLDDOWN ARM RELEASE		CENTER ENGINE CUTOFF		OUTBOARD ENGINE CUTOFF		S-IC/S-II SEPARATION	
	PRED	ACT	PRED	ACT	PRED	ACT	PRED	ACT	PRED	ACT
RANGE TIME--SEC	-6.40	-6.40	0.30	0.30	137.96	137.85	162.09	161.76	163.60	163.50
DRY STAGE	288015.	287855.	288015.	287855.	288015.	287855.	288015.	287855.	288015.	287855.
LOX IN TANK	3263854.	3264664.	3195279.	3180760.	385193.	377024.	2900.	2006.	1737.	1527.
LOX BELOW TANK	46552.	46562.	48227.	48237.	48192.	48201.	33783.	32022.	29089.	27880.
LOX ULLAGE GAS	419.	419.	520.	499.	634.	630.	7574.	7543.	7590.	7555.
FUEL IN TANK	1431500.	1430356.	1408902.	1401215.	186695.	18708.	15112.	16496.	12139.	15741.
FUEL BELOW TANK	9509.	9538.	13219.	13246.	13219.	13248.	13136.	13169.	13136.	13169.
FUEL ULLAGE GAS	70.	69.	70.	77.	465.	463.	525.	525.	528.	529.
H2 PURGE GAS	80.	80.	80.	80.	43.	43.	43.	43.	43.	43.
HELIUM IN BOTTLE	636.	636.	636.	627.	240.	242.	181.	180.	177.	176.
FROST	1400.	1400.	1400.	1400.	750.	750.	750.	750.	750.	750.
RETROCKET PROP	2264.	2264.	2264.	2264.	2264.	2264.	2264.	2264.	2264.	2264.
OTHER	528.	528.	528.	528.	528.	528.	528.	528.	528.	528.
TOTAL STAGE	5044826.	5044373.	4959142.	4936793.	932140.	924231.	364414.	365318.	359995.	357715.
TOTAL S-IC/S-II IS	10097.	10091.	10097.	10091.	10097.	10091.	10097.	10091.	10097.	10091.
TOTAL S-II STAGE	1089054.	1088062.	1089054.	1088062.	1089566.	1087574.	1089566.	1087574.	1089566.	1087574.
TOT S-II/S-IVB IS	8062.	8055.	8062.	8055.	8062.	8055.	8062.	8055.	8062.	8055.
TOTAL S-IVB STAGE	265425.	265041.	265425.	265041.	265225.	265041.	265225.	265041.	265225.	265041.
TOTAL INSTRU UNIT	4527.	4502.	4527.	4502.	4527.	4502.	4527.	4502.	4527.	4502.
TOTAL SPACECRAFT	116401.	116314.	116401.	116314.	116401.	116314.	116401.	116314.	116401.	116314.
TOTAL UPPERSTAGE	1493967.	1492865.	1493967.	1492865.	1492879.	1492177.	1492879.	1492177.	1492879.	1492177.
TOTAL VEHICLE	6536395.	6537238.	6452709.	6429658.	241020.	2416409.	1897293.	1857495.	1848874.	1849897.

Table 16-3. Total Vehicle Mass - S-II Burn Phase - Kilograms

EVENTS	S-IC IGNITION		S-II IGNITION		S-II MAINSTAGE		S-II ENGINE CUTOFF		S-II/S-IVB SEPARATION	
	PRED	ACT	PRED	ACT	PRED	ACT	PRED	ACT	PRED	ACT
RANGE TIME--SEC	-6.40	-6.40	165.90	165.20	167.70	167.40	559.21	559.54	560.20	560.60
S-IC/S-II SMALL IS	616.	616.	0.	0.	0.	0.				
S-IC/S-II LARGE IS	3963.	3960.	3963.	3960.	3963.	3960.				
S-IC/S-II PROPELLANT	0.	0.	0.	0.	0.	0.				
TOTAL S-IC/S-II IS	4579.	4577.	3963.	3960.	3963.	3960.				
DRY STAGE	36458.	36451.	36458.	36451.	36458.	36451.	36458.	36451.	36458.	36451.
LOX IN TANK	383563.	383073.	383563.	383073.	383073.	383112.	382622.	637.	637.	541.
LOX BELOW TANK	737.	737.	737.	737.	800.	800.	787.	787.	787.	787.
LOX ULLAGE GAS	136.	136.	136.	136.	136.	139.	1865.	1896.	1891.	1900.
FUEL IN TANK	72672.	72719.	72666.	72713.	72454.	72501.	1293.	1184.	1238.	1144.
FUEL BELOW TANK	104.	104.	110.	111.	127.	127.	123.	123.	123.	123.
FUEL ULLAGE GAS	43.	43.	44.	44.	45.	45.	780.	758.	782.	761.
INSULATION PURGE GAS	17.	17.	0.	0.	0.	0.				
FROST	204.	204.	0.	0.	0.	0.				
START TANK	13.	13.	13.	13.	2.	2.	2.	2.	2.	2.
OTHER	34.	34.	34.	34.	34.	34.	34.	34.	34.	34.
TOTAL S-II STAGE	493986.	493536.	493765.	493315.	493174.	492724.	42002.	41877.	41859.	41748.
TOT S-II/S-IVB IS	3656.	3653.	3656.	3653.	3656.	3653.	3656.	3653.	3656.	3653.
TOTAL S-IVB STAGE	120394.	120583.	120304.	120492.	120304.	120492.	120304.	120492.	120302.	120490.
TOTAL IU	2053.	2042.	2053.	2042.	2053.	2042.	2053.	2042.	2053.	2042.
TOTAL SPACECRAFT	52798.	52759.	52798.	52759.	52798.	52759.	48656.	48601.	48656.	48601.
TOTAL UPPER STAGE	178903.	179038.	178813.	178947.	178813.	178947.	174671.	174789.	174669.	174787.
TOTAL VEHICLE	677470.	677152.	676541.	676223.	675950.	675632.	216674.	216666.	216529.	216535.

Table 16-4. Total Vehicle Mass - S-II Burn Phase - Pounds

EVENTS	S-IC IGNITION		S-II IGNITION		S-II MAINSTAGE		S-II ENGINE CUTOFF		S-II/S-IVB SEPARATION	
	PRED	ACT	PRED	ACT	PRED	ACT	PRED	ACT	PRED	ACT
RANGE TIME--SEC	-6.40	-6.40	165.90	165.20	167.70	167.40	559.21	559.54	560.20	560.60
S-IC/S-II SMALL IS	1360.	1359.	0.	0.	0.	0.				
S-IC/S-II LARGE IS	8737.	8732.	8737.	8732.	8737.	8732.				
S-IC/S-II PROPELLANT	0.	0.	0.	0.	0.	0.				
TOTAL S-IC/S-II IS	10097.	10091.	8737.	8732.	8737.	8732.				
DRY STAGE	80377.	80362.	80377.	80362.	80377.	80362.	80377.	80362.	80377.	80362.
LOX IN TANK	845613.	844532.	845613.	844532.	844617.	843537.	1404.	1405.	1193.	1196.
LOX BELOW TANK	1625.	1625.	1624.	1624.	1764.	1764.	1736.	1736.	1736.	1736.
LOX ULLAGE GAS	301.	301.	301.	301.	307.	307.	4157.	4181.	4169.	4190.
FUEL IN TANK	160216.	160320.	160202.	160306.	159734.	159838.	2851.	2612.	2730.	2524.
FUEL BELOW TANK	231.	231.	244.	244.	282.	282.	272.	272.	272.	272.
FUEL ULLAGE GAS	96.	96.	97.	97.	99.	99.	1720.	1673.	1725.	1678.
INSULATION PURGE GAS	38.	38.	0.	0.	0.	0.				
FROST	450.	450.	0.	0.	0.	0.				
START TANK	30.	30.	30.	30.	5.	5.	5.	5.	5.	5.
OTHER	76.	76.	76.	76.	76.	76.	76.	76.	76.	76.
TOTAL S-II STAGE	1089054.	1088062.	1088566.	1087574.	1087262.	1086271.	92600.	92323.	92285.	92039.
TOT S-II/S-IVB IS	8062.	8055.	8062.	8055.	8062.	8055.	8062.	8055.	8062.	8055.
TOTAL S-IVB STAGE	265425.	265841.	265225.	265641.	265225.	265641.	265225.	265641.	265220.	265636.
TOTAL IU	4527.	4502.	4527.	4502.	4527.	4502.	4527.	4502.	4527.	4502.
TOTAL SPACECRAFT	116401.	116314.	116401.	116314.	116401.	116314.	107270.	107147.	107270.	107147.
TOTAL UPPER STAGE	394419.	394712.	394215.	394512.	394215.	394512.	385084.	385345.	385079.	385340.
TOTAL VEHICLE	1493967.	1492888.	1491519.	1490818.	1491215.	1489515.	477685.	477668.	477384.	477379.

Table 16-5. Total Vehicle Mass - S-IVB First Burn Phase - Kilograms

EVENTS	S-IC IGNITION		S-IVB IGNITION		S-IVB MAINSTAGE		S-IVB ENGINE CUTOFF		S-IVB END DECAY	
	PRED	ACT	PRED	ACT	PRED	ACT	PRED	ACT	PRED	ACT
RANGE TIME--SEC	-6.40	-6.40	963.30	963.60	965.80	966.10	705.48	706.21	705.70	706.40
DRY STAGE	11377.	11384.	11354.	11361.	11354.	11361.	11293.	11300.	11293.	11300.
LOX IN TANK	88284.	88452.	88282.	88452.	88154.	88223.	82689.	82840.	82657.	82721.
LOX BELOW TANK	166.	166.	166.	166.	166.	166.	166.	166.	166.	166.
LOX ULLAGE GAS	11.	12.	12.	12.	14.	14.	92.	93.	92.	94.
FUEL IN TANK	19809.	19815.	19804.	19808.	19755.	19761.	14576.	14528.	14565.	14517.
FUEL BELOW TANK	21.	19.	26.	23.	26.	23.	26.	23.	26.	23.
FUEL ULLAGE GAS	17.	18.	17.	16.	17.	17.	53.	57.	53.	57.
ULLAGE ROCKET PROP	53.	53.	9.	9.						
APS PROPELLANT	285.	299.	285.	299.	285.	299.	283.	298.	283.	298.
HELIUM IN BOTTLES	204.	197.	203.	197.	203.	197.	186.	174.	184.	174.
FROST	136.	136.	45.	45.	45.	45.	45.	45.	45.	45.
START TANK GAS	2.	2.	2.	2.	0.	0.	3.	2.	3.	2.
OTHER	25.	25.	25.	25.	25.	25.	25.	25.	25.	25.
TOTAL S-IVB STAGE	120395.	120583.	120237.	120422.	120083.	120250.	89454.	89560.	89411.	89432.
TOTAL IU	2053.	2042.	2053.	2042.	2053.	2042.	2053.	2042.	2053.	2042.
TOTAL SPACECRAFT	48656.	48601.	48656.	48601.	48656.	48601.	48656.	48601.	48656.	48601.
TOTAL UPPERSTAGE	90710.	90643.	90710.	90643.	90710.	90643.	90710.	90643.	90710.	90643.
TOTAL VEHICLE	171105.	171226.	170947.	171066.	170773.	170893.	140164.	140203.	140122.	140075.

Table 16-6. Total Vehicle Mass - S-IVB First Burn Phase - Pounds Mass

EVENTS	S-IC IGNITION		S-IVB IGNITION		S-IVB MAINSTAGE		S-IVB ENGINE CUTOFF		S-IVB END DECAY	
	PRED	ACT	PRED	ACT	PRED	ACT	PRED	ACT	PRED	ACT
RANGE TIME--SEC	-6.40	-6.40	963.30	963.60	965.80	966.10	705.48	706.21	705.70	706.40
DRY STAGE	25084.	25099.	25033.	25048.	25033.	25048.	24898.	24913.	24898.	24913.
LOX IN TANK	194633.	195005.	194630.	195005.	194366.	194719.	138206.	138540.	138136.	138278.
LOX BELOW TANK	367.	367.	367.	367.	397.	397.	397.	397.	397.	397.
LOX ULLAGE GAS	25.	28.	28.	28.	31.	31.	203.	185.	203.	186.
FUEL IN TANK	43672.	43685.	43660.	43670.	43553.	43567.	32136.	32029.	32112.	32006.
FUEL BELOW TANK	48.	42.	58.	52.	58.	52.	58.	52.	58.	52.
FUEL ULLAGE GAS	37.	40.	37.	37.	38.	39.	118.	126.	118.	127.
ULLAGE ROCKET PROP	118.	117.	22.	22.						
APS PROPELLANT	630.	661.	630.	661.	630.	661.	626.	658.	626.	658.
HELIUM IN BOTTLES	450.	435.	449.	435.	448.	435.	406.	385.	406.	385.
FROST	300.	300.	100.	100.	100.	100.	100.	100.	100.	100.
START TANK GAS	5.	5.	5.	5.	1.	1.	7.	5.	7.	5.
OTHER	56.	57.	56.	57.	56.	57.	56.	57.	56.	57.
TOTAL S-IVB STAGE	265425.	265841.	265077.	265487.	264494.	265107.	197213.	197447.	197119.	197164.
TOTAL IU	4527.	4502.	4527.	4502.	4527.	4502.	4527.	4502.	4527.	4502.
TOTAL SPACECRAFT	107270.	107147.	107270.	107147.	107270.	107147.	107270.	107147.	107270.	107147.
TOTAL UPPERSTAGE	111797.	111649.	111797.	111649.	111797.	111649.	111797.	111649.	111797.	111649.
TOTAL VEHICLE	377222.	377444.	376874.	377136.	376491.	376756.	309010.	309096.	308916.	308813.

Table 16-7. Total Vehicle Mass - S-IVB Second Burn Phase - Kilograms

EVENTS	S-IVB IGNITION		S-IVB MAINSTAGE		S-IVB ENGINE CUTOFF		S-IVB END DECAY		SPACECRAFT SEPARATION	
	PRED	ACT	PRED	ACT	PRED	ACT	PRED	ACT	PRED	ACT
RANGE TIME--SEC	9215.90	9216.50	9218.00	9219.00	9560.21	9558.42	9560.40	9558.60	14359.80	14440.00
DRY STAGE	11293.	11300.	11293.	11300.	11293.	11300.	11293.	11300.	11293.	11300.
LOX IN TANK	62620.	62670.	62494.	62543.	1665.	1574.	1632.	1542.	1960.	1469.
LOX BELOW TANK	166.	166.	180.	180.	180.	180.	180.	180.	166.	166.
LOX ULLAGE GAS	111.	98.	111.	99.	185.	200.	181.	200.	190.	184.
FUEL IN TANK	13575.	13569.	13525.	13522.	922.	980.	909.	969.	576.	577.
FUEL BELOW TANK	26.	23.	26.	23.	26.	23.	26.	23.	21.	17.
FUEL ULLAGE GAS	131.	184.	132.	184.	247.	269.	244.	270.	87.	116.
APS PROPELLANT	238.	246.	238.	246.	236.	246.	236.	246.	212.	229.
HELIUM IN BOTTLES	167.	162.	167.	161.	108.	102.	108.	102.	108.	30.
FROST	45.	45.	45.	45.	45.	45.	45.	45.	45.	45.
START TANK GAS	2.	2.	0.	0.	3.	2.	3.	2.	3.	0.
OTHER	25.	25.	25.	25.	25.	25.	25.	25.	25.	25.
TOTAL S-IVB STAGE	88404.	88495.	88240.	88334.	14939.	14951.	14887.	14909.	14292.	14161.
TOTAL IU	2053.	2042.	2053.	2042.	2053.	2042.	2053.	2042.	2053.	2042.
TOTAL SPACECRAFT	48656.	48601.	48656.	48601.	48656.	48601.	48656.	48601.	625.	625.
TOTAL UPPERSTAGE	50710.	50643.	50710.	50643.	50710.	50643.	50710.	50643.	2679.	2668.
TOTAL VEHICLE	139114.	139139.	138990.	138978.	65649.	65594.	65598.	65552.	16971.	16829.

Table 16-8. Total Vehicle Mass - S-IVB Second Burn Phase - Pounds Mass

EVENTS	S-IVB IGNITION		S-IVB MAINSTAGE		S-IVB ENGINE CUTOFF		S-IVB END DECAY		SPACECRAFT SEPARATION	
	PRED	ACT	PRED	ACT	PRED	ACT	PRED	ACT	PRED	ACT
RANGE TIME--SEC	9215.90	9216.50	9218.00	9219.00	9560.21	9558.42	9560.40	9558.60	14359.80	14440.00
DRY STAGE	24898.	24913.	24898.	24913.	24898.	24913.	24898.	24913.	24898.	24913.
LOX IN TANK	138054.	138169.	137776.	137885.	3671.	3472.	3600.	3400.	3441.	3230.
LOX BELOW TANK	367.	367.	397.	397.	397.	397.	397.	397.	367.	367.
LOX ULLAGE GAS	244.	217.	245.	220.	408.	441.	401.	442.	420.	406.
FUEL IN TANK	29929.	29916.	29819.	29813.	2033.	2161.	2005.	2138.	1270.	1273.
FUEL BELOW TANK	58.	52.	58.	52.	58.	52.	58.	52.	48.	42.
FUEL ULLAGE GAS	290.	407.	291.	407.	545.	595.	538.	596.	193.	257.
APS PROPELLANT	526.	543.	526.	543.	522.	543.	522.	543.	469.	506.
HELIUM IN BOTTLES	369.	358.	368.	357.	240.	227.	240.	226.	240.	68.
FROST	100.	100.	100.	100.	100.	100.	100.	100.	100.	100.
START TANK GAS	5.	5.	1.	1.	7.	5.	7.	5.	7.	1.
OTHER	56.	57.	56.	57.	56.	57.	56.	57.	56.	57.
TOTAL S-IVB STAGE	194898.	195100.	194537.	194745.	32935.	32963.	32822.	32869.	31509.	31220.
TOTAL IU	4527.	4502.	4527.	4502.	4527.	4502.	4527.	4502.	4527.	4502.
TOTAL SPACECRAFT	107270.	107147.	107270.	107147.	107270.	107147.	107270.	107147.	1380.	1380.
TOTAL UPPERSTAGE	111797.	111649.	111797.	111649.	111797.	111649.	111797.	111649.	5907.	5882.
TOTAL VEHICLE	306695.	306749.	306336.	306394.	144732.	144612.	144619.	144518.	37416.	37102.

Table 16-9. Flight Sequence Mass Summary

MASS HISTORY	PREDICTED		ACTUAL	
	KG	LBM	KG	LBM
S-IC STAGE, TOTAL	2288294.	5044828.	2288088.	5044373.
S-IC/S-II IS, TOTAL	4579.	10097.	4577.	10091.
S-II STAGE, TOTAL	493986.	1089054.	493536.	1088062.
S-II/S-IVB IS, TOTAL	3656.	8062.	3653.	8055.
S-IVB STAGE, TOTAL	120394.	265425.	120583.	265841.
INSTRUMENT UNIT	2053.	4527.	2042.	4502.
SPACECRAFT, TOTAL	52798.	116401.	52759.	116314.
1ST FLT STG AT IGN	2965765.	6538395.	2965240.	6537238.
THRUST BUILDUP	-38866.	-85686.	-48797.	-107580.
1ST FLT STG AT HDAR	2926898.	6452709.	2916443.	6429658.
FROST	-294.	-650.	-294.	-650.
MAINSTAGE	-2082676.	-4591518.	-2072221.	-4568469.
N2 PURGE GAS	-16.	-37.	-16.	-37.
THRUST DECAY-IE	-954.	-2104.	-862.	-1900.
ENG EXPENDED PROP	-189.	-418.	-189.	-418.
S-II INSUL PURGE	-17.	-38.	-17.	-38.
S-II FROST	-204.	-450.	-204.	-450.
S-IVB FROST	-90.	-200.	-90.	-200.
THRUST DECAY-OE	0.	0.	0.	0.
1ST FLT STG AT OECO	842453.	1857293.	842545.	1857495.
THRUST DECAY-OE	-3818.	-8419.	-3448.	-7602.
S-IC/S-II ULL RKT	0.	0.	0.	0.
1ST FLT STG AT SEP	838635.	1848874.	839096.	1849892.
STG AT SEPARATION	-161476.	-355995.	-162256.	-357715.
S-IC/S-II SMALL IS	-616.	-1360.	-616.	-1359.
S-IC/S-II ULL RKT	0.	0.	0.	0.
2ND FLT STG AT SSC	676541.	1491519.	676223.	149081.
FUEL LEAD	0.	0.	0.	0.
S-IC/S-II ULL RKT	0.	0.	0.	0.
2ND FLT STG AT IGN	676541.	1491519.	676223.	1490818.
THRUST BUILDUP	-579.	-1278.	-579.	-1278.
START TANK	-11.	-25.	-11.	-25.
S-IC/S-II ULL RKT	0.	0.	0.	0.
2ND FLT STG AT MS	675950.	1490215.	675632.	1489515.
MAINSTAGE	-451118.	-994545.	-450797.	-993838.
LES	-4141.	-9131.	-4158.	-9167.
S-IC/S-II LARGE IS	-3963.	-8737.	-3960.	-8732.
TD & ENG PROP	-52.	-116.	-49.	-108.
2ND FLT STG AT COS	216674.	477685.	216666.	477668.
THRUST DECAY	-142.	-315.	-128.	-283.
S-IVB ULL RKT PROP	-2.	-5.	-2.	-5.
2ND FLT STG AT SEP	216528.	477364.	216535.	477379.
STG AT SEPARATION	-41859.	-92285.	-41748.	-92039.
S-II/S-IVB IS DRY	-3176.	-7002.	-3169.	-6988.
S-II/S-IVB PROP	-480.	-1060.	-483.	-1067.
S-IVB AFT FRAME	-21.	-48.	-21.	-48.
S-IVB ULL RKT PROP	-1.	-3.	-1.	-3.
S-IVB DET PKG	-1.	-3.	-1.	-3.

Table 16-9. Flight Sequence Mass Summary (Continued)

MASS HISTORY	PREDICTED		ACTUAL	
	KG	LBM	KG	LBM
3RD FLT STG 1ST SSC	170987.	376963.	171109.	377231.
ULLAGE ROCKET PROP	-39.	-88.	-39.	-87.
FUEL LEAD	-0.	-1.	-3.	-8.
3RD FLT STG 1ST IGN	170947.	376874.	171066.	377136.
ULLAGE ROCKET PROP	-9.	-22.	-9.	-22.
START TANK	-1.	-4.	-1.	-4.
THRUST BUILDUP	-162.	-357.	-160.	-354.
3RD FLT STG 1ST MS	170773.	376491.	170893.	376756.
ULLAGE ROCKET CASE	-61.	-135.	-61.	-135.
MAINSTAGE	-30545.	-67341.	-30627.	-67522.
APS	-1.	-4.	-1.	-3.
3RD FLT STG 1ST COS	140164.	309010.	140103.	309096.
THRUST DECAY	-42.	-93.	-128.	-283.
3RD FLT STG 1ST ETD	140122.	308916.	140075.	308813.
ENGINE PROP	-18.	-40.	-18.	-40.
FUEL TANK LOSS	-901.	-1987.	-818.	-1803.
LOX TANK LOSS	-23.	-51.	-39.	-87.
APS	-45.	-100.	-52.	-115.
START TANK	-0.	-2.	0.	0.
O2/H2 BURNER	-7.	-16.	-7.	-16.
3RD FLT STG 2ND SSC	139125.	306719.	139139.	306751.
FUEL LEAD	-10.	-23.	-0.	-2.
3RD FLT STG 2ND IGN	139114.	306695.	139139.	306749.
START TANK	-1.	-4.	-1.	-4.
THRUST BUILDUP	-162.	-357.	-159.	-351.
3D FLT STG 2ND MS	138950.	306334.	138977.	306394.
MAINSTAGE	-73299.	-161598.	-73383.	-161782.
APS	-1.	-4.	0.	0.
3RD FLT STG 2ND COS	65649.	144732.	65594.	144612.
THRUST DECAY	-48.	-106.	-42.	-94.
3RD FLT STG 2ND ETD	65598.	144619.	65552.	144518.
JETTISON SLA	-1170.	-2581.	-1170.	-2581.
CSM	-30437.	-67104.	-30367.	-66949.
S-IVB STAGE LOSS	-318.	-703.	-492.	-1086.
STRT TRANS/DOCK	33670.	74231.	33521.	73902.
CSM	30437.	67104.	30367.	66949.
END TRANS/DOCK	64108.	141335.	63888.	140851.
CSM	-30437.	-67104.	-30367.	-66949.
LM	-16422.	-36205.	-16436.	-36237.
S-IVB STAGE LOSS	-276.	-610.	-255.	-563.
LAU VEH AT S/C SEP	16971.	37416.	16829.	37102.
S/C NOT SEPARATED	-625.	-1380.	-625.	-1380.
IU	-2053.	-4527.	-2042.	-4502.
S-IVB STAGE	-14292.	-31509.	-14161.	-31220.

Table 16-10. Mass Characteristics Comparison

EVENT	MASS		LONGITUDINAL C.G. (X STA.)		RADIAL C.G.		ROLL MOMENT OF INERTIA		PITCH MOMENT OF INERTIA		YAW MOMENT OF INERTIA	
	KILO POUNDS	O/O DEV.	METERS INCHES	DELTA INCHES	METERS INCHES	DELTA INCHES	KG-M2 X10-6	O/O DEV.	KG-M2 X10-6	O/O DEV.	KG-M2 X10-6	O/O DEV.
S-IC STAGE DRY	130641.		9.316		0.0642							
	PRED 288015.		366.8		2.5298		2.560		16.553		16.553	
S-IC STAGE DRY	130569.		9.316		0.000		0.0000		0.0000		0.0000	
	ACTUAL 287855.	-0.05	366.8		0.00 2.5298		0.0000	2.558	-0.05	16.564	-0.05	16.564
S-IC/S-II INTER-STAGE TOTAL	4580.		41.765		0.1512							
	PRED 10097.		1644.3		5.9548		0.115		0.071		0.071	
S-IC/S-II INTER-STAGE TOTAL	4577.		41.765		0.000		0.0000		0.0000		0.0000	
	ACTUAL 10091.	-0.05	1644.3		0.00 5.9548		0.0000	0.115	-0.05	0.071	-0.05	0.071
S-II STAGE DRY	36458.		47.886		0.1670							
	PRED 80377.		1885.3		6.5764		0.597		1.990		1.990	
S-II STAGE DRY	36452.		47.873		-0.012		0.0000		0.0000		0.0000	
	ACTUAL 80362.	-0.01	1884.8		-0.50 6.5764		0.0000	0.597	-0.01	1.989	-0.01	1.989
S-II/S-IVB INTER-STAGE TOTAL	3657.		66.451		0.0672							
	PRED 8062.		2616.2		2.6476		0.065		0.044		0.044	
S-II/S-IVB INTER-STAGE TOTAL	3654.		66.451		0.000		0.0000		0.0000		0.0000	
	ACTUAL 8055.	-0.08	2616.2		0.00 2.6476		0.0000	0.064	-0.08	0.044	-0.08	0.044
S-IVB STAGE DRY	11378.		72.557		0.2241							
	PRED 25084.		2856.6		8.8255		0.082		0.299		0.299	
S-IVB STAGE DRY	11385.		72.557		0.000		0.0000		0.0000		0.0000	
	ACTUAL 25099.	0.06	2856.6		0.00 8.8255		0.0000	0.082	0.06	0.299	0.06	0.299
VEHICLE INSTRUMENT UNIT	2053.		82.410		0.4748							
	PRED 4527.		3244.5		18.6954		0.019		0.010		0.010	
VEHICLE INSTRUMENT UNIT	2042.		82.410		0.000		-0.0044		-0.0044		-0.0044	
	ACTUAL 4502.	-0.54	3244.5		0.0018 5.205		-0.1749	0.019	-0.54	0.010	-0.54	0.009
SPACECRAFT TOTAL	52799.		91.442		0.0980							
	PRED 116401.		3600.1		3.8600		0.099		1.680		1.680	
SPACECRAFT TOTAL	52759.		91.440		-0.002		-0.0004		-0.0004		-0.0004	
	ACTUAL 116314.	-0.06	3600.0		-0.09 3.8418		-0.0181	0.099	-0.06	1.681	0.11	1.681



Table 16-10. Mass Characteristics Comparison (Continued)

EVENT	MASS		LONGITUDINAL C.G. (X STA.)		RADIAL C.G.		ROLL MOMENT OF INERTIA		PITCH MOMENT OF INERTIA		YAW MOMENT OF INERTIA	
	KILO POUNDS	O/O DEV.	METERS INCHES	DELTA	METERS INCHES	DELTA	KG-M2 X10-6	O/O DEV.	KG-M2 X10-6	O/O DEV.	KG-M2 X10-6	O/O DEV.
1ST FLIGHT STAGE AT IGNITION	PRED	2965766. 6538394.	30.458 1199.1		0.0051 0.2024		3.655		395.899		895.834	
	ACTUAL	2965241. 6537238.	30.458 1199.1	0.000 0.00	0.0045 0.1802	-0.0005 -0.0222	3.641	-0.39	909.607	1.53	909.542	1.53
1ST FLIGHT STAGE AT HOLDDOWN ARM RELEASE	PRED	2926899. 6452708.	30.404 1197.0		0.0052 0.2059		3.691		896.911		896.846	
	ACTUAL	2916444. 6429658.	30.402 1196.9	-0.002 -0.07	0.0045 0.1802	-0.0006 -0.0256	3.676	-0.39	908.268	1.27	908.203	1.27
1ST FLIGHT STAGE AT OUTBOARD ENGINE CUTOFF SIGNAL	PRED	842454. 1857292.	46.820 1843.3		0.0177 0.6977		3.675		444.578		444.517	
	ACTUAL	842546. 1857495.	46.788 1842.0	-0.031 -1.22	0.0157 0.6191	-0.0019 -0.0785	3.659	-0.40	445.788	0.27	445.727	0.27
1ST FLIGHT STAGE AT SEPARATION	PRED	838635. 1848873.	46.985 1849.8		0.0177 0.6977		3.673		439.422		439.361	
	ACTUAL	839097. 1849892.	46.939 1848.0	-0.045 -1.78	0.0157 0.6191	-0.0019 -0.0785	3.658	-0.40	441.097	0.38	441.035	0.38
2ND FLIGHT STAGE AT START SEQUENCE COMMAND	PRED	676542. 1491519.	55.926 2201.8		0.0187 0.7397		0.981		140.078		140.090	
	ACTUAL	676224. 1490818.	55.933 2202.1	0.007 0.27	0.0187 0.7382	-0.0000 -0.0015	0.981	-0.04	140.115	0.03	140.131	0.03
2ND FLIGHT STAGE AT MAINSTAGE	PRED	675950. 1490215.	55.926 2201.8		0.0187 0.7397		0.983		140.072		140.085	
	ACTUAL	675633. 1489515.	55.934 2202.1	0.008 0.31	0.0187 0.7382	-0.0000 -0.0015	0.982	-0.04	140.107	0.02	140.122	0.03
2ND FLIGHT STAGE AT CUTOFF SIGNAL	PRED	216674. 477684.	71.414 2811.6		0.0562 2.2153		0.881		45.462		45.473	
	ACTUAL	216667. 477668.	71.418 2811.7	0.004 0.15	0.0563 2.2190	0.0000 0.0037	0.880	-0.04	45.392	-0.14	45.407	-0.14

16-10

Table 16-10. Mass Characteristics Comparison (Continued)

EVENT	MASS		LONGITUDINAL C.G. (X STA.)		RADIAL C.G.		ROLL MOMENT OF INERTIA		PITCH MOMENT OF INERTIA		YAW MOMENT OF INERTIA	
	KILO POUNDS	O/O DEV.	METERS INCHES	DELTA	METERS INCHES	DELTA	KG-M2 X10-6	O/O DEV.	KG-M2 X10-6	O/O DEV.	KG-M2 X10-6	O/O DEV.
2ND FLIGHT STAGE AT SEPARATION	PRED	216529. 477364.	71.431 2812.2		0.0565 2.2252			0.881	45.364		45.376	
	ACTUAL	216536. 477379.	71.434 2812.4	0.003 0.11	0.0566 2.2289	0.0000 0.0037	0.880	-0.04	45.301	-0.13	45.316	-0.12
3RD FLIGHT STAGE AT 1ST START SEQUENCE COMMAND	PRED	170988. 376963.	77.310 3043.7		0.0387 1.5239		0.207		13.960		13.957	
	ACTUAL	171109. 377231.	77.299 3043.2	-0.011 -0.44	0.0382 1.5065	-0.0004 -0.0173	0.207	0.00	13.946	-0.09	13.943	-0.09
3RD FLIGHT STAGE AT 1ST IGNITION	PRED	170947. 376874.	77.311 3043.7		0.0387 1.5239		0.207		13.959		13.956	
	ACTUAL	171066. 377136.	77.299 3043.2	-0.011 -0.46	0.0382 1.5065	-0.0004 -0.0173	0.207	0.00	13.945	-0.09	13.941	-0.09
3RD FLIGHT STAGE AT 1ST MAINSTAGE	PRED	170773. 376490.	77.313 3043.8		0.0387 1.5239		0.207		13.958		13.954	
	ACTUAL	170894. 376755.	77.301 3043.3	-0.011 -0.46	0.0382 1.5065	-0.0004 -0.0173	0.207	0.01	13.944	-0.09	13.940	-0.09
3RD FLIGHT STAGE AT 1ST CUTOFF SIGNAL	PRED	140165. 309010.	78.212 3079.2		0.0467 1.8417		0.206		13.125		13.121	
	ACTUAL	140203. 309095.	78.197 3078.6	-0.015 -0.59	0.0463 1.8266	-0.0003 -0.0151	0.206	0.00	13.116	-0.06	13.112	-0.06
3RD FLIGHT STAGE AT 1ST END THRUST DECAY, START COAST	PRED	140122. 308916.	78.214 3079.2		0.0467 1.8417		0.206		13.123		13.120	
	ACTUAL	140075. 308812.	78.202 3078.8	-0.011 -0.44	0.0463 1.8266	-0.0003 -0.0151	0.206	0.00	13.110	-0.09	13.107	-0.09
3RD FLIGHT STAGE AT 2ND START SEQUENCE COMMAND	PRED	139125. 306719.	78.224 3079.7		0.0468 1.8439		0.205		13.117		13.114	
	ACTUAL	139140. 306750.	78.215 3079.3	-0.009 -0.36	0.0463 1.8266	-0.0004 -0.0173	0.205	-0.02	13.103	-0.10	13.099	-0.10

16-11

Table 16-10. Mass Characteristics Comparison (Continued)

EVENT	MASS		LONGITUDINAL C.G. (X STA.)		RADIAL C.G.		ROLL MOMENT OF INERTIA		PITCH MOMENT OF INERTIA		YAW MOMENT OF INERTIA	
	KILO POUNDS	O/O DEV.	METERS INCHES	DELTA	METERS INCHES	DELTA	KG-M2 X10-6	O/O DEV.	KG-M2 X10-6	O/O DEV.	KG-M2 X10-6	O/O DEV.
3RD FLIGHT STAGE AT 2ND IGNITION	PRED	139115. 306695.	78.221 3079.5		0.0468 1.8439		0.205		13.120		13.117	
	ACTUAL	139139. 306748.	78.212 3079.2	-0.009 -0.36	0.0463 1.8266	-0.0004 -0.0173	0.705	-0.02	13.106	-0.10	13.103	-0.10
3RD FLIGHT STAGE AT 2ND MAINSTAGE	PRED	138951. 306333.	78.226 3079.7		0.0470 1.8536		0.205		13.117		13.114	
	ACTUAL	138978. 306393.	78.216 3079.4	-0.009 -0.36	0.0466 1.8363	-0.0004 -0.0173	0.205	-0.02	13.103	-0.10	13.100	-0.10
3RD FLIGHT STAGE AT 2ND CUTOFF SIGNAL	PRED	65649. 144731.	86.033 3387.1		0.0975 3.8421		0.204		5.265		5.262	
	ACTUAL	65595. 144611.	86.028 3386.9	-0.005 -0.20	0.0967 3.8102	-0.0008 -0.0318	0.204	-0.01	5.252	-0.23	5.249	-0.24
3RD FLIGHT STAGE AT 2ND END THRUST DECAY	PRED	65598. 144618.	86.045 3387.6		0.0975 3.8421		0.204		5.252		5.249	
	ACTUAL	65552. 144517.	86.039 3387.3	-0.006 -0.25	0.0967 3.8102	-0.0008 -0.0318	0.204	-0.01	5.241	-0.20	5.238	-0.21
CSM SEPARATED	PRED	33394. 73620.	79.219 3118.8		0.0956 3.7670		0.146		1.664		1.659	
	ACTUAL	33522. 73902.	79.208 3118.4	-0.011 -0.46	0.0893 3.5174	-0.0063 -0.2495	0.146	-0.21	1.668	0.26	1.663	0.23
CSM DOCKED	PRED	63832. 140724.	85.590 3369.7		0.1175 4.6281		0.196		4.617		4.611	
	ACTUAL	63889. 140851.	85.563 3368.6	-0.027 -1.06	0.1133 4.4629	-0.0041 -0.1652	0.195	-0.22	4.627	0.23	4.621	0.23
SPACECRAFT SEP- ARATED	PRED	16971. 37415.	73.780 2904.7		0.1650 6.4970		0.111		0.606		0.602	
	ACTUAL	16829. 37102.	73.796 2905.3	0.015 0.59	0.1560 6.1424	-0.0090 -0.3545	0.111	-0.30	0.605	-0.09	0.601	-0.16

SECTION 17  
LUNAR IMPACT

17.1 SUMMARY

All aspects of the S-IVB/IU Lunar Impact Mission objectives were accomplished successfully except the precise determination of the impact point and time of impact. Preliminary analysis of available tracking data plus calculations based upon three lunar seismometer recordings of the impact indicate the S-IVB/IU was successfully maneuvered to impact the lunar surface within 350 kilometers (189 n mi) of the target. The loss of tracking data at 97,799 seconds (27:09:59) has precluded determining the impact time and location within the mission objectives of one second and five kilometers (2.7 n mi), but these objectives may be eventually determined by analytical techniques not previously used.

Based upon analysis to date the S-IVB/IU impacted the lunar surface at 270,482 seconds (75:08:02) at approximately 2.1 degrees north latitude and 22.1 degrees west longitude with a velocity of 2,655 meters per second (8,711 ft/s). This preliminary impact point is approximately 320 kilometers (173 n mi) from the target of 2.3 degrees south latitude and 31.7 degrees west longitude.

Real time targeting activities were changed considerably from preflight planned operations because of the following real time indications:

- (1) IU GN<sub>2</sub> cooling pressurant leakage,
- (2) unanticipated IU velocity accumulations during Timebase 7 (later identified as primarily platform biases),
- (3) suspected early S-IVB APS Module 1 propellant depletion (later identified as a He leakage problem), and
- (4) unsymmetrical APS ullage performance.

Because of these indications, a more efficient LOX dump attitude was selected to reduce the APS targeting burn requirement. Due to the problems with the vehicle, there would have been no opportunity to perform a second APS burn even if it had been required.

17.2 TRANSLUNAR COAST MANEUVERS

Following Command and Service Module (CSM)/Launch Vehicle (LV) separation at 11,099 seconds (3:04:59), the CSM was docked with the Lunar Module (LM)

at 12,113 seconds (3:21:53) and the CSM/LM was then ejected from the S-IVB/IU at 14,355 seconds (3:59:15). After CSM/LM ejection, the S-IVB/IU was maneuvered to the inertially-fixed attitude required for the evasive burn. Timebase 8 (Tg) was initiated 293 seconds earlier than nominal at 15,487 seconds (4:18:07). The APS ullage engines were started 1 second following Tg and burned for 80 seconds. Table 17-1 shows the actual evasive velocity increment was greater than real time expected or preflight planned. The direction of the actual velocity change was considerably off-nominal due to unsymmetrical APS performance.

Because of a suspected early depletion of the APS Module 1 propellant and the unsymmetrical APS performance, the Lunar Impact Team (LIT) at the Huntsville Operations Support Center (HOSC) decided in real time to place the S-IVB/IU in a more efficient LOX dump attitude than preflight planned. This attitude change was to reduce later APS burn requirements. The commands for this maneuver were sent from the Mission Control Center at Houston (MCC-H) by the Booster Systems Engineer (BSE) to the S-IVB/IU.

Following the maneuver to the updated Continuous Vent System (CVS) and LOX dump attitude, the initial lunar targeting velocity changes were accomplished by means of a 300-second CVS vent starting 1,000 seconds after Tg and a 48-second LOX dump starting 1,280 seconds after Tg. Table 17-1 shows the CVS vent and LOX dump maneuver changes from preflight planned to real time expected as well as the postflight actual values.

A significantly revised APS lunar impact targeting burn was then determined in real time by the LIT. The commands for this APS burn (described in Table 17-1) were sent from the MCC-H by the BSE to the S-IVB/IU. At 4,920 seconds following Tg (5:40:07) a 54-second APS burn was initiated. Table 17-1 again shows the unsymmetrical APS performance obtained during the maneuver.

Because of limited APS capability and problems within the IU, the LIT decided to terminate the real time lunar impact operations. Therefore, no second APS targeting burn was attempted. The three-axis passive thermal control (PTC) maneuver was then initiated at 21,306 seconds (5:55:06) and the flight control computer was turned off.

Figure 17-1 presents line-of-sight range rate residuals from a Goldstone DSN (GDSW) tracking station and depicts graphically the major S-IVB/IU velocity changes and the PTC tumbling. Residuals are obtained by differencing observed range rate data with calculated range rate data (observed minus calculated). The calculated range rate data is developed from a sophisticated orbital model which is statistically fitted to portions of the observed data. Figure 17-2 verifies the reconstruction of the maneuvers presented in Table 17-1 by showing the residuals resulting from the same Goldstone tracking data but with the reconstructed

Table 17-1. Translunar Coast Maneuvers

PARAMETER	ACTUAL	REAL TIME EXPECTED	PREFLIGHT PLANNED	ACT-RTE	RTE-PFP
TIMEBASE B INITIATION					
GRT Time 16 April, hr:min:sec	22:12:07	22:12:06	22:17:00	0:00:01	-0:04:54
Range Time, hr:min:sec (sec)	4:18:07 (15,487)	4:18:06 (15,486)	4:23:06 (15,780)	0:00:01 (1)	-0:04:54 (-294)
APS EVASIVE BURN					
Initiation, sec from T <sub>0</sub>	1	1	1	0	0
Duration, sec	80	80	80	0	0
Velocity Increment, m/s (ft/s)	3.36 (11.02)	3.12 (10.24)	2.98 (9.78)	0.24 (0.78)	0.14 (0.46)
Pitch Attitude*, deg. inertial (local)	67.36	55.44 (175.96)	55.44 (175.96)	11.92	0 (0)
Yaw Attitude*, deg. inertial (local)	40.83	40.00 (40.87)	40.00 (40.87)	0.83	0 (0)
CVS VENT					
Initiation, sec from T <sub>0</sub>	1,000	1,000	1,000	0	0
Duration, sec	300	300	300	0	0
Velocity Increment, m/s (ft/s)	0.52 (1.71)	0.37 (1.21)	0.37 (1.21)	0.15 (0.50)	0.00 (0.00)
Pitch Attitude*, deg. inertial (local)	119.60	112.66 (237.00)	64.66 (189.00)	6.94	48.00 (48.00)
Yaw Attitude*, deg. inertial (local)	12.26	4.98 (6.00)	12.98 (14.00)	7.28	-8.00 (-8.00)
LOF DUMP					
Initiation, sec from T <sub>0</sub>	1,280	1,280	1,280	0	0
Duration, sec	48	48	48	0	0
Velocity Increment, m/s (ft/s)	8.07 (26.48)	8.05 (29.04)	8.91 (29.23)	-0.78 (-2.56)	-0.06 (-0.19)
Pitch Attitude*, deg. inertial (local)	115.35	112.27 (237.00)	64.27 (189.00)	3.08	48.00 (48.00)
Yaw Attitude*, deg. inertial (local)	6.97	4.91 (6.00)	12.91 (14.00)	2.06	-8.00 (-8.00)
APS LUNAR IMPACT BURN					
Initiation, sec from T <sub>0</sub>	4,920	4,913	4,020	7	893
Duration, sec	54	54	158	0	-104
Velocity Increment, m/s (ft/s)	2.54 (8.33)	2.44 (8.01)	6.66 (21.85)	0.10 (0.32)	-4.22 (-13.04)
Pitch Attitude*, deg. inertial (local)	90.00	82.00 (213.00)	58.00 (189.00)	7.20	24.00 (24.00)
Yaw Attitude*, deg. inertial (local)	-30.81	-34.87 (-33.00)	12.93 (14.00)	3.26	-47.00 (-47.00)

\* Attitudes are the velocity increment direction.

NOTE: ACT is an abbreviation for ACTUAL  
RTE is a mnemonic for REAL TIME EXPECTED  
PFP is a mnemonic for PREFLIGHT PLANNED

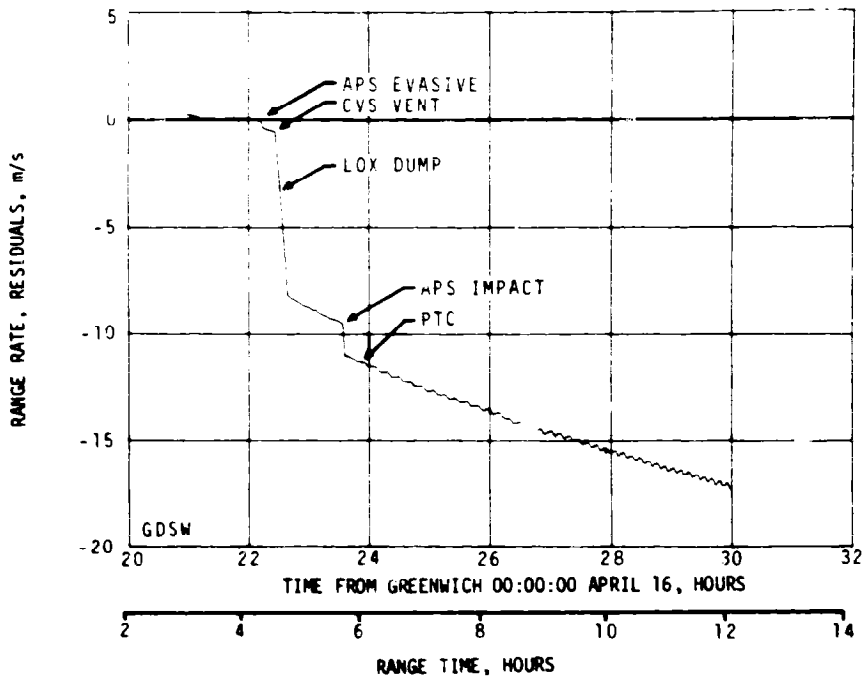


Figure 17-1. Translunar Coast Maneuvers Overview

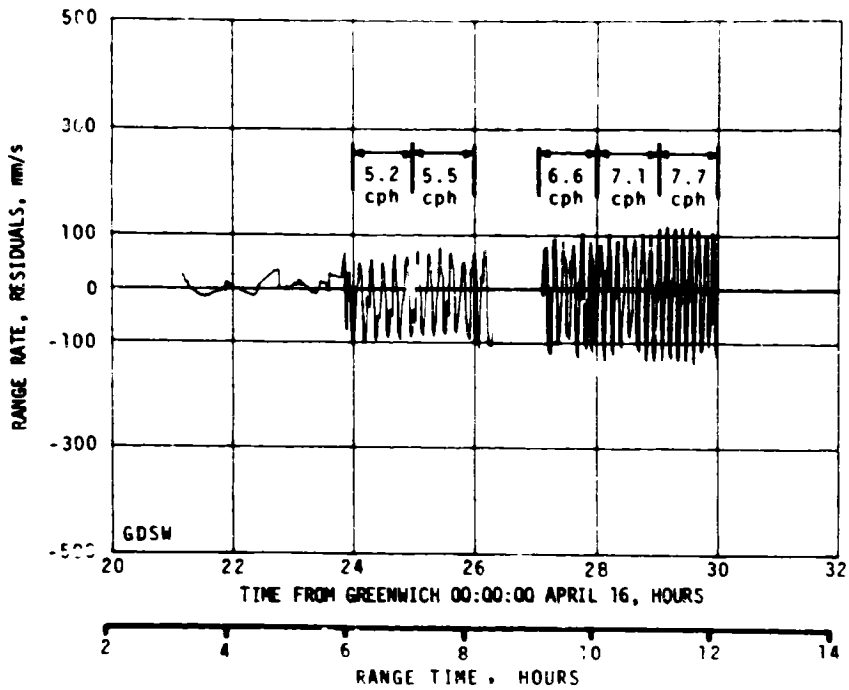


Figure 17-2. Modeled Translunar Coast Maneuvers and Early PTC Residuals

maneuvers used in the orbital model to account for the velocity changes. It is to be noted that telemetered IU platform accelerometer data was used to obtain the velocity and attitude data presented in Table 17-1.

### 17.3 TRAJECTORY EVALUATION

Table 17-2 presents the actual and nominal geocentric orbital parameters of the S-IVB/IU trajectory after the APS targeting burn.

Figure 17-2 shows the initiation and early portion of the PTC tumbling. The tumble, as seen by the Goldstone station, starts at approximately 5.2 cycles per hour (cph) and increases gradually. The 5.2 cph is equivalent to 0.52 degree per second which is close to the commanded pitch, yaw, and roll tumble rates. Figure 17-3 shows the later portion of the PTC tumbling, as seen by a Madrid DSN (MADW) tracking station, decreasing gradually with a rather significant frequency change occurring over a 3-hour period starting at approximately 22 hours range time. Further analysis is required on the PTC tumbling residuals from the several tracking stations observing the vehicle before final conclusions can be reached about the significance of these frequency changes. It is to be noted that the amplitude of the range rate modulations for the AS-511 S-IVB/IU is twice as great as for the AS-510 S-IVB/IU. This factor coupled with the loss of tracking data at approximately 27 hours range time may preclude a precise determination of the impact trajectory.

Table 17-2. Geocentric Orbit Parameters Following APS Impact Burn

PARAMETER	ACTUAL	NOMINAL	A.T-NOM
Semi-Major Axis, km (n mi)	232,057 (125,301)	234,663 (126,708)	-2,606 (-1,407)
Eccentricity	0.971884	0.972549	-0.000665
$C_3^*$ , km <sup>2</sup> /s <sup>2</sup> (n mi <sup>2</sup> /s <sup>2</sup> )	-1.717695 (-0.500800)	-1.698616 (-0.495237)	-0.019079 (-0.005563)
Perigee Radius, km (n mi)	6,525 (3,523)	6,442 (3,478)	83 (45)

\* $C_3$  is twice the specific energy of orbit.

### 17.4 LUNAR IMPACT CONDITIONS

Figure 17-4 presents the lunar landmarks of interest relative to the preliminary estimate of the S-IVB/IU impact. Tracking analyses to date indicate the S-IVB/IU impacted the moon at 2.1 degrees north latitude and 22.1 degrees west longitude at 21:02:03 GMT on April 19, 1972 (75:08:03). This impact point is accurate within about 60 kilometers (32 n mi) in



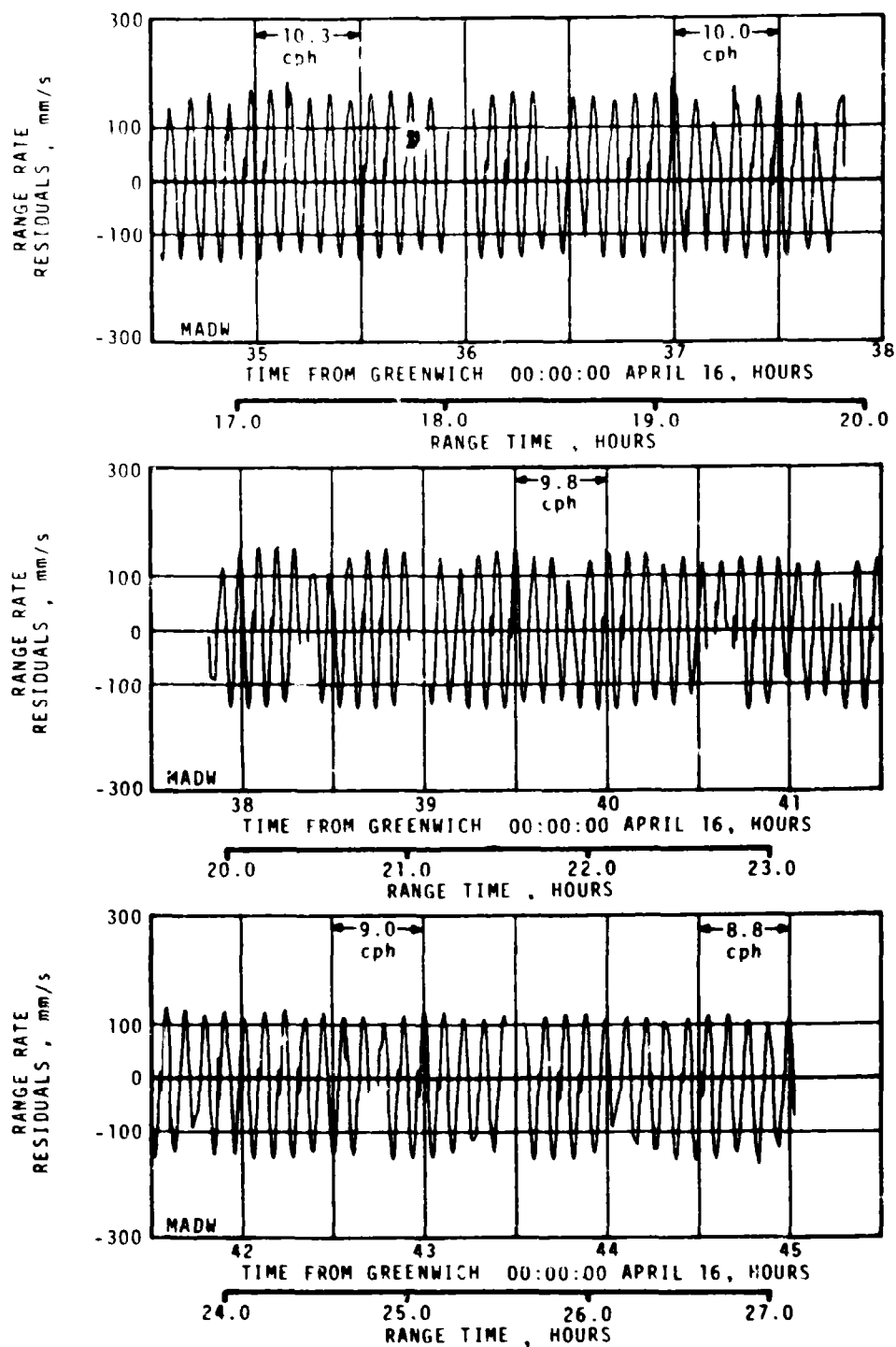


Figure 17-3. Late Residuals Showing PTC Frequency Decrease

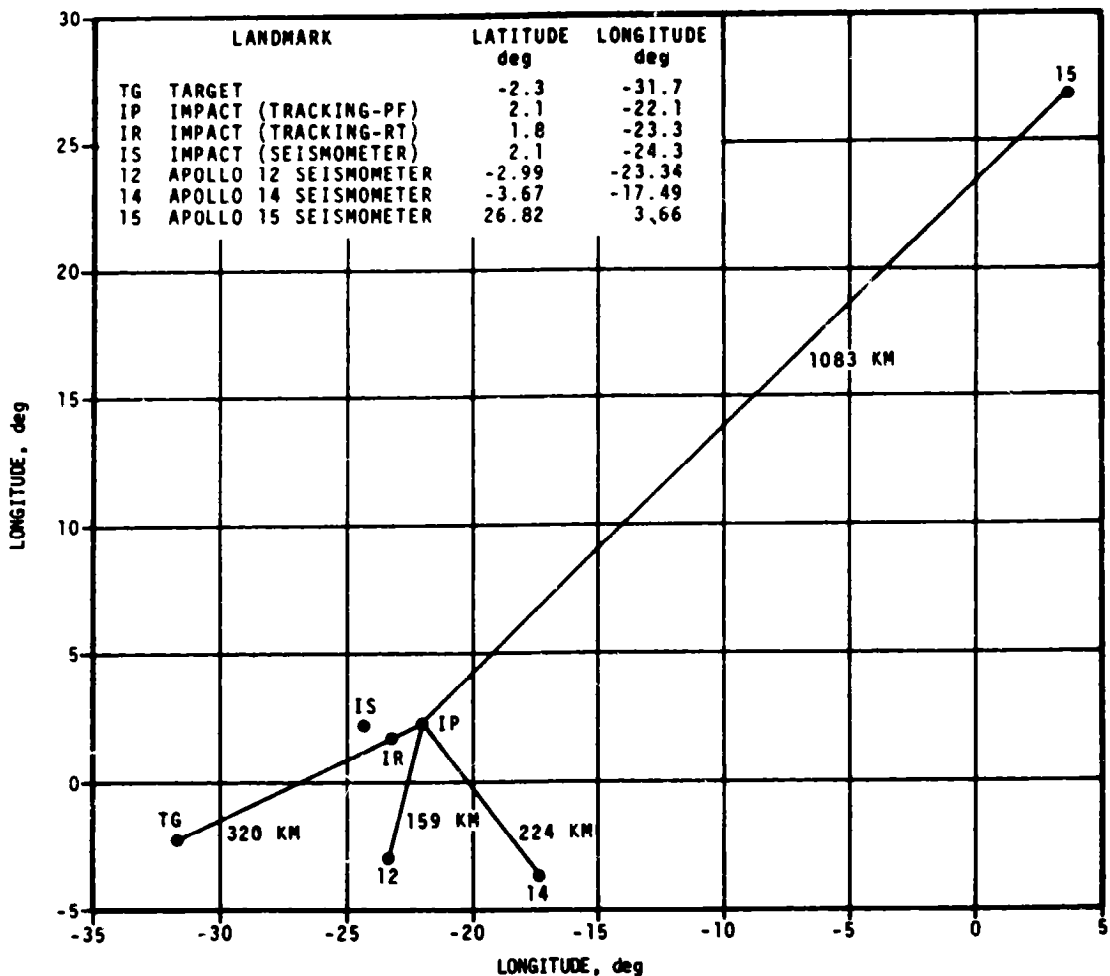


Figure 17-4. Lunar Landmarks of Scientific Interest

position. Further analysis, currently in work, will refine the impact conditions. It may not be possible to determine the impact point within the 5-kilometer (2.7 n mi) and 1-second mission objectives because of the high tumble amplitude and the loss of tracking data. Figure 17-4 presents impact results from MSC's real time analysis of tracking data, from past flight analyses, and from seismometer recordings.

Comparison of impact parameters with the OT and miss distances from the lunar landmarks of interest as derived from postflight analyses are presented in Table 17-3. The distance from the impact point to the target is 320 kilometers (173 n mi) which is within the 350-kilometer (189 n mi) mission objective. Table 17-4 presents the Apollo 12, 14, and 15 seismometer actuation times due to the impact. Calculations by the principal seismic experiment investigator give a derived impact point which is 2.2 degrees west of the preliminary tracking point. The calculated time of impact given in Table 17-4 is taken as the best estimate of the lunar

impact time and is the basis for the time quoted in the summary. The principle seismic investigator reports an accuracy of  $\pm 2$  seconds in the impact time.

### 17.5 TRACKING DATA

Figure 17-5 shows the tracking data available to the trajectory determination. Table 17-5 shows the tracking site locations and configuration. Both C-Band and S-Band data of good quality were received. However, as indicated in Figure 17-5, tracking stopped at 97,799 seconds (27:09:59). Hence, following CSM separation, approximately 24 hours of data are available for analysis on the AS-511 whereas for the AS-509 vehicle 79.5 hours of data were available and for the AS-510 vehicle 76 hours of data were available.

Table 17-3. Lunar Impact Conditions

PARAMETER AT IMPACT	ACTUAL	NOMINAL	ACT-NOM
Stage Mass, kg (lbm)	$\sim 13,973$ ( $\sim 30,805$ )	13,973 (30,805)	$\sim 0$ ( $\sim 0$ )
Velocity Relative to Surface, m/s (ft/s)	2,655 (8,711)	2,565 (8,415)	90 (296)
Impact Angle Measured From Vertical, deg	16.6	11.2	5.4
Incoming Heading Angle Measured From North to West, deg	104.7	96.9	7.8
Selenographic Latitude, deg	2.1	-2.3	4.4
Selenographic Longitude, deg	-22.1	-31.7	9.6
Impact Time, GMT 19 April	21:02:03	20:24:08	00:37:55
Distance to Target, km (n mi)	320 (173)	0 (0)	320 (173)
Distance to Apollo 12 Seismometer, km (n mi)	159 (86)	255 (138)	-96 (-52)
Distance to Apollo 14 Seismometer, km (n mi)	224 (121)	433 (234)	-209 (-113)
Distance to Apollo 15 Seismometer, km (n mi)	1,083 (585)	1,390 (751)	-307 (-166)
Note: Real time analysis of tracking data gave impact at 1.8° latitude, -23.3° longitude, and 21:01:03 GMT 19 April.			

Table 17-4. Lunar Impact Seismic Data

SEISMOMETER	LOCATION		IMPACT SIGNAL RECEPTION TIME GMT 19 APRIL, 1972
	LATITUDE deg	LONGITUDE deg	
Apollo 12	-2.99	-23.34	21:02:32
Apollo 14	-3.67	-17.49	21:02:40
Apollo 15	26.82	3.66	21:04:30

NOTE: The derived Apollo 16 S-IVB/IU impact conditions are 2.1° latitude, -24.3° longitude, and 21:02:02 GMT 19 April (75:08:02 range time).

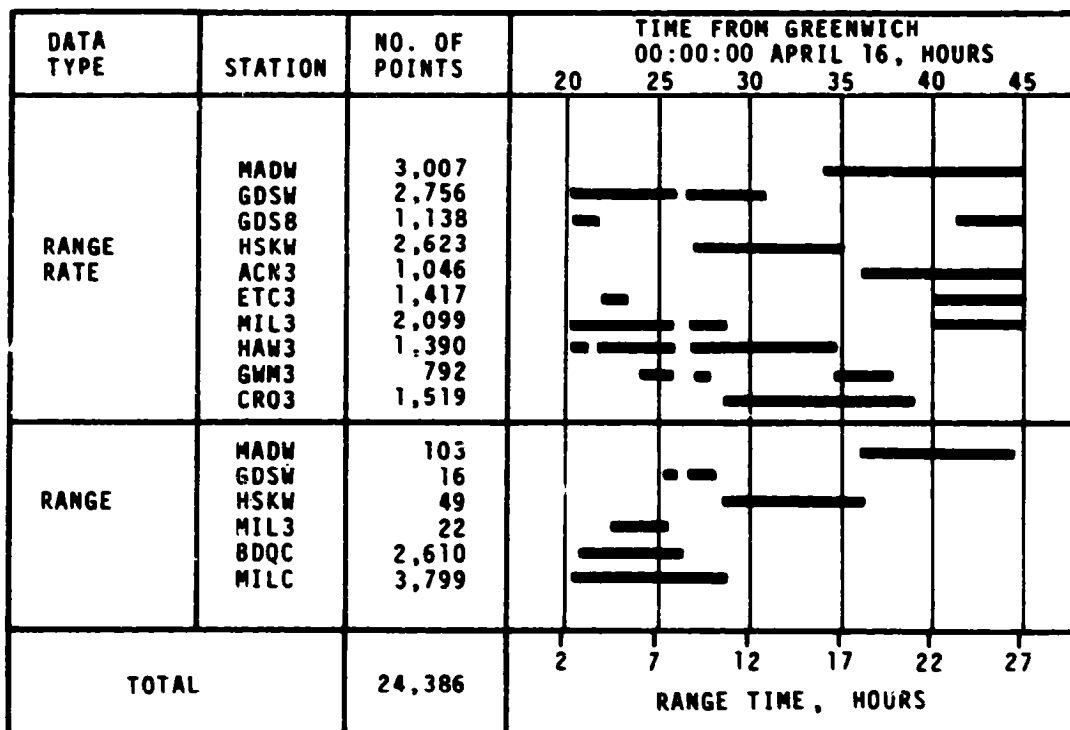


Figure 17-5. Tracking Data Availability

Table 17-5. S-IVB/IU Tracking Stations

STATION LOCATION	CONFIGURATION	ABBREVIATION
Madrid, Spain	DSN 85' S-Band	MADW
Madrid, Spain	MSFN 85' S-Band	MAD8
Ascension Island	MSFN 30' S-Band	ACN3
Bermuda Island	MSFN 30' S-Band	BDA3
Merritt Island, Florida	MSFN 30' S-Band	MIL3
Greenbelt, Maryland	MSFN 30' S-Band	ETC3
Goldstone, California	DSN 85' S-Band	GDSW
Goldstone, California	MSFN 85' S-Band	GDS8
Kauai, Hawaii	MSFN 30' S-Band	HAW3
Guam Island	MSFN 30' S-Band	GWM3
Carnarvon, Australia	MSFN 30' S-Band	CRO3
Tidbinbilla, Australia	DSN 85' S-Band	HSKW
Canberra, Australia	MSFN 85' S-Band	HSK8
Bermuda Island	FPQ-6 C-Band	BDQC
Merritt Island, Florida	TPQ-18 C-Band	MILC

## SECTION 18

### SPACECRAFT SUMMARY

The spacecraft was manned by Captain John W. Young, Commander; Lt. Commander Thomas K. Mattingly II, Command Module Pilot; and Lt. Colonel Charles M. Duke, Jr., Lunar Module Pilot. The spacecraft/S-IVB combination was inserted into a parking orbit for systems checkout and preparation for the translunar injection maneuver. The command and service module was separated from the S-IVB at about 3 hours and docked with the lunar module.

The crew observed that the thermal coating was flaking from the surface of the lunar module directly below the docking target. Because of this, an unscheduled ingress was made into the lunar module to verify that the spacecraft systems were functioning normally.

The only translunar midcourse correction was made at the midcourse No. 2 option time to reduce the closest approach to the moon to 71.4 n mi. During translunar coast, a significant command and service module systems problem was encountered. A false indication of inertial measurement unit gimbal lock was received by the computer; therefore, a software program was provided to inhibit the computer from responding to such indications during critical operations. Prior to lunar orbit insertion, the scientific instrument module door was jettisoned. The spacecraft was inserted into a lunar orbit of 170 by 58 n mi. following a service propulsion firing of 374.9 seconds. Four hours later, the descent orbit insertion maneuver was performed to lower the spacecraft orbit to 58 x 11 miles.

The crew entered the lunar module at 93 1/2 hours to prepare for descent to the lunar surface. While activating the lunar module systems, the S-band steerable antenna was found to be inoperative in the yaw plane; therefore, the two omnidirectional antennas were used for most of the remaining lunar operations. A pressure regulation problem in system A of the reaction control system was also discovered; however, the condition had no significant effect on the mission.

The lunar landing was delayed approximately 5 3/4 hours because of oscillations detected in a secondary yaw gimbal actuator on the service propulsion system engine during systems checks. Tests and analyses showed that the system was still usable and safe. Following the problem assessment, the command and service module successfully performed the circularization maneuver on the primary gimbal servo system.

The lunar module powered descent proceeded normally and the spacecraft

landed 276 meters northwest of the planned landing site at about 104 1/2 hours. About 100 seconds of hover time remained at touchdown. The best estimate of lunar surface position is 8 degrees 59 minutes 29 seconds south latitude and 15 degrees 30 minutes 52 seconds east longitude.

The lunar surface activity was rescheduled because of the later-than-planned landing and the surface stay was initiated with an 8-hour rest period.

The first extravehicular activity began at 119 hours. Television coverage of surface activity was delayed until after the Lunar Roving Vehicle (LRV) systems were activated because of the loss of the steerable antenna on the lunar module. The experiments package were deployed but accidental breakage of the electronics cable on the heat flow equipment caused the loss of that experiment. All planned stations were visited and samples were obtained in the vicinity of Flag and Spook Craters. The crew activated the active seismic experiment and transferred about 42 pounds of samples into the lunar module. The extravehicular activity duration was 7 hours and 11 minutes.

One station was eliminated from the second traverse. During this extravehicular activity, geological investigations and lunar sampling were conducted first at Stone Mountain, and then at several craters on the return traverse. About 71 pounds of samples were obtained during the 7 hour and 23 minute activity.

The third extravehicular activity was reduced in time and scope due to the late landing. The rim of North Ray Crater was examined in detail, as was an area about 3/4 kilometer from the crater. About 100 pounds of lunar samples were obtained during this 5 hour and 40 minute extravehicular activity.

The lunar surface activities lasted 20 hours and 14 minutes and an estimated 213 pounds of samples were collected. The total distance traveled in the LRV was about 27 kilometers. The crew remained on the lunar surface approximately 71 hours.

While the lunar module crew was on the surface, the Command Module Pilot operated the lunar orbit experiments. Some problems were encountered with the laser altimeter and the panoramic camera.

Lunar ascent was initiated at 175 1/2 hours and was followed by a normal rendezvous and docking. The lunar module had no attitude control at jettison; consequently, a de-orbit maneuver was not possible. The estimated orbital life of the lunar module is about 1 year.

The particles and fields subsatellite was launched into lunar orbit and normal systems operation is indicated. The mass spectrometer deployment boom stalled during a retract cycle and was therefore jettisoned prior to transearth injection. The second plane change maneuver and

some orbital science photography were deleted, thus allowing transearth injection to be performed about 24 hours early. Transearth injection was initiated at about 200 1/2 hours with a 162.3-second firing of the service propulsion system.

The transearth coast phase of the mission included photography for Skylab contamination studies and visual light flash phenomenon investigation. A 1 hour and 24 minute transearth extravehicular activity was conducted during which the Command Module Pilot retrieved the film cassettes from the scientific instrument module cameras, visually inspected the equipment, and performed the microbial response in space environment experiment. Two midcourse corrections were made on the return flight.

Entry and landing were normal. The command module was viewed on television while on the drogue parachutes and continuous coverage was provided through crew recovery. The spacecraft landed at 0 degrees 42 minutes south latitude and 156 degrees 12 minutes 48 seconds west longitude, as determined by the onboard computer. Total time for the Apollo 16 mission was 265 hours, 51 minutes, and 5 seconds.



## SECTION 19

### APOLLO 16 INFLIGHT DEMONSTRATION

One inflight demonstration was conducted as proposed by the Marshall Space Flight Center to demonstrate Electrophoretic Separation in a zero g environment. The Electrophoretic Separation Demonstration, a chemical separation process based on the motion of particles in a fluid due to the force of an electric field, was conducted to show the advantages of the almost weightless environment.

On earth, electrophoresis has to contend with sedimentation and thermal convective mixing which limits its usefulness for high molecular weight materials and large volume samples. The demonstration was expected to show that electrophoresis in space is not limited by molecular weight and volume.

The test instrument was a 4 by 5 by 6-inch box, weighing 7 pounds and requiring 32 watts of 115 volts, 400 cycle power for one hour. A viewing window was provided so that the action in the test tubes could be photographed employing a series of twelve 70mm Hasselblad exposures spaced 20 seconds apart. The electrical system included white fluorescent lights, pump motor, and 300 vdc rectified power for the electrophoresis electrodes in the ends of the tubes. The fluid system included a peristaltic pump, filter, gas phase separator and tubing to flush the electrodes. The flowing fluid was separated from the passive fluid in the test tubes by dialysis membranes, although a dilute boric acid solution was used throughout.

The preliminary assessment of the demonstration indicates that the electrophoresis was more distinct than on earth and fluid convection effects were minimal. The photographs were clear and sharp and the crew commentary thorough.

## SECTION 20

### LUNAR ROVING VEHICLE

#### 20.1 SUMMARY

The Lunar Roving Vehicle (LRV) satisfactorily supported the lunar exploration objectives. The total odometer distance traveled during the three traverses was 26.9 kilometers at an average velocity of 7.8 km/hr. Refer to Figure 20-1 for LRV traverse map. The maximum velocity attained was 17.0 km/hr and the maximum slope negotiated was 20 degrees. The average LRV energy consumption rate was 2.1 amp-hours/km with a total consumed energy of 88.7 amp-hours (including the Lunar Communication Relay Unit (LCRU) out of an approximate total available energy of 242 amp-hours. The navigation system gyro drift and closure error at the Lunar Module (LM) were negligible.

Controllability was good. There were no problems with steering, braking, or obstacle negotiation, except downslope at speeds above 10 kph, where the vehicle reacted like an "auto driven on ice." Brakes were used at least partially on all downslopes. Driving down sun was difficult because of poor visibility of the "washed out" terrain.

All interfaces between crew and LRV and between LRV and stowed payload were satisfactory.

The following anomalies were noted during lunar surface operation:

- a. The LRV battery cooldown between EVA's 1 and 2 and between EVA's 2 and 3 was insufficient causing battery over temperature before the end of the mission (reference paragraph 20.12).
- b. Subsequent to control panel reconfigurations, the crew reported after Station 9 that the navigation system distance, range, and bearing indications were not updating (reference paragraph 20.10) and during an amps check between Stations 6 and 8 on EVA 2, Battery #2 read zero amps (Reference paragraph 20.8.2).
- c. In the LRV instrumentation system, the crew reported at post deployment checkout that four of six meters were off scale low (reference paragraph 20.8.3) and that the rear steering system was inoperative (reference paragraph 20.8.4). On EVA 2 the vehicle attitude indicator pitch scale debonded and fell off (reference paragraph 20.10). Also, on EVA 2 the amp-hour meter #2 indication increased and the amp-hour meter #1 indication decreased much faster than expected (reference paragraph 20.8.5). On EVA 3 the Battery #1 temperature meter indicated

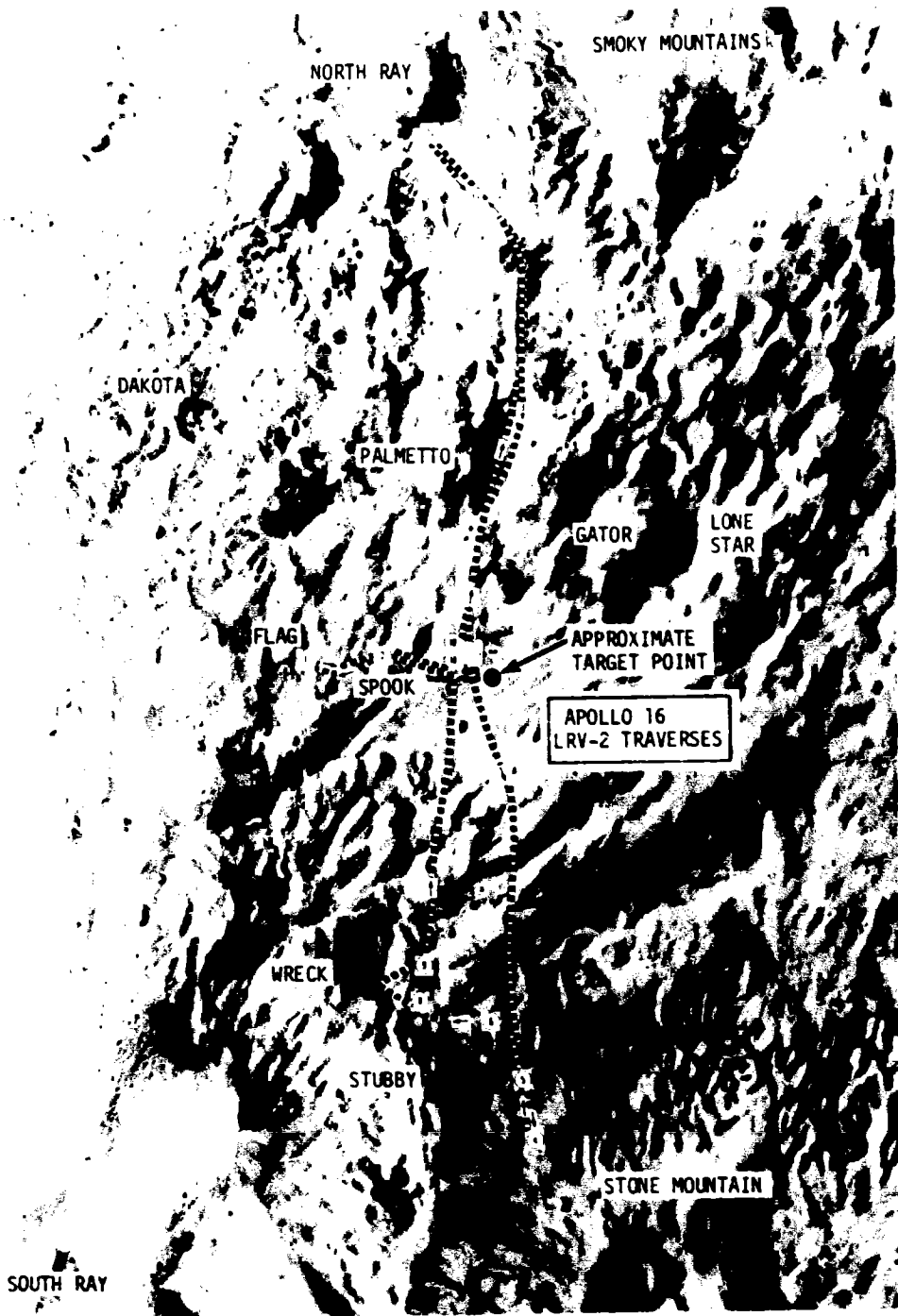


Figure 20-1. Apollo 16 LRV-2 Traverses

off scale low (Reference paragraph 20.8.3).

- d. The right rear fender extension was bumped by a crewman and knocked off on EVA 2.

## 20.2 DEPLOYMENT

Deployment of the LRV from the LM was completed successfully using less than 10 minutes of crew time. The operation was smooth and no significant problems were encountered. The landing attitude of the LM was favorable (less than 3° inclination) and did not adversely affect the operation. Three minor irregularities were noticed; (1) both walking hinges were unlatched and had to be latched by the crew prior to beginning deployment, (2) the aft wheels did not lock during the course of the operation and were locked by the crew, however, the wheels would have eventually locked when the LRV reached the lunar surface, and (3) the chassis lock pins did not seat fully in place but the crew had no difficulty in seating the pins by using the deployment assist tool. Even though these occurrences were deviations from design performance, they were anticipated and normal deployment procedures were adequate to handle them.

LRV set up and checkout required less than 9 minutes of crew time. During checkout four of six meters and rear steering were inoperative. These are discussed in paragraphs 20.8.3 and 20.8.4, respectively.

## 20.3 LRV TO STOWED PAYLOAD INTERFACE

The interfaces between the stowed payloads and LRV were satisfactory.

## 20.4 LUNAR TRAFFICABILITY ENVIRONMENT

The terrain created no unusual operating problems for the LRV. In general, the lunar surface character was gently undulated, hummocky, and abundantly cratered. It was littered in some areas by boulders (see Figure 20-2), often up to 25 centimeters in diameter which contributed to the higher average wander factor of 22.2 percent (see Performance Table 20-1). Pre-mission planning assumed a wander factor of 10 percent based on Apollo 15 data and on surface details that were discernible on 20 meter resolution photographs. The high wander factor seen on EVA 1 (40 percent) is attributed to the initial driving conservatism and to the zig-zag steering mode employed to compensate for poor visibility caused by driving down sun.


The crew reported driving was easy on a level surface relatively free of obstacles. On this type of surface the indicated vehicle speed ranged between 11 kph and 14 kph.

On the basis of crew debriefings and EVA photographic coverage, it appears that the LRV was operated uphill and downhill on slopes of 20 degrees or more. Because of its light weight and the excellent traction



Figure 20-2. Lunar Surface Photographs

Table 20-1. LRV Performance Summary

	EVA 1	EVA 2	EVA 3	TOTAL	PRE-MISSION
Drive Time (HR:MIN:SEC)	00:43	1:31	1:12	3:26	3:41
Odometer Distance (KM)	4.2	11.3 (Estimated)	11.4	26.9	27.67
Map Distance (KM)	3.0	9.0	10.0	22.0	25.0
Ride Time (MIN)	Approx. 43	Approx. 91	Approx. 72	--	--
Park Time (MIN)	Approx. 219	Approx. 236	Approx. 146	--	--
Total Time of Traverse (MIN)	Approx. 262	Approx. 327	Approx. 218	--	--
Average Velocity (KM/HR)	5.87	7.43	9.5	7.8	7.5
Mobility Rate (KM/HR)	4.17	5.92	8.3	6.36	7.3
Energy Rate (Amp-Hr/Km - LRV Only)	2.2	2.26	1.9	2.1	3.0
Amp-Hours Consumed LRV	9.2 (13.9)	25.6 (43.00)	21.76 (21.76)	56.6 (88.7)	114
LCRU	14.7	17.4	0	32.1	
Maximum Speed Reported (KPH)	11	11	11-14 (17 Down)	--	--
Maximum Slope Reported (Degrees)	--	20°	15° Up and Down	--	--
Number of Navigation Checks	0	1	0	1	3
Number of Navigation Updates	0	0	0	0	3
Navigation Closure Error (M)	0		0	0	0.2
Maximum Position Error (M)	100	100	100	--	280
Gyro Drift Rate (Degrees/Per Hour)	None	None	None	None	1.6
Gyro Misalignment	Small	Small	Small	--	--
Wander Factor & Slip (Percent)	40	26	14	22.2	10.0

Definitions

Map Distance - Map distance traveled, neglecting deviations around small craters.

Total Ride Time - The time spent riding, including minor stops, Grand Prix Runs, from departure to arrival at the LM.


Ride Time - Total ride time minus Grand Prix and minor stops.

Average Velocity - The odometer reading at the end of the traverse divided by the ride time.

Mobility Rate - The map distance divided by the ride time.

Navigation Closure Error - The position error in the navigation system at the end of the traverse.

Wander Factor & Slip =  $\frac{\text{speed} - \text{mobility rate}}{\text{mobility rate}} \times 100\%$

 Navigation readouts stopped incrementing at a range of 2.6 Km.

obtained, the general performance of the vehicle on these slopes was satisfactory. Maneuvering the vehicle on slopes did not present any serious problems. It was reported that the vehicle could be controlled more easily on upslope than down-slope. Maximum speed reached was 17 kph down-slope. Vehicle traverse cross slope caused crew discomfort and was avoided whenever possible.

## 20.5 WHEEL SOIL INTERACTION

As on Apollo 15, the LRV made only a shallow imprint on the lunar surface. This crew observation is supported by numerous photographs obtained during the lunar surface EVA's. The depth of the wheel tracks averaged 1-1/2 cm (1/2 in) for a fully loaded LRV (vehicle, crew, payload). The LRV wheels (wire mesh/Chevron 50 percent by area) developed excellent traction in the lunar surface material. In most cases a sharp imprint of the Chevron tread was clearly discernible, indicating that the surface soil possessed a small amount of cohesion and the amount of wheel slip was minimal. The shallow wheel track indicates the good flotation provided by the Chevrons and also indicates that the primary energy losses were due to compaction and rolling resistance and that bulldozing was minimal. This observation is supported by the small error of traverse closure in the navigation system.

## 20.6 LOCOMOTION PERFORMANCE

The locomotion performance of the LRV was satisfactory and met all of the demands required by the Apollo 16 mission. Comparison of the LRV amp-hour integrator readings with pre-flight predictions indicates that the LRV power usage was slightly less than expected. This comparison is shown in Figure 20-3. Locomotion performance is contained in Table 20-1.

Amp-hour readings received beyond Station 9, EVA 2 were questionable due to an amp-hour integrator problem (refer to paragraph 20.8.5). Enough data points had been obtained to allow the assumption of a soil type for use in post mission analysis. This same soil type, which seems to give excellent results for Apollo 16, also gave the best overall results for the post Apollo 15 analysis. This consistency of soil characteristics should permit improved prediction of power consumption for Apollo 17.

## 20.7 MECHANICAL SYSTEMS

### 20.7.1 Harmonic Drive

The harmonic drive performed satisfactorily; no excessive power consumption or temperatures were noted nor was any mechanical malfunction apparent.

### 20.7.2 Wheels and Suspension

The wheels and suspension systems performed as expected. The maximum vehicle speed/obstacle size encountered was 8-10 kph over an obstacle 30 centimeters high. The suspension was noted to "bottom out." This also occurred during the Apollo 15 mission and is considered normal whenever the LRV is traveling at a relatively high velocity and encounters obstacles approximately

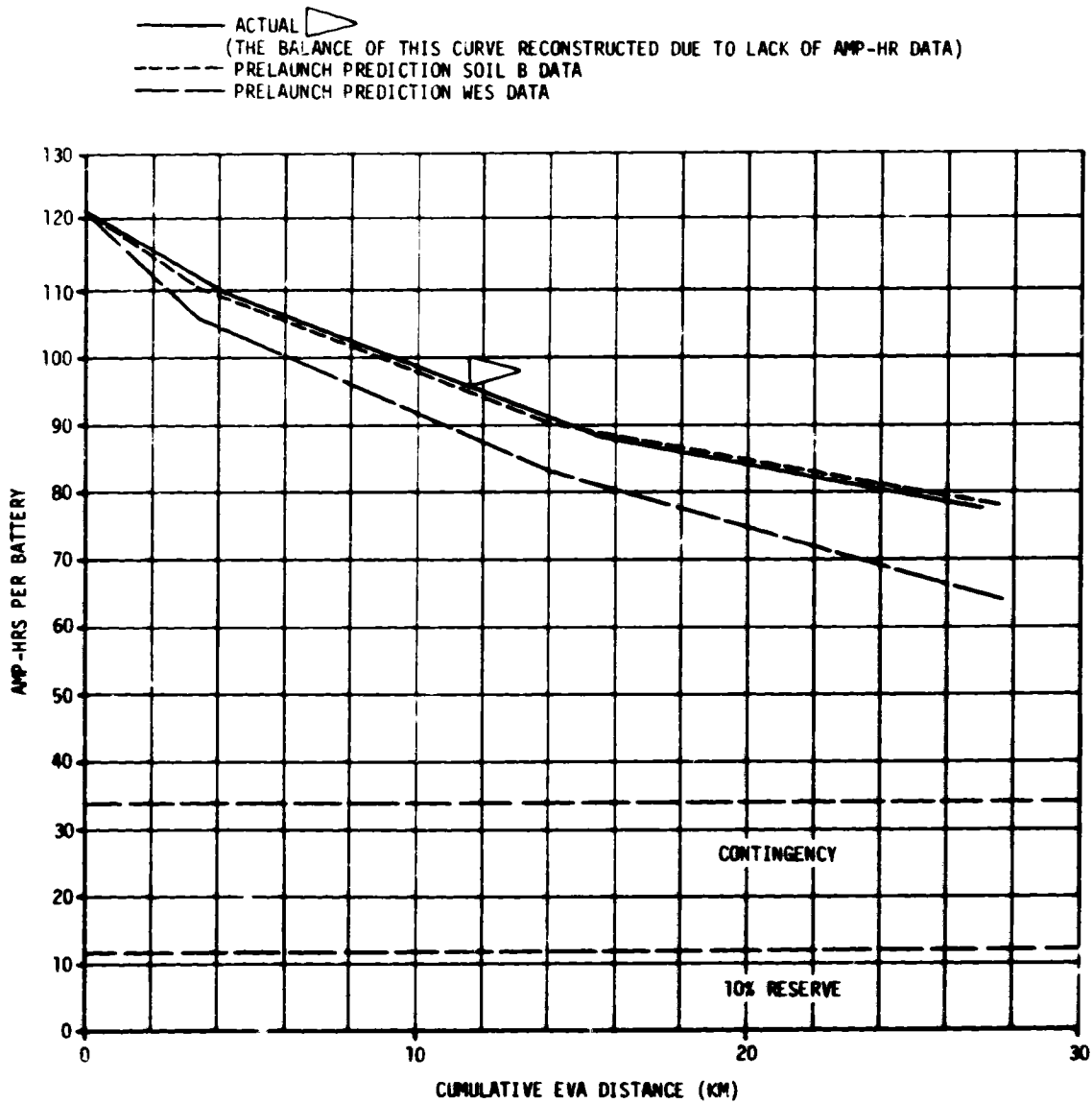


Figure 20.3 LRV Power Usage



30 centimeters high.

### 20.7.3 Brakes

The LRV braking capability was reported to be excellent. The wheels tended to completely lock and the vehicle came to a complete stop within one to three vehicle lengths. There was no instance of "fade" even during prolonged down-slope braking.

### 20.7.4 Stability

The LRV was stable and had no tendency to roll. The response was predominantly a pitching motion producing a low frequency "rocking" type ride. The wheels became airborne occasionally, but did not cause a controllability problem. Driving cross slope, although stable, proved to be an uncomfortable driving condition.

### 20.7.5 Hand Controller

The hand controller performed satisfactorily.

### 20.7.6 Loads

Instrumentation was not available on the LRV to ascertain induced loads. No evidence of load problems was reported.

## 20.8 ELECTRICAL SYSTEMS

The LRV electrical systems performed with no major impact on the mission. Electrical anomalies are elaborated on in the following paragraphs.

### 20.8.1 Batteries

The battery capacity was more than adequate for the mission. Amp-hour measurements were erratic after Station 9 of EVA 2, but amp-hour usage including LCRU, was estimated to be 88.7 out of a nominal capacity of 242 amp-hours for the two batteries.

### 20.8.2 Traction Drive System

The traction drive system performed satisfactorily. There were no indications of any off nominal conditions within the traction drives and all four units performed as expected. The maximum temperature of any traction drive unit was 225°F which occurred on EVA 3.

During amps checks between Stations 6 and 8 on EVA 2, Battery #2 ammeter read zero. During a malfunction procedure at Station 8, the crew found that the Pulse Width Modulator (PWM) Select Switch had been inadvertently tripped from PWM "Both" to PWM "1", in spite of it being a guarded switch. This prevented a drive enable pulse from being received by the rear drive,

therefore no current was being drawn from Battery #2. The switch was probably hit during retrieval of the stowed LMP seat belt or during operation of the 16mm Data Acquisition Camera. There was no mission impact. Rear drive enable was switched to PWM-1 for the remainder of EVA 2 and the console was returned to normal configuration for start of EVA 3.

### 20.8.3 Distribution System

The electrical distribution system provided power to all functions as required. The following two instrumentation anomalies were noted:

- a. At post deployment checkout, amp-hour Meter #2, Battery #2 voltmeter, Battery #1 and Battery #2 temperature meter failed to indicate. All meters operated satisfactorily upon leaving the Modularized Equipment Stowage Assembly (MESA) stop. No single failure point has been identified that would explain all the meter malfunctions. Tests on four similar meters were performed at MSFC in an attempt to duplicate the anomaly. The meters were first checked in a thermal vacuum chamber to -60°F after which they responded to an applied voltage without failure. A cold soak in the chamber to -30°F for four days was conducted, again with no failures. A cold soak test of the LRV Qualification Unit will be conducted in an attempt to duplicate the failure.
- b. Battery #1 temperature meter was off scale low at the end of EVA 3. Possible causes are meter or sensor failure. The exact cause cannot be determined because of lack of data.

### 20.8.4 Steering

The LRV steering performed satisfactorily for all three EVA's. However, on the initial drive from post deployment checkout to the MESA stop, the crew reported no rear steering. Upon leaving the MESA, both steering systems were operational. The cause has not been determined, however, it may be associated with the meter concerns in paragraph 20.8.3. Investigation is continuing. At the beginning of EVA 1, the crew found the double Ackerman steering very sensitive, and after a short drive crew reported the steering mode excellent.

### 20.8.5 Amp-Hour Integrator

The amp-hour integrator readings diverged during EVA 2. At Station 9 the amp-hour meter #2 indication increased (i.e., battery charging which is not possible). Also, Battery #1 amp-hour meter indication decreased much faster than expected based on previously observed power usage. This condition existed for the remainder of the mission. No explanation has been developed for the amp-hour integrator behavior. No single failure has been identified which would cause both amp-hour integrators to perform as they did. There was no impact to the Apollo 16 mission as a power consumption trend had already been established from prior EVA 1 and EVA 2 data. Investigation is continuing.

## 20.9 CONTROL AND DISPLAY CONSOLE

The control and display console displays proved adequate. All switches and circuit breakers were satisfactory and within reach of the Commander (CDR). However, some difficulty was apparently experienced during panel switch/circuit breaker reconfiguration. This is discussed in paragraph 20.10, Navigation System.

## 20.10 NAVIGATION SYSTEM

The Navigation System satisfactorily supported the Apollo 16 Mission except for the loss of distance, range, and bearing calculations during EVA 2. The Navigation System stayed well within the mission planning value for position error (100 meters) during EVA's 1 and 3 and did not require an update during lunar operation. Table 20-1 contains a summary of navigation performance.

After leaving Station 9, EVA 2, (approximately 1.2 km traveled) the crew reported that the distance, range, and bearing indications were not updating. This condition remained for the balance of EVA 2. To be operative, the odometer logic requires inputs from at least three powered wheels. Refer to Figure 20-4 for Navigation System Block Diagram.

Post flight analysis using crew photographs and mission transcripts substantiate crew navigation readouts from Station 8 to Station 9 and the final readout on reaching Station 9, indicating that the Navigation System problem was due to an occurrence at Station 9.

Heading and speed indicators operated normally throughout EVA 2, indicating that power was on the Navigation System, that pulses were being received from the right rear (RR) wheel, the 400 Hz inverter was operating, and the +16 vdc power supply was operative. At the Apollo Lunar Surface Experiments Package (ALSEP) site the navigation reset was activated and all indicators reset to zero, indicating that power was available at the counters and that they were not mechanically bound. The front wheel temperatures were off scale low and the rear wheel temperatures were 210°F indicating higher use of rear wheels. This was the only time any wheel temperature indicated above 200°F (lowest indication on temperature scale) on EVA 2.

At Station 9, in an attempt to control battery temperatures, all LRV power was removed from Battery #2 by pulling Bus D circuit breaker. Refer to Figure 20-5 for an LRV power schematic. Previously, at Station 8, Bus C circuit breaker had been pulled to switch LCRU power to Battery #1 (Bus C and D circuit breakers control all power from Battery #2; Bus A and B circuit breakers control all power from Battery #1). Refer to Figure 20-6 for a Control and Display Panel configuration and circuit breaker location. Loss of front wheel power could have resulted from either (a) the two front drive power switches (refer to Figure 20-6) being switched from Bus A to some

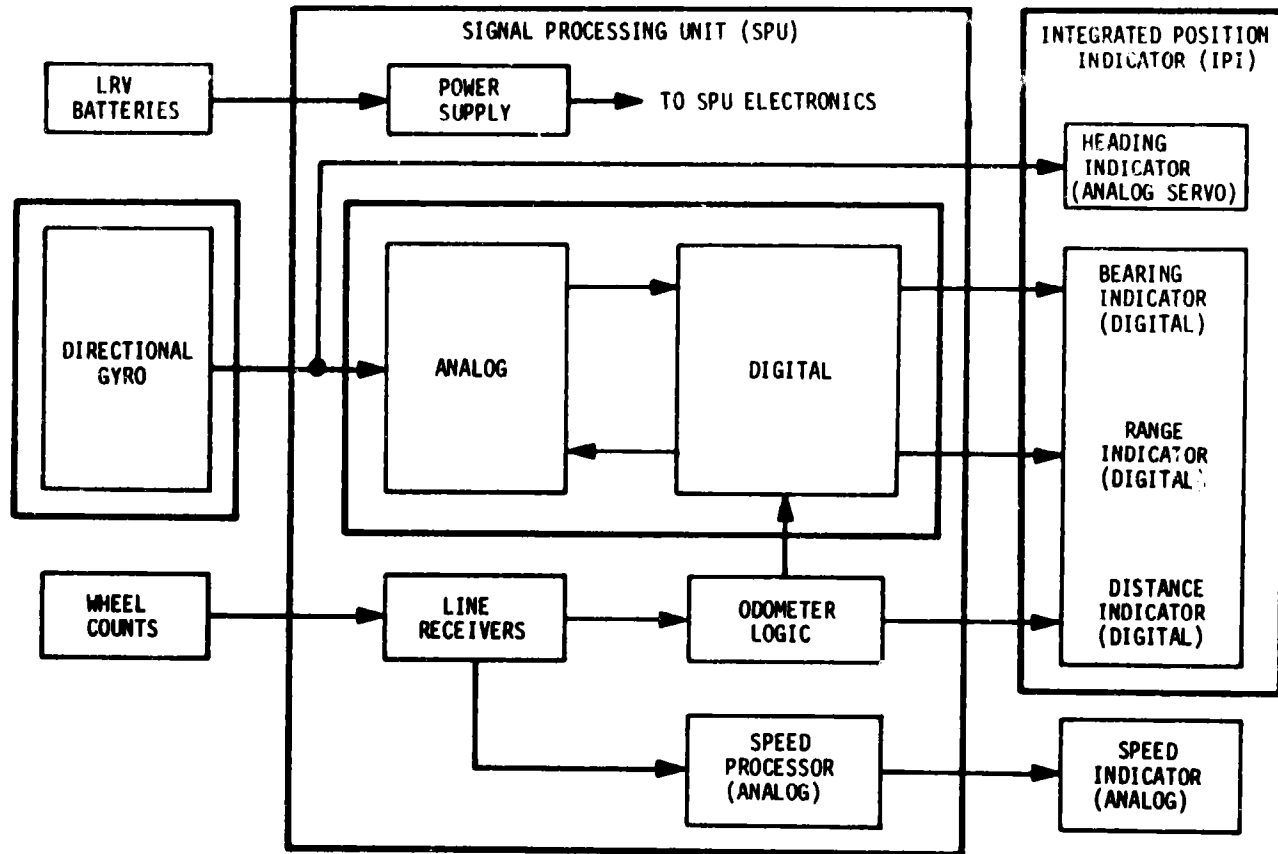


Figure 20-4. Navigation Subsystem Block Diagram

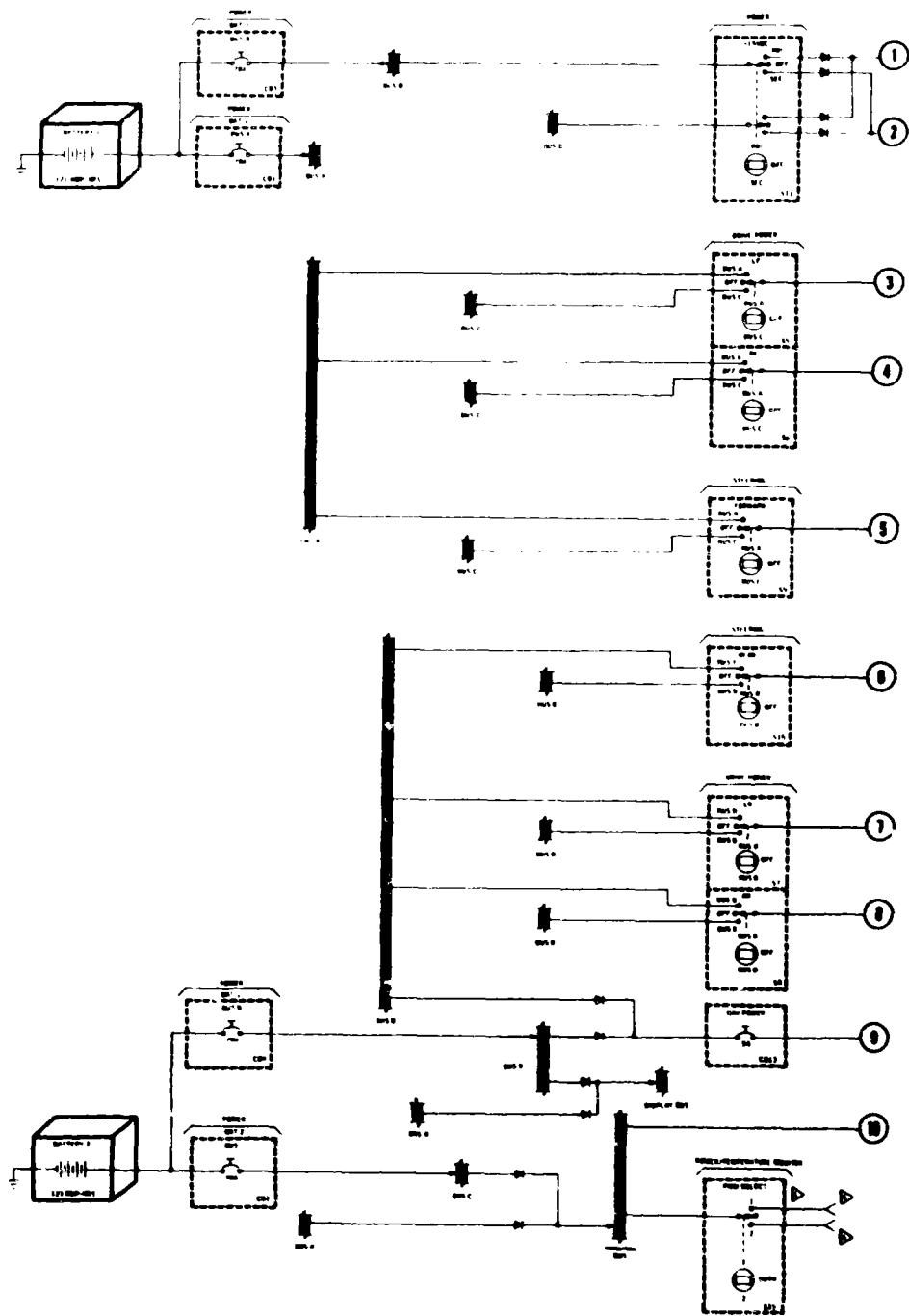


Figure 20-5. LRV Power Schematic (Sheet 1 of 2)

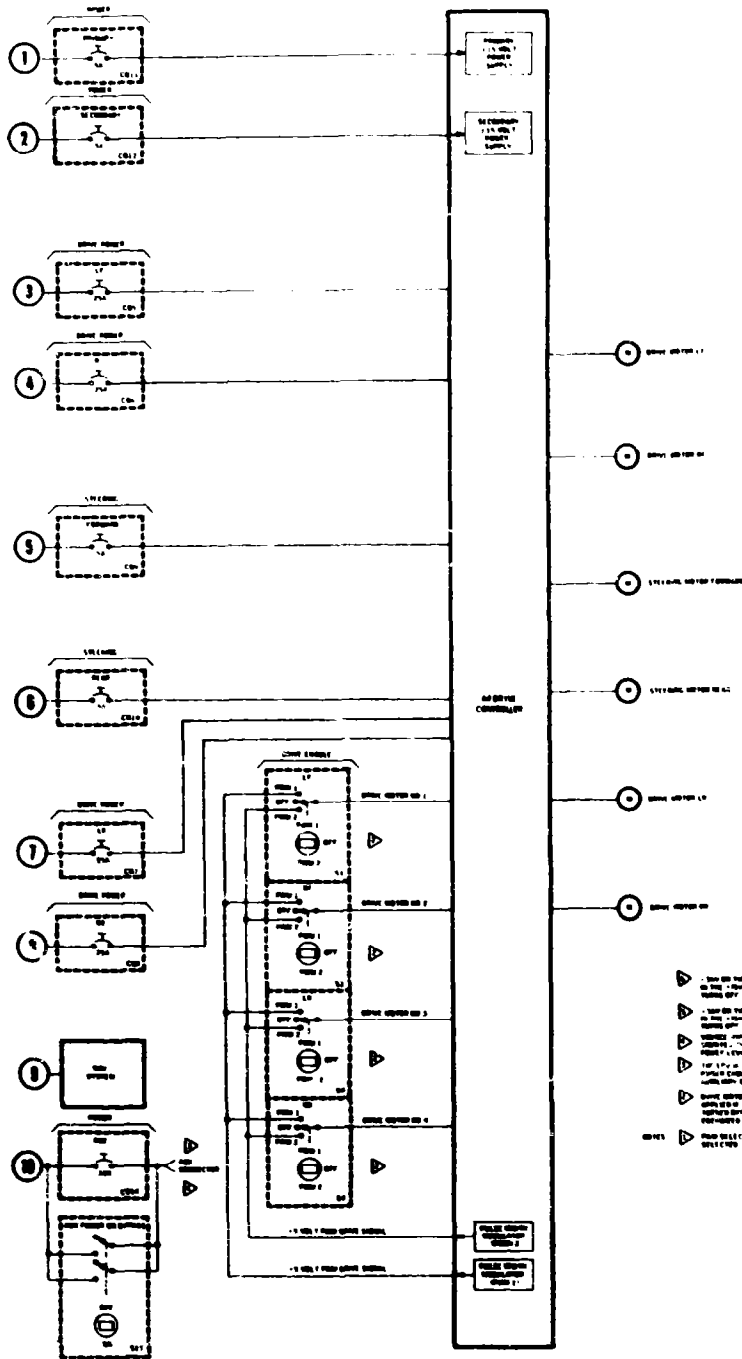


Figure 20-5. LRV Power Schematic (Sheet 2 of 2)

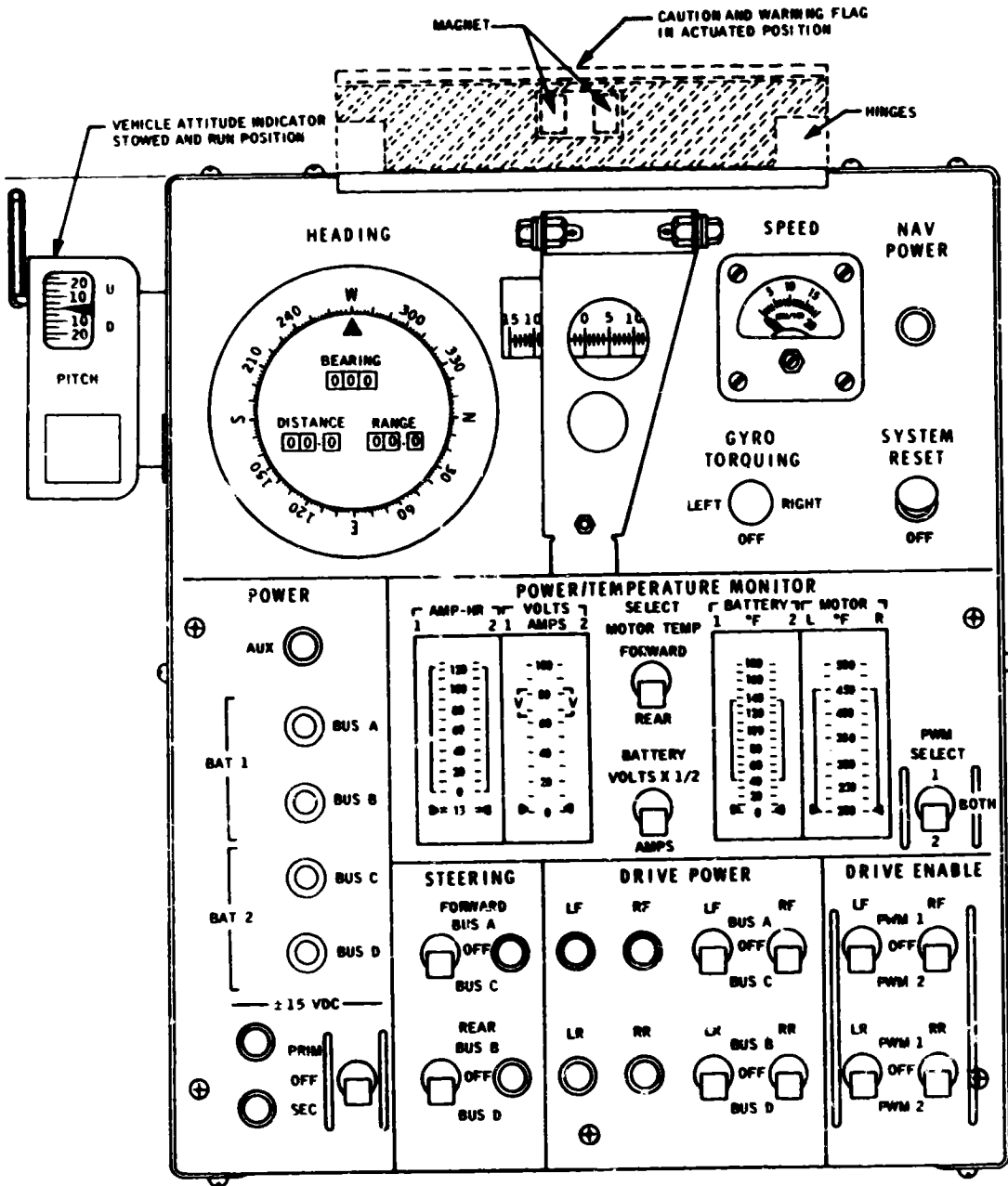


Figure 20-6. Control and Display Panel Configuration

other position or (b) an intermittent component or wiring failure to the front drive power system.

The probability of a component or wiring failure is considered low because the Navigation System operated normally through EVA 3 when the Control and Display Panel was returned to normal configuration. The most probable cause is the inadvertent switching of the front drive power switches.

Laboratory tests on the Qual Vehicle and on a subsystem breadboard indicate that the only failures within the Navigation Subsystem which would result in conditions experienced (i.e., lack of distance, bearing, and range update) would be a malfunction in the third-fastest-wheel selection logic or the five volt power supply. The only condition tested on the Qualification Vehicle which reproduced the anomaly was the removal of power from the two front wheels by switching the front drive power switches from Bus A. This permits only two odometer signals to be received by the odometer logic circuit, thus preventing selection of the third-fastest-wheel for the distance, range, or bearing calculations.

There was no indication from the crew (through review of flight transcript or crew debriefing) that power was removed from the front wheels at Station 9. However, no other explanation has been developed which would account for this condition.

Also on EVA 2, the LRV vehicle attitude indicator pitch scale debonded and fell off. There was no impact on the mission as the pointer worked and the crew could estimate a reading adequately. A similar problem occurred during Qualification test of the LRV, and a new adhesive was incorporated for all flight units (LRV-1 through -3). No deficiencies in the LRV-3 bonding procedure have been identified and no change is planned for LRV-3. The LRV-3 vehicle attitude indicator will undergo visual inspection during prelaunch checkout at Kennedy Space Center (KSC).

## 20.11 CREW STATION

The crew reported no problem with the basic crew station. The new seat belt design functioned satisfactorily. The adjustments determined during the KC-135, 1/6 G test flights proved to be very good, with only minor adjustments required on the lunar surface. Access and stowage was adequate, however, retrieval of the LMP belt from its stowage loop on the camera staff could have caused the PWM select switch condition discussed in paragraph 20.8.2.

The Velcro used to tie down the seat in stowed position was described as difficult to remove. The mated surface of the Velcro is 2 inches by 3.5 inches. No changes are planned for LRV-3 at this time.



The crew reported that the right rear fender extension was bumped and knocked off while working around the aft end of the LRV. This created a significant problem in that excessive dust was thrown forward onto the crew and LRV by the rear wheel. A redesign of the fender extension stop is being incorporated to eliminate this problem.

## 20.12 THERMAL

### 20.12.1 Summary

The thermal control system performed satisfactorily, during the transportation phase. On the lunar surface, higher battery temperatures than predicted were noted and special operating procedures were implemented in an attempt to control battery temperature. In spite of these procedures, the temperatures of both batteries exceeded specification (125°F) before the end of EVA 3.

### 20.12.2 Transportation Phase

Analysis indicates all LRV components were maintained within storage temperature limits during the transportation phase (translunar coast, lunar orbit, pre-deployment attitude).

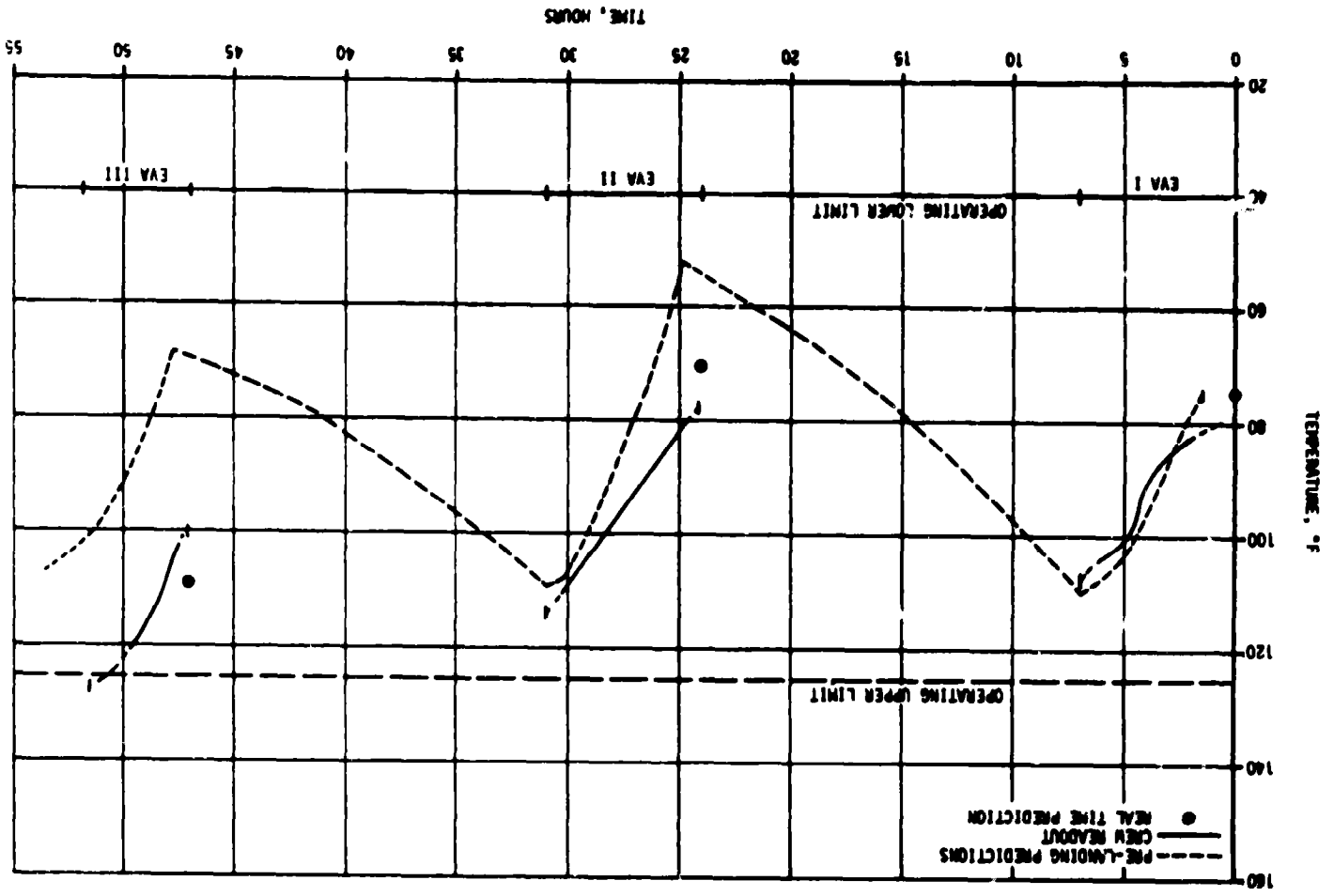
### 20.12.3 Extravehicular Activity Periods

All LRV components remained within operational temperature limits throughout the three lunar surface EVA's with the exception of the batteries. As predicted, motor temperatures were off-scale low throughout most of the EVA's. The actual and predicted maximum motor temperatures were 225°F (107°C) and 228°F (109°C), respectively.

The battery cooldown between EVA's 1 and 2 and between EVA's 2 and 3 was insufficient causing battery over temperature before the end of the mission. Refer to Figures 20-7 and 20-8 for temperature profile. The indicated battery temperatures at EVA 1 initiation were 82°F (28°C), slightly higher than the 75°F (24°C) that was predicted based on delayed landing time. During EVA 1, Battery #1 and #2 temperatures increased to 104°F (40°C) and 105°F (41°C) respectively, essentially as expected. At the beginning of EVA 2, the temperatures of both batteries was much higher than expected. Refer to Figures 20-7 and 20-8.

During EVA 2, battery load switching was performed to prevent Battery #2 from exceeding the 125°F (52°C) operating limit (refer to paragraph 20.10). At the end of EVA 2, Battery #1 and #2 temperatures were 110°F (43°C) and 120°F (49°C). Again, at the beginning of EVA 3, both battery temperatures were much higher than the pre-landing predictions. Battery load switching (all power except Navigation System removed from Battery #2 at Station 11) was again tried during EVA 3 in an attempt to control battery temperature. However, both batteries exceeded the 125°F (52°C) design limit (Battery #2 at Station 11 and Battery No. 1 at Station 13). It was recommended that the battery dust covers be opened at Station 11,

Figure 20-7. Battery No. 1 Temperature



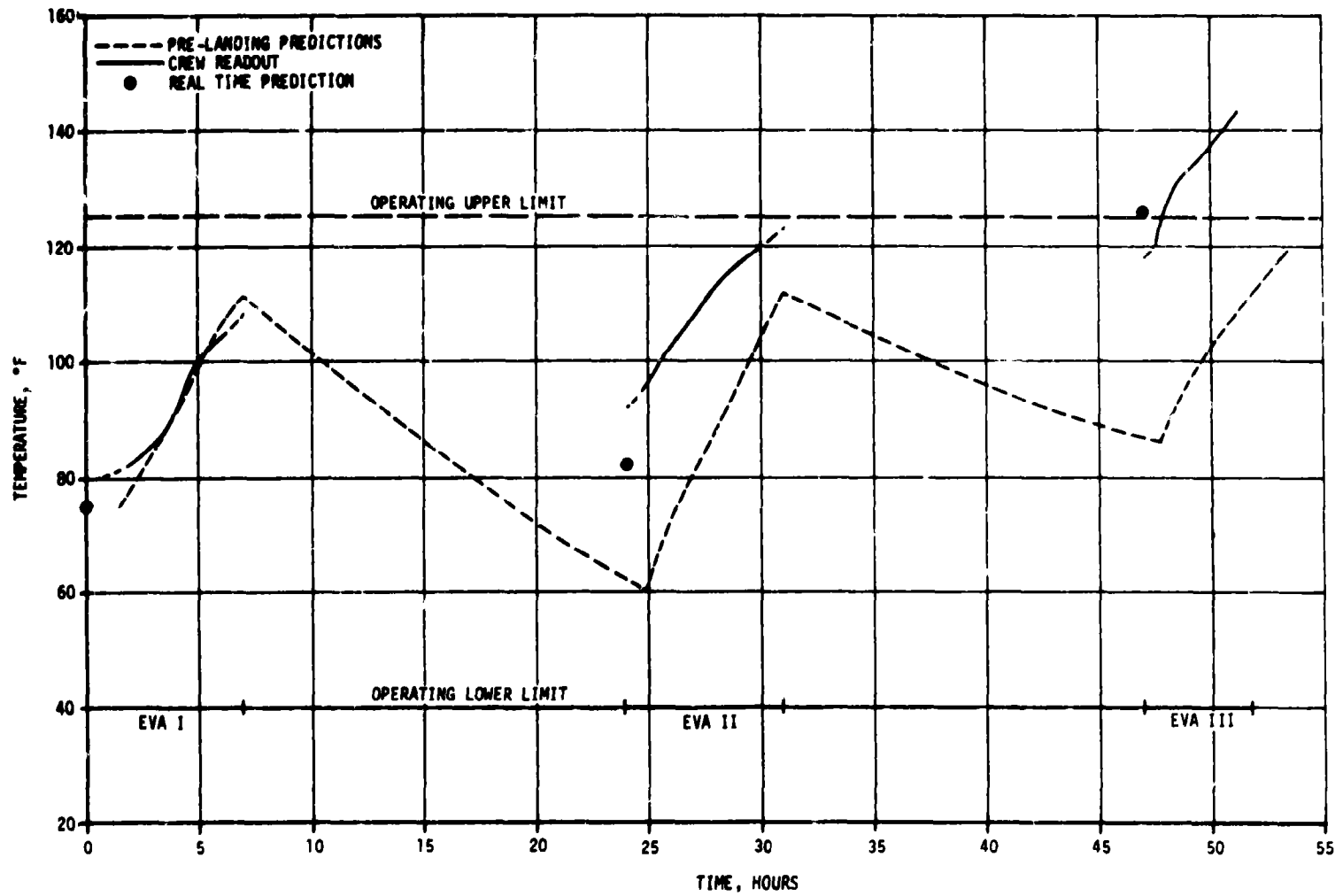


Figure 20-8. Battery No. 2 Temperature

but crew timeline limitations prevented the implementation.

Battery #2 indicated a closeout reading of 143°F (62°C), however, it was still functional. Battery #1 indicator read off scale low at the end of EVA 3 (refer to paragraph 20.8.3b), but the battery was still functional. Battery temperature was estimated to be 130°F (54°C).

Two conditions have been identified as prime contributors to the insufficient battery cooldown between EVA's 1 and 2 and EVA's 2 and 3.

- a. Dust accumulation on LRV battery mirrors degraded normal cooldown. The crew reported at the end of both EVA 1 and EVA 2 that the LRV battery mirrors remained dust covered after having been brushed as well as possible. At best the value of dusting is limited and every precaution should be taken to preclude getting dust on the mirrors.
- b. The LRV was parked too close to the LM between EVA's causing radiant heating from the LM to the LRV. A heading orientation was imposed and followed by the crew, but no distance constraint from the LM was included in the parking requirements. This parking condition was observed from television coverage at the closeout of EVA 2. The crew had already exceeded the seven hour EVA time, however, and were not asked to repark the LRV. Video tapes of EVA 1 parking were subsequently reviewed and it was concluded the LM radiant heating could also have contributed to the post EVA 1 cooldown degradation. A parking limitation relative to the LM will be incorporated for the LRV-3 mission.

### 20.13 STRUCTURAL

There was no structural damage to the load bearing members of the LRV but a crewman bumped and dislodged a rear fender extension (refer to paragraph 20.11).

### 20.14 LUNAR ROVING VEHICLE CONFIGURATION

LRV-2 was essentially unchanged from LRV-1 which was flown on Apollo 15. Refer to Saturn V Launch Vehicle Flight Evaluation Report - AS-510, Apollo 15 Mission for Vehicle Description.

Significant configuration changes are contained in Table 20-3.

Table 20-2. LRV Significant Configuration Changes

SYSTEM	CHANGE	REASON
Payload	Stow gnomon bag on LRV prior to launch rather than on lunar surface.	Reduce crew operation on lunar surface.
Crew Station	Revised seat belt	Seat belt operation on LRV-1 was very time consuming. Seat belt was revised for LRV-2 to prevent belt hangup on console test connector and to reduce fastening time.
Payload/Electrical	Replace auxiliary power 7.5 amp circuit breaker with 10.0 amp circuit breaker	MSC thermal analysis indicated 7.5 amp auxiliary power circuit breaker not adequate should LRV battery power be required for LCRU power on EVA-3.
Payload/Electrical	Add auxiliary power circuit breaker bypass switch	Added to prevent LCRU TV dropout after LM liftoff. Switch will be used after EVA 3 to disable auxiliary power circuit breaker and hardwire LCRU to LRV battery power.
Thermal	Add dust seal and thermal reflective tape to LRV forward chassis	Added to reduce temperature of forward chassis (battery, Signal Processing Unit, Drive Control Electronics).
Electrical	Replace existing shunts of 1 millivolt/amp scale factor with shunt of 2 millivolts/amp scale factor	To gain more accurate engineering data. LRV-1 amp meter readings were off scale low.
Electrical	Use of LRV battery to power LCRU on EVA 1 and EVA 2.	To conserve crew time. Crew will not have to change out LCRU batteries on EVA 1 or EVA 2.

## APPENDIX A

### ATMOSPHERE

#### A.1 SUMMARY

This appendix presents a summary of the atmospheric environment at launch time of the AS-511. The format of these data is similar to that presented on previous launches of Saturn vehicles to permit comparisons. Surface and upper levels winds, and thermodynamic data near launch time are given.

#### A.2 GENERAL ATMOSPHERIC CONDITIONS AT LAUNCH TIME

At launch time, the Cape Kennedy launch area was experiencing fair weather resulting from a ridge of high pressure extending westward, from the Atlantic, through central Florida. See Figure A-1.

Surface winds in the Cape Kennedy area were light and southwesterly as shown in Table A-1. Wind flow aloft is shown in Figure A-2 (500 millibar level). The maximum wind belt was located north of Florida, giving less intense wind flow aloft over the Cape Kennedy area.

#### A.3 SURFACE OBSERVATIONS AT LAUNCH TIME

At launch time, total sky cover was 2/10, consisting of scattered cumulus at 0.9 kilometers (3,000 ft). Surface ambient temperature was 304°K (88.2°F). During ascent the vehicle did not pass through any clouds. All surface observations at launch time are summarized in Table A-1. Solar radiation data are not given due to instrumentation problems.

#### A.4 UPPER AIR MEASUREMENTS

Data were used from three of the upper air wind systems to compile the final meteorological tape. Table A-2 summarizes the wind data systems used. Only the Rawinsonde and the Loki Dart meteorological rocket data were used in the upper level atmospheric thermodynamic analyses.

##### A.4.1 Wind Speed

Wind speeds were light, being 6.3 m/s (12.2 knots) at the surface and increasing to a peak of 26.1 m/s (50.7 knots) at 11.85 kilometers

(38,880 ft). The winds began decreasing above this altitude, becoming relatively light to 61.0 kilometers (200,129 ft) altitude as shown in Figure A-3. Maximum dynamic pressure occurred at 14.31 kilometers (46,948 ft). At max Q altitude, the wind speed and direction was 11.2 m/s (21.8 knots), from 265 degrees.

#### A.4.2 Wind Direction

At launch time, the surface wind direction was 269 degrees. The wind direction varied, between south and west, with increasing altitude over the entire profile. Figure A-4 shows the complete wind direction versus altitude profile. As shown in Figure A-4, wind directions were quite variable at altitudes with low wind speeds.

#### A.4.3 Pitch Wind Component

The pitch wind velocity component (component parallel to the horizontal projection of the flight path) at the surface was a tailwind of 6.0 m/s (11.7 knots). A maximum tailwind of 26.0 m/s (50.5 knots) was observed at 11.85 kilometers (38,880 ft) altitude. See Figure A-5.

#### A.4.4 Yaw Wind Component

The yaw wind velocity component (component normal to the horizontal projection of the flight path) at the surface was a wind from the left of 1.8 m/s (3.6 knots). The peak yaw wind velocity in the high dynamic pressure region was from the left of 12.5 m/s (24.2 knots) at 15.50 kilometers (50,850 ft). See Figure A-6.

#### A.4.5 Component Wind Shears

The largest component wind shear ( $\Delta h = 1000$  m) in the altitude range of 8 to 16 kilometers (26,247 to 52,493 ft) was a pitch shear of  $0.0095 \text{ sec}^{-1}$  at 13.65 kilometers (44,780 ft). The largest yaw wind shear, at these lower levels, was  $0.0114 \text{ sec}^{-1}$  at 15.50 kilometers (50,850 ft). See Figure A-7.

#### A.4.6 Extreme Wind Data in the High Dynamic Region

A summary of the maximum wind speeds and wind components is given in Table A-3. A summary of the extreme wind shear values ( $\Delta h = 1000$  meters) is given in Table A-4.

### A.5 THERMODYNAMIC DATA

Comparisons of the thermodynamic data taken at AS-511 launch time with the annual Patrick Reference Atmosphere, 1963 (PRA-63) for temperature, pressure, density, and Optical Index of Refraction are shown in Figures A-8 and A-9, and are discussed in the following paragraphs.

### A.5.1 Temperature

Atmospheric temperature differences were small, generally deviating less than 4 percent from the PRA-63, below 59 kilometers (193,570 ft) altitude. Temperatures did deviate to -4.88 percent of the PRA-63 value at 18.75 km (61,515 ft). Air temperatures were generally warmer than the PRA-63 from the surface through 15 kilometers (49,210 ft). Above this altitude, temperatures became cooler than the PRA-63 values through 29.5 km (96,780 ft). Above this level temperatures were again warmer than the PRA-63. See Figure A-8 for the complete profile.

### A.5.2 Atmospheric Density

Atmospheric density deviations were small, being within 5 percent of the PRA-63 for nearly all altitudes. Surface density was 1.85 percent less than the PRA-63 density value. The density deviation reached a maximum of 7.34 percent greater than the PRA-63 value at 18.75 kilometers (61,515 ft) as shown in Figure A-9.

### A.5.3 Optical Index of Refraction

Optical Index of Refraction was  $11.4 \times 10^{-6}$  units lower than the corresponding value of the PRA-63. The deviation became less negative with altitude, and it approximated the PRA-63 at high altitudes, as is shown in Figure A-9. The maximum value of the Optical Index of Refraction was  $1.94 \times 10^{-6}$  units greater than the PRA-63 at 17.2 kilometers (56,430 ft).

## A.6 COMPARISON OF SELECTED ATMOSPHERIC DATA FOR SATURN V LAUNCHES

A summary of the atmospheric data for each Saturn V launch is shown in Table A-5.



Table A-1. Surface Observations at AS-511 Launch Time

LOCATION	TIME AFTER T-0 (MIN)	PRES-SURE N/CM <sup>2</sup> (PSIA)	TEMPERATURE °K (°F)	DEW POINT °K (°F)	VISI-BILITY KM (STAT MI)	AMOUNT (TENTHS)	SKY COVER TYPE	HEIGHT OF BASE METERS (FEET)	WIND*	
									SPEED M/S (KNOTS)	DIR (DEG)
NASA 150 m Ground Wind Tower	0	10.183 (14.77)	304.4 (88.2)	290.2 (52.6)	16 (10)	2	Cumulus	914 (3,000)	3.2 <sup>***</sup> (6.2 <sup>***</sup> )	232 <sup>***</sup>
Cape Kennedy Rawinsonde Measurements	10	10.180 (14.76)	302.5 (84.7)	294.2 (69.8)	--	--	--	--	5.0 (9.7)	150
Pad 38A Lightpole 18.3 m (60.0 ft) <sup>**</sup>	0	--	--	--	--	--	--	--	6.3 (12.2)	269
LUT Pad 38A 161.5 m (530 ft) <sup>**</sup>	0	--	--	--	--	--	--	--	5.1 (10.0)	256

\* Instantaneous readings at T-0, unless otherwise noted.  
<sup>\*\*</sup> Above natural grade.  
<sup>\*\*\*</sup> 10 minute average about T-0.

Table A-2. Systems Used to Measure Upper Air Wind Data for AS-511

TYPE OF DATA	RELEASE TIME		PORTION OF DATA USED			
	TIME (UT)	TIME AFTER T-0 (MIN)	START		END	
			ALTITUDE M (ft)	TIME AFTER T-0 (MIN)	ALTITUDE M (ft)	TIME AFTER T-0 (MIN)
FPS-16 Jimsphere	1812	18	150 (492)	18	16,000 (52,493)	72
Rawinsonde	1804	10	16,250 (53,313)	63	25,750 (84,481)	95
Loki Dart	1924	90	61,000 (200,129)	90	26,000 (85,301)	115

Table A-3. Maximum Wind Speed in High Dynamic Pressure Region for Apollo/Saturn 501 through Apollo/Saturn 511 Vehicles

VEHICLE NUMBER	MAXIMUM WIND			MAXIMUM WIND COMPONENTS			
	SPEED M/S (KNOTS)	DIR (DEG)	ALT KM (FT)	PITCH ( $W_x$ ) M/S (KNOTS)	ALT KM (FT)	YAW ( $W_z$ ) M/S (KNOTS)	ALT KM (FT)
AS-501	26.0 (50.5)	273	11.50 (37,700)	24.3 (47.2)	11.50 (37,700)	12.9 (25.1)	9.00 (29,500)
AS-502	27.1 (52.7)	255	12.00 (42,600)	27.1 (52.7)	12.00 (42,600)	12.9 (25.1)	15.75 (51,700)
AS-503	34.8 (67.6)	284	15.22 (49,900)	31.2 (60.6)	15.10 (49,500)	22.6 (43.9)	15.80 (51,800)
AS-504	76.2 (148.1)	264	11.73 (38,480)	74.5 (144.8)	11.70 (38,390)	21.7 (42.2)	11.43 (37,500)
AS-505	42.5 (82.6)	270	14.18 (46,520)	40.8 (79.3)	13.80 (45,280)	18.7 (36.3)	14.85 (48,720)
AS-506	9.6 (18.7)	297	11.40 (37,400)	7.6 (14.8)	11.18 (36,680)	7.1 (13.8)	12.05 (39,530)
AS-507	47.6 (92.5)	245	14.23 (46,670)	47.2 (91.7)	14.23 (46,670)	19.5 (37.9)	13.65 (44,780)
AS-508	55.6 (108.1)	252	13.58 (44,540)	55.6 (108.1)	13.58 (44,540)	15.0 (29.1)	12.98 (42,570)
AS-509	52.8 (102.6)	255	13.33 (43,720)	52.8 (102.6)	13.33 (43,720)	24.9 (48.5)	10.20 (33,460)
AS-510	18.6 (36.2)	063	13.75 (45,110)	17.8 (34.6)	13.73 (45,030)	7.3 (14.2)	13.43 (44,040)
AS-511	26.1 (50.7)	257	11.85 (38,880)	26.0 (50.5)	11.85 (38,880)	12.5 (24.2)	15.50 (50,850)

Table A-4. Extreme Wind Shear Values in the High Dynamic Pressure Region for Apollo/Saturn 501 through Apollo/Saturn 511 Vehicles

( $\Delta h = 1000 \text{ m}$ )				
VEHICLE NUMBER	PITCH PLANE		YAW PLANE	
	SHEAR (SEC <sup>-1</sup> )	ALTITUDE KM (FT)	SHEAR (SEC <sup>-1</sup> )	ALTITUDE KM (FT)
AS-501	0.0066	10.00 (32,800)	0.0067	10.00 (32,800)
AS-502	0.0125	14.90 (48,900)	0.0084	13.28 (43,500)
AS-503	0.0103	16.00 (52,500)	0.0157	15.78 (51,800)
AS-504	0.0248	15.15 (49,700)	0.0254	14.68 (48,160)
AS-505	0.0203	15.30 (50,200)	0.0125	15.53 (50,950)
AS-506	0.0077	14.78 (48,490)	0.0056	10.30 (33,790)
AS-507	0.0183	14.25 (46,750)	0.0178	14.58 (47,820)
AS-508	0.0166	15.43 (50,610)	0.0178	13.98 (45,850)
AS-509	0.0201	13.33 (43,720)	0.0251	11.85 (38,880)
AS-510	0.0110	11.23 (36,830)	0.0071	14.43 (47,330)
AS-511	0.0095	13.65 (44,780)	0.0114	15.50 (50,850)

Table A-5. Selected Atmospheric Observations for Apollo/Saturn 501 through Apollo/Saturn 511 Vehicle Launches at Kennedy Space Center, Florida

VEHICLE NUMBER	VEHICLE DATA			SURFACE DATA						IMFLIGHT CONDITIONS		
	DATE	TIME NEAREST MINUTE	LAUNCH COMPLEX	PRESSURE N/CM <sup>2</sup>	TEMPERATURE °C	RELATIVE HUMIDITY PERCENT	WIND*		CLOUDS	MAXIMUM WIND IN 8-16 KM LAYER		
							SPEED M/S	DIRECTION DEG		ALTITUDE KM	SPEED M/S	DIRECTION DEG
AS-501	9 Nov 67	0700 EST	39A	10.261	17.6	55	8.0	70	1/10 cumulus	11.50	26.0	273
AS-502	4 Apr 68	0700 EST	39A	10.200	20.9	83	5.4	132	5/10 stratocumulus, 1/10 cirrus	13.00	27.1	255
AS-503	21 Dec 68	0751 EST	39A	10.207	15.0	88	1.0	360	4/10 cirrus	15.22	34.8	284
AS-504	3 Mar 69	1100 EST	39A	10.095	19.6	61	6.9	160	7/10 stratocumulus, 10/10 altostratus	11.73	76.2	264
AS-505	18 May 69	1249 EDT	39B	10.190	26.7	75	8.2	125	4/10 cumulus, 2/10 altocumulus, 10/10 cirrus	14.18	42.5	270
AS-506	16 Jul 69	0932 EDT	39A	10.203	29.4	73	3.3	175	1/10 cumulus, 2/10 altocumulus, 9/10 cirrostratus	11.40	9.6	297
AS-507	14 Nov 69	1122 EST	39A	10.081	20.0	92	6.8	280	10/10 stratocumulus with rain	14.23	47.6	245
AS-508	11 Apr 70	1413 EST	39A	10.119	24.4	57	6.3	105	4/10 altocumulus 10/10 cirrostratus	13.58	55.6	252
AS-509	31 Jan 71	1603 EST	39A	10.102	21.7	86	5.0** 8.5**	255** 275**	7/10 cumulus 2/10 altocumulus	13.33	52.8	255
AS-510	26 Jul 71	0934 EDT	39A	10.196	29.8	68	5.1** 5.4**	156** 158**	7/10 cirrus	13.75	18.6	063
AS-511	16 Apr 72	1254 EST	39A	10.183	31.2	44	6.3 5.1	269 256	2/10 cumulus	11.85	26.1	257

\*Instantaneous readings from charts at T-0 (unless otherwise noted) from anemometers on launch pad 39 (A & B) light pole at 18.3 m (60.0 ft). Beginning with AS-509, wind measurements were required at the 161.5 m (530 ft) level from anemometer charts on the LUT. These instantaneous LUT winds are given directly under the listed pad light pole winds. Heights of anemometers are above natural grade.

\*\*Not instantaneous, but one minute average about T-0.

A-8

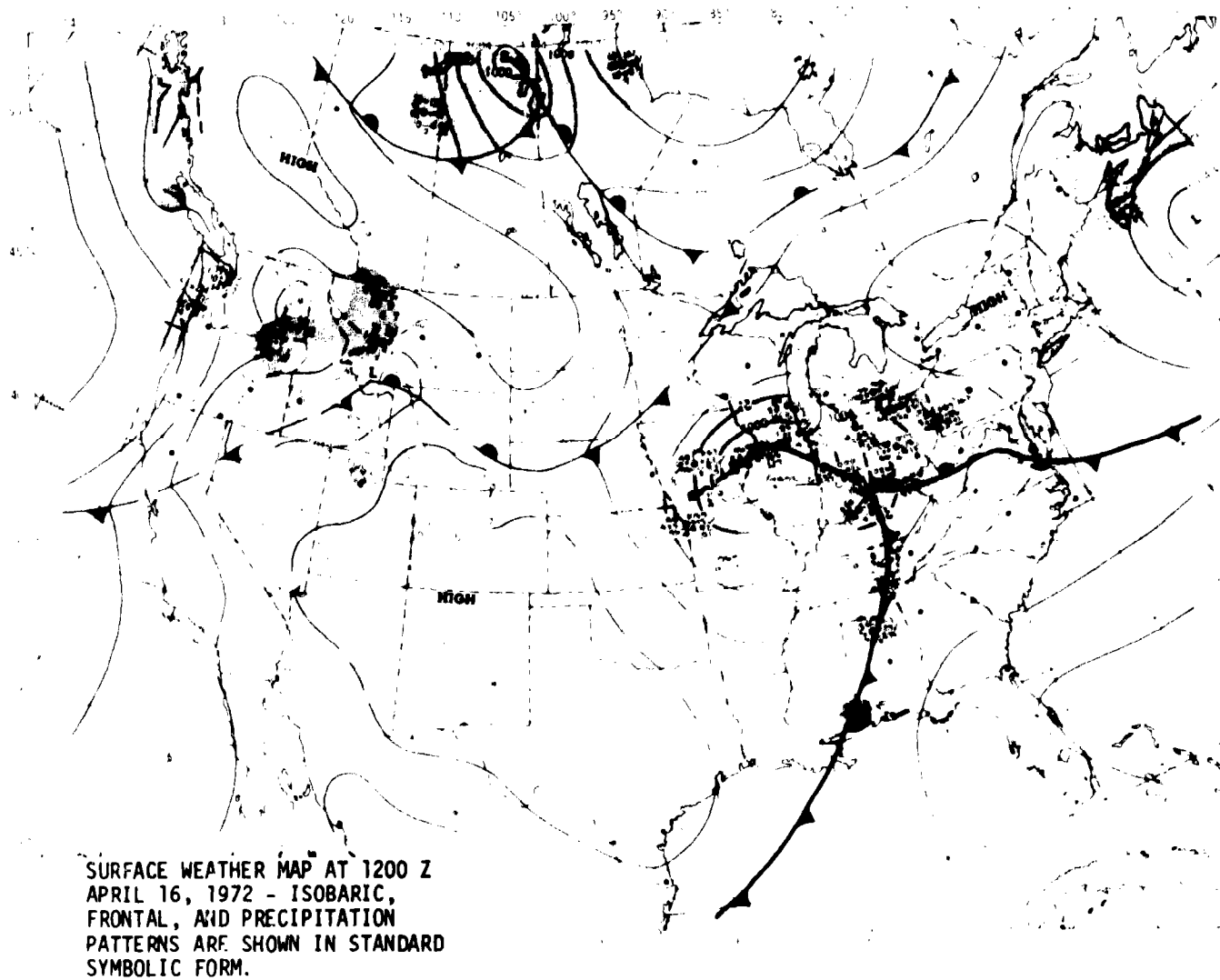
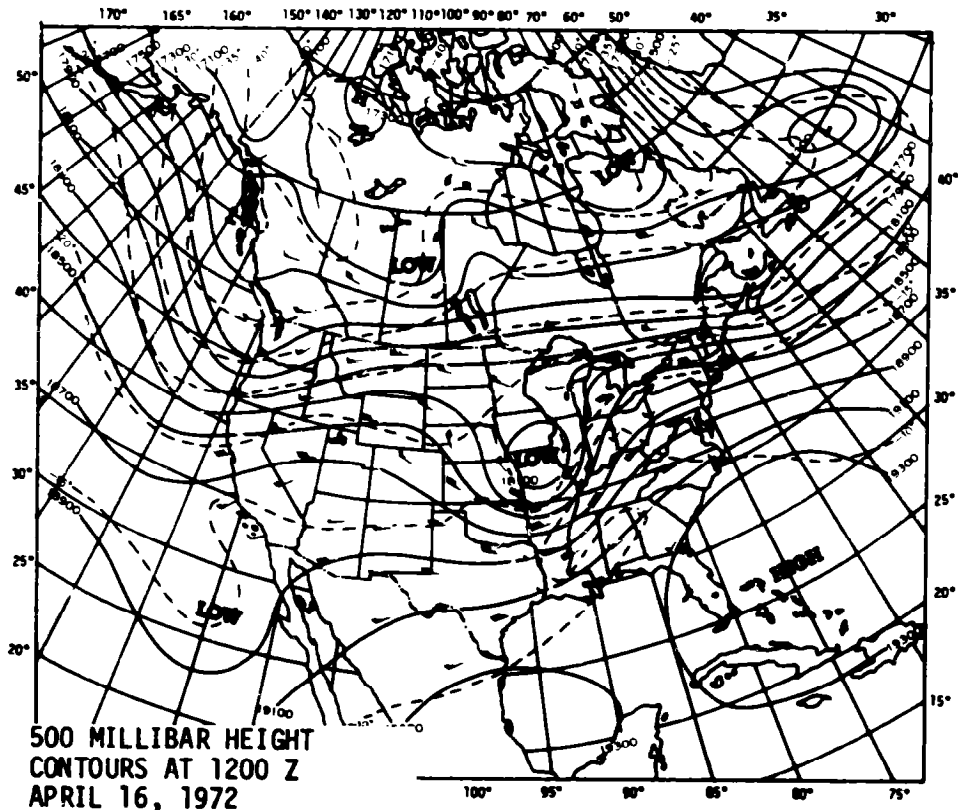


Figure A-1. Surface Weather Map Approximately 6 Hours Before Launch of AS-511

REPRODUCIBILITY OF THE ORIGINAL PAGE IS POOR



CONTINUOUS LINES INDICATE HEIGHT CONTOURS IN FEET ABOVE SEA LEVEL. DASHED LINES ARE ISOTHERMS IN DEGREES CENTIGRADE. ARROWS SHOW WIND DIRECTION AND SPEED AT THE 500 MB LEVEL. (ARROWS SAME AS ON SURFACE MAP).

Figure A-2. 500 Millibar Map Approximately 6 Hours Before Launch of AS-511

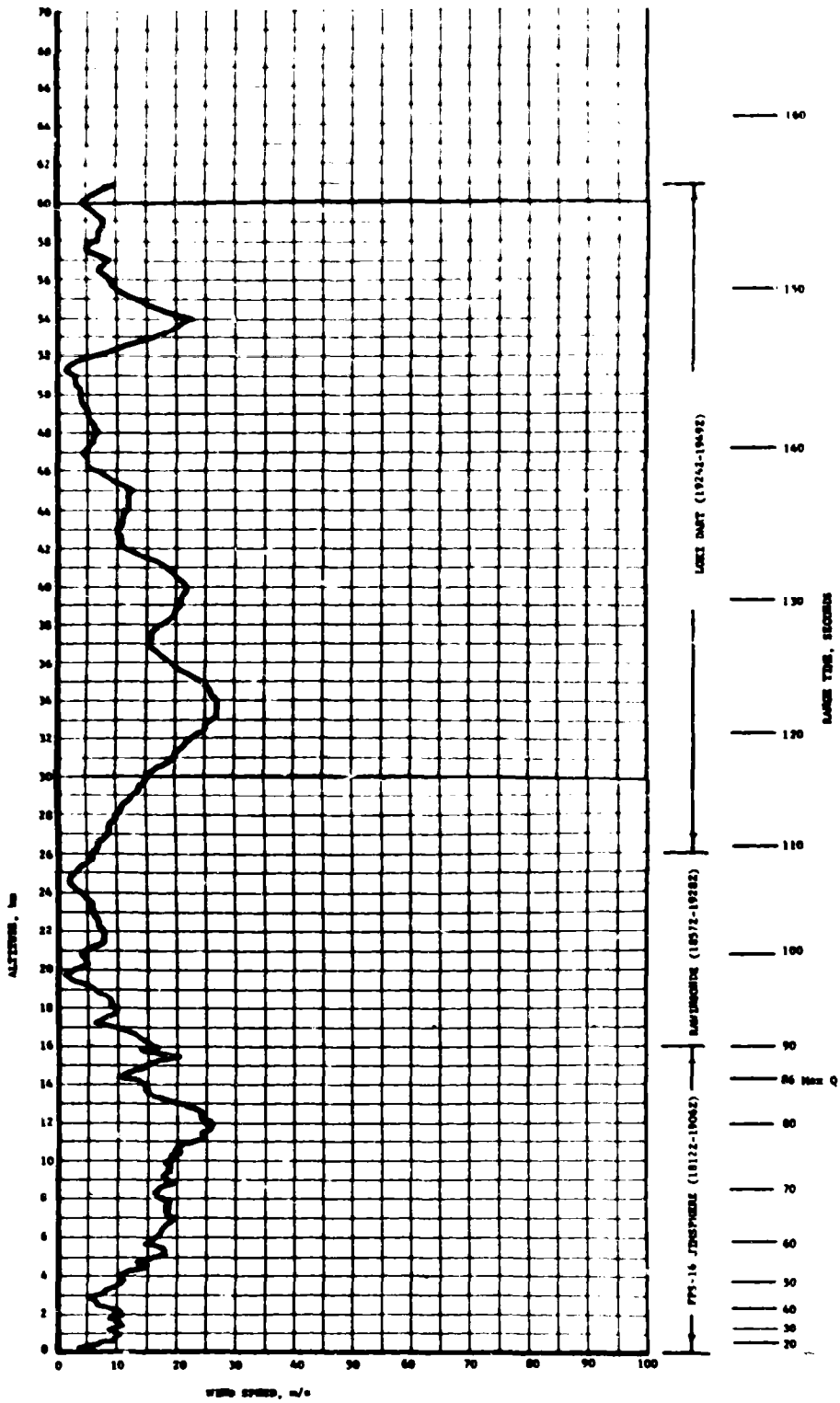


Figure A-3. Scalar Wind Speed At Launch Time of AS-511

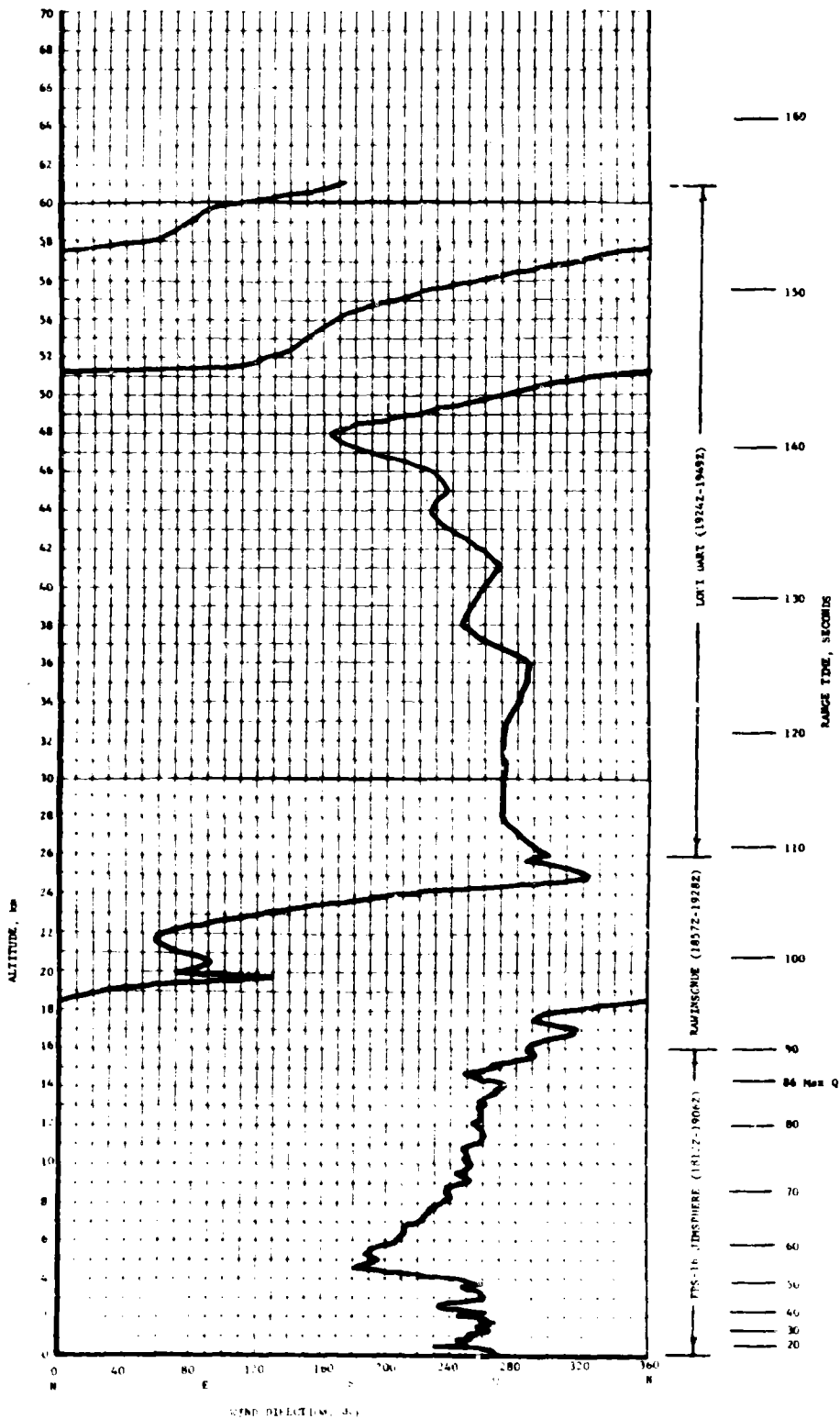


Figure A-4. Wind Direction at Launch Time of AS-511



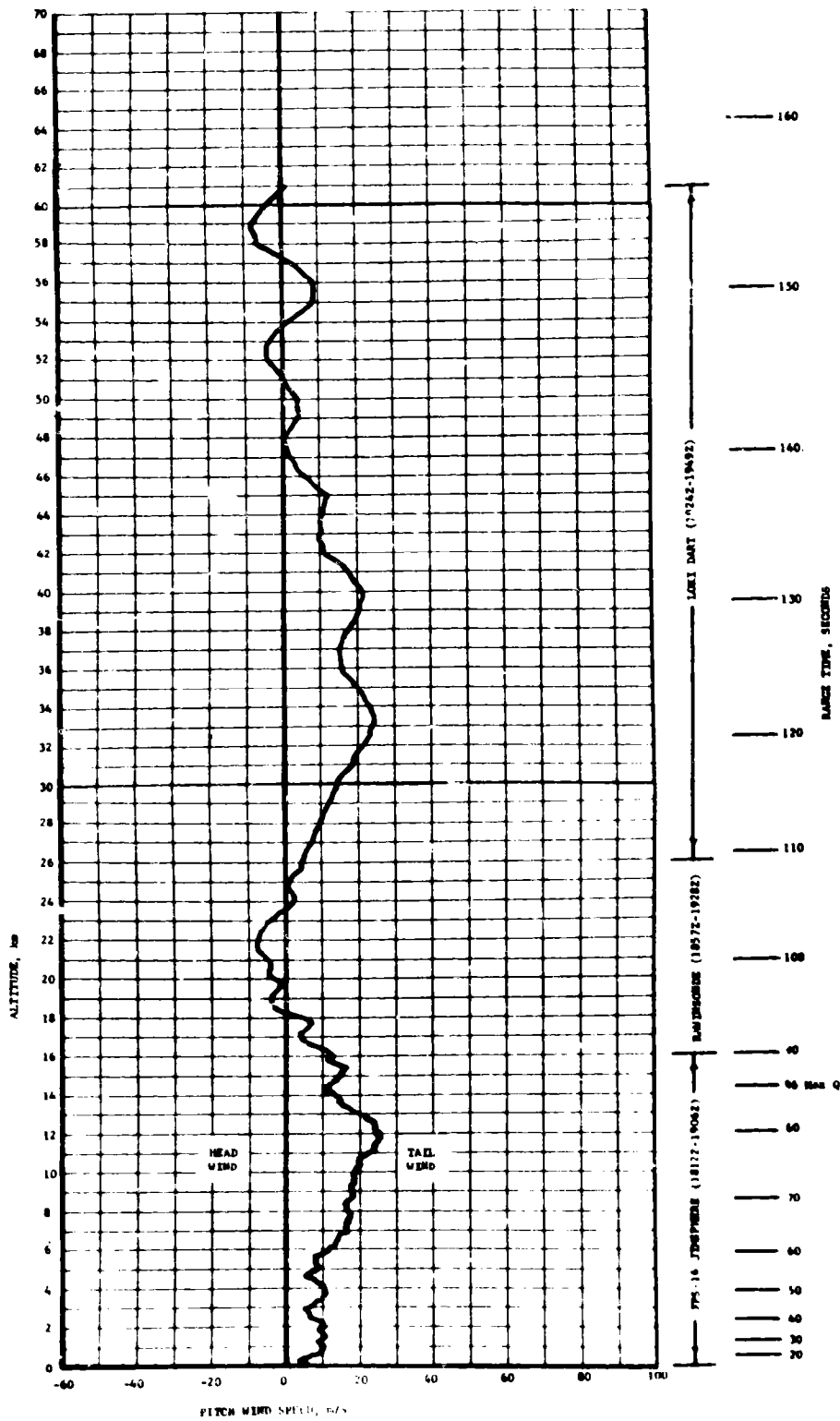


Figure A-5. Pitch Wind Velocity Component ( $W_x$ ) at Launch Time of AS-511

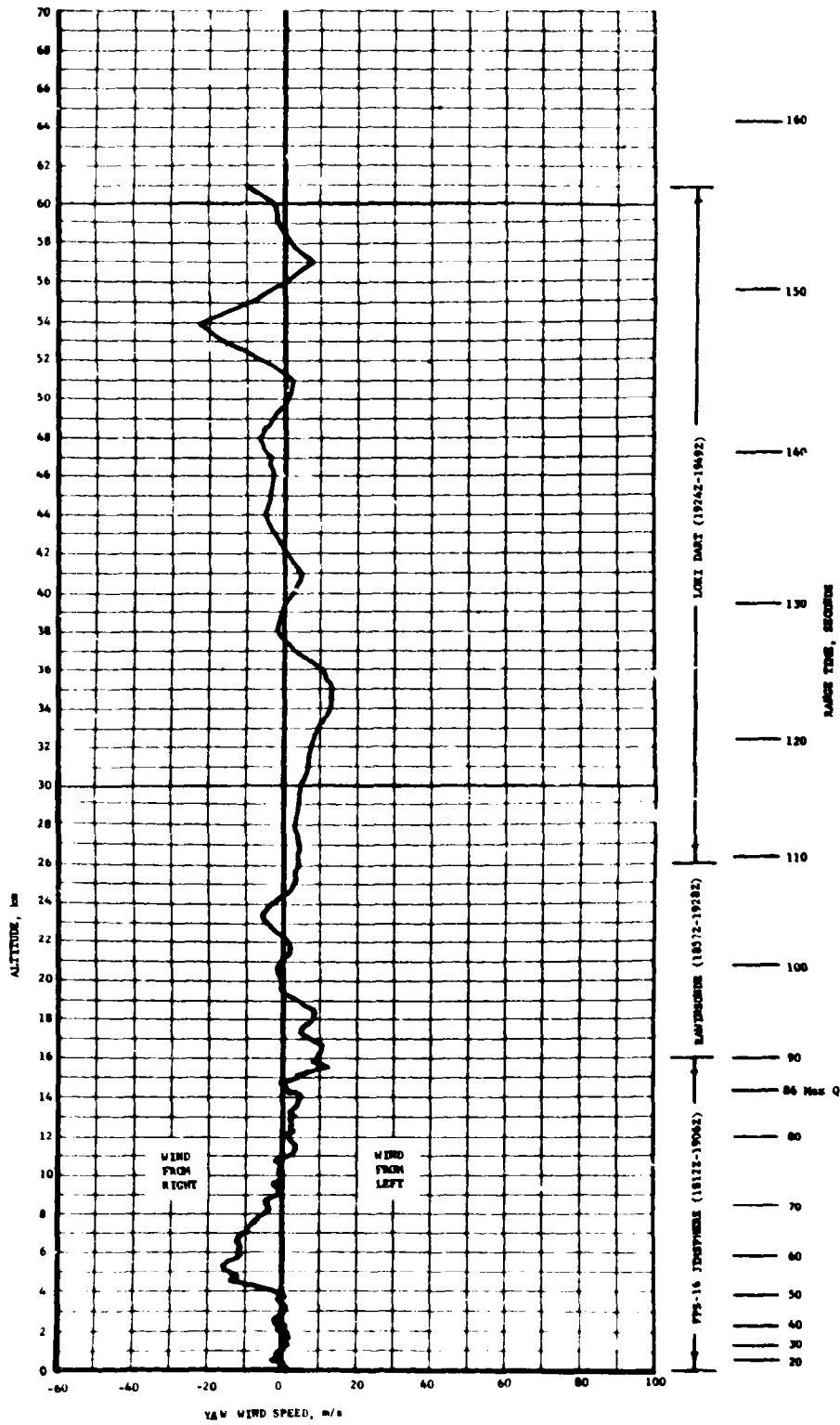


Figure A-6. Yaw Wind Velocity Component ( $W_2$ ) at Launch Time of AS-511

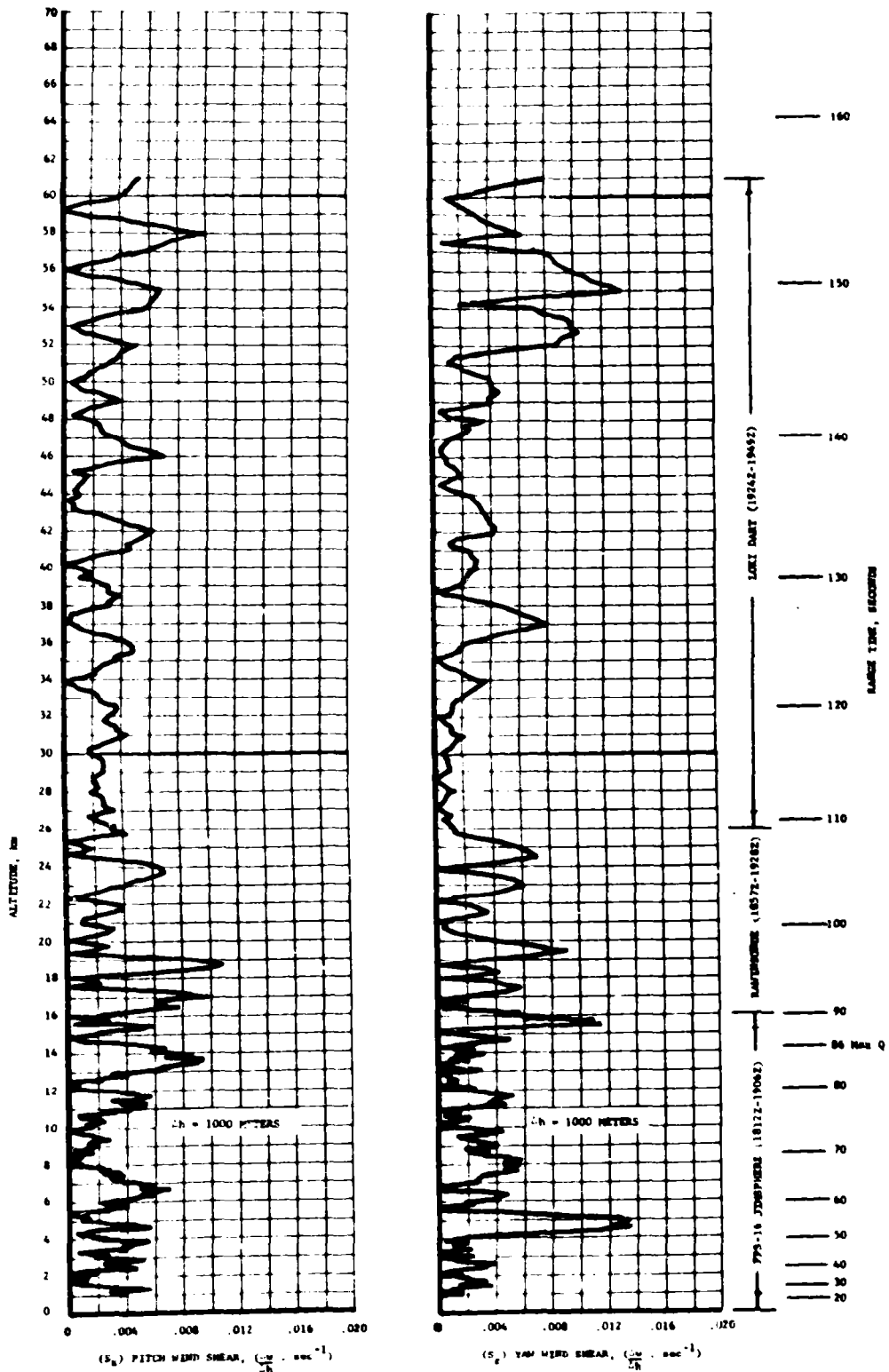


Figure A-7. Pitch (S<sub>x</sub>) and Yaw (S<sub>z</sub>) Component Wind Shears at Launch Time of AS-511

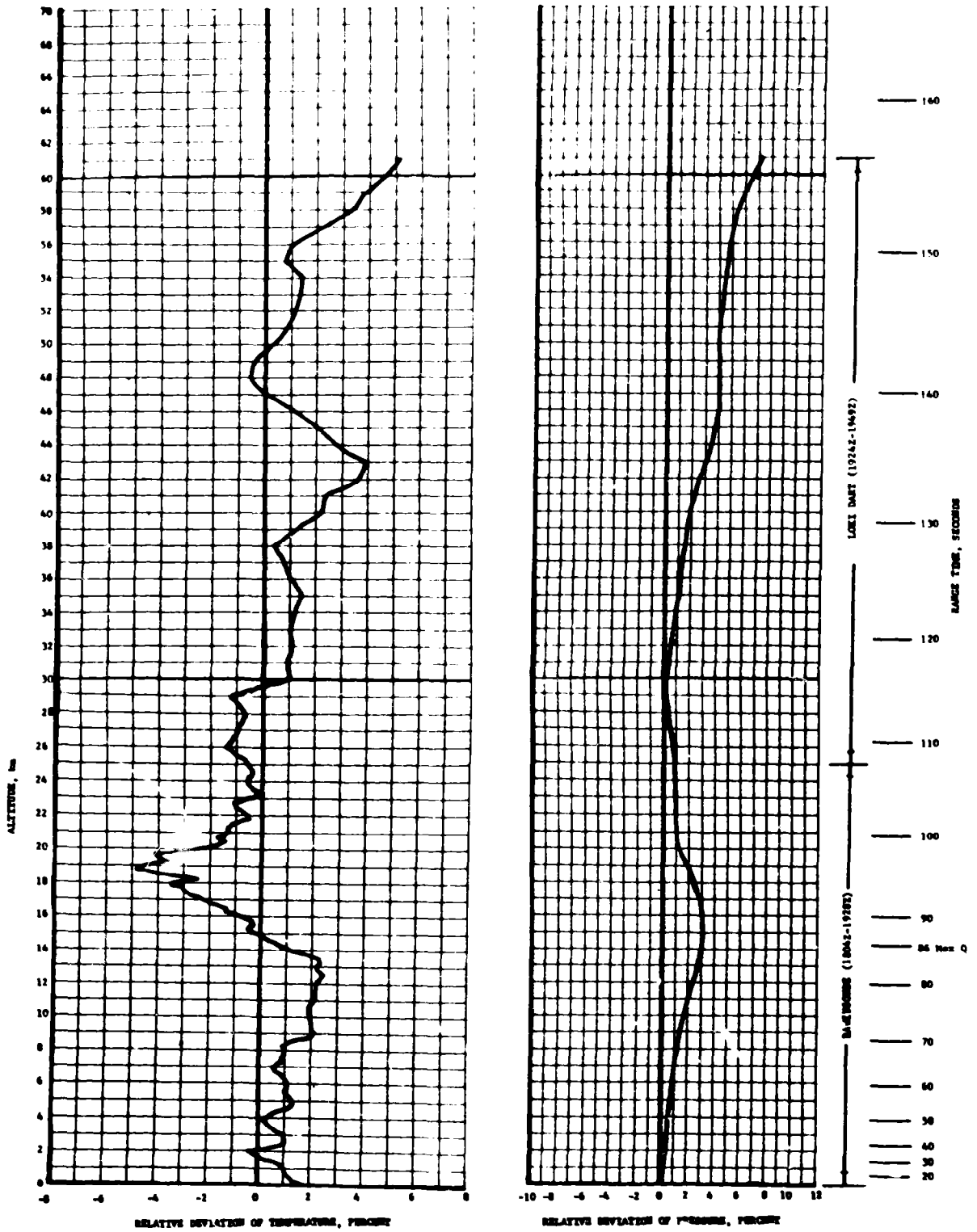


Figure A-8. Relative Deviation of Temperature and Pressure from the PRA-63 Reference Atmosphere, AS-511

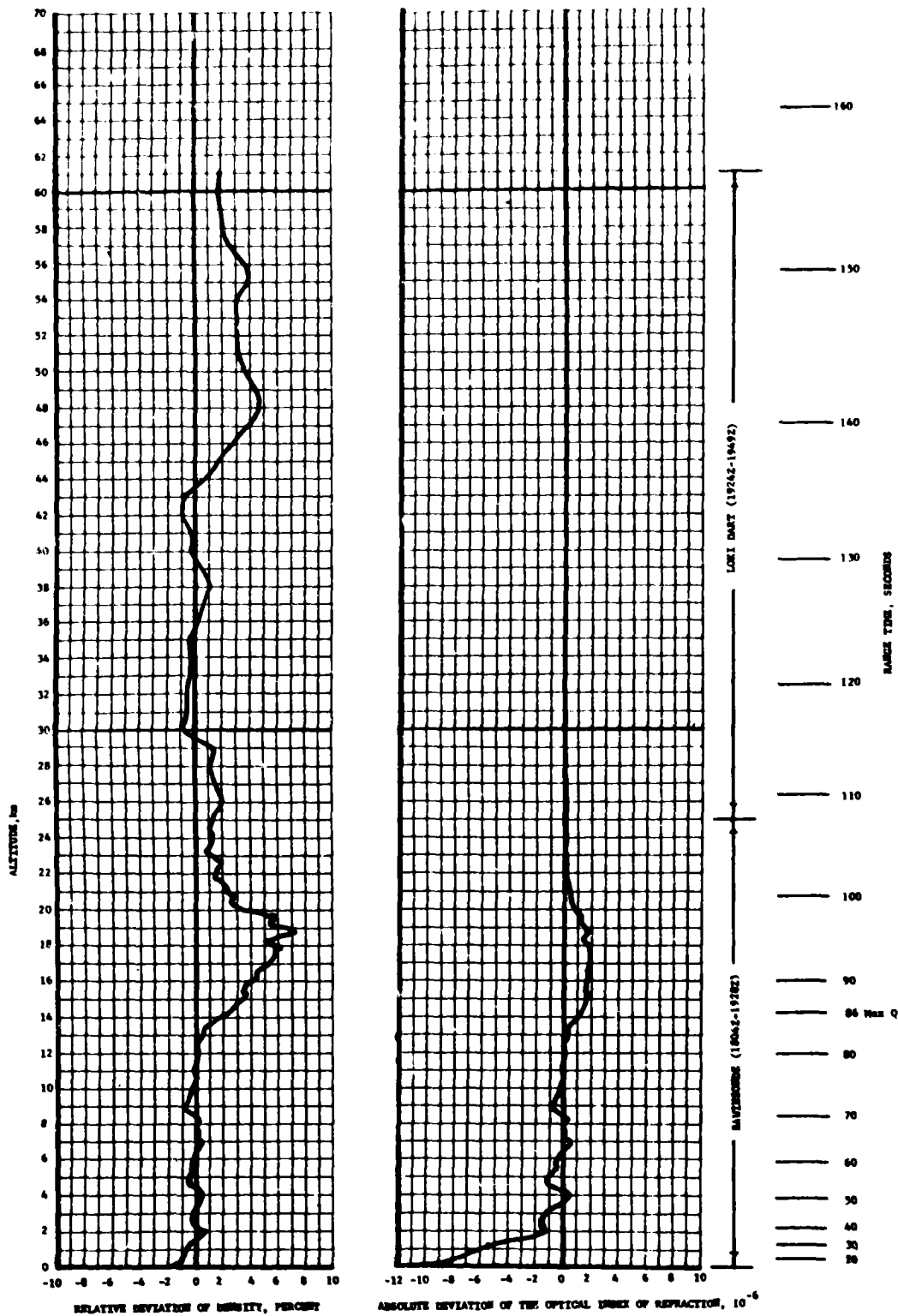


Figure A-9. Relative Deviation of Density and Absolute Deviation of the Index of Refraction From the PRA-63 Reference Atmosphere, AS-511

## APPENDIX B

### AS-511 SIGNIFICANT CONFIGURATION CHANGES

#### B.1 INTRODUCTION

The AS-511, eleventh flight of the Saturn V series; was the ninth manned Apollo Saturn V vehicle. The AS-511 launch vehicle configuration was essentially the same as the AS-510 with significant exceptions shown in Tables B-1 through B-4. The Apollo 16 spacecraft structure and components were essentially unchanged from the Apollo 15 configuration. The basic launch vehicle description is presented in Appendix B of the Saturn V Launch Vehicle Flight Evaluation Report, AS-504, Apollo 9 Mission, MPR-SAT-FE-69-4.

**Table B-1. S-IC Significant Configuration Changes**

SYSTEM	CHANGE	REASON
Propulsion	Replacement of lead alloy plated K-seal on inboard QOX line with gold plated K-seal.  Incorporate F-1 engine series lube system utilizing turbopump #1 and #2 thrust bearing cavity drainage to splash lubricate turbopump #3 turbine bearing.	Lead alloy plated K-seal was not LOX compatible.  To simplify turbopump lubrication configuration and reduce leakage possibilities by employing internal lube lines.
Guidance & Control	Redesign of MOOG servomotor electrical filter assembly.  Redesign of servomotor 3" limit detection device connector.	To incorporate filter which is compatible with flight amplifiers.  To minimize possibility of failure from physical abuse.
Separation	Added four retro motors to S-IC stage.	To reduce possibility of collision between S-IC/S-II stages after separation.
Electrical	Added redundant hardware command line through the umbilical for each engine start control valve.	To provide redundant start command path.

Table B-2. S-II Significant Configuration Changes

SYSTEM	CHANGE	REASON
Propulsion	Addition of helium purge to LOX tank ullage pressure sensing line.	To preclude a LOX/GOX compatibility situation within the LOX pressure switch.
Instrumentation	Deletion of Stillwell propellant level monitor point sensor system and addition of point sensors for propellant loading.	To provide redundant propellant loading monitoring capability, to simplify system, and to reduce cost and weight.
Guidance and Control	Addition of a mechanical clamp to the Engine Actuation System (EAS) servoactuator to hold the manual cylinder bypass valve in the closed position.	To provide positive retention of the EAS bypass valve actuation button and thus to prevent possible loss of ability to control engine position.
Electrical	Addition of redundant circuits for engines start/cutoff and installation of simplified power system wiring.	To eliminate single failure points and reduce wiring congestion.
Structural	Incorporate heavy-weight design by changing material of unpressurized structures from 2020-T6 to 7075-T6.  Move the weld joining LH <sub>2</sub> tank cylinder #1 to #2 0.4 inch forward.	Eliminate 2020-T6 material not available and obtain or approach a factor of safety of 1.4.  To compensate for preloading in excess of design limitations due to LH <sub>2</sub> tank fabrication tolerance problem.

Table B-3. S-IVB Significant Configuration Changes

SYSTEM	CHANGE	REASON
Instrumentation	Addition of measurement D0265-403 to the port provided by the new design of the Solar LOX Low Pressure Feed Duct.	To determine the effects of Low Frequency Vibration on duct during burn.
Propulsion	Changed LOX and LH <sub>2</sub> low pressure feed ducts from one ply bellows to two ply bellows.  Mission significant tubing assemblies previously fabricated with MC 125 sleeves replaced by tubing assemblies which utilize A286 material.	To provide increased safety margin in case of flow resonance.  To prevent potential leakage through sleeves which might fail due to low temperature exposure.
Structures	Replace electrical bonding strap on LOX Tank Vent Line.	To provide a LOX compatible material for the bonding strap.
Hydraulics	Replace the AVCO Hydraulic Accumulator Charging Valve with a valve manufactured by Schrader.	Improve reliability by eliminating a single point leak path.

Table B-4. IU Significant Configuration Changes

SYSTEM	CHANGE	REASON
Environmental Control	Relocate snubber assembly upstream of the hydraulic pressure switch.	To reduce sensitivity of pressure switch reaction to transient coolant pressure changes.
Networks	Removed K69 and K70 relays from the EDS Distributor and added continuous monitoring of the S-IVB LOX tank pressure in the CM by direct wiring through the EDS Distributor.  Modified control distributor to provide an upper S-IC engines 2 or 3 out discrete and a lower engines 1 or 4 out discrete.  Modified Control and EDS Distributors to provide redundant IU umbilical paths for functions that could cause or prevent engine cutoff after ignition.	To allow crew to monitor S-IVB LOX tank pressure prior to S-II/S-IVB separation rather than S-II fuel tank pressure prior to separation.  To allow the flight program to handle upper and lower S-IC outboard engine out situations by different methods.  To improve reliability.
Instrumentation and Communications	Command Decoder solder joint redesigned.  410 Multiplexer Power Supply Card changed to new configuration.  Added measurements  H10-603 Z Accelerometer H11-603 X Accelerometer H12-603 Y Accelerometer  Deleted measurements  H17-603 Z Accelerometer H21-603 X Accelerometer H24-603 Y Accelerometer	Decrease possibility of cracked solder joint.  Improve thermal and vibrational characteristics to reduce risk of data loss.  For continuous monitoring of the ST-124 M platform accelerometer pickup prior to and during liftoff.  To make room for added measurements.
LVDA/LVDC	Added a periodic rather than continuous monitor of the TLC set control of the Firing Commit Inhibit latches.	To lessen the possibility of setting DO-13 or error monitor bit 10 as a result of noise.
Flight Program	<u>BOOST INITIALIZE</u>  Provide extra accelerometer read out from $T_0 + 3.0$ to $T_1 + 10.0$ seconds.  Liftoff time guard changed to $T_0 + 17.4$ seconds.  <u>BOOST</u>  Tilt arrest and CHI freeze changed to allow correction for upper, lower, or center engine out in S-IC stage.  APS control failure test in S-IVB stage for roll.	To allow more complete postflight analysis of vibration and acceleration effects in the time period around liftoff.  Modification changes the preset search enable time to delay the recognition of the discrete, D124, thereby decreasing mission exposure to a single point failure mode.  Capability added to distinguish between an upper (2 or 3) or lower (1 or 4) outboard S-IC engine out. This allows different adjustments for upper and lower engines out, allowing contingency logic to be more nearly optimized for the actual failure situation occurring.  Attitude testing added to detect divergences between commanded and actual vehicle attitudes characteristic of a Control Signal Processor null shift. A DCS ground command has been added to provide capability to change ladder magnitude limits if telemetry indicates a null shift has occurred.



Table B-4. IU Significant Configuration Changes (Continued)

SYSTEM	CHANGE	REASON
Flight Program	<p style="text-align: center;"><u>ORBIT</u></p> <p>State Vector Telemetry at change from boost to orbital guidance</p> <p>Attitude command rate limit changed to 0.14 degrees/sec in TB5.</p> <p>Redesign of solar heating avoidance maneuver.</p> <p>APS Control Failure Test added in all channels to provide capability for setting ladder magnitude limits during the periods of flight when the vehicle is under APS control.</p>	<p>On past flights, a DCS command has been required to determine the state at orbital initialize. On the AS-510 flight, the state vector was not dumped and the data was never obtained. This change causes the state vector to be telemetered automatically without DCS action.</p> <p>By decreasing the attitude command rate in TB5, the slosh modes will be decreased such that the propellant will not be vented in liquid state through the gaseous vent orifices. The command rates will be restored to nominal values at TB6 start.</p> <p>The pre-programmed AS-510 maneuver was modified to allow the vehicle to remain at a stable attitude longer and to minimize ground command dependence.</p> <p>Attitude testing has been added to detect divergences between commanded and actual vehicle attitudes characteristic of a CSP null shift. A DCS ground command has been added to provide capability to change ladder magnitude limits if telemetry indicates a null shift has occurred.</p>

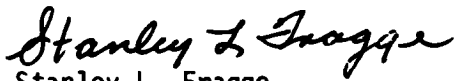
APPROVAL

SATURN V LAUNCH VEHICLE FLIGHT EVALUATION REPORT

AS-511, APOLLO 16 MISSION

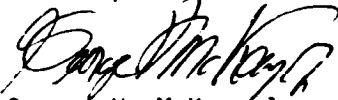
By Saturn Flight Evaluation Working Group

The information in this report has been reviewed for security classification. Review of any information concerning Department of Defense or Atomic Energy Commission programs has been made by the MSFC Security Classification Officer. The highest classification has been determined to be unclassified.

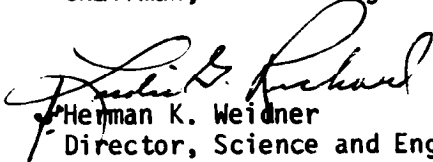


Stanley L. Fragge  
Security Classification Officer

This report has been reviewed and approved for technical accuracy.



George H. McKay, Jr.  
Chairman, Saturn Flight Evaluation Working Group



Herman K. Weidner  
Director, Science and Engineering



Richard G. Smith  
Saturn Program Manager

**END  
DATE  
FILMED**

DEC 17 1973